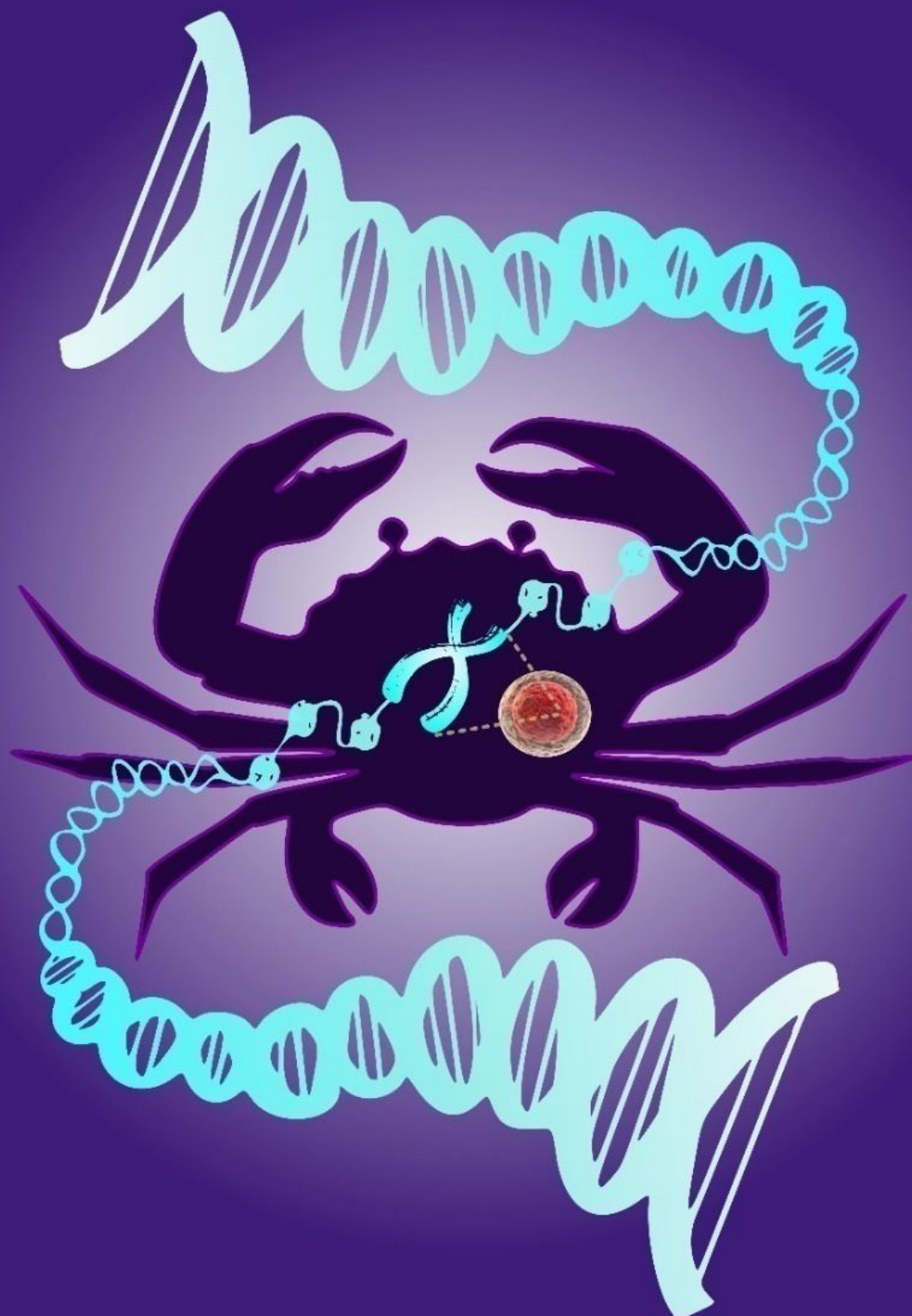




# Current Oncological Abstract Service

COAS (Monthly)

October 2025, Volume 2 Issue 10



Compiled by:  
Chittaranjan National Cancer Institute Library, Kolkata  
(An Autonomous Body under Govt. of India, Ministry of Health & Family Welfare)

## Current Oncological Abstract Service (COAS)

---

### Monthly

---

#### Aims of the Abstracts

The Current Oncological Abstract Service (COAS) aims to provide timely, curated abstracts from a broad spectrum of oncological literature. The objectives of the service are:

1. To deliver concise, up-to-date abstracts of recently published oncological research, covering various subfields such as medical oncology, radiation oncology, anesthesiology, surgical oncology, and hematology.
2. To assist healthcare professionals, researchers, and students in staying informed about the latest advances and trends in oncology.
3. To support clinical and research-based decision-making by providing quick access to relevant, high-impact studies.
4. To foster knowledge exchange across disciplines, promoting a broader understanding of cancer-related topics.

#### Scope of the Abstracts

1. COAS includes abstracts from areas such as cancer biology, genetics, epidemiology, clinical trials, and treatment modalities (e.g., chemotherapy, immunotherapy, and targeted therapies), as well as patient care practices.
2. Abstracts are sourced from global research publications, offering a comprehensive view of international advancements in oncology.
3. Priority is given to high-impact studies, systematic reviews, meta-analyses, and research with significant implications for clinical practice.
4. In addition to core oncology, abstracts may cover related fields such as molecular biology, pharmacology, palliative care, and psychological support in oncology, reflecting the interdisciplinary nature of cancer care.

#### Layout

The "Current Oncological Abstract Service" is designed as a targeted information resource that provides clinicians, researchers, and students in oncology with the latest research abstracts and developments in cancer-related fields. It offers a regularly updated collection of abstracts from recently published articles, journals, and reports in oncology to keep users informed about current research trends, treatments, diagnostic methods, and advancements in oncology. The service is delivered monthly via email and as a downloadable PDF available on the CNCI website.

**Content Sections** - The COAS includes summaries of:

- The latest and most impactful research papers.
- Updates on new treatments, drugs, and clinical trials.
- Abstracts on new diagnostic tools, biomarkers, and techniques.
- Insights into cancer prevention research and epidemiological studies.
- Information on palliative care, patient management, and supportive therapies.

**Abstract Formatting** Each entry in the Current Oncological Abstract Service (COAS) includes:

- The title of the article or study.
- Authors and publication details.
- A summary focused on key findings and relevance.
- Keywords for easier navigation.
- A direct link to the original source (if online access is available).

### **User Navigation**

- An index organized by cancer types, treatment methods, and research areas to facilitate easy navigation.
- A searchable database on the web platform, allowing users to quickly locate relevant abstracts.

### **User Engagement**

- **Feedback Mechanism:** Users can provide feedback on abstracts and suggest improvements.
- **Personalization:** Users can subscribe to specific categories or topics of interest.

### **Bibliographical Citation:**

**Title**-The title of the paper is invariably given in English and non-English titles are translated into English.

**Author**-A maximum of ten author's names are given. In case of more than ten authors, names of first ten authors are given followed by et al.

**Details**-The title of the paper is followed by volume number, issue number (in parenthesis), pagination and the of publication. Late publication or late receipt of the journals (if any), language(s) and number of references cited in the publication are given in parenthesis.

**Abstract**-Abstracts are informative and comprehensive. New data or findings are specifically indicated.

**Current Oncological Abstract Service (COAS)**

---

**Editorial Board Members**

---

**Dr. Jayanta Chakrabarti**

**Director & HOD, Surgical Oncology**

**Chittaranjan National Cancer Institute**

**Kolkata**

**Dr. Suparna Mazumdar**

**HOD, Radio-diagnosis**

**Chittaranjan National Cancer Institute**

**Kolkata**

**Dr. Aniruddha Dam**

**HOD, Head & Neck Oncology**

**Chittaranjan National Cancer Institute**

**Kolkata**

**Dr. Sankar Sengupta**

**MS & HOD, Laboratory Services**

**Chittaranjan National Cancer Institute**

**Kolkata**

**Dr. Deepa Chakrabarti**

**HOD, Anaesthesiology & Critical Care**

**Chittaranjan National Cancer Institute**

**Kolkata**

**Dr. Debarshi Lahiri**

**Specialist (SAG), Radiation Oncology**

**Chittaranjan National Cancer Institute**

**Kolkata**

**Dr. Sutapa Mukherjee**

**Senior Scientific Officer**

**Chittaranjan National Cancer Institute**

**Kolkata**

---

**Compiled by Central Library, Chittaranjan National Cancer Institute, Kolkata**

**Published by Chittaranjan National Cancer Institute Library, Kolkata**

---

**Current Oncological Abstract Service (COAS)**

---

**Monthly Abstracting Journal**

---

**VOLUME 2**

**ISSUE 10**

**OCTOBER 2025**

---

**Compiler:**

**Dr. Sanmoy Chakraborty**

Assistant Library & Information Officer

**&**

**Mr. Ganesh Gorai**

Assistant Library & Information Officer

Phone: 033 2475-9313, 033 3506-0600

Website: <https://www.cnci.ac.in/>

Email: [cnci.library@gmail.com](mailto:cnci.library@gmail.com)

**DTP and Computer Processing:**

CNCI Central Library

The purpose of the Current Oncological Abstract Service (COAS) is to provide users with valuable, curated oncology-related abstracts for research, educational, and informational purposes. Access to COAS materials is granted only to authorized users within CNCI, Kolkata. Use of COAS content is restricted to non-commercial, academic, and research-oriented purposes. Every effort is made to present the abstracts accurately but COAS assumes no liability for any errors and omissions.

**Current Oncological Abstract Service (COAS)**

---

**Monthly Abstracting Journal**

---

**VOLUME 2**

**ISSUE 10**

**OCTOBER 2025**

---

**Contents**

**Page No.**

**Anesthesiology**

**1- 18**

**Cancer Research**

**19- 110**

**Diagnostic Services**

**(Pathology, Cancer Screening & Radio-diagnosis)**

**111- 144**

**Medical Oncology**

**(Chemotherapy, Hematology & Radiotherapy)**

**145- 203**

**Surgical Oncology**

**204- 272**

**List of Serials**

**273**

**Anesthesiology****25COASOCT01:****Title: Positive End-Expiratory Pressure and Atelectasis after Bronchial Blockade One-Lung Ventilation in Infants: A Randomized Controlled Study,**

Ling-Shan Yu, Xiu-Hua Chen, Si-Jia Zhou, Zeng-Chun Wang,

Journal of Cardiothoracic and Vascular Anesthesia, Volume 39, Issue 10, 2025, Pages 2760-2768,

<https://doi.org/10.1053/j.jvca.2025.06.025>.

**Abstract:** This study aimed to evaluate the effect of positive end-expiratory pressure (PEEP) combined with 100% oxygen on atelectasis during emergence from anesthesia after one-lung ventilation (OLV) with a bronchial blocker in infants receiving thoracoscopic lobectomies. This was a randomized controlled study. This study was performed in a teaching hospital. Infants who received thoracoscopic lobectomies in our hospital from June 2024 to December 2024 were included in this study. Sixty-nine infants (Group A) with bronchial blocker OLV thoracoscopic lobectomies received no PEEP but maintained intraoperative oxygen levels ( $\text{FiO}_2$  0.6-0.8) after the removal of the bronchial blocker until extubation during emergence from anaesthesia. Another 69 infants who met the inclusion criteria and received PEEP of 5 to 6  $\text{cmH}_2\text{O}$ , combined with 100% oxygen, after removal of the bronchial blocker until extubation during emergence from anesthesia, were included in Group B. The inclusion criteria were as follows: (1) These infants were diagnosed with congenital cystic adenomatoid malformation and received bronchial blockade OLV thoracoscopic lobectomies; (2) American Society of Anesthesiologists (ASA) class I to II (ASA class I means a normal healthy patient; class II means a patient with mild systemic disease); and (3) age younger than 1 year. The exclusion criteria were as follows: (1) preoperative chest computed tomography or ultrasound suggestive of atelectasis; (2) intraoperative ventilation mode was changed to bilateral lung ventilation; (3) intraoperative  $\text{FiO}_2$  greater than 0.9; (4) cardiorespiratory dysfunction; (5) large cysts causing significant mediastinal shift or compressing cardiac chambers; and (6) declined to participate. There were no significant differences in the preoperative general condition, perioperative hemodynamics, duration of operation, or length of postoperative hospital stay between the two groups ( $P > 0.05$ ). There were no significant differences in the oxygenation index, alveolar-arterial oxygen differential pressure, or oxygen saturation ( $\text{SpO}_2$ ) at T1 (the completion of surgery) ( $p > 0.05$ ). At T2 (30 minutes after extubation), the oxygenation index and  $\text{PaO}_2$  level were greater, the alveolar-arterial oxygen differential pressure was lower, and the lowest postoperative  $\text{SpO}_2$  level within 30 minutes after extubation was better in Group B than in Group A ( $p < 0.05$ ). The time from bronchial blocker removal to extubation was shorter in Group B than in Group A ( $p < 0.05$ ). Compared with those of Group A, the proportions of patients with lung ultrasound scores of 3 (juxtapleural consolidation, large-sized consolidations and B-lines, white lung) and bedside chest radiography atelectasis scores of 3 (lobar atelectasis) in both lungs after extubation were lower in Group B ( $p < 0.05$ ). The prevalence of hypoxemia (after extubation,  $\text{SpO}_2 < 90\%$ ) was 46 (66.7%) in Group A and 14 (20.3%) in Group B, and the differences were statistically significant ( $p < 0.05$ ). The duration of oxygen administration after extubation in Group B was shorter than that in Group A ( $p < 0.05$ ). There was a statistically



significant correlation between lung ultrasound scores and the chest radiographic atelectasis score in both groups ( $p < 0.05$ ). In one-lung ventilation using bronchial blockers performed during thoracoscopic lobectomies in infants, applying PEEP at 5 to 6 cmH<sub>2</sub>O combined with 100% oxygen ventilation after the removal of the bronchial blocker until extubation was associated with improved oxygenation and did not appear to increase the risk of atelectasis during emergence from anesthesia. However, further studies are needed to evaluate the safety of this strategy.

**Keywords:** one lung ventilation; bronchial blockade; PEEP; atelectasis

## 25COASOCT02:

### **Title: The Association Between Coping Styles, Meaning in Life, Death Preparedness of Advanced Cancer Patients,**

Xi Zhang, Jingxin Wang, Mei Liu, Feng Li, Tieying Zeng,

Journal of Pain and Symptom Management, Volume 70, Issue 4, 2025, Pages 363-370,

<https://doi.org/10.1016/j.jpainsymman.2025.07.001>.

**Abstract:** The current level of death preparedness in advanced cancer patients is low. However, death preparedness is an important prerequisite for quality of life and quality of death for these patients. This study aimed to explore the unique relationship between coping styles, meaning in life, and death preparedness in advanced cancer patients, and whether meaning in life mediates the relationship between coping styles and death preparedness. A cross-sectional study design was used. A convenience sampling method was used to recruit 1100 advanced cancer patients from seven hospitals in Hubei and Anhui provinces, China. Data were collected using the medical coping modes questionnaire, the meaning in life questionnaire, and the death preparedness scale. Pearson's correlation was used to examine the relationship between coping styles, meaning in life, and death preparedness. Mediation analyses examined whether meaning in life mediated the relationship between coping styles and death preparedness. The coping style of confrontation and meaning in life are positively correlated with death preparedness. The coping style of avoidance is negatively correlated with death preparedness. Meaning in life plays a partial mediating role between the coping styles of confrontation, avoidance and death preparedness. These findings provide new knowledge and perspectives to promote death preparedness in advanced cancer patients. Meaning in life played a partial mediating role between coping styles of confrontation, avoidance and death preparedness. Therefore, to improve patients' death preparedness, taking effective measures to enhance patients' meaning in life is particularly important.

**Keywords:** Coping styles; meaning in life; death preparedness; advanced cancer patients; mediator

## 25COASOCT03:

### **Title: Understanding and Predicting End-of-Life Care Preferences Among Urban-Dwelling Older Adults in China,**

Chuqian Chen, Robert Jiqi Zhang,

Journal of Pain and Symptom Management, Volume 70, Issue 4, 2025, Pages 379-391.e3,

<https://doi.org/10.1016/j.jpainsymman.2025.07.009>.



**Abstract:** Understanding older adults' preferences for end-of-life care (EoLC) is vital for respecting their wishes and informing effective service planning and policy development. Previous research has examined factors influencing different dimensions of EoLC preferences separately, but few studies have explored these dimensions as interconnected patterns and viewed older adults as heterogeneous using a person-centered approach. This study aims to: 1) identify heterogeneous latent patterns across seven dimensions of EoLC preferences among Chinese older adults; 2) describe and explain these patterns; and 3) predict membership within these patterns.: Survey data from 646 urban-dwelling older adults aged 60 and above across 26 provincial-level administrative divisions in Mainland China were analyzed. EoLC preferences regarding willingness to know diagnosis, willingness to know prognosis, decision-maker, treatment goals, place of care, caregiver, and setting advance directives were assessed alongside demographics, resources, knowledge and attitudes, and caregiving/bereavement experiences. Latent class analysis (LCA), 3-step regressions, and Catboost machine learning models were employed to identify subgroups, examine between-group differences, and predict subgroup membership, respectively. LCA identified three latent patterns: "low self-determination, quality-goal, family-oriented care" (9.1%), "high self-determination, quality-goal, family-oriented care" (54.0%), and "high self-determination, quantity-goal, professional-oriented care" (36.9%). Significant between-group differences were found in education, marital status, living arrangements, family income, social support, EoLC knowledge, general trust, and professional-patient trust. Machine learning models revealed that high general trust predicts membership in the high self-determination, quality-goal, family-oriented care group, while low filial piety expectations predict membership in the high self-determination, quantity-goal, professional-oriented care group. Among Chinese older adults, three EoLC preference patterns were found, which were characterized by low family connections, low trust in professionals combined with adequate resources, and extensive knowledge, respectively. High general trust and low filial piety expectations were key predictors for two of the three patterns.

**Keywords:** End-of-life care preferences; Chinese; Older adults; Latent class analysis; Machine learning

#### 25COASOCT04:

**Title: Variations in End-of-Life Symptom Management Medication Prescribing Among Home Care Recipients in Ontario, Canada,**

Deena Fremont, James Downar, Hsien Seow, Peter Tanuseputro, Colleen Webber,  
Journal of Pain and Symptom Management, Volume 70, Issue 4, 2025, Pages 341-350.e6,  
<https://doi.org/10.1016/j.jpainsymman.2025.06.013>.

**Abstract:** Nearing the end of life (EOL), a variety of medications can be prescribed for symptom management during the dying process. To describe the prescribing of subcutaneous symptom management medications during the last six weeks of life among home care recipients in Ontario, Canada, and to assess the association of prescribing medications with EOL outcomes. This retrospective cohort study included individuals in Ontario who died between January 1, 2017, and March 17, 2020, aged 66–105 at death and who received publicly-funded home care at least one month prior to death. End-of-life symptom management medications were identified based on an extensive literature review and

consultation with Ontario palliative care physicians. We measured the proportion of decedents prescribed an EOL medication in the last six weeks of life. We used log-binomial regression models to evaluate the association between EOL medication prescribing and emergency department visits and hospitalizations in the last two weeks of life, and location of death (community vs. institution). Of the 55,903 home care decedents identified, 28.6% received an EOL symptom management prescription. Those who received a prescription had a decreased risk of dying in an institution (adjusted risk ratio (aRR): 0.59, 95% confidence interval (CI): 0.57–0.60), having an emergency department visit (aRR: 0.22, CI: 0.20–0.24), and being hospitalized (aRR: 0.20, CI: 0.18–0.22) compared to those without a prescription. Our findings suggest that EOL prescribing is associated with a decreased risk of late acute care use and death in hospital among home care decedents.

**Keywords:** Administrative health data; End-of-life care; Prescribing; Home care; Health system measures

## 25COASOCT05:

### **Title: Development of an Explanatory Model of Resuscitation Preference Decision Making,**

Mark Goldszmidt, Rachelle Lassaline, Kristen A. Bishop, Ravi Taneja,  
Journal of Pain and Symptom Management, Volume 70, Issue 4, 2025, Pages 351-362,  
<https://doi.org/10.1016/j.jpainsymman.2025.06.012>.

**Abstract:** Establishing resuscitation preferences prior to a medical emergency is a well-recognized component of hospital practice. When done effectively, these help to ensure that care received aligns with patient wishes. In practice however, these conversations can be challenging and influences on choice are not well understood. Objectives: The purpose of this study was to identify influences on patient resuscitation preferences and their relationship to each other, with the aim of developing an explanatory model. Constructivist grounded theory was used to analyze 107 clinical notes from a dataset of detail-rich resuscitation preference conversation narratives. Sampling was purposeful and focused on maximum variation. Iterative data collection and analysis and constant comparison was used to enhance rigor as was the incorporation, in later stages of the analysis, of existing theories and models. Twenty-seven coding categories were developed and integrated into the resuscitation preferences conversation model that described the interaction and relationship between influences. Within the model, three categories (Ability to Engage in Meaningful Activity, Trajectory, and Perceptions and Beliefs) informed patient and Substitute Decision Maker (SDM) preferences, while an additional two categories (Social and Knowing, and Experiences) informed substitute decision maker choice. The developed model builds on prior work and helps explain the relationship between influences and preferences. The integration of both patient and substitute decision maker perspective into the model shows the complexity of the substitute decision maker role in decision-making. The model should be used in conjunction with existing conversation guides to support effective resuscitation preference conversations.

**Keywords:** Resuscitation preferences; resuscitation preferences model; decision-making; internal medicine; constructivist grounded theory

**25COASOCT06:****Title: Measuring the Complexity of Palliative Care: A Single-Center Retrospective Study,**

Hironori Ohinata, Mitsunori Miyashita, Isseki Maeda,

Journal of Pain and Symptom Management, Volume 70, Issue 4, 2025, Pages 371-378.e2,

<https://doi.org/10.1016/j.jpainsymman.2025.07.007>.

**Abstract:** International guidelines recommend specialized palliative care for patients with complex care needs. However, scales assessing patient complexity should be modified according to each country and its healthcare systems. This study aimed to develop a scale for assessing the complexity of palliative care needs among patients referred to a palliative care unit and to determine its validity. We developed an 8-item COMPLEX scale (with each item scored 0–3 points) to assess patient complexity based on physicians' clinical reasoning and a literature review. Data were collected from a palliative care unit at a Japanese hospital between September 2022 and March 2023. The inclusion criteria were: (1) referral to a palliative care unit, and (2) any age, sex, or primary cancer focus. A total of 305 patients were included in the analysis. During the data collection period, 148 patients (48.5%) died. Regarding survival time analysis, patients were stratified into three groups based on their COMPLEX scale scores. At the time of referral to the palliative care unit, the mean survival time was 62.0 days for those with a score of  $\leq 8$ , 51.1 days for those with scores of 9–10, and 48.8 days for those with a score of  $\geq 11$ . Overall, patients with higher scores had significantly shorter survival times than those with lower scores ( $P = 0.037$ ). The COMPLEX scale demonstrated meaningful associations with external indicators, such as survival time. Future studies should validate its reliability across diverse clinical settings, among various raters, and in relation to other external indicators.

**Keywords:** Complexity; palliative care; palliative care unit; care needs; advanced cancer

**25COASOCT07:****Title: The Italian Version of the FAMCARE-P13 Questionnaire: A Validation Study,**

Giacomo Massa, Gabriele Tinè, Ernesto Zecca, Rosalba Miceli, Alessandra Pigni,

Journal of Pain and Symptom Management, Volume 70, Issue 4, 2025, Pages 392-399.e2,

<https://doi.org/10.1016/j.jpainsymman.2025.07.017>.

**Abstract:** The FAMCARE-P13 is a tool designed to evaluate patients' satisfaction with received healthcare. This self-reported questionnaire has already been adapted and validated in different languages but not Italian. The study aims to examine the cultural adaptation of the Italian version of the FAMCARE-P13 questionnaire and evaluate its psychometric properties in outpatients with advanced cancer. The FAMCARE-P13, a questionnaire of 13 items scored on a 5-point Likert scale (from 1 = “very dissatisfied” to 5 = “very satisfied”), was culturally adapted into Italian through forward-back translation by native Italian and English speakers. The questionnaire was then administered to a balanced sample of outpatients with five advanced cancer histologies. The following psychometric analyses were performed: Confirmatory Factor Analysis to test the presence of a single latent factor, Cronbach's  $\alpha$  to test internal consistency, intraclass correlation coefficient to evaluate test-retest reliability after 3 days, and a known-group validity analysis. A total of 300 patients completed the questionnaire. Confirmatory factor analysis fully supported a one-factor structure of the tool,

with the model exhibiting robust fit indices, specifically a comparative fit index of 0.96 and a Tucker-Lewis Index of 0.95. The satisfaction was closely related to doctors' availability and availability to communicate. Cronbach's  $\alpha$  was 0.95 (95% CI: 0.94–0.95), showing satisfactory internal consistency. Test-retest analysis showed stability over time, with a global intraclass correlation coefficient of 0.91 (P-value < 0.0001). The Italian version of the FAMCARE-P13 questionnaire appears valid for assessing the satisfaction with the care received by patients with advanced cancer.

**Keywords:** Patient satisfaction; PREMs; FAMCARE-P13; validation; palliative care

## 25COASOCT08:

### **Title: Minimal Clinically Important Difference in the Integrated Palliative Care Outcome Scale for Cancer Dyspnea,**

Yoshinobu Matsuda, Masanori Mori, Akihiro Tokoro, Yoshihiko Taniguchi, Sayo Aiki, Yusuke Takagi,

Journal of Pain and Symptom Management, Volume 70, Issue 4, 2025, Pages 335-340,

<https://doi.org/10.1016/j.jpainsymman.2025.06.010>.

**Abstract:** Dyspnea is a common and distressing symptom in patients with cancer. The Integrated Palliative care Outcome Scale (IPOS) provides health care providers with a proxy tool for assessing dyspnea; however, the minimal clinically important difference (MCID) in the IPOS for dyspnea is unknown. To determine the MCID in the IPOS improvement for dyspnea, this secondary analysis used data from a multicenter prospective observational study initially designed to evaluate the effectiveness and safety of opioids for dyspnea in patients with cancer. We included patients with available IPOS scores and Patient's Global Impression (PGI) at baseline and 24, 48, and 72 h after starting opioid therapy, comprising cohorts 1, 2, and 3, respectively. The MCID for IPOS improvement in dyspnea was determined using a sensitivity-specificity approach, specifically Youden's J statistic and the top-left approach. A total of 354, 308, and 272 patients were included in cohorts 1, 2, and 3, respectively. Based on Youden's J statistic, the optimal MCID cutoff for improvement in the IPOS score for dyspnea was  $\geq +1$  in all cohorts. The sensitivities of these cutoffs were 0.86, 0.885, and 0.909 and the specificities were 0.770, 0.593, and 0.560 for cohorts 1, 2, and 3, respectively. The top-left approach confirmed this MCID cutoff of  $\geq +1$  in all cohorts. The MCID for IPOS improvement in dyspnea was determined to be  $\geq +1$  across all time points. This can facilitate the design and interpretation of future studies using IPOS scores as study outcomes.

**Keywords:** Minimal clinically important difference; Integrated palliative care outcome scale; dyspnea; Cancer

## 25COASOCT09:

### **Title: Bone cement implantation syndrome: a scoping review,**

Karen E. Brokke, Manon Graman, Sjoerd Servaas, Inger N. Sierevelt, Monique A.H. Steegers, Peter A. Nolte,

British Journal of Anaesthesia, Volume 135, Issue 4, 2025, Pages 1038-1050,

<https://doi.org/10.1016/j.bja.2025.05.041>.

**Abstract:** Bone cement implantation syndrome comprises the occurrence of hypoxaemia, hypotension, unexpected loss of consciousness, or cardiac arrest occurring around the time of cementation, prosthesis insertion, or reduction of the joint in arthroplasty. As the yearly number of arthroplasties will increase, the number of complications including bone cement implantation syndrome is also expected to increase. Therefore, a good understanding of this syndrome is important. This scoping review aims to provide a comprehensive overview of the current knowledge of bone cement implantation syndrome. This scoping review was conducted based on the PRISMA-ScR Checklist. A literature search was done in PubMed, Cochrane, and Embase. A total of 85 studies were included in the study. The incidence of bone cement implantation syndrome during cemented hip or knee arthroplasty varied from 15.4% to 46.7% and 27.5% to 70.7%, respectively. The incidence in shoulder arthroplasty was 16.2%. In uncemented hip arthroplasty, the incidence ranged from 0.0% to 21.8%. Risk factors identified for bone cement implantation syndrome included advanced age, ASA physical status 3 or 4, and primary lung cancer or lung metastasis. Bone cement implantation syndrome is a potentially severe complication that can occur during both cemented and uncemented arthroplasty. Moreover, the occurrence of bone cement implantation syndrome is not dependent on the use of cement. However, the severity does seem to have an association with the fixation method.

**Keywords:** bone cement implantation syndrome; cementation; cemented arthroplasty; desaturation; hypotension; hypoxia; uncemented arthroplasty

## 25COASOCT10:

**Title:** Factors associated with a reduction in the preventive effect of intravenous dexamethasone on rebound pain after axillary brachial plexus block,

Nassim Touil, Athanasia Pavlopoulou, Olivier Barbier, Xavier Libouton, Damien Gruson, Jean-Luc Gala, Patricia Lavand'homme,

British Journal of Anaesthesia, Volume 135, Issue 4, 2025, Pages 1059-1066,

<https://doi.org/10.1016/j.bja.2025.05.055>.

**Abstract:** Rebound pain after regional anaesthesia remains a significant clinical problem. Intravenous dexamethasone is commonly used as an adjuvant to prevent rebound pain although its effectiveness varies among patients. We aimed to identify phenotypic and biological factors influencing glucocorticoid sensitivity contributing to dexamethasone resistance in the prevention of rebound pain. Patients undergoing ambulatory upper limb surgery with an axillary brachial plexus block were enrolled prospectively to receive dexamethasone (0.1 mg kg<sup>-1</sup> i.v.) before surgery. Preoperative factors analysed encompassed clinical aspects (central sensitivity, anxiety, and pain scores) and biological parameters (salivary cortisol, annexin-A1, and blood inflammatory markers). Postoperative outcomes comprised rebound pain incidence (numerical rating scale >7 within the first 24 h) and persistent pain at 3 months. Of the 104 patients included, 36 (34.6%) developed rebound pain. Preoperative nocturnal awakening pain (odds ratio [OR]=3.09, P=0.03), severe anxiety (OR=3.54, P=0.01), high catastrophising score (OR=4.14, P=0.01), and low salivary cortisol levels (<1147 pg ml<sup>-1</sup>) (OR=3.33, P=0.02) were associated with an increased risk of rebound pain. Persistent pain at 3 months (27%) was associated with the presence of postoperative rebound pain (P=0.04). Preoperative nocturnal pain, severe anxiety, high catastrophising, and



low salivary cortisol levels are factors that might reduce the efficacy of dexamethasone in preventing rebound pain. These findings support the development of personalised preventive strategies.

**Keywords:** axillary brachial plexus block; dexamethasone; orthopaedic surgery; peripheral nerve block; rebound pain

#### 25COASOCT11:

**Title:** Association between pyramidal neurone spiking in the medial prefrontal cortex and the sedative potency of volatile anaesthetics in mice,

Yu Leng, Yaixin Yang, Qian Li, Yujie Wu, Han Huang, Peng Liang, Donghang Zhang, Cheng Zhou, Hugh C. Hemmings,

British Journal of Anaesthesia, Volume 135, Issue 4, 2025, Pages 965-976,

<https://doi.org/10.1016/j.bja.2025.07.046>.

**Abstract:** The mechanisms underlying volatile anaesthetic-induced unconsciousness remain unclear. Glutamatergic pyramidal neurones and fast-spiking interneurons in cerebral cortex circuits play distinct roles in cortical network dynamics under volatile anaesthesia. We investigated the roles of medial prefrontal cortex (mPFC) pyramidal and fast-spiking interneurons in volatile anaesthetic-induced hypnosis. The electrophysiological properties of pyramidal and fast-spiking parvalbumin (PV+) neurones were explored by in vivo multichannel recordings and in vitro patch-clamp electrophysiological recordings. Chemogenetic manipulation was used to test the role of pyramidal neurones in the mPFC in volatile anaesthetic-induced unconsciousness. Nav1.1 knockdown in PV+ neurones was used to regulate activities of pyramidal neurones by PV+-dependent disinhibition and to investigate the role of pyramidal neurone activation in volatile anaesthetic-induced unconsciousness. Regular-spiking pyramidal neurones and fast-spiking PV+ neurones in the mPFC were identified with distinct spiking properties. Sevoflurane suppressed pyramidal neurone firing frequency and action potential characteristics. Chemogenetic inhibition of pyramidal neurones in the mPFC enhanced the potency of volatile anaesthetics, whereas chemogenetic activation produced the opposite results. Sevoflurane also suppressed the firing of fast-spiking PV+ neurones, with a greater inhibition ratio than that in regular pyramidal neurones; however, sevoflurane did not affect the action potential properties of PV+ neurones. Nav1.1 knockdown in PV+ neurones enhanced sevoflurane-mediated suppression of PV+ neurone activity, leading to pyramidal neurone disinhibition and reduced hypnotic potency. The excitability of pyramidal neurones in the mPFC primarily determines the sedative potency of volatile anaesthetics in mice.

**Keywords:** action potential; medial prefrontal cortex; neuronal spiking; pyramidal neurones; parvalbumin neurones; volatile anaesthetics

#### 25COASOCT12:

**Title:** The amnesic effects of propofol on functional connectivity in the hippocampus determined by functional magnetic resonance imaging in volunteers,

David Lindsay, Ram M. Adapa, David K. Menon, Emmanuel A. Stamatakis,

British Journal of Anaesthesia, Volume 135, Issue 4, 2025, Pages 930-940,

<https://doi.org/10.1016/j.bja.2025.04.032>.

**Abstract:** One of the primary actions of general anaesthetic agents, apart from inducing a state of unconsciousness, is reversible impairment of memory formation during the period of administration. Failure to induce and maintain amnesia can result in recall of accidental intraoperative awareness and contribute to adverse psychological health outcomes. The precise mechanisms of action by which general anaesthetics achieve their amnesic effects are not fully understood. To this end, we focused on the hippocampus, a region critical for the formation of new episodic explicit long-term memories of the type normally inhibited by general anaesthetics. We enrolled 25 healthy adult volunteers who underwent functional magnetic resonance neuroimaging (fMRI) whilst sedated with a plasma target-controlled infusion of the anaesthetic agent propofol. The functional connectivity (synchronised neuronal activity with other brain regions) of the hippocampus and microanatomical hippocampal subregions was assessed at baseline, under sedation, and during recovery. Serial plasma propofol concentrations and responses to an auditory stimulus semantic decision task were measured. Post-scanning memory testing was conducted, and memory performance was related to the fMRI data. Functional connectivity changes associated with an amnesic but subhypnotic depth of propofol sedation were predominantly characterised by a reduced connectivity signature of the hippocampus stratum radiatum, stratum lacunosum, stratum moleculare, CA1 stratum pyramidalis, and CA4/dentate gyrus subfields with the precuneus. We provide evidence for differential actions of propofol on hippocampal subdivisions and limbic circuits related to amnesic efficacy, which suggests a more significant role of the precuneus in long-term memory consolidation than previously thought.

**Keywords:** amnesia; fMRI; general anaesthesia; hippocampus; memory; propofol; sedation

## 25COASOCT13:

**Title:** Human neutrophil-derived extracellular vesicles induce renal endothelial inflammation in critical illness: an ex vivo investigation,

Jonny R. Stephens, Yoichi Iki, Tomoaki Yasuda, Elizabeth Brown, Diianeira Tsiridou, Ashleigh Green,

British Journal of Anaesthesia, Volume 135, Issue 4, 2025, Pages 920-929,

<https://doi.org/10.1016/j.bja.2025.06.030>.

**Abstract:** Circulating neutrophil-derived extracellular vesicles (NEVs) may contribute to the pathophysiology of acute kidney injury by causing glomerular endothelial inflammation. NEVs were first isolated from ex vivo, lipopolysaccharide stimulation of whole blood taken from healthy volunteers (median age [interquartile range {IQR}]: 32 [26–42] yr; 47% female), and also from plasma of COVID-19 patients with acute respiratory distress syndrome (median age [IQR]: 59 [52–66] yr; 45% female). NEVs were incubated for 4 h in a co-culture of peripheral blood mononuclear cells and either human umbilical vein endothelial cells or renal glomerular endothelial cells. Enzyme-linked immunoassays (tumour necrosis factor- $\alpha$  [TNF]) and flow cytometry (median fluorescence intensity [MFI]) were used to quantify cell-specific markers of inflammation/activation, in the presence/absence of pharmacological inhibitors. NEVs were internalised by monocytes, leading to their activation via the p38 mitogen-activated protein kinase pathway and increased release of TNF (median [IQR]: 676 [474–1731] pg ml<sup>-1</sup> after NEV internalisation, compared with controls (27 [18–29] pg ml<sup>-1</sup>,  $P=0.003$ ). This proinflammatory response increased cell adhesion molecule



expression (E-selectin) on human umbilical vein endothelial cells (median MFI [IQR]; NEVs: 4120 [3671–4858] vs untreated: 1438 [1252–1708],  $P=0.008$ ) and human renal glomerular endothelial cells (median MFI [IQR]; NEVs: 2960 [2471–4991] vs untreated: 931 [881–1181],  $P=0.003$ ). NEVs contained substantial amounts of matrix metalloproteinase-8 and -9, inhibitors of which (doxycycline, MMP-8 inhibitor or MMP-9 inhibitor) prevented endothelial cell inflammation.

Circulating NEVs may contribute to acute kidney injury through renal endothelial inflammation in a monocyte-dependent fashion in patients with acute respiratory distress syndrome.

**Keywords:** COVID-19; critical illness; extracellular vesicle; matrix metalloproteinase (MMP); renal glomerular inflammation

#### 25COASOCT14:

**Title:** Pharmacokinetic modelling and simulation for prolonged infusion of levobupivacaine with or without epinephrine in transversus abdominis plane and erector spinae plane blocks: a randomised controlled trial and analysis of pooled data,

Andrea Araneda, J.C. De la Cuadra, Marcia Corvetto, Detlef Balde, René de la Fuente, Mauricio Ibacache,

British Journal of Anaesthesia, Volume 135, Issue 4, 2025, Pages 1051-1058,

<https://doi.org/10.1016/j.bja.2025.05.047>.

**Abstract:** Interfacial blocks often require large volumes of local anaesthetic, raising concerns about systemic absorption and potential toxicity. This study examined the pharmacokinetics of levobupivacaine with and without epinephrine during thoracic erector spinae plane (ESP) or transversus abdominis plane (TAP) blocks, simulating reported 48-h dosing regimens to evaluate safety. Data from three studies were analysed. Study 1 included 38 patients receiving an ESP block before video-assisted thoracoscopy, whereas Study 2 analysed published data on TAP blocks. Both studies used 20 ml of levobupivacaine 0.25% with or without epinephrine ( $5 \mu\text{g ml}^{-1}$ ), measuring arterial concentrations over 90 min. Study 3 involved intravenous bupivacaine administration in 10 healthy volunteers. Pharmacokinetic analysis used NONMEM software, with significance set at  $P<0.05$ . We analysed 258 ESP samples, 150 TAP samples, and 190 bupivacaine i.v. samples. A one-compartment model described the data, with a mean distribution volume of 41.9 L (coefficient of variation, 47%) and clearance rate of  $0.288 \text{ L min}^{-1}$  (coefficient of variation, 38%). Epinephrine reduced bioavailability (54.3% vs 32.8%) and prolonged absorption half-life (0.84 min vs 1.55 min;  $P<0.05$ ). Simulated doses of 50 mg plus 300 mg per 24 h over 48 h remained below toxic thresholds. Similar dosing regimens for ESP and TAP blocks are supported by this pharmacokinetic analysis, with epinephrine effectively reducing systemic drug concentrations by prolonging absorption half-life and lowering bioavailability. The findings suggest that extended 300 mg per 24 h dosing for 48 h is likely to be safe. Further studies in broader patient populations are warranted to evaluate safety.

**Keywords:** erector spinae plane block; interfacial block; local anaesthetic; pharmacokinetic modelling; regional anaesthesia; systemic toxicity; transversus abdominis plane block

**25COASOCT15:**

**Title: Drug-specific recovery of long-term memory and visual discrimination after anaesthetic-induced unconsciousness in rats,**

David P. Obert, Gwi H. Park, Kathleen F. Vincent, Ken Solt,

British Journal of Anaesthesia, Volume 135, Issue 4, 2025, Pages 953-964,

<https://doi.org/10.1016/j.bja.2025.05.058>.

**Abstract:** Perioperative neurocognitive disorders represent a growing public health concern. To improve the translatability of preclinical findings, it is important to use similar research methods across species. In this study, we used a touchscreen-based cognitive testing system to train rats on the paired-associate learning (PAL) task, which assesses long-term visuospatial associative memory. The goal was to capture the time course of cognitive recovery after receiving mechanistically distinct anaesthetic drugs. Adult Sprague–Dawley rats (eight males, eight females) were trained on the interference PAL (iPAL) task. After reaching proficiency, loss of righting was induced with propofol (10 mg kg<sup>-1</sup> i.v.), sevoflurane (20 min at 3 vol%), dexmedetomidine (20 µg kg<sup>-1</sup> i.v.), ketamine (50 mg kg<sup>-1</sup> i.v.), or fentanyl (50 µg kg<sup>-1</sup> i.v.). We evaluated time to return of righting reflex (RORR) and time to cognitive recovery, defined as 4/5 correct on the first try. Data are presented as median (first quartile–third quartile). The number of sessions to achieve proficiency was 51 (45–57). Latency to RORR was 11.5 (7.2–12.7) min after propofol, 4.9 (3.6–7.9) min after sevoflurane, 63.7 (48.6–72.0) min after dexmedetomidine, 31.6 (27.0–35.9) min after fentanyl, and 28.1 (19.3–32.3) min after ketamine. Compared with baseline, time to reach 4/5 correct was prolonged after all drugs (all  $P < 0.001$ ). Although animals recovered cognition within 60 min after RORR after propofol and sevoflurane, it took 2–3 h after ketamine, dexmedetomidine, and fentanyl. All animals returned to baseline performance within 24 h. We found distinct recovery profiles of neurocognitive function after the different drugs, consistent with their distinct pharmacologic properties. The iPAL touchscreen-based cognitive testing system allows evaluation of long-term visuospatial memory after drug-induced unconsciousness, providing a robust, translatable method for future studies of perioperative neurocognitive disorders.

**Keywords:** cognition; cognitive recovery; general anaesthesia; paired-associate learning; perioperative neurocognitive disorders

**25COASOCT16:**

**Title: Use of smart glasses imaging for interscalene brachial plexus block: a randomised clinical trial,**

Ping Liu, Jiaqi Qiu, Furui Wang, Rui Li, Ye Zhang, Yun Wu, Lingling Jiang,

British Journal of Anaesthesia, Volume 135, Issue 4, 2025, Pages 1067-1074,

<https://doi.org/10.1016/j.bja.2025.06.040>.

**Abstract:** Smart glasses can provide real-time ultrasonographic images without additional head–eye movement. We investigated whether smart glasses combined with ultrasonography could improve interscalene brachial plexus block (ISB) procedural efficiency. This prospective, randomised trial enrolled 151 patients undergoing upper limb surgery requiring interscalene brachial plexus block. Four anaesthesiologists received standardised training in smart glasses-assisted (smart glasses group) or conventional (control group) ultrasound

guidance. The primary outcome was total procedure time. Five participants were excluded, and 146 participants were included in the analysis. The total puncture time was shorter in the smart glasses group compared with the control group (124.0 [98.0–155.5] s vs 153.0 [123.0–197.5] s;  $P<0.001$ ). In addition, the ultrasound probe imaging time was better in the smart glasses group than in the control group (19.0 [13.5–30.0] s vs 31.0 [20.0–51.0] s;  $P<0.001$ ), and the period from the first skin puncture to reaching the target area was also shorter (16.0 [12.5–24.5] s vs 26.0 [18.5–33.5] s;  $P<0.001$ ). Hand–eye coordination was significantly better in the smart glasses group compared with the control group, which included fewer operator head movements (1.0 [1.0–2.0] vs 5.0 [3.0–8.0];  $P<0.001$ ); more consistent needle redirections (3.00 [2.0–3.0] vs 3.0 [2.0–4.0];  $P=0.004$ ). Pain scores remained similarly low in both groups, with no significant differences in adverse event rates. Ergonomic satisfaction scores (rated 4 or 5) were higher in the smart glasses group (56.2% [41/73] vs 24.7% [18/73];  $P<0.001$ ). Smart glasses reduced the procedure time for experienced anaesthetists performing interscalene brachial plexus block compared with the control group, and improved their hand–eye coordination and satisfaction.

**Keywords:** hand–eye coordination; interscalene brachial plexus block; regional anaesthesia; smart glasses; ultrasound

## 25COASOCT17:

**Title:** Orexin signalling in the nucleus accumbens promotes arousal from isoflurane anaesthesia and restores communication between the nucleus accumbens and frontal cortex,

Jia Huo, Huiming Li, Dan Wang, Sa Wang, Xinxin Zhang, Hailong Dong, Jiannan Li,  
British Journal of Anaesthesia, Volume 135, Issue 4, 2025, Pages 941–952,  
<https://doi.org/10.1016/j.bja.2025.03.042>.

**Abstract:** Orexin can induce arousal from general anaesthesia; however, the underlying mechanisms are not fully understood. Nucleus accumbens (NAc), a downstream target of orexinergic neurones, plays a role in regulating consciousness. We aimed to clarify whether and how the NAc mediates the arousal effects of orexin. Fibre photometry was used to track changes of orexinergic afferent activity during isoflurane anaesthesia and arousal from anaesthesia. Optogenetics was used to study the effects of orexinergic afferents to the NAc. Neuropharmacology approaches were used to assess receptor mechanisms. Optogenetics and in vivo electrophysiology were used to assess the influence of orexin on NAc neuronal firing and communication between the NAc and the frontal cortex. Orexinergic afferents in the NAc were wake-active during isoflurane anaesthesia and the arousal process. Optogenetic activation of orexinergic terminals in the NAc prolonged the time to induction, shortened time to emergence, and reduced the burst suppression ratio (from 67.4% [2.5%] to 14.5% [1.0%];  $n=6$ ,  $P<0.001$ ) during 1.4 vol% isoflurane anaesthesia. Microinjection of orexin-A into the NAc promoted arousal from isoflurane anaesthesia. Orexin-1 receptors were primarily expressed in NAc D1 receptor-positive (D1R+) neurones. Optogenetic activation of orexinergic terminals increased D1R+ neuronal firing (from 0.77 [0.54] spikes  $s^{-1}$  to 2.53 [0.46] spikes  $s^{-1}$ ;  $n=24$ ,  $P=0.0194$ ) and restored NAc-to-frontal cortex coherence during isoflurane anaesthesia. Orexin restores communication between the NAc and frontal cortex by

upregulating the activity of D1R+ neurones, thereby promoting arousal from isoflurane anaesthesia.

**Keywords:** arousal; coherence; D1 receptor; general anaesthesia; isoflurane; nucleus accumbens; orexin

## 25COASOCT18:

**Title:** Training and assessment of skills in neuraxial space access: a scoping review of educational approaches to lumbar puncture, epidural anaesthesia, and spinal anaesthesia,

Martine Siw Nielsen, Frederik Veitland Ilkjær, Anders Morten Grejs, Anders Bo Nielsen, Lars Konge, Anne Craveiro Brøchner,

British Journal of Anaesthesia, Volume 135, Issue 4, 2025, Pages 1026-1037,

<https://doi.org/10.1016/j.bja.2025.06.008>.

**Abstract:** Neuraxial space access, including lumbar puncture, spinal anaesthesia, and epidural anaesthesia, is important in clinical practise for diagnostics and anaesthesia. Despite frequent use, standardised educational recommendations for training and assessing proficiency in these procedures are not well-integrated. The following research question was formulated: what is known from published literature to guide future educational recommendations for training and skills assessment of neuraxial space access with and without the use of ultrasound? On May 7, 2024, searches were performed in the Cochrane Library, MEDLINE (Ovid), Scopus, PubMed, CINAHL (EBSCO), and EMBASE (Ovid). Studies were eligible if they involved physicians, medical students, or nurses and focused on training or assessment of neuraxial space access skills. No comparator was required, and all study designs were included if outcomes could be assessed using Kirkpatrick framework. There were no restrictions on language or publication date. Methodological quality was assessed using the Medical Education Research Study Quality Instrument (MERSQI). The review included 99 studies, and overall, 28 (28%) of the included studies were of low quality with a MERSQI score <9, whereas 22 (22%) were of high quality with a MERSQI score of ≥14. The designs were primarily cohort studies (68%) and RCTs (24%). Specialities represented were mainly anaesthesia (22%) and paediatrics (17%), but many were not reported (30%). Training modalities varied, predominantly using low-fidelity manikins (55%). Simulation-based methods enhanced procedural confidence and technical skills. Studies on education in neuraxial space access show substantial variation in educational approaches and assessment. Consistent findings indicate that simulation-based training enhances outcomes across multiple Kirkpatrick levels, although the studies generally have low methodological quality. Further high-quality research is needed, especially linking training and assessment to patient outcomes.

**Keywords:** assessment; education; epidural anaesthesia; lumbar puncture; neuraxial access; spinal anaesthesia; training

## 25COASOCT19:

**Title:** Comparison of the efficiency of high flow nasal cannula oxygen and conventional nasal cannula oxygen in pediatric patients under sedation for gastrointestinal endoscopy: A prospective observational study,

Sami Olcay Ozbay, Mehmet Yilmaz, Merve Yazici Kara, Ayse Zeynep Turan Civraz, Nurseda Dundar, Ayten Saracoglu, Kemal Tolga Saracoglu, Trends in Anaesthesia and Critical Care, Volume 64, 2025, 101591, <https://doi.org/10.1016/j.tacc.2025.101591>.

**Abstract:** Oxygenation during upper gastrointestinal (GI) endoscopy in pediatric patients is essential to prevent hypoxia and complications. High-flow nasal cannula oxygenation (HFNO) effectively improves oxygenation compared to conventional nasal cannula oxygenation (NCO). This study compares the efficacy of HFNO and NCO in minimizing hypoxia during sedation. This prospective observational study included 82 pediatric patients aged 4–18 years with ASA scores I or II, all undergoing upper GI endoscopy under sedation. Patients received either HFNO or NCO, maintaining SpO<sub>2</sub> above 93 %. The primary outcome was hypoxia incidence, while secondary outcomes included hypoxia duration, minimum SpO<sub>2</sub> levels, and recovery measures. Statistical significance was set at  $p < 0.05$ . Hypoxia occurred significantly less in the HFNO group (4.9 %) than in the NCO group (22.0 %,  $p = 0.023$ ). HFNO also led to shorter hypoxia duration and higher minimum SpO<sub>2</sub> values (88.5 % vs. 68.4 %,  $p = 0.034$ ). There were no significant differences in procedure or recovery times, or vomiting rates. The HFNO group maintained better hemodynamic stability, including mean arterial pressure and respiratory rate. HFNO proved more effective in reducing hypoxia incidence and duration compared to NCO in pediatric patients undergoing upper GI endoscopy. It also enhanced respiratory and hemodynamic stability, indicating its promise as a safer oxygenation method in practice.

**Keywords:** Pediatric anesthesia; Gastrointestinal endoscopy; Outpatient; Hypoxia; Oxygenation; SpO<sub>2</sub>

## 25COASOCT20:

**Title:** Development of a multiple logistic regression model to predict depth of the cricothyroid membrane in the adult surgical population,

Umair Ansari, Clementine Stubbs, Siew Wan Hee, Shubha Srinivasa Reddy, Cyprian Mendonca,

Trends in Anaesthesia and Critical Care, Volume 64, 2025, 101584, <https://doi.org/10.1016/j.tacc.2025.101584>.

**Abstract:** To adequately prepare for a difficult airway requiring emergency front of neck access, it is recommended that anaesthetists identify the cricothyroid membrane (CTM) before the induction of anaesthesia. In addition, the technique and success of eFONA depends on the depth of CTM. This study aims to develop a multiple logistic regression model using patient characteristics and airway assessment parameters to predict depth of the CTM. The study was performed at University Hospitals Coventry and Warwickshire NHS Trust from October 2018 to February 2022. Following written informed consent and detailed airway assessment, ultrasonography of the neck was performed and depth of CTM was measured in supine neck extended position. We inspected the relationship of age, sex, weight, BMI, Mallampati score, thyromental distance, sternomental distance, inter-incisor distance, jaw protrusion, CTM palpability, neck extension and neck circumference with CTM depth. Each of these covariates were included in simple univariate logistic regression model as predictor with binary CTM as the response. Covariates that showed significance at p-value of



0.10 were included in a multiple logistic regression model. We analysed the data from 2578 patients. The mean (SD) depth of the CTM in male patients was 9.4 (2.7) mm and in female patients was 9.7 (3.1) mm. In simple univariate logistic regression, we found sex, weight, BMI, Mallampati score, sternomental distance, CTM palpability and neck circumference all to have a statistically significant relationship with CTM depth. There was a strong positive correlation between neck circumference and CTM depth. We have developed a multiple logistic regression model for predicting CTM depth  $\leq 13$  mm based on sex, BMI, CTM palpability, sternomental distance and neck circumference with good sensitivity (0.80) and specificity (0.85).

**Keywords:** eFona; CTM; Predictive model

## 25COASOCT21:

**Title:** Comparative study on prediction of paediatric endotracheal tube size by ultrasonography little finger breadth and age based formula: A prospective observational study,

Mathew Antony, V. Arun, Gaurang J. Kothari,

Trends in Anaesthesia and Critical Care, Volume 64, 2025, 101586,

<https://doi.org/10.1016/j.tacc.2025.101586>.

**Abstract:** Ultrasound is said to be a reliable, safe and non-invasive modality for evaluation of upper airways and a useful tool for estimating the proper size of the ET tube. Transverse subglottic diameter measured by ultrasound may be used to choose the correct size of tracheal tube by predicting the outer diameter of ET tube. There are studies comparing ultrasonography with age-based formulas and ultrasonography with little finger breadth for ET tube estimation. But there are no studies comparing all three techniques. In this study we wanted to find the utility of ultrasound to predict ET tube size in paediatric population. This was a prospective observational study involving 30 paediatric patients aged 6 months to 6 years undergoing elective surgery. Preoperatively, the breadth of the distal phalanx of little finger at level of distal inter-phalangeal groove of all patients was measured with the help of a calliper. Measurement of transverse subglottic diameter at cricoid level was performed using a portable ultrasound machine. An uncuffed ET tube with the OD close to the subglottic diameter measured by ultrasound was used to intubate the patient. Mean values for age and weight were  $2.25 \pm 1.87$  and  $11.10 \pm 3.65$ , respectively. Mean values for USG guided MTDSA (Minimal Transverse Diameter of Subglottic Airway) diameter vs. O.D (Outer diameter) of ET tube were  $6.51 \pm 0.91$  vs.  $6.33 \pm 0.88$ , respectively. Mean values for age-based formula size vs. I.D (Inner diameter) of ET tube were  $4.35 \pm 0.56$  vs.  $4.62 \pm 0.64$ , respectively. Mean values for little finger breadth vs. O.D. of ET tube were  $6.52 \pm 1.04$  vs.  $6.33 \pm 0.88$ , respectively. The scatter plot showed a correlation (r) between USG-guided MTDSA measurement and the OD of the ET tube used (r value = 0.95) and Bland-Altman analysis (mean bias of 0.16). The correlation between little finger breadth and OD of the ET tube showed a correlation (r) of 0.83 in the scatter plot. The mean bias shown by Bland-Altman analysis using the little finger breadth method was 0.17. The scatter plot between age-based formula and ID of ET tube showed a correlation (r) of 0.92, and Bland-Altman analysis showed a mean bias of 0.27. The highest level of correlation was observed between ultrasound measurement and OD of the ET tube used (r = 0.95). Least bias was found

between ultrasound measurement and OD of ET tube used ( $-0.16$ ). Ultrasound predicted the correct tube size in 80 % of the population. Ultrasound is a better tool compared to conventional age-based formulas and the little finger breadth method in predicting the appropriate size of the ET tube in paediatric population.

**Keywords:** Paediatric-ET tube size; Ultrasound; MTDSA; Little finger breadth; Age-based formula

## 25COASOCT22:

**Title:** The long-term influence of green nudges on the consumption of desflurane and on the carbon footprint of general anaesthesia: A retrospective study,

Leonard Santen, Florian Windler, Mark Coburn, Birgit Bette, Se-Chan Kim, Christian Bode, Philippe Kruse,

Trends in Anaesthesia and Critical Care, Volume 64, 2025, 101592,

<https://doi.org/10.1016/j.tacc.2025.101592>.

**Abstract:** The medical sector is responsible for a significant share of greenhouse gas emissions. It is imperative that a transition towards ecological sustainability takes place. Nevertheless, initiatives for healthcare providers to reduce emissions remain limited in clinical practice, and climate-damaging behaviour persists. A salient example is the regular use of desflurane in anaesthesia. In order to promote sustainable clinical practice, the implementation of behavioural decision support mechanisms, so called nudges, could be a promising approach. A retrospective study was conducted to analyse the effectiveness of nudges to reduce the consumption of desflurane. The nudges comprised structural modifications to the workplace, with desflurane vaporisers being replaced with those for sevoflurane and isoflurane. The effectiveness of the nudges was evaluated by analysis of the desflurane's order volume. In addition, the emissions of greenhouse gases were normalised to the number of surgical procedures performed. Finally, the economic benefit of reduced desflurane consumption was investigated based on the purchase price. Following the implementation, desflurane was no longer utilised in the long term. Overall, these nudges resulted in a 91 % reduction in emissions of volatile anaesthetics per quarter, equivalent to 219 t CO<sub>2</sub>e. Consequently, the average greenhouse gas emissions per surgical procedure were reduced by 42.2 kg CO<sub>2</sub>e. Furthermore, the costs for volatile anaesthetics decreased by 63.9 %, amounting to a reduction of €18,237.28. The implementation of nudges has been demonstrated to lead to a cessation of desflurane consumption, thereby supporting the green transformation of the healthcare sector. In the future, green nudges favouring sustainable clinical practice are poised to assume greater significance as a cost-effective and readily implementable sustainability measure.

**Keywords:** Structural workplace adjustments; Desflurane; Climate change; Sustainability strategies; Volatile anaesthetics; Behaviour change tools

## 25COASOCT23:

**Title:** The modified renal angina index and renal outcomes in critically ill patients: a prospective cohort study,

P. Mohamed Anas, Vishal Shanbhag, Attur Ravindra Prabhu, Shankar Prasad Nagaraju, Dharshan Rangaswamy,



Trends in Anaesthesia and Critical Care, Volume 64, 2025, 101587,  
<https://doi.org/10.1016/j.tacc.2025.101587>.

**Abstract:** Existing risk prediction tools for acute kidney injury (AKI) have focused on the prediction of AKI occurrence, but few have addressed clinically meaningful outcomes such as the need for dialysis, mortality and kidney recovery. We sought to study the performance of the modified renal angina index (mRAI) for prediction of major adverse kidney events 30 (MAKE30). This prospective single-centre observational study was conducted in the medical ICUs of a tertiary care hospital in India from March 2023 to July 2024. We included consecutive adult ICU patients with hospital stays  $\geq 48$  h, excluding those with end-stage kidney disease, prior kidney transplantation, or needing dialysis at admission. The mRAI was calculated 24 h after ICU admission based on condition scores and changes in serum creatinine, as described by Matsuura et al. The primary outcome was MAKE30, a composite of in-hospital mortality, new renal replacement therapy (RRT) initiation, or persistent renal dysfunction by discharge or day 30. The area under the receiver operating curve (AUROC) was used to assess the performance of the mRAI for MAKE30 prediction and compared with other scores. Among 750 eligible patients, 326 (43.4 %) experienced MAKE30. The mRAI had an AUROC of 0.75 (95 % CI: 0.70–0.78) for MAKE30 prediction, which was numerically higher than that of the SEA-MAKE score (AUROC 0.70), SOFA score (AUROC 0.70) and APACHE II score (AUROC 0.68). The mRAI demonstrated good discriminative ability for MAKE30 prediction in critically ill patients. While this may be a promising tool to guide clinical decision-making, further research is warranted.

**Keywords:** Renal angina index; Major adverse kidney events; Acute kidney injury; Renal replacement therapy; Critical care

## 25COASOCT24:

**Title:** Impact of fluid removal rate on patients receiving continuous renal replacement therapy for acute kidney injury,

Samantha Gunning, Muhammad Mire, George Gulotta, Jay Koyner,  
Journal of Critical Care, Volume 89, 2025, 155161,  
<https://doi.org/10.1016/j.jcrc.2025.155161>.

**Abstract:** Fluid accumulation in severe acute kidney injury (AKI) has been associated with dialysis dependence and mortality. Less is known about the impact of fluid removal and its optimal rate with continuous dialysis. We conducted a single-center retrospective cohort study amongst adult patients admitted to the intensive care unit at the University of Chicago with AKI treated with continuous veno-venous hemodialysis (CVVHD) from April 1, 2016 to March 31, 2020. We collected baseline demographics, daily fluid balances, and patient outcomes. Weight adjusted fluid removal rates were calculated using the cumulative fluid balance over the first three days of CVVHD. Low fluid removal rate was defined as less than or equal to 1.01 mL/kg/h and high fluid removal rate as greater than 1.75 mL/kg/h. We identified 1242 AKI patients treated with CVVHD. Baseline characteristics were compared on the basis of fluid removal rates. There were significant differences in rates of congestive heart failure, baseline weight, and cumulative fluid balance prior to CVVHD between the groups. 90-day mortality was highest (74 %) amongst those with low fluid removal rates. In an adjusted hazards model, low fluid removal rate was significantly associated with 90-day

mortality (AHR 2.74(1.58–4.76)) but high fluid removal rate was not (AHR 0.50(0.30–1.03)). In a large single center cohort, low fluid removal rate was an independent risk factor for 90-day mortality. High fluid removal rates may improve, but certainly do not worsen, outcomes. Clinical trials are needed to further investigate the optimal rates for fluid removal.

**Keywords:** Fluid removal; Fluid overload; Acute kidney injury; Continuous dialysis; Ultrafiltration

## 25COASOCT25:

**Title:** Pulse oximetry beyond oxygen saturation: Early waveform characteristics in sepsis patients with adverse outcomes - A proof-of-concept study,

Sanne Ter Horst, Raymond J. van Wijk, Anna D. Schoonhoven, Anouk de Lange, Jan C. ter Maaten, Hjalmar R. Bouma,

Journal of Critical Care, Volume 89, 2025, 155115,

<https://doi.org/10.1016/j.jcrc.2025.155115>.

**Abstract:** Sepsis is a life-threatening disorder with an in-hospital mortality rate of 10–40 %. Identifying patients at risk for deterioration is critical in guiding clinical decisions for patients with infection at the emergency department (ED). While pulse oximetry is known for estimating oxygen saturation, we hypothesize that photoplethysmography (PPG) can reflect early cardiovascular changes in sepsis. This study explores the potential use of pulse oximetry - PPG as a tool for predicting clinical deterioration in patients with early sepsis. We conducted a secondary analysis of prospectively obtained data from the Acutelines data-biobank, involving 576 patients with early sepsis at the ED. Clinical and demographic data, vital signs, laboratory values, and PPG waveforms were collected. Groups were determined by a composite endpoint of intensive care unit (ICU) admission and/or in-hospital mortality within 48 h. PPG features were calculated and differences between groups were analyzed. Within our study cohort, 9.7 % of patients were admitted to the ICU and/or deceased within 48 h after ED arrival. During the first 20 min after ED arrival, patients who deteriorated showed lower systolic peak amplitude (SPA: 1218 vs. 1490 AU,  $p < 0.001$ ), lower diastolic peak amplitude (DPA: 462 vs. 621 AU,  $p < 0.001$ ), and shorter pulse intervals (PI: 0.540 vs. 0.609 s,  $p < 0.001$ ) on PPG. Additionally, the APG b/a ratio was lower ( $-0.881$  vs.  $-0.802$ ,  $p < 0.001$ ). In contrast, systolic blood pressure (SBP: 123 vs. 129 mmHg,  $p = 0.186$ ), diastolic blood pressure (DBP: 78 vs. 76 mmHg,  $p = 0.400$ ), mean arterial pressure (MAP: 88 vs. 95 mmHg,  $p = 0.111$ ) did not differ between groups. Heart rate (HR: 111 vs. 99 bpm,  $p = 0.001$ ) and PPG-derived PI were both significantly different and strongly correlated ( $\rho = -0.921$ ), as both reflect the duration of one interbeat interval. This study highlights the potential use of PPG as a valuable tool for detecting early cardiovascular changes in sepsis. These findings hold significance for developing novel tools that can facilitate early identification of patients at risk for deterioration, thereby improving clinical decisions and outcomes for ED patients with early sepsis.

**Keywords:** Sepsis; Emergency department; Pulse oximetry; Waveform; Photoplethysmography; Intensive care unit; Mortality

**Cancer Research****25COASOCT01****Title: Synchronous Presentation and Management of Abdominal Aortic Aneurysm and Renal Neoplasm: A Case Series Analysis**

Priscilla Nardi, Greta D'onofrio, Valeria Iacoucci, Elena Marcelli et.al.

Anticancer Research October 2025, 45 (10) 4607-4616;

<https://doi.org/10.21873/anticancerres.17806>

**Abstract:** The concomitant presence of abdominal aortic aneurysm (AAA) and renal cancer is a rare but increasingly diagnosed condition, often found incidentally. Despite distinct etiologies, both pathologies share common risk factors making their coexistence relevant in an increasingly comorbid population. The lack of established guidelines necessitates careful multidisciplinary planning for optimal therapeutic choice. **Patients and Methods:** From March 2010 to March 2025, 11 consecutive patients with coexisting AAA and renal neoplasm underwent surgical procedures at Policlinico Umberto I, Rome. Interventions included simultaneous or staged surgical approaches. The primary endpoints of this study were overall survival (OS) and disease-free survival (DFS). The secondary endpoints included: 30-day postoperative myocardial infarction (MI), postoperative acute kidney injury (AKI), surgical complications, endoleak occurrence, operative time, and length of hospital stay. **Results:** Overall survival (OS) at 24 and 36 months was 90.0% and 77.1%, respectively, with similar disease-free survival (DFS) rates. One patient (9.1%) had neoplastic recurrence at 24 months. Median operative time for simultaneous procedures was 200 min [interquartile range (IQR)=142.5-242.5]. For staged procedures, endovascular aortic repair (EVAR) median time was 100 min (IQR=45-165), and nephrectomy was 102.5 min (IQR=45-165). The overall median hospital stay was eight days (IQR=1-17). No postoperative myocardial infarctions, acute lower limb ischemia, or significant intraoperative hemorrhages occurred. One patient (9.1%) developed acute kidney injury managed conservatively. Three patients (27.3%) experienced type II endoleaks without requiring intervention. **Conclusion:** Managing concomitant AAA and renal neoplasm is complex due to its rarity and lack of clear guidelines. This study demonstrates that both simultaneous and staged surgical approaches (EVAR and nephrectomy) yield excellent long-term survival and low postoperative morbidity, underlining the importance of a multidisciplinary approach and personalized therapy.

**25COASOCT02****Title: Significance of Preoperative Chemotherapy and Chemoradiotherapy in Patients With Locally Advanced and Borderline Resectable Pancreatic Cancer**

Masaaki Murakawa, Rei Kanemoto, Tatsuya Kanai et.al.

Anticancer Research October 2025, 45 (10) 4585-4596;

<https://doi.org/10.21873/anticancerres.17804>

**Abstract:** Multi-agent chemotherapy regimens have improved the survival of patients with pancreatic adenocarcinoma (PDAC). However, only a few studies have compared multi-regimen treatments with single-regimen followed by curative-intent resection. This study aimed to explore optimal treatment strategies and clarify the role of radiotherapy in borderline resectable PDAC (BRPC) and locally advanced PDAC (LAPC) treatment. **Patients**

and Methods: Consecutive patients who underwent pancreatectomy for PDAC at our institution between January 2013 and December 2022, diagnosed with BRPC and LAPC, and subjected to radical resection following preoperative chemotherapy or chemoradiotherapy were included in this study. We divided the cohort into preoperative multiple regimen (MR) and single regimen (SR) groups to compare survival. Results: Of the 527 patients with PDAC, 68 who responded favorably to neoadjuvant therapy and subsequently underwent curative-intent or conversion resection were included in the analysis. In terms of overall survival, the 5-year survival rate was significantly higher in the MR group (80.8%) than in the SR group (20.3%). Multivariate analysis identified R0 resection, preoperative carbohydrate antigen 19-9 levels <80 U/ml, and preoperative treatment with multiple regimens as factors associated with better prognosis. Conclusion: Treatment with multiple regimens may improve the prognosis of patients with LAPC or BRPC. The addition of chemoradiotherapy as a treatment modality may have a positive impact on prognosis.

### 25COASOCT03

#### **Title: Epidemiological Analysis of Malignant Bone and Cartilage Tumors in the Hand With Focus on Chondrosarcoma: A Twenty-year Study with a Focus on Surgical Treatment Outcomes**

André S. Alves, Adriano Fabi And Carlo M. Oranges

Anticancer Research October 2025, 45 (10) 4535-4546;

<https://doi.org/10.21873/anticancer.17800>

**Abstract:** Malignant bone and cartilage tumors of the hand are rare and complex, significantly affecting patient quality of life. This study examined the epidemiology and surgical outcomes of these patients with a focus on chondrosarcoma as well as the critical role of surgery. Patients and Methods: A population-based study was performed by analyzing data from the Surveillance, Epidemiology, and End Results (SEER) database, covering all hand-related bone and cartilage malignant tumors from 22 registries between 2000 and 2020. Descriptive analysis characterized demographic and pathophysiological features. Overall survival (OS) was assessed using the log-rank test. Multivariable Cox regression identified independent prognostic factors. Results: The study involved 315 patients [163 (51.75%) females, average age  $45.83 \pm 22.41$  years], with chondrosarcoma being the most prevalent diagnosis (52.06%), followed by osteosarcoma, giant cell tumor, and Ewing sarcoma. Most tumors were right-hand localized (55.56%) and at a localized stage (45.08%). Surgical intervention was performed in 72.06% of cases, with survival rates starting at 96.37% at one year and declining to 60.56% at twenty years. In chondrosarcoma cases, radical surgery demonstrated notably better outcomes with no deaths, significantly outperforming amputation ( $p=0.018$ ). Survival differences based on surgical approach were statistically significant in localized chondrosarcoma ( $p=0.012$ ), particularly with radical surgery showing the highest survival for localized Grade I and II tumors ( $p=0.034$ ). Multivariate analysis highlighted age, higher tumor grade, and advanced stage as predictors of worse outcomes, whereas radical surgery consistently predicted better survival compared to amputation. Conclusion: Early and aggressive surgical management for enhancing patient survival is essential, particularly in cases of localized and low-grade chondrosarcomas. The findings highlight the need for ongoing research on new treatment strategies seeking to improve outcomes for these rare but impactful tumors.

**25COASOCT04****Title: Cost-effectiveness Analysis of Atezolizumab Plus Bevacizumab Versus Lenvatinib in Intermediate-stage Hepatocellular Carcinoma: A Real-world Retrospective Study**

Akifumi Kuwano, Masayoshi Yada, Kosuke Tanaka et.al.

Anticancer Research October 2025, 45 (10) 4627-4636;

<https://doi.org/10.21873/anticancerres.17808>

**Abstract:** The optimal systemic therapy for intermediate-stage (BCLC-B) hepatocellular carcinoma (HCC) remains undefined. While transarterial chemoembolization (TACE) has long been the standard of care, increasing use of molecular-targeted agents and immune checkpoint inhibitors (ICIs), including atezolizumab plus bevacizumab (Atez/Bev) and lenvatinib (LEN), has shifted therapeutic paradigms. This study compared real-world effectiveness, safety, and cost-effectiveness of Atez/Bev versus LEN for BCLC-B HCC in Japan. **Patients and Methods:** This single-center, retrospective cohort study analyzed 55 consecutive patients with BCLC-B HCC: 33 received Atez/Bev and 22 received lenvatinib. Clinical outcomes, treatment-related adverse events, total healthcare expenditures (drugs costs, hospitalization, procedures, imaging, laboratory tests, supportive care) were assessed. Life-years gained (LYG) were estimated using mean overall survival, and incremental cost-effectiveness ratios (ICERs) were calculated. **Results:** Baseline age and body weight were comparable between groups. The Atez/Bev cohort had larger tumors and more impaired liver function. No significant differences were observed in tumor response, median overall survival (OS), or progression-free survival (PFS). Mean total healthcare expenditures per patient were significantly lower with lenvatinib (\$65,227.9) than with Atez/Bev (\$101,480.1;  $p=0.036$ ), primarily as a result of reduced drug acquisition costs (Atez/Bev: \$70,000; LEN: \$33,241.4;  $p=0.007$ ). Life-years lost with Atez/Bev versus LEN totaled 0.46 years (mean OS: Atez/Bev: 17.82 months; LEN: 23.27 months). LEN dominated Atez/Bev (ICER=−\$161,896.5 per LYG). **Conclusion:** Although Atez/Bev and LEN confer similar survival in BCLC-B HCC, lenvatinib offers superior cost-effectiveness in the Japanese healthcare setting. These findings underscore the importance of integrating economic considerations into treatment selection for intermediate-stage HCC.

**25COASOCT05****Title: High Claudin 18.2 Expression Predicts Favorable Outcomes in Pancreatic Ductal Adenocarcinoma After Curative Resection**

Hyebin Cha, Eden Demere Amare, Yun Kyung Jung et.al.

Anticancer Research October 2025, 45 (10) 4565-4573;

<https://doi.org/10.21873/anticancerres.17802>

**Abstract:** Pancreatic ductal adenocarcinoma (PDAC) exhibits aggressive clinical behavior and poor prognosis, primarily due to late-stage diagnosis, early metastasis, and treatment resistance. Current therapeutic approaches, including operation, chemotherapy, and radiotherapy, demonstrate limited efficacy, underscoring the urgent need for novel targeted approaches. Claudin 18.2 (CLDN18.2) has emerged as a promising monoclonal antibody target, such as zolbetuximab; however, limited studies have examined its role in PDAC. This study investigated the association between CLDN18.2 expression and patient outcomes to inform potential therapeutic strategies. **Materials and Methods:** CLDN18.2 expression was evaluated by immunohistochemistry (IHC) on tissue microarrays from 95 patients with



PDAC and quantified using the H-score method. Samples were categorized into high-expression (H-score  $\geq 200$ ) and low-expression (H-score  $< 200$ ) groups. Results: High CLDN18.2 expression was identified in 20 (21.1%) of 95 cases and was significantly associated with better tumor differentiation ( $p=0.016$ ), absence of lymphatic invasion ( $p<0.001$ ), lower lymph node ratio ( $p=0.028$ ), and lower N stage ( $p=0.002$ ). Survival analyses revealed that patients with high CLDN18.2 expression had prolonged overall survival ( $p=0.026$ , log-rank test) and recurrence-free survival ( $p=0.009$ , log-rank test) compared to those with low expression. Among patients receiving curative resection with adjuvant chemotherapy, high CLDN18.2 expression correlated with improved recurrence-free survival ( $p=0.010$ ). Conclusion: High CLDN18.2 expression is associated with favorable clinicopathologic characteristics and improved survival outcomes in PDAC, especially among patients receiving adjuvant chemotherapy, suggesting its potential as a therapeutic and prognostic marker.

## 25COASOCT06

### **Title: Clinical Significance of Molar Count in Esophageal Squamous Cell Carcinoma: Propensity Score Matching Study**

Tenshi Makiyama, Yasunori Matsumoto, Takeshi Toyozumi et.al.

Anticancer Research October 2025, 45 (10) 4597-4606;

<https://doi.org/10.21873/anticancer.17805>

**Abstract:** Emerging evidence suggests that oral health influences the prognosis of esophageal squamous cell carcinoma, with tooth loss linked to poorer outcomes and higher risk of postoperative pneumonia. While the number of teeth has been associated with esophageal squamous cell carcinoma risk, the prognostic role of molars, which play key roles in masticatory function, remains underexplored. Therefore, this study evaluated the prognostic significance of the number of remaining molars in patients undergoing esophagectomy for esophageal squamous cell carcinoma. Patients and Methods: This retrospective study analyzed data from 272 patients with esophageal squamous cell carcinoma who underwent surgery and preoperative dental assessment. The patients were categorized into two groups based on the number of molars ( $\geq 7$  vs.  $< 7$ ), and propensity score matching was applied to control for confounding variables. Survival outcomes were analyzed using Kaplan–Meier curves and Cox regression analysis. Results: After propensity score matching, 68 matched pairs were analyzed. The group with  $\geq 7$  molars showed significantly better overall survival (57.0% vs. 36.1%,  $p=0.0284$ ) and recurrence-free survival (RFS; 52.3% vs. 32.2%,  $p=0.0498$ ) compared with the group with  $< 7$  molars. Multivariate analysis identified postoperative pneumonia and advanced pathological stage as independent predictors of poor survival. Conclusion: The number of remaining molars could serve as a prognostic marker in patients with esophageal squamous cell carcinoma. Maintaining molars may improve clinical outcomes, emphasizing the role of oral health in the perioperative management of esophageal cancer.

## 25COASOCT07

### **Title: Urinary phthalate metabolites associate with blood levels of estrogen quinone-derived hemoglobin adducts in Taiwanese pregnant women**

Shu-Li Wang, Dar-Ren Chen, Sheng-Yen Hsu

Toxicology Letters, Volume 412, October 2025

<https://doi.org/10.1016/j.toxlet.2025.07.1409>

**Abstract:** In this study, we aimed to analyze the background levels of estrogen quinone-derived adducts in hemoglobin (Hb) obtained from pregnant women in Taiwan (n = 394) and to investigate the associations of these adducts with levels of urine metabolites of phthalates. Both 17 $\beta$ -estradiol-2,3-quinone (E2-2,3-Q) and 17 $\beta$ -estradiol-3,4-quinone (E2-3,4-Q) are reactive metabolites of estrogen that are thought to be responsible for the estrogen-induced genotoxicity and carcinogenicity. Results confirmed that levels of estrogen quinone-derived adducts in pregnant women, including E2-3,4-Q-2-S-Hb and E2-2,3-Q-4-S-Hb, were detected at concentrations comparable with those of non-pregnant women with mean levels at 165 (range 108–428) and 97.2 (range 34.9–251) pmol/g, respectively. Levels of E2-3,4-Q-2-S-Hb correlated significantly with those of E2-2,3-Q-4-S-Hb (correlation coefficient  $r = 0.543$ ,  $p < 0.001$ ). The ratios of primary (mono-2-ethylhexyl-phthalate) to secondary (mono (2-ethyl-5-hydroxyhexyl phthalate), mono (2-ethyl-5-oxohexyl) phthalate) metabolites of di-2-ethylhexyl phthalate (DEHP), positively correlated with levels of E2-2,3-Q-4-S-Hb and/or E2-2,3-Q-4-S-Hb plus E2-3,4-Q-2-S-Hb ( $p < 0.05$ ). One of the urinary metabolites of phthalates, mono-isobutyl phthalate, a metabolite of diisobutyl phthalate (DiBP), positively correlated with those of E2-3,4-Q-2-S-Hb ( $r = 0.110$ ,  $p = 0.034$ ) and E2-2,3-Q-4-S-Hb plus E2-3,4-Q-2-S-Hb ( $r = 0.123$ ,  $p = 0.018$ ). Overall, this evidence suggests that levels of these estrogen quinone-derived Hb adducts associate with environmental exposure to phthalates, in particular DEHP and DiBP. We hypothesized that environmental exposure to phthalates may enhance bioactivation of estrogen to quinones leading to accumulation of reactive quinonoid metabolites in pregnant.

## 25COASOCT08

**Title: Protective effect of glucocorticoid receptor against lung inflammation induced by nicotine-derived nitrosamine ketone is mediated by suppression of the ROS-mediated cyclooxygenase-2/prostaglandin E2 pathway in human distal lung epithelial A549 cells**

MyeongKuk Shim, Wonchung Lim

Toxicology Letters, Volume 412, October 2025

<https://doi.org/10.1016/j.toxlet.2025.07.1416>

**Abstract:** Cigarette smoking is a significant risk factor for lung cancer. The cyclooxygenase-2 (COX-2)/prostaglandin E2 (PGE2) pathway is a well-established key player in inflammation and tumorigenesis, both of which are linked to cigarette smoking. Nevertheless, the function of glucocorticoid receptors (GR) in the context of the COX-2/PGE2 pathway induced by nicotine-derived nitrosamine ketones (NNK) remains to be elucidated. The NNK-induced increase in COX-2 expression and PGE2 production was inhibited by glucocorticoids, and this effect was antagonized by the GR antagonist, RU38486. Notably, the induction of COX-2 by NNK correlated with NNK's ability to increase reactive oxygen species (ROS). The ROS scavenger N-acetylcysteine inhibited the NNK-induced increase in COX-2 mRNA levels and promoter activity. Furthermore, dexamethasone significantly inhibited NNK-induced cell invasion. Conclusively, the data collectively indicate that NNK-induced ROS activates the COX-2/PGE2 pathway and cell invasion in lung cancer cells. These findings elucidate the pathophysiological connection between NNK, GR, inflammatory responses, and cell metastasis.



**25COASOCT09****Title: The role of endoplasmic reticulum stress in Atrazine-induced hepatic lipid accumulation**

Honghao Qian, Shuping Ren, Haotang Zhao

Toxicology Letters, Volume 412, October 2025

<https://doi.org/10.1016/j.toxlet.2025.07.1410>

**Abstract:** Atrazine (ATR) is an extensively applied triazine herbicide which belongs to the persistent environmental endocrine disruptors. ATR is capable of penetrating the body and disrupting lipid metabolism, but its underlying mechanism is still unclear. L02 hepatocytes were exposed to ATR (0 (Con), 10, 50, 100  $\mu$ M) and 0.02 % DMSO (VCon) for 24 h. Lipid levels were measured using colorimetry. The lipid droplet accumulation level and detection of  $\text{Ca}^{2+}$  levels by fluorescent staining. Real-Time PCR and Western blot were used to measure mRNA and protein levels. The results showed that groups treated with ATR exhibited elevated levels of lipid. Both intracellular lipid droplet accumulation and  $\text{Ca}^{2+}$  levels increased proportionally with higher ATR dosages. Additionally, the levels of genes linked to lipid metabolism (DGAT2, ACC1, PPAR $\gamma$ , and SCD1) were upregulated. Endoplasmic reticulum stress (ERS) was triggered, leading to augmented gene expression in the IRE1 $\alpha$ /XBP1 signaling pathway, as well as enhanced expression of GRP78 and GRP94. ERS was inhibited by 4-phenylbutyric acid (4-PBA), IRE1 $\alpha$  was silenced by lentivirus transfection. Notably, the upregulation of IRE1 $\alpha$ , XBP1, GRP78, and GRP94, alongside the ATR-induced lipid elevations, were significantly reversed upon ERS inhibition or IRE1 $\alpha$  gene silencing. This study demonstrated that ATR exposure caused ERS in L02 hepatocytes, and induced lipid metabolism disorders by activation the key ERS signal pathway IRE1 $\alpha$ /XBP1, resulting in hepatic lipid accumulation.

**25COASOCT10****Title: KCNQ1OT1/miR-140–5p/PTP4A3 axis is involved in endosulfan-induced vascular endothelial cell migration linking to atherosclerosis**

Boxiang Zhang , Qing Li, Yanyuan Lu et.al.

Toxicology Letters, Volume 412, October 2025

<https://doi.org/10.1016/j.toxlet.2025.07.1415>

**Abstract:** Endosulfan, an organochlorine pesticide, is implicated in human cardiovascular diseases. Protein-tyrosine phosphatase 4A3 (PTP4A3) has been identified to play a critical role in endothelial cell migration when exposure to endosulfan. In the present study, we aim to explore the epigenetic mechanism by which endosulfan upregulates PTP4A3 expression to enhance cell migration in human umbilical vein endothelial cells (HUVECs). Bioinformatics analysis showed that there were complementary sequences in the 3'-UTR of PTP4A3 and lncRNA KCNQ1OT1 to the seed regions of miR-140–5p. Dual luciferase reporter assay confirmed that miR-140–5p had potential binding capacity to PTP4A3 and KCNQ1OT1. Endosulfan upregulated PTP4A3 and KCNQ1OT1, but downregulated miR-140–5p expression, promoting cell migration through the activation of MAPK/ERK and PI3K/AKT pathways in HUVECs, which were inhibited by miR-140–5p overexpression or KCNQ1OT1 silencing. Anti-Ago2 RNA immunoprecipitation experiments confirmed the binding interaction between miR-140–5p and KCNQ1OT1. Transfection of miR-140–5p mimics downregulated PTP4A3 and KCNQ1OT1, while si-KCNQ1OT1 downregulated PTP4A3 and

upregulated miR-140–5p in HUVECs. Either miR-140–5p mimic or si-KCNQ1OT1 attenuated cell migration and influenced MAPK/ERK and PI3K/AKT signaling pathways in HUVECs, which were counteracted by co-transfection with pEGFP-PTP4A3 or anti-miR-140–5p. We observed the upregulation of PTP4A3 and KCNQ1OT1, as well as the downregulation of miR-140–5p in the aorta of the ApoE<sup>-/-</sup> atherosclerotic mice. These findings suggest the involvement of KCNQ1OT1/miR-140–5p/PTP4A3 axis in endosulfan-induced cell migration, providing new insights into the epigenetic mechanisms of endothelial dysfunction in cardiovascular diseases when exposure to endosulfan.

## 25COASOCT11

**Title: Gentamicin aggravates renal injury by affecting mitochondrial dynamics, altering renal transporters expression, and exacerbating apoptosis**

Mingkang Zhang, Yan Zhou, Xiujuan Wang et.al.

Toxicology Letters, Volume 412, October 2025

<https://doi.org/10.1016/j.toxlet.2025.07.1418>

**Abstract:** Drug-induced nephrotoxicity has developed as a prevalent trigger in patients with hospital-acquired AKI. Gentamicin, a broad-spectrum bactericidal aminoglycoside antibiotic, is used clinically in synergy with other antibiotics. However, the presence of nephrotoxicity greatly limits their widespread clinical application. The kidney is one of the most energy intensive organs in the body, second to the heart in mitochondrial content and oxygen consumption. In particular, the mitochondria-rich proximal renal tubules are highly susceptible to be damaged by metabolic wastes or exogenous substances, and many studies have considered mitochondrial dysfunction as a targeted therapeutic strategy for the treatment of AKI. In this study, the results of in vitro experiments revealed that gentamicin could damage renal tubular epithelial cells in a dose- or time-dependent manner and resulted in impaired mitochondrial structure, decreased membrane potential, and reactive oxygen species (ROS) accumulation. Moreover, gentamicin aggravated renal injury by altering renal transporters expression, impairing mitochondrial homeostatic balance by affecting the expression of mitochondrial dynamics (e.g., OPA1, Mitofusin1/2, and DRP1), and promoting apoptosis through the Bax/Bcl2-Caspase3 pathway. It is worth noting that changes in serum creatinine or blood urea nitrogen (BUN) levels could not accurately identify early renal injury caused by gentamicin, and the road to finding an early diagnosis of kidney injury is still long. Our study provided a theoretical basis for gentamicin-induced renal injury and also contributed to the clinical application of gentamicin.

## 25COASOCT12

**Title: Imidacloprid and its major metabolites blocks the alpha subunit of the human hERG (KV11.1) channel: Evidence from in-silico and fluorescence polarization studies**

Vankadoth Umakanth Naik, Ajay Godwin Potnuri, Swati Sharma et.al.

Toxicology Letters, Volume 412, October 2025

<https://doi.org/10.1016/j.toxlet.2025.08.001>

**Abstract:** Neonicotinoids are high affinity agonists of insect Nicotinic Acetyl Choline Receptors (nAChRs) resulting in insect paralysis and death. Although they are assumed to have relatively low affinity towards mammalian and other non-insect nAChRs, studies have shown that they can cause neuro-endocrine toxicity, immunotoxicity and endocrine toxicity.

Moreover, as a result of bioaccumulation the levels of neonicotinoids can be even traced in non-farming population at an significant level. KCHN2 gene encodes ERG1 or hERG or KV11.1 which is responsible for I<sub>Kr</sub> current. Multiple chemical molecules can block this KV11.1-alpha sub unit and can result in prolongation of QT interval causing Drug induced Long QT Syndrome (DI-LQTS). This could potentially trigger Torsades de Pointes (TdP), a unique form of the premature ventricular complex which are spontaneous in origin and often result in Sudden Cardiac Death (SCD). Imidacloprid (IMI) is highly bioavailable and undergoes biotransformation by cytochrome p450 monooxygenases (CYP) and aldehyde oxidases (AOX) forming Desnitro-Imidacloprid (DNI) and Imidacloprid-Olefin (IOL). Interestingly, acute poisoning with IMI can result in cardiac features such as ventricular tachyarrhythmias with severe hypotension. Nonetheless, despite of the evidence regarding the toxic bioaccumulation of neonicotinoids, a little is known about their cardiovascular toxicity. Henceforth, the current study aims to understand the effect of imidacloprid and its major metabolites on hERG (KV11.1) channel blockade using molecular docking studies. Findings of the study highlighted that IMI, DNI and IOL can potentially bind to residues like Tyr652 and Phe656 in the pore forming domain and can cause hERG (KV 11.1) blockade.

## 25COASOCT13

### **Title: In silico toxicity assessment and trace level quantification of potential genotoxic impurities in imipramine hydrochloride**

Vighnesh Pradeep Nalawade, Ravindra Kulkarni, Faiz Hussain Sayyed et.al.

Toxicology Letters, Volume 412, October 2025

<https://doi.org/10.1016/j.toxlet.2025.08.002>

**Abstract:** Since the adoption of the ICH M7 guidelines in 2014, pharmaceutical industries have been mandated to screen all reagents and chemicals used in drug synthesis for genotoxicity. Genotoxic impurities (GTIs) have the potential to induce mutations in DNA, which may lead to cancer. Unlike routine impurities, the threshold for controlling GTIs is extremely low. Imipramine hydrochloride (IH) is a commonly used antidepressant; however, the genotoxicity of both the drug and their impurities remain unknown. In this study, we systematically investigate the raw materials, intermediates, and known impurities involved in the synthesis pathway of IH for their potential genotoxicity. We employed in silico prediction tools to evaluate the toxicity of the impurities, intermediates, and raw materials used in the synthesis of IH, in accordance with ICH M7 guidelines. In silico prediction results revealed two specific impurities, 2,2-dinitro-1,2-diphenylethane (DNB) and 2,2-amino-1,2-diphenylethane (DAB), as potentially genotoxic. Furthermore, molecular docking and simulation studies were conducted to evaluate the specific interactions of these impurities with DNA. The results demonstrated consistent interactions of these impurities with the dG-rich region of the DNA duplex, particularly at the minor groove. Both in silico predictions and molecular docking studies corroborated the genotoxic nature of these impurities. As part of our risk assessment and control strategy, we developed and validated an HPLC-UV method in accordance with ICH guidelines to identify both GTIs in the final active pharmaceutical ingredient (API) of imipramine. This study will assist manufacturers of IH in controlling these genotoxic impurities to ensure its safe consumption.

**25COASOCT14****Title: Cuproptosis is involved in small intestinal toxicity in the paraffins during pregnancy**

Juan Tang, Zemin Xu, Mengna Jiang et.al.

Toxicology Letters, Volume 412, October 2025

<https://doi.org/10.1016/j.toxlet.2025.08.006>

**Abstract:** Short-chain chlorinated paraffins (SCCPs) is generally regarded as an emerging persistent organic pollutant. So far, small intestine injury in the progeny of adult mice exposed to SCCPs during pregnancy has not yet been the subject of any research. To investigate potential intestinal injury in the progeny of adult mice exposed to SCCPs during pregnancy. There were no noticeable variations in litter size, sex ratio, or the birth weight of male and female mice. However, SCCPs gestational exposure significantly reduced the adult body weight of female and male mice. In addition, we discovered that SCCPs exposure resulted in histological alterations in the small intestines of both female and male newborns. Furthermore, the small intestines of SCCPs-treated female and male mice showed a significantly elevated superoxide dismutase (SOD) activity and reduced glutathione (GSH) activity compared to control group. Moreover, SCCPs exposure led to downregulation of FDX1 protein level and upregulation the protein levels of DLAT and SLC31A1, indicating initiation of coppers. Interestingly, the alterations in FDX1, DLAT, and LIAS mRNA expression levels varied between female and male progeny. Even while none of the phenotypes showed the typical dose-dependent effects, the findings suggest that female offspring are more susceptible to small intestine toxicity than male offspring. According to our findings, SCCPs exposure during pregnancy might develop sex-specific small intestine toxicity, which may lead to reactive oxygen species activation and following coppers. In summary, this study demonstrated that exposure to SCCPs during pregnancy had deleterious effects on the offspring's small intestine.

**25COASOCT15****Title: Skin penetration and decontamination efficacy following in vitro human skin exposure to sulfur mustard**

K. Höjer Holmgren, E. Wigenstam, L. Öberg, A. Bucht et.al.

Toxicology Letters, Volume 412, October 2025

<https://doi.org/10.1016/j.toxlet.2025.07.1412>

**Abstract:** Sulfur mustard (HD) is a chemical warfare agent. Dermal injuries are most common following exposure and only supportive treatment exists. Consequently, skin decontamination is important to avoid severe injuries. In the present study, selected decontamination protocols were evaluated following in vitro human skin exposure to HD. The degradation kinetics of HD in receptor solution was also evaluated and a sample analysis method was developed. Rapid HD-degradation to thiodiglycol (TDG) was observed in the standard receptor solution (ethanol and water; 1:3). No intact HD was detected after 2 h. Low HD-degradation was detected in 100 % ethanol during 20 h (90 % intact agent). Subsequently, both HD and TDG was measured in all skin penetration samples. HD skin penetration experiments using the standard receptor solution or 100 % ethanol as receptor solution indicated that agent degradation primarily occurred in the receptor solution and not during agent penetration through skin. Reactive Skin Decontamination Lotion (RSDL)

followed by wet decontamination displayed the highest decontamination efficacy following skin exposure to neat HD. Dry removal using an absorbent pad followed by wet decontamination and wet decontamination alone resulted in a significant efficacy, of which, wet decontamination alone resulted in the lowest efficacy. RSDL has displayed the highest decontamination efficacy following skin exposure to both HD and the nerve agent VX in experiments using the same skin penetration model. The present study supports previously reported benefits of dry removal prior to wet decontamination and should be recommended to enable rapidly initiated decontamination if specific resources are lacking.

## 25COASOCT16

### **Title: Associations of semen essential/non-essential elements with the risk of male infertility: A systematic review and meta-analysis**

Jianfeng Chen, Wenwen Tan, Zhilian Chen et.al.

Toxicology Letters, Volume 412, October 2025

<https://doi.org/10.1016/j.toxlet.2025.08.007>

**Abstract:** Defective sperm function is the leading cause of male infertility, and epidemiological studies have revealed that various trace elements are linked to declining semen quality. However, differences in study quality and the heterogeneity of findings complicate the interpretation of the clinical significance of essential and non-essential elements in semen, especially ultra-trace elements. **Methods:** Essential and non-essential elements in the semen of male infertility were systematically searched within eight databases (Embase, Cochrane, PubMed, MedLine, Web of Science, Chinese Knowledge Infrastructure (CNKI), China Science and Technology Journal Database, and Wanfang database) up to November 2024. **Results:** A total of 38 studies involving 5070 patients (male fertility: 3061 vs. healthy control: 2009) were included. Thirty-eight studies measuring five essential elements (Zinc, Zn; Iron, Fe; Manganese, Mn; Selenium, Se; Copper, Cu) and four non-essential elements (Calcium, Ca; Magnesium, Mg; Lead, Pb; Cadmium, Cd) in the semen of men with infertility were included. Random-effect results indicated that the semen Cu (SMD = 0.505; 95 % CI: 0.246–0.764; P = 0.000) and Cd (SMD = 0.725; 95 % CI: 0.534–0.916; P = 0.000) levels in the male infertility group were higher than those of the control group. No significant differences in male infertility patient cases and healthy controls were found for Zn, Fe, Mn, Se, Ca, Mg, and Pb in semen. **Conclusion:** Elevations of Cu and Cd in semen were associated with the risk of male infertility. Investigation of essential and non-essential elements in semen may help to understand the pathogenesis of male infertility and could also be useful to plan treatment strategies in the future.

## 25COASOCT17

### **Title: Zinc and titanium nanoparticles exposure intensifies the risk of skin issues by elevating cytokine gene expression despite following current international safety protocols**

Vahid Babaei , Azadeh Ashtarinezhad, Maryam Torshabi et.al.

Toxicology Letters, Volume 412, October 2025

<https://doi.org/10.1016/j.toxlet.2025.08.004>

**Abstract:** Objectives: The growing use of nanomaterials in daily life has raised concerns about their biological effects and potential toxicity. This study examines the impact of Zinc



oxide (ZnO) and Titanium dioxide (TiO<sub>2</sub>) nanoparticles (NPs) on the expression of cytokine genes related to inflammation and their effects on skin abnormalities. Methods: Conducted in Iran in November 2021, this study involved 110 factory workers, all adhering to international safety protocols when handling nanomaterials. Workers were classified by their years of experience in the warehouse and production lines. Skin complications were assessed by physicians, alongside measurements of inflammatory cytokines (IL-4, IL-6, IL-8, TNF- $\alpha$ ) using RT-PCR, and CRP levels using a diagnostic kit. These workers were compared with a control group of administrative employees unexposed to nanoparticles. The concentrations of Zn and Ti nanoparticles in the workers were measured before and after their shifts. Results: The concentrations of Zn and Ti nanomaterials in these individuals were measured before and after their daily work shifts. Results were modeled with skin manifestations in Network Pharmacology, drawing on previous studies. Blood nanoparticle measurements before and after work shifts indicated that current protective methods are inadequate to prevent NP penetration into the body. Conclusion: The results show a strong correlation between years of exposure to nanoparticles and increased inflammatory gene expression, CRP, and skin manifestations, with p values less than 0.0001. The results highlight the need for enhanced safety measures when using nanomaterials in industries like cosmetics, hygiene products, and food, to prevent potential health risks from prolonged exposure.

## 25COASOCT18

**Title:** Exploring the impact of lysis conditions on the alkaline standard and Fpg-modified in vivo comet assay

M. Colia, E. Saenz-Martinez, A. Vettorazzi et.al.

Toxicology Letters, Volume 412, October 2025

<https://doi.org/10.1016/j.toxlet.2025.08.003>

**Abstract:** The comet assay is a method used to detect DNA lesions. The protocol involves cell lysis and electrophoresis of the DNA once the cells are embedded in agarose. In this study, we investigated how lysis duration and pH affect Wistar rat tissues. A single oral dose of 200 mg/kg methyl methanesulfonate (MMS) to induce DNA strand breaks (SBs), or 5 mg/kg MMS or 400 mg/kg potassium bromate (KBrO<sub>3</sub>) to induce Fpg-sensitive sites, was administered to male Wistar rats (n = 3 rats/group). The negative control rats received saline solution. After 3 h, the rats were sacrificed and different tissues were analysed after necropsy or snap-frozen in liquid nitrogen before analysis. The tested duration of lysis was from no lysis to overnight (pH 10). Different pH (i.e. 7 and 10) were tested in longer lysis (up to 1 week) in the case of the standard assay and in 1-hour lysis in the case of the Fpg- modified assay. No significant differences in SBs were found among the lysis lengths, including no lysis, but, after applying longer lysis in frozen samples, up to 1 -week, an increase in SBs was seen in the samples from treated rats. A neutral pH seems to slightly increase the % DNA in tail obtained. In the case of using Fpg a 5-min lysis was needed to detect Fpg-sensitive sites. The detection of Fpg-sensitive sites in MMS-treated rats was time and pH dependent. On the contrary, there were no differences in KBrO<sub>3</sub> detected lesions.

## 25COASOCT19

**Title:** Dose-dependent hepatotoxicity in Norway rat: Investigating the effects of methadone and morphine on liver gene expression and function

Hamid Norioun, Saeedeh Ghiasvand

Toxicology Letters, Volume 412, October 2025

<https://doi.org/10.1016/j.toxlet.2025.08.005>

**Abstract:** Methadone and morphine are two widely prescribed opioids for pain management and opioid substitution therapy. While both are pharmacologically effective, their long-term use may induce hepatotoxic effects. This study aimed to evaluate the hepatotoxic potential of methadone and morphine through an integrative approach combining experimental and bioinformatics analyses. Male Norway rats were administered methadone and morphine at doses of 3 and 7 mg/kg for 30 days. Liver tissues were analyzed using qRT-PCR to assess the expression of key metabolic genes (Cyp2b3, Cyp1a2, Cyp3a2, Cyp7a1, and Ugt2b), and serum liver enzyme levels (SGOT and SGPT) were measured as markers of liver injury. To further elucidate the molecular mechanisms underlying drug-induced liver injury, RNA sequencing (RNA-seq) data were analyzed to identify differentially expressed genes and enriched biological pathways. The bioinformatics data were sourced from the Gene Expression Omnibus (GEO) database with the accession number GSE250058. Bioinformatics analysis using DESeq2 revealed significant alterations in gene expression profiles, especially within immune regulation, oxidative stress, and metabolic detoxification pathways. KEGG and GO enrichment analyses highlighted the involvement of apoptosis, autophagy, and inflammation-related processes. These findings were supported by observed elevations in liver weight and liver enzymes, particularly in the high-dose methadone group. Overall, our results demonstrate that high-dose methadone induces more severe hepatic metabolic stress and gene dysregulation compared to morphine, indicating its greater hepatotoxic potential. This integrative study underscores the importance of combining experimental data with transcriptomic analyses to enhance our understanding of opioid-induced liver injury and inform future therapeutic strategies.

## 25COASOCT20

**Title: Cluster-based read-across of ToxCast data identifies buprofezin as a partial PPAR $\gamma$  agonist with obesogenic potential**

Seokyoung Hwang, Soyeon Oh, Seungchan An et.al.

Toxicology Letters, Volume 412, October 2025

<https://doi.org/10.1016/j.toxlet.2025.08.011>

**Abstract:** The identification of environmental obesogens has become increasingly urgent amid rising rates of metabolic disorders linked to chemical exposures. Here, we employed a cluster-based read-across framework that integrates structural descriptors with high-throughput screening (HTS) data from the ToxCast database to systematically identify potential obesogens. A total of 8971 chemicals were represented in a 2,217-dimensional structure–activity matrix, combining 1905 chemical fingerprints and 312 bioactivity endpoints, which were reduced and clustered into 135 distinct chemical groups. Among these, Cluster 14 was notably enriched with compounds affecting lipid metabolism pathways and included buprofezin, a thiadiazine insecticide not previously linked to obesogenic activity. Functional assays in human bone marrow-derived mesenchymal stem cells (hBM-MSCs) demonstrated that buprofezin promotes adipogenesis. Despite its classification as inactive in PPAR $\gamma$ -specific ToxCast assays, mechanistic studies revealed that buprofezin acts as a partial agonist of PPAR $\gamma$  ( $K_i = 14.8 \mu\text{M}$ ), enhancing SRC1 coactivator recruitment.



These findings underscore the limitations of current HTS data in capturing partial agonist activities and demonstrate the value of integrated read-across approaches in uncovering hidden chemical hazards. Given buprofezin's environmental persistence and widespread agricultural use, its potential metabolic health risks require further investigation.

## 25COASOCT21

### **Title: LncRNA SNHG15 sponges miR-3143/FOXO3 to regulate autophagy in ovarian dysfunction induced by benzene exposure**

Zhongming Ye, Qihao Huang , Haipeng Wu et.al.

Toxicology Letters, Volume 412, October 2025

<https://doi.org/10.1016/j.toxlet.2025.08.009>

**Abstract:** Benzene, a recognized carcinogen, is utilized in synthesizing various chemicals. Epidemiological studies have established a positive correlation between benzene exposure and increased incidences of abnormal menstruation and dysmenorrhea. This exposure might also pose risks to the fetal hematopoietic system. However, the precise molecular mechanisms underlying these effects are not fully understood. In this study, a chronic benzene exposure model was established through dynamic inhalation. We assessed the autophagy levels in mouse ovarian granulosa cells and human ovarian granulosa cells treated with 1,4-benzoquinone using molecular biology techniques such as qPCR, Western blot, and transmission electron microscopy (TEM), etc. The experimental results show that Benzene-exposed mice exhibited autophagy, a reduced number of ovarian granulosa cells, and vacuolar lesions in the fallopian tubes. Cell-based experiments demonstrated that benzene exposure significantly upregulated SNHG15 expression in human ovarian granulosa cells ( $P < 0.05$ ). The upregulation of SNHG15 enhanced FOXO3 expression via the miR-3143/FOXO3 axis, which in turn increased the transcription of autophagy-related proteins such as Atg5 ( $P < 0.05$ ), ultimately leading to excessive autophagy in granulosa cells and ovarian dysfunction. Benzene and its metabolite benzoquinone increase autophagy in ovarian granulosa cells. The lncRNA SNHG15 regulates this autophagy induced by benzene exposure through sponge-like binding to miR-3143/FOXO3, thus impairing ovarian function. Inhibiting SNHG15, miR-3143, and FOXO3 expression markedly reduced autophagy in granulosa cells and ameliorated ovarian dysfunction resulting from benzene exposure. These results suggest that the ceRNA axis involving SNHG15 may be a potential clinical therapeutic target.

## 25COASOCT22

### **Title: Cyclin-dependent kinase inhibitor abemaciclib-induced cutaneous responses mediated by inflammation**

Tugce Boran ,Özce Pala Çamlı , Mahmoud Abudayyak et.al.

Toxicology Letters, Volume 412, October 2025

<https://doi.org/10.1016/j.toxlet.2025.08.013>

**Abstract:** Abemaciclib is a cyclin-dependent kinase (CDK) enzyme inhibitor approved by the FDA for advanced and metastatic breast cancer therapy. Abemaciclib has caused some adverse reactions, such as dermatitis and skin reactions; however, the underlying cellular mechanism is still not obvious. In the current study, human keratinocyte HaCaT cells were treated with 0–10  $\mu$ M abemaciclib for 24 h. The cytotoxic, apoptosis/necrosis, oxidative

stress, and inflammation-inducing potentials of abemaciclib were evaluated. Abemaciclib induced cytotoxicity and the half-maximal inhibitory concentration (IC<sub>50</sub>) was computed to be  $\geq 24.18 \mu\text{M}$ . It significantly induced apoptosis and oxidative damage in the lowest treatment group ( $0.1 \mu\text{M}$ ). The time-dependent effects show that the highest effects were seen after 24 h. The study on low concentrations indicated that the maximum effects were seen in the  $0.1 \mu\text{M}$  treatment group. There was a notable rise in the secretion of MCP-1, IL-6, and IL-8 at  $0.1 \mu\text{M}$ , while it decreased at  $1\text{--}10 \mu\text{M}$ . Similarly, the levels of other mediators were increased solely at  $0.1 \mu\text{M}$ ; however, no changes in the higher concentrations. The increase in TNF- $\alpha$  was significant at  $5 \mu\text{M}$ ; however, the increase diminished at the highest treatment concentration. It could be concluded that abemaciclib-induced toxicity could be via oxidative inflammation leading to cell death in human keratinocytes. No effect was detected in the higher concentrations, while the effect was observed in the lowest treatment group. These findings underscore the need for further comprehensive studies of the spectrum of activity and risk profile of abemaciclib and encourage future research in this area.

## 25COASOCT23

### **Title: Human in vitro metabolism of an environmental mixture of polycyclic aromatic hydrocarbons (PAH) found at the Portland Harbor Superfund Site**

Kari A. Gaither, Kimberly Tyrrell, Whitney Garcia et.al.

Toxicology Letters, Volume 412, October 2025

<https://doi.org/10.1016/j.toxlet.2025.08.010>

**Abstract:** Polycyclic aromatic hydrocarbons (PAHs) are widespread environmental contaminants that pose health risks to humans. Toxicity testing approaches of PAHs have evolved from traditional rodent models to New Approach Methodologies (NAMs), such as high-throughput screening in zebrafish, enabling rapid evaluation of chemical hazards. However, translating toxicity findings from laboratory systems to humans remains difficult due to complexity and species-specific differences. Chemical dosimetry modeling offers a quantitative framework to bridge this gap, but its accuracy depends on robust knowledge of PAH metabolism. The objective of this study was to measure human metabolism rates of Supermix-10, the ten most abundant PAHs found at the Portland Harbor Superfund Site, to support development of human pharmacokinetic models. We incubated individual PAHs from Supermix-10 in pooled human liver microsomes and quantified parent PAH disappearance using high-performance liquid chromatography (HPLC) with UV and fluorescent detection. To assess the potential of mixture interactions, we also measured metabolism of all 10 compounds in an equimolar mixture and compared rates of parent disappearance to those observed for individual PAHs. All Supermix-10 PAHs demonstrated rapid parent compound disappearance in human hepatic microsomes. PAHs grouped into three metabolism patterns: high metabolism rates and capacity (2-methylnaphthalene, acenaphthylene, fluorene, naphthalene), high affinity metabolism that rapidly achieves low-level saturation (benzo[a]anthracene, chrysene), and moderate metabolism rates and capacity (fluoranthene, pyrene, retene, phenanthrene). Smaller PAHs exhibited faster metabolism, and higher metabolism rates correlated inversely with molecular weight. When incubated in an equimolar mixture, Supermix-10 demonstrated significantly slower metabolism (47–89%) compared to metabolism of individual PAHs at the same concentration. These findings enhance our understanding of PAH metabolism in humans and demonstrate significant

mixture interactions under the conditions tested. Our findings offer insights into the metabolic behavior of Supermix-10 and provide critical metabolism rate data to support the development of physiological based pharmacokinetic (PBPK) models. Dosimetry models can translate PAH chemical dosimetry from high-throughput testing platforms, like zebrafish and cellular system assays, to human exposures enhancing the accuracy and reliability of PAH risk assessments.

## 25COASOCT24

### **Title: Cytokine profile and early immune response to SARS-CoV-2 in occupationally lead-exposed individuals: A cross-sectional study**

Marta Jeziorska, Sławomir Kasperczyk, Michał Słota

Toxicology Letters, Volume 412, October 2025

<https://doi.org/10.1016/j.toxlet.2025.08.008>

**Abstract:** The adaptive immune response to severe acute respiratory syndrome coronavirus 2 (SARS-CoV-2) is characterized by the production of various antibodies, with immunoglobulin M (IgM) being the initial isotype synthesized. Lead (Pb), a toxic heavy metal, accumulates in biological systems and disrupts multiple biochemical processes, potentially modulating immune function through alterations in cytokine production and antibody levels. **Objective:** This study aimed to elucidate the early immune response to SARS-CoV-2 in lead-exposed individuals by examining antibody profiles and associated immunological parameters. **Methods:** A cohort of 277 male employees from a zinc and lead smelting facility in Poland was evaluated for SARS-CoV-2-specific IgM, IgG, and IgA antibodies prior to COVID-19 vaccination. Participants were stratified into IgM-positive ( $n = 13$ ) and IgM/IgG/IgA-negative ( $n = 149$ ) groups. Biomarkers of inflammation, hematological parameters, and oxidative stress were analyzed. **Results:** The IgM-positive group exhibited significantly elevated levels of cytokines, including a proliferation-inducing ligand (APRIL), B cell activating factor (BAFF), interleukin-20 (IL-20), pentraxin-3 (PTX-3), and soluble tumor necrosis factor receptor 2 (sTNF-R2). A significantly higher level of IgM antibody levels was observed in individuals with higher zinc protoporphyrin (ZPP) concentrations. However, no significant differences in blood lead levels (PbB), oxidative stress markers, or hematological parameters were detected between the groups. **Conclusion:** Elevated levels of APRIL, BAFF, IL-20, sTNF-R2, and PTX-3 in lead-exposed individuals with recent SARS-CoV-2 infection may indicate robust dendritic cell and B cell activation and enhanced modulation of tumor necrosis factor-alpha (TNF- $\alpha$ ) activity. These findings contribute to our understanding of the complex interplay between environmental lead exposure and the immune response to SARS-CoV-2 infection.

## 25COASOCT25

### **Title: Skin-targeted AhR activation by microbial and synthetic indoles: Insights from the AhaRaCaT reporter cell line**

Radim Vrzal, Aneta Grycová, Aneta Vrzalová

Toxicology Letters, Volume 412, October 2025

<https://doi.org/10.1016/j.toxlet.2025.09.001>

**Abstract:** Disruption of the epidermal barrier contributes to skin disorders such as atopic dermatitis and psoriasis. The aryl hydrocarbon receptor (AhR), a ligand-activated

transcription factor, plays a key role in skin homeostasis and immune regulation. While traditionally associated with toxicity, AhR has emerged as a promising therapeutic target, particularly via tryptophan-derived indoles. To support AhR research in a dermatological context, we developed AhaRaCaT, a stable luciferase-based reporter cell line derived from human keratinocytes (HaCaT), enabling the assessment of AhR transcriptional activity in a skin-relevant model. We characterized the inducibility of AhaRaCaT in response to model AhR ligands (TCDD, BaP, FICZ) in dose- and time-dependent assays. Antagonist profiling with MNF, CH223191, GNF, carvone, and jasmonone yielded IC<sub>50</sub> values over 4- and 24-hour exposures. A panel of indoles previously studied in other models was evaluated for AhR activation, revealing a robust luciferase response at 4 h that declined at 24 h, consistent with trends observed in other cell types. Selected indoles also induced CYP1A1 mRNA expression and reversed cytokine-induced downregulation of filaggrin in HaCaT cells, highlighting their potential in mitigating inflammation-associated skin barrier defects. In summary, the AhaRaCaT cell line offers a sensitive and physiologically relevant tool for studying AhR signaling in skin, with broad applications in toxicology, dermatological research, and the development of AhR-targeted therapies for inflammatory skin diseases.

## 25COASOCT26

### **Title: Establishing scientific confidence in a two-chamber co-culture system to evaluate androgenic response in the presence of hepatic metabolism**

Tessa C.A. van Tongeren, Susan J. Hall, Samantha J. Madnick

Toxicology Letters, Volume 412, October 2025

<https://doi.org/10.1016/j.toxlet.2025.08.014>

**Abstract:** For the in vitro determination of toxicity on target organs in the presence of physiologically relevant human metabolism, we recently developed a two-chamber liver-target organ co-culture system in a medium-throughput 96-well format. Our proof-of-concept study using human HepaRG microtissues cultured in three-dimension (3D) and AR-CALUX reporter cells demonstrated the significantly reduced testosterone (T)-mediated androgen receptor (AR) responses in the presence of human liver metabolism. The present study further increased the scientific confidence in this two-chamber co-culture system as a flexible and robust tool to capture androgen-mediated responses by incorporating alternate AR reporter cell systems as the target and examining additional androgenic compounds. The system generated concordant metabolism-dependent changes in T- and 5 $\alpha$ -dihydrotestosterone (DHT)-mediated AR responses using two different AR reporter cell systems (AR-CALUX, AR-INDIGO). The AR reporters had different sensitivity ranges and required media optimization. We demonstrated that this two-chamber co-culture system with integrated hepatic biotransformation can be used to evaluate endocrine activity with potential metabolism modulation of parent compounds.

## 25COASOCT27

### **Title: Characterization of formaldehyde-induced hepatotoxicity based on proteometabolomic analysis**

Sanjita Paudel, Hyunchae Sim, Eunjoo Kang et.al.

Toxicology Letters, Volume 412, October 2025

<https://doi.org/10.1016/j.toxlet.2025.09.003>

**Abstract:** Formaldehyde (FA) is a well-known environmental toxicant used in various industries, including biomedical, agriculture, and textiles, but poses significant health risks. Despite extensive research, the exact hepatotoxic mechanism of FA remains unclear. This study investigated FA-induced liver toxicity through an integrative analysis of proteomics and metabolomics in rat models, identifying 84 differentially expressed proteins and 66 metabolites. Using xMWAS and Reactome software, the study highlighted ferroptosis as a key pathway in FA-induced liver damage. STAT3/HO-1 were identified as crucial protein biomarkers, leading to ferroptosis via lipid peroxide accumulation through iron efflux. Validation through qPCR, western blot, and cell experiments confirmed the involvement of genes like Stat3, Hmox-1, and coagulation-related genes (Fga, Fgb, Fgg, Serpina1, and A2M). This research reveals a novel FA hepatotoxic mechanism involving ferroptosis and complement and coagulation pathways, offering potential for therapeutic interventions.

## 25COASOCT28

### **Title: Clozapine-associated perturbation of arachidonic acid metabolism: A future direction for clozapine-induced cardiotoxicity**

Ellen Kingston, Kathryn Burns, Malcolm Tingle

Toxicology Letters, Volume 412, October 2025

<https://doi.org/10.1016/j.toxlet.2025.09.005>

**Abstract:** Clozapine is an effective antipsychotic medication utilised for treatment-resistant schizophrenia. However, clinical use of clozapine is limited due to the risk of cardiotoxicities, including clozapine-induced myocarditis. Oxidation of clozapine and reduction of clozapine-N-oxide can be catalysed by the cardio-selective cytochrome P450 (CYP) isoforms CYP2J2, CYP1A1 and CYP1B1, which are also reported to metabolise arachidonic acid. Any interaction with CYP-catalysed arachidonic acid metabolism may perturb the balance of pro-inflammatory hydroxyeicosatetraenoic acids and anti-inflammatory epoxyeicosatrienoic acids, priming the heart to an inflammatory state. Thereby making it more susceptible to the damage that may induce clozapine-induced myocarditis. The purpose of this preliminary study was to investigate whether an interaction between arachidonic acid and clozapine or clozapine-N-oxide occurs at CYP2J2, CYP1A1 and CYP1B1, in comparison to the hepatic isoform CYP2C19. Our results demonstrated a clear perturbation of CYP1B1 catalysed arachidonic acid metabolism, with a concentration-dependent decrease in metabolite formation in the presence of clozapine and clozapine-N-oxide. Each isoform also had decreased N-desmethylozapine formation relative to incubations with clozapine alone and impaired clozapine and clozapine-N-oxide REDOX cycling capacity. Although limited by analytical sensitivity, these data provide clear evidence of a metabolic interaction between arachidonic acid and clozapine. This offers a novel hypothesis to explain patient susceptibility and a feasible mechanism for the cardiac-selective inflammation observed in clozapine-induced myocarditis.

## 25COASOCT29

### **Title: Toxicological effects of micro/nano-plastics on human reproductive health: A review**

Amirreza Talaie , Sanaz Alaei, Elham Hosseini et.al.

Toxicology Letters, Volume 412, October 2025



<https://doi.org/10.1016/j.toxlet.2025.06.021>

**Abstract:** Micro/Nano-plastics (MNPs), including microplastics (MPs; <5 mm) and nanoplastics (NPs; <100 nm), have become pervasive environmental pollutants due to extensive plastic production and insufficient recycling practices. These particles originate from the degradation of larger plastic materials through processes such as photo-oxidation, thermo-oxidation, and incomplete biodegradation, resulting in chemically reactive fragments that persist in air, water, and food. Once released, MNPs enter the human body primarily via ingestion, inhalation, and dermal absorption, ultimately accumulating in various tissues, including reproductive organs. This review provides a comprehensive summary of current knowledge regarding the toxicological effects of MNPs on male and female reproductive health, with a focus on mammalian models and relevance to human exposure. In males, MNPs have been associated with testicular damage, impaired spermatogenesis, reduced sperm count and motility, and disruptions in the hypothalamic-pituitary-gonadal axis. In females, exposure has been linked to altered folliculogenesis, disrupted ovarian hormone levels, impaired oocyte quality, and placental dysfunction. These effects are largely driven by mechanisms involving oxidative stress, inflammation, endocrine disruption, mitochondrial dysfunction, and apoptosis. Furthermore, MNPs have been shown to disrupt gut microbiota composition, contributing to systemic inflammation and reproductive dysfunction through emerging pathways such as the gut–testis axis. Given their widespread presence and multifaceted modes of action, MNPs pose a serious threat to human reproductive health. Therefore, there is an urgent need for stricter environmental regulations, improved waste management, and further research to understand the long-term and transgenerational consequences of MNP exposure.

## 25COASOCT30

### **Title: Haematopoietic ageing in health and lifespan**

Rebecca Andersson, Eva Mejia-Ramirez & Maria Carolina Florian

Nature Cell Biology volume 27, pages1398–1410 (2025)

<https://doi.org/10.1038/s41556-025-01739-1>

**Abstract:** Ageing of the haematopoietic system is characterized by phenotypic and functional impairments that are driven by alterations of haematopoietic stem cells and of the bone marrow niche. Haematopoietic stem cells are responsible for the production of all the different cell types that constitute the blood, and their maintenance and differentiation must be tightly regulated during the whole life of an organism. Exciting new data emphasize that central aspects of blood ageing, ranging from inflammageing and immunosenescence to clonal haematopoiesis, are mechanistically linked to dysfunction and ageing of other tissues, supporting a central role for the haematopoietic system in this context. Here we review some of the recent findings with a focus on ageing of the haematopoietic system and provide an overview of its role in driving healthspan and lifespan of the whole organism.

## 25COASOCT31

### **Title: Genome-wide CRISPR screen identifies Menin and SUZ12 as regulators of human developmental timing**

Nan Xu, Hyein S. Cho, James O. S. Hackland et.al.

Nature Cell Biology volume 27, pages1411–1421 (2025)



<https://doi.org/10.1038/s41556-025-01751-5>

**Abstract:** Embryonic development follows a conserved sequence of events across species, yet the pace of development is highly variable and particularly slow in humans. Species-specific developmental timing is largely recapitulated in stem cell models, suggesting a cell-intrinsic clock. Here we use directed differentiation of human embryonic stem cells into neuroectoderm to perform a whole-genome CRISPR-Cas9 knockout screen and show that the epigenetic factors Menin and SUZ12 modulate the speed of PAX6 expression during neural differentiation. Genetic and pharmacological loss-of-function of Menin or SUZ12 accelerate cell fate acquisition by shifting the balance of H3K4me3 and H3K27me3 at bivalent promoters, thereby priming key developmental genes for faster activation upon differentiation. We further reveal a synergistic interaction of Menin and SUZ12 in modulating differentiation speed. The acceleration effects were observed in definitive endoderm, cardiomyocyte and neuronal differentiation paradigms, pointing to chromatin bivalency as a general driver of timing across germ layers and developmental stages.

## 25COASOCT32

**Title:** A multichaperone condensate enhances protein folding in the endoplasmic reticulum

Anna Leder, Guillaume Mas, Viktória Szentgyörgyi et.al.

Nature Cell Biology volume 27, pages1422–1430 (2025)

<https://doi.org/10.1038/s41556-025-01730-w>

**Abstract:** Protein folding in the endoplasmic reticulum (ER) relies on a network of molecular chaperones that facilitates the folding and maturation of client proteins. How the ER chaperones organize in a supramolecular manner to exert their cooperativity has, however, remained unclear. Here we report the discovery of a multichaperone condensate in the ER lumen, which is formed around the chaperone PDIA6 during protein folding homeostasis. The condensates form in a Ca<sup>2+</sup>-dependent manner and we resolve the underlying mechanism at the atomic and cellular levels. The PDIA6 condensates recruit further chaperones—Hsp70 BiP, J-domain protein ERdj3, disulfide isomerase PDIA1 and Hsp90 Grp94—which constitute some of the essential components of the early folding machinery. The chaperone condensates enhance folding of proteins, such as proinsulin, and prevent protein misfolding in the ER lumen. The PDIA6-scaffolded chaperone condensates hence provide the functional basis for spatial and temporal coordination of the dynamic ER chaperone network.

## 25COASOCT33

**Title:** The intrinsically disordered regions of organellophagy receptors are interchangeable and control organelle fragmentation, ER-phagy and mitophagy flux

Mikhail Rudinskiy, Carmela Galli, Andrea Raimondi

Nature Cell Biology volume 27, pages1431–1447 (2025)

<https://doi.org/10.1038/s41556-025-01728-4>

**Abstract:** Organellophagy receptors control the generation and delivery of portions of their homing organelle to acidic degradative compartments to recycle nutrients, remove toxic or aged macromolecules and remodel the organelle upon physiologic or pathologic cues. How they operate is not understood. Here we show that organellophagy receptors are composed of

a membrane-tethering module that controls organellar and suborganellar distribution and by a cytoplasmic intrinsically disordered region (IDR) with net cumulative negative charge that controls organelle fragmentation and displays an LC3-interacting region (LIR). The LIR is required for lysosomal delivery but is dispensable for organelle fragmentation. Endoplasmic reticulum (ER)-phagy receptors' IDRs trigger DRP1-assisted mitochondrial fragmentation and mitophagy when transplanted at the outer mitochondrial membrane. Mitophagy receptors' IDRs trigger ER fragmentation and ER-phagy when transplanted at the ER membrane. This offers an interesting example of function conservation on sequence divergency. Our results imply the possibility to control the integrity and activity of intracellular organelles by surface expression of organelle-targeted chimeras composed of an organelle-targeting module and an IDR module with net cumulative negative charge that, if it contains a LIR, eventually tags the organelle portions for lysosomal clearance.

### 25COASOCT34

**Title: A chaperone-proteasome-based fragmentation machinery is essential for aggrephagy**

Mario Mauthe, Nicole van de Beek, Muriel Mari et.al.

Nature Cell Biology volume 27, pages1448–1464 (2025)

<https://doi.org/10.1038/s41556-025-01747-1>

**Abstract:** Perturbations in protein quality control lead to the accumulation of misfolded proteins and protein aggregates, which can compromise health and lifespan. One key mechanism eliminating protein aggregates is aggrephagy, a selective type of autophagy. Here we reveal that fragmentation is required before autophagic clearance of various types of amorphous aggregates. This fragmentation requires both the 19S proteasomal regulatory particle and the DNAJB6-HSP70-HSP110 chaperone module. These two players are also essential for aggregate compaction that leads to the clustering of the selective autophagy receptors, which initiates the autophagic removal of the aggregates. We also found that the same players delay the formation of disease-associated huntingtin inclusions. This study assigns a novel function to the 19S regulatory particle and the DNAJB6-HSP70-HSP110 module, and uncovers that aggrephagy entails a piecemeal process, with relevance for proteinopathies.

### 25COASOCT35

**Title: CHIP protects lysosomes from CLN4 mutant-induced membrane damage**

Juhyung Lee, Natalie Chin, Jizhong Zou et.al.

Nature Cell Biology volume 27, pages1465–1481 (2025)

<https://doi.org/10.1038/s41556-025-01738-2>

**Abstract:** Understanding how cells mitigate lysosomal damage is critical for unravelling pathogenic mechanisms of lysosome-related diseases. Here we generate and characterize induced pluripotent stem cell (iPSC)-derived neurons (i3Neuron) bearing ceroid lipofuscinosis neuronal 4 (CLN4)-linked DNAJC5 mutations, which revealed extensive lysosomal abnormality in mutant neurons. In vitro membrane-damaging experiments establish lysosomal damages caused by lysosome-associated CLN4 mutant aggregates, as a critical pathogenic linchpin in CLN4-associated neurodegeneration. Intriguingly, in non-neuronal cells, a ubiquitin-dependent microautophagy mechanism downregulates CLN4

aggregates to counteract CLN4-associated lysotoxicity. Genome-wide CRISPR screens identify the ubiquitin ligase carboxyl terminus of Hsc70-interacting protein (CHIP) as a central microautophagy regulator that confers ubiquitin-dependent lysosome protection. Importantly, CHIP's lysosome protection function is transferrable: ectopic CHIP improves lysosomal function in CLN4 i3Neurons and effectively alleviates lipofuscin accumulation and cell death in a *Drosophila* CLN4 disease model. Our study establishes CHIP-mediated microautophagy as a key organelle guardian that preserves lysosome integrity, offering new insights into therapeutic development for lysosome-related neurodegenerative diseases.

## 25COASOCT36

**Title: Hbo1 and Msl complexes preserve differential compaction and H3K27me3 marking of active and inactive X chromosomes during mitosis**

Dounia Djeghloul, Sherry Cheriyankunnel, Bhavik Patel et.al.

Nature Cell Biology volume 27, pages1482–1495 (2025)

<https://doi.org/10.1038/s41556-025-01748-0>

**Abstract:** In mammals, chromosome-wide regulatory mechanisms ensure a balance of X-linked gene dosage between males (XY) and females (XX). In female cells, expression of genes from one of the two X chromosomes is curtailed, with selective accumulation of Xist-RNA, Xist-associated proteins, specific histone modifications (for example, H3K27me3) and Barr body formation observed throughout interphase. Here we show, using chromosome flow-sorting, that during mitosis, Xist-associated proteins dissociate from inactive X (Xi) chromosomes, while high levels of H3K27me3 and increased compaction of the Xi relative to active X (Xa), are retained. Proteomic comparison of mitotic Xi and Xa revealed that components of Hbo1 and Msl/Mof histone acetyltransferase complexes are significantly enriched on Xa as compared to Xi and autosomes. By contrast, inhibitors of histone acetylation co-enrich with Xi. Furthermore, inhibition of Hbo1 or deletion of Msl/Mof components functionally abolishes mitotic differences in H3K27me3 marking and chromosome compaction. These data uncover critical roles for acetylation pathways in preserving X chromosome properties during mitosis.

## 25COASOCT37

**Title: Synthetic ZFTA fusions pinpoint disordered protein domain acquisition as a mechanism of brain tumorigenesis**

Arabzade, H. K. Shirnekhi, S. Varadharajan et.al.

Nature Cell Biology volume 27, pages1496–1509 (2025)

<https://doi.org/10.1038/s41556-025-01745-3>

**Abstract:** Over 95% of ependymomas that arise in the cortex are driven by a gene fusion involving the zinc finger translocation-associated (ZFTA) protein. Here, using super-resolution and lattice light-sheet microscopy, we demonstrate that the most frequent fusion variant, ZFTA–RELA (ZR), forms dynamic nuclear condensates that are required for oncogene expression and tumorigenesis. Mutagenesis studies of ZR reveal a key intrinsically disordered region (IDR) in RELA that governs condensate formation. Condensate-modulating IDR mutations introduced into ZR impaired its genomic occupancy at oncogenic loci and inhibited the recruitment of transcriptional effector proteins, such as MED1, BRD4 and RNA polymerase II. Using nuclear magnetic resonance spectroscopy, we examined the

DNA-binding residues of the critical zinc finger (ZF1) found in ZR and characterized their significance for condensate formation, genomic binding and oncogene activation. We generated synthetic ZFTA fusion proteins where IDRs from known condensate-forming proteins were grafted into ZR. Synthetic ZFTA fusion oncoproteins utilizing IDRs from EWS and FUS restored condensate formation, oncogene transcription and tumour initiation in mice. These findings provide key insights into the oncogenic mechanism of ZR and the importance of IDR acquisition in fusion oncoproteins in brain cancer.

## 25COASOCT38

### **Title: RNA-binding proteins mediate the maturation of chromatin topology during differentiation**

Bondita Dehingia, Małgorzata Milewska-Puchała, Marcin Janowski et.al.

Nature Cell Biology volume 27, pages1510–1525 (2025)

<https://doi.org/10.1038/s41556-025-01735-5>

**Abstract:** Topologically associating domains (TADs) and chromatin architectural loops impact promoter–enhancer interactions, with CCCTC-binding factor (CTCF) defining TAD borders and loop anchors. TAD boundaries and loops progressively strengthen upon embryonic stem (ES) cell differentiation, underscoring the importance of chromatin topology in ontogeny. However, the mechanisms driving this process remain unclear. Here we show a widespread increase in CTCF–RNA-binding protein (RBP) interactions upon ES to neural stem (NS) cell differentiation. While dispensable in ES cells, RBPs reinforce CTCF-anchored chromatin topology in NS cells. We identify Pantr1, a non-coding RNA, as a key facilitator of CTCF–RBP interactions, promoting chromatin maturation. Using acute CTCF degradation, we find that, through its insulator function, CTCF helps maintain neuronal gene silencing in NS cells by acting as a barrier to untimely gene activation during development. Altogether, we reveal a fundamental mechanism driving developmentally linked chromatin structural consolidation and the contribution of this process to the control of gene expression in differentiation.

## 25COASOCT39

### **Title: MLKL PARylation in the endothelial niche triggers angiocrine necroptosis to evade cancer immunosurveillance and chemotherapy**

Nan Yang, Xiaoxue Li, Wenwen Huang et.al.

Nature Cell Biology volume 27, pages1526–1542 (2025)

<https://doi.org/10.1038/s41556-025-01740-8>

**Abstract:** Chemoresistance is the leading cause of cancer-related death. How chemotherapy subjugates the cellular crosstalk in the tumour microenvironment to cause chemoresistance remains to be defined. Here we find chemotherapy enables immunosuppressive SDF1+ endothelial niche to evade immunosurveillance in ovarian and breast cancers. We integrated human patient data and mouse models to show that chemotherapy selectively activates PARP1–SDF1 axis in tumour endothelial cells (ECs). This angiocrine SDF1 interferes with antitumour interplay between CXCL10+ macrophages and CXCR3+CD8+ T cells and promotes tumour progression in ovarian and breast cancers. Proteome-based screening revealed that endothelial PARP1 PARylates MLKL, a key necroptosis effector to upregulate angiocrine SDF1 in ECs. In sum, we identify PARylation-dependent necroptosis in tumour

ECs as an important step in subverting the tumour microenvironment to evade immunosurveillance.

## 25COASOCT40

### **Title: Durotaxis is a driver and potential therapeutic target in lung fibrosis and metastatic pancreatic cancer**

Taslim A. Al-Hilal, Maria-Anna Chrysovergi, Paula E. Grasberger et.al.

Nature Cell Biology volume 27, pages1543–1554 (2025)

<https://doi.org/10.1038/s41556-025-01697-8>

**Abstract:** Durotaxis, cell migration along stiffness gradients, is linked to embryonic development, tissue repair and disease. Despite solid in vitro evidence, its role in vivo remains largely speculative. Here we demonstrate that durotaxis actively drives disease progression in vivo in mouse models of lung fibrosis and metastatic pancreatic cancer. In lung fibrosis, durotaxis directs fibroblast recruitment to sites of injury, where they undergo mechano-activation into scar-forming myofibroblasts. In pancreatic cancer, stiffening of the tumour microenvironment induces durotaxis of cancer cells, promoting metastatic dissemination. Mechanistically, durotaxis is mediated by focal adhesion kinase (FAK)–paxillin interaction, a mechanosensory module that links stiffness cues to transcriptional programmes via YAP signalling. To probe this genetically, we generated a FAK-FATL994E knock-in mouse, which disrupts FAK–paxillin binding, blocks durotaxis and attenuates disease severity. Pharmacological inhibition of FAK–paxillin interaction with the small molecule JP-153 mimics these effects. Our findings establish durotaxis as a disease mechanism in vivo and support anti-durotactic therapy as a potential strategy for treating fibrosis and cancer.

## 25COASOCT41

### **Title: CD160 dictates anti-PD-1 immunotherapy resistance by regulating CD8+ T cell exhaustion in colorectal cancer**

Tongsen Zheng, Chujie Ding, Shihui Lai et.al.

Nature Cell Biology volume 27, pages1555–1571 (2025)

<https://doi.org/10.1038/s41556-025-01753-3>

**Abstract:** The colon exhibits higher propensity for tumour development than ileum. However, the role of immune microenvironment differences in driving this disparity remains unclear. Here, by comparing paired ileum and colon samples from patients with colorectal cancer (CRC) and healthy donors, we identified ileum-enriched CD160+CD8+ T cells with previously unrecognized characteristics, including resistance to terminal exhaustion and strong clonal expansion. The transfer of CD160+CD8+ T cells significantly inhibits tumour growth in microsatellite instability-high and inflammation-induced CRC models. Cd160 knockout accelerates tumour growth, which is mitigated by transferring CD160+CD8+ T cells. Notably, in microsatellite instability-high and anti-PD-1-resistant CRC models, CD160+CD8+ T cells improve anti-PD-1 efficacy and overcome its resistance by increasing tumour-infiltrating progenitor-exhausted T cells, nearly eradicating tumours. Mechanistically, we uncover a CD160–PI3K (p85 $\alpha$ ) interaction that promotes Fc $\epsilon$ R1 $\gamma$  and 4-1BB expression via the AKT–NF- $\kappa$ B pathway, thereby enhancing CD8+ T cell cytotoxicity. Our study reveals CD160 as a crucial regulator of CD8+ T cell function and proposes an innovative

immunotherapy strategy of transferring CD160+CD8+ T cells to overcome anti-PD-1 resistance.

## 25COASOCT42

### **Title: LncSNHGs: new targets in osteosarcoma**

Yining Zhang, Jinfa Wu & Jiaming Liu

Cancer Gene Therapy volume 32, pages1031–1041 (2025)

<https://doi.org/10.1038/s41417-025-00952-2>

**Abstract:** Long non-coding RNAs (lncRNAs) have attracted significant attention for their role in tumor initiation and progression. Specifically, studying lncRNA small nucleolar RNA host genes (lncSNHGs) has opened up new possibilities for the treatment of osteosarcoma (OS). This review aims to give a thorough overview of the state of research on the biological roles, molecular mechanisms, and expression of the lncRNA SNHG family in OS. Through an extensive analysis, it is demonstrated that members of the SNHG family exhibit dysregulated expression patterns in OS. These dysregulations affect multiple oncogenic processes, including tumor proliferation, metastasis, apoptosis, autophagy, and chemotherapy resistance. The lncRNA SNHG family promises to identify novel strategies and targets for diagnosing, treating, and prognosis OS.

## 25COASOCT43

### **Title: PANoptosis in cancer: molecular mechanisms and therapeutic potential**

Xi Pu, Yuting Wu, Chen Peng

Cancer Gene Therapy volume 32, pages1042–1053 (2025)

<https://doi.org/10.1038/s41417-025-00940-6>

**Abstract:** Tumorigenesis is closely related to an imbalance in cell death regulation. PANoptosis is a recently characterized form of programmed cell death that integrates the molecular features of cellular pyroptosis, apoptosis and necrotic apoptosis through the assembly of a multiprotein complex termed the PANoptosome. Beyond its role in cancer initiation and progression, PANoptosis is intricately linked to immune responses within the tumor microenvironment, thus offering new avenues for therapeutic intervention. The present review outlines the interplay among different cell death pathways, highlights the defining characteristics and assembly mechanisms of PANoptosis, as well as discusses its functional roles in cancer biology. Additionally, the implications of PANoptosis in tumor immunity and the potential of targeting this pathway in cancer therapy are explored.

## 25COASOCT44

### **Title: Real-world outcomes of Adjuvant De Gramont versus Xelox chemotherapy in reSected gasTric canCER: a propensity score-matched analysis (ASTER study)**

Ina Valeria Zurlo, Fausto Rosa, Diana Giannarelli et.al.

Cancer Gene Therapy volume 32, pages1054–1061 (2025)

<https://doi.org/10.1038/s41417-025-00945-1>

**Abstract:** The role of adjuvant chemotherapy (aCT) in gastric and esophago-gastric junction cancer (GC/EGJC) remains controversial. This study (ASTER study) aimed to compare the clinical outcomes of De Gramont (DG) versus XELOX/FOLFOX (OXA) regimens in a European real-world setting. This retrospective, bicentric study included patients treated with



aCT between January 2001 and January 2018. A propensity score-matched (PSM) analysis was performed to compare oncological outcomes between DG and OXA regimens. Primary endpoints were disease-free survival (DFS) and overall survival (OS). Statistical analyses included the chi-square test, Kaplan–Meier method, and Cox proportional hazards modeling. Among 255 patients (127 DG, 128 OXA), 160 were matched (80 per arm) by PSM. Median DFS and OS did not differ significantly between groups (mDFS: 102.3 vs. 85.4 months,  $p=0.91$ ; mOS: 119.5 vs. 89.8 months,  $p=0.69$ ). In PSM-adjusted analysis, DG showed a trend towards longer DFS ( $p=0.052$ ) and significantly improved OS ( $p=0.016$ ). Multivariate analysis confirmed age, ECOG PS, resection margins, and stage as major prognostic factors. DG and OXA regimens demonstrated similar efficacy in the adjuvant treatment of resected GC/GEJC in a European cohort. Further prospective studies are warranted to optimize regimen selection and refine patient stratification.

## 25COASOCT45

### **Title: Engineered L-asparaginase variants with enhanced therapeutic properties to improve treatment of childhood acute lymphatic leukemia**

Mainak Biswas, Soumika Sengupta, Khushboo A. Gandhi et.al.

Cancer Gene Therapy volume 32, pages1062–1075 (2025)

<https://doi.org/10.1038/s41417-024-00865-6>

**Abstract:** Escherichia coli L-asparaginase (EcA), a key component of a multi-drug acute lymphatic leukemia (ALL) treatment regimen, has several limitations that reduce its therapeutic efficacy. The major disadvantages include immunogenicity, serum instability, shorter half-life, and accompanying glutaminase activity that causes neurotoxicity and pancreatitis. Pegylated asparaginase and Erwinase have better therapeutic potential, but they are expensive. Using site-directed mutagenesis, we created several EcA variants by substituting specific amino acid residues at the dimer-dimer interface and B-cell epitope regions. After several rounds of screening and selection, we identified two EcA variants viz. K288S/Y176F (KSY-17) and K288S/Y176F/W66Y (KSYW-17), which showed comparable asparaginase activity to wild-type (WT) and significantly less glutaminase activity (30.36 U/mg for WT vs 1.54 and 0.99 U/mg for KSY-17 and KSYW-17). KSYW-17 was less immunogenic than WT, eliciting 4.8–5.3-fold and 2.4–3.8-fold less IgG and IgM responses, respectively. Compared to WT EcA, we also observed significantly less (~1.5-2-fold) binding of these variants to pre-existing antibodies in ALL patients' serum. Pharmacokinetic studies showed that KSY-17 ( $213.3 \pm 6.5$  min) and KSYW-17 ( $244.8 \pm 35.5$  min) had longer plasma half-lives than WT ( $101.1 \pm 5.1$  min). Both variants showed no toxicity up to 5000 IU/kg (single dose) and 1600 IU/kg (repeat dose) in mice. ALL xenograft mice studies showed a 90% and 70% reduction in leukemia burden in KSY-17 and KSYW-17 administered mice, respectively, as compared to 30% for WT after repeat dose administration, accompanied by significantly higher mice survival (100% vs. 70% vs. 10% for KSY-17 vs. KSYW-17 vs. WT). Overall, the engineered EcA variants' showed improved therapeutic efficacy, thus making them promising candidates for primary and relapsed ALL treatment.

## 25COASOCT46

### **Title: Targeting MCM10 disrupts cancer stemness and counteracts sorafenib resistance in hepatocellular carcinoma**

Ziyun Zhang, Lu Liang, Yi Li et.al.

Cancer Gene Therapy volume 32, pages1076–1089 (2025)

<https://doi.org/10.1038/s41417-025-00946-0>

**Abstract:** Hepatocellular carcinoma (HCC) is the most prevalent primary malignant tumor, with sorafenib as the main treatment for advanced cases. However, the development of resistance to sorafenib, often driven by cancer stemness, significantly limits its therapeutic efficacy. Minichromosome maintenance complex component 10 (MCM10), a critical regulator of DNA replication and tumor progression, has been implicated in cancer stemness and therapeutic resistance. This study utilized datasets from TCGA and ICGC alongside in vitro and vivo experiments on clinical HCC tissues and sorafenib-resistant cell lines to evaluate MCM10's role in HCC. The Connectivity Map (CMap) was employed to identify TW-37, a potential gene silencing agent targeting MCM10 transcription. The effects of TW-37 on MCM10 expression, cancer stemness, and sorafenib sensitivity were assessed. Elevated MCM10 expression was observed in sorafenib-resistant HCC cell lines and was associated with poor patient outcomes. MCM10 knockout diminished cancer stemness and restored sorafenib sensitivity in resistant cells. Furthermore, TW-37, identified via CMap, effectively downregulated MCM10, reduced cancer stemness, and enhanced sorafenib efficacy, offering a promising therapeutic approach. MCM10 plays a pivotal role in promoting cancer stemness and sorafenib resistance in HCC. Targeting MCM10 transcription with TW-37 represents a novel strategy to overcome sorafenib resistance and improve therapeutic outcomes in HCC patients.

## 25COASOCT47

**Title: NK cells mediate preventive efficacy of intravenous BCG against lung metastasis in mice**

Claudia Guerrero, Marta Casal, Cristina Alierta et.al.

Cancer Gene Therapy volume 32, pages1090–1097 (2025)

<https://doi.org/10.1038/s41417-025-00948-y>

**Abstract:** Lung metastases frequently arise from primary tumors, including bladder cancer, and represent a critical negative prognostic factor. Natural Killer (NK) cells have shown to play a vital role in controlling metastasis. Consequently, tumor cells have evolved specific mechanisms to evade NK cell-mediated immune surveillance, promoting metastasis and resistance to immunotherapy. In this study, we investigated the prophylactic and therapeutic potential of intravenous Bacillus Calmette–Guerin (BCG) in preventing lung metastases from bladder cancer cells using a murine model. We demonstrated that prophylactic BCG administration significantly reduced tumor burden and prolonged survival, largely through NK cell activation. However, BCG treatment was ineffective when administered over established tumors, likely due to tumor-driven immune evasion mechanisms. Our results revealed the contribution of interferon-gamma (IFN- $\gamma$ ) to tumor resistance. Tumor cells exposed to IFN- $\gamma$  were more resistant to BCG in vivo, which correlated with the overexpression of immune checkpoint molecules, whereas disruption of the IFN- $\gamma$  signaling pathway in tumor cells partially restored the therapeutic efficacy of BCG. Our findings highlight the importance of understanding tumor immune escape mechanisms and suggest that BCG could be a promising treatment for preventing lung metastases in bladder cancer.

**25COASOCT48****Title: METTL3 facilitates colorectal cancer growth through altering the abundance of intestinal Akkermansia muciniphila**

Ling Wu, Weidong Lian, Rui Bai et.al.

Cancer Gene Therapy volume 32, pages1098–1106 (2025)

<https://doi.org/10.1038/s41417-025-00949-x>

**Abstract:** Colorectal cancer (CRC) is a prevalent malignant tumor that poses a significant threat to human health; however, the precise mechanism underlying its onset remains elusive. In this study, we utilized metagenomic sequencing to reveal the dysregulation of intestinal microbiota caused by CRC. Single-cell sequencing data showed elevated mRNA expression of methyltransferase-like protein 3 (METTL3) in CRC, which was correlated with the abundance of intestinal microbiota. Furthermore, we found that METTL3 promotion of CRC progression is microbiota-dependent. Using induced METTL3<sup>fl/fl</sup> Vill1-cre<sup>+/-</sup> mice, we identified the microbiota regulated by METTL3 in CRC. Our research indicates that METTL3 leads to high expression of HIF1 $\alpha$ , which promotes the expression of lipocalin 2 (LCN2) in CRC cells, inhibiting the abundance of Akkermansia muciniphila, thereby promoting CRC progression.

**25COASOCT49****Title: The involvement of lncRNA EMSLR in the disulfidptosis and progression of endometrial carcinoma**

Yixuan Sun, Ruiwen Wang, Xinzhu Li et.al.

Cancer Gene Therapy volume 32, pages1107–1119 (2025)

<https://doi.org/10.1038/s41417-025-00918-4>

**Abstract:** The incidence of endometrial cancer (EC) continues to rise. Disulfidptosis, a novel form of cell death, may represent a potential therapeutic target in EC. Through bioinformatic analysis of The Cancer Genome Atlas (TCGA) database, E2F1 mRNA-stabilizing lncRNA (EMSLR) was identified as a lncRNA related to disulfidptosis in EC. Functional assays, including cell proliferation and xenograft assays, demonstrated that knockdown of EMSLR significantly impeded EC cell proliferation, whereas overexpression of EMSLR promoted cell viability. Additionally, EMSLR was found to be associated with glucose uptake and NADPH production in glucose-restricted culture conditions. Moreover, downregulation of EMSLR markedly increased cell death and induced cytoskeletal collapse under glucose deprivation, as evidenced by F-actin and cell death staining. Notably, we observed a strong correlation between EMSLR and the c-MYC-GLUT1 pathway. Mechanistically, EMSLR was found to mediate the expression and nuclear translocation of c-MYC, thereby regulating the progression of EC and its associated disulfidptosis. In conclusion, EMSLR is identified as a disulfidptosis-related gene in endometrial cancer. Elucidating the function and molecular mechanisms of EMSLR in EC presents a promising avenue for therapeutic intervention in patients.

**25COASOCT50****Title: Abemaciclib impairs glioblastoma sphere formation by targeting the GSK3 $\beta$ -mediated transcriptional regulation of CD44 and TCF7L2**

Muh-Lii Liang, Chun-Han Chen, Ya-Ching Lin et.al.

Cancer Gene Therapy volume 32, pages1120–1132 (2025)

<https://doi.org/10.1038/s41417-025-00955-z>

**Abstract:** Glioblastoma multiforme (GBM) is an aggressive brain tumor partly driven by cancer stem cells (CSCs). Abemaciclib demonstrates the potential for treating GBM, although its mechanisms beyond RB phosphorylation are not fully understood. This study reveals that Abemaciclib diminishes GBM sphere formation by influencing EMT pathways via GSK3 $\beta$ -mediated regulation of CD44 and TCF7L2. Treatment with Abemaciclib significantly hindered sphere formation in GBM cells, and transcriptomic analysis indicated EMT pathways suppression. Mechanistically, Abemaciclib consistently lowered the expression of CD44 and TCF7L2 in both parental and sphere cells by inhibiting GSK3 $\beta$  phosphorylation. A pharmacological GSK3 $\beta$  inhibitor produced similar effects, reinforcing the existence of a GSK3 $\beta$ -CD44/TCF7L2 axis. Moreover, orthotopic xenografts confirmed reduced tumor growth and CD44 expression in vivo. Analyses of TCGA and CGGA datasets revealed that the mesenchymal GBM subtype (MES-GBM), linked with poor outcomes, exhibits elevated EMT gene expression. Treatment of MES-like LN229 cells with Abemaciclib resulted in decreased phosphorylation of GSK3 $\beta$  and reductions in EMT-related gene expression. Our findings highlight a novel EMT-suppressive action of Abemaciclib, illustrating its therapeutic potential for targeting the CSCs and for treating the MES-GBM. This research provides mechanistic insights and justification for repurposing Abemaciclib as targeted therapies for aggressive glioblastoma.

## 25COASOCT51

### **Title: BCL-xL dependency in chromophobe renal cell carcinoma**

Nadine Mahmoud, Xingping Qin, Wafaa Bzeih et.al.

Cancer Gene Therapy volume 32, pages1133–1143 (2025)

<https://doi.org/10.1038/s41417-025-00953-1>

**Abstract:** Chromophobe renal cell carcinoma (ChRCC) is the third most common subtype of kidney cancer, with limited therapeutic options. Using BH3 profiling to screen ChRCC-derived cell lines, we discovered that BH3 peptides targeting BCL-xL promote apoptosis in ChRCC. Downregulation of BCL2L1 is sufficient to induce apoptosis in ChRCC-derived cells, consistent with our screening results. BCL2L1, encoding BCL-xL, is fourfold upregulated in ChRCC compared to normal kidney and has the second highest expression in The Cancer Genome Atlas. BCL2L1 downregulation enhances MCL-1 expression, suggesting a possible compensatory role for MCL-1. Based on these results, we evaluated two BH3 mimetics, A-1331852 (targeting BCL-xL) and S63845 (targeting MCL-1). Their combination resulted in 80% cell death. DT2216, a proteolysis-targeting chimera (PROTAC) that targets BCL-xL for degradation, induced cleaved PARP and caspase 3, indicators of apoptosis. ChRCC cells are known to be highly sensitive to ferroptosis. We combined A-1331852 and S63845 with IKE or RSL3 (ferroptosis-inducing drugs). BCL-xL and MCL-1 inhibition enhanced the susceptibility to ferroptosis, suggesting a link between apoptosis and ferroptosis in ChRCC. These data indicate that BCL-xL maintains ChRCC cell survival by suppressing apoptosis. The BCL-xL-specific PROTAC DT2216, currently in clinical trials, may provide an opportunity for ChRCC therapy.

**25COASOCT52****Title: Avelumab combined with axitinib for patients with advanced thymoma B3 and thymic carcinoma**

Fabio Conforti, Laura Pala, Chiara Catania et.al.

Cancer, Volume131, Issue18, 2025

<https://doi.org/10.1002/cncr.70092>

**Abstract:** Introduction: Patients with advanced thymoma B3 (TB3) and thymic carcinoma (TC) resistant to chemotherapy have limited treatment options. The final overall survival (OS) results of the CAVEATT trial are presented. Methods: The CAVEATT was a single-arm, multicentric, phase II trial testing the combination of avelumab (anti-PD-L1) and axitinib (antiangiogenesis) in patients with advanced TB3 or TC, who had progressed after at least one line of platinum-based chemotherapy. Patients could have received prior antiangiogenesis drugs but not immune checkpoint inhibitors. Results: Thirty-two patients were enrolled: 27 had TC, 3 TB3, and 2 a mixed TB3/TC. Most (91%, 29/32) had Stage IVB disease, and 41% (13/32) had prior antiangiogenesis treatment. After a median follow-up for overall survival (OS) of 48.9 months (range, 2.5–61.1), 23 deaths occurred. Median OS was 23.4 months (95% CI, 16.5–31.1), with 12- and 24-month OS rates of 77.7% (95% CI, 58.8–88.7) and 48.5% (95% CI, 30.3–64.6), respectively. No significant OS differences emerged across most subgroups, except for patients without liver metastases (OS hazard ratio [OS-HR], 0.39; 95% CI, 0.17–0.89) and lower lactate dehydrogenase levels (OS-HR, 0.25; 95% CI, 0.10–0.65), who had significantly longer survival compared to patients with liver metastases and with higher lactate dehydrogenase levels, respectively. Conclusions: The combination of avelumab and axitinib demonstrated long-term efficacy in heavily pretreated patients with TC and TB3. This finding underscores the meaningful impact of immune checkpoint inhibitors and antiangiogenesis drugs on the prognosis of this patient population.

**25COASOCT53****Title: Determinants of geographic variation in the incidence of adult nonmalignant meningioma in the United States, 2010–2019**

Diana R. Withrow PhD, Joseph Boyle PhD, Martha S. Linet MD et.al.

Cancer, Volume131, Issue18, 2025

<https://doi.org/10.1002/cncr.70042>

**Abstract:** US incidence rates of nonmalignant brain tumors are 3-fold higher in highest versus lowest incidence states. A county-level analysis was conducted to assess whether geographic variation in nonmalignant meningioma (NMM) incidence is related to demographics, cancer registry, health care, and other factors. Methods: Age-adjusted incidence rates of NMM in US counties during 2010–2019 were modeled with data from the Central Brain Tumor Registry of the United States. Demographic, geographic, cancer registry, environmental, health care, health, lifestyle, and socioeconomic factors at the county level were drawn from numerous data sources. Bayesian index regression models were fit containing spatial random effects. Results: Three domains were significantly associated with rates of NMM at the county level: cancer registry practices (funding source and % radiographically confirmed), socioeconomic status index (higher levels with percent working in white-collar occupations as an important contributor), and demographics (% Black and % female). No associations were observed for general health or environmental factors. In the



fully adjusted model, the number of counties with significantly elevated and lowered spatial random effects decreased by 33% and 28%, respectively, compared to a no-covariate model. **Conclusions:** Although general health and environmental factors cannot be ruled out in explaining the geographic variation in NMM incidence rates, results suggest that socioeconomic factors, certain demographic characteristics, and cancer diagnosis and registry practices may all play a significant role in driving such variation. These results may have implications for other tumor types diagnosed primarily radiographically or outside hospital settings, where variation in detection and reporting may affect incidence rates.

## 25COASOCT54

### **Title: The utility of artificial intelligence in gastrointestinal oncology: A systematic review of randomized controlled trials**

Luke E. Sorensen MD, Vanessa A. Moore BS, Jared L. Gregston BS et.al.

Cancer, Volume131, Issue18, 2025

<https://doi.org/10.1002/cncr.70043>

**Abstract:** In the field of gastrointestinal oncology, the development of novel artificial intelligence (AI) processes may help with multiple aspects of cancer care delivery. However, a comprehensive understanding of the current utility of AI in gastrointestinal oncology is lacking. The authors conducted searches in the following databases: MEDLINE (Ovid), Embase (Ovid), and CINAHL (Cumulative Index of Nursing and Allied Health) Ultimate (EBSCO). The analysis focused on publication trends and outcomes of randomized controlled trials (RCTs) that used AI to manage gastrointestinal malignancies. From our initial search retrieval of 3730 studies, 27 RCTs (with a total of 29,895 patients) were identified that met inclusion criteria. The first RCT was published in 2019, followed by five in 2020, four in 2021, six in 2022, and 11 in 2023. Colorectal malignancies comprised the majority of the literature (23 of 27 studies; 85%), with other studies focused on gastric cancer (three of 27 studies; 11%) and hepatocellular carcinoma (one of 27 studies; 4%). Of the included RCTs, 25 (93%) had a primary outcome focused on lesion/cancer detection throughout the gastrointestinal tract using endoscopy or ultrasound, with others focused on algorithmic-based AI assistance with postoperative pain management or histologic diagnosis. Overall, 22 of 27 studies (81%) met their primary end point with a statistically significant result. In this systematic review, the authors observed a recent increase in the number of RCTs focused on AI within the field of gastrointestinal oncology and identified specific areas in which AI is being used. Findings from this work should help to inform further investigations to develop and test innovative AI uses, enhance care delivery, and improve patient outcomes.

## 25COASOCT55

### **Title: Preoperative intensity-modulated radiation therapy in lower extremity soft tissue sarcomas with and without dose avoidance of uninvolved skin/subcutaneous tissue**

Siyer Roohani MD, Anthony M. Griffin MSc, Zhihui Amy Liu PhD et.al.

Cancer, Volume131, Issue18, 2025

<https://doi.org/10.1002/cncr.70049>

**Abstract:** The objective of this study was to evaluate whether dosimetric sparing of uninvolved normal tissues, including skin/subcutaneous flaps, affects acute and late toxicities in preoperative image-guided intensity-modulated radiation therapy (IG-IMRT) for lower



extremity soft tissue sarcomas (LE-STS).Methods: Patients with LE-STS from a phase 2 preoperative IG-IMRT trial (flap-sparing-IMRT, 2005–2009) and a prospectively maintained institutional database (standard-IMRT, 2005–2020) were propensity matched by age, sex, tumor size, grade, location, wound closure, and interval from IG-IMRT to surgery; all received 50 Gy in 25 fractions preoperatively. The primary outcome was major wound complication (MWC). Secondary outcomes were late Radiation Therapy Oncology Group toxicities, functional scores (Toronto Extremity Salvage Score [TESS]; Musculoskeletal Tumor Society scales [MSTS-87 or MSTS-93]), and oncologic outcomes. Kaplan–Meier estimates, cumulative incidence functions, and linear, logistic, and Cox regression were used, as appropriate.Results: Fifty-five patients who received flap-sparing-IMRT were 1:5 matched to 275 patients who received standard-IMRT (median follow-up, 104 vs. 56 months, respectively). Regression analyses identified no significant association between treatment technique and MWCs (29% vs. 27%; odds ratio, 0.92;  $p = .77$ ), late grade 2 or greater toxicities: subcutaneous fibrosis (15% vs. 8%), joint stiffness (5% vs. 2%), edema (11% vs. 10%), fracture (2% vs. 4%), or functional outcomes (TESS, 87 vs. 89; MSTS-87, 33 vs. 33; and MSTS-93, 93 vs. 97; all  $p > .1$ ). Five-year overall survival (83.6% vs. 75.2%), disease-free survival (65.5% vs. 64.1%), local recurrence (5.2% vs. 7.3%), distant metastasis (29.1% vs. 30.1%) were also comparable ( $p > .1$ ).Conclusions: Flap-sparing-IMRT with specific avoidance of uninvolved skin/subcutaneous tissues demonstrated minimal differences in MWCs, late toxicity, and functional and oncologic outcomes compared with standard-IMRT in patients with LE-STS.

## 25COASOCT56

### **Title: Clinical and biological factors associated with response to immune checkpoint inhibitors in advanced sarcomas: IMPRESARC, a French retrospective multicenter cohort study**

Mina Fazel MD, Romain Varnier MD, H  l  ne Vanacker MD et.al.

Cancer, Volume131, Issue18, 2025

<https://doi.org/10.1002/cncr.70052>

**Abstract:** Immune checkpoint inhibitors (ICIs) in unselected sarcomas yield limited response rates and tumor control. Long-term responders have however been reported, suggesting a critical challenge in refining patient selection, by identifying reliable predictive factors for response.Methods: The authors conducted a multicenter, retrospective study of patients with advanced sarcomas treated with ICIs in six French reference sarcoma centers. The study assessed efficacy and safety, as well as clinical and biological variables associated with objective response rate (ORR), progression-free survival (PFS), and overall survival (OS).Results: A total of 272 patients were included in the analysis. The ORR was 17%, with 16% partial responses and 1% complete responses. Stable disease (SD) occurred in 33% of patients, resulting in a disease control rate of 49%. Median PFS was 2.7 months (95% confidence interval [CI], 2.5–3.4), with 28% of patients showing PFS >6 months and 13% with PFS >12 months. Median OS was 13.5 months (95% CI, 11.0–17.3). The safety profile was consistent with that of clinical trials, with 5% of patients experiencing grade  $\geq 3$  adverse events and 10% discontinuing treatment due to toxicity. Poorer outcomes were associated with high Eastern Cooperative Oncology Group performance status ( $\geq 1$ ), cyclophosphamide coadministration, and high derived neutrophil-to-lymphocyte ratio. Anti-programmed death-

ligand 1 (PD-L1) therapies were associated with shorter OS compared to anti-PD-1. Histotypes such as alveolar soft part sarcoma (ASPS) had better survival, whereas dedifferentiated liposarcoma had poorer outcomes. Conclusions: Despite a short median PFS, certain histological subtypes, including ASPS, chordomas, SMARCA4-deficient tumors, gastro-intestinal stromal tumor, and NF1 mutations, showed strong activity signals, indicating long-term responses in some patients.

## 25COASOCT57

### **Title: Association of patient and physician characteristics with androgen-deprivation-therapy intensification in patients with de novo hormone-sensitive metastatic prostate cancer: A population-based study**

David-Dan Nguyen MDCM MPH, Raj Satkunasivam MD MS, Khatereh Aminoltehari MD MSc et.al.

Cancer, Volume131, Issue18, 2025

<https://doi.org/10.1002/cncr.70070>

**Abstract:** Introduction: Treatment intensification with androgen receptor signaling inhibitors and/or chemotherapy is guideline recommended for patients with de novo metastatic hormone-sensitive prostate cancer (mHSPC). However, most patients only receive androgen deprivation therapy monotherapy. The aim was to identify physician-, patient-, and tumor-related factors associated with the receipt of treatment intensification. Methods: A population-based cohort study was conducted in Ontario, Canada, which included men  $\geq 66$  years newly diagnosed with de novo mHSPC between January 2014 and December 2022. Hierarchical regression modeling was used to examine the association of physician, patient, and tumor characteristics with the receipt of treatment intensification, defined as the initiation of an androgen receptor signaling inhibitor, docetaxel, or both within six months of diagnosis. Darlington's method was used to assess predictor importance via standardized regression coefficients (SRC). Results: Among 6099 eligible older men newly diagnosed with de novo mHSPC, 1475 (24.2%) received treatment intensification. In multivariable modeling, patients initiated on androgen deprivation therapy by radiation oncologists were less likely to receive treatment intensification (odds ratio [OR]. 0.48; 95% CI, 0.37–0.61;  $p < .01$ ; SRC: 19.46;  $p < .01$ ) whereas those by medical oncologists were more likely to receive treatment intensification (OR, 1.64; 95% CI, 1.21–2.22;  $p < .01$ ; SRC: 9.56;  $p < .01$ ), each compared to urologists. Older patients were significantly less likely to receive treatment intensification (OR 0.94 per year over age 66; 95% CI, 0.93–0.95;  $p < .01$ ; SRC: –36.21;  $p < .01$ ). Conclusion: Patient and physician characteristics significantly influence variation in the use of treatment intensification for de novo mHSPC. These findings inform targeted interventions and policies to enhance the delivery of life-prolonging mHSPC care.

## 25COASOCT58

### **Title: Sexual health among Danish cancer survivors and individuals with no history of cancer: Baseline findings from the nationwide Project SEXUS cohort study**

Cecilie H. Madsen MD, Christian Graugaard MD, PhD, Susanne O. Dalton MD et.al.

Cancer, Volume131, Issue18, 2025

<https://doi.org/10.1002/cncr.70074>

**Abstract:** Introduction: Being diagnosed with and treated for cancer often results in physical

symptoms and psychosocial distress that may affect sexual health. This population-based study in Denmark aimed to compare the sexual health of cancer survivors across multiple cancer sites with that of individuals with no history of cancer. **Methods:** Data were used from 4085 cancer survivors and 58,590 individuals without cancer aged 15 to 89 years, who participated in the nationally representative Project SEXUS cohort study. Prevalence estimates for sexual outcomes were calculated, and logistic regression analyses yielded confounder-adjusted odds ratios (aORs) with 95% confidence intervals (CIs) for associations of cancer survivorship with sexual outcomes, both overall and across cancer sites. **Results:** Cancer survivors experienced significantly more sexual challenges than individuals without cancer, both overall and in the first 5 years after their most recent cancer diagnosis. This difference was seen across multiple cancer sites and regardless of age at diagnosis (<60 vs. ≥60 years). Among several statistically significant findings, particularly high aORs were noted for dissatisfaction with breast appearance (aOR: 1.89; CI, 1.49–2.41) and genital pain dysfunction (aOR: 1.74; CI, 1.32–2.28) among women and lack of sexual needs (aOR: 1.93; CI, 1.61–2.30) and erectile dysfunction (aOR: 2.79; CI, 2.30–3.38) among men. **Conclusion:** Compared to individuals with no history of cancer, sexual health was significantly affected among cancer survivors of both sexes and across cancer sites, time since diagnosis, and age at diagnosis. Health care professionals should recognize and routinely address the sexual challenges experienced by cancer survivors to enhance their biopsychosocial recovery.

## 25COASOCT59

### **Title: The 3P-CP model: Expanding our conceptualization of cancer pain**

Desiree R. Azizoddin PsyD, Jian Zhao PhD, Tamara J. Somers PhD et.al.

Cancer, Volume131, Issue18, 2025

<https://doi.org/10.1002/cncr.70080>

**Abstract:** Cancer pain is a complex, multifactorial, and growing public health challenge affecting millions of Americans. Effective pain management is essential for comprehensive cancer care, influencing physical and mental health, quality of life, and functional ability. However, progress in cancer pain management is hindered by the complexity of the issue and a fragmented understanding of the myriad factors shaping the pain experience. Additionally, traditional pain terminology—“acute” (<6 months) and “chronic” pain (≥6 months)—offers limited utility in cancer contexts, highlighting the need for a more nuanced framework. To address this gap, we propose the 3P-CP model, which conceptualizes cancer pain through three interconnected phases: predisposing factors that increase cancer pain risk, precipitating factors that trigger cancer pain onset, and perpetuating factors that sustain or exacerbate cancer pain over time. This model provides a structured approach to assess the dynamic nature of cancer pain across the entirety of the cancer trajectory. In this paper, key factors associated with each phase of the 3P-CP model are outlined and their implications for research and clinical care explored. Aligning with the oncology field's shift toward precision medicine, the 3P-CP model has the potential to guide comprehensive assessment, risk mitigation, prevention, and intervention strategies—supporting efforts to deliver the right targeted and tailored treatments, to the right patients, at the right time.

## 25COASOCT60

### **Title: Meta-analysis evaluating the efficacy and safety of various Bruton tyrosine kinase**

**(BTK) inhibitors for central nervous system lymphoma: Novel covalent BTK inhibitors, except for ibrutinib, also demonstrate good efficacy in the treatment of primary central nervous system lymphoma**

Shuai Tan MD, PhD, Huizhen He MS, Jing Ni MD, PhD et.al.

Cancer, Volume131, Issue18, 2025

<https://doi.org/10.1002/cncr.70083>

**Abstract:** Central nervous system lymphoma (CNSL) is aggressive, and treatment with Bruton tyrosine kinase (BTK) inhibitors (BTKis) plays a key role. For this systematic review and meta-analysis, the authors evaluated BTKis for the treatment of primary CNSL (PCNSL) and secondary CNSL (SCNSL). **Methods:** By May 1, 2025, the authors conducted a systematic search of databases, including PubMed, EMBASE, etc. Included studies were those that investigated BTKi-treated CNSL and analyzed the overall response rate (ORR) as well as the complete response (CR) and partial response (PR) rates using systematic review and meta-analysis software. **Results:** Forty studies (935 patients) were included in the meta-analysis. The pooled ORR and CR and PR rates were 73%, 49%, and 28%, respectively. The pooled ORR and CR rates for BTKi monotherapy were 60% and 34%, respectively; whereas the rates for BTKi plus chemotherapy or immunochemotherapy were 79% and 55%, respectively. For PCNSL, the pooled ORR and PR rates were 73% and 49%, respectively. For SCNSL, the pooled ORR and CR rates reached 75% and 53%, respectively. Among patients with PCNSL, zanubrutinib achieved pooled ORR and CR rates of 85% and 54%, respectively. Ibrutinib had pooled ORR and CR rates of 67% and 46%, respectively; whereas orelabrutinib demonstrated pooled ORR and CR rates of 70% and 59%, respectively. For SCNSL, zanubrutinib achieved pooled ORR and CR rates of 77% and 62%, respectively; whereas ibrutinib achieved rates of 72% and 54%, respectively. Hematologic toxicities and transaminase increases were grade 3–5 toxicities according to common toxicity criteria. **Conclusions:** The combination of BTKis with traditional chemotherapy or immunochemotherapy offers superior response rates compared with BTKis alone, and the safety profile is acceptable. Efficacy varies by BTKi type and should be selected based on patient condition. Specifically, for PCNSL, the response rates of zanubrutinib and obinutuzumab are better; for SCNSL, there is a minimal difference in efficacy among the various BTKis; and, overall, regardless of whether it is PCNSL or SCNSL, the off-target effects and side effects of covalent BTKis (zanubrutinib, obinutuzumab), except for ibrutinib, have improved.

**25COASOCT61****Title: Influence of biologic sex and obesity on liver recurrence and survival in patients undergoing upfront surgery for pancreatic adenocarcinoma**

Sean J. Judge MD, Emily Manin MD, Joanne Chou MPH et.al.

Cancer, Volume131, Issue18, 2025

<https://doi.org/10.1002/cncr.70088>

**Abstract:** The influence of obesity and sex on outcomes in pancreatic adenocarcinoma (PDAC) remains unclear. The association between obesity (body mass index [BMI],  $\geq 30$ ) and biologic sex (male or female) for outcomes in patients with PDAC undergoing a surgery-first approach was investigated. **Methods:** A prospectively maintained pancreatic cancer database at the Memorial Sloan Kettering Cancer Center was queried to identify all patients

undergoing surgery with a pathologic diagnosis of PDAC. Clinicodemographic variables, outcomes, and tumor mutational analyses for all available patients were collected. Cumulative incidence of first recurrence involving the liver was estimated via a cumulative incidence function. Multivariable Cox regression was used to investigate the association between BMI and sex for overall survival. Results: From 2012 to 2022, 939 patients were identified who underwent surgery with a final pathologic diagnosis of PDAC. Median age was 70 years, 52% were male, and 24% were obese (BMI,  $\geq 30$ ). When dichotomized by sex and obesity status (BMI,  $<30$  or  $\geq 30$ ), females with obesity had the lowest cumulative incidence of liver recurrence at 12 and 24 months postsurgery compared to all other groups (13% [95% CI, 7.2%–20%] and 15% [8.7%–23%], respectively). Females with obesity had the longest median overall survival at 37 months. Conclusions: After curative surgery for pancreatic cancer, females with obesity have a significantly lower rate of liver recurrence and the longest median overall survival. This does not appear to be related to surgical quality, receipt of adjuvant therapy, or tumor mutational profile. Investigation into host immune, metabolic, and hormonal parameters is paramount to understanding these differences.

## 25COASOCT62

**Title: The impact of opioid use associated with curative-intent cancer surgery on safe opioid prescribing practice among veterans: An observational study**

Marilyn M. Schapira MD, MPH, Sumedha Chhatre PhD, Patience M. Dow PhD et.al.

Cancer, Volume 131, Issue 18, 2025

<https://doi.org/10.1002/cncr.70009>

**Abstract:** Opioid exposure during cancer therapy may increase long-term unsafe opioid prescribing. This study sought to determine the rates of coprescription of benzodiazepine and opioid medications and new persistent opioid use after surgical treatment of early-stage cancer. Methods: A retrospective cohort study was conducted among a US veteran population via the Veterans Affairs Corporate Data Warehouse database. Participants were opioid-naïve persons aged  $\geq 21$  years with a new diagnosis of stage 0–III cancer between January 1, 2015, and December 31, 2016. Outcomes were days of coprescription of benzodiazepines and opioids in the 13 months posttreatment and new persistent opioid use. The exposure was total morphine milligram equivalents (MMEs) attributed to treatment and prescribed from 30 days before through 14 days after the index surgical procedure. Results: Among 9213 veterans, coprescription of benzodiazepines and opioids occurred in 366 patients (4.0%) and new persistent opioid use in 981 patients (10.6%). In a linear model adjusting for patient, clinical, and geographic factors, persons in the highest quartile compared to no opioid exposure had increased days with coprescription of benzodiazepines and opioids (mean difference, 1.0; 95% CI, 0.3–1.7). In a discrete time survival analysis, persons in the highest quartile of MME exposure compared to none had a greater risk of new persistent opioid use (hazard ratio, 1.6; 95% CI, 1.3–1.9). Conclusions: More than one of 10 opioid-naïve veterans undergoing curative-intent surgical treatment for cancer developed new persistent opioid use. Optimizing cancer treatment pain management strategies to mitigate long-term opioid-related health risks is crucial.

## 25COASOCT63

**Title: HSV-1 hijacks mitochondrial dynamics: potential molecular mechanisms linking**



**viral infection to neurodegenerative disorders**

Siping Kuang, Zhiyang He, Jingjing Zhang et.al.

Apoptosis, Volume 30, pages 1913–1930, (2025)

<https://doi.org/10.1007/s10495-025-02142-9>

**Abstract:** Herpes simplex virus type 1 (HSV-1), a neurotropic virus, hijacks the critical neuronal organelle—mitochondria—to establish lifelong latent infection and potentially accelerate neurodegenerative pathologies. Research indicates that HSV-1 infection disrupts mitochondrial dynamics, impairs its bioenergetic function, and compromises interorganellar communication. This disruption is primarily achieved through the degradation of mitochondrial DNA (mtDNA) and the functional alteration of key proteins, leading to excessive production of reactive oxygen species (ROS), intracellular calcium dysregulation, and abnormal energy metabolism. These alterations not only diminish cellular energy production and exacerbate oxidative damage but also readily trigger neuronal cell death. Crucially, the virus specifically interferes with mitochondrial-endoplasmic reticulum contact sites (MERCs) to evade immune surveillance while simultaneously promoting its own replication. In severe encephalitis, mitochondrial damage is closely associated with neuroinflammation. For Alzheimer's disease (AD), HSV-1 may synergize with amyloid-beta pathology through ROS and viral proteins (such as glycoprotein B (gB) and glycoprotein I (gI)), exacerbating disease progression. Paradoxically, HSV-1 also inhibits immediate cell death to sustain host cell survival, facilitating latent viral reactivation. Research elucidating how the virus exploits mitochondria for pathogenesis suggests that future therapeutic strategies could combine classical antiviral drugs with agents that protect mitochondrial function (e.g., antioxidants). This combined approach holds promise for combating acute infection and potentially mitigating the progression of associated neurodegenerative diseases.

**25COASOCT64****Title: Exploiting autophagy and related pathways: pioneering new horizons in cataract therapy**

Mehrdad Hashemi, Pezhman Shafiei Asheghabadi, Mahdi Moassesfar et.al.

Apoptosis, Volume 30, pages 1931–1960, (2025)

<https://doi.org/10.1007/s10495-025-02134-9>

**Abstract:** Autophagy is a critical catabolic pathway that facilitates the degradation of intracellular components through lysosomal activity, originally recognized for its role in nutrient recycling during starvation. Recent research has expanded our understanding of autophagy, revealing its involvement in various physiological processes essential for cellular, tissue, and organismal homeostasis. Dysregulation of autophagy has been linked to numerous diseases, including ocular conditions such as cataracts. In human lens fibers, autophagic vesicles containing mitochondria or mitochondrial fragments have been identified, underscoring the importance of autophagy in maintaining lens integrity and transparency. Disruptions in organelle elimination can lead to increased reactive oxygen species (ROS), altering lens homeostasis and contributing to cataract formation. Recent studies have highlighted the complex interplay between autophagy and lens epithelial cells (LECs) in both age-related and diabetic cataract development. In age-related cataracts, increased autophagic activity coincides with elevated apoptosis in LECs, suggesting a bidirectional regulatory role of autophagy in cellular senescence. Additionally, the degradation of SQSTM1/p62 during



oxidative stress implicates autophagy in the apoptotic processes associated with senile cataracts. In diabetic cataracts, high glucose levels disrupt the relationship between autophagy and epithelial-mesenchymal transition (EMT) in LECs via the Notch signaling pathway, leading to impaired autophagic function and subsequent cataractogenesis. These findings indicate that autophagy dysregulation is a significant contributor to the pathophysiology of various cataract types. Future research should focus on exploring the therapeutic potential of modulating autophagy to prevent or treat cataracts, investigating specific signaling pathways involved, and identifying biomarkers for early detection. By elucidating the molecular mechanisms underlying autophagy's role in cataract formation, novel targeted therapies may emerge, providing hope for improved management and prevention of this prevalent ocular pathology.

## 25COASOCT65

### **Title: Disrupting membranes, controlling cell fate: the role of pore-forming proteins in cell death and therapy**

Sonia Iranpour, Maryam Arif & Eva Szegezdi

Apoptosis, Volume 30, pages 1961–1988, (2025)

<https://doi.org/10.1007/s10495-025-02133-w>

**Abstract:** Pore-forming proteins (PFPs), characterized by their ability to form pores or disrupt membranes are now recognized as key executioners of cell death, either as effectors of the immune system (non-cell-autonomous function), or of regulated cell death programs (cell autonomous function). To perforate membranes, most PFPs transition from water-soluble monomers or oligomers into multimeric and often supramolecular complexes, a process achieved via substantial structural transition of the PFP. Although they share the general ability to perforate cellular or intracellular membranes, PFPs differ in their membrane-binding preferences, the structural and functional characteristics of the pores they form (such as pore size, pore structure and ability to trigger membrane rupture) and the cell death mechanism they induce or execute. Herein, we review the specific traits of all key human PFPs, including their membrane specificity, regulation of their activity and the structure of the membrane pores they form, followed by insights into the therapeutic potential of PFPs and harnessing their abilities for cancer therapy.

## 25COASOCT66

### **Title: Targeting pyroptosis in myocardial inflammation and fibrosis: molecular mechanisms and therapeutic strategies**

Yixiang Hu, Ying Huang, Jincai Guo et.al.

Apoptosis, Volume 30, pages 1989–2007, (2025)

<https://doi.org/10.1007/s10495-025-02151-8>

**Abstract:** Pyroptosis is an inflammatory form of programmed cell death (PCD), driven by the activation of inflammasomes and inflammatory caspases. These molecular events trigger the proteolytic cleavage of gasdermin proteins, leading to membrane pores formation, cell lysis, and the subsequent release of cellular contents. Induction of pyroptosis amplifies inflammation, contributing to severe inflammatory responses and accelerating the pathogenesis of various chronic inflammation-related diseases. Myocardial fibrosis (MF) is characterized by the deposition of scar tissue in the heart, stemming from an aberrant wound

healing response to inflammatory damage. It is a prevalent pathological feature in a range of cardiovascular diseases. Given the complex nature of wound repair and fibrosis following myocardial injury, treatments that target only specific contributors to disease pathogenesis show limited efficacy in mitigating fibrosis. While significant progress has been made in understanding the mechanisms underlying pyroptosis, its regulatory processes in MF remain incompletely understood, and strategies to improve clinical outcomes are still lacking. This review provides an in-depth examination of the latest insights into the regulatory mechanisms of pyroptosis, newly identified influencing factors, and its role in myocardial inflammation and fibrosis. Additionally, we discuss potential anti-fibrotic therapies targeting pyroptosis for the management of MF, highlighting challenges and future directions in this field.

## 25COASOCT67

### **Title: Precision Synthesis of Polyrotaxanes Using Cascade Metathesis Polymerization**

Jiaqi Han, Seung Eun Choi, Xin Jiang et.al.

J. Am. Chem. Soc. 2025, 147, 39, 35871–35880

<https://doi.org/10.1021/jacs.5c09098>

**Abstract:** Mechanically interlocked polymers (MIPs), such as polyrotaxanes (PRs) and polycatenanes, represent intriguing synthetic macromolecules distinguished by their unique architectures and topology. These MIPs, characterized by their mechanical bonds and movable component parts, have been extensively utilized across various contemporary fields of chemistry, presenting opportunities for the design of functional materials with enhanced mechanical properties. However, the precision synthesis of MIPs, specifically PRs, with controlled molecular weights and narrow dispersity remains a significant challenge, hindering the progression of well-defined mechanically interlocked materials that exhibit a clear structure–property relationship. Herein, we disclose the controlled chain-growth synthesis of main-chain PRs through cascade metathesis polymerization by employing a catenane-based monomer. A series of PRs with targeted molecular weights, narrow dispersities, and tunable mechanical properties was successfully prepared by adjusting the monomer-to-catalyst feed ratio. The “livingness” of this polymerization was validated through kinetic studies, and the detailed structural characteristics of the synthesized PRs were supported by <sup>1</sup>H NMR spectroscopy and mass spectrometry. Both block and statistical copolymers were produced in a controlled manner through the copolymerization of the catenane-based monomer with other monomers that can undergo ring-opening metathesis polymerization (ROMP), allowing for easy access to PRs featuring different architectures and, most importantly, tunable ring densities. This work significantly advances beyond the majority of previously reported studies concerning the controlled synthesis of PRs, paving the way for the rational design and synthesis of mechanically interlocked materials with desired functionalities.

## 25COASOCT68

### **Title: Targeting ASK1 signaling in neurodegeneration: molecular insights and therapeutic promise**

Nasreen Sulthana, Piyush Mittal, Ahsas Goyal et.al.

Apoptosis, Volume 30, pages 2019–2041, (2025)

<https://doi.org/10.1007/s10495-025-02148-3>

**Abstract:** Apoptosis signal-regulating kinase 1 (ASK1), a redox-sensitive member of the

mitogen-activated protein kinase kinase kinase (MAP3K) family, is a master regulator of neuronal apoptosis as well as neuroinflammation in neurodegenerative disorders (NDs). Under oxidative and endoplasmic reticulum stress conditions, ASK1 sets off a series of pathways, ultimately leading to impairment of cellular functions and the cell's demise. The comprehensive review focuses on the diverse contributions of ASK1 to neurodegeneration driven by Alzheimer's disease (AD), Parkinson's disease (PD), Huntington's disease (HD), amyotrophic lateral sclerosis (ALS), and multiple sclerosis (MS). Human and animal evidence links dysregulated ASK1 signaling is related to amyloid deposition, tau hyperphosphorylation, neuroinflammation, abnormal protein folding, and subsequent neurodegeneration. ASK1 plays a role in tau hyperphosphorylation and amyloid-beta-induced neurotoxicity in AD. ASK1-mediated apoptosis of dopaminergic neurons caused by oxidative stress and aggregation of  $\alpha$ -synuclein contributes to PD. Furthermore, ASK1 activation is associated with motor neuron degeneration in ALS related to endoplasmic reticulum stress caused by mutant SOD1. Moreover, the pathogenesis of HD involves the activation of ASK1 by the cellular stress caused by mutant huntingtin protein. ASK1 signaling potentiates inflammatory signals in MS because it is involved in demyelination and neuronal injury. Nonetheless, obstacles persist such as developing brain-targeted therapies, reducing adverse systemic effects, and defining disease-stage-specific functions of ASK1. This review aims to comprehensively examine the role of ASK1 signaling in major NDs, discuss its upstream and downstream regulatory mechanisms, and evaluate the current and emerging therapeutic strategies targeting ASK1.

## 25COASOCT69

### **Title: Mitochondrial bioenergetics and networks in melanoma: an update**

Gaia Giannitti, Alyssa Julia Jennifer Paganoni, Sara Marchesi et.al.

Apoptosis, Volume 30, pages 2042–2056, (2025)

<https://doi.org/10.1007/s10495-025-02155-4>

**Abstract:** Melanoma is the most aggressive and deadly form of skin cancer. However, advances in the understanding of its biology have led to the development of several new therapeutic approaches. One of these novel treatment strategies is based on the targeting of the mitochondrial bioenergetic and networks responsible for tumor initiation and progression. Indeed, it has recently emerged that changes in mitochondrial metabolism, dynamics, redox homeostasis, and apoptosis are strictly associated with tumor growth, metastasis, and drug resistance. In this review, we summarize current evidence about the multiple biological functions exerted by mitochondria in melanoma, also focusing on the role of these organelles as promising targets for pharmacological intervention.

## 25COASOCT70

### **Title: Pyroptosis: inflammatory cell death mechanism and its pathological roles in neurological diseases and injuries**

Haonan Ma, Yapei Zhu, Xuan Zhao et.al.

Apoptosis, Volume 30, pages 2057–2076, (2025)

<https://doi.org/10.1007/s10495-025-02160-7>

**Abstract:** Neurological disorders represent a major global public health challenge, causing significant impairments in motor, sensory, and cognitive functions. Among these disorders,

Alzheimer's disease, cerebrovascular diseases, and Parkinson's disease are notably prevalent. Despite their widespread impact, effective therapeutic interventions remain limited. Recently, pyroptosis—a highly pro-inflammatory form of programmed cell death characterized by cell swelling, membrane perforation, and the release of cellular contents—has gained considerable attention. While pyroptosis plays a crucial role in host defense against pathogen infections, its excessive activation can trigger sustained inflammatory responses and has been implicated in the pathogenesis and progression of various neurological disorders. This review provides an overview of pyroptosis, including its definition, key molecular components, and associated signaling pathways, while examining its mechanistic roles in neuroinflammation, neurological disorders, cerebrovascular diseases, and neural tumors. Additionally, it explores the influence of other systemic dysregulations on the development of neurological disorders. Research has demonstrated that pyroptosis drives the death of neurons and glial cells through inflammasome activation and the Caspase-Gasdermin pathway, thereby amplifying neuroinflammation and influencing disease progression. Notably, excessive pyroptosis activation exacerbates neural damage in conditions such as Alzheimer's disease, Parkinson's disease, and ischemic brain injury. Consequently, targeting pyroptosis signaling pathways may present promising therapeutic strategies for neurological disorders. This review consolidates recent advancements in the field, offering valuable insights for the development of effective interventions.

## 25COASOCT71

### **Title: Emerging role of RNA m6A modifications in laryngeal squamous cell carcinoma: insights into tumorigenesis and therapeutic potential**

Guotong Zheng, Jing Bi, Yangyan Yan et.al.

Apoptosis, Volume 30, pages 2077–2089, (2025)

<https://doi.org/10.1007/s10495-025-02159-0>

**Abstract:** Laryngeal squamous cell carcinoma (LSCC) is one of the major malignant cancers worldwide. Emerging evidence has demonstrated that N6-methyladenosine (m6A) modification affects gene expression by regulating RNA metabolic processes, dynamically and reversibly regulated by its “writers”, “erasers” and “readers”. m6A modification plays an important role in the occurrence and development of various tumors. Recent studies have shown that m6A modifications are abnormally expressed in LSCC cells and tissues and participate in the malignant phenotypes of LSCC including cell proliferation, invasion, metastasis and chemotherapy resistance by mediating m6A regulators. This fundings may provide new directions for the molecular classification and targeted treatment of LSCC. In this review, we will focus on the molecular mechanism and potential clinical function of m6A modification in LSCC and emphasize its potential as a biomarker for the clinical diagnosis, prognosis, and treatment of LSCC.

## 25COASOCT72

### **Title: Emerging role of RNA m6A modifications in laryngeal squamous cell carcinoma: insights into tumorigenesis and therapeutic potential**

Guotong Zheng, Jing Bi, Yangyan Yan et.al.

Apoptosis, Volume 30, pages 2077–2089, (2025)

<https://doi.org/10.1007/s10495-025-02159-0>

**Abstract:** Laryngeal squamous cell carcinoma (LSCC) is one of the major malignant cancers worldwide. Emerging evidence has demonstrated that N6-methyladenosine (m6A) modification affects gene expression by regulating RNA metabolic processes, dynamically and reversibly regulated by its “writers”, “erasers” and “readers”. m6A modification plays an important role in the occurrence and development of various tumors. Recent studies have shown that m6A modifications are abnormally expressed in LSCC cells and tissues and participate in the malignant phenotypes of LSCC including cell proliferation, invasion, metastasis and chemotherapy resistance by mediating m6A regulators. This fundings may provide new directions for the molecular classification and targeted treatment of LSCC. In this review, we will focus on the molecular mechanism and potential clinical function of m6A modification in LSCC and emphasize its potential as a biomarker for the clinical diagnosis, prognosis, and treatment of LSCC.

### 25COASOCT73

**Title: Comprehensive analysis of regulated cell death pathways: intrinsic disorder, protein–protein interactions, and cross-pathway communication**

Oleksandr Sorokin, Frank Hause, Alice Wedler et.al.

Apoptosis, Volume 30, pages 2110–2162, (2025)

<https://doi.org/10.1007/s10495-025-02161-6>

**Abstract:** Regulated cell death (RCD) pathways—once viewed as linear, independent processes—are now recognized as components of a dynamic, interconnected molecular network that dictates cellular fate in health and disease. This study presents a systematic meta-analysis of thirteen major RCD pathways, examining their molecular mechanisms, triggers, and interconnections through protein–protein interaction (PPI) networks. Using custom bioinformatics approaches, we unveiled the interactome of proteins involved in apoptosis, autophagy-dependent cell death, cellular senescence, mitotic catastrophe, entotic cell death, ferroptosis, cuproptosis, immunogenic cell death, lysosome-dependent cell death, mitochondrial permeability transition-driven necrosis, necroptosis, neutrophil extracellular trap formation-related cell death (NETosis), parthanatos, and pyroptosis. By integrating data from an extensive literature review with STRING database analyses, we identified previously unrecognized cross-pathway interactions and regulatory nodes where special attention was given to the role of intrinsically disordered proteins (IDPs) in these pathways. Our findings reveal a complex interplay between different RCD mechanisms and highlight potential therapeutic targets for diseases characterized by dysregulated cell death programs, including cancer and autoimmune disorders. This comprehensive analysis provides new insights into the molecular architecture of RCD pathways and their cooperative functions in maintaining cellular homeostasis.

### 25COASOCT74

**Title: Targeting cuproptosis in liver cancer: Molecular mechanisms and therapeutic implications**

Yun-Fei Zhou, Yi-Wen Zhu, Meng-Yuan Hao et.al.

Apoptosis, Volume 30, pages 2163–2190, (2025)

<https://doi.org/10.1007/s10495-025-02150-9>

**Abstract:** Liver cancer (LC) stands as one of the most prevalent and highly malignant tumors

globally, with persistently elevated mortality rates. For advanced-stage LC, identifying efficacious treatment modalities remains a critical imperative. Cuproptosis, a newly identified form of regulated cell death, exhibits therapeutic potential for impeding LC progression. However, the current clinical evidence remains limited, meriting further in-depth investigation by researchers. Existing literature has summarized copper homeostasis, the molecular mechanisms of cuproptosis, and its roles in certain cancers. However, key challenges in clinical translation haven't been included in the research scope, such as the mechanistic complexity, poor targeting specificity, lack of mature biomarkers, and risk of therapeutic resistance. Notably, the lessons from failed clinical trials have not been fully integrated into ongoing investigations. This review systematically delineates cuproptosis-associated biomarkers in LC, critically analyzes the challenges of targeting cuproptosis for LC therapy and discusses potential solutions. By highlighting current research gaps, we aim to provide actionable research directions for future investigations.

## 25COASOCT75

### **Title: Research progress on programmed cell death of cardiomyocytes in pressure-overload hypertrophic cardiomyopathy**

Fei Xiao, Hui-Li Li, Jia-Rui Wang et.al.

Apoptosis, Volume 30, pages 2191–2224, (2025)

<https://doi.org/10.1007/s10495-025-02146-5>

**Abstract:** Pressure overload hypertrophic cardiomyopathy (PO-HCM), a prevalent cardiovascular condition, is characterized by the heart's adaptive response to chronic pressure overload. However, excessive pressure overload contributes to cardiomyocyte dysfunction and pathological hypertrophy. The pathological hallmarks of PO-HCM include the abnormal enlargement of cardiomyocytes (hypertrophy) and structural remodeling of myocardial tissue. The pathogenesis is multifaceted and involves hemodynamic alterations, imbalances in neurohumoral regulation, and intracellular signaling pathway abnormalities. Within this pathological context, programmed cell death is critically involved in cardiomyocytes. This review synthesizes current research on programmed cell death mechanisms in PO-HCM—including apoptosis, necroptosis, pyroptosis, autophagy, and ferroptosis—to inform translational research and guide future therapeutic development.

## 25COASOCT76

### **Title: Acute high-altitude hypoxia induced NLRP3 inflammasome activation in pulmonary artery smooth muscle cells by BMAL1 targeting mitochondrial VDAC1-mediated MtDNA leakage**

Si-Yuan He, Ying-Rui Bu, Jin Xu et.al.

Apoptosis, Volume 30, pages 2225–2237, (2025)

<https://doi.org/10.1007/s10495-025-02138-5>

**Abstract:** Hypoxia-induced inflammatory injury is an important pathological mechanism underlying the progression of acute mountain sickness (AMS). Recent studies reported that molecular clock could control mitochondrial pathways to involve hypoxic and inflammatory responses. Excessively released mitochondrial DNA (mtDNA) acts as a damage-associated molecular pattern (DAMP) to trigger inflammation in many diseases. Herein, we subjected mice at a simulated altitude of 5500 m for 3 days and found that the expression levels of



inflammatory cytokines were significantly increased in mouse pulmonary arteries, accompanied by mtDNA release and NLRP3 inflammasome activation in the pulmonary artery smooth muscle cells (PASMCs). RNA-sequencing and loss- and gain-of function experiments indicated that the core clock component BMAL1 regulated mtDNA leakage in PASMCs, and smooth muscle-specific Bmal1 knockout significantly alleviated the pulmonary arterial inflammation under acute high-altitude hypoxia. Mechanically, BMAL1 as a transcription factor directly promoted the transcriptional expression of Voltage-dependent anion channel 1 (VDAC1) and exacerbated the VDAC1-mediated mtDNA leakage under hypoxia, which activated NLRP3 inflammasome signaling in PASMCs and induced vascular inflammation. Our work provides mechanistic insights into the hypoxia-induced inflammation in PASMCs and may provide a novel therapeutic approaching for targeting BMAL1-VDAC1 in AMS.

## 25COASOCT77

### **Title: DNA damage repair inhibitors boost targeted radionuclide therapy and immunotherapy of prostate cancer**

Bin Xu, Lei Tao, Juan Sun et.al.

Apoptosis, Volume 30, pages 2238–2253, (2025)

<https://doi.org/10.1007/s10495-025-02136-7>

**Abstract:** Targeted radionuclide therapy (TRT) has emerged as a valuable treatment for metastatic castration-resistant prostate cancer (mCRPC) patients. The radioresistance coupled with heterogeneity and immunosuppressive tumor microenvironment of mCRPC, however, greatly restricts the clinical response and anticancer immunity. Here, we found that DNA damage repair inhibitors, in particular ATM inhibitor (ATMi), effectively boost TRT and immunotherapy of prostate cancer. ATMi significantly amplified TRT-induced DNA damage and immunogenic cell death in tumor cells, by impairing double-strand break repair and arresting cell cycle progression, which reshaped the tumor microenvironment and markedly improved tumor inhibition and survival rate in murine RM-1-hPSMA tumor model. Intriguingly, addition of  $\alpha$ CTLA-4 antibody further resulted in 71% mice complete regression. TRT in combination with ATMi and  $\alpha$ CTLA-4 appeared to boost adaptive and long-lasting anticancer immunity. Our results signify that ATM inhibitor not only sensitizes targeted radionuclide therapy but also effectively augments immune checkpoint inhibitor therapy.

## 25COASOCT78

### **Title: Aspirin-Inspired 6-O-Carboxymethyl-N-Acetylglucosamine: A potent antitumor agent with enhanced efficacy**

Ziwen Qiao, Guangmin Zhang, Xin Chen et.al.

Apoptosis, Volume 30, pages 2254–2268, (2025)

<https://doi.org/10.1007/s10495-025-02139-4>

**Abstract:** Aspirin, widely recognized for its anti-inflammatory and cardioprotective effects, has also shown potential as a cancer therapeutic. However, its clinical application is hindered by severe adverse effects. Here, we explore 6-O-Carboxymethyl-N-Acetylglucosamine (CM-NAG) a novel derivative of N-acetylglucosamine, designed to mimic the structural and functional properties of aspirin. CM-NAG significantly inhibits the viability of both

colorectal and pancreatic cancer cells. In colorectal cancer cells, CM-NAG also suppressed migration and invasion and induced apoptosis more effectively than aspirin. Mechanistically, CM-NAG upregulated phosphoenolpyruvate carboxykinase 2 (PCK2), a key regulator of gluconeogenesis in colorectal cancer cells. In a xenograft model, CM-NAG reduced tumor size and improved histopathological outcomes, while showing no significant toxicity in major organs. The expression of PCK2 in CRC tissues was significantly lower than in cancer-adjacent tissues, according immunohistochemistry analysis. Clinical analysis revealed high PCK2 expression in colorectal cancer tissues correlates with better disease-free survival, supporting PCK2 as a promising therapeutic target. These findings suggest that CM-NAG may represent a next-generation antitumor agent with enhanced efficacy and safety compared to aspirin, offering new prospects for cancer treatment.

## 25COASOCT79

### **Title: TSLP mitigates post-infarction myocardial remodeling by promoting eosinophil recruitment and inhibiting JAK1–STAT5-mediated ferroptosis**

Yunzhe Wang, Chenxi Cao, Tinglan Fu, et.al.

Apoptosis, Volume 30, pages 2269–2286, (2025)

<https://doi.org/10.1007/s10495-025-02137-6>

**Abstract:** Acute myocardial infarction (AMI) remains a leading cause of morbidity and mortality globally, often leading to heart failure due to excessive inflammation and fibrosis. Thymic stromal lymphopoietin (TSLP), a cytokine primarily involved in immune regulation, has recently been identified as a key player in cardiovascular health. However, its role in modulating inflammation and fibrosis after AMI is not fully understood. This study investigates how TSLP mediates anti-inflammatory effects and reduces fibrosis, ultimately improving heart function in a mouse model of AMI. We established a TSLP knockout mouse strain and performed left anterior descending (LAD) coronary artery ligation to create an AMI model. This was used to investigate the role of TSLP in eosinophil (EOS) recruitment and fibrosis alleviation. Additionally, EOS depletion, JAK-STAT pathway inhibition, and ferroptosis were employed to analyze potential mediating factors. The extent of cardiac tissue fibrosis was evaluated using histological staining. Inflammatory cytokine levels and EOS were assessed through ELISA and flow cytometry. Western blotting was conducted to detect proteins related to ferroptosis and the JAK-STAT pathway. TSLP deficiency significantly exacerbated myocardial remodeling in AMI mice, while TSLP treatment markedly reduced cardiac fibrosis following AMI, with a notable decrease in collagen deposition within the heart tissue. In Transwell assays, TSLP effectively recruited EOSs, and in vivo experiments demonstrated that TSLP promoted the resolution of acute-phase inflammation (within one week), a process that could be blocked by EOS depletion. TSLP promotes the resolution of post-infarction inflammation and inhibits fibrosis by recruiting EOSs to the heart. This highlights the potential of targeting the TSLP-EOS axis as a therapeutic strategy to improve cardiac function and reduce post-AMI complications.

## 25COASOCT80

### **Title: Microplastics promote chemoresistance by mediating lipid metabolism and suppressing pyroptosis in colorectal cancer**

Dongzhi Hu, Hui Liu, Yaoyang Guo et.al.

Apoptosis, Volume 30, pages 2287–2300, (2025)

<https://doi.org/10.1007/s10495-025-02143-8>

**Abstract:** Microplastics are ubiquitous environmental contaminants worldwide. Although studies have shown their potential to harm human health, the relationship between microplastics and tumors remains unclear. The intestine is the primary site for microplastics absorption, thus the impact of microplastics on colorectal cancer merits further investigation. Our results indicate that the endocytosis protein clathrin, highly expressed in cancer cells, plays a crucial role in the massive ingestion of microplastics. Further research reveals that microplastics ingestion enhances lipid absorption in colorectal cancer cells by activating the NF- $\kappa$ B signaling pathway. Accumulation of lipids, in turn, suppresses pyroptosis by inhibiting NLRP3/Caspase-1/GSDMD axis, thereby promoting cellular drug resistance. Moreover, microplastics accelerate colorectal cancer development in mice and enhance tumor resistance to oxaliplatin. In summary, microplastics regulate lipid metabolism and pyroptosis in colorectal cancer, emerging as a novel contributor to chemotherapy resistance in colorectal cancer against the backdrop of escalating microplastics pollution.

## 25COASOCT81

**Title: Melatonin alleviates sodium sulfite-induced osteoporosis in mice via suppression of the ferroptosis pathway**

Qiuping He, Lei Xie, Haining Peng et.al.

Apoptosis, Volume 30, pages 2301–2315, (2025)

<https://doi.org/10.1007/s10495-025-02135-8>

**Abstract:** Sodium sulfite (SS) is a common food additive that is widely absorbed and distributed throughout the body, but its excessive intake has been linked to adverse health effects. Here, we investigate the impact of chronic SS exposure on bone tissue and the underlying mechanisms. Using a mouse model, we demonstrate that prolonged SS exposure induces significant bone loss, which correlates with alterations in ferroptosis-related markers. In vitro, SS exposure activates ferroptosis, which is characterized by elevated reactive oxygen species levels and impaired osteogenic differentiation in MC3T3 cells. Notably, melatonin, a potent endogenous antioxidant, mitigates SS-induced oxidative stress, inhibits ferroptosis, restores osteoblast function, and alleviates bone loss in mice. These findings highlight ferroptosis as a critical contributor to SS-induced osteoporosis and identify melatonin as a promising therapeutic agent for its prevention and treatment.

## 25COASOCT82

**Title: Kim-1-targeted multimodal nanoprobes for early diagnosis and monitoring of sepsis-induced acute kidney injury**

Qingjie Chen, Jianbo Yang, Mei Yang et.al.

Apoptosis, Volume 30, pages 2316–2339, (2025)

<https://doi.org/10.1007/s10495-025-02141-w>

**Abstract:** Sepsis-induced acute kidney injury (AKI) is a critical condition characterized by high mortality and limited early diagnostic tools. This study presents the development of a novel multimodal nanoprobe,  $^{68}\text{Ga}/^{99\text{m}}\text{Tc}@\text{LTH-SPIONs}$ , for targeted detection and monitoring of sepsis-induced AKI. By combining PET/SPECT imaging capabilities of radiolabeled isotopes ( $^{68}\text{Ga}$  and  $^{99\text{m}}\text{Tc}$ ) with the anatomical resolution of superparamagnetic

iron oxide nanoparticles (SPIONs) for MRI, the nanoprobe facilitates precise and non-invasive imaging. Surface modification with the LTH peptide, which specifically targets Kidney Injury Molecule-1 (Kim-1), enhances the nanoprobe's diagnostic specificity. Extensive in vitro and in vivo evaluations revealed low cytotoxicity, excellent biocompatibility, and effective renal targeting, with metabolites predominantly cleared through urine. In a sepsis AKI mouse model, the nanoprobe provided sensitive and specific imaging, enabling early detection of kidney injury. This study underscores the potential of Kim-1-targeted nanoprobe as a powerful tool for elucidating cellular injury mechanisms and monitoring therapeutic interventions in AKI.

### 25COASOCT83

#### **Title: AIM2-PANoptosome-driven PANoptosis in hepatic lipid dysregulation induced by $\beta$ -HCH and nanoplastics co-exposure**

Qizhuan Lin, Helei Cai, Fan Yu et.al.

Apoptosis, Volume 30, pages 2340–2357, (2025)

<https://doi.org/10.1007/s10495-025-02147-4>

**Abstract :** Environmental pollutants pose an increasing threat to human health and ecosystems, with persistent organic pollutants (POPs) and nanoplastics (NPs) drawing significant attention due to their resistance to degradation, high mobility, and bioaccumulation.  $\beta$ -Hexachlorocyclohexane ( $\beta$ -HCH), a typical POP, poses a serious threat to organisms due to its long-term environmental persistence, despite being banned. In this study, we investigated the molecular mechanisms underlying hepatic lipid metabolism disorders induced by combined exposure to  $\beta$ -HCH and NPs using a zebrafish model and Hep G2 cell experiments. Histological staining, RT-qPCR, Western blotting, and immunofluorescence staining demonstrated that  $\beta$ -HCH and NPs co-exposure triggered multiple forms of programmed cell death (PCD), including apoptosis, pyroptosis, and necroptosis, through activation of the pyroptosis, apoptosis and necroptosis (PANoptosis) pathway mediated by the Absent in Melanoma 2 (AIM2)-PANoptosome complex, ultimately leading to lipid metabolism disturbances. RNA interference and gene overexpression experiments further revealed that down or overexpression of AIM2 significantly impacted PANoptosis, confirming the central regulatory role of AIM2 in this process. This study firstly elucidates the regulatory role of the AIM2-PANoptosome complex in the PANoptosis pathway under  $\beta$ -HCH and NPs co-exposure conditions. It provides valuable insights for developing intervention strategies targeting AIM2 for lipid metabolic diseases.

### 25COASOCT84

#### **Title: Novel L-type chiral metal(II) complexes inhibit breast cancer growth through synergistic effects of anti-angiogenesis, anti-inflammatory, apoptosis induction and cuproptosis**

Nan Jin, Bing-Bing Xu, Hong-Yu Lin et.al.

Apoptosis, Volume 30, pages 2358–2384, (2025)

<https://doi.org/10.1007/s10495-025-02149-2>

**Abstract:** Breast cancer ranks first among female malignant tumors and is the largest cancer worldwide. Recently, research on chiral metal-based complexes for cancer treatment has significantly increased. This study synthesized an L-copper(II) complex Cu-1 and a pair of

chiral nickel(II) complexes Ni-1 (L-type) and Ni-2 (D-type). The antiproliferative activities of Cu-1, Ni-1, and Ni-2 against female malignant tumor cells (MCF-7, MDA-MB-231, SKOV3, Hela) were evaluated. Among them, the L-type complexes Cu-1 and Ni-1 exhibited superior bioactivity compared to the D-type Ni-2. Further mechanistic studies demonstrated that Cu-1 and Ni-1 could effectively inhibit the growth of MCF-7 cells. Additionally, in vivo experiments in nude mice verified that Cu-1 could exert anti-tumor effects through the synergistic action of multiple pathways. In summary, Cu-1 and Ni-1 possess multiple functions including anti-tumor angiogenesis, anti-inflammatory, apoptosis, and copper-induced death, providing theoretical reference for the development of breast cancer drugs.

## 25COASOCT85

### **Title: GSDME-dependent astrocyte pyroptosis promotes the progression of neuroinflammation in experimental cerebral malaria**

Jun Wang, Qinghao Zhu, Guodong Tong et.al.

Apoptosis, Volume 30, pages 2385–2400, (2025)

<https://doi.org/10.1007/s10495-025-02140-x>

**Abstract:** Cerebral malaria (CM), a life-threatening neurological complication of *Plasmodium falciparum* infection, is characterized by severe neuroinflammation and long-term neurological sequelae. Central nervous system inflammation, driven by brain-infiltrated CD8<sup>+</sup> T cells, represents a hallmark pathological feature of CM. In this study, we demonstrate that astrocytes, a critical component of the blood–brain barrier and neurovascular unit, exhibit a robust interferon- $\gamma$  response during CM, facilitating CD8<sup>+</sup> T cell recruitment into the brain parenchyma and antigen presentation to these immune cells. Importantly, we identify gasdermin E (GSDME)-dependent pyroptosis in astrocytes, a process triggered by brain-infiltrated CD8<sup>+</sup> T cells. This pyroptotic pathway amplifies neuroinflammation and exacerbates neuronal injury. Genetic ablation of *Gsdme* or pharmacological inhibition of GSDME activation by mannose significantly attenuated brain inflammation and damage in a murine CM model. Our findings establish, for the first time, that GSDME-dependent astrocyte pyroptosis critically exacerbates neuroinflammation in CM. These results highlight GSDME as a novel therapeutic target for mitigating CM and related neuroinflammatory diseases.

## 25COASOCT86

### **Title: Dual-functional Anti-hPSMAEC domain nanocapsules for targeted inhibition of prostate tumor growth**

Heng Yang, Jian He, Yujun Chen et.al.

Apoptosis, Volume 30, pages 2401–2420, (2025)

<https://doi.org/10.1007/s10495-025-02163-4>

**Abstract:** Addressing prostate cancer, particularly in its aggressive forms, poses challenges that call for innovative treatment modalities. Our research focuses on developing a nanotechnological solution to enhance targeted cancer therapy. We have synthesized advanced nanocapsules embedded with indocyanine green (ICG) and conjugated with the Anti-hPSMAEC domain to improve specificity towards prostate cancer cells. These nanocapsules are engineered to perform dual-mode phototherapy through photothermal and photodynamic mechanisms. In vitro experiments demonstrated the nanocapsules effectively



target and induce apoptosis in prostate cancer cells upon exposure to near-infrared light. Furthermore, in vivo assessments in murine models revealed excellent tumor localization and a substantial reduction in tumor volume with minimal impact on healthy tissues. This innovative approach underscores the potential of nanotechnology to transform the therapeutic landscape of prostate cancer by achieving precise targeting and reducing systemic side effects. Such nanocapsule systems' continued development and refinement may substantially improve clinical outcomes and provide promising therapeutic strategies for treating complex cancers.

## 25COASOCT87

**Title: High-dose tamoxifen impairs the homeostasis of the intestinal stem cell niche by enhancing fatty acid degradation and damaging mitochondria**

Lu Xu, Xiangjun Liu, Jianhua Feng et.al.

Apoptosis, Volume 30, pages 2421–2434, (2025)

<https://doi.org/10.1007/s10495-025-02153-6>

**Abstract:** Tamoxifen is therapeutically employed for breast and ovarian cancers, and it is also widely utilized to activate Cre recombinase in transgenic mice containing Cre-ERT locus. However, high dose tamoxifen (HDTAM) has been reported to induce many side effects in several organs and tissues. Intestinal stem cells (ISCs) play pivotal roles in sustaining the epithelial homeostasis and intestinal functionality. In this study, we systematically investigated the influences of HDTAM on ISCs and their niche. It was found that HDTAM treatment decreased the body weight and the length of small intestines (SI), damaged the gross and histological morphology of SI. Notably, HDTAM dramatically inhibited the proliferation, differentiation, gene expression of ISCs in vivo and in vitro. RNA-Seq results demonstrated that these changes caused by HDTAM were significantly correlated with the degradation of intestinal fatty acids and the process of fatty acid oxidation. Mechanistically, HDTAM impaired the morphology and function of mitochondria of intestinal epithelial cells, increased the endoplasmic reticulum (ER) contents in Paneth cells. Therefore, we concluded that HDTAM could result in a disruption for the function and homeostasis of ISCs, and the interruption of fatty acid utilization might be responsible for these effects. This study implicates a careful use and evaluation of tamoxifen is in necessity when it's used for intestinal research.

## 25COASOCT88

**Title: Bioactivity of mycosynthesized nanoparticles assists photothermal therapy of breast cancer cells**

Aya Ezzat, Marwa A. Ramadan, Jehane I. Eid et.al.

Apoptosis, Volume 30, pages 2435–2454, (2025)

<https://doi.org/10.1007/s10495-025-02145-6>

**Abstract:** Chaga mushroom (*Inonotus obliquus*) exhibits cytotoxic effects against breast cancer cells. Mycosynthesized nanoparticles, owing to their biodegradability, biocompatibility, and low toxicity, present a promising therapeutic approach. This study explored the cytotoxic potential of gold nanoparticles synthesized using Chaga mushroom extract (AuCh-NPs) combined with Light Emitting Diode (LED) irradiation (530 nm) on human breast cancer (MCF-7) cells, aiming to develop a safe and effective sensitizer for

photothermal therapy. The AuCh-NPs were characterized using UV–visible spectroscopy, FTIR, TEM, particle size analysis, and zeta potential measurements. Cytotoxicity was evaluated via MTT assay under LED irradiation with total light exposure 325.8 and 488.7 J cm<sup>-2</sup>, alongside mechanistic studies involving wound healing, autophagy, cell cycle arrest, annexin V analysis, real-time PCR, and comet assays. TEM revealed spherical AuCh-NPs with sizes ranging from 15.4 to 28.9 nm. The MTT assay demonstrated enhanced cytotoxicity under LED irradiation, with AuCh-NPs exhibiting a lower IC<sub>50</sub> (5.56 μM) than citrate-capped gold nanoparticles (AuCit-NPs, 7 μM). Cell cycle analysis revealed significant arrest in G<sub>0</sub>/G<sub>1</sub> (91.68%) and S (7.55%) phases, while annexin V analysis confirmed apoptosis induction. Real-time PCR showed upregulation of the pro-apoptotic genes BAX, and the comet assay indicated increased double-strand DNA damage in MCF-7 cells treated with AuCh-NPs compared to AuCit-NPs. These findings highlight the superior selective cytotoxicity of AuCh-NPs against MCF7 cells, positioning them as a promising targeted agent for photothermal therapy in breast cancer treatment.

## 25COASOCT89

### **Title: FOXP2/SOS1/AKT negative feedback loop inhibits cell proliferation in KRAS-mutant colorectal cancer**

Jinpu Liu, Yayun Wang, Yuya Liu et.al.

Apoptosis, Volume 30, pages 2455–2465, (2025)

<https://doi.org/10.1007/s10495-025-02154-5>

**Abstract:** FOXP2, a member of the Forkhead box transcription factor family, has been implicated in diverse biological processes and malignancies. However, its role in colorectal cancer (CRC), particularly in the context of KRAS mutations, remains poorly defined. Here, we analyzed FOXP2 expression in CRC datasets and clinical specimens, and conducted functional assays—including colony formation, cell viability, EdU incorporation, and cell cycle analysis—in KRAS-mutant CRC cell lines with FOXP2 overexpression or knockdown. Western blotting, dual-luciferase reporter assays, and in vivo xenograft models were used to explore the underlying mechanisms. FOXP2 was significantly downregulated in CRC tissues and its high expression correlated with favorable prognosis in KRAS-mutant patients. Functionally, FOXP2 overexpression suppressed cell proliferation, induced G<sub>0</sub>/G<sub>1</sub>-phase arrest, and inhibited PI3K/AKT signaling. Mechanistically, FOXP2 transcriptionally repressed SOS1, thereby attenuating downstream AKT activation. Notably, AKT activation enhanced FOXP2 expression, indicating a FOXP2/SOS1/AKT negative feedback loop. Collectively, our findings suggest that FOXP2 inhibits proliferation in KRAS-mutant CRC by suppressing SOS1-mediated PI3K/AKT signaling, and may serve as a prognostic biomarker and potential therapeutic target in KRAS-driven CRC.

## 25COASOCT90

### **Title: Endothelial HMGB1-AIM2 axis worsens myocardial ischemia—reperfusion injury by regulating endothelial pyroptosis**

Rui Chen, Junying Duan, Ye Zhou et.al.

Apoptosis, Volume 30, pages 2466–2479, (2025)

<https://doi.org/10.1007/s10495-025-02162-5>

**Abstract:** This study investigates mechanisms related to endothelial cells in myocardial

ischaemia–reperfusion (I/R) injury, focusing on the role of high-mobility group box 1 (HMGB1) protein in these cells. Using a murine model, we observed elevated levels of HMGB1 in both the heart and circulation following I/R, with a portion originating from cardiac vascular endothelial cells and cardiomyocytes. Endothelial cell-specific HMGB1 knockout preserved cardiac function after I/R by reducing infarct size, mitigating myocardial damage, maintaining endothelial cell barrier function, and attenuating inflammatory and oxidative stress responses. Single-cell analysis revealed that HMGB1 endothelial knockout altered cardiac cell composition by decreasing the proportion of endothelial cells with high fatty acid-binding protein 4 expression. Mechanistically, HMGB1 endothelial knockout significantly inhibited the expression of absent in melanoma 2 (AIM2)-associated inflammasome- and pyroptosis-related proteins after I/R, whereas AIM2 overexpression exacerbated myocardial injury, inflammation, and the expression of pyroptosis-related proteins. Our findings demonstrate that the endothelial HMGB1-AIM2 axis worsens I/R injury by regulating endothelial cell pyroptosis, suggesting a novel pathway involved in microcirculatory dysfunction during myocardial I/R injury.

## 25COASOCT91

### **Title: Biomarkers in cystic lesions of the pancreas: Controversies and advances**

Longyu Liu, Zhiyao Fan, Hanxiang Zhan

BBA, Volume 1880, Issue 5, October 2025, 189392

<https://doi.org/10.1016/j.bbcan.2025.189392>

**Abstract:** Pancreatic cystic lesions (PCLs) represent a highly heterogeneous category of pancreatic abnormalities with an increasing prevalence due to advances in imaging modalities and an aging population. While the majority of PCLs are benign, a subset harbors a variable risk of malignant transformation. Current guidelines rely primarily on imaging features for risk stratification, but limitations in diagnostic accuracy have led to many unnecessary surgical procedures and conversely, missed opportunities for timely resection in cases that progress to malignancy. Recent advances in biomarker discovery hold great promise for improving the management of PCL. In this review, we focus on comparing the diagnostic efficacy of classical tumor markers, highlighting the controversies and challenges associated with each. In addition, we explore the heterogeneous expression of mucins in different subtypes of intraductal papillary mucinous neoplasms (IPMNs) and review the role of common genetic mutations and next-generation sequencing (NGS) in the genomic assessment of PCLs. Importantly, we summarize the results of several novel gene panels and evaluate their diagnostic performance and clinical potential. Although accurate diagnosis and risk stratification of PCLs remain challenging, advances in biomarkers and molecular techniques continue to reveal their potential in precision medicine, with promising implications for clinical translation.

## 25COASOCT92

### **Title: Targeting the triad: phenotypic plasticity, tumor microenvironment and bone microenvironment in prostate cancer bone-metastatic events**

Ma Chi-Cheng, Ou-Yang Ao-Rong, Chen Zi-Xian et.al.

BBA, Volume 1880, Issue 5, October 2025, 189388

<https://doi.org/10.1016/j.bbcan.2025.189388>

**Abstract:** The incidence and mortality rates of prostate cancer are increasing annually, indicating that it poses a serious threat to men's health. Previous studies have demonstrated that bone-metastatic tumor cells undergo four hallmark bone-metastatic events, including colonization, dormancy, reactivation and bone reconstruction. However, most advanced patients experience four stages of progression and undergo advanced bone reconstruction—the “vicious circle”—which is irreversible. These patients have a poor prognosis and can even die. Therefore, determining how various components in the tumor and bone microenvironments affect the progression and events of bone metastasis is crucial. Here, we integrate the latest mechanisms of phenotypic plasticity and microenvironment interactions, proposing potential therapeutic targets to disrupt the ‘vicious cycle’ in advanced bone metastasis. We look forward to providing direction and guidance for the future treatment of prostate cancer bone metastasis.

### 25COASOCT93

**Title: Metabolic reprogramming in breast cancer: Pathways driving progression, drug resistance, and emerging therapeutics**

Pankaj Garg, Gargi Singhal, David Horne et.al.

BBA, Volume 1880, Issue 5, October 2025, 189396

<https://doi.org/10.1016/j.bbcan.2025.189396>

**Abstract:** Breast cancer (BC), one of the most frequent causes of cancer-related death in women, is known to be a highly heterogeneous disease in regard to molecular subtypes, which seem to possess different metabolic profiles. Aberrant metabolism is well understood as one of the hallmarks of cancer and it contributes to BC progression, therapeutic resistance, and metastasis. Here, we analyze BC metabolism and how certain cancer types, such as hormone receptor-positive, HER2-positive, and triple-negative BC, use glycolysis, lipid metabolism, amino acid compulsion, and mitochondrial biogenesis to feed and proliferate. These metabolic hallmarks, in the context of the tumor microenvironments, are illustrated to highlight the metabolic byproducts that are derived from reprogrammed pathways and are vital to immunosuppression and tumor survival under low oxygen and nutrient availability. Furthermore, we emphasize novel trends in anticancer drugs designed to strike on these metabolic dependencies to suppress tumor growth. In addition to summing up current knowledge about metabolic reprogramming in BC, this review reveals new targets for specific treatments that might enhance prognosis in certain types of BC. This review aims to bridge basic scientific insights and clinical perspectives, guiding future metabolic interventions in BC toward clinically relevant, subtype-specific therapeutic strategies.

### 25COASOCT94

**Title: TXNIP in cancer: Unlocking biological insights and tackling clinical challenges**

Piercarlo Del Console, Luca Gelsomino, Cinzia Giordano

BBA-Review on Cancer, Volume 1880, Issue 5, October 2025, 189394

<https://doi.org/10.1016/j.bbcan.2025.189394>

**Abstract:** Cancer remains a major global health challenge and one of the leading causes of mortality worldwide. Its development and progression involve complex genetic and molecular alterations, including the activation of oncogenes, as well as the inactivation of tumor suppressor genes (TSGs). These TSGs play critical roles in regulating cell cycle,

genomic stability, and apoptotic pathways, with their dysfunction widely contributing to tumorigenesis and therapy response. Among the TSGs, Thioredoxin Interacting Protein (TXNIP) has gained attention as a key regulator with multifaceted roles in cancer biology. Mechanistic insights have identified TXNIP as a broad-acting protein involved in a variety of cellular responses, including oxidative stress, metabolism, immune regulation, and tumor suppression. This literature review critically examines the emerging clinical and experimental evidence of TXNIP's functions in cancer, with a particular focus on breast cancer, the most frequently diagnosed malignancy in women. Furthermore, it explores promising therapeutic advances aimed at restoring TXNIP tumor-suppressive functions to slow cancer progression and improving patient outcomes.

## 25COASOCT95

**Title: From unearthing to an intriguing cancer-fighting target: the human BCL-2 promoter G-quadruplex and i-motif.**

Pronamika Chetia, Amit Kumar

BBA-Review on Cancer, Volume 1880, Issue 5, October 2025, 189391

<https://doi.org/10.1016/j.bbcan.2025.189391>

**Abstract:** Cancer is a global burden that calls for creative solutions. Among the several hallmarks of cancer, overexpression of the BCL-2 oncogene serves as a factor for cancer cell proliferation and progression. Targeting the transcription machinery of the BCL-2 oncogene is an effective approach against cancer since chemotherapy causes huge problems due to its catastrophic toxicity and accompanying side effects. Transcription of the BCL-2 gene is primarily controlled by the P1 promoter and its upstream region, which is G-rich and can fold into G-quadruplexes (G4 or GQ), and i-motif structures. G4 and i-motif are secondary structures of nucleic acids that provide a platform for binding proteins, small molecules, peptide nucleic acids, etc. Such secondary structures can be targeted and have been extensively studied in the past few years. Therefore, it is reasonable to carry out an in-depth investigation of the G4 and i-motif structures in the BCL-2 gene and its potential as a therapeutic target. Here, we will overview the discovery and structure of BCL-2 G4 and i-motif structure and the proteins that bind to P1 promoter. Lastly, we will discuss BCL-2 G4 and i-motif binding small molecules/ligands, and their anticancer activities and examine their potential for innovative cancer treatments.

## 25COASOCT96

**Title: Multidimensional regulation of the microbe-TLR4 signaling Axis in colorectal cancer: From molecular mechanisms to microbe-targeted therapies**

Caihou Zhang , Haimin Geng, Yurong Tan et.al.

BBA-Review on Cancer, Volume 1880, Issue 5, October 2025, 189397

<https://doi.org/10.1016/j.bbcan.2025.189397>

**Abstract:** Colorectal cancer (CRC), the third most common cancer globally, arises from complex interactions between genetic predisposition, environmental factors, and gut microbiota dysbiosis. This review systematically analyzes the multidimensional regulatory mechanisms of the microbe-TLR4 signaling axis in CRC, including key pathways such as TLR4/NF- $\kappa$ B, MAPK, TRIF/IRF3, Keap1/NRF2/CYP2J2, and ceramide/ $\beta$ -catenin/SOAT1. These pathways drive tumor progression through metabolic reprogramming, immune



modulation, and genotoxic effects. Therapeutic strategies targeting this axis encompass natural compounds (e.g., terpenoids, polysaccharides, saponins), traditional Chinese medicine formulas (e.g., Ganluyin, Xiao-Chai-Hu-Tang), microbiota therapies (probiotics, engineered bacteria, oncolytic viruses), and dietary and metabolic regulation (dietary fiber, methionine), exerting anti-tumor effects by inhibiting excessive TLR4 activation, repairing intestinal barriers, and regulating microbial balance. The review highlights challenges such as the complexity of signaling pathways, precise microbiota modulation, and drug delivery. At the same time, emerging technologies like single-cell multi-omics and artificial intelligence prediction models offer new directions for precision interventions. Targeting the microbe-TLR4 axis holds promise as an innovative strategy for CRC treatment.

## 25COASOCT97

### **Title: Advances in the combination of immunoadjuvants and tumor ablation: Mediating immune effects to enhance anti-tumor efficacy**

Duo Yu a, Yang Zuo, Mengdi Qi et.al.

BBA-Review on Cancer, Volume 1880, Issue 5, October 2025, 189393

<https://doi.org/10.1016/j.bbcan.2025.189393>

**Abstract:** Percutaneous tumor ablation is a minimally invasive treatment for tumors. The release of tumor neoantigens after ablation not only remodels the local tumor microenvironment, but also achieves abscopal effects by mediating local and systemic immune effects. However, studies have shown that a single ablation technique is not sufficient to achieve the desired anti-tumor immune effect. Numerous studies have shown that the combination of immunoadjuvants and tumor ablation can transform immunologically “cold” tumors into “hot” tumors, significantly improving the suppressive anti-tumor immune properties of the local microenvironment, while enhancing systemic anti-tumor immunity and the abscopal effect. At the same time, it enhances the systemic anti-tumor immunity and abscopal effect. This paper reviews the immune responses induced by different ablation techniques, including thermal ablation, cryoablation, high-frequency focused ultrasound, photodynamic therapy, and irreversible electroporation. The research progress in recent years on the combination of immunoadjuvants and ablation techniques in improving anti-tumor efficiency and enhancing immune effects is reviewed, mainly including traditional immunomodulators such as immune checkpoint inhibitors, adoptive cellular therapies, Toll-like receptor agonists, STING agonists, as well as emerging immunoadjuvants that are expected has great advantage in further enhance the synergistic anti-tumor efficiency and immune effects, such as tumor ablation in-situ vaccines, nano-metallic organic frameworks, polylactic acid-hydroxyacetic acid copolymers (PLGA), hydrogels and other nanomaterials. This paper discusses recent research advances in the use of immunoadjuvants in combination with ablation, demonstrating the immense immune effects of this synergistic therapy and its promising application in clinical oncology treatment.

## 25COASOCT98

### **Title: Targeting hormone-related signals to reprogram the antitumor immune response in breast cancer: Research progress and application prospects**

Shunchao Yan, Zhijie Zhang, Jiale Ji et.al.

BBA-Review on Cancer, Volume 1880, Issue 5, October 2025, 189390

<https://doi.org/10.1016/j.bbcan.2025.189390>

**Abstract:** Breast cancer is a heterogeneous disease with varying responses to hormonal therapies and immunotherapies. It is commonly characterized as a “cold” tumor; however, increasing evidence demonstrates the immunomodulatory effects of hormonal signals and an evolving tumor immune microenvironment following treatment. Several investigations have shown that anti-hormone treatment enhances the capacity of antitumor immune cells while reducing the population of immunosuppressive cells. Understanding the effects and mechanisms of hormone and anti-hormone therapies on the antitumor immune response is crucial for developing novel cancer treatment strategies. This review explores the complex interplay between hormonal signals and antitumor immune responses in breast cancer and outlines the research progress and potential applications of targeting hormone-related signals to reprogram the immune response against breast cancer. We also address the challenges, opportunities, and future directions in regulating hormonal signals to improve the efficacy of immunotherapy for individuals with breast cancer.

## 25COASOCT99

### **Title: Mechanism of interleukin-6 cytokine family in bone metastasis of lung cancer and prospects for its application**

Jinbai Huang, Qingting Zhang, Yuanshan Yang et.al.

BBA-Review on Cancer, Volume 1880, Issue 5, October 2025, 189398

<https://doi.org/10.1016/j.bbcan.2025.189398>

**Abstract:** Bone metastasis is a significant clinical problem for lung cancer patients. Current studies have reported a strong relationship between the progression of bone metastases from lung cancer and inflammatory cytokines, which can modulate the tumor microenvironment (TME) and promote the migration of tumor cells. Interleukin-6 (IL-6) family cytokines are critical components of the immune microenvironment secreted by several cell types in vivo. They can regulate immune homeostasis, inflammatory response, etc., and activate multiple signal pathways involved in tumor progression. Some of these factors (e.g., IL-6 and IL-11) increase the serum expression levels of patients with bone metastases from lung cancer; the level of expression correlates with a poor prognosis in patients with lung cancer. However, the role of this family of novel cytokines in lung cancer bone metastasis remains unclear. Besides, limited studies exist on the related regulatory mechanisms, and there is a lack of direct evidence for their relationship with bone metastasis. Thus, this review discusses the current roles and potential mechanisms of all IL-6 family members in lung cancer bone metastasis, as well as the potential of blocking the IL-6 family, its receptors, and signaling pathways for treating lung cancer bone metastasis. This is geared towards providing prospective treatment targets for bone metastases from lung cancer and possible future research directions.

## 25COASOCT100

### **Title: Research advances on amino acid starvation interventions for hepatocellular carcinoma**

Yanqi Li, Lin Li, Yongyong Hou et.al.

BBA-Review on Cancer, Volume 1880, Issue 5, October 2025, 189400

<https://doi.org/10.1016/j.bbcan.2025.189400>

**Abstract:** Hepatocellular carcinoma (HCC) is an aggressive malignancy associated with high mortality. Numerous endeavors have been undertaken to develop more effective pharmaceutical interventions. Metabolic reprogramming is recognized as a hallmark of cancer for adapting to heightened bioenergetic and biosynthetic demands. Amino acid (AA) metabolism dysregulation plays a crucial role in the tumor initiation and progression of HCC, resulting in high reliance on AA availability. This makes HCC cells vulnerable to AA starvation, implying that restricting AA supply and utilization may offer a promising nutritional strategy in HCC therapy. We delineate the pivotal physiological functions and aberrant alterations of various AA metabolisms in HCC. We systematically summarize the recent advances in agents, targets, antineoplastic effects, and mechanisms of various AA starvation strategies in HCC, including dietary restriction, circulating depletion, transporter blockade, and metabolic enzyme inhibition. We further discussed a suite of adaptive responses that enable HCC cells to survive with AA shortage. Targeting these adaptive pathways in combination with AA starvation may enhance the efficacy of HCC treatment. This review aims to provide a comprehensive overview of progress in the field of AA starvation for HCC therapy and to explore novel therapeutic opportunities and strategies through nutritional intervention for HCC therapy.

## 25COASOCT101

### **Title: Lactylation: A new direction for tumor-targeted therapy**

Dan Deng, Yan Luo, Yun Hong et.al.

BBA-Review on Cancer, Volume 1880, Issue 5, October 2025, 189399

<https://doi.org/10.1016/j.bbcan.2025.189399>

**Abstract:** Lactate, a central metabolite generated during glycolysis, functions not only as a by-product but also as a critical signalling mediator, profoundly influencing tumor progression and cellular destiny. Among the post-translational modifications, lactylation—a novel modification driven by lactate—has emerged as a transformative discovery, reshaping our understanding of lactate's role within the tumor microenvironment (TME). This modification bridges metabolic reprogramming and epigenetic regulation, unveiling previously unexplored dimensions of tumor biology. Recent findings demonstrate that protein lactylation in tumor cells, cancer stem cells, and immune cells infiltrating the TME can modulate transcriptional activities, thereby influencing tumor initiation, progression, and immune evasion. These insights position lactylation as a promising target for new therapeutic strategies in cancer. This review expounds on the underlying mechanisms of lactylation, including the identification of the “writers” and “erasers” involved in protein lactylation, and highlights the physiological significance of lactylation across diverse biological contexts. Furthermore, the paper emphasized on the latest advancements in understanding the modulatory functions of protein lactylation within pathological processes, the potential for targeting lactylation sites, and underscores the scientific significance for future investigative endeavours.

## 25COASOCT102

### **Title: Dietary sugar intervention: A promising approach for cancer therapy**

Xinyi Zhou, Yujia Song, Zhen Wang et.al.

BBA-Review on Cancer, Volume 1880, Issue 5, October 2025, 189402

<https://doi.org/10.1016/j.bbcan.2025.189402>

**Abstract:** Cancer constitutes a significant global health challenge, with altered metabolism being a hallmark feature of cancer cells. Diet can directly modulate systemic metabolite levels, thereby exerting both direct and indirect influences on tumor progression. The primary mechanisms include: (1) directly altering signaling pathways related to tumor cell proliferation or apoptosis, (2) indirectly affecting tumor progression by modulating nutrient availability or immune cell function in the tumor microenvironment, and (3) influencing tumor development through changes in gut microbiota composition or metabolic activity. Dietary sugars, as integral components of nutritional intake, play crucial roles in providing energy and participating in metabolism and signaling processes. Building upon this understanding, our discussion delves into the impact and mechanisms of dietary sugars, including glucose, fructose, and mannose, on tumors, and investigates potential dietary interventions. We also summarize current clinical applications of these dietary interventions, hoping to contribute to the conceptualization of personalized dietary treatment plans for individuals grappling with cancer.

### 25COASOCT103

**Title: Gynecological malignancy organoids: A game changer for personalized medicine**

Ziyang Ding, Xingyu Chang, Xinyu Qu et.al.

BBA-Review on Cancer, Volume 1880, Issue 5, October 2025, 189405

<https://doi.org/10.1016/j.bbcan.2025.189405>

**Abstract:** Recently, the incidence of gynecological malignancies has increased annually, posing a serious threat to women's health. Historically, the emergence and progression of gynecological cancers have primarily been studied using cell lines and animal models. However, these models often fail to accurately reflect tumor characteristics because genetic mutations frequently occur during long-term cultivation. Also, the complex tumor microenvironment is difficult to replicate. Consequently, these models have limitations in translating research findings into clinical applications. Organoids successfully retain key characteristics of primary tumors, including histological structure, genomic landscape, expression profiles, and intratumor heterogeneity. They provide new solutions to these challenges and have been effectively applied in drug development and personalized therapy. This review describes several common culture systems for organoids of gynecological malignancies. It discusses the latest technologies related to organoids and their applications in gynecological oncology. Despite limitations, organoids are ideal preclinical models and a promising platform for tumor research.

### 25COASOCT104

**Title: Decoding the key hallmarks of chemoresistance: A proteomic tale from breast cancer research**

Praneeta Pradip Bhavsar, Bhargab Kalita, Khushman Taunk et.al.

BBA-Review on Cancer, Volume 1880, Issue 5, October 2025, 189404

<https://doi.org/10.1016/j.bbcan.2025.189404>

**Abstract:** Chemoresistance denotes the intricate, multifactorial molecular mechanisms by which malignant cells subvert the cytotoxicity of chemotherapeutic agents, thereby impeding therapeutic efficacy. This phenomenon is orchestrated through a confluence of processes,

which we propose as the major hallmarks of chemoresistance in cancer. Dysregulation of drug transporters, activation of pro-survival pathways, cancer stem cell driven proliferation, DNA damage and repair mechanisms, evasion of apoptosis, autophagy induction, secretion of extracellular vesicles, and metabolic reprogramming represents the major mechanisms of chemoresistance in cancer. Breast cancer is one of the most common and aggressive types of cancer, with significant challenges in treatment due to its heterogeneity. Despite progress in various treatment regimens, chemoresistance continues to be a significant challenge in the effective management of breast cancer. In this context, high-throughput proteomic methodologies, which quantitatively assess proteome-wide alterations and explore post-translational modifications, can provide an unbiased framework for unraveling the molecular intricacies of chemotherapy resistance. This article comprehensively reviews the application of advanced proteomic techniques in elucidating the pathophysiological mechanisms of chemoresistance in breast cancer. Additionally, it highlights promising protein signatures uncovered via proteomic tools, as well as therapeutic strategies targeting chemoresistant hallmarks to overcome drug resistance in breast cancer. By leveraging the mightiness of proteomic technologies, we move closer to efficient, potent and personalized therapeutic interventions for chemoresistant breast cancer.

## 25COASOCT105

### **Title: Clinical aspect of combined immunotherapy and radiotherapy effect on tumor immune microenvironment in hepatobiliary and pancreatic cancers**

Jun-Jie Cheng, Qiu-Yi Zheng, Yi-Lan Huang et.al.

BBA-Review on Cancer, Volume 1880, Issue 5, October 2025, 189406

<https://doi.org/10.1016/j.bbcan.2025.189406>

**Abstract:** Hepatobiliary and pancreatic cancers (HBPCs) remain among the most aggressive nature and lethal malignancies, presenting formidable challenges in their treatment. Surgical resection remains the cornerstone of curative treatment for early-stage HBPCs; however, advanced cases often necessitate a multidisciplinary systematic approach incorporating radiotherapy and immunotherapy. In recent years, innovations in radiotherapy technology have facilitated the precise and targeted delivery of tumoricidal doses, minimizing damage to surrounding normal tissue and expanding the application of radiotherapy in treating HBPCs. Moreover, the intricate impact of radiotherapy on the tumor immune microenvironment (TIME) is being increasingly understood. Synergizing radiotherapy with immunotherapy to induce a robust and sustained antitumor immune response, both locally at the irradiated site and systemically throughout the body, represents a promising and increasingly critical avenue of current research. This review begins by delineating the heterogeneity of the TIME in HBPCs and discusses how radiotherapy can either stimulate or suppress the TIME under various conditions. It also highlights recent preclinical and clinical advances in combining radiotherapy with immunotherapy, which have shown potential in improving local control rates and inducing systemic antitumor responses. This emerging paradigm warrants sustained research to fully realize its therapeutic potential in HBPC management.

## 25COASOCT106

### **Title: Taurine and cancer: Biological properties and multifaceted roles in cancer progression**



Rong Liu, Xinze Li, Zhenyu Hua et.al.

BBA-Review on Cancer, Volume 1880, Issue 5, October 2025, 189403

<https://doi.org/10.1016/j.bbcan.2025.189403>

**Abstract:** Cancer remains one of the leading causes of mortality worldwide and poses a major threat to global health. Recent insights into the tumor microenvironment (TME) have highlighted the pivotal role of amino acid metabolism—one of the three core metabolic pathways—in driving tumor proliferation, metastasis, and resistance to therapy. Taurine, a conditionally essential amino acid abundantly present in various tissues, does not participate in protein synthesis but exhibits multiple biological functions, including antioxidant, anti-inflammatory, and cytoprotective effects. These properties are increasingly recognized as relevant in both physiological regulation and pathological conditions such as cancer. Emerging evidence suggests that taurine modulates tumor growth and progression through diverse mechanisms, including regulation of immune responses, redox homeostasis, cellular metabolism, and the TME. This review summarizes the multifaceted roles of taurine in tumorigenesis and its potential applications in cancer therapy, providing new perspectives for targeted intervention.

## 25COASOCT107

**Title: The immunosuppressive microenvironment modulated by glioma-associated mesenchymal stem cells: Current status and potential strategies**

Yuyi Wu, Qiang Liu , Wei Xiang et.al.

BBA-Review on Cancer, Volume 1880, Issue 5, October 2025, 189410

<https://doi.org/10.1016/j.bbcan.2025.189410>

**Abstract:** Glioma, the most prevalent primary malignant tumor of the central nervous system, exhibits aggressive progression and poor prognosis, largely due to its highly immunosuppressive tumor microenvironment (TME). Glioma-associated mesenchymal stem cells (GA-MSCs), a key component of the glioma TME, play a dual and context-dependent role in tumor biology. On one hand, GA-MSCs actively shape immunosuppression by interacting with various immune cells—including T cells, B cells, natural killer (NK) cells, dendritic cells (DCs), and macrophages—via soluble factors (e.g., TGF- $\beta$ , PGE2, miR-21) and cell-contact mechanisms, thereby facilitating tumor immune evasion. They also promote glioma progression by enhancing the stemness, invasiveness, and chemoresistance of glioma stem cells (GSCs) through pathways such as IL-6/STAT3 and mitochondrial transfer, while contributing to pathological angiogenesis via differentiation into pericytes and secretion of pro-angiogenic factors like VEGF. On the other hand, GA-MSCs possess therapeutic potential: genetically engineered GA-MSCs can secrete pro-inflammatory cytokines (e.g., IL-12, IFN- $\beta$ ) or immune checkpoint blockers (e.g., scFv-PD1) to reverse immunosuppression, serve as carriers for targeted delivery of chemotherapeutics, miRNAs, suicide genes, or oncolytic viruses, and enhance anti-tumor immune responses. However, clinical translation is hindered by challenges including residual immunosuppressive activity, unstable transgene expression, limited migration efficiency, and safety concerns. This review summarizes the complex mechanisms by which GA-MSCs modulate the glioma TME, highlights their bidirectional roles in tumor progression and immunotherapy, and discusses potential strategies to overcome current limitations, aiming to provide insights for developing novel therapies targeting GA-MSCs and their interactions within the glioma microenvironment.

**25COASOCT108****Title: Anoikis and NETosis in colorectal cancer liver metastasis: the relationship and perspectives**

Ruoyu Zhang, Yunfei Tan, Dedi Jiang et.al.

BBA-Review on Cancer, Volume 1880, Issue 5, October 2025, 189401

<https://doi.org/10.1016/j.bbcan.2025.189401>

**Abstract:** Colorectal cancer (CRC) is a leading cause of cancer-related mortality, with metastatic spread being the primary reason for fatalities. Anoikis, a form of programmed cell death triggered by cell detachment from the extracellular matrix (ECM), and NETosis, a neutrophil cell death mode releasing extracellular traps (NETs), play critical roles in CRC liver metastasis (CRCLM). This review explores the mechanisms of anoikis and NETosis, their interplay, and genetic underpinnings in CRCLM. Anoikis resistance in CRC cells allows survival during metastasis in the initial stage, while NETs promote tumor progression by facilitating immune evasion, ECM remodeling, and angiogenesis. Meanwhile, through bioinformatics analysis and summary, we elaborated on the relationship between anoikis and NETosis as well as the potential interaction mechanisms, exploring the connecting links between them. The crosstalk between these processes is analyzed, highlighting shared signaling pathways (e.g., PI3K/AKT, MAPK, EMT) and potential biomarkers (e.g., MUC13, GLI2, SIRT6, FASN). Therapeutic strategies targeting anoikis and NETosis, including inhibitors of integrins, EGFR, and NET components (e.g., DNase I, CXCR2 antagonists), inhibitors of autophagy (e.g., CQ, HCQ, azithromycin) are discussed. This comprehensive analysis advances understanding of CRCLM pathogenesis and provides novel perspectives for targeted interventions.

**25COASOCT109****Title: Reprogramming of amino acid metabolism in breast cancer**

Meijin Wang, Yunlu Zhang, Zhenhua Li et.al.

BBA-Review on Cancer, Volume 1880, Issue 5, October 2025, 189412

<https://doi.org/10.1016/j.bbcan.2025.189412>

**Abstract:** Breast cancer is one of the most prevalent malignant tumours, representing a significant health risk for women. Subtyping of breast cancer is based on gene expression profiles, with five distinct subtypes identified Luminal A, Luminal B, HER2-positive, basal-like and normal-like. The heterogeneity of breast cancer represents a significant challenge to its treatment, while drug resistance limits the effectiveness of existing therapies. There is widespread amino acid metabolic reprogramming in breast cancer, and the altered amino acid metabolism observed in breast cancer cells exhibits a heterogeneous metabolic phenotype that differs from normal cells. Consequently, targeting the metabolic differences between breast and normal cells may represent a promising novel anti-cancer strategy. In this article, we review the alterations in the metabolism of amino acids such as glutamine, cystine, serine, glycine, tryptophan and arginine in breast cancer and explore the specific mechanisms by which the aberrant expression of various amino acid metabolism-related enzymes leads to alterations in the proliferative, invasive and metastatic capacities of cancer cells. Finally, we summarise the drugs targeting amino acid metabolism in breast cancer that are currently in preclinical and clinical trials, providing a theoretical basis for targeted therapy of amino acid metabolism.

**25COASOCT110****Title: Metabolic insights into TAMs and the tumor immune microenvironment: Regulatory mechanisms and therapeutic interventions**

Lei Yang, Yingying Shao, Zewen Zhang et. al.

BBA-Review on Cancer, Volume 1880, Issue 5, October 2025, 189411

<https://doi.org/10.1016/j.bbcan.2025.189411>

**Abstract:** Tumor-associated macrophages (TAMs) are pivotal regulators of the tumor immune microenvironment exhibiting a dual role in tumor therapy by functioning as both pro-tumorigenic effectors and anti-tumor agents. Tumor cells reprogram macrophages towards the pro-tumorigenic M2 phenotype through the induction of signaling molecules and manipulation of metabolic pathways. Recent evidence indicates that the interplay between TAM functional polarization and metabolic reprogramming profoundly influences anti-tumor immunity across multiple dimensions. TAMs, in turn, collectively modulate the immunosuppressive niche via a complex interaction network involving dynamic metabolite exchange, immune checkpoint signaling, and sensing of the physical microenvironment. In this review, we integrate current understanding of TAM metabolic networks, elucidate key mechanisms by which they remodel the immunosuppressive microenvironment through metabolic crosstalk, and outline emerging therapeutic strategies targeting TAMs to overcome current treatment limitations.

**25COASOCT111****Title: GABAergic signaling in colorectal cancer: Mechanistic insights, tumor microenvironment crosstalk, and therapeutic opportunities**

Donghao Tang, Paola Orlandi, Qijie Li et.al.

BBA-Review on Cancer, Volume 1880, Issue 5, October 2025, 189414

<https://doi.org/10.1016/j.bbcan.2025.189414>

**Abstract:**  $\gamma$ -Aminobutyric acid (GABA) and its receptors have emerged as critical modulators of colorectal cancer (CRC) progression and the tumor microenvironment (TME). Although GABA is traditionally recognized as an inhibitory neurotransmitter in the central nervous system, recent studies have uncovered its complex and sometimes paradoxical roles in cancer biology. In vivo, elevated GABA levels in CRC tissues have been associated with enhanced tumor growth, immune evasion, and metabolic adaptation. In contrast, in vitro studies suggest that exogenous GABA and GABA receptor agonists can inhibit CRC cell proliferation, highlighting a context-dependent role for GABAergic signaling. This duality may stem from variations in GABA receptor subtype expression, tumor-intrinsic metabolic reprogramming, and immune modulation within the TME. A better understanding of these mechanisms may offer new therapeutic opportunities. In this review, we summarize recent advances in the field, focusing on the molecular mechanisms, immune and metabolic interactions, and therapeutic potential of targeting GABAergic signaling in colorectal cancer.

**25COASOCT112****Title: Targeting lipid metabolism to enhance cancer immunotherapy**

Dan Zhao, Lei Wu, Yongsheng Li et.al.

BBA-Review on Cancer, Volume 1880, Issue 5, October 2025, 189416

<https://doi.org/10.1016/j.bbcan.2025.189416>

**Abstract:** In recent years, the interaction between lipid metabolism and immune checkpoint inhibitors (ICIs) has become a key area of research in cancer treatment. Tumor cells utilize lipid metabolism reprogramming to promote rapid proliferation, evade immune surveillance, and develop resistance to treatment, highlighting the significant role of lipid metabolism in cancer progression and immune regulation. This review analyzes the mechanisms by which lipid metabolism reshapes the tumor microenvironment (TME) and collaborates with ICIs to enhance therapeutic effects. We discussed how lipid metabolism regulates tumor phenotypes and summarized the impact of dysregulated lipid metabolism on infiltrating immune cells in the TME. We propose that targeting lipid metabolism may be a promising strategy for improving immunotherapy. Furthermore, we suggest that lipid metabolism can serve as a predictive biomarker for the response to immunotherapy and guide the immunotherapy process. Finally, we outline future research directions, including the development of innovative drugs targeting lipid metabolism to enhance the effectiveness of immunotherapy.

### 25COASOCT113

**Title: Histological transformation in lung cancer: Mechanisms, clinical characteristics, and therapeutic approaches**

Shiyi Liu, Tao Xu, Xiaojing Cao et.al.

BBA-Review on Cancer, Volume 1880, Issue 5, October 2025, 189413

<https://doi.org/10.1016/j.bbcan.2025.189413>

**Abstract:** Lung cancer, the leading cause of cancer-related mortality globally, exhibits remarkable histological plasticity, with non-small cell lung cancer (NSCLC) frequently transforming into small cell lung cancer (SCLC) as a resistance mechanism to targeted therapies and immunotherapies. The molecular mechanisms and treatments for SCLC transformation remain unclear. This review analyzes the mechanisms, molecular features, and treatment landscape of histological transformation, particularly in EGFR-mutant NSCLC. Key findings include: (1) RB1 and TP53 co-inactivation is a hallmark of transformed SCLC, enabling lineage plasticity via epigenetic and neuroendocrine changes; (2) the tumor immune microenvironment becomes immunosuppressive during transformation; and (3) new therapies targeting DLL3 and AURKA show promise in early trials. This study offers a comprehensive framework to understand histological transformation in lung cancer. It underscores the importance of routine re-biopsies for early detection and supports the development of biomarker-guided therapies. Future research should validate predictive biomarkers and optimizing combination therapies for transformed SCLC.

### 25COASOCT114

**Title: From infection to immune exhaustion: The Epstein-Barr virus and its contribution to Immunosenescence**

Longtai Hu, Tongxi Zhu, Jingyi Long et.al.

BBA-Review on Cancer, Volume 1880, Issue 5, October 2025, 189421

<https://doi.org/10.1016/j.bbcan.2025.189421>

**Abstract:** Epstein-Barr virus (EBV), a common herpesvirus, is linked to chronic infections and malignancies like lymphomas and nasopharyngeal carcinoma. EBV's evasion of immune surveillance and induction of immune dysfunction are critical for disease progression. This review explores how EBV drives immune exhaustion and immunosenescence, focusing on its

effects on T and NK cells. Chronic EBV infection causes persistent antigenic stimulation and upregulation of immune checkpoint molecules (PD-1, LAG-3, TIM-3, CTLA-4), leading to reduced T and NK cell proliferation, cytokine secretion, and cytotoxicity-hallmarks of immune exhaustion. EBV also modulates cytokines (IL-10, IL-18, IL-6, TNF- $\alpha$ ), further disrupting immune surveillance and promoting tumor growth within the tumor microenvironment. Furthermore, EBV infection is associated with expanded populations of exhausted immune cells (CD28<sup>-</sup> CD8<sup>+</sup> T cells and CD56dim NK cells), markers of immune dysfunction and aging. Immunotherapies, such as checkpoint inhibitors, offer promise for reversing EBV-induced immune exhaustion and restoring anti-tumor immunity. This review highlights EBV's role in immune regulation and the therapeutic potential of targeting EBV-driven immune dysfunction.

### 25COASOCT115

#### **Title: Inhibition of nucleotide excision repair proteins associated with cancer chemotherapy**

Francesco Gentile, Emeline Cros-Perrial, Lars Petter Jordheim

BBA-Review on Cancer, Volume 1880, Issue 5, October 2025, 189408

<https://doi.org/10.1016/j.bbcan.2025.189408>

**Abstract:** DNA repair is involved in the cellular response to alkylating agents used for the treatment of various cancers, decreasing the damages induced by the compounds and thus limiting the efficacy of the drugs. The inhibition of DNA repair should therefore increase the cytotoxic effect of alkylating agents, and this has been suggested as a therapeutic approach to increase clinical success. In this review, we focus on proteins involved in Nucleotide Excision Repair (NER) with a particular emphasis on the heterodimer ERCC1/XPF, and give an overview of preclinical and clinical studies underlying this therapeutic approach, as well as details on studies and compounds with notable activities. We also discuss the use of computer-aided methods to develop small molecule inhibitors targeting NER-related proteins, with a focus on structure-based virtual screening, and reflect on future perspectives on this topic. Although interesting results are obtained on cell models with various molecules, we believe new efforts are needed in order to validate the proof of concept in vivo and to translate the use of NER inhibitors in cancer patients.

### 25COASOCT116

#### **Title: Liquid-liquid phase separation: A dynamic driver of hepatocellular carcinoma**

Tianle Zhou, Lei Li, Yuping Chen

BBA-Review on Cancer, Volume 1880, Issue 5, October 2025, 189418

<https://doi.org/10.1016/j.bbcan.2025.189418>

**Abstract:** Liquid-liquid phase separation (LLPS) is a physicochemical phenomenon prevalent in eukaryotic cells, mediating the compartmentalization of discrete subcellular regions through the formation of membrane-less organelles and biomolecular condensates and thereby enabling precise spatiotemporal regulation of cellular physiological processes. LLPS dysregulation constitutes a pathogenic mechanism underlying various diseases, with accumulating evidence demonstrating its critical involvement in hepatocellular carcinoma (HCC) progression. Here, we summarize the biophysical principles governing LLPS and the biological characteristics of intracellular phase separation, and primarily discuss the



mechanistic contributions of aberrant LLPS to HCC pathogenesis, including disrupted gene expression, signal transduction, stress adaptation, etc. We further propose future research directions on LLPS in HCC and highlight its therapeutic potential through pharmacological modulation, aiming to provide novel perspectives for understanding the pathology of HCC and offer new therapeutic targets to facilitate effective strategies for HCC treatment.

## 25COASOCT117

**Title: STIM1-mediated calcium signalling in cancer: Its relation to tumour aggressiveness and therapeutic horizons**

Songling Fang, Yan Wang, Zixian Huang et.al.

BBA-Review on Cancer, Volume 1880, Issue 5, October 2025, 189420

<https://doi.org/10.1016/j.bbcan.2025.189420>

**Abstract:** Calcium ions (Ca<sup>2+</sup>), pivotal regulators of tumour progression, drive cancer metastasis and therapy resistance via STIM1-mediated store-operated calcium entry (SOCE). This review focuses on the role of STIM1 and SOCE-mediated calcium signalling in various cancer types, with particular emphasis on oral cancer as a key area of our research, and future research directions in these areas are proposed. Specifically, this review reveals the mechanism by which the STIM1/Orai1 complex activates calmodulin (CaM)-dependent effectors to promote epithelial–mesenchymal transition (EMT) and remodelling of the cytoskeleton and immunosuppressive microenvironment. Clinically, STIM1 overexpression is correlated with advanced tumour stage, chemoresistance, and a poor prognosis, highlighting its dual role as a prognostic biomarker and therapeutic target. Although preclinical studies have demonstrated that calcium release-activated calcium (CRAC) channel inhibitors suppress tumour growth, challenges such as calcium signalling complexity and tissue-specific toxicity persist. Future research should integrate emerging technologies and systematic approaches to clarify the mechanisms underlying the dynamic regulation of calcium signalling networks, which will ultimately accelerate their clinical translation and therapeutic application.

## 25COASOCT118

**Title: Targeting cholesterol metabolism in tumor and its immune microenvironment: opportunities and challenges**

Ziyi Wang, Xinyan Li , Xiangyu Sun et.al.

BBA-Review on Cancer, Volume 1880, Issue 5, October 2025, 189422

<https://doi.org/10.1016/j.bbcan.2025.189422>

**Abstract:** Cholesterol metabolism provides cell and organelle membrane components, and its precursors and derivatives exert a variety of biological functions. Dysregulated cholesterol metabolism has emerged as a hallmark of tumors. In the tumor microenvironment, cell-intrinsic and cell-extrinsic cues reprogram cholesterol metabolism to drive tumorigenesis and tumor development. Clinical studies and mechanistic investigations into cholesterol metabolism pathways have uncovered novel metabolic vulnerabilities that hold promise for cholesterol metabolism-targeted therapies for cancer. Moreover, recent studies highlight that manipulating cholesterol metabolism could reshape the immunological landscape and re-boost anti-tumor immunity. Thus, it is critical to deeply discuss the role of cholesterol metabolism in tumors and immune microenvironment to extend this knowledge into current

immunotherapies. In this review, we summarize current insights into reprogrammed cholesterol metabolism in tumors and explore the complex interplay between cholesterol metabolism and anti-tumor immunity in diverse immune components within the tumor microenvironment. These findings may provide novel clinical strategies for targeting cholesterol metabolism in the context of cancers.

## 25COASOCT119

### **Title: Olfactomedin 4 in cancer development and progression**

Wenli Liu, Griffin P. Rodgers

BBA-Review on Cancer, Volume 1880, Issue 5, October 2025, 189423

<https://doi.org/10.1016/j.bbcan.2025.189423>

**Abstract:** Olfactomedin 4 (OLFM4) is endogenously expressed in several normal human tissues and exerts its biological functions through its diverse binding partners on both the cell surface and intracellularly. OLFM4 is involved in multiple cellular functions, such as proliferation, apoptosis, and adhesion. OLFM4 is also a target gene in several important inflammation- and cancer-related pathways, and OLFM4 plays important roles in both infectious and inflammatory diseases and a variety of cancers. Studies of OLFM4 expression and function in cancer development and progression in numerous cancers indicate that OLFM4 exerts tumor-suppressing or tumor-promoting effects depending on the tissue and cellular context, and that OLFM4 is aberrantly expressed and functionally involved in multiple human cancers through different mechanisms. In cancers where OLFM4 is upregulated or plays a tumor-promoting role, therapies designed to inhibit OLFM4 expression may be clinically beneficial. OLFM4 could also have utility as a biomarker for early detection and diagnosis of precancerous states in several human cancers.

## 25COASOCT120

### **Title: Integrating multi-omics proteomic approaches in deciphering the tumor microenvironment and therapeutic resistance mechanisms in prostate cancer**

Yutao Wang, Fan Wang, Qi Pan et.al.

BBA-Review on Cancer, Volume 1880, Issue 5, October 2025, 189426

<https://doi.org/10.1016/j.bbcan.2025.189426>

**Abstract:** Prostate cancer (PCa) is one of the main causes of cancer-related mortality. The tumor microenvironment (TME) and the development of drug resistance pose significant challenges to effective cancer therapy. This review explores the integration of multi-omics proteomic approaches to decipher the complex interactions within the TME and the mechanisms driving resistance in PCa. We discuss how proteomics and genomics, transcriptomics, and metabolomics enhance our understanding of the molecular drivers of cancer progression, immune evasion, and treatment failure. Emphasis is placed on recent advances in proteomic profiling of the TME, including extracellular matrix components and immune regulators, and how single-cell proteomics provides insights into tumor heterogeneity. We also highlight the multi-omics role in identifying post-translational modifications and kinase pathways contributing to therapeutic resistance, and its implications for biomarker discovery and personalized medicine. The review concludes by addressing the clinical potential of multi-omics approaches and their future role in improving outcomes for prostate cancer patients.

**25COASOCT121****Title: The dysregulated YY1-EZH2-RKIP axis in cancer cells and immune evasion**

Talia Festekdjian, Benjamin Bonavida

BBA-Review on Cancer, Volume 1880, Issue 5, October 2025, 189424

<https://doi.org/10.1016/j.bbcan.2025.189424>

**Abstract:** We have recently witnessed several milestones in the treatment of a subset of cancer patients with immunotherapy and resulting in significant clinical responses. However, there is a subset that is unresponsive due to resistant factors in the cancer cells that are responsible for immune evasion. The characterization of such factors might lead to novel targeted therapies to restore the anti-tumor immunotherapies. We describe three dysregulated gene products, namely, Yin Yang1 (YY1), EZH2, and RKIP (PEBP1), that play pivotal roles in immune evasion. We report on the various molecular regulatory roles and signaling pathways that lead to the overexpression of YY1 and EZH2 and under expression of RKIP in cancer cells and established cross-talk signaling pathways amongst these three gene products. Such cross-talks established the dysregulated YY1-EZH2-RKIP axis and its pivotal role in the regulation of immune evasion. Thus, this axis is a potentially new therapeutic target to inhibit immune evasion by targeting the inhibition of YY1 or EZH2 or the induction of RKIP. Various agents are discussed to target each of these gene products, alone or in combination, to be investigated preclinically. However, the specific targeting to the tumor cells and sparing normal tissues is challenging, though new approaches are feasible.

**25COASOCT122****Title: Elucidating cellular origins and TME dynamic evolution in NSCLC through multi-omics technologies**

Ning Ning Chao, Li Zhang

BBA-Review on Cancer, Volume 1880, Issue 5, October 2025, 189425

<https://doi.org/10.1016/j.bbcan.2025.189425>

**Abstract:** Non-small cell lung cancer (NSCLC) is a leading cause of cancer mortality. Despite progress in targeted therapies and immunotherapy, resistance driven by tumor heterogeneity and dynamic tumor microenvironment (TME) remodeling persists. Multi-omics (single-cell/spatial transcriptomics) reveals lung adenocarcinoma (LUAD) origins in alveolar type 2 (AT2) cells and lineage plasticity via SOX2/WNT/YAP pathways driving aggressive subtypes. The TME, a dynamic ecosystem of immune cells and fibroblasts, evolves through immune-editing phases and cancer-associated fibroblasts (CAF)/tumor-associated macrophage (TAM) crosstalk to foster immunosuppression. Multi-omics identifies key immune subsets (CXCL13+CD8+T cells, M1/M2 macrophages) and antigen-presenting cancer-associated fibroblasts (apCAFs) as therapeutic targets. Emerging strategies targeting lineage plasticity, TME reprogramming, and microbiome modulation may overcome immune checkpoint blockade (ICB)/tyrosine kinase inhibitor (TKI) resistance. Challenges in spatiotemporal heterogeneity resolution call for artificial intelligence (AI)-driven TME modeling to guide precision interventions. This review highlights multi-omics in bridging NSCLC evolution with clinical translation for personalized therapies.

**25COASOCT123****Title: Multidimensional technological advances in cervical cancer screening: From**

**standardized processes to precision medicine**

Xiang Li, Jiaxin Zheng, Chang Liu

BBA-Review on Cancer, Volume 1880, Issue 5, October 2025, 189432

<https://doi.org/10.1016/j.bbcan.2025.189432>

**Abstract:** Cervical cancer is a common malignancy among women worldwide. To address this significant public health issue, the World Health Organization launched the “Eliminating Cervical Cancer” initiative. Effective screening of cervical cancer is crucial for reducing its morbidity and mortality. With continuous technological advancements, cervical cancer screening has evolved from traditional cytology and human papillomavirus (HPV) testing models to a new era of multidimensional, multilevel, and precise screening. This comprehensive review focuses on the core progress of screening technology in recent years, including the innovation of traditional screening methods, noninvasive optical imaging, molecular diagnosis from the perspective of precision medicine, and the deep integration and empowerment of artificial intelligence in the entire screening process. Cervical liquid-based cytology, combined with automated cell sorting technology and intelligent whole-slide image analysis, has achieved high-throughput identification of abnormal cells. The accuracy and specificity of HPV and multiomic biomarker detection technologies have significantly improved, providing a new basis for the accurate triage of patients with high-risk infections. Noninvasive cervical imaging technology already offers early identification of cervical precancerous lesions at the molecular level, combining ease of use with good patient acceptance. Notably, artificial intelligence technology is being integrated into multiple screening processes, leveraging horizontal integration and cross-platform capabilities in image recognition, risk assessment, auxiliary diagnosis, and automated testing processes, becoming a key driver of innovation in screening systems.

**25COASOCT124****Title: Role of mesenchymal stem cells in modulating cytokine networks and immune checkpoints in gastric cancer therapy**

Zakari Shaibu, Isah Adamu Danbala , Zhihong Chen et.al.

BBA-Review on Cancer, Volume 1880, Issue 5, October 2025, 189433

<https://doi.org/10.1016/j.bbcan.2025.189433>

**Abstract:** Gastric cancer (GC) remains a leading cause of cancer-related mortality worldwide, driven by a complex tumor microenvironment (TME) that promotes disease progression and therapeutic resistance. This review explores the pivotal roles of mesenchymal stem cells (MSCs), cytokines, and immune checkpoint inhibitors (ICIs) in shaping the immunosuppressive GC TME, with emphasis on their interaction and implications for immunotherapy. MSCs secrete cytokines such as IL-6, TGF- $\beta$ , and IL-10, fostering an immunosuppressive milieu that enables tumor growth, immune evasion, and resistance to ICIs. We synthesize current knowledge on how MSC-derived cytokines regulate immune checkpoint expression, suppress anti-tumor immunity, and contribute to TME heterogeneity. Additionally, we discuss therapeutic strategies targeting MSC-cytokine-immune checkpoint interactions to enhance ICI efficacy and improve clinical outcomes. Emerging approaches including MSC reprogramming, exosome-based therapies, and multi-omics technologies are highlighted as promising avenues to decipher TME complexity and develop personalized immunotherapies. By elucidating mechanisms of MSC-mediated

immune modulation in GC, this review aims to inspire novel strategies to overcome therapeutic resistance in this challenging disease.

## 25COASOCT125

**Title: Molecular mechanisms of TAM-regulated tumorigenesis and progression in various types of radiotherapy and future prospects of radiation-immunotherapy combinations**

Luyu Liao , Yuzhao Jin, Wei Mao et.al.

BBA-Review on Cancer, Volume 1880, Issue 5, October 2025, 189434

<https://doi.org/10.1016/j.bbcan.2025.189434>

**Abstract:** Although conventional photon radiotherapy can eradicate tumors, the presence of radioresistance has limited treatment efficacy. Nowadays the multiple radiotherapies carried out around different physics beam types will provide more options for tumor treatment. Under the current trend of anti-tumor immunotherapy, tumor-associated macrophages (TAMs), as an important component of the tumor microenvironment, significantly influence tumor progression and prognosis of comprehensive tumor therapy through reciprocal regulation with radiotherapy. The aim of this review is to summarize the influence of radiotherapy with various beam types on the biological effects of TAMs, and to explore the physiological basis for the conjunction of radiotherapy and immunotherapy based on TAMs. Ultimately, these data will provide an evidence-based medical rationale and translational research basis for optimizing the combination of radiotherapy and immunotherapy as a treatment modality for tumors in the future.

## 25COASOCT126

**Title: Unlocking the power of innate lymphoid cell plasticity in the tumor microenvironment: A revolutionary pathway for cancer immunotherapy**

Peng Yin , Pei Cao , Yu Liang et.al.

BBA-Review on Cancer, Volume 1880, Issue 5, October 2025, 189430

<https://doi.org/10.1016/j.bbcan.2025.189430>

**Abstract:** Innate lymphoid cells (ILCs) are emerging as powerful players in the immune system, capable of dramatically influencing tumor immunity. Their extraordinary plasticity, which allows them to adapt to dynamic changes in the tumor microenvironment, positions them as a double-edged sword in cancer immunotherapy. While they can drive anti-tumor immune responses, they can also promote tumor progression under certain conditions. In this review, we delve into the multifaceted roles of ILCs—focusing on ILC1, ILC2, and ILC3—and explore how their functional plasticity can be harnessed to shift their activities from immune suppression to potent anti-tumor actions. We highlight groundbreaking therapeutic strategies aimed at modulating ILC plasticity, such as metabolic reprogramming, cytokine therapy, and CAR-ILC1 therapy, each designed to enhance the anti-tumor potential of these cells. Despite the immense promise, challenges remain, including immune suppression within the TME and the short-lived efficacy of cytokines. However, targeting ILC plasticity offers a transformative approach to overcome these hurdles, presenting an opportunity to personalize cancer treatment and create tailored immunotherapies that dynamically modulate the immune response. This review underscores the game-changing potential of ILC-based therapies and provides insights into the next generation of cancer immunotherapies that could revolutionize



the fight against cancer.

### 25COASOCT127

**Title: Testicular germ cell tumors and infertility: Exploring epigenetic dysregulation in the journey of the male germ cell towards new biomarkers and therapeutics**

Bruno Oliveira-Lopes , Nuno Tiago Tavares , Rui Henrique et.al.

BBA-Review on Cancer, Volume 1880, Issue 5, October 2025, 189437

<https://doi.org/10.1016/j.bbcan.2025.189437>

**Abstract:** The development of male germ cells comprises a series of differentiation events that culminate in the formation of spermatozoa. From the primordial germ cell (PGC) to the spermatid, an array of epigenetic events take place in different stages of life. Disruptions in these mechanisms due to external factors can ultimately lead to decreased fertility and to testicular germ cell tumors (TGCTs). In this review, we highlight how DNA methylation, histone modifications and non-coding RNAs (ncRNAs) contribute to normal male germ cell development and discuss how disturbances in this epigenetic machinery can compromise fertility and induce neoplasia. Furthermore, the bidirectional relationship between infertility and TGCTs is discussed. Finally, we disclose the utility of “epidrugs” and ncRNAs as promising therapeutic options and TGCT biomarkers, respectively.

### 25COASOCT128

**Title: The role of clonal hematopoiesis of indeterminate potential in non-hematological malignancies of various origins**

Bo Zheng , Jie He , Wanqian Hu et.al.

BBA-Review on Cancer, Volume 1880, Issue 5, October 2025, 189442

<https://doi.org/10.1016/j.bbcan.2025.189442>

**Abstract:** Clonal hematopoiesis of indeterminate potential (CHIP) bridges hematopoietic clonality and solid tumorigenesis, unveiling a systemic dimension of somatic mutagenesis in cancer biology. Generally, population studies demonstrate CHIP carriers face elevated risks of cancer and poorer survival outcomes. This review consolidates current knowledge on the role of CHIP as potential biomarkers in the prediction/early detection/prognosis evaluation of various non-hematological cancers. We provide an overview of recent studies demonstrating the clinical consequences of CHIP including mosaic chromosomal alterations (mCA) across multiple cancer types. Furthermore, we collected the lab studies focusing on the impact of CHIP genes gain/loss in myeloid/lymphoid cells in non-hematological cancers, highlighting the underlying molecular mechanism and therapeutic targets. This review underscores the clinical impact of CHIP in non-hematological cancers, also the complicated cancer-regulating role of CHIP, highlighting targeting CHIP-associated pathways or integrating CHIP status into clinical decision-making could revolutionize precision oncology.

### 25COASOCT129

**Title: Osteoblasts in bone metastasis: Key players in the tumor microenvironment and therapeutic targets**

Lingxiao Jin, Zhenxuan Shao, Zhaoming Ye et.al.

BBA-Review on Cancer, Volume 1880, Issue 5, October 2025, 189435

<https://doi.org/10.1016/j.bbcan.2025.189435>

**Abstract:** Osteoblasts, recognized for their role in bone formation and mineral metabolism, are emerging as pivotal, although underexplored, regulators within the bone tumor microenvironment (TME). Despite increasing evidence of their involvement, their precise contributions to metastatic progression remain underappreciated. Recent studies reveal that osteoblasts orchestrate metastasis through dynamic, stage-specific interactions. In early colonization, they may attract tumor cells via CXCL12/CXCR4 signaling and remodel the metastatic niche. During dormancy, osteoblast-derived factors such as LIF, TGF $\beta$ 2, and BMP7, along with adhesion molecules such as N-cadherin, promote therapy resistance. Subsequently, osteoblasts can drive metastatic outgrowth through metabolic coupling (e.g., Ca<sup>2+</sup> transfer) and mTOR pathway activation. Beyond these direct effects on tumor cells, osteoblasts modulate the TME by interacting with osteoclasts and immune cells, suppressing CD8<sup>+</sup> T/NK cell activity while skewing macrophage polarization to promote immune evasion. Tumor-derived signals including PTHrP, BMPs, and ET-1, further reprogram osteoblasts into a tumor-supportive phenotype. Therapeutic approaches, such as RANKL inhibition, CXCL12 pathway blockade, TGF- $\beta$  superfamily antagonism, and osteoblast-targeted immunotherapies, offer promising directions for clinical intervention. Recognizing osteoblasts as central players in bone metastasis may provide new frontiers in bone-targeted cancer therapy.

## 25COASOCT130

**Title: Unveiling anaphylatoxins: Pioneering cancer therapies through complement system insights**

Jiamu Li , Xinqiao Li , Jinpeng Hu et.al.

BBA-Review on Cancer, Volume 1880, Issue 5, October 2025, 189436

<https://doi.org/10.1016/j.bbcan.2025.189436>

**Abstract:** The complement system, a cornerstone of innate immunity, plays pivotal roles in both defense and pathology, particularly through its anaphylatoxins, C3a and C5a. These small peptides, generated during complement activation, not only mediate pro-inflammatory responses but also contribute to the progression of various cancers by modulating the tumor microenvironment (TME). Anaphylatoxins influence tumor cell proliferation, epithelial-mesenchymal transition, angiogenesis, immune suppression, and therapy resistance via key signaling pathways such as PI3K/AKT, MEK/ERK, and p38 MAPK. This review summarizes recent findings on the roles of C3a and C5a in different tumor types, including glioma, lung cancer, melanoma, breast cancer, and hematological malignancies, highlighting their potential as biomarkers and therapeutic targets. Additionally, we discuss the development of anaphylatoxin inhibitors, their clinical applications, and the synergistic effects of combining these inhibitors with immune checkpoint blockade therapies. A deeper understanding of anaphylatoxin-mediated mechanisms may provide novel strategies for cancer diagnosis, prognosis, and treatment, paving the way for targeted and combination therapies to overcome tumor progression and immune evasion.

## 25COASOCT131

**Title: The CD39-CD73-adenosine axis: Master regulator of immune evasion and therapeutic target in pancreatic ductal adenocarcinoma**

Xiaolong Liu , Qingzhu Ding , Han Zhang et.al.

BBA-Review on Cancer, Volume 1880, Issue 5, October 2025, 189443

<https://doi.org/10.1016/j.bbcan.2025.189443>

**Abstract:** Pancreatic ductal adenocarcinoma (PDAC) exhibits persistent resistance to immunotherapy, with a 5-year survival rate around 10 %. The CD39-CD73-adenosine axis emerges as a critical mediator of immune evasion in PDAC, generating pathologically elevated adenosine concentrations that systematically suppress anti-tumor immunity. This purinergic pathway operates through sequential ATP hydrolysis by CD39 and CD73 ectonucleotidases, producing adenosine that engages four G-protein-coupled receptors (A1, A2A, A2B, A3) to orchestrate comprehensive immunosuppression. A2A and A2B receptors mediate the predominant immunosuppressive effects through cAMP-PKA signaling, inhibiting CD8<sup>+</sup> T cell and NK cell cytotoxicity while enhancing regulatory T cells, myeloid-derived suppressor cells, and M2-like tumor-associated macrophages. Cancer-associated fibroblasts and tumor cells contribute to adenosine production and respond to its signaling, establishing self-reinforcing immunosuppressive networks. Current therapeutic strategies demonstrate promising early clinical results, with multiple CD73 inhibitors, CD39 antagonists, and adenosine receptor antagonists under evaluation in PDAC trials. However, critical challenges remain: CD73's non-enzymatic functions promote chemoresistance independently of adenosine production, explaining why enzymatic inhibitors fail to enhance chemotherapy sensitivity. The spatial adenosine gradient within tumors, receptor-specific paradoxical effects, and compensatory resistance mechanisms through AMP accumulation further complicate therapeutic targeting. Multi-targeted approaches combining adenosine pathway inhibition with checkpoint blockade, chemotherapy, and stromal modulation show enhanced efficacy. Future directions include developing predictive biomarker panels, optimizing combination sequences, and designing inhibitors targeting both enzymatic and structural functions of purinergic enzymes. Understanding these complex interactions provides the foundation for transforming the adenosine pathway from an immunosuppressive barrier into a therapeutic opportunity in PDAC.

## 25COASOCT132

### **Title: Calcium and cancer metastasis: Discoveries from zebrafish xenografts**

Ghazala Rahman, Anamika Bhargava

BBA-Review on Cancer, Volume 1880, Issue 5, October 2025, 189446

<https://doi.org/10.1016/j.bbcan.2025.189446>

**Abstract:** Cancer metastasis remains the leading cause of cancer-related deaths, highlighting the urgent need for therapies targeting metastatic processes. Dysregulated calcium (Ca<sup>2+</sup>) signaling is increasingly linked to metastasis and offers a promising, underexplored therapeutic target. The zebrafish xenograft model has emerged as a powerful tool for studying cancer due to its optical transparency, genetic similarity to humans, and rapid development. This review outlines how zebrafish xenografts have been employed to investigate Ca<sup>2+</sup> signaling in cancer progression, revealing roles for ORAI1 in nasopharyngeal carcinoma, TRPM8 in prostate cancer, VDAC1 and TMBIM6 in breast cancer, and TRPV1 in gastric cancer. These studies highlight the zebrafish xenograft model's advantages in visualization, cost, and throughput over traditional systems. Despite its promise, the zebrafish xenograft model remains underutilized in Ca<sup>2+</sup>-related metastasis research. Future work using transgenic lines like tg-EGFP:flk1 and tg-GCaMP, CRISPR knockouts, morpholinos or

optogenetic approaches could unlock deeper insights and guide novel metastasis-targeting therapies.

### 25COASOCT133

#### **Title: Innate immune cells in oral squamous cell carcinoma: Characteristics and therapeutic potential**

Yinjie Jiang , Jingyi Cheng , Jianjun Wu et.al.

BBA-Review on Cancer, Volume 1880, Issue 5, October 2025, 189444

<https://doi.org/10.1016/j.bbcan.2025.189444>

**Abstract:** Innate immune cells play an important role in the immune system and are mainly responsible for the rapid response to foreign pathogens, damaged tissues, or abnormal cells. However, their immunophenotype in oral squamous cell carcinoma (OSCC) is altered due to the influence of various components within the tumour microenvironment, including tumour cells, cancer associated fibroblasts, and the extracellular matrix. This immunophenotypic shift results in the suppression of anti-tumour-related immune functions and active participation in further remodelling of the tumour microenvironment. These remodelled innate immune cells are further involved in crosstalk with other components within the tumour microenvironment (TME), resulting in tumour immune reprogramming via multiple pathways in a positive feedback manner. This process facilitates tumour development, metastasis, and immune evasion, while impeding the efficacy of tumour immunotherapy. Consequently, disrupting the positive feedback loop through which innate immune cells are remodelled and actively reprogrammed within the tumour microenvironment may improve therapeutic outcomes and prognosis of patients with OSCC. Therefore, this article aimed to provide an overview of the reprogramming patterns of innate immune cells within the TME of OSCC, and the major pathways through which these cells participate in the regulation of TME. Additionally, this review summarises and discusses therapeutic approaches targeting innate immune cells in OSCC, and provides novel insights for the development of treatment strategies targeting the functions of innate immune cells in OSCC.

### 25COASOCT134

#### **Title: Raf-kinase inhibitor protein (RKIP): A therapeutic target in colon cancer**

Seema Kumari , Sujatha Peela , Pallaval Veera Bramhachari et.al.

BBA-Review on Cancer, Volume 1880, Issue 5, October 2025, 189387

<https://doi.org/10.1016/j.bbcan.2025.189387>

**Abstract:** Raf-kinase inhibitor protein (RKIP) plays a significant role in maintaining cell homeostasis, and its downregulation is a hallmark of various cancers, including colorectal cancer (CRC). It modulates several signals, including MAPK (Raf/MEK/ERK), NF- $\kappa$ B, STAT3, cell cycle, and GPCR signaling by modulating phosphorylation state. It's binding to Raf-1 inhibits phosphorylation and makes the signaling molecules inactive. In the case of NF- $\kappa$ B, which plays a central role in drug resistance, RKIP interacts with I $\kappa$ B $\alpha$  and inhibits IKK $\alpha$ , IKK $\beta$ , and NIK by preventing their phosphorylation, thereby maintaining NF- $\kappa$ B in an inactive state. A reduction in the expression level of RKIP increases the metastasis and promotes the signaling associated with cancer progression. This review examines the role of RKIP in the aggressiveness and metastasis of CRC. Several signal pathways influenced by changes in the expression level of RKIP are discussed in detail. Strategies like the use of

inhibitors, understanding the role of miRNA, immunotherapy, and combined therapies have been discussed in detail, along with the clinical implications of RKIP in CRC.

### 25COASOCT135

#### **Title: Targeting the YY1-Bcl2-c-Myc Axis in the treatment of non-Hodgkin lymphoma**

Mai P. Ho , Evagelia Skouradaki , Stavroula Baritaki et.al.

BBA-Review on Cancer, Volume 1880, Issue 5, October 2025, 189395

<https://doi.org/10.1016/j.bbcan.2025.189395>

**Abstract:** Non-Hodgkin lymphoma (NHL) presents a complex therapeutic challenge due to its heterogeneous nature and the high incidence of relapse following initial treatment. As such, patients who are more susceptible to treatment resistance face a poor prognosis with limited treatment options. With recent advances, the direct targeting of overexpressed gene products is a novel therapeutic approach to overcome resistance mechanisms in unresponsive NHL patients. In the pathogenesis of NHL, we suspect aberrant deregulations amongst three major oncogenes: Yin Yang 1 (YY1), B-cell lymphoma 2 (Bcl-2), and Myelocytomatosis oncogene (c-Myc). Through analyses of the reported literature data, we have determined, indeed, multiple cross-talk signaling pathways (i.e. with factors MDM2, NF- $\kappa$ B, SENP1, TGF- $\beta$ , p53, ERK) for YY1, Bcl-2, and c-Myc that enable malignant cells to evade immune surveillance, promote tumor aggressiveness, and maintain resistance against various treatment modalities. In addition, we also present various approaches and agents to target each of the gene products, with discussion of challenges faced to generate such agents that specifically target the tumor cells.

### 25COASOCT136

#### **Title: Yin yang 1: a potential regulator of immune related diseases and cancer immunity**

Yutong Tan , Dan Ye, Cheng Qian et.al.

BBA-Review on Cancer, Volume 1880, Issue 5, October 2025, 189389

<https://doi.org/10.1016/j.bbcan.2025.189389>

**Abstract:** Yin Yang (YY1) is a context-dependent bifunctional transcription factor, activating or repressing target gene transcription via transcriptional or post-translational way, participate in multiple physiological processes including development, cell proliferation, differentiation, DNA repair and cell apoptosis. Recent reports show that YY1 also functions as a key transcription factor in immune response. Immune system dysfunction is closely related to various disease such as autoimmunity and cancer progression, how YY1 modulates immune related disease progression has not been systematically discussed. In addition, although YY1 has been widely reviewed to be a tumor promoter or suppressor, the role of YY1 in cancer immune microenvironment modulation and immune escape is not completely clear. This review provides an overview about the role of YY1 in immune related disease progression, and focused on discussing how YY1 affects cancer immune escape. Then we talked about recent strategies explored for YY1-targeted therapy including both preclinical and clinical studies. Finally, the challenges and limitations via targeting YY1 in future research is also discussed.



**25COASOCT137****Title: Role of YY1 in pancreatic ductal adenocarcinoma: Mechanisms and therapeutic perspectives**

Pallavi Pellakuru , Rachael Guenter , Niharitha Hariharan et.al.

BBA-Review on Cancer, Volume 1880, Issue 5, October 2025, 189415

<https://doi.org/10.1016/j.bbcan.2025.189415>

**Abstract:** YY1 (Yin Yang 1) is a transcription factor (TF) widely conserved across normal biological cells and solid tumors. It plays a key role in inflammation-related diseases and cancer, particularly pancreatic ductal adenocarcinoma (PDAC). In preclinical investigations, YY1 suppression has shown the ability to reduce PDAC growth, sensitize PDAC cells to chemotherapy, and induce apoptosis. Recent investigations have suggested the combination of YY1 inhibition with an immune checkpoint inhibitor for increased therapeutic effects; nevertheless, clinically, YY1-targeted treatment has yet to be adapted for PDAC. The current review summarizes YY1, its function in inflammation, PDAC progression, and the strategies for YY1-directed therapy involving small molecule inhibitors, gene editing, and RNA interference.

**25COASOCT138****Title: Heparanase as a therapeutic target for mitigating cancer progression**

Yogesh Kumar , Lokesh Gambhir , Gaurav Sharma

BBA-Review on Cancer, Volume 1880, Issue 5, October 2025, 189441

<https://doi.org/10.1016/j.bbcan.2025.189441>

**Abstract:** Cancer has been one of the primary causes of mortality for the last three decades across the globe, with contemporary treatment modalities often falling short due to limitations viz. drug resistance, toxicity, and the inability to target molecular mechanisms of tumor progression. Among various intracellular mediators implicated in cancer progression, heparanase, a heparan sulfate degrading enzyme, has been pivotal by facilitating tumor invasion, angiogenesis, and metastasis. Inhibiting the activity of heparanase is a promising therapeutic approach that can potentially curtail tumor growth and metastasis, offering a novel strategy to curb cancer progression. The present review underpins the discovery, structural features, and functional roles of heparanase, with a focus on its differential expression in normal and cancer cell state. Further, the review provides an insight in several classes of heparanase inhibitors including nucleic acid-based inhibitors, polysulfated saccharides, vaccines, miRNA, monoclonal antibodies, natural compounds and small molecule inhibitors along with their mechanism of action and potential benefits in cancer therapy. Recent advancements in heparanase inhibitor development, especially those agents that have moved into clinical trials and received patents is also highlighted thereby underscoring their therapeutic potential and commercial viability. The present review emphasizes over the potential of heparanase as a therapeutic agent and provides an extensive summary of actual endeavors to develop effective inhibitors that may substantiate the forthcoming landscape of cancer treatment.

**25COASOCT139****Title: The role of tissue factor in the tumor microenvironment and targeted therapy**

Ying Yan , Yifan Li , Dan Zou et.al.

BBA-Review on Cancer, Volume 1880, Issue 5, October 2025, 189409

<https://doi.org/10.1016/j.bbcan.2025.189409>

**Abstract:** Tissue factor (TF) serves as a pivotal initiator of coagulation and has been extensively acknowledged for its substantial involvement in cancer progression and metastasis. Recent evidence suggests that targeting TF can enhance the infiltration of immune effector cells, thereby reshape the tumor microenvironment (TME). Despite these advancements, a comprehensive review of TF's role within the TME has yet to be conducted. This review uniquely synthesizes emerging evidence on TF-mediated immunosuppression mechanisms and evaluates cutting-edge targeting strategies to overcome therapy resistance.

## 25COASOCT140

**Title: Mechanical stress and mechanosensitive protein in skin tumors**

Baixin Li, Shuang Zhao, Lingling Zhang et.al.

BBA-Review on Cancer, Volume 1880, Issue 5, October 2025, 189419

<https://doi.org/10.1016/j.bbcan.2025.189419>

**Abstract:** The skin is highly susceptible to external physical stimuli, and mechanical stresses contribute to certain skin tumors. Focusing on keloid, basal cell carcinoma, cutaneous squamous cell carcinoma and melanoma, we systematically examined the roles and mechanisms between mechanical stresses, such as tensile stress and matrix stiffness, and mechanosensitive proteins, including Piezo, transient receptor potential (TRP), integrin family, Yes-associated protein (YAP) and transcriptional coactivator with PDZ-binding motif (TAZ), in skin tumor progression. Additionally, we analyze existing research challenges and bottlenecks in this field. This review aims to further deepen the knowledge of skin tumorigenesis from the perspective of mechanical stress, which may help identify diagnostic and prognostic biomarkers and develop novel therapies, ultimately optimizing clinical management of skin tumors.

## 25COASOCT141

**Title: Mammary adipose dysfunction in the dual epidemic of obesity and breast cancer**

Elvina Jeyakumar, Sathyavathi Sundararaju, Stephanie Annett et.al.

Carcinogenesis, Volume 46, Issue 3, September 2025,

<https://doi.org/10.1093/carcin/bgaf053>

**Abstract:** Breast cancer (BC) is one of the leading causes of death among women, with obesity being a significant factor. Mammary adipose tissue (MAT) dysfunction in obesity creates a tumor-supportive environment, leading to increased risk. In obesity, MAT undergoes significant changes, including increased adiposity, chronic inflammation, aromatase overexpression, insulin resistance, and altered adipokine signaling, collectively fostering a protumorigenic microenvironment. The interaction between adipocytes and cancer cells further exacerbates BC progression through metabolic crosstalk and immune evasion. This review examines the role of MAT dysfunction in BC incidence and progression, in obesity. Interestingly, obesity appears to have a paradoxical effect on BC risk, offering a potentially protective role in premenopausal women, but increased risk in postmenopausal women, primarily due to differences in estrogen levels. Addressing the metabolic, inflammatory, and hormonal abnormalities in obese MAT can aid in enabling the development of precision therapies that reduce BC risk and improve treatment outcomes in

obese patients.

## 25COASOCT142

### **Title: Core transcriptional regulatory circuit-regulated IGF2BP3 stabilizes E2F2 mRNA via m6A modification in neuroblastoma**

Pengcheng Yang, Jianwei Wang, Ziheng Wu et.al.

Carcinogenesis, Volume 46, Issue 3, September 2025, bgaf040,

<https://doi.org/10.1093/carcin/bgaf040>

**Abstract:** Neuroblastoma (NB) is a pediatric tumor with diverse outcomes and unknown underlying mechanisms. The core transcriptional regulatory circuit (CRC) and N6-methyladenosine (m6A) are key factors that control cell identity and fate. IGF2BP3 is an m6A reader protein that is transcriptionally regulated by CRC transcription factors (TFs). In NB, this molecule is abundantly expressed, and there is a clear correlation between its expression and a bad prognosis. We mechanistically demonstrated that IGF2BP3 promotes E2F2 mRNA expression through m6A, which is correlated with high risk and poor prognosis in NB patients. We showed that the CRC TF-IGF2BP3-E2F2 regulatory axis forms an oncogenic network that drives NB development and progression. Overall, we investigated the molecular mechanism by which IGF2BP3, a m6A-reading protein that is regulated by CRC TFs, regulates E2F2 mRNA expression in an m6A-dependent manner. This study highlights the therapeutic potential of disrupting this axis with m6A-targeted interventions.

## 25COASOCT143

### **Title: Expression profile of Claudins 3, 4, and 7 in breast tumors and its correlation with clinicopathological features**

Reena Yadav, Sumit Goel, Laxmi Kumari et.al.

Carcinogenesis, Volume 46, Issue 3, September 2025, bgaf049,

<https://doi.org/10.1093/carcin/bgaf049>

**Abstract:** Claudins, integral components of tight junctions, play a pivotal role in maintaining cellular adhesion and polarity. Aberrant expression of claudins has been implicated in the progression of various malignancies, including breast cancer (BC). This study aims to elucidate the clinical relevance of claudins by studying the expression of Claudins 3, 4, and 7 in BC cell lines (CLs) and cancer tissues and correlating it with cellular properties and clinicopathological parameters. The transcriptional expression of Claudins 3, 4, and 7 was assessed in four BCCLs (MDA-MB-231, MDA-MB-468, T47D, and SKBR-3) and tumor tissues by using quantitative PCR. Correlations between claudin expression profiles and clinicopathological parameters, including tumor grade, lymph node involvement, and proliferative index, were evaluated in patient samples. Compared to normal breast tissue, all BCCLs exhibited downregulated expression of Claudins 3, 4, and 7. Differential expression was observed among CLs, with MDA-MB-231 exhibiting the lowest and MDA-MB-468 the highest levels. Among BC patient samples (n = 65), 97% demonstrated significant ( $P < 0.05$ ) dysregulation in the expression of one or more of these claudins. Prevalence of Claudins 3, 4, 7-low and -high tumors was found to be 29.23% and 21.53% respectively, in our patients. The former correlated significantly with adverse prognostic factors, including higher grade, nodal metastasis, and elevated proliferative indices. The pharmacological induction of Claudin 4 by celecoxib was found to attenuate cell viability, proliferation, and migration in

aggressive claudin-low BC cells. These findings underscore the potential utility of modulating claudins as a therapeutic strategy for managing claudin-low BCs.

#### 25COASOCT144

**Title: A novel serum biomarker Enhancer RNA RASSF8-AS1 promotes the progression of gastric cancer**

Xun Li, Xiaojue Chen, Bairong Chen et.al.

Carcinogenesis, Volume 46, Issue 3, September 2025, bgaf050,

<https://doi.org/10.1093/carcin/bgaf050>

**Abstract:** Gastric cancer (GC) is globally recognized as one of the most widespread malignant tumors. As the symptoms of patients with early GC are ambiguous, the majority of patients are given a diagnosis of advanced GC. Therefore, this necessitates the search for new biomarkers to be utilized in the early diagnosis and screening of GC. Enhancer RNA (eRNA) is a non-coding RNA in transcription by enhancers that is tumor-specific and has a critical function in cancer progression. Our research investigates new eRNAs as bio-diagnostic markers for GC. Four eRNAs with good differential expression in GC were screened by TCGA and University of California, Santa Cruz databases. Quantitative real-time PCR was utilized for testing the level of RASSF8-AS1. The diagnostic effect of RASSF8-AS1 was evaluated using the receiver operating characteristic (ROC). Functional experiments were used to detect the ability of RASSF8-AS1 to affect the metastasis and proliferation in GC cells. The expression of RASSF8-AS1 was obviously elevated in both GC tissues and serum, whereas it was decreased in the serum levels of postoperative GC patients. ROC showed that RASSF8-AS1 was more diagnostically efficient than common diagnostic biomarkers for GC and that diagnostic effectiveness could be better than combining them. The findings of in vitro experiments showed that knocking down the level of RASSF8-AS1 clearly suppressed the ability of growth and metastasis in GC cells. Studies have shown that serum RASSF8-AS1 has the potential to contribute to the progression of GC as a biomarker for diagnosis and prognostic monitoring of GC.

#### 25COASOCT145

**Title: HECTD3 E3 ligase mediates ubiquitination of AKT-phosphorylated CMTM3 in HER2-overexpressed breast cancer cells**

Jun Wang, Delong Wang, Xinxing Zhang et.al.

Carcinogenesis, Volume 46, Issue 3, September 2025, bgaf048,

<https://doi.org/10.1093/carcin/bgaf048>

**Abstract:** CKLF-like MARVEL transmembrane domain-containing (CMTM) proteins play pivotal roles in tumorigenesis and cancer progression across various malignancies. However, their expression profiles and regulatory mechanisms in distinct subtypes of breast cancer remain largely undefined. In this study, we systematically analysed the expression of all nine CMTM family members across major molecular subtypes of breast cancer, including Luminal A, Luminal B, HER2-positive (HER2+), and triple-negative breast cancer (TNBC). Among these, CMTM3 was uniquely downregulated in Luminal B and HER2+ breast cancer cells and functioned as a tumor suppressor. Overexpression of HER2 in normal breast epithelial cell lines led to the phosphorylation of CMTM3. Molecular and biochemical analyses revealed that HER2 overexpression activated the downstream phosphoinositide 3-

kinase (PI3K)/protein kinase B (also known as RAC-Alpha Serine/Threonine-Protein Kinase, AKT) signaling pathway in Luminal B and HER2+ breast cancer cells. AKT1 directly phosphorylated CMTM3 at serine 181 (Ser181), a modification that facilitated its recognition and ubiquitination by the E3 ligase HECT domain E3 ubiquitin protein ligase 3 (HECTD3), ultimately targeting CMTM3 for proteasomal degradation. Functional assays demonstrated that either knockdown of HECTD3 or pharmacological inhibition of PI3K/AKT signaling stabilized CMTM3 protein levels. Moreover, reintroducing a nonphosphorylatable CMTM3 mutant (CMTM3S181A) into CMTM3 knockout breast cancer cells resulted in significantly reduced proliferation, colony formation, invasive capacity, and in vivo tumor growth compared with cells expressing wild-type CMTM3 (CMTM3WT). Collectively, these findings reveal a previously unrecognized posttranslational regulatory mechanism of CMTM3 and suggest that targeting the PI3K/AKT–HECTD3–CMTM3 axis may offer a promising therapeutic approach for treating HER2+ breast cancers.

## 25COASOCT146

**Title: Targeted sequencing and functional interrogation identified novel variant at 12q14.2 associated with risk of ovarian cancer in Han Chinese women**

Yanrui Zhao, Wei Geng, Wei Liu et.al.

Carcinogenesis, Volume 46, Issue 3, September 2025, bgaf037,

<https://doi.org/10.1093/carcin/bgaf037>

**Abstract:** Chromosome 12q14.2 has been reported as a potential risk locus for epithelial ovarian cancer (EOC) in genome-wide association study (GWAS). We performed targeted sequencing around the rs11175194 at chromosome 12q14.2 and identified five potential risk variants. The association between these five variants and EOC risk was evaluated in 893 EOC cases and 1292 controls. We identified that rs11175195 ( $P = 1.94 \times 10^{-6}$ , OR = 1.36, 95% CI = 1.20–1.54) was significantly associated with EOC risk in validation study and after meta-analysis with previous GWAS data, rs11175195 reached genome-wide significant level ( $P < 5 \times 10^{-8}$ ). Functional annotation and expression quantitative trait loci analysis prioritized rs11175194 as a causal variant at this locus. The presence of G-rs11175194 risk allele increased binding affinity of the transcription factor NR1H4 and upregulate SRGAP1 gene expression. Overexpression of SRGAP1 promotes the proliferation and invasion in ovarian cancer cell lines. In conclusion, we identified a novel susceptibility locus of ovarian cancer and revealed a potential molecular mechanism for ovarian cancer carcinogenesis. These results may provide a potential biomarker and therapeutic target for ovarian cancer.

## 25COASOCT147

**Title: Associations of prediagnostic serum liver enzyme levels with lung cancer risk in predominantly low-income African and European Americans**

Shuai Xu, Hui Cai, Jie Wu et.al.

Carcinogenesis, Volume 46, Issue 3, September 2025, bgaf052,

<https://doi.org/10.1093/carcin/bgaf052>

**Abstract:** Previous studies have linked liver diseases to lung cancer (LC) risk; however, few studies evaluated the associations of circulating liver enzyme levels with LC risk. We conducted a study of 353 incident LC cases and 646 matched controls with baseline serum alanine aminotransferase (ALT) and of 548 cases and 1032 matched controls with baseline



serum alkaline phosphatase (ALP) nested within the Southern Community Cohort Study. Conditional logistic regression and generalized linear models were used to estimate adjusted odds ratios (ORs) and 95% confidence intervals (CIs) among all study participants and by stratification of potential effect modifiers. Most participants had clinically normal liver enzyme levels. Higher serum ALT levels were associated with reduced LC risk. Compared with the lowest tertile, participants in the second and third tertiles had OR (95% CI) of 0.74 (0.48–1.14) and 0.47 (0.28–0.78) (Ptrend < .01), respectively. The inverse association was observed in African Americans (AAs) and European Americans, which was especially prominent among men, and was seen in both those diagnosed within [ORT3 versus T1 = 0.41 (0.19–0.88)] and beyond [ORT3 versus T1 = 0.35 (0.17–0.73)] a median follow-up time of 39 months. Higher serum ALP levels were associated with increased LC risk among AA men only [ORT3 versus T1 = 2.01 (1.19–3.39)] (Ptrend < .01). Our results indicate that in a predominantly low-income American population, higher serum ALT levels may be related to lower LC risk. Further studies are warranted to confirm our findings and elucidate the potential underlying biological mechanisms of the associations.

## 25COASOCT148

### **Title: Epithelial Ikk $\beta$ deletion modulates immune responses and the IFN $\gamma$ /CXCL9 axis during early esophageal carcinogenesis**

Nathan Hodge, Marie-Pier T  treault

Carcinogenesis, Volume 46, Issue 3, September 2025, bgaf055,

<https://doi.org/10.1093/carcin/bgaf055>

**Abstract:** Esophageal cancer is a major cause of cancer-related death, often preceded with chronic inflammation and injuries. The NF $\kappa$ B/IKK $\beta$  pathway plays a central role in inflammation, yet its role in early esophageal carcinogenesis remains unclear. This study investigated the role of epithelial IKK $\beta$  in early esophageal carcinogenesis. Mice were treated with the carcinogen 4-nitroquinoline-1-oxide (4-NQO) or a vehicle for one month to induce precancerous lesions. Esophagi were harvested and examined through histological, protein, flow cytometry, and RNA analyses. Histological analysis revealed that 4-NQO treatment led to increased inflammation, intraepithelial CD45<sup>+</sup> immune cells, and elevated IKK $\beta$  phosphorylation levels. Mice with esophageal epithelial-specific Ikk $\beta$  deletion (4-NQO/Ikk $\beta$ EEC-KO) showed delayed progression to a precancerous state, with reduced immune cell recruitment compared to 4-NQO/controls. Immunophenotyping showed decreased recruitment of T cells, including CD4<sup>+</sup>, CD8<sup>+</sup> and regulatory (Tregs) T cells, and increased recruitment of macrophages in 4-NQO/Ikk $\beta$ EEC-KO mice compared with 4-NQO/controls. RNA sequencing data identified 262 differentially expressed genes in 4-NQO/Ikk $\beta$ EEC-KO mice, implicating pathways related to inflammation and wound healing. Notably, the chemokine CXCL9, a T cell chemoattractant, was significantly upregulated in 4-NQO control mice, but not in 4-NQO/Ikk $\beta$ EEC-KO mice. Further analysis identified IFN $\gamma$  as an upstream regulator of Cxcl9 expression, and neutralization of IFN $\gamma$  reduced Cxcl9 expression levels in 4-NQO treated mice. Additionally, in vitro studies demonstrated that IFN $\gamma$  upregulates Cxcl9 in an NF $\kappa$ B dependent manner in esophageal keratinocytes. These findings suggest that epithelial IKK $\beta$  regulates the immune microenvironment in early esophageal carcinogenesis through the IFN $\gamma$ /CXCL9 axis and influencing T cell recruitment and inflammatory responses.

**25COASOCT149****Title: Longitudinal single-cell RNA model aids prediction of EGFR-TKI resistance**

Guoxin Hou, Zhimin Lu, Dongqiang Zeng et.al.

Carcinogenesis, Volume 46, Issue 3, September 2025, bgaf038,

<https://doi.org/10.1093/carcin/bgaf038>

**Abstract:** Resistance is inevitable and a major challenge in treating lung adenocarcinoma (LUAD) patients with EGFR mutations. This study aimed to investigate the mechanism of EGFR-TKI resistance in LUAD using longitudinal single-cell RNA sequencing (scRNA-seq) data. We collected tumour samples of LUAD patients before and after EGFR inhibitor treatment and performed single-cell RNA sequencing. We used machine learning models for cell annotation and classified cells into subgroups. The inferCNV algorithm was used for CNV score calculation and tumour cell identification, and metabolic analysis was done using a gene-scoring approach. EGFR resistance score (ERscore), a gene signature derived from resistant tumour cells, was established to evaluate the predictiveness to EGFR-TKI inhibitors. The investigation classified subgroups of cells and identified three tumour cell types as critical cells mediating EGFR-TKI resistance. Our data also analysed the metabolic aspects of EGFR-TKI resistance using a single-cell approach. It showed that some tumour cell subtypes had a consistent metabolic profile, significantly up-regulating purine metabolism, oxidative phosphorylation, glycogen, and lipid metabolism. An assessment system called ERscore was established to evaluate the association between EGFR-TKI resistance and tumour ecosystem. The analysis showed a significant correlation between the ERscore and EGFR-TKI resistance, lung cancer phenotype, and prognosis. The findings suggest that the molecular mechanisms driving EGFR-TKI resistance in lung cancer may also contribute to poorer prognosis, particularly in lung adenocarcinomas with high EGFR mutation rates. Overall, the study provides important insights into the mechanisms of EGFR-TKI resistance in lung cancer at the single-cell level.

**25COASOCT150****Title: FZD6 promotes 5-fluorouracil resistance through inhibiting pyroptosis in colorectal cancer**

Zilong He, Jing Yang, Yu Zhang et.al.

Carcinogenesis, Volume 46, Issue 3, September 2025, bgaf041,

<https://doi.org/10.1093/carcin/bgaf041>

**Abstract:** Resistance to 5-fluorouracil (5-FU) causes treatment failure in most colorectal cancer (CRC) cases. Pyroptosis is associated with chemotherapy resistance, although its role in 5-FU resistance in CRC is not well understood. To investigate this, we performed proteomic sequencing and bioinformatics analysis on wild-type and 5-FU-resistant CRC cell lines. Subsequently, Frizzled receptor 6 (FZD6) knockdown and overexpression cell lines were established using a lentiviral system. CCK-8, colony formation, and EdU assays were performed to assess the viability and proliferative potential of 5-FU-treated cells. The morphological changes associated with pyroptosis were examined by microscopic imaging and electron microscopy. The nuclear expression of  $\beta$ -catenin was examined by immunofluorescence and western blotting. These findings indicated that FZD6 protein was upregulated in the 5-FU-resistant CRC cells compared with the corresponding wild-type cell lines, an observation further validated through immunohistochemical analysis of clinical

samples. Additionally, 5-FU treatment induced NLRP3/caspase-1/GSDMD-mediated classical pyroptosis in the wild-type CRC cells and decreased their viability, while the pyroptosis inhibitor Ac-FITD-CMK enhanced drug resistance. Furthermore, overexpression of FZD6 promoted nuclear translocation of  $\beta$ -catenin, reduced pyroptosis, and increased 5-FU resistance. In contrast, 5-FU treatment did not induce significant pyroptosis in drug-resistant cells, while pyroptosis inducers (nigericin or LPS + ATP) significantly reduced cell viability regardless of 5-FU. Moreover, knockdown of FZD6 decreased nuclear translocation of  $\beta$ -catenin, enhanced pyroptosis, and reduced 5-FU resistance. Finally,  $\beta$ -catenin knockdown enhanced pyroptosis and decreased 5-FU resistance. Thus, FZD6 promotes 5-FU resistance in CRC cells by inhibiting pyroptosis through increased nuclear translocation of  $\beta$ -catenin.

### 25COASOCT151

#### **Title: Generative Design of Functional Metal Complexes Utilizing the Internal Knowledge and Reasoning Capability of Large Language Models**

Jieyu Lu, Zhangde Song, Qiyuan Zhao et.al.

J. Am. Chem. Soc. 2025, 147, 36, 32377–32388

<https://doi.org/10.1021/jacs.5c02097>

**Abstract:** Large language models (LLMs) have shown promise in science, such as structure–property prediction and acting as AI agents, yet their intrinsic knowledge and reasoning capability for scientific discovery remains underexplored. We introduce LLM-EO, an integration of LLMs into evolutionary optimization, and demonstrate its success in optimizing transition metal complexes (TMCs). LLM-EO demonstrates advantages in few-sample learning due to the intrinsic chemical knowledge embedded within LLMs and their ability to leverage entire historical data collected during optimizations. Through natural language instructions, LLM-EO offers enhanced accessibility for multiobjective optimizations, potentially lowering barriers for experimental chemists without extensive programming expertise. As generative models, LLM-EO possesses the capability to propose novel ligands and TMCs with unique chemical properties by amalgamating both internal knowledge and external chemistry data, thus combining the benefits of efficient optimization and generation. With advancements in LLMs, both in their capacity as pretrained foundational models and new strategies in post-training inference, we anticipate broad applications of LLM-EO in chemistry and materials design.

### 25COASOCT152

#### **Title: Cosmic Blueprint to Nanoscale Design: Hoag’s Object-Like Polyoxovanadate Encapsulated by a Hierarchical Silver Nanocluster**

Wei-Dan Si, Hao Liang, Seung-Hyun Ji et.al.

J. Am. Chem. Soc. 2025, 147, 36, 32458–32467

<https://doi.org/10.1021/jacs.5c04995>

**Abstract:** The pervasive presence of toroidal architectures across scales, from molecular assemblies to cosmic formations, reveals a universal design principle that integrates aesthetic symmetry with functional topology in nature. Yet, constructing such hierarchical toroidal organization at the nanoscale, particularly for metal nanoclusters, remains an unmet challenge. We present an unprecedented wheel-shaped silver nanocluster,

[(V6O19C<sub>2</sub>V22O66)@Ag<sub>96</sub>(tBuPhC≡C)<sub>56</sub>(SO<sub>4</sub>)<sub>2</sub>(DMF)<sub>12</sub>]<sup>6+</sup> (Ag<sub>96</sub>), encapsulating an unparalleled hierarchical toroidal [V<sub>6</sub>O<sub>19</sub>C<sub>2</sub>V<sub>22</sub>O<sub>66</sub>]<sub>30</sub><sup>−</sup> polyoxovanadate (POV). The hierarchical toroidal [V<sub>6</sub>O<sub>19</sub>C<sub>2</sub>V<sub>22</sub>O<sub>66</sub>]<sub>30</sub><sup>−</sup> mirrors the core-shell geometry of Hoag's Object, a rare ring galaxy, with a Lindqvist-type [V<sub>6</sub>O<sub>19</sub>]<sub>8</sub><sup>−</sup> core enclosed by a macrocyclic [V<sub>22</sub>O<sub>66</sub>]<sub>22</sub><sup>−</sup> shell. This work constitutes a unique astronomical morphology in coinage metal nanoclusters, uncovering the universal principles of hierarchical self-assembly at the nanoscale. Leveraging the flexibility of POVs, we further isolated a bowl-shaped [(SO<sub>4</sub>@V<sub>15</sub>O<sub>42</sub>)@Ag<sub>46</sub>(tBuPhC≡C)<sub>31</sub>(DMF)<sub>2</sub>]<sup>4+</sup> (Ag<sub>46</sub>), encapsulating an open-cage [SO<sub>4</sub>@V<sub>15</sub>O<sub>42</sub>]<sub>11</sub><sup>−</sup> template by regulating the stoichiometric ratio. Due to their distinct structural configurations, these nanoclusters exhibit markedly different photothermal conversion performance when exposed to visible or near-infrared (NIR) lasers. This breakthrough positions POVs as versatile templates for engineering complex metal nanoclusters, opening new frontiers in materials science and nanotechnology.

## 25COASOCT153

### Title: Determination of Mn Valence States in Nanocatalysts During Sustainable Syngas Conversion

Zhiping Li, Duohua Liao, Guo Tian et.al.

J. Am. Chem. Soc. 2025, 147, 36, 32548–32559

<https://doi.org/10.1021/jacs.5c06550>

**Abstract:** Constructing structure–activity relationships (SAR) between nanocatalysts under reactive atmospheres makes them indispensable for chemical synthesis, energy transformation, and environmental remediation. However, this structure sensitivity remains ambiguous for metals/metal oxides due to dynamic changes in metal valences under a reductive atmosphere. Herein, this study delves into the complexities of Mn-based nanocatalysts, focusing on the impact of the Mn valence state in a test reaction converting sustainable syngas to aromatics—a process highly sensitive to the catalyst's redox environment and active site characteristics. We conducted a thorough SAR analysis and discovered a direct correlation between the Sabatier effect, CO adsorption, and the space-time yields of aromatics. Notably, Mn in the +2-oxidation state emerged as the optimal valence for achieving the highest catalytic performance, with a maximum yield of 1.6 mmol·h<sup>−1</sup>·g<sub>cat</sub><sup>−1</sup>. Our findings provide critical insights into the role of the catalyst's intrinsic properties in dictating the selectivity and efficiency of CO hydrogenation for the rational design of nanocatalysts that can sustainably transform small molecules into valuable chemicals and fuels.

## 25COASOCT154

### Title: Photochemical Generation of Peroxynitrite: Concurrent Inhibition of Glycolysis and Glutamine Metabolism for Enhanced Metabolic Therapy

Lizhen Yuan, Liang Yang, Wen Song et.al.

J. Am. Chem. Soc. 2025, 147, 36, 32610–32624

<https://doi.org/10.1021/jacs.5c07860>

**Abstract:** Disrupting homeostasis within tumor cells by interfering with their diverse metabolic pathways is an attractive tumor treatment method. However, current methods generally focus on one pathway within tumor cells, such as glycolysis or the glutamine (Gln)

metabolic pathway, overlooking potential strong correlations between different cellular pathways and preventing a comprehensive blockade of the tumor energy supply, thereby compromising therapeutic efficacy. Herein, a photochemistry-activated peroxynitrite (ONOO<sup>−</sup>) nanogenerator, capable of simultaneously inhibiting glycolysis and Gln metabolism in tumor cells, is proposed to achieve enhanced metabolic therapy. Specifically, the ONOO<sup>−</sup> nanogenerator is constructed by loading the thermally sensitive nitric oxide (NO) donor BNN-6 onto dual-function Prussian blue (PB) nanocubes through electrostatic interaction, followed by coating with tumor cell membranes to achieve homologous targeting. Under near-infrared light irradiation, PB decomposes hydrogen peroxide (H<sub>2</sub>O<sub>2</sub>) to produce oxygen, while the converted heat induces BNN-6 decomposition to generate NO. Subsequently, NO reacts with oxygen to form nitrite, and then with H<sub>2</sub>O<sub>2</sub> to yield ONOO<sup>−</sup> under acidic conditions. ONOO<sup>−</sup> achieves simultaneous inhibition of glycolysis and Gln metabolism through the nitration of key proteins. More importantly, the former effectively reduces lactate levels, and the latter increases Gln levels, which both, in turn, remodel the tumor microenvironment and stimulate a strong immune response. The *in vitro* and *in vivo* data demonstrated that these changes significantly inhibited the growth and spread of primary and distant metastatic tumors in a mouse model. This approach takes advantage of tumor-specific physicochemical properties to enable localized and highly efficient ONOO<sup>−</sup> synthesis, offering promise for enhanced metabolic therapy.

## 25COASOCT155

### **Title: Allenes as Stimuli-Responsive Chromophores for Visible to Near-Infrared Optical Modulation**

Jiaoyan Zhao, Lin Jiao, Lilia Kinziabulatova et.al.

J. Am. Chem. Soc. 2025, 147, 36, 32710–32716

<https://doi.org/10.1021/jacs.5c08383>

**Abstract:** Despite their rigid, orthogonal  $\pi$ -systems and synthetic modularity, allenes remain underexplored in functional material design. Here, we report that tetraaryl-substituted allenes undergo clean and reversible protonation at the central sp-hybridized carbon, triggering substantial  $\pi$ -electron reorganization. To investigate how substitution patterns modulate the halochromic response, we synthesized a series of five tetraaryllallenes, enabling a systematic structure–property relationship study of their optoelectronic behavior. Protonation induces large bathochromic shifts in absorption of up to 500 nm, with extinction coefficients exceeding 30,000 M<sup>−1</sup> cm<sup>−1</sup> in the near-infrared region. Frontier molecular orbital (FMO) analysis and time-dependent density functional theory (TD-DFT) calculations reveal pronounced delocalization upon protonation, resulting in polymethine-like electronic structures with tunable donor–acceptor character. Protonation occurs even with weak acids such as acetic acid, and the process remains fully reversible through base-mediated deprotonation. UV–vis–NIR spectroscopy and ultrafast transient absorption spectroscopy confirm the formation of charge-transfer states. These findings establish allenes as a synthetically accessible and tunable platform for reversible, stimuli-responsive optical modulation across the visible to NIR spectrum.

## 25COASOCT156

### **Title: The Radical S-Adenosyl-L-methionine Enzyme HydE Forms an Fe(I)Fe(I) Dimer**



**En Route to the [FeFe] Hydrogenase H-Cluster**

Guodong Rao, Lizhi Tao, Xin Yu et.al.

J. Am. Chem. Soc. 2025, 147, 36, 32737–32744

<https://doi.org/10.1021/jacs.5c08533>

**Abstract:** [FeFe] hydrogenases are highly efficient metalloenzymes that catalyze hydrogen conversion via a sophisticated active site cofactor known as the H-cluster. Biosynthesis of its [2Fe]H subcluster, which contains CO, CN<sup>−</sup>, and azadithiolate ligands, requires the action of several dedicated enzymes, including the radical S-adenosyl-l-methionine (rSAM) enzyme HydE. HydE has been proposed to convert a mononuclear [Fe(II)(cysteinate)(CO)<sub>2</sub>(CN)]<sup>−</sup> precursor into a dimeric [Fe<sub>2</sub>(SH)<sub>2</sub>(CO)<sub>4</sub>(CN)<sub>2</sub>]<sup>2−</sup> complex, yet direct characterization of this product species has remained elusive. Here, we report spectroscopic identification of the dimeric product of the HydE reaction in its one-electron oxidized, mixed-valent Fe<sup>1.5+</sup>Fe<sup>1.5+</sup> (S = 1/2) state. Continuous wave and pulse <sup>13</sup>C ENDOR spectroscopy confirm the presence of two nonequivalent CN<sup>−</sup> ligands and delocalized spin density across the diiron core. Oxidation of a synthetic [Fe<sub>2</sub>(SH)<sub>2</sub>(CO)<sub>4</sub>(CN)<sub>2</sub>]<sup>2−</sup> complex reproduces similar electron paramagnetic resonance features only when it is preincubated with HydE, supporting in situ formation and stabilization of the dimer by the enzyme. These findings implicate the FeI/FeI dimer as the terminal product of HydE and strongly suggest its central role in H-cluster assembly, expanding our understanding of rSAM enzyme catalysis in metallocofactor biosynthesis.

**25COASOCT157****Title: Phosphorus-Doped Cu/Fe<sub>2</sub>O<sub>3</sub> Electrocatalysts with Optimized Synergy between the Different Sites for Efficient Urea Electrosynthesis**

Ting Deng, Shuaiqiang Jia, Cheng Xue et.al.

J. Am. Chem. Soc. 2025, 147, 36, 32924–32931

<https://doi.org/10.1021/jacs.5c09805>

**Abstract:** Urea electrosynthesis from the coelectrolysis of CO<sub>2</sub> and NO<sub>3</sub><sup>−</sup> (UECN) has emerged as a promising sustainable alternative to traditional energy-intensive methods; however, the rational design of advanced electrocatalysts capable of achieving concurrent optimization of Faradaic efficiency (FE) and urea yield rates continues to pose a fundamental challenge in this field. Herein, we developed a phosphorus-doped Cu/Fe<sub>2</sub>O<sub>3</sub> electrocatalyst (denoted as P-Cu/Fe<sub>2</sub>O<sub>3</sub>), where phosphorus atoms partially substitute for oxygen atoms within the Cu/Fe<sub>2</sub>O<sub>3</sub> heterostructure. This engineered electrocatalyst achieves exceptional urea electrosynthesis performance, delivering a very high Faradaic efficiency of 73.81% with a corresponding yield rate of 62.74 mmol h<sup>−1</sup> g<sup>−1</sup>cat. at −0.68 V vs RHE, which are superior to most UECN electrocatalysts reported to date. Notably, the urea yield rate can be further boosted to 97.11 mmol h<sup>−1</sup> g<sup>−1</sup>cat. at −0.88 V vs RHE. Operando spectroscopic characterization and density functional theory (DFT) simulations indicated that P doping modulates the electronic structure of the electrocatalyst surface, which promotes the formation of \*CO and \*NO, lowers the energy barrier for the coupling of \*CO and \*NO, and increases \*H coverage to facilitate the hydrogenation process during UECN. This multisite cooperative mechanism establishes a new paradigm for designing high-performance electrocatalysts, demonstrating substantial potential for industrial-scale urea production.

**25COASOCT158****Title: Importance of Selective Quenching of the Triplet Excited State of Thermally Activated Delayed Fluorescence (TADF) Photosensitizers in Redox-Photosensitized Reactions: Case Studies on Photocatalytic CO<sub>2</sub> Reduction**

Yusuke Tamaki, Kei Kamogawa, Rei Inoue et.al.

J. Am. Chem. Soc. 2025, 147, 36, 33010–33022

<https://doi.org/10.1021/jacs.5c10614>

**Abstract:** Redox photosensitizers exhibiting thermally activated delayed fluorescence (TADF) are widely used in the various research fields. We investigated the roles of the singlet and triplet excited states of such molecules in photocatalytic CO<sub>2</sub> reduction. Two TADF compounds (4DPAIPN and 3DPAFIPN) were used in combination with a manganese(I) complex as a catalyst and 1,3-dimethyl-2-phenyl-2,3-dihydro-1H-benzo[d]imidazole (BIH) and triethanolamine (TEOA) as sacrificial electron donors. In the case of 4DPAIPN, the quantum yield of CO<sub>2</sub> reduction ( $\Phi_{\text{CO}+\text{HCOO}^-}$ ) was negatively correlated with the concentration of BIH, equaling 43.2% and 20.3% at [BIH] = 5 and 200 mM, respectively. The reduction of the singlet excited state by BIH afforded a singlet geminate ion pair, 1(4DPAIPN<sup>•-</sup>...BIH<sup>•+</sup>), which experienced a markedly faster backward electron transfer affording the ground state than the corresponding triplet, 3(4DPAIPN<sup>•-</sup>...BIH<sup>•+</sup>). The escape yield of the singlet state was approximately 10 times lower than that of the triplet state. High BIH concentrations favored the quenching of the singlet excited state and disfavored the formation of the triplet excited state, resulting in low photocatalytic efficiencies. Although the system with 3DPAFIPN exhibited a similar tendency, the maximum  $\Phi_{\text{CO}+\text{HCOO}^-}$  was lower (11.9% at [BIH] = 10 mM) because of its greater oxidizing power resulting in the efficient quenching of its singlet excited state by TEOA. Based on these results, we extracted the reaction conditions and molecular designs of TADF photosensitizers suitable for constructing efficient photocatalysts, namely those minimizing the quenching of the singlet excited state and maximizing the quenching of the triplet excited state.

**25COASOCT159****Title: Cyclization Decoded: Engineering Amylomaltase for Efficient  $\alpha$ -Glucan Transformations**

Han Liu, Tianwen Shang, Scott Mazurkewich et.al.

J. Am. Chem. Soc. 2025, 147, 36, 33162–33176

<https://doi.org/10.1021/jacs.5c11260>

**Abstract:**  $\alpha$ -Glucan, broadly distributed in nature or produced artificially by biotransformation, is fundamental to life. Amylomaltases (AMs) can modulate the biochemical properties of  $\alpha$ -glucan through a distinctive cyclization feature to form  $\alpha$ -1,4-glucoside-linked large-ring polysaccharides (cycloamyloses; CAs), endowing  $\alpha$ -glucan with significant health benefits and medical value. While the industrial application of CAs continues to progress, the mechanistic intricacies of the cyclization process—and its nuanced interplay with hydrolysis—remain only partially understood. Here, we harness large-scale computations in synergy with biochemical experiments to unravel, at atomic resolution, the full covalent and noncovalent catalytic mechanism of AMs, revealing that cyclization (12.8 kcal/mol) outcompetes hydrolysis (17.5 kcal/mol) as the dominant pathway. Furthermore, we

identify that postglycosylation noncovalent polysaccharide chain transfer emerges as the decisive factor in cyclization, particularly for AM–degree of polymerization (DP) greater than 30 substrate complexes, where this noncovalent step ( $\geq 13.6$  kcal/mol) dictates the rate of CA production. 57 variants with enhanced activity (up to a 2.3-fold increase) were engineered in our biochemical experiments by strategically modulating the chain transfer step. Enzyme kinetics results suggest that the improvement in enzyme performance largely stems from the decrease in enzyme–substrate affinity along the substrate transfer pathway. Additionally, through mass spectrometry, CAs with DP ranging from 22 to 61 were detected, confirming our theoretical results. We also quantify the kinetic competitive balance between cyclization and hydrolysis, providing clear engineering blueprints for the AM family. This work delivers a systematic, molecular-level understanding of CA biosynthesis from an industrial-performance perspective, paving the way for next-generation CA innovations.

### 25COASOCT160

**Title: Dimension-Tunable Supramolecular Organic Frameworks with Chiral Pore Channels for Selective Guest Encapsulation and Enhanced Circularly Polarized Luminescence**

Tiejun Li, Dian Niu, Jingdan Zhang et.al.

J. Am. Chem. Soc. 2025, 147, 36, 33223–33231

<https://doi.org/10.1021/jacs.5c11407>

**Abstract:** Here, we report a dimension-tunable supramolecular organic framework (SOF) with chiral pore channels, which shows selective guest encapsulation and enhanced circularly polarized luminescence (CPL). SOFs from a chiral para-substituted bis-naphthalene bis-urea (PNU) are fabricated by both vapor diffusion crystallization and an antisolvent self-assembly approach, leading to the formation of one-dimensional (1D) micrometer-sized single crystal and two-dimensional (2D) plate-like and three-dimensional (3D) octahedral self-assembled microstructures, respectively. The similar permanent porosity of these dimension-tunable chiral SOFs is collectively proved by N<sub>2</sub> adsorption–desorption experiments, single-crystal structure, high-resolution transmission electron microscopy (HR-TEM), and density functional theory (DFT) calculations. By soaking octahedral SOFs in aqueous dye solutions, the chiral porous channels effectively absorb size-matched guest dyes and impart their chirality, leading to enhanced CPL with a dissymmetry factor of  $1.6 \times 10^{-2}$ . This work provides insights for the efficient synthesis of chiral SOFs with pore channels from a single component, which also deepens our understanding of size-selective adsorption and chirality transfer in confined space, as well as the enhancement of circularly polarized luminescence.

### 25COASOCT161

**Title: Interfacial Curvature, not Simply Size, Controls Spontaneous Hydrogen Peroxide Formation in Water Microdroplets**

Kyoungmun Lee, Masoud A. Mehrgardi, Richard N. Zare

J. Am. Chem. Soc. 2025, 147, 36, 33240–33247

<https://doi.org/10.1021/jacs.5c11575>

**Abstract:** Micron-sized water droplets promote redox reactions that are absent in bulk water, yet the kinetics of these interfacial processes remain poorly understood. Here we use real-time fluorescence imaging to monitor spontaneous hydrogen peroxide (H<sub>2</sub>O<sub>2</sub>) generation in

individual microdroplets. Both the apparent production rate and equilibrium concentration of H<sub>2</sub>O<sub>2</sub> increase with decreasing droplet size, even after normalizing for surface area, revealing an intrinsic curvature-dependent enhancement. This effect arises from the geometry-driven amplification of interfacial electric fields, and this enhancement of electric field strength accelerates redox processes. Modulating interfacial electrostatics further alters reactivity: organic surfactants suppress H<sub>2</sub>O<sub>2</sub> formation to varying degrees, whereas simple salts like NaCl and KCl have minimal impact, even at relatively high concentrations. These results highlight curvature and interfacial charge as key determinants of microdroplet reactivity, governed by mesoscale electrostatic fields that drive chemical transformations at and near the surface of the microdroplet.

## 25COASOCT162

### **Title: A Highly Versatile Enantiodifferentiating Polyglutamate Alignment Medium to Measure Residual Dipolar Couplings in Non-Polar and Polar Solvents**

Lukas Laux, Marcel Alcaraz Janßen, Christina M. Thiele

J. Am. Chem. Soc. 2025, 147, 37, 33634–33642

<https://doi.org/10.1021/jacs.5c09152>

**Abstract:** Helical structures are ubiquitous in nature and exhibit fascinating properties. They are inherently chiral, and many rely on hydrogen bonds to stabilize their conformation. Homopolypeptides of the glutamate type form  $\alpha$ -helical secondary structures and are considered rigid-rod polymers. They form lyotropic liquid crystalline phases in helicogenic solvents. Over the past decade, this property has been exploited in the NMR-based structure elucidation of organic compounds, making anisotropic NMR observables, such as residual dipolar couplings (RDCs), accessible. However, many alignment media are limited in their compatibility, especially with polar (nonhelicogenic) solvents like DMSO, and thus also in their analyte compatibility. Herein, we present poly- $\gamma$ -(4-propargyloxybenzyl)-l-glutamate (PPOBLG) as an exceptionally versatile alignment medium compatible with several organic solvents, including DMSO and acetone. The polymer not only allows extraction of RDCs in all these solvents but also provides linearly independent orientations of a model compound by simple variation of the solvent. Moreover, a remarkably high enantiodifferentiation is observed. We furthermore show that these improved properties make it compatible with various natural products containing a wide variety of functional groups.

## 25COASOCT163

### **Title: Divergent Synthesis of 1-Azabicyclo[n.1.1]alkane Bioisosteres via Photoinduced Palladium Catalysis**

Ying Zhang, Kai-Dian Li, Song Yu et.al.

J. Am. Chem. Soc. 2025, 147, 37, 33700–33710

<https://doi.org/10.1021/jacs.5c09500>

**Abstract:** Nitrogen heterocycles are indispensable structural motifs in pharmaceuticals, agrochemicals, and materials science. However, the development of new synthetic methods to access these frameworks remains a significant challenge. Here, we describe a switchable radical approach for the synthesis of 1-azabicyclo[2.1.1]hexanes and 1-azabicyclo[4.1.1]octenes through the coupling of azabicyclo[1.1.0]butanes with 1,3-dienes, mediated by a visible-light-driven palladium photocatalytic system. This method exhibits a

broad substrate scope, excellent functional group compatibility, and the capacity to assemble complex architectures, underscoring its utility in accessing valuable aza-bioisosteres. The strategy has also been employed successfully in DNA-encoded library (DEL) synthesis. Mechanistic studies, synthetic applications, and computational analyses corroborate the proposed open-shell pathway, revealing that allylic palladium intermediate formation and regiodivergent nucleophilic addition are key to achieving divergent synthesis.

## 25COASOCT164

### **Title: Molecular Simulations with a Pretrained Neural Network and Universal Pairwise Force Fields**

Adil Kabylda, J. Thorben Frank, Sergio Suárez-Dou et.al.

J. Am. Chem. Soc. 2025, 147, 37, 33723–33734

<https://doi.org/10.1021/jacs.5c09558>

**Abstract:** Machine Learning Force Fields (MLFFs) promise to enable general molecular simulations that can simultaneously achieve efficiency, accuracy, transferability, and scalability for diverse molecules, materials, and hybrid interfaces. A key step toward this goal has been made with the GEMS approach to biomolecular dynamics [Unke et al., Sci. Adv. 2024, 10, eadn4397]. This work introduces the SO3LR method that integrates the fast and stable SO3krates neural network for semilocal interactions with universal pairwise force fields designed for short-range repulsion, long-range electrostatics, and dispersion interactions. SO3LR is trained on a diverse set of 4 million neutral and charged molecular complexes computed at the PBE0+MBD level of quantum mechanics, ensuring broad coverage of covalent and noncovalent interactions. Our approach is characterized by computational and data efficiency, scalability to 200 thousand atoms on a single GPU, and reasonable to high accuracy across the chemical space of organic (bio)molecules. SO3LR is applied to study units of four major biomolecule types, polypeptide folding, and nanosecond dynamics of larger systems such as a protein, a glycoprotein, and a lipid bilayer, all in explicit solvent. Finally, we discuss future challenges toward truly general molecular simulations by combining MLFFs with traditional atomistic models.

## 25COASOCT165

### **Title: Surface-Driven Electron Localization and Defect Heterogeneity in Ceria**

Xingfan Zhang, Akira Yoko, Yi Zhou et.al.

J. Am. Chem. Soc. 2025, 147, 37, 33888–33902

<https://doi.org/10.1021/jacs.5c10679>

**Abstract:** The exceptional performance of ceria (CeO<sub>2</sub>) in catalysis and energy conversion is fundamentally governed by its defect chemistry, particularly oxygen vacancies. The formation of each oxygen vacancy (VO<sup>••</sup>) is assumed to be compensated by two localized electrons on cations (Ce<sup>3+</sup>). Here, we show by combining theory with experiment that while this 1 VO<sup>••</sup>: 2Ce<sup>3+</sup> ratio accounts for the global charge compensation, it does not apply at the local scale, particularly in nanoparticles. Hybrid quantum mechanical/molecular mechanical (QM/MM) defect calculations, together with synchrotron X-ray photoelectron spectroscopy (XPS) measurements, show that electrons have a strong preference to localize and segregate on surfaces, which can overcome the trapping force from the VO<sup>••</sup> sites in the bulk. At a given Fermi level, the surface VO<sup>••</sup> tends to trap more electrons than those in bulk, resulting



in a higher Ce<sup>3+</sup> to VO<sup>••</sup> ratio on surfaces than that in the bulk, driven by the preferential localization of electrons and enhanced VO<sup>••</sup>–Ce<sup>3+</sup> coupling. Large-scale unbiased Monte Carlo simulations on ceria nanoparticles confirmed this trend and further show that the surface segregation of electrons is more pronounced at low reduction levels and in smaller nanoparticles. In highly reduced ceria nanoparticles, however, the enhanced repulsive interactions lead to a less significant extent of defect heterogeneity or even reverse the location preference of defects in some nanoparticles. Our findings underscore the need to consider both the overall nonstoichiometry and local defect behavior in easily reducible oxides, with direct relevance to their performance in catalytic and energy applications.

## 25COASOCT166

### **Title: Cation Dehydration by Surface-Grafted Phenyl Groups for Enhanced C<sub>2</sub><sup>+</sup> Production in Cu-Catalyzed Electrochemical CO<sub>2</sub> Reduction**

Miyeon Chang, Suhwan Yoo, Wenchao Ma et.al.

J. Am. Chem. Soc. 2025, 147, 37, 34001–34010

<https://doi.org/10.1021/jacs.5c11313>

**Abstract:** The challenge to produce multicarbon (C<sub>2</sub><sup>+</sup>) products in high current densities in the electrochemical reduction of carbon dioxide (CO<sub>2</sub>RR) has motivated intense research. However, the ability of solvated cations to tune and activate water for C<sub>2</sub><sup>+</sup> production in the CO<sub>2</sub>RR has been overlooked. In this study, we report the incorporation of a covalently grown layer of functionalized phenyl groups on the Cu surface that leads to a 7-fold increase in ethylene production (to –530 mA cm<sup>–2</sup>) and a 6-fold increase in C<sub>2</sub><sup>+</sup> products (to –760 mA cm<sup>–2</sup>). Our mechanistic study, notably by in situ infrared, isotope effect, and electrochemical impedance spectroscopy, reveals that the surface grafting provokes the reduction of the hydration shell around alkali cations at the electrode–electrolyte interface. This reduction weakens the hydrogen bond network and thus enhances water dissociation to provide a proton for the CO<sub>2</sub>RR. Moreover, it increases cation density at the outer Helmholtz plane, resulting in a larger local electric field that further stabilizes intermediates en route to C<sub>2</sub><sup>+</sup> production. Our study brings to light the crucial role of cations in modulating the interfacial water structure, which has to be optimal for efficient C<sub>2</sub><sup>+</sup> production in CO<sub>2</sub>RR.

## 25COASOCT167

### **Title: Enantioselective Assembly of (Hetero)aryl Alkyl Sulfilimines via Copper-Catalyzed S-Arylation of S-Alkyl Sulfenamides with (Hetero)aryl Iodides**

Rongxing Zhang, Tongkun Wang, Mingchuang He et.al.

J. Am. Chem. Soc. 2025, 147, 37, 34126–34131

<https://doi.org/10.1021/jacs.5c12689>

**Abstract:** Currently, most sulfoximine clinical candidates feature both S-aryl and S-alkyl substituents. The asymmetric synthesis of these compounds typically relies on oxidizing corresponding enantioenriched sulfilimines. Herein, we describe an effective catalytic system comprising CuI and an azabicyclo[2.2.1] carboxylic acid-derived amide ligand. This system enables the highly enantioselective coupling of S-alkyl sulfenamides with (hetero)aryl iodides to afford aryl alkyl sulfilimines. A wide range of functionalized (hetero)aryl iodides and S-alkyl sulfenamides are compatible under the reaction conditions, providing an attractive approach for assembling enantioenriched aryl alkyl sulfilimines. The utility of this method is

demonstrated by the gram-scale asymmetric synthesis of clinical candidate TNG 260 and the formal asymmetric synthesis of three additional drug candidates.

## 25COASOCT168

### **Title: Discovery of RNA-Reactive Small Molecules Guides the Design of Electrophilic Modules for RNA-Specific Covalent Binders**

Noah A. Springer, Patrick R. A. Zanon, Amirhossein Taghavi et.al.

J. Am. Chem. Soc. 2025, 147, 38, 34271–34282

<https://doi.org/10.1021/jacs.5c06802>

**Abstract:** RNA is a key drug target that can be modulated by small molecules; however, covalent binders of RNA remain largely unexplored. Using a high-throughput mass spectrometry screen of 2,000 electrophilic compounds, we identified ligands that react with RNA in a binding-dependent manner. RNA reactivity was influenced by both the reactive group and the noncovalent RNA-binding scaffold. In addition to known RNA-reactive electrophiles such as N-acylimidazoles and bis(2-chloroethyl)amines, covalent screening enabled the surprising discovery that common thiol-reactive electrophiles (chloroacetamide) and rarely characterized electrophiles (3-chloropivalamide) cross-linked to RNA. These results suggest that electrophiles commonly used for protein targeting can also covalently modify RNA, potentially contributing to both on- and off-target effects. This insight enabled the design of an RNA-specific covalent compound by modifying a bis-benzimidazole scaffold, originally identified to bind DNA, to react selectively with the expanded triplet repeat RNA, r(CUG)<sub>exp</sub>, that causes myotonic dystrophy type 1 (DM1). Selectivity appears to arise from differences in the RNA and DNA binding modes, revealing that proper positioning of the electrophile toward the nucleophilic guanine residue is important for efficient covalent bond formation. Overall, this study highlights the potential of rationally designing covalent RNA-targeting small molecules.

## 25COASOCT169

### **Title: Photosynthetic Biohybrid System for Enhanced Abiotic N<sub>2</sub>-to-NH<sub>3</sub> Conversion under Ambient Conditions**

Jinhyeong Jang, Yuzi Liu, David J. Gosztola et.al.

J. Am. Chem. Soc. 2025, 147, 38, 34477–34486

<https://doi.org/10.1021/jacs.5c08453>

**Abstract:** Photosynthetic biohybrid systems (PBSs) offer an eco-friendly approach to transforming solar energy into value-added products by integrating biological entities with inorganic semiconductors. However, the chemical conversion capacity of most PBSs has inherent limitations, as whole-cell bacteria and isolated enzymes require fine-tuning of environmental conditions. Here, we report a new PBS developed by introducing free-standing ceria nanoparticles into the purple membrane (PM) of *Halobacterium salinarum* archaea, which can unidirectionally transfer charge carriers in response to incident photons, even after separation from living archaea at various conditions. Our microscopy, spectroscopy, and synchrotron X-ray scattering analyses confirm that the electrostatic assembly between ceria and PM creates seamless interfacial contact, thereby enhancing the photocatalytic capacity of ceria. Although the conversion of dinitrogen (N<sub>2</sub>) to ammonia (NH<sub>3</sub>) is thermodynamically challenging due to the triple bond in N<sub>2</sub> and a series of charge-transfer reactions, our PM–

ceria (PMC) hybrid nanoparticle efficiently produces NH<sub>3</sub> by reducing N<sub>2</sub> using solar energy even under atmospheric pressure and room temperature while simultaneously converting glycerol into value-added derivatives. Additionally, our PMC nanoparticle involves neither toxic/precious metals nor bioengineering processes to achieve enhanced photocatalytic N<sub>2</sub>-to-NH<sub>3</sub> conversion. This study sheds light on the new aspect of PBSs by employing PM to potentially resolve the global energy and environmental challenges posed by the conventional Haber–Bosch process.

## 25COASOCT170

### **Title: Synthesis of Diverse Glycosyl Bicyclo[1.1.1]pentanes Enabled by Electrochemical Functionalization of [1.1.1]Propellane**

Jiandong Liu, Rajeshwaran Purushothaman, Fabian Hinrichs et.al.

J. Am. Chem. Soc. 2025, 147, 38, 34813–34822

<https://doi.org/10.1021/jacs.5c10732>

**Abstract:** Over the past decade, bicyclo[1.1.1]pentanes (BCPs) have emerged as valuable bioisosteres of aromatic rings, offering unique three-dimensional architectures for medicinal chemistry. Meanwhile, glycosyl derivatives play a pivotal role in chemical biology and drug discovery due to their widespread presence in biologically active molecules; however, the potential of bicyclo[1.1.1]pentanes (BCPs) as versatile scaffolds in glycoscience remains largely unexplored. Herein, we report an electrochemistry strategy for the synthesis of BCP–glycosides via the functionalization of [1.1.1]propellane. By leveraging an electrochemical halogen-atom transfer (e-XAT) process, we achieved a one-step, three-component reaction of glycosyl bromides, [1.1.1]propellane, and radical acceptors under mild conditions, enabling the construction of glycosyl BCP–iodides, glycosyl BCP–H, and glycosyl BCP–pinacolboronic esters (Bpins) with exceptional functional group tolerance and scalability. Mechanistic studies suggested that the electrochemical process facilitated the generation of radical intermediates, which underwent selective addition to [1.1.1]propellane, followed by trapping with radical acceptors. This study establishes a versatile platform for late-stage functionalization and streamlined access to privileged scaffolds in drug discovery and chemical biology.

## 25COASOCT171

### **Title: Atomic Exploration of the Fluorination-Driven Structural Rearrangement of Carbon Electrocatalysts toward Efficient Oxygen Reduction Reactions**

Yang Li, Zhen Cao, Cailing Chen et.al.

J. Am. Chem. Soc. 2025, 147, 38, 34933–34943

<https://doi.org/10.1021/jacs.5c11417>

**Abstract:** The atom arrangement in carbon electrocatalysts is crucial for enhancing the intrinsic activity toward oxygen reduction reactions (ORRs), a key process in multiple renewable energy systems. However, the challenge of designing electrocatalysts with improved performance by manipulating atomic arrangement has been limited by synthetic constraints and a lack of understanding of the catalytic phase formation. Herein, we gain atomic-level insight into the origin of a highly active site by creating a model catalyst with a heteroatom-decorated carbon matrix of a specific configuration. The introduction of fluorine (F) during the synthesis of the nitrogen (N)-decorated carbon matrix induces structural

rearrangement, converting most pyrrolic-N (Pr-N) into highly stable graphitic-N (G-N), thereby achieving a N configuration predominantly composed of pyridinic nitrogen (Py-N) and G-N. The multidopant synergistic effect of F, Py-N, and G-N causes a destabilized  $\pi$ -conjugated electron network of the carbon matrix, resulting in a more localized electronic structure. As a result, multiple dopant configurations with high ORR activity have been explored, among which the asymmetric Py-N and G-N configurations feature the lowest theoretical ORR overpotential, ultimately enabling the optimized F@NC catalyst to exhibit excellent oxygen reduction activity. This work establishes a foundation for the rational design of metal-free carbon-based electrocatalysts toward ORR.

## 25COASOCT172

### Title: Hydrogen Activation by a $\sigma\sigma^*$ -Carbene Through Quantum Tunneling

Virinder Bhagat, Jan Meisner, J. Philipp Wagne et.al.

J. Am. Chem. Soc. 2025, 147, 39, 35275–35282

<https://doi.org/10.1021/jacs.5c06016>

**Abstract:** The electronic structure of carbenes arises from the occupation of a  $\sigma$  and a  $\pi$  frontier orbital. While parent methylene possesses a triplet ground state ( $\sigma^1\pi^1$ ), substituents are capable of stabilizing the singlet as the ground state ( $\sigma^2\pi^0$  or  $\sigma^0\pi^2$ ) by altering the frontier orbital energies. Here, we reveal that the 1,2[I]-shift isomer of 2-iodopyridine, the N-iodo Hammick intermediate, features a resonance between its carbene  $\sigma$  and N–I bond  $\sigma^*$  orbitals, rendering them frontier orbitals. This singlet carbene is efficiently generated via UV photolysis of 2-iodopyridine in solid neon at 4.4 K and reacts with molecular hydrogen – but not deuterium – via N–I bond cleavage enabled by quantum tunneling. Instanton theory computations demonstrate the preference for a concerted hydrogen addition mechanism at elevated temperatures, while hydrogen atom abstraction dominates below 100 K despite a higher kinetic barrier for this process. Our findings introduce an unprecedented carbene class, unlocking new opportunities for reactivity and electronic structure explorations.

## 25COASOCT173

### Title: Multicyclic Peptides Targeting PD-L1 for Radiotheranostics: From Discovery to Clinical Proof-of-Concept

Xueting Cheng, Shuo Jiang, Xingtong Peng et.al.

J. Am. Chem. Soc. 2025, 147, 39, 35638–35654

<https://doi.org/10.1021/jacs.5c11292>

**Abstract:** Radiotheranostics holds transformative potential for precision oncology by integrating diagnostic imaging with targeted radionuclide therapy. However, advancements in this field are significantly hindered by the limited availability of high-affinity ligands that are capable of engaging challenging cell-surface antigens, particularly flat, low-druggability targets such as programmed death-ligand 1 (PD-L1). Here, we overcome this barrier through de novo discovery and rational engineering of a disulfide-directed multicyclic peptide (DDMP), dmp10, which achieves a picomolar affinity for PD-L1 by leveraging conformationally constrained structural scaffolds. By combining disulfide-directed library design with iterative directed evolution, we successfully generated dmp10, a ~3 kDa multicyclic peptide that establishes unprecedented shape complementarity to the expansive binding interface of PD-L1. Preclinical evaluations demonstrated that  $^{68}\text{Ga}$ -labeled dmp10

enables high-contrast PET imaging of PD-L1+ tumors in murine models, achieving a tumor uptake of 13.27 %ID/g at 4 h post-injection. The therapeutic counterpart, <sup>177</sup>Lu-labeled dmp10, effectively eradicated 92.47% of established tumors in tumor models while sparing healthy tissues, thereby validating its dual radiotheranostic utility. The translational relevance of our findings was further confirmed in a first-in-human pilot study, where <sup>68</sup>Ga-labeled dmp10 was well tolerated and allowed visualization of PD-L1+ lesions in patients with solid tumors. This work not only establishes DDMPs as a versatile platform for targeting geometrically complex antigens but also delivers a promising radiotheranostic agent that bridges molecular imaging and precision radionuclide therapy for PD-L1-driven malignancies. Our findings advance current strategies for designing ultrahigh-affinity peptide binders and underscore the untapped potential of multicyclic architectures in overcoming longstanding challenges in cancer theranostics.



**Diagnostic Services****(Pathology, Cancer Screening & Radio-diagnosis)****25COASOCT01****Title: Low-Grade Endometrial Stromal Sarcoma Clinicopathologic and Prognostic Features in a Cohort of 102 Tumors**Devins, Kyle M. MD<sup>\*</sup>; Mendoza, Rachelle P. MD et.al.

The American Journal of Surgical Pathology 49(10):p 977-991, October 2025.

<https://doi.org/10.1097/PAS.0000000000002428>

**Abstract:** Low-grade endometrial stromal sarcomas (LG-ESS) are the second most common malignant uterine mesenchymal tumors, but in contrast to the more common leiomyosarcomas, they are often characterized by a prolonged and relatively indolent course. However, a subset of patients experience significant morbidity or die of disease, and it is difficult to predict which tumors will behave aggressively, with most published studies limited in either the number of tumors or the depth of pathologic parameters evaluated. Thus, we studied the clinicopathologic features of LG-ESS in 102 patients ranging from 21 to 74 (median: 47) years. All were treated with hysterectomy and staged according to both the FIGO 2018 system (stage IA=22, IB=36, I-not otherwise specified=5, II=16, III=13, IV=10) and the FIGO 1988 system (stage I=62, II=1, III=17, IV=22). Tumors measured 1.2-49 (median: 7) cm. Microscopically, 69 involved the endometrium while 33 were centered in the myometrium. Thirteen showed only minimal infiltration of the myometrium while the rest displayed the typical extensive myometrial permeation. The cervical stroma was involved in 18, the uterine serosa in 27, and the parametrium in 22. Conventional morphology resembling proliferative endometrial stroma was seen in 95, fibroblastic appearance in 35, smooth muscle differentiation in 23, sex cord-like differentiation in 21, stromal hyalinization in 21, and myxoid stroma in 9. Less common features included glandular differentiation resembling adenomyosis (n=5), pseudopapillary pattern (n=1), deciduoid appearance (n=2), adipocytic differentiation (n=2), multinucleated cells (n=2), and rhabdomyoblastic differentiation (n=1). Mitoses ranged from <1 to 20 per 10 high-power fields (median=3). Lymphovascular invasion and infarct-type necrosis were present in 64 and 23, respectively. Follow-up was available in all patients ranging from 16 to 358 (median: 79) months. Forty-six received adjuvant treatment as hormonal therapy (n=34), radiation (n=4), radiation and hormonal therapy (n=4), chemotherapy (n=3), or chemotherapy and radiation (n=1). Three patients had persistent unresected tumor following surgery, and an additional 34 had recurrences at intervals of 3 to 272 (median: 79) months, including 2 tumors with minimal infiltration. At last follow-up, 75 patients were alive with no evidence of disease, 14 were alive with disease, and 9 died of disease at intervals of 16 to 167 (median=70) months. Four died of unrelated causes without recurrence. Five-year recurrence-free survival (RFS) and disease-specific survival (DSS) were 80% and 94%, while 10-year RFS and DSS were 51% and 87%, respectively. On statistical analysis, cervical stromal involvement ( $P=0.018$ ) and myxoid stroma ( $P<0.001$ ) were associated with shorter recurrence-free survival. Tumors lacking a conventional component had worse disease-specific survival ( $P=0.048$ ). All other clinical and morphologic features, including stage, were not significantly associated with outcome. On multivariate analysis, only cervical stromal involvement remained an independent predictor of recurrence-free survival ( $P=0.047$ ; HR: 16.939) and no factors were independently

predictive of disease-specific survival. Our findings highlight the difficulty in predicting outcomes in these tumors, likely due to slow progression and frequent treatment responses even in the recurrent setting. We confirm the potential for recurrence even in tumors initially showing minimal infiltration. Cervical stromal involvement and lack of conventional morphology are potential novel risk factors that should be further evaluated in subsequent studies.

## 25COASOCT02

### **Title: HPV42 A Common Low-Risk HPV Type Associated With Distinctive Cervicovaginal and Cutaneous Neoplasia**

Talia, Karen L.\*; Hawkes, David PhD<sup>†</sup>

The American Journal of Surgical Pathology 49(10):p 992-1003, October 2025. |

<https://doi.org/10.1097/PAS.0000000000002420>

**Abstract:** Seborrheic keratosis-like lesion (SKLL) is an extremely rare, morphologically distinct lesion occurring in the cervix and vagina that differs histologically from other squamous intraepithelial lesions in these sites due to its unique morphology, including close resemblance to cutaneous seborrheic keratosis and lack of viral cytopathic effect (koilocytosis). We report a series of 17 cases, describe in detail the morphology and add to the evidence linking SKLL with low-risk human papillomavirus (LRHPV), specifically HPV42, which was detected in 13 cases; in 3 cases, an additional single HPV type (HPV6, 16, 61) was detected. In 2 of the SKLLs, a component of high-grade morphology and block-type p16 immunoreactivity were observed, prompting speculation as to the oncogenic potential of HPV42. Nineteen cases of papillary immature metaplasia, another distinctive LRHPV-associated lesion with some morphologic overlap with SKLL, were HPV42 negative. Independently, HPV42 has recently been implicated as the cause of a rare, aggressive cutaneous tumour, digital papillary adenocarcinoma (DPA), with experimental molecular data supporting the transforming capacity of this virus. These findings, along with the observation that rare anogenital squamous cell carcinomas are associated with HPV42, demonstrate the rare carcinogenic potential of this LRHPV. The association of HPV42 with these 2 unique and distinctive tumours (SKLL and DPA) also illustrates the incompletely understood diversity of HPV genotype-phenotype associations and virus-host interactions and highlights the importance of HPV typing of novel genital and cutaneous tumours.

## 25COASOCT03

### **Title: Clinicopathologic and Genomic Features of Gastric-Type Intraductal Papillary Neoplasm of the Bile Duct Potential Role of *STK11* in Malignant Progression**

Shimada, Yuki MD<sup>\*,†</sup>; Yamamoto, Takeo MD, PhD

The American Journal of Surgical Pathology 49(10):p 1004-1014, October 2025. |

<https://doi.org/10.1097/PAS.0000000000002451>

**Abstract:** Gastric-type intraductal papillary neoplasm of the bile duct (G-type IPNB) remains an underexplored subtype of IPNBs, with limited molecular characterization. This study aimed to elucidate the clinicopathologic and genomic features of G-type IPNB to better understand its malignant potential and progression. Eighty-three IPNB cases, including 21 G-type IPNBs, were analyzed. The clinicopathologic features and prognosis of G-type IPNB were compared with those of other subtypes. Targeted sequencing was performed in 15 G-type cases,

comprising 5 with high-grade dysplasia (HGD), 6 with invasive carcinoma (INV), and 4 with lymph node metastasis (LNM). The samples displayed varying histologic grades. The G-type frequently exhibited HGD; however, invasive G-type IPNBs showed significantly higher rates of lymph node metastasis compared with the other subtypes ( $P=0.044$ ). Recurrent mutations were detected in *KRAS* (60%), *STK11* (40%), *KMT2C* (40%), *APC* (20%), *CTNNB1* (13%), and *TP53* (13%). Mutational profiles remained highly concordant across histologic grades, with no significant new mutations accumulating during tumor progression. *KRAS* mutations were predominantly found in preinvasive lesions, supporting their role in early tumorigenesis. *STK11* mutations were exclusive to INV and LNM cases, but not detected in HGD cases. Notably, identical mutations were uniformly carried over from preinvasive lesions to invasive carcinoma and metastatic lymph node lesions. Immunohistochemically, aberrant STK11 expression was specific to the G-type compared with other subtypes ( $P=0.030$ ). These findings highlight the unique clinicopathologic and molecular features of G-type IPNB, including the association of *STK11* mutations with invasive behavior and their potential as indicators of tumor progression.

#### 25COASOCT04

##### **Title: Dedifferentiated Solitary Fibrous Tumor: A Clinicopathologic, Immunohistochemical, and Molecular Characterization of 25 Cases**

Simon, Adrian Georg MD\*; Mariño-Enríquez, Adrian MD, PhD

The American Journal of Surgical Pathology 49(10):p 1015-1027, October 2025.

<https://doi.org/10.1097/PAS.0000000000002417>

**Abstract:** Dedifferentiated solitary fibrous tumor (DDSFT) is a rare and clinically aggressive malignancy with a poor prognosis. It represents the progression of solitary fibrous tumor to a high-grade, morphologically nondistinctive sarcoma. This study characterizes the clinicopathologic and molecular features of 25 DDSFT. The study cohort comprised 13 males and 12 females with a median age of 63 years (range 31 to 84). Tumors were most common in the pelvic cavity (8/25), thoracic cavity (6/25), and trunk (4/25). Histologically, DDSFT demonstrated remarkably variable morphology, including pleomorphic, epithelioid, spindle cell, and round cell features. Heterologous elements were present in 4/25 (16%). Immunohistochemical expression of STAT6 was completely lost in 8/22 (36%) tumors. Targeted DNA sequencing demonstrated that in most tumors (10/13; 77%), the *NAB2::STAT6* fusion variant resulted in a truncated STAT6 (STAT6-TAD) in the fusion protein. Recurrent secondary alterations involved *TP53* (10/14; 71%), *TERT* (8/14; 57%), and *RBI* (3/14; 21%). Statistical analysis of the study cohort and 55 cases reported in the literature demonstrated that complete loss of STAT6 in DDSFT is associated with shorter disease-specific survival (HR 12.69,  $P=0.023$ ).

#### 25COASOCT05

##### **Title: Psammomatous Calcifications Identified in Targeted Needle Biopsies and Radical Prostatectomy From *IDH1* Mutant Prostatic Adenocarcinoma**

Zong, Yang MD, PhD\*; Sharobim, Mark MD

The American Journal of Surgical Pathology 49(10):p 1090-1096, October 2025. |

<https://doi.org/10.1097/PAS.0000000000002461>

**Abstract:** IDH1 mutant prostatic adenocarcinoma represents a small fraction of prostate cancer with distinct epigenetic changes, characterized by genome-wide DNA hypermethylation. Recently, prostatic adenocarcinoma with intratumoral psammomatous calcifications was found to frequently harbors *IDH1* R132 mutations. However, the association with *IDH1* hotspot mutations and psammomatous calcifications in prostate cancer remains controversial. Here we report another rare case of *IDH1* R132H mutant prostatic adenocarcinoma, showing intratumoral psammomatous calcifications identified in targeted needle biopsies as well as subsequent radical prostatectomy specimen. This case provides independent evidence for identification of *IDH1* mutant prostate cancer by combined histologic features, including intratumoral psammomatous calcifications, anterior tumor location, and high Gleason score. In addition, to our knowledge, this is the first case of multifocal prostate cancer reported in the literature, with the co-existence of spatially disparate and genetically distinct tumor foci harboring *IDH1* R132H mutation or *TMPRSS2-ERG* gene fusion in the same prostate.

## 25COASOCT06

### **Title: Localised rectal cancer: ESMO Clinical Practice Guideline for diagnosis, treatment and follow-up<sup>★</sup>**

Hofheinz, R.-D. et al.

Annals of Oncology, Volume 36, Issue 9, 1007 - 1024

<https://doi.org/10.1016/j.annonc.2025.05.528>

**Abstract:** This ESMO Clinical Practice Guideline (CPG) focusses on localised rectal cancer. The management of advanced and metastatic rectal cancer is covered in the ESMO CPG on metastatic colorectal cancer (CRC).<sup>1-3</sup> Incidence and epidemiology- Rectal cancer has an incidence rate of 13.9 cases per 100 000 per year in males and 8.6 cases per 100 000 in females, reflecting almost one-third of all CRCs.<sup>4</sup> Incidence is increasing, particularly in individuals aged 50-64 years, with rectal cancer accounting for 4 out of 10 CRCs in this age group.<sup>4</sup> Notably, mortality rates have decreased in countries with better access to screening, early diagnosis and high levels of care. Delayed diagnosis and slow adoption of modern therapy may, at least in part, explain the higher mortality rates in central and eastern European countries. Lifestyle factors, including excess body weight, obesity, consequent diabetes, lack of exercise and dietary habits, which are associated with CRC, have influenced these trends. Diagnosis, pathology and molecular biology- Diagnosis-Rectal cancer can present with symptoms; however, it is increasingly being identified via population screening programmes. After a positive screening test, colonoscopy can provide an accurate histological diagnosis of the primary tumour via biopsy or, if appropriate based on pit pattern assessment during advanced endoscopy, direct local excision (LE). Pathology- Subsequent diagnostic work-up focusses on establishing the locoregional status. The diagnostic work-up for rectal cancer is summarised in Supplementary Table S1, available at <https://doi.org/10.1016/j.annonc.2025.05.528>. Depth of tumour invasion can determine whether the tumour is locally excisable, surgically resectable or requires neoadjuvant therapy. Further assessment of locally excised tumours can determine the risk of lymph node metastases and/or local recurrence. Risk features include tumour size, invasion depth, type, grade, presence of tumour budding, lymphatic and vascular invasion and status of resection margins. The presence of two or more of these features serves as an indication for radical

resection, although this depends on national guidelines. Molecular biology- Assessment of mismatch repair (MMR) proteins on biopsies or LE specimens can identify patients with sporadic microsatellite instability-high (MSI-H) tumours or Lynch syndrome, who may benefit from treatment with immunotherapy and, in the case of Lynch syndrome, referral for genetic counselling [see ESMO Scale for Clinical Actionability of molecular Targets (ESCAT) for further details – Supplementary Table S2, available at <https://doi.org/10.1016/j.annonc.2025.05.528>]. As neoadjuvant therapy can disrupt MMR staining or diminish the number of evaluable tumour cells, baseline biopsy material is preferred. Analysis of *RAS*, *BRAF* V600E, *NTRK* and human epidermal growth factor receptor 2 (HER2) status currently has no impact on the treatment of localised tumours.

## 25COASOCT07

### **Title: Long-term development of 12- and 15-year-old offspring after maternal cancer diagnosis during pregnancy: a prospective multicentre cohort study**

Huis in 't Veld, E.A. et al.

Annals of Oncology, Volume 36, Issue 9, 1025 – 1034

<https://doi.org/10.1016/j.annonc.2025.04.011>

**Abstract:** Evidence is lacking on the long-term effects of prenatal exposure to maternal cancer and its treatment on adolescent neurocognitive, cardiac, and physical health. **Methods-** In a multicentre cohort study, children aged 12 and/or 15 years, prenatally exposed to maternal cancer (treatment), underwent clinical, echocardiographic, and neurocognitive evaluations. Standardized assessments were used, and associations between neurocognitive outcomes and covariates were examined using one-way and multivariable analysis of variance. Further analyses examined the need for extra support and the impact of chemotherapy exposure on puberty onset. **Results-** Of 166 children, 122 were exposed to chemotherapy, 17 to surgery alone, 14 to radiotherapy, 1 to trastuzumab, 1 to rituximab, and 21 to no treatment. Cardiac function was within normal ranges, with a median ejection fraction of 56.7% (z-score: -1.6) and two cases showed mild systolic dysfunction (ejection fraction <50%). Neurocognitive outcomes, including intelligence, memory, and attention, were also within normal limits. Nine children, however, had lower verbal memory scores linked to chemotherapy exposure ( $\beta = -0.52, P = 0.044$ ). Visuospatial memory was negatively correlated with maternal death ( $\beta = -0.55, P = 0.019$ ), and attention was influenced by prematurity ( $\beta = 0.034$  per gestational week,  $P = 0.020$ ) and male sex ( $\beta = -0.17, P = 0.024$ ). Extra support was needed in 21 children, primarily associated with lower intelligence, attention, and executive function scores, as well as prematurity. Pubertal development was within standard ranges, with no significant associations found between chemotherapy exposure and puberty onset. **Conclusion-** Overall, no significant disruptions were found in the neurocognitive, cardiac, or physical development of adolescents prenatally exposed to maternal cancer and its treatment. Observed vulnerabilities, such as lower verbal memory and attention scores, were primarily linked to prematurity and maternal death rather than maternal cancer or its treatment. Ongoing monitoring is recommended to understand long-term outcomes into adulthood.

## 25COASOCT08

### **Title: Twenty-year survival of advanced gastrointestinal stromal tumours treated with**



**imatinib: exploratory long-term follow-up of the BFR14 trial**

Blay, J.-Y. et al.

Annals of Oncology, Volume 36, Issue 9, 1035 - 1046

<https://doi.org/10.1016/j.annonc.2025.05.535>

**Abstract:** Gastrointestinal stromal tumours (GIST) are driven by mutations in KIT and platelet derived growth factor receptor A (PDGFRA) kinases in >75% of patients. Imatinib, a tyrosine kinase inhibitor, has shown efficacy in metastatic GIST but the long-term survival impact remains less understood, especially after extended treatment durations. Patients and methods-The BFR14 study, initiated in 2002, is a multicentric randomized phase III clinical trial involving 434 patients with advanced or unresectable GIST, treated with imatinib. This long-term follow-up ed to assess the survival outcomes of the patients prospectively included in this study. Patient demographics, mutation status, overall survival (OS) and response rates were collected. Results-With a median follow-up of 219 months, median OS was 75.3 months. Survival rates at 10, 15, and 20 years were 33.9%, 19.8%, and 13.1%, respectively. Factors significantly associated with better survival included female sex, gastric tumour location, smaller primary tumour size, and *KIT* exon 11 mutations. Complete response to imatinib and complete surgical resection of metastases with R0 resections are associated with a doubling of median survival and a significantly prolonged OS. Conclusions- This long-term follow-up of the BFR14 trial shows long-term efficacy of imatinib in patients with advanced GIST. Complete resection of metastasis and achievement of complete response is associated with a doubling of median survival.

**25COASOCT09****Title: Ultrasensitive detection and tracking of circulating tumor DNA to predict relapse and survival in patients with locally advanced cervical cancer: phase III CALLA trial analyses**

Mayadev, J. et al.

Annals of Oncology, Volume 36, Issue 9, 1047 - 1057

<https://doi.org/10.1016/j.annonc.2025.05.533>

**Abstract:** After chemoradiotherapy (CRT), 30%-50% of patients with locally advanced cervical cancer (LACC) relapse, highlighting the unmet need for prognostic biomarkers. In the global randomized CALLA trial (NCT03830866), the addition of durvalumab during and after CRT did not significantly improve progression-free survival (PFS) in a biomarker-unselected intent-to-treat population. We analyzed the association of ultrasensitive circulating tumor DNA (ctDNA) and circulating human papillomavirus (cHPV) DNA detection with relapse and survival in the largest dataset in LACC to date. Patients and method- CALLA, adult women with stage IB2-IIB node-positive or IIIA-IVA any node-status LACC were randomized 1 : 1 to receive durvalumab + CRT or CRT alone. The NeXT Personal® (Personalis) ultrasensitive tumor-informed assay with up to 1800 patient-specific variants was used for ctDNA and cHPV DNA analysis at baseline, cycle 3 day 1 (C3D1, post-CRT), and C6D1 (3 months post-CRT). Correlations were analyzed between ctDNA/cHPV DNA detection and outcomes [PFS, overall survival (OS)]. Results-ctDNA was detected in 98.9% (183/185) of baseline samples, with no difference between treatment arms. Detection levels of ctDNA were predictive of disease progression and survival at baseline: hazard ratios (95% confidence intervals) comparing PFS and OS, respectively, in the ctDNA less than median

versus ctDNA greater than median subgroups were 0.61 (0.28-1.35) and 0.55 (0.23-1.35) with durvalumab + CRT, and 0.49 (0.26-0.95) and 0.65 (0.33-1.28) with CRT. Post-treatment trends were similar and independent of stage or lymph node status. ctDNA detection at C3D1 occurred a median of 164 days (95% confidence interval 85-250) days before clinical progression. Baseline cHPV DNA levels were similar but were only predictive following treatment. Conclusions-This study demonstrates the potential utility of ultrasensitive detection of ctDNA as a predictive and prognostic marker of disease progression and OS in LACC independent of disease stage.

## 25COASOCT10

### **Title: Enzalutamide plus radium-223 in metastatic castration-resistant prostate cancer: results of the EORTC 1333/PEACE-3 trial**

Tombal, B. et al.

Annals of Oncology, Volume 36, Issue 9, 1058 – 1067

<https://doi.org/10.1016/j.annonc.2025.05.011>

**Abstract:** The EORTC 1333 ‘PEACE-3’ study investigated the combination of enzalutamide and 6 monthly injections of radium-223 (Ra223) in patients with metastatic castration-resistant prostate cancer (mCRPC) and bone metastases. Materials and methods From November 2015 to March 2023, 446 patients, including 11 who received abiraterone, were randomized to enzalutamide (without placebo) or enzalutamide combined with six cycles of Ra223. As of March 2018, the co-administration of zoledronic acid or denosumab was mandatory. The primary endpoint was radiological progression-free survival (rPFS) by investigator assessment. Key secondary endpoints included overall survival (OS), time to subsequent systemic treatment, pain progression, and symptomatic skeletal event. Results- The hazard ratio (HR) for rPFS was 0.69 [95% confidence interval (CI) 0.54-0.87,  $P = 0.0009$ ], with a median rPFS of 16.4 months (95% CI 13.8-19.2 months) in the enzalutamide arm and 19.4 months (95% CI 17.1-25.3 months) in the combination arm. At the preplanned interim analysis conducted at 80% of the OS events, the HR for OS was 0.69 (95% CI 0.52-0.90,  $P = 0.0031$ ), with a median OS of 35.0 months (95% CI 28.8-38.9 months) in the enzalutamide arm and 42.3 months (95% CI 36.8-49.1 months) in the combination arm. Due to non-proportional hazards, this will be tested further at the final OS analysis. Treatment-emergent adverse events (TEAEs)  $\geq$  grade 3 were recorded in 55.8% and 65.6% of the patients in the enzalutamide and combination arms, respectively. The most frequent grade  $\geq 3$  TEAEs in the combination arm were hypertension (34%), fatigue (6%), fracture (5%), anemia (5%), and neutropenia (5%). Fractures [either treatment-emergent or post-treatment, symptomatic or pathologic, or with or without bone-protecting agent (BPA) use] were reported in 30 (13.4%) patients in the enzalutamide arm and 53 patients (24.3%) in the combination arm. Conclusion- PEACE-3 demonstrates that combining enzalutamide with Ra223 as first-line therapy for mCRPC significantly improves rPFS. Although statistically significant at the OS interim boundary, the study will continue to the final OS analysis.

## 25COASOCT11

**Title: Association of the circulating lipid panel, PCPro, with clinical outcomes in metastatic hormone-sensitive prostate cancer: *post hoc* analysis of the ENZAMET phase III randomised trial (ANZUP 1304)**

Lin, H.-M. et al.

Annals of Oncology, Volume 36, Issue 9, 1068 - 1077

<https://doi.org/10.1016/j.annonc.2025.05.529>

**Abstract:** Enzalutamide significantly improves overall survival (OS) of patients with metastatic hormone-sensitive prostate cancer (mHSPC). However, ~10% of patients will die within 2 years. PCPro is a plasma lipid panel associated with decreased OS in metastatic castration-resistant prostate cancer. In this study, we assessed the association between PCPro and clinical outcomes in mHSPC by carrying out a *post hoc* analysis of ENZAMET, the landmark phase III trial comparing enzalutamide with nonsteroidal anti-androgen (NSAA). Patients and methods- PCPro status was determined by liquid chromatography–mass spectrometry analysis of plasma samples from 866 participants (77% of the ENZAMET trial cohort), before treatment ( $n = 866$ ) and at first progression ( $n = 282$ ). Outcomes examined were OS and clinical progression-free survival (clinPFS). Results-Participants with a positive PCPro status at baseline (13.4%) had a significantly shorter OS and clinPFS compared with those with a negative PCPro status [OS hazard ratio (HR) 1.81, 95% CI 1.40-2.33, clinPFS HR 1.65, 95% CI 1.32-2.07,  $P < 0.0001$ ]. PCPro is an independent prognostic factor when modelled with key clinical prognostic factors ( $P < 0.001$ ). Enzalutamide (compared with NSAA) improved the OS of PCPro-negative participants (HR 0.61,  $P < 0.0001$ ), but not the survival of PCPro-positive participants (HR 1.10,  $P = 0.69$ ; interaction  $P = 0.024$ ). Participants who were PCPro positive at progression have a shorter OS than those who were negative, irrespective of baseline status (median OS 24-28 months versus 42-45 months). Conclusions-PCPro status is a prognostic biomarker and predictive of the lack of OS benefit from enzalutamide compared with NSAA in mHSPC. These findings provide a rationale for testing therapeutic agents that can modify circulating lipid profiles in mHSPC.

## 25COASOCT12

**Title: Copenhagen Prospective Personalized Oncology (CoPPO)—impact of comprehensive genomic profiling in more than 2000 patients in a phase I setting**

Belcaid, L. et al.

Annals of Oncology, Volume 36, Issue 9, 1078 - 1087

<https://doi.org/10.1016/j.annonc.2025.04.004>

**Abstract:** Targeted therapy based on the molecular characterization of tumors has been among the most remarkable advances in cancer medicine. In this article, we report the impact of almost 10 years of comprehensive genomic profiling in >2000 patients with advanced solid tumors at the Phase I Unit, Department of Oncology, Rigshospitalet, Copenhagen, Denmark. Materials and methods-A prospective, single-center, single-arm open-label study (NCT02290522) was conducted, enrolling patients with advanced cancer referred to a phase I unit. Fresh tumor tissue was obtained for whole-genome or -exome sequencing (germline and somatic), RNA sequencing, and single nucleotide polymorphism (SNP) array. In cases where fresh tumor tissue was unavailable, archived formalin-fixed paraffin-embedded tumor tissue or circulating tumor DNA extracted from plasma were obtained for targeted panels. Genomic reports were reviewed and discussed by a multidisciplinary tumor board and actionable alterations were classified according to the European Society for Medical Oncology Scale for Clinical Actionability of molecular Targets (ESCAT). When possible, patients were treated with regimen matched to the genomic profile. Results-A total of 2147 patients with advanced

cancer and exhausted treatment options were enrolled from April 2013 to December 2021. Genomic profiles were obtained in 1866 patients (87%). At least one actionable target was identified in 1062 patients (57%) with a total of 1614 actionable alterations including high RNA *CEACAM5* expression ( $n = 559$ , 35%), homologous recombination deficiency (HRD) alteration ( $n = 314$ , 20%), and tumor mutational burden-high ( $n = 84$ , 5%). Overall, 256 patients (24% of the patients with an actionable target) were treated with targeted therapy and among these 14 patients were treated with more than one line of targeted therapy. In total, 274 targeted treatment regimens were initiated, and 259 treatments were evaluable with an overall response (OR) rate of 25% (95% confidence interval 0.20% to 0.30%). ESCAT I/II was associated with improved OR, along with better progression-free survival (PFS) and overall survival (OS). Conclusion-This large-scale study demonstrates that genomic profiling is efficient in identifying actionable targets and in matching patients to targeted therapies.

## 25COASOCT13

**Title: Avelumab plus sacituzumab govitecan versus avelumab monotherapy as first-line maintenance treatment in patients with advanced urothelial carcinoma: JAVELIN Bladder Medley interim analysis<sup>★</sup>**

Hoffman-Censits, J. et al.

Annals of Oncology, Volume 36, Issue 9, 1088 - 1095

<https://doi.org/10.1016/j.annonc.2025.05.010>

**Abstract:** Avelumab first-line maintenance is a recommended treatment option for patients with locally advanced or metastatic urothelial carcinoma (la/mUC) without progression following platinum-based chemotherapy (PBC). The JAVELIN Bladder Medley phase II trial is investigating the efficacy and safety of maintenance treatment with avelumab combined with other antitumor agents versus avelumab monotherapy. We report an interim analysis of avelumab plus sacituzumab govitecan (SG) versus avelumab monotherapy. Patients and methods- Patients with la/mUC without progression after first-line PBC were randomized 2 : 1 to receive avelumab (800 mg every 2 weeks) plus SG (10 mg/kg on days 1 and 8 of 21-day cycles) or avelumab monotherapy (800 mg every 2 weeks). Primary endpoints are investigator-assessed progression-free survival (PFS) and safety. For PFS and overall survival (OS), data in the avelumab monotherapy arm were extended per protocol using propensity score-weighted JAVELIN Bladder 100 data. Results-At data cut-off (16 September 2024), 38/74 patients (51.4%) in the avelumab plus SG arm and 10/37 patients (27.0%) in the avelumab monotherapy arm were still receiving study treatment. Median PFS with avelumab plus SG versus avelumab monotherapy was 11.17 versus 3.75 months, respectively [hazard ratio (HR) 0.49, 95% confidence interval (CI) 0.31-0.76; prespecified efficacy boundary:  $HR \leq 0.60$ ]. OS data were immature; median OS was not reached versus 23.75 months, respectively (HR 0.79, 95% CI 0.42-1.50). In patients treated with avelumab plus SG or avelumab monotherapy, any-grade treatment-related adverse events (TRAEs) occurred in 97.3% versus 63.9% (grade  $\geq 3$  in 69.9% versus 0%), respectively. Conclusion- In patients with la/mUC without progression after first-line PBC, PFS was prolonged with avelumab plus SG versus avelumab monotherapy as maintenance treatment. TRAEs were more frequent with the combination and were consistent with known safety profiles of SG and avelumab. Combining avelumab with anti-Trop-2 antibody-drug conjugates may be a promising strategy to improve patient outcomes in la/mUC.

**25COASOCT14****Title: Spatiotemporal T-cell tracking for personalized T-cell receptor T-cell therapy designs in childhood cancer**

Sentís, I. et al.

Annals of Oncology, Volume 36, Issue 9, 1096 - 1106

<https://doi.org/10.1016/j.annonc.2025.05.530>

**Abstract:** Immune checkpoint inhibition (ICI) has revolutionized oncology, offering extended survival and long-term remission in previously incurable cancers. While highly effective in tumors with high mutational burden, lowly mutated cancers, including pediatric malignancies, present low response rate and limited predictive biomarkers. Patients and methods- We present a framework for the identification and validation of tumor-reactive T cells as a biomarker to quantify ICI efficacy and as candidates for a personalized T-cell receptor T-cell (TCR-T) therapy. Therefore, we profiled a pediatric malignant rhabdoid tumor patient with complete remission after ICI therapy using deep single-cell T-cell receptor (TCR) repertoire sequencing of the tumor microenvironment (TME) and the peripheral blood. Results Tracking T-cell dynamics longitudinally from the tumor to cells in circulation over a time course of 12 months revealed a systemic response and durable clonal expansion of tumor-resident and ICI-induced TCR clonotypes. We functionally validated tumor reactivity of TCRs identified from the TME and the blood by co-culturing patient-derived tumor cells with TCR-engineered autologous T cells. Here, we observed unexpectedly high frequencies of tumor-reactive TCR clonotypes in the TME and confirmed T-cell dynamics in the blood post-ICI to predict tumor reactivity. Conclusions- These findings strongly support spatiotemporal tracking of T-cell activity in response to ICI to inform therapy efficacy and to serve as a source of tumor-reactive TCRs for personalized TCR-T designs.

**25COASOCT15****Title: Immune checkpoint inhibitor-induced gastrointestinal injury: prevalence of cytomegalovirus, adenovirus and Epstein-Barr virus**Chornenkyy Y, LaBoy C, De Hoyos SX, *et al**Journal of Clinical Pathology* 2025;78:583-590.<https://doi.org/10.1136/jcp-2024-209621>

**Abstract:** Widespread use of immune checkpoint inhibitors (ICIs) for treatment of advanced malignancies led to an increase in number of immune-related adverse events such as ICI gastrointestinal (GI) injury (ICIGI). The resulting immune dysregulation of the GI mucosa is believed to predispose patients to viral infections. We characterised the histopathological features of ICIGI and the frequency of viral infections such as cytomegalovirus (CMV), adenovirus, and Epstein-Barr virus (EBV). Methods Single-centre retrospective study (2011–2020). Results 81 GI biopsies from 31 patients with ICIGI (65% male (20/31), 35% female (11/31)) with advanced malignancies were reviewed. Most patients received ipilimumab and nivolumab (14/31, 45%), followed by pembrolizumab (9/31, 29%), ipilimumab (4/31, 13%), nivolumab (2/31, 6%) and combination of all three medications (2/31, 6%). Average regimen prior to incidence of diarrhea was three cycles. Evidence of colitis or erythema by endoscopy was present in 77% of cases, while 23% showed normal endoscopy. Histologically, the predominant ICIGI findings were active inflammation (84%), including cryptitis (77%), crypt abscesses (65%), lymphocytic colitis-like (LCL) pattern (61%), increase in epithelial



apoptosis (74%) and/or surface injury (81%). Only one case showed diffuse CMV positivity (3%) with characteristic CMV viral cytopathic effects present on H&E stain and four cases were positive for rare EBV (13%). Adenovirus infection was not identified. Conclusion While our cohort is small, ICI GI generally demonstrates active inflammation including cryptitis and crypt abscesses in the colon, LCL pattern, and an increase in epithelial apoptosis. Upfront immunohistochemistry for viral infection without high-degree of clinical and histologic suspicion is not recommended.

## 25COASOCT16

**Title: “Find Your Y”: histological differences in early stage (pT) and post-treatment (ypT) oesophageal adenocarcinoma with implications for salvage endoscopic resection**

Pacheco RR, Lee G, Yang Z, *et al*

Journal of Clinical Pathology 2025; 78:591-598.

<https://doi.org/10.1136/jcp-2024-209688>

**Abstract:** Current guidelines offer limited strategies for managing recurrent/persistent oesophageal adenocarcinoma (EAC). Salvage endoscopic mucosal/submucosal resection (ER) shows promise in oesophageal squamous cell carcinoma, however its success in EAC is limited. We ed to elucidate histological characteristics influencing salvage ER success in patients with low-stage, pretreated EAC. Methods We retrospectively reviewed 272 EAC tumours postoesophagectomy from five US centres and collected clinicopathological data including discontinuous growth (DG), defined as separate tumour foci  $\geq 2$  mm from the main tumour. We selected 101 patients with low-stage disease and divided them into treatment-naïve (n=70) and neoadjuvant therapy (n=31) groups. We compared the two groups and differences in clinical, histological and outcome characteristics were identified. Results In the entire cohort (n=272), DGs were identified in 22% of cases. Multivariate analysis revealed DGs as an independent prognostic factor for recurrence and positive oesophagectomy margins. Lymphovascular invasion (LVI) and background intestinal metaplasia predicted DG presence and absence, respectively. Compared with the treatment-naïve low T-stage subgroup, the pretreated subgroup exhibited higher incidence of poorly differentiated carcinoma (16% vs 46%, p=0.007), larger tumours (14 vs 30 mm, p<0.001), higher tumour, node, metastases stage (7% vs 30%, p=0.004), more nodal disease (7% vs 36%, p<0.001) and frequent DGs (1% vs 13%, p=0.030). Conclusions In treated low T-stage EACs, DGs may contribute to suboptimal outcomes following salvage ER. Presence of LVI (as a surrogate for DGs) and poor differentiation in the absence of intestinal metaplasia in biopsy samples may serve as histological poor prognosticators in treated patients with EAC being considered for salvage ER.

## 25COASOCT17

**Title: Clinicopathological features of EBV-positive polymorphic B-cell lymphoproliferative disorders involving central nervous system in people living with HIV**

Wang J, Zeng D, Song F, *et al*

Journal of Clinical Pathology 2025;78:599-604.

<https://doi.org/10.1136/jcp-2024-209958>

**Abstract:** To investigate the histomorphological, immunophenotypic and molecular

pathological features of Epstein-Barr virus (EBV)-positive polymorphic B-cell lymphoproliferative disorders (LPD) of the central nervous system (CNS) in people living with HIV. Methods Seven HIV-positive patients with primary CNS lesions were retrospectively analysed. According to the 5th edition of the WHO Classification of Haematolymphoid Tumours and 2022 International Consensus Classification of mature B-cell lymphomas, these patients were pathologically diagnosed based on their H&E staining, immunohistochemistry, immunoglobulin heavy chain (IGH) clonality analysis, EBV-encoded RNA (EBER) fluorescence in situ hybridisation (FISH) and clinical data. Results MRI revealed lesions in the frontal lobe, cerebellar vermis, occipital lobe, temporal lobe, basal ganglia and thalamus, with four patients exhibiting lesions in multiple locations. Histopathological examination revealed polymorphic lymphocytic infiltrates in brain tissue, including lymphocytes, histiocytes, immunoblasts, plasma cells, atypical large B-cell and Hodgkin-Reed-Sternberg-like cells, with B-cell predominantly. Lymphocytic infiltration was mainly perivascular, with focal coagulative necrosis observed in four cases. Immunohistochemistry identified B-cell (CD20+, CD79a+), large B-cell and immunoblasts (CD30+), T-cell (CD3+), histiocytes (CD68+) and plasma cells (CD138+). All cases were positive for BCL-2 and Ki67 (20%–60%+), with three cases positive for EBNA2. All cases were negative for LMP1, HHV8, Bcl-6 and CD15. EBER in situ hybridisation was positive in all cases, and five cases showed IGH clonal rearrangement. FISH testing for IGH breakage recombination was negative in all seven cases. Conclusion Accurate diagnosis of EBV-positive polymorphic B-cell LPD in the CNS of HIV patients requires a comprehensive approach including histology, immunophenotyping, molecular testing, and clinical information.

## 25COASOCT18

### **Title: Identification of immune cell markers associated with ulcerative colitis histological disease activity in colonic biopsies**

Lefevre PLC, Wang Z, Teft W, *et al*

Journal of Clinical Pathology 2025;78:605-613.

<https://doi.org/10.1136/jcp-2023-209327>

**Abstract:** Accurate determination of histological activity in ulcerative colitis (UC) is essential given its diagnostic and prognostic importance. Data on the relationship between histology and immune cell markers are limited. We ed to evaluate the association between histological disease activity and immune cell marker concentration in colonic biopsies from patients with UC. Methods Sigmoid colon biopsies from 20 patients with UC were retrospectively assessed using the Robarts Histopathology Index (RHI). Targeted mass spectrometry determined the concentration of 18 immune cell markers (cluster of differentiation (CD) 4, CD8, CD19, CD20, CD40, CD56, CD68, CD103, forkhead box p3 (FOXP3), human leucocyte antigen, DR alpha chain (HLA-DRA), interleukin 10 (IL-10), IL-23 subunit alpha (IL-23A), IL-23 receptor (IL-23R), IL-2 receptor alpha chain (IL-2RA), Ki67, lymphocyte-activation gene 3 (LAG-3), programmed cell death protein 1 (PD-1) and PD ligand 1 (PD-L1)). The association between RHI score and immune cell marker concentration was quantified using Spearman's rank correlation coefficient ( $\rho$ ) and related 95% CIs. Results Fourteen of the 18 immune cell marker proteins were detected, with tissue concentration ranging from 0.003 to 11.53 fmol/ $\mu$ g. The overall RHI score was positively

correlated with CD19, CD20, CD40, FOXP3, LAG-3, PD-1 and PD-L1 concentration ( $p=0.596-0.799$ ) and negatively correlated with CD56 concentration ( $p=-0.460$ ). There was no significant association between RHI score and CD4, CD8, CD68, CD103, HLA-DRA or Ki67 concentration. **Conclusions** This study provides insight into the correlation between immune cell marker expression and histological disease activity and the possible molecular and immunological determinants underlying microscopic disease activity in UC.

## 25COASOCT19

**Title:** In triple-negative breast cancer, fibrotic focus, the mitotic activity index and tumour-infiltrating lymphocytes have independent prognostic value: an observational population-based cohort study with very long follow-up

Kiraz U, Rewcastle E, Pettersen KB, *et al*

Journal of Clinical Pathology 2025;78:614-622.

<https://doi.org/10.1136/jcp-2024-209855>

**Abstract:** Triple-negative breast cancer (TNBC) is prognostically and therapeutically heterogeneous. The mitotic activity index (MAI) and fibrotic focus (FF) have been established as predictors in non-TNBC but not in TNBC. Late distant metastases occur in TNBC, but previous studies had short follow-up. High stromal tumour-infiltrating lymphocytes (sTILs) are prognostically favourable, but prognostic sTILs-thresholds are not well assessed. We evaluated prognostic/predictive characteristics in an observational population-based cohort of 231 consecutive TNBC patients with long follow-up. **Methods** MAI, FF, sTILs and other characteristics were analysed with standard receiver operating characteristic curve analysis, percentile-derived prognostic thresholds, univariate and multivariate survival methods. A TNBC index and decision tree were assessed for distant metastasis-free survival. **Results** Long follow-up was decisive: 7% of patients developed late distant metastases. In agreement with the aggressive nature of TNBC, the strongest prognostic MAI-threshold was 5 ( $p=0.001$ ), lower than that for non-TNBC phenotypes. Lymph-node (LN) status ( $p=0.0003$ ), FF ( $p=0.002$ ), MAI5 ( $p=0.009$ ) and sTILs (threshold 40%,  $p=0.003$ ) were multivariable based significant and independent prognosticators, but no other characteristics (age, tumour size and grade). LN status was the strongest prognosticator, followed by FF, MAI5 and sTILs40. Subgroup analyses of patients undergoing adjuvant chemotherapy (ACT) showed that only FF and sTILs had significant prognostic value, while LN-positivity and the combination of LN-positivity and  $MAI \geq 5$  could be a predictive factor for ACT outcome. **Conclusions** LN status, MAI5, FF and sTILs40 are prognostic factors in TNBC patients. In TNBC patients who have undergone ACT, the combination of LN-positivity and MAI5 is predictive for response to treatment.

## 25COASOCT20

**Title:** CD31 expression in human cancers: a pan-cancer immunohistochemical study

Ito A, Ito Y, Ikeda H, *et al*

Journal of Clinical Pathology 2025;78:623-628.

<https://doi.org/10.1136/jcp-2024-210009>

**Abstract:** CD31 (platelet endothelial cell adhesion molecule 1) is a transmembrane glycoprotein involved in cell adhesion and signal transduction that is primarily expressed in vascular endothelial cells, platelets, neutrophils, and certain tumour cells. We investigated

CD31 expression in cancer cells by conducting a pan-cancer gene expression analysis using data from cancer cell lines as well as an immunohistochemical analysis of surgically resected cancer specimens. The goal was to elucidate the frequency and distribution of CD31 expression across cancer types and its diagnostic significance. Methods Gene expression data from 1073 cancer cell lines were analysed to determine the frequency of CD31 expression across different cancer types. Immunohistochemical analysis was performed on 358 resected cancer specimens, focusing on adenocarcinomas and squamous cell carcinomas. The analysis compared the frequency of CD31 expression among specific cancer subtypes and between histological types. Results In gene expression analyses, adenocarcinomas showed a higher frequency of CD31 expression than did squamous cell carcinomas. Immunohistochemically, CD31 expression was observed in breast apocrine carcinomas (40.0%), hepatocellular carcinomas (18.8%), uterine endometrioid adenocarcinomas (31.6%), ovarian high-grade serous carcinomas (20.0%), ovarian clear cell carcinomas (40.0%) and urothelial carcinomas (25.0%). No CD31 expression was detected in oesophageal, renal, prostate or cervical cancers. Conclusions CD31 expression is more frequent in adenocarcinomas than in squamous cell carcinomas, with variability among cancer subtypes. Recognising CD31-positive cancers is critical to avoid misdiagnosing them as endothelial-derived tumours. The mechanisms underlying CD31 expression in cancer remain unclear and warrant further investigation.

## 25COASOCT21

**Title: If you provide them, they will come: an observational study of online pathology report access by patients at a large, academic, tertiary care hospital in Canada**

Ranot J, Noghani P, Rothwell D, et al

Journal of Clinical Pathology 2025;78:636-640.

<https://doi.org/10.1136/jcp-2025-210065>

**Abstract:** Patients of The Ottawa Hospital (TOH) are given immediate access to their pathology reports via an online patient portal. The purpose of this study was to determine how often patients accessed their reports, the sociodemographic and pathologic variables associated with access and the latency between sign out and access. Methods This retrospective cross-sectional observational study was conducted on the first 250 consecutive pathology reports published in 2023 from 10 different subspecialties in anatomical pathology at TOH. Data regarding date/time of report publication and access, as well as demographic data, and variables related to the individual report contents were extracted from the hospital's electronic health records. Results Of the 2500 patients included in this study, 1315 (52.6%) accessed their report online. Patients under 65 years of age, female patients and those residing within Ottawa were more likely to access their reports. Biopsies and reports with malignant diagnoses were accessed at higher rates than resections and benign cases, respectively. 463 (36.0%) patients accessed their reports within 24 hours; 822 (68.5%) accessed them within the first week. In 53% of cases, the patient accessed their report before the treating physician. Conclusions These findings highlight that while over half of patients accessed their pathology reports online, significant differences in access rates were observed based on age, gender, location and report type. The high proportion of patients reviewing their reports before their treating physician underscores the need for patient-centred strategies to enhance understanding and support timely communication of results.

**25COASOCT22****Title: Characterising the challenges of managing difficult red blood cell alloantibodies in liver transplant recipients**Chornenkyy Y, Fink MC, Felicelli C, *et al*

Journal of Clinical Pathology 2025;78:641-647.

<https://doi.org/10.1136/jcp-2024-209399>

**Abstract:** Formation of red blood cell alloantibodies (RBCAs) complicates transfusion support in liver transplantation (LT). Difficult RBCAs (DAs, >3 antibodies or antibodies for which <25% donors are antigen negative) further challenge care. This study characterises DA outcomes relative to non-difficult RBCAs (NDAs). Methods Single-centre, retrospective analysis of LT patients (2002–2021). RBCAs were defined as clinically significant antibodies. DAs were compared with NDAs. Results 89 patients had clinically significant RBCAs (DA=50, NDA=39). More DAs were anti-Jka, anti-M; fewer were anti-E, anti-K (all  $p<0.05$ ). DA patients often had multiple antibodies (44% vs 12.8% NDA,  $p=0.0022$ ). Probability of finding antigen-negative blood was lower for DAs (17.4% vs 68.1% NDA,  $p<0.0001$ ) as was RBCs received (9.4 vs 14.7 units in NDA,  $p=0.0036$ ). Although survival was similar, patients with DAs had more adverse reactions (8% vs 0%,  $p=0.128$ ). Some antibodies appeared to occur with specific liver diseases (such as primary sclerosing cholangitis, alcoholic steatohepatitis and recurrent disease); however, due to low sample size, definitive conclusions cannot be made.

Conclusions DA LT recipients contain >1 RBCA, have a lower probability of finding antigen negative blood and may experience more adverse transfusion event (ATE). Despite this, the incidence of ATEs was still quite low.

**25COASOCT23****Title: Paediatric Crohn's disease: histologic findings at initial presentation**Spasic S, Pankaj A, Kaplan JL, *et al*

Journal of Clinical Pathology 2025;78:659-666.

<https://doi.org/10.1136/jcp-2024-209535>

**Abstract:** Background Diagnosing paediatric Crohn's disease (CD) based on histology can present challenges. We evaluate the histological spectrum of treatment-naïve biopsies from children with CD and assess these findings' diagnostic and predictive value. Methods Three cohorts were identified: (1) 137 patients with CD, (2) 116 patients with ulcerative colitis (UC) and (3) 50 patients without inflammatory bowel disease. Biopsies from the gastrointestinal (GI) tract were re-examined for signs of active and chronic inflammation, including lymphocyte-pattern oesophagitis, focal enhancing gastritis and indicators of chronicity. Additionally, granulomas and microgranulomas (defined as clusters of 4–9 epithelioid histiocytes) were evaluated. Results Lymphocyte-pattern oesophagitis was observed in 15% of patients ( $n=20$ ). Moderate-to-severe diffuse gastritis was noted in 50.4% of patients ( $n=68$ ), while focal enhancing gastritis was identified in 11.1% ( $n=15$ ). In terminal ileal biopsies, 46.1% exhibited activity and 5.3% showed features of chronicity. Active colitis was present in 73% of patients ( $n=100$ ), with chronic colitis seen in 11.7% ( $n=16$ ). Granulomas and microgranulomas were observed in 31.4% (43/137) and 48.9% (67/137) of patients, respectively. Notably, 30.7% (42/137) of patients with microgranulomas were without granulomas. Previously undetected microgranulomas were found in 20 of 27 cases.



2.5% of patients with UC and none of the control cohort showed microgranulomas. Lymphocyte-pattern oesophagitis was associated with an increased need for anti-tumor necrosis factor (TNF) therapy ( $p=0.007$ ). Conclusions GI microgranulomas, often overlooked, are specific to CD in the proper clinical context. Oesophageal lymphocytosis may predict a need for more aggressive treatment. The study brings to light under-recognised aspects of CD's histological diagnosis, including the oversight of microgranulomas, the high prevalence of diffuse gastritis and low prevalence of focal enhancing gastritis, the frequent absence of terminal ileitis and the infrequent occurrence of chronic colitis.

## 25COASOCT24

### **Title: Clinicopathological significance and prognostic analysis of p21 and EGFR in colorectal cancer: a retrospective analysis on 12 319 cases in China**

Fei Y, Ma M, Gan L, *et al*

Journal of Clinical Pathology 2025;78:667-672.

<https://doi.org/10.1136/jcp-2024-209450>

**Abstract:** Colorectal cancer (CRC) is the third most common malignancy worldwide. Accurate pathological diagnosis and predictive abilities for treatment response and prognosis are crucial for patients with CRC. This study to analyse the expressions of p21 and EGFR in CRC and their relationships with clinicopathological characteristics and prognosis to enhance diagnostic and prognostic evaluations. Methods This study conducted a retrospective analysis of p21 and EGFR expressions in 12 319 Chinese patients with CRC using immunohistochemistry. The relationships between these expressions and clinicopathological characteristics and survival outcomes were explored through statistical and survival analyses. Results Differential expressions of p21 and EGFR in CRC were closely related to clinicopathological characteristics and significantly impacted overall survival (OS). p21 expression was associated with the primary tumour site, mucinous subtype, lymphovascular invasion, perineural invasion, circumferential resection margin, T stage, N stage, tumour, node, metastases (TNM) stage, and mismatch repair status. EGFR expression was related to mucinous subtype, tumour differentiation, lymphovascular invasion, perineural invasion, tumour size, T stage, N stage, TNM stage and *BRAF* gene mutation. p21 and EGFR expressions were positively correlated ( $r=0.11$ ). High p21 expression correlated with favourable OS, whereas high EGFR expression predicted poorer OS. A prognostic nomogram incorporating these biomarkers and clinical variables demonstrated robust predictive power for patient survival rates. Conclusion p21 and EGFR serve as potential indicators for pathological diagnosis, risk stratification, and predicting treatment efficacy and prognosis in patients with CRC. The study's findings provide valuable references for personalised treatment and prognosis evaluation in clinical practice.

## 25COASOCT25

### **Title: Lymph node threshold in colorectal cancer: surgeons' perspectives and practices**

Padmanabha N, Chornenkyy Y, Pan W, *et al*

Journal of Clinical Pathology 2025;78:673-677.

<https://doi.org/10.1136/jcp-2025-210290>

**Abstract:** Background Current guidelines emphasise examining at least 12 lymph nodes (LN) in colorectal cancer resections. This study surveyed surgeon perspectives on suboptimal

LN yield (<12) to assess interpretive variability and beliefs regarding its clinical impact. **Methods** A voluntary 19-question electronic survey was distributed to colorectal and general surgeons, exploring clinical, pathological and molecular considerations in cases with low LN yield. **Results** Among 168 respondents (58% colorectal surgeons; 32% general surgeons), most practised in academic or mixed settings, and 73% had over 10 years of experience. While 71% reported suboptimal LN yields as infrequent, 29% encountered them more regularly. A majority (92%) contacted pathology when LN yield was low; however, opinions diverged on next steps—particularly when maximum N-stage was already achieved or when considering total fat submission. Nearly half (49%) believed that low LN yield rarely alters treatment decisions, yet many acknowledged its association with poorer outcomes. Regarding potential contributing factors, 56% cited neoadjuvant therapy, 47% noted specimen length or sidedness, but most did not consider mismatch repair status, age or body mass index to significantly impact LN yield. **Conclusion** Despite the ‘12-node rule’, surgeon perspectives vary regarding the significance, aetiology and clinical consequences of suboptimal LN yield. The overarching message for pathology is that thoughtful communication among surgeons and pathologists is critical to understand the idiosyncrasies around individualised care and nuances around factors that may influence LN yield, with the ultimate hope to best manage resources and optimise patient care.

## 25COASOCT26

**Title: Relationship between adenovirus infection and intussusception via pathological evidence confirms**

Lin L, Huang C, Lo C, *et al*

Journal of Clinical Pathology 2025;78:678-683.

<https://doi.org/10.1136/jcp-2025-210194>

**Abstract:** Although some cases of intussusception in older children are associated with pathological changes such as lymphoma or polyps, the cause of most cases in infants is unknown. Several reports have identified an association between adenovirus infection and intussusception in children. However, much of the evidence is indirect, such as stool samples or throat swab data. Our study analysed intestinal tissue, which may be more direct evidence of the relationship between adenovirus infection and intussusception. **Methods** We retrospectively reviewed children <6 years of age with intussusception who underwent surgery for failed reduction. The pathological tissue was processed into formalin-fixed paraffin-embedded (FFPE) sections. Adenovirus immunohistochemistry (IHC) and PCR testing were performed to obtain direct evidence of the relationship between adenovirus infection and intussusception. **Results** Our study included 29 patients, 27 appendiceal and 8 intestinal tissues. Only eight appendix specimens were successfully processed into FFPE tissue. IHC testing was positive in three cases (37.5%), and PCR testing was positive for adenovirus type C in four cases (50%). The control group consisted of eight children <6 years who underwent incidental appendectomies, and all control subjects had negative IHC and PCR analyses. PCR is as useful and reliable as IHC in diagnosing adenovirus in intussusception and has greater sensitivity than IHC. **Conclusion** We directly confirmed the relationship between adenovirus infection and intussusception through IHC analysis and PCR detection of pathological evidence. PCR is more sensitive than IHC for diagnosing adenovirus in intussusception.

**25COASOCT27****Title: Can polycythaemia vera disease be predicted from haematologic parameters? A machine learning-based study**

Haskul M, Kaya E, Kurtoğlu A

Journal of Clinical Pathology 2025;78:684-690.

<https://doi.org/10.1136/jcp-2025-210087>

**Abstract:** The of this research is to diagnose polycythaemia vera (PV) disease using different machine learning (ML) algorithms with complete blood count (CBC) parameters before further investigations such as Janus kinase 2 (*JAK2*), erythropoietin (EPO) and bone marrow biopsy (BMB). **Methods** The study included 1484 patients who presented to the adult haematology clinic with elevated haemoglobin. Participants were retrospectively screened for *JAK2*, EPO and BMB results, and patients were categorised as PV group (n=82) and non-PV (other) (n=1402). First, the synthetic minority oversampling technique (SMOTE) method was used to avoid data imbalance. Then, classification predictions were made using Random Forest, Support Vector Machine Technique, Extreme Gradient Boosting (XGBoost) and K-Nearest Neighbours algorithms according to the participants' CBC parameters of white cell count (WBC), haematocrit (HCT), haemoglobin (HGB) and platelet (PLT). **Results** The XGBoost algorithm was found to be the most effective ML algorithm in predicting the model (area under the curve=0.99, accuracy=0.94, F1-Score=0.94). In addition, the most effective parameter in the prediction of the model was PLT with 42.4%. As a result of the t-test, there was a highly significant difference between the WBC, PLT, HGB, HCT, EPO, *JAK2* and bone marrow density results of PV and other groups ( $p<0.001$ ). **Conclusion** ML algorithms can diagnose PV with CBC parameters with high accuracy, thus emphasising the potential to reduce the dependence on costly diagnostic methods such as *JAK2*, EPO and BMB.

**25COASOCT28****Title: Use of quality checks and processes across digital histopathology: an initial survey from the Bigpicture consortium**Pye H, Brett DS, Lyons C on behalf of the Bigpicture consortium, *et al*

Journal of Clinical Pathology 2025;78:691-696.

<https://doi.org/10.1136/jcp-2024-210010>

**Abstract:** In the end-to-end digital pathology workflow, variability can be introduced at each step, resulting in differences in the final image dataset. The effectiveness of quality control processes at each step of the workflow will impact the extent and relevance of this variability. **Methods** To assess the maturity of whole slide imaging (WSI) quality processes for the whole digital pathology workflow, we conducted an online questionnaire across 19 digitally active members of the Bigpicture consortium. **Results** A key finding was that a lower proportion of centres are implementing rigorous quality processes and checks processes at the post-scanning steps of the WSI workflow, such as 'digital reporting and display' (44%) and computational analysis (34%), when compared with pre-scanning steps such as 'pre-staining' (72%) and 'staining' (77%). **Conclusions** This information allows us to identify priorities for quality improvement of the overall WSI workflow.

**25COASOCT29****Title: Increased PI3K pathway activity is associated with recurrent breast cancer in**

**patients with low and intermediate 21-gene recurrence score**Lin LH, Wesseling-Rozendaal Y, Vasudevaraja V, *et al*

Journal of Clinical Pathology 2025;78:697-702.

<https://doi.org/10.1136/jcp-2023-209344>

**Abstract:** We investigated key signalling pathways' activity and mutational status of early-stage breast carcinomas with low and intermediate 21-gene recurrence score (RS) to identify molecular features that may predict recurrence. **Methods** This is a retrospective case–control study of 18 patients with recurrent breast carcinoma with low and intermediate 21-gene RS (<25) and control group of 15 non-recurrent breast cancer patients. DNA and mRNA were extracted from tumour tissue. mRNA expression of genes involved in oestrogen receptor (ER), androgen receptor (AR), PI3K and MAPK signalling pathways was measured by real-time quantitative reverse transcription-qPCR (OncoSIGNa G4 test, InnoSIGN). Tumour mutational landscape was assessed by targeted DNA sequencing (OncoPrint Precision Assay). **Results** There were no statistical differences between the groups' demographic and clinicopathological characteristics. PI3K pathway showed significantly higher activity in cases compared with controls ( $p=0.0014$ ). Receiver operating characteristic curve analysis showed an area under the curve of 0.79 for PI3K pathway activity in the prediction of recurrent disease in low and intermediate 21-gene RS breast cancer. There was no difference in ER, AR and MAPK pathway activity. *PIK3CA* alterations were the most common driver mutations, but no difference was found between the groups ( $p=0.46$ ) and no association with PI3K pathway activity ( $p=0.86$ ). Higher *Ki67* gene expression was associated with recurrences ( $p=0.042$ ). **Conclusion** Increased PI3K pathway activity, independent of *PIK3CA* mutations, may play a role in the recurrence of early-stage breast cancer with low and intermediate 21-gene RS. Pathway analysis can help to identify high-risk patients in this setting.

**25COASOCT30****Title: Genomic discordances and heterogeneous mutational burden, PD-L1 expression and immune infiltrates of non-small cell lung cancer metastasis**Wu J, Mao L, Lei W, *et al*

Journal of Clinical Pathology 2025;78:703-710.

<https://doi.org/10.1136/jcp-2023-209328>

**Abstract:** To investigate the genomic discordances and heterogeneous mutational burden, PD-L1 expression and immune cell (IC) infiltrates of non-small cell lung cancer (NSCLC) metastasis. **Methods** Surgical samples from 41 cases of NSCLC with metastatic tumours (MTs) and paired primary tumours (PTs) were collected. PD-L1 expression and ICs were quantified using image-based immunohistochemistry profiling. Whole exome sequencing was employed to explore discrepancies in genomic characteristics, tumour mutational burden (TMB) and tumour neoantigen burden (TNB) in 28 cases. **Results** Non-synonymous mutations in MTs were slightly more than in PTs, with only 42.34% of mutations shared between paired PTs and MTs. The heterogeneity of TMB showed no significant difference ( $p=0.785$ ) between MTs and PTs, while TNB significantly increased in MTs ( $p=0.013$ ). MTs generally exhibited a higher density of PD-L1+ cells and a higher tumour proportion score with a lower density of IC infiltrates. Subgroup analysis considering clinicopathological factors revealed that the heterogeneity of immune biomarkers was closely associated with the

histology of lung adenocarcinoma, metastatic sites of extrapulmonary, time intervals and treatment history. Prognosis analysis indicated that a high density of CD8+ T cells was a low-risk factor, whereas a high density of PD-L1+ cells in MTs was a high-risk factor for cancer-related death in metastatic NSCLC. Conclusions The mutational burden, PD-L1 expression and IC infiltrates undergo changes during NSCLC metastasis, which may impact the immunotherapeutic benefits in patients with NSCLC with metastatic progression and should be monitored according to clinical scenarios.

### 25COASOCT31

**Title: Quantitative assessment of red blood cell surface molecules in hereditary spherocytosis**

More TA, Kedar PS

Journal of Clinical Pathology 2025;78:711-716.

<https://doi.org/10.1136/jcp-2025-210055>

**Abstract:** Hereditary spherocytosis (HS) refers to a heterogeneous disorder varying in genotypic and phenotypic features manifested by the production of spherocytes. The diseased cells can be eliminated from the circulatory system either by macrophages in the spleen in the extravascular pathway or the intravascular pathway via the complement cascade. This study ed to investigate the status of red blood cell (RBC) surface molecules CD55 (decay accelerating factor), CD35 (complement receptor type 1–CR1), CD59 (MACIF), CD47 (marker of self) and CD71 (transferrin receptor) from individuals diagnosed with HS. Methods This study to quantitatively assess RBC surface molecules (CD35, CD55, CD59, CD47 and CD71) on peripheral RBCs from 42 HS patients and 30 healthy controls, carried out by flow cytometry using monoclonal antibodies. Results Our findings show that HS patients had a significant 58% decrease in anti-CD35 binding compared with healthy controls. This is the first study to demonstrate the presence of erythrocytes with reduced CD35 levels in HS patients. Compared with the control group, HS patients had comparable levels of CD59 and CD47, but their CD55 levels were significantly reduced, with a 30% decrease in anti-CD55 binding. The expression level of CD71 was higher in HS patients (3.33%) compared with healthy controls in our study. Conclusion The diminished levels of CD35 and CD55 in HS patients may influence RBC clearance, possibly through mechanisms that remain fully understood and require further investigation, including their potential role in haemolytic crises. Further research employing molecular techniques is required to clarify their exact role in HS.

### 25COASOCT32

**Title: Low-grade oncocytoid neoplasm in the Milan system: Tips for the diagnosis of Warthin tumor and other differential diagnostic considerations**

Esther Diana Rossi MD, PhD, Christopher C. Griffith MD

Cancer Cytopathology, vol.-133, issue -10.

<https://doi.org/10.1002/cncy.70037>

**Abstract:** The current review article deals with the evaluation of the oncocytic/oncocytoid lesions in the salivary gland. The authors will focus on the diagnosis of Warthin tumor (WT) as a launching point to detail important morphologic findings that should prompt designation of an aspirate as oncocytic salivary gland neoplasm of uncertain malignant potential or other



Milan categories. Oncocytic cells are defined as cells with a moderate to abundant amount of eosinophilic finely granular cytoplasm, round-to-oval nuclei, and large-distinct nucleoli. In contrast, the term oncocytoid is also frequently used in this discussion and indicates tumor cells with similarly abundant and sometimes granular cytoplasm but lacking all the definitive features of a true oncocyte. Several helpful tips are provided in hopes of improving an accurate diagnosis of WT on an aspirate sample. Using these types allows for consideration of important differential diagnoses, including both benign and malignant entities, when faced with an oncocytic salivary gland neoplasm. The morphological criteria as well as the possible application of ancillary techniques are also discussed.

### 25COASOCT33

**Title: American College of Radiology–Developed Thyroid Imaging Reporting and Data System 3, 4, and 5 thyroid nodules are distinctive by cytology, genetic imprints, and histology**

Sanhong Yu MD, PhD et.al.

Cancer Cytopathology, vol.-133, issue -10.

<https://doi.org/10.1002/cncy.70050>

**Abstract:** Thyroid nodules, found in up to 68% of adults, can be risk-stratified by high-resolution ultrasound. This study evaluates the concordance between “suspicious” Thyroid Imaging Reporting and Data System (TI-RADS) 3–5 nodules and cytologic and molecular findings from fine-needle aspiration. **Methods**—A total of 1199 suspicious thyroid nodules stratified as TI-RADS 3 ( $n = 384$ ), TI-RADS 4 ( $n = 569$ ), and TI-RADS 5 ( $n = 246$ ) were studied. Cytopathologic and molecular results were correlated with clinical data from electronic medical records. **Results**—Cytology, histology, and molecular testing revealed a lower risk of malignancy in TI-RADS 3 and 4 nodules compared to TI-RADS 5. Among TI-RADS 3 nodules, 75% (287 of 384) were cytologically benign, with only one case diagnosed as papillary thyroid carcinoma (PTC), and 8 of 48 resected nodules (17%) confirmed as carcinoma. In TI-RADS 4, 10% (56 of 569) were suspicious for or diagnosed as PTC by cytology, with 85 of 130 (65%) resected nodules confirmed as carcinoma. In TI-RADS 5, 44% (109 of 246) were cytologically suspicious for or diagnosed as PTC, and 129 of 154 (84%) resected nodules were malignant. High-risk mutations were more frequent in TI-RADS 5 than in TI-RADS 3 and 4. Overall malignancy rates were 2.0% (eight of 384) for TI-RADS 3, 14% (77 of 569) for TI-RADS 4, and 52% (129 of 246) for TI-RADS 5 nodules. **Conclusion**—TI-RADS 3, 4, and 5 nodules demonstrate distinct cytologic, molecular, and histologic features. TI-RADS 3 and 4 nodules are associated with lower malignancy risks, whereas TI-RADS 5 nodules exhibit a high risk of malignancy and are associated with higher mortality.

### 25COASOCT34

**Title: *DICER1* mutations in Bethesda III/IV thyroid cytology samples: A multicenter observational study**

Afreen Karimkhan MD et.al.

Cancer Cytopathology, vol.-133, issue -10.

<https://doi.org/10.1002/cncy.70045>

**Abstract:** Mutations in *DICER1* are uncommon, poorly understood, and infrequently found

in thyroid nodules. **Methods-**The objective of this study was to investigate category III/IV thyroid nodules according to The Bethesda System for Reporting Thyroid Cytopathology with *DICER1* gene mutations detected in fine-needle aspiration cytology samples using ThyroSeq v3 molecular testing, with a focus on an exploration of the clinical and histopathologic outcomes of these nodules. In this multicenter study spanning more than 6 years, nodules were retrospectively analyzed for patient demographics, clinical course, cytologic features, and histopathology, where available. **Results-** In total, 88 patients with somatic *DICER1* mutations were included, with a mean age of 39.6 years and a female predominance. All mutations were in the somatic hotspot region, most commonly at the codon 5437 site. Most excised nodules showed benign histologic features (65.9%). Interestingly, the rate of malignancy was higher in this cohort compared with that in the national average. **Conclusions-***DICER1* mutations appear to confer a higher risk of malignancy, but are not associated with any specific cytological or histopathological distinguishing features.

### 25COASOCT35

#### **Title: Diagnostic approach to FNA biopsy of cystic lesions of the head and neck**

Stefen Andrianus MD, Olivia Leung MD, Zubair Baloch MD, PhD

Cancer Cytopathology, vol.-133, issue -10.

<https://doi.org/10.1002/cncy.70036>

**Abstract:** Cystic lesions of the head and neck encompass a wide spectrum of benign and malignant entities, which often presents diagnostic challenges as a result of the region's complex anatomy. Despite extensive literature, variability persists in diagnostic strategies and approaches. Fine-needle aspiration biopsy is a commonly used and highly effective method for the initial assessment of these lesions by offering a minimally invasive technique to collect cellular material for diagnostic evaluation. A multidisciplinary approach integrating clinical, radiologic, and cytologic findings is essential in diagnosing cystic lesions of the head and neck. This review provides readers with an organ-based algorithmic approach for integrating anatomic location (central vs. lateral neck), radiologic features, and cytomorphology to refine diagnoses and guide patient management.

### 25COASOCT36

#### **Title: Infections Due to *Corynebacterium kroppenstedtii* With Focus on Granulomatous Lobular Mastitis for Tissue Specificity, Pathogenesis, Bacteriologic Workup, and Treatment.**

Qiong Gan, Yang Ding et.al.

Arch Pathol Lab Med 26 August 2025; 149 (9): 812–821.

<https://doi.org/10.5858/arpa.2024-0365-OA>

**Abstract:** *Corynebacterium kroppenstedtii*-may cause granulomatous lobular mastitis (GLM). Yet, current understanding is limited regarding its overall clinical significance, cultivation practice, GLM pathogenesis, and antimicrobial treatment. **Objective-**To report the isolation and significance of *C kroppenstedtii*, features of patients with GLM, pathologic findings and mechanism, bacteriologic workup, and optimal treatment. **Design.-** Analysis of the cases with *C kroppenstedtii* at The University of Texas MD Anderson Cancer Center from 2016 to March 2024 for mechanistic insights. **Results-**During a period of 8 years, isolates

of *C. kroppenstedtii* were obtained from 10 women and 7 men. All of the women, with an average age of 34 years (range, 18–61 years), presented with chronic or subacute mastitis, and were subsequently diagnosed with GLM. The men, with an average age of 66 years, had neoplastic diagnoses with the bacterium being commensal in 6 cases. Thus, *C. kroppenstedtii* shows a predilection to infect the female breast ( $P < .001$ ). Predisposing risks for GLM included childbirth in 8 women and nipple inversion in 2 women. Histopathology revealed xanthogranulomatous inflammation and Gram-positive bacilli within fat droplets or extracellularly. From GLM aspirates or tissue, the liquid culture media and/or anaerobic incubation yielded 9 of 10 isolates. Up to 14 tested strains were susceptible to vancomycin, linezolid, rifampin, and gentamicin. Nine women received extensive antimicrobial therapy. Conclusions- *C. kroppenstedtii* is a rare commensal, is mammophilic, and causes GLM. Liquid culture media and/or anaerobic incubation offer the best culture recovery. The inflamed fatty milieu of the breast forms xanthogranulomas. Several antibiotics likely render effective treatment, particularly lipophilic rifampin, which penetrates the bacteria-laden fat droplets. The genus *Corynebacterium* comprises a large group of Gram-positive bacilli that are common commensals found on the surface of human skin and mucosa. These bacteria are club-shaped facultative anaerobes and commonly require nutritionally rich media for cultivation. Among roughly 110 *Corynebacterium* spp, half are medically significant. *Corynebacterium diphtheriae*, described in 1896, was the well-known cause of diphtheria in children before the vaccination era, whereas all other *Corynebacterium* spp are usually opportunistic but assume more significance nowadays with better recognition and/or increasing populations with comorbidities.

## 25COASOCT37

### **Title: Concomitant Waldenström Macroglobulinemia/Lymphoplasmacytic Lymphoma and Non-Immunoglobulin M Plasma Cell Neoplasm: A Report of 14 Cases With Laboratory Evidence of Biclonal B-Cell Neoplasms in Individual Patients**

Yue Zhao, MD, PhD; Philip Petersen, MD, PhD et.al.

Arch Pathol Lab Med (2025) 149 (9): 822–830.

<https://doi.org/10.5858/arpa.2024-0270-OA>

**Abstract:** The co-occurrence of plasma cell neoplasm (PCN) and lymphoplasmacytic lymphoma (LPL) is rare, and their clonal relationship remains unclear. Objective-To evaluate the clinicopathologic characteristics of concomitant LPL/PCN. Design-Retrospectively analyzed clinical and laboratory data of 14 cases. Results-Three patients initially presented with immunoglobulin (Ig) M paraprotein, 1 with IgG paraprotein, and 10 had simultaneous diagnoses of PCN and LPL. In 13 cases, flow cytometry detected both LPL and PCN in marrow biopsies. Furthermore, immunohistochemistry highlighted the 2 neoplastic populations, demonstrating an increased proportion of plasma cells and their expression of cyclin D1, CD56, and/or a non-IgM isotype restriction. All cases exhibited discordant heavy-chain isotypes between LPL and PCN. Thirteen of the 14 cases (92.9%) had concordant light-chain restrictions between the 2 neoplasms, and the remaining case (7.1%) showed discordant light-chain restrictions. Of the 12 patients with follow-up, 5 were treated with myeloma regimens, 2 with LPL regimens, 3 with combined therapy, and 2 with observation alone. Follow-up ranged from 2 to 146 months (median, 12.5 months). One patient died of PCN progression, one died of comorbidity, and 10 patients were alive with or without disease.

Survival analysis showed no significant difference from the control. Conclusions- The discordant heavy-chain isotype restrictions between PCN and LPL suggest biclonal B-cell neoplasms, which is supported by PCN's phenotypic distinction, such as the expression of cyclin D1 and/or CD56. However, our series exhibited a tendency toward concordant light-chain restrictions between the 2 neoplasms, raising the possibility that PCN may evolve from LPL through class switching. Lymphoplasmacytic lymphoma/Waldenström macroglobulinemia (LPL/WM) is a type of indolent small mature B-cell neoplasm that typically exhibits plasmacytoid differentiation.<sup>1</sup> Conversely, plasma cell neoplasm (PCN) is a neoplasia of terminally differentiated B cells, devoid of clonal B-cell component. Both neoplasms have a propensity to involve the bone marrow and often present with serum paraproteinemia. In both instances, serum paraprotein may present early as monoclonal gammopathy of undetermined significance, years before the disease progresses to either LPL/WM or symptomatic PCN. Despite these shared clinical and laboratory features, these 2 neoplasms develop at different stages of B-cell ontogeny and manifest distinctive clinical presentations and disease courses. Consequently, the current therapeutic approaches differ between LPL/WM and PCN, and the pathologic diagnosis of each entity is usually straightforward. Interestingly, PCN has been reported to coexist with other mature B-cell neoplasms, most frequently with chronic lymphocytic leukemia (CLL), but its concurrence with LPL is relatively rare. In particular, the co-occurrence of LPL and PCN in the bone marrow of the same individual is rarely reported, being limited to sporadic case reports or small series in the literature. This may be because a plasmacytoid component is naturally present in LPL,<sup>1</sup> and PCN concurrent with LPL in the bone marrow is susceptible to being misclassified as a plasmacytic component of LPL, leading to underrecognition of cases with this type of composite B-cell neoplasms. Consequently, the clinicopathologic features and pathogenesis of concomitant LPL/WM and PCN remain to be well delineated. Herein, we report our retrospective analysis of 14 cases of concomitant LPL/WM and PCN in individual patients.

## 25COASOCT38

### **Title: The Development and Evaluation of a Convolutional Neural Network for Cutaneous Melanoma Detection in Whole Slide Images**

Emily L. Clarke, MBBS, PGDip(HR), PhD

Arch Pathol Lab Med (2025) 149 (9): 831–837.

<https://doi.org/10.5858/arpa.2024-0094-OA>

**Abstract:** The current melanoma staging system does not account for 26% of the variance seen in melanoma-specific survival, therefore our ability to predict patient outcome is not fully elucidated. Morphology may be of greater significance than in other solid tumors, with Breslow thickness remaining the strongest prognostic indicator despite being subject to high levels of interobserver variation. The application of convolutional neural networks to whole slide images affords objective morphologic metrics, which may reveal new insights into patient prognosis. Objective-To develop and evaluate a convolutional neural network for invasive cutaneous melanoma detection in whole slide images for the generation of objective prognostic biomarkers based on tumor morphology. Design-One thousand sixty-eight whole slide images containing cutaneous melanoma from 5 data sets were used in the initial development and evaluation of the convolutional neural network. A 2-class tumor

segmentation network with a fully convolutional architecture was trained using sparse annotations. The network was evaluated at per-pixel and per-tumor levels as compared to manual annotation, as well as variation across 3 scanning platforms. Results-The convolutional neural network located conventional cutaneous invasive melanoma tissue with an average per-pixel sensitivity and specificity of 97.59% and 99.86%, respectively, across the 5 test sets. There were high levels of concordance between the tumor dimensions generated by the model as compared to manual annotation, and between the tumor dimensions generated by the model across 3 scanning platforms. Conclusions-We have developed a convolutional neural network that accurately detects invasive cutaneous conventional melanoma in whole slide images from multiple data sources. Future work should assess the use of this network to generate metrics for survival prediction.

### 25COASOCT39

#### **Title: Intraoperative Evaluation of Pediatric Bone and Soft Tissue Lesions: Retrospective Analysis of 595 Frozen Sections With Emphasis on Discrepancy and Diagnostic Pitfalls**

Benjamin L. Coiner, MD; Hernán Correa, MD et.al.

Arch Pathol Lab Med (2025) 149 (9): 838–845.

<https://doi.org/10.5858/arpa.2024-0329-OA>

**Abstract:** Frozen section (FS) evaluation of pediatric bone and soft tissue (BST) lesions is infrequently encountered and may pose considerable diagnostic challenges. Limited data exist about the accuracy and related diagnostic difficulties. Objective-To identify and analyze discrepancies between the FS diagnosis and final diagnosis in order to increase the awareness of common diagnostic pitfalls in FS evaluation of pediatric BST lesions. Design-We retrospectively reviewed 595 consecutive FSs of pediatric BST lesions from 373 patients and analyzed the accuracy and causes for interpretation errors. Results-Discrepant diagnoses were found in 23 of 595 FSs (3.9%). Discrepancy rates were slightly higher in benign soft tissue lesions and FSs requested for diagnosis/adequacy, although no statistically significant difference was observed. Pathologist misinterpretation contributed to discrepancy in 17 of 23 FSs (73.9%), which were classified into 6 patterns of error. For margin, 3 patterns were found: normal hematopoietic elements versus malignant cells in Ewing sarcoma bone marrow margin (n = 3), prominent sinonasal vasculature and stroma versus sinonasal tract angiofibroma (n = 3), and atrophic skeletal muscles versus malignant cells in rhabdomyosarcoma and Ewing sarcoma (n = 2). For diagnosis, another 3 patterns were identified: misclassification of benign bone tumors (n = 5), misclassification of benign spindle neoplasms (n = 2), and vascular malformation versus normal tissue (n = 2). Conclusions-FS is a valuable tool for guiding surgical management of pediatric BST lesions, which can be challenging entities and represent significant diagnostic pitfalls. Awareness of these FS pitfalls may help in further increasing diagnostic accuracy.

### 25COASOCT40

#### **Title: Optimization of Current Procedural Terminology Coding in Complex Genitourinary Surgical Specimens**

David B. Behrman, MD; Robert Achram, MD et.al.

Arch Pathol Lab Med (2025) 149 (9): 846–851.



<https://doi.org/10.5858/arpa.2024-0118-OA>

**Abstract:** Complex surgical specimens are associated with complex Current Procedural Terminology (CPT) coding. Objective-To assess and optimize the accuracy of CPT coding of complex genitourinary specimens at our institution. Design-Baseline CPT codes for nephrectomy and cystectomy surgical pathology specimens were examined during a 3-month period. Pathology reports were reviewed for accurate CPT coding, and commensurate tests of change were implemented. Post-test-of-change data were re-collected, analyzed, and compared to the baseline data. Results-Baseline data consisted of 71 genitourinary specimens (April to June 2021) and demonstrated undercoding in 46% (n = 33 of 71) of specimens, mostly in specimens with 2 or more billable organs. From findings in baseline data, we implemented test-of-change efforts consisting of awareness, education, and increased documentation and communication between all involved parties. Marked improvement was noted in the coding accuracy of specimens with 2 billable organs (pretest: n = 4 of 21, 19%; posttest: n = 14 of 21, 67%) and 3 or more billable organs (pretest: n = 0 of 16, 0%; posttest: n = 7 of 12, 58%) ( $P$  value = .002). Problematic areas included nephrectomy specimens resected with adrenal glands (pretest: n = 2 of 12, 17%; posttest: n = 12 of 14, 86%) and ureters for urothelial carcinoma (pretest: n = 0 of 10, 0%; posttest: n = 3 of 6, 50%), as well as regional lymph nodes commingled with resection specimens (pretest: n = 0 of 11, 0%; posttest: n = 7 of 9, 78%). Conclusions-A comprehensive approach involving all stakeholders is necessary for CPT coding of complex surgical specimens. Documentation and familiarity with coding rules, specifically bundling and unbundling, as well as clinical indications for resection, are important factors in optimizing CPT coding.

## 25COASOCT41

### **Title: The Impact of Scoring Method on Accuracy and Reproducibility of Hans Cell-of-Origin Prediction in Excisional Biopsies of Diffuse Large B-Cell Lymphoma, Not Otherwise Specified**

Oleksandr Yanko, MD; Andrew G. Lytle, MD, PhD et.al.

Arch Pathol Lab Med (2025) 149 (9): 852–858.

<https://doi.org/10.5858/arpa.2024-0366-OA>

**Abstract:** Aided by tissue microarray (TMA) technology, several RNA-correlated immunohistochemistry-based algorithms have been developed for cell-of-origin (COO) prediction in diffuse large B-cell lymphoma, not otherwise specified (DLBCL-NOS). However, there is currently no empirical evidence to guide the optimal application of these algorithms to whole tissue sections (WTSs). Objective-To assess the impact of various scoring methods on the accuracy and reproducibility of the popular Hans algorithm. Design-We compared 3 different WTS-based scoring methods, designated as *global*, *selective*, and *hotspot* scoring, to a matched TMA evaluation and gold standard RNA analysis (Lymph2Cx; germinal center B cell n = 64; activated B cell/unclassified n = 68) using a representative series of 132 excisional biopsies of de novo DLBCL-NOS. Positivity scores (10% increments) were submitted by 3 expert lymphoma pathologists, with 30% or more defining positivity. Results-Sixty-eight of the 132 cases of DLBCL-NOS (52%) exhibited variation in Hans immunohistochemistry marker phenotype as a consequence of scoring method and/or interscorer discordance. Although this led to changes in Hans COO assignment in 27 of 132 cases (20%), none of the WTS-based scoring methods were

statistically inferior to one another in terms of raw accuracy. Hotspot scoring yielded the lowest proportion of borderline scores (20%–40% range) for BCL6 transcription repressor (BCL6) and IRF4 transcription factor (MUM1) but negatively impacted the balance between sensitivity and specificity for these markers. Selective scoring was associated with significantly worse interscorer concordance compared to TMA evaluation, which it was designed to replicate. Conclusions-Overall, our data favor the use of global scoring for its noninferior accuracy, solid interscorer concordance, nonnegative influence on individual Hans markers, and current widespread use.

## 25COASOCT42

### **Title: A Multicenter Study to Evaluate Diagnostic Accuracy by Pathologists Using the Aperio GT 450 DX in Local and Remote Viewing Stations Open Access**

Alexander D. Borowsky, MDCorresponding Author; Dylan V. Miller, MD et.al.

Arch Pathol Lab Med (2025) 149 (9): 859–867.

<https://doi.org/10.5858/arpa.2024-0204-OA>

**Abstract:** The adoption of digital pathology may enable pathologists to perform primary diagnosis in both local and remote whole slide image viewing settings, improving logistics and convenience. Objective-To test the performance of a new whole slide imaging system (Aperio GT 450 DX), both local intranet-based and remote internet-based viewing were compared with manual glass slide light microscopy. Design- A total of 1161 curated cases, enriched with difficult clinical diagnoses, were enrolled in this accuracy study and digitally scanned on 3 Aperio GT 450 DX instruments at 3 clinical sites. Ten reading pathologists across the 3 study sites viewed images either locally (directly connected to the image server) or remotely (viewed over an internet connection). Each diagnosis was scored (concordant, minor discrepancy, or major discrepancy) by a separate team of 3 adjudication pathologists. The diagnostic accuracy of the Aperio GT 450 DX was tested by comparing the whole slide image review diagnosis with the conventional light microscope manual slide review diagnosis. Results-The difference in the major discrepancy rate between whole slide image review diagnosis and manual slide review diagnosis was 2.40% (95% CI, 1.40%–3.39%), meeting the predefined acceptance criterion of the 95% CI upper bound of 4% or less. Secondary end points were also met, including an upper bound of 7% or less and both local-only and remote-only upper-bound discrepancy rates of 4% or less. Major discrepancies were slightly lower for the remotely viewed cases (2.17%) compared with local direct server connection (2.61%), and time per read was not different. Conclusions-The diagnoses made using the Aperio GT 450 DX, using both local and remote access image data, were noninferior to the diagnoses made using conventional light microscopy.

## 25COASOCT43

### **Title: Prognostic Implications of the Bethesda System in Fine-Needle Aspiration for Follicular Thyroid Carcinoma**

Hyunju Park, MD, PhD; Young Lyun Oh, MD, PhD

Arch Pathol Lab Med (2025) 149 (9): 868–873.

<https://doi.org/10.5858/arpa.2024-0304-OA>

**Abstract:** Fine-needle aspiration is an effective tool for sampling thyroid nodules; its results are classified according to the Bethesda System for Reporting Thyroid Cytopathology

(BSRTC), whose categories define malignancy risks. Objective- To compare the histologic outcomes and disease-free survival (DFS) with the preceding BSRTC categories, we hypothesized that the initial cytologic categories may reflect long-term outcomes in follicular thyroid carcinoma (FTC), similar to those observed in papillary thyroid carcinoma. Design- This retrospective study enrolled 134 patients with FTC who underwent preoperative cytology between April 2011 and December 2020. Results were classified into 6 categories according to the BSRTC: nondiagnostic, benign, atypia of uncertain significance (AUS), follicular neoplasm (FN), suspicious for malignancy, or malignant. Results-Overall, 8 of 134 patients (6.0%) were categorized as having a nondiagnostic FTC, 35 of 134 (26.1%) as benign, 51 of 134 (38.1%) as AUS, and 40 of 134 (29.9%) as FN. No lesions were classified as suspicious for malignancy or malignant. The nondiagnostic, AUS, and FN categories were associated with a progressively higher risk of vascular invasion, disease recurrence, and high-risk FTC, based on the 2022 World Health Organization classification ( $P$  for trend = .01, .01, and .01, respectively). Disease-free survival was lower in the FN group (log-rank  $P$  = .01). Conclusions-The initial BSRTC results may reflect not only the risk of malignancy but also the presence of vascular invasion and poor prognosis when the thyroid nodule is diagnosed as FTC. These results may provide prognostic information for therapeutic decision-making and clinical management of FTC.

## 25COASOCT44

### Title: The Effect of Window Size on Pathologists' Search for Rare Elements in a Digital Pathology Setting

Alana Lopes, BSc Corresponding Author; Sean Rasmussen, MD et.al.

Arch Pathol Lab Med (2025) 149 (9): 874–879.

<https://doi.org/10.5858/arpa.2024-0378-OA>

**Abstract:** Digital pathology requires pathologists to assess tissue digitally rather than on an analog microscope, which has been the mainstay tool for tissue assessment for more than a century. The impact of different digital interaction configurations on pathologists' performance is not well understood. This work focuses on the impact of the display window size for diagnostic assessment. Objective- To determine the effect of digital image viewer window size on pathologists' diagnostic performance when searching for tumors in lymph nodes while under a time limit. Design- Six pathologists assessed 8 breast lymph node whole slide images using 4 digital image viewer window sizes (8, 14, 24, and 32 inches) for tumors in lymph nodes while under a time limit. Eye-gaze data were collected. Pathologists were subsequently asked to rate their preference of window sizes. Results-The fraction of window not covered with foveated vision was significantly associated with window size ranging from 43% for 32 inches to 5% for 8 inches ( $P$  < .001). There was no statistically significant relationship between the number of false negatives or assessment time and window size ( $P$  = .21 and  $P$  = .28, respectively). The distance traversed per panning instance ranged from 301 pixels for 32-inch to 193 pixels for 8-inch windows ( $P$  = .002). All pathologists preferred the largest window size as it provided more context for diagnostic assessment. Conclusions- Window size does not significantly affect pathologists' diagnostic performance when searching for tumors in lymph nodes. However, pathologists adapted their slide navigation approach to accommodate the amount of context the window size permitted.

**25COASOCT45****Title: Improved Performance on Longitudinal Knowledge Assessment in Continuing Certification: The ABPath CertLink Strategy**

Gary W. Procop, MD Corresponding Author; Tyler Sandersfeld, PhD et.al.

Arch Pathol Lab Med (2025) 149 (9): 880–883.

<https://doi.org/10.5858/arpa.2024-0318-OA>

**Abstract:** All member boards of the American Board of Medical Specialties have continuing certification (ie, maintenance of certification) programs. The efficacy of these programs has been questioned and, therefore, warrants study. Objective- To determine if the American Board of Pathology CertLink program, as structured, is associated with an improvement in the performance of participants on the assessment of content that was previously missed (ie, inaccurately answered). Design- We reviewed the performance of American Board of Pathology CertLink participants from January 2022 through December 2023 on the readministration of the content from 110 036 multiple-choice items that were previously missed by the participants in a program with enhanced learning strategies and incentives. Results-The correct response rate upon the assessment of readministered content that was previously missed increased from 0% to 62.2% (68 394 of 110 036), which exceeds that which would be achieved by guessing ( $P < .001$ ). Conclusions-The American Board of Pathology CertLink program, which incentivizes learning and was constructed from adult learning principles and modern educational precepts to improve knowledge retention, interrupt forgetting, and introduce practice-relevant content, is associated with an improvement in the performance of diplomates on continuing certification knowledge assessments.

**25COASOCT46****Title: Addition of Lay Language Comments in Placental Pathology Reports Increases Provider Understanding and Comfort Open Access**

Linda M. Ernst, MD, MHS Corresponding Author; Alexa A. Freedman, PhD

Arch Pathol Lab Med (2025) 149 (9): 884–888.

<https://doi.org/10.5858/arpa.2024-0105-OA>

**Abstract:** Placental pathology reports may contain terminology that obstetric providers do not feel comfortable discussing with their patients. Objective-To determine if lay language comments appended to the placental pathology report increase provider comfort and understanding of the report. Design-We drafted a priori lay language comments explaining the major pathologic findings in the placenta. To test the acceptability and value of the comments, we designed an anonymous and randomized survey ed to assess provider understanding of the terminology in the pathology report and comfort with explaining the report to their patients. Survey respondents were randomly assigned to receive 2 hypothetical placental pathology reports, one with and one without lay language comments. Respondents were asked to rate their understanding and comfort level explaining the report to their patients on a scale of 1 to 4. Within-provider differences in understanding and comfort by report type and pathology type were assessed by using repeated measures analysis of variance. Results-Thirty-one providers responded to the survey. Providers reported greater complete understanding of the report when reading the report with lay language comments as compared to the report without the comments (mean comfort of 3.5 for lay language versus

2.97 for original report,  $P < .001$ ), as well as greater comfort with the report (mean comfort of 3.29 for lay language versus 2.81 for original report,  $P = .002$ ). There was no difference in provider understanding or comfort by the pathology findings represented ( $P = .66$ ). Conclusions—Our survey results indicate that the inclusion of lay language comments in the placental pathology report can improve provider understanding of the placental findings and therefore improve their comfort when discussing the findings with a patient and considering future treatment options.

## 25COASOCT47

### **Title: Associations of Breast Cancer Method of Detection With Tumor Characteristics, Treatments, and Overall Survival: A Propensity-Score-Matched Analysis**

Steven J. Chen, MD, Azwade Rahman, MD, MPH et al.

American Journal of Roentgenology, Vol. 225, No. 3

<https://doi.org/10.2214/AJR.25.33245>

**Abstract:** A contributor to variable breast cancer screening guidelines has been limited research assessing associations of the method of cancer detection with cancer outcomes. The purpose of this study is to compare tumor characteristics, treatments, and survival outcomes between patients with breast cancer detected by mammographic screening versus by clinical symptoms. This retrospective study included patients with biopsy-proven breast cancer from January 1, 2010, to January 1, 2020. For each patient, the method of detection was classified as screening-detected (i.e., screening mammography in the absence of symptoms) or clinically detected (i.e., presentation with symptoms leading to diagnostic imaging). Propensity-score matching was performed between the screening-detected and clinically detected cohorts by age, race, ethnicity, insurance status, and year of diagnosis. Tumor characteristics, treatments, and overall survival rates were compared between cohorts. Overall survival was compared between cohorts using Kaplan-Meier curves, incorporating a 0.5-year lead time bias adjustment in the screening-detected cohort. Before propensity-score matching, the analysis included 1460 patients with breast cancer (screening-detected cohort, 932 patients; clinically detected cohort, 528 patients). After propensity-score matching, each cohort included 507 patients (mean age in the screening-detected and clinically diagnosed cohorts of 61.2 and 62.0 years, respectively). Tumor size measured 1–10 mm in 42.0% of screening-detected cancers versus in 13.0% of clinically detected cancers ( $p < .001$ ). Frequencies of noninvasive disease, localized disease, regional disease, and distant metastatic disease were 35.5%, 54.0%, 9.9%, and 0.0% in the screening-detected cohort versus 8.9%, 47.3%, 34.1%, and 7.7% in the clinically detected cohort, respectively ( $p < .001$ ). Screening-detected and clinically detected cohorts showed significant differences in frequencies of surgical therapies (lumpectomy, 66.1% vs 39.3%; mastectomy, 22.1% vs 34.3%;  $p < .001$ ), radiation therapy (50.1% vs 41.2%;  $p = .006$ ), and chemotherapy (15.0% vs 40.2%;  $p < .001$ ). The screening-detected in comparison with the clinically detected cohort showed significantly greater 5-year survival rate (94.4% vs 79.6%;  $p < .001$ ) and 10-year survival rate (82.7% vs 66.1%;  $p < .001$ ). Kaplan-Meier curves indicated significantly greater overall survival in the screening-detected cohort ( $p < .001$ ), with a progressively increasing difference in survival with increasing time since diagnosis. Screening-detected cancers in comparison with clinically detected cancers were associated with smaller size, earlier stage, less-invasive therapies, and improved overall survival.



**25COASOCT48****Title: From Detection to Survival: Strengthening the Case for Screening Mammography**

Derek L. Nguyen, MD

American Journal of Roentgenology, Vol. 225, No. 3

<https://doi.org/10.2214/AJR.25.33435>

**Abstract:** This study delivers timely evidence supporting the value of screening mammography by showing that the method of detection is not just a data point, but a determinant of outcomes. The study isolates the impact of screening detection versus clinical detection based on tumor characteristics, treatment strategies, and long-term survival. For practicing clinicians and patients, the take-home message is clear: screening mammography is effective. For radiologists, the data reinforce the importance of early detection through routine mammographic screening, especially in patients at average risk who might otherwise delay or skip screening. Radiologists can leverage these statistics in patient conversations to demonstrate asymptomatic screening's critical value in catching smaller, lower grade, and earlier stage cancers, translating to less-aggressive therapy and better survival. Importantly, the findings also empower radiology advocacy. When discussing the rationale for screening with referring providers or hesitant patients, we often rely on population-level data or mortality modeling. This study provides concrete patient-level survival data with 10-year follow-up results. The statistics strengthen our voice in advocating for annual screening beginning at age 40, matching American College of Radiology and Society of Breast Imaging recommendations. They also offer additional weight in ongoing discussions with payers and policymakers about resource allocation for screening services. Lastly, this study highlights disparities in detection that should prompt reflection and action. Clinically detected cancers were more common among patients with Medicaid insurance, mirroring real-world inequities in screening access. Radiologists are uniquely positioned to work with health systems to increase outreach, improve access, and eliminate disparity barriers to mammography. In summary, this study provides not just an academic analysis but a road map for clinical and systemic change. By making the method of detection visible, the authors give radiologists a powerful tool to better serve patients, inform practice, and strengthen the evidence for annual screening mammography.

**25COASOCT49****Title: Real-World Diagnostic Performance and Clinical Utility of Artificial Intelligence–Assisted Interpretation for Detection of Lung Metastasis on CT in Patients With Colorectal Cancer**

Sowon Jang, MD, Junghoon Kim, MD et.al.

American Journal of Roentgenology, Vol. 225, No. 3

<https://doi.org/10.2214/AJR.25.33063>

**Abstract:** Studies of artificial intelligence (AI) for lung nodule detection on CT have primarily been conducted in investigational settings and/or focused on lung cancer screening. The purpose of this study was to evaluate the impact of AI assistance on radiologists' diagnostic performance for detecting lung metastases on chest CT in patients with colorectal cancer (CRC) in real-world clinical practice and to assess the clinical utility of AI assistance in this setting. This retrospective study included patients with CRC who underwent chest CT as surveillance for lung metastasis from May 2020 to December 2020 (conventional

interpretation) or May 2022 to December 2022 (AI-assisted interpretation). Between the two periods, the institution implemented a commercial AI lung nodule detection system. During the second period, radiologists interpreted examinations concurrently with AI-generated reports, using clinical judgment regarding whether to report AI-detected nodules. The reference standard for metastasis incorporated pathologic and clinical follow-up criteria. Diagnostic performance (i.e., sensitivity, specificity, accuracy) and clinical utility (i.e., diagnostic yield, false-referral rate, management changes after positive reports) were compared between groups based on clinical radiology reports. Net benefit was estimated using a decision curve analysis equation. Stand-alone AI interpretation was evaluated. The conventional interpretation group included 647 patients (mean age,  $64 \pm 11$  [SD] years; 394 men, 253 women; metastasis prevalence, 4.3%); the AI-assisted interpretation group included 663 patients (mean age,  $63 \pm 12$  years; 381 men, 282 women; metastasis prevalence, 4.4%). The AI-assisted interpretation group compared with the conventional interpretation group showed higher sensitivity (72.4% vs 32.1%, respectively;  $p = .008$ ), accuracy (98.5% vs 96.0%,  $p = .005$ ), and frequency of management changes (55.2% vs 25.0%,  $p = .02$ ), without significant difference in specificity (99.7% vs 98.9%,  $p = .11$ ), diagnostic yield (3.2% vs 1.4%,  $p = .30$ ), or false-referral rate (0.3% vs 1.1%,  $p = .10$ ). AI-assisted interpretation had positive estimated net benefit across outcome ratios. Stand-alone AI correctly detected metastasis in 24 of 29 patients but had 381 false-positive detections in 634 patients without metastasis; only one AI false-positive was reported as positive by interpreting radiologists. AI assistance yielded increased sensitivity, accuracy, and frequency of management changes, without significantly changed specificity. False-positive AI results minimally impacted radiologists' interpretations.

## 25COASOCT50

### **Title: Cervical Cancer Reporting Lexicon: A Collaboration by the SAR Uterine and Ovarian Cancer DFP, ESUR Female Pelvic Imaging Working Group, and Asian Society of Abdominal Radiology**

Lauren A. Roller, MD, Aradhana M. Venkatesan, MD et.al.

American Journal of Roentgenology, Vol. 225, No. 3

<https://doi.org/10.2214/AJR.25.33087>

**Abstract:** Cervical cancer treatment involves multidisciplinary care teams composed of gynecologic surgeons, gynecologic oncologists, radiation oncologists, pathologists, and radiologists. The 2018 update of the FIGO cervical cancer staging system incorporated imaging as a source of staging information, reflecting the critical role of imaging in evaluating patients with cervical cancer before and after therapy. However, the lack of standardized terminology has led to challenges in the updated system's application, including ambiguity in management decisions. This collaborative project between the Society of Abdominal Radiology Uterine and Ovarian Cancer Disease-Focused Panel, the European Society of Urogenital Radiology Female Pelvic Imaging Working Group, and the Asian Society of Abdominal Radiology led to develop a list of standardized consensus-based terms and definitions for reporting imaging findings in the initial staging, follow-up, and treatment planning of cervical cancer, as well as a report template leveraging the lexicon terms. The lexicon and report template were developed by 20 committee members (17 radiologists, two gynecologic oncologic surgeons, and one radiation oncologist), representing 19 institutions

from North America, Europe, and Asia. These tools are intended to improve consistency in the reporting of cervical cancer imaging, to enhance communication among care teams and optimize patient management.

## 25COASOCT51

### **Title: Role of Neuroimaging in Cancer-Treatment Neurotoxicity**

Alvand Hassankhani, MD

American Journal of Roentgenology, Vol. 225, No. 3

<https://doi.org/10.2214/AJR.25.33139>

**Abstract:** As cancer therapies evolve and become increasingly targeted, the spectrum of treatment-related neurotoxicities presents a growing challenge. This Review highlights important neurotoxic complications associated with commonly used and emerging cancer therapies, emphasizing the critical role of neuroimaging in their detection and differentiation from disease progression and other entities. The specific entities considered include neurologic immune-related adverse events, immune effector cell–associated neurotoxicity syndrome, and tumor inflammation–associated neurotoxicity. Imaging techniques, such as perfusion MRI, vessel wall imaging, and amino acid PET, are complementary in improving performance in diagnosing neurotoxicity syndromes and guiding timely clinical decision-making and intervention. A multidisciplinary approach integrating oncology, neurology, and imaging is crucial for balancing therapeutic benefits with neurotoxicity risk. Early recognition and intervention are essential; although many treatment-induced neurotoxicities are reversible, delayed diagnosis can result in long-term disability or even death. By recognizing characteristic imaging patterns, radiologists play a central role in identifying emerging treatment-related neurotoxicity syndromes, thereby supporting safe, high-quality, patient-centered cancer care.

## 25COASOCT52

### **Title: Diagnostic Performance of Ultrasound for Diagnosing Midgut Malrotation and Volvulus in Children: A Multiinstitutional Retrospective Review**

HaiThuy N. Nguyen, MD

American Journal of Roentgenology, Vol. 225, No. 3

<https://doi.org/10.2214/AJR.25.32660>

**Abstract:** The reported diagnostic performance of ultrasound (US) for midgut malrotation and volvulus varies. The purpose of this study was to evaluate the diagnostic performance of US for midgut malrotation and volvulus separately and to assess individual sonographic signs for each diagnosis. This multicenter, retrospective, cross-sectional study included children (who were defined as individuals 0–18 years old) who had US performed as the first imaging test for evaluation of suspected midgut malrotation or volvulus from January 1, 2018, to June 30, 2021. Clinical data were extracted from medical records. Blinded reviewers measured the proximal duodenum and assessed for malrotation and volvulus as well as for specific sonographic signs. Nondiagnostic and equivocal studies were excluded. The reference standards used for malrotation included surgery, upper gastrointestinal (UGI) series, and CT and/or MRI. Volvulus reference standards included the same plus clinical follow-up (minimum, 28 days). Sensitivity, specificity, and accuracy were calculated to evaluate diagnostic performance; the Wilcoxon rank sum test was used to compare median values.

Malrotation analysis included 384 examinations; median patient age was 32 days (IQR, 5–182 days). Volvulus analysis included 900 examinations; median patient age was 60 days (IQR, 9–573 days). The sensitivity and specificity of US for malrotation were 93% (95% CI, 81–98%) and 96% (95% CI, 92–98%) by original report and 97% (95% CI, 87–100%) and 99% (95% CI, 97–100%) by blinded research review. The sensitivity and specificity of US for volvulus were 97% (95% CI, 85–100%) and 98% (95% CI, 96–99%) by original report and 97% (95% CI, 86–100%) and 99% (95% CI, 98–100%) by blinded research review. The most accurate sonographic signs were the intraperitoneal position of the third portion of the duodenum for malrotation (accuracy = 98%) and the whirlpool sign for volvulus (accuracy = 99%). The median proximal duodenal diameter was greater in children with volvulus (13 mm [IQR, 7–18 mm] versus 6 mm [IQR, 4–8 mm],  $p < .001$ ). The performance of US for diagnosing both midgut malrotation and volvulus is excellent in the setting of a diagnostic imaging study.

**Medical Oncology**

(Chemotherapy, Hematology &amp; Radiotherapy)

**25COASOCT01****Title: Astaxanthin promotes apoptosis by suppressing growth signaling pathways in HT-29 colorectal cancer cells.**Taştumur, Ş., Kaleci, A.O., Öztürk, A. *et al.**Med Oncol* 42, 426 (2025).<https://doi.org/10.1007/s12032-025-02978-w>

**Abstract:** Colorectal cancer (CRC) is the third most frequently diagnosed malignancy globally and ranks second in cancer-related mortality. Despite advancements in therapeutic approaches, the need for novel, effective and less toxic treatment strategies remains critical. Astaxanthin (ATX), a naturally occurring xanthophyll carotenoid, has attracted attention due to its strong antioxidant, anti-inflammatory and anti-cancer properties. This study aimed to evaluate the antiproliferative and pro-apoptotic effects of ATX on CRC through its influence on key molecular pathways, involved in tumorigenesis. The human colorectal adenocarcinoma cell line HT-29 was treated with varying concentrations of ATX (10 µM and 20 µM) for 24 h. Cell viability was assessed using the XTT assay. The expression levels of HER2, EGFR, ERK1, ERK2 and mTOR were quantified via enzyme-linked immunosorbent assay (ELISA). Immunofluorescence staining was used to evaluate the expression of EGFR and caspase-3 proteins. ATX exhibited significant antiproliferative and pro-apoptotic effects on HT-29 cells, with an IC<sub>50</sub> value of 10.98 µM at 24 h. Treatment with ATX (10.98 µM) led to a marked increase in caspase-3 expression and a significant reduction in EGFR levels. Additionally, HER2, ERK1 and ERK2 levels were significantly downregulated, while mTOR expression remained unaffected. Flow cytometry analysis revealed a significant increase in apoptotic cell populations following ATX treatment, compared to the control group. ATX exerts notable antiproliferative and pro-apoptotic effects on CRC cells, potentially through modulation of the EGFR/HER2/ERK signaling pathway. These findings suggest that ATX may serve as a promising candidate for further investigation as an adjunctive or standalone therapeutic agent in the treatment of CRC.

**25COASOCT02****Title: 18F-FDG PET/CT-based deep radiomic models for enhancing chemotherapy response prediction in breast cancer.**Jiang, Z., Low, J., Huang, C. *et al.**Med Oncol* 42, 425 (2025).<https://doi.org/10.1007/s12032-025-02982-0>

**Abstract:** Enhancing the accuracy of tumor response predictions enables the development of tailored therapeutic strategies for patients with breast cancer. In this study, we developed deep radiomic models to enhance the prediction of chemotherapy response after the first treatment cycle. 18F-Fludeoxyglucose PET/CT imaging data and clinical record from 60 breast cancer patients were retrospectively obtained from the Cancer Imaging Archive. PET/CT scans were conducted at three distinct stages of treatment; prior to the initiation of chemotherapy (T1), following the first cycle of chemotherapy (T2), and after the full chemotherapy regimen (T3). The patient's primary gross tumor volume (GTV) was



delineated on PET images using a 40% threshold of the maximum standardized uptake value (SUVmax). Radiomic features were extracted from the GTV based on the PET/CT images. In addition, a squeeze-and-excitation network (SENet) deep learning model was employed to generate additional features from the PET/CT images for combined analysis. A XGBoost machine learning model was developed and compared with the conventional machine learning algorithm [random forest (RF), logistic regression (LR) and support vector machine (SVM)]. The performance of each model was assessed using receiver operating characteristics area under the curve (ROC AUC) analysis, and prediction accuracy in a validation cohort. Model performance was evaluated through fivefold cross-validation on the entire cohort, with data splits stratified by treatment response categories to ensure balanced representation. The AUC values for the machine learning models using only radiomic features were 0.85(XGBoost), 0.76 (RF), 0.80 (LR), and 0.59 (SVM), with XGBoost showing the best performance. After incorporating additional deep learning-derived features from SENet, the AUC values increased to 0.92, 0.88, 0.90, and 0.61, respectively, demonstrating significant improvements in predictive accuracy. Predictions were based on pre-treatment (T1) and post-first-cycle (T2) imaging data, enabling early assessment of chemotherapy response after the initial treatment cycle. Integrating deep learning-derived features significantly enhanced the performance of predictive models for chemotherapy response in breast cancer patients. This study demonstrated the superior predictive capability of the XGBoost model, emphasizing its potential to optimize personalized therapeutic strategies by accurately identifying patients unlikely to respond to chemotherapy after the first treatment cycle.

## 25COASOCT03

**Title: Anticancer efficacy of sericin (silkworm protein) and sericin chitosan conjugated silver nanoparticles against colorectal cancer.**

Ijaz, F., Ali, S., Pervaiz, A. *et al.*

*Med Oncol* 42, 423 (2025).

<https://doi.org/10.1007/s12032-025-02974-0>

**Abstract:** Sericin is a globular protein known to have antioxidant potential due to presence of amino, carboxyl and hydroxyl groups in its structure. This study was designed to investigate the antiproliferative and apoptotic potential of sericin and sericin chitosan conjugated silver nanoparticles against colorectal cancer cells. To investigate the antiproliferative and apoptotic activity of sericin and sericin chitosan conjugated silver nanoparticles (SChiAgNPs), three human colorectal cancer cell lines (SW480, SW620, HCT116) were used. Sericin was isolated by the degumming process followed by the characterization by using FTIR, UV, XRD, and SEM techniques to confirm the isolation process and successful synthesis of SChiAgNPs. MTT assay was carried out to analyze the antiproliferative activities, while expression profiling of the genes i.e., GADD45A, BCL2, and TNF was assessed by qRT-PCR analysis. Sericin (S-Ext) and SChiAgNPs showed significant antiproliferative activities in SW480, SW620 and HCT 116 cells. Overall, there was 29–34 inhibition of viability for sericin S-Ext and 35–43 for SChiAgNPs in the three cell lines in comparison to untreated control. Expression profiling indicated the significant stimulation of GADD45A, BCL-2 and TNF genes expression in SW480, SW620 and HCT 116 cells. The GADD 45 A showed induction by 1.43–1.71-fold in SW480, 1.09–1.56-fold in SW620 and 1.25–4.55-fold in HCT

116 cells in response to treatment groups. The BCL2 showed the induction by 1.35–2.53, 1.38–3.1, and 2.32–3.76-fold in SW480, SW620, and HCT116 cells, respectively. TNF was induced by a factor of 3.9–6.43, 2.53–5.41, and 2.7–5.31-fold in SW480, SW620, and HCT116 cells, respectively, after the exposure with compounds. Sericin and S-ChiAgNPs, showed significant growth inhibition and gene expression profiling modifications in the colorectal cancer cells. The findings provide evidence about sericin and its nanoparticle conjugates as potential anticancer medicine for colorectal cancer.

#### 25COASOCT04

**Title: Tanshinone IIA is synergistic with the PARP inhibitor olaparib in inducing BRCA-proficient and -deficient triple-negative breast cancer cell apoptosis.**

Liu, Q., Zhou, Q., Yang, X. *et al.*

*Med Oncol* 42, 419 (2025).

<https://doi.org/10.1007/s12032-025-02968-y>

**Abstract:** Poly ADP-ribose Polymerase (PARP) inhibitor-based targeted therapy benefits the triple-negative breast cancer (TNBC) patients with Breast cancer susceptibility genes (BRCA) mutation. However, only about 50% BRCA-mutated TNBC patients respond to PARP inhibitor treatment and 80% TNBC patients are BRCA proficient, which limit clinical application of PARP inhibitor for TNBC treatment. Ataxia-telangiectasia mutated (ATM) is a DNA double-strand break (DSB) sensor to detect and facilitate DSB repair. ATM deficiency sensitizes cancer cells to PARP inhibitor. Currently, none of ATM inhibitor is approved for clinical use largely due to toxicity. Tanshinone IIA (Tan IIA) is a natural compound derived from *Salvia miltiorrhiza* and has been approved for clinical application for cardiovascular diseases treatment in China. This study aims to evaluate whether Tan IIA could sensitize both BRCA-proficient and -deficient TNBC cells to PARP inhibitor (olaparib) and explore the underlying molecular mechanisms. We report that Tan IIA synergistically enhances the cytotoxic effects of olaparib in both BRCA-proficient and -deficient TNBC cells. Tan IIA increases DSBs in TNBC cells and subsequently triggers apoptosis by destabilizing ATM. The results suggest that Tan IIA is a potential combinatory drug to enhance PARP inhibitor efficacy in TNBC treatment.

#### 25COASOCT05

**Title: Induction of ER stress-mediated apoptosis in breast cancer cell line by the powerful alkylating agent bendamustine and insights into its molecular mechanisms.**

Sankaralingam, G., Subramaniyan, K., Ezhilarasi, K. *et al.*

*Med Oncol* 42, 416 (2025).

<https://doi.org/10.1007/s12032-025-02981-1>

**Abstract:** Bendamustine, an alkylating agent used in treating hematological cancers like non-Hodgkin's lymphoma (NHL) and chronic lymphocytic leukemia (CLL), has recently garnered attention for its potential in breast cancer therapy. This study explores its anticancer effects and molecular mechanisms in breast cancer cells. MDA-MB-231 cells were exposed to various concentrations of bendamustine (0–50  $\mu$ M), and cytotoxicity was assessed using Alamar Blue and LDH assays, revealing a dose-dependent reduction in cell viability with an IC<sub>50</sub> value of 16.98  $\mu$ M at 24 h ( $p < 0.001$ ). Intracellular reactive oxygen species (ROS) were quantified by DCF-DA flow cytometry, showing a significant elevation following treatment

( $p < 0.01$ ). Downregulation of major antioxidant enzymes (SOD, CAT, GPx1, GST;  $p < 0.01$ ) and upregulation of TRPC6 (1.8-fold at 10  $\mu\text{M}$ , 2.5-fold at 20  $\mu\text{M}$ ;  $p < 0.01$ ) were detected by qPCR. Markers of apoptosis were evaluated by Annexin V/PI staining, revealing significant increases in both early and late apoptotic cell populations ( $p < 0.01$ ), and by gene expression analysis showing increased BAX:BCL-2 ratio (1.5-fold at 10  $\mu\text{M}$ , 7.8-fold at 20  $\mu\text{M}$ ;  $p < 0.01$ ). CHOP mRNA, an ER stress-related pro-apoptotic gene, was significantly upregulated (2.5-fold at 20  $\mu\text{M}$ ;  $p < 0.01$ ), supporting activation of the ER stress pathway. The results demonstrated that bendamustine exerted a dose-dependent cytotoxic effect, decreasing cell viability and increasing LDH release. It significantly increased ROS levels and altered the expression of apoptotic genes, promoting apoptosis in breast cancer cells. Furthermore, bendamustine-induced ER stress, shown by upregulated Chop expression, suggests that ER stress plays a role in its anticancer activity. These findings highlight bendamustine as a promising therapeutic agent for breast cancer treatment.

## 25COASOCT06

**Title: Next-generation nanoformulation: *Glycyrrhiza glabra*-based chitosan–curcumin MgO/Fe<sub>2</sub>O<sub>3</sub> nanocomposite for targeted lung cancer therapy with dual antioxidant action.**

Elmetwalli, A., Abdelsayed, S., Elsayed, A. *et al.*

*Med Oncol* 42, 414 (2025).

<https://doi.org/10.1007/s12032-025-02977-x>

**Abstract:** This study aims to develop and evaluate *Glycyrrhiza glabra*-based magnesium oxide/iron oxide nanocomposite (NC) functionalized with chitosan and curcumin to enhance therapeutic efficacy against lung cancer and oxidative stress. This is the first report integrating *G. glabra* extract with chitosan and curcumin functionalization into a MgO/Fe<sub>2</sub>O<sub>3</sub> nanocomposite for enhanced antioxidant and anticancer effects. The developed nanocomposite demonstrated strong biocompatibility and in vitro therapeutic efficacy, as evidenced by low cytotoxicity in normal cells and significant inhibitory effects against A549 lung cancer cells. In this study, bioactive phytochemical-loaded *G. glabra* extract was used as a green capping and reducing agent to synthesize MgO/Fe<sub>2</sub>O<sub>3</sub> NC. The nanomaterials were also functionalized with curcumin and chitosan to promote stability, bioavailability, and site-specific pharmacological activity. The synthesis process was carried out under green conditions, in which the nanocomposite was characterized using FTIR, UV–Vis spectroscopy, EDX analysis, zeta potential analysis, HR-TEM, and XRD. The antioxidant potential was assessed through the DPPH free radical scavenging activity, whereby MgO/Fe<sub>2</sub>O<sub>3</sub>–chitosan–curcumin NCs yielded the maximum inhibition of free radicals ( $\text{IC}_{50} = 0.0977 \text{ mg/mL}$ ) when compared to other nanomaterials. Antimicrobial activity was assessed against Gram-negative and Gram-positive bacteria, wherein MgO/Fe<sub>2</sub>O<sub>3</sub> NC showed moderate activity, and chitosan and curcumin functionalization reduced this to some extent by possibly controlled release behavior or protection of active sites. Cytotoxicity against A549 human lung cancer cells showed strong inhibition by the MgO/Fe<sub>2</sub>O<sub>3</sub>–chitosan–curcumin NC ( $\text{IC}_{50} = 10 \text{ }\mu\text{g/mL}$ ), confirmed by changes in morphology in accordance with apoptosis. In addition, in silico ADME simulation suggested favorable bioavailability and low toxicity, which is an indicator of the therapeutic potential of these NCs. To the best of our knowledge, this is the first report on *G. glabra*-mediated green synthesis with dual

functionalization of chitosan and curcumin in a MgO/Fe<sub>2</sub>O<sub>3</sub> nanocomposite. The formulation has synergistic antioxidant and anticancer activity with vast potential in lung cancer therapy. As a whole, the findings address the dual antioxidant and anticancer properties of *G. glabra*-derived MgO/Fe<sub>2</sub>O<sub>3</sub>-chitosan-curcumin NC and their green potential as agents in the treatment of lung cancer. In vivo studies are recommended to confirm efficacy and safety.

## 25COASOCT07

**Title: Evaluation of the efficacy and safety of HyperArc stereotactic radiotherapy for the treatment of lung cancer brain metastasis.**

Zhu, Y., Chen, Z., Zhu, L. *et al.*

*Med Oncol* 42, 408 (2025).

<https://doi.org/10.1007/s12032-025-02970-4>

**Abstract:** This study assessed the efficacy and safety of HyperArc (HA) stereotactic radiotherapy (SRT) in 48 patients with lung cancer brain metastases (LCBM) while identifying prognostic factors and high-risk predictors for symptomatic cerebral radiation necrosis (sCRN). We enrolled 48 patients diagnosed with LCBM at the People's Hospital Affiliated to Jiangsu University between February 2021 and February 2025, assigning 44 to the SRT group and 4 to the WBRT-boost group. Clinical data were collected, and all patients underwent HA stereotactic radiotherapy. The WBRT-boost group additionally received a local HA boost. Prescription doses of 24–30 Gy were administered in 3–5 fractions at 5 fractions weekly, tailored to lesion characteristics. We evaluated both the efficacy and safety of HA treatment for LCBM. The 1-year overall survival (OS), intracranial distant progression-free survival (iDPFS), and intracranial local progression-free survival (iLPFS) rates for the entire cohort were 76.1, 64.5, and 69.4%, respectively. For out-of-field distant metastases, the cumulative intracranial objective response rate (icORR) and intracranial disease control rate (icDCR) reached 52.1 and 64.6%, compared with 81.2 and 97.9% for in-field metastases. The WBRT-boost group exhibited a median OS of 6.6 months, while the SRT group achieved superior 1-year outcomes (OS:79.1%; iDPFS:67.0%; iLPFS:71.8%). Compared with WBRT-boost, SRT showed significantly better local control (iLPFS,  $P=0.044$ ) and overall survival (OS,  $P=0.036$ ), though distant control (iDPFS,  $P=0.086$ ) did not differ significantly. Multivariate analysis identified V12 > 10 cc (HR 12.52,  $P=0.011$ ) and female sex (HR 11.66,  $P=0.026$ ) as independent prognostic factors. All 12 symptomatic radiation necrosis cases (27.3%) occurred in the SRT group. Logistic regression demonstrated that higher BED3 (HR 57.0,  $P=0.009$ ) independently increased sCRN risk, whereas targeted therapy (HR 0.08,  $P=0.024$ ) significantly reduced it. HyperArc-based fractionated stereotactic radiotherapy proves safe and feasible for managing brain metastases from lung cancer, achieving effective intracranial tumor control. Compared with WBRT + boost, SRT yields superior therapeutic outcomes despite requiring careful monitoring for symptomatic radiation necrosis. Further investigations should examine combined approaches incorporating targeted agents and optimized dose distribution.

## 25COASOCT08

**Title: Cardio-oncology in focus: novel molecular signatures of lung adenocarcinoma-driven cardiac cachexia.**

Fu, Z., Lin, Z., Chen, S. *et al.*

*Med Oncol* 42, 406 (2025).

<https://doi.org/10.1007/s12032-025-02933-9>

**Abstract:** Cardiac cachexia linked to lung adenocarcinoma (LCACC) is a clinically important yet under-researched issue in cardio-oncology. LCACC is caused directly by the progression of the tumor, unlike cardiotoxicity induced by therapy. We proposed that LCACC myocardium exhibits unique transcriptomic and immunometabolic profiles. Objective-To thoroughly analyze the molecular alterations in the myocardium associated with LCACC and pinpoint possible regulatory genes and therapeutic targets. Methods-We conducted a comprehensive bioinformatics analysis using publicly accessible myocardial RNA-seq data ( $n = 4 + 4$ ) from LCACC and control mice. The analyses comprised differential gene expression (DEG), immune deconvolution using xCell, gene set enrichment analysis (GSEA), weighted gene co-expression network analysis (WGCNA), and protein–protein interaction (PPI) networks. Results-In LCACC, the myocardium exhibited metabolic reprogramming characterized by increased oxidative phosphorylation (OXPHOS) and protein synthesis pathways, while cell cycle and inflammatory signaling (such as NF- $\kappa$ B) were downregulated. The analysis of immune profiles indicated a rise in fibroblasts and megakaryocyte–erythroid progenitors, while conventional dendritic and memory B cells were reduced. Five central genes (CCL2, CDC20, MKI67, CX3CR1, CXCL1) were discovered, grouped within chemokine signaling and cell division pathways, and linked to actionable upstream transcription factors, miRNAs, and possible drugs. Conclusion-This research offers the initial comprehensive map of transcriptomic and immunometabolic changes in LCACC. These results emphasize that LCACC involves active, regulated biological processes, indicating it is not just a passive result of cachexia, and they pave the way for further mechanistic and translational studies.

## 25COASOCT09

**Title:** ALDH1A1 promotes colorectal cancer metastasis through activating the notch signaling pathway.

Wang, X., Wen, X., Hu, X. *et al.*

*Med Oncol* 42, 403 (2025).

<https://doi.org/10.1007/s12032-025-02958-0>

**Abstract:** Aldehyde dehydrogenase 1 family member A1 (ALDH1A1) gene is a member of aldehyde dehydrogenase (ALDH) family, and it is closely associated with cancer metastasis. However, the exact mechanism remains to be clarified. In the present study, we aimed to explore the specific mechanism and role of ALDH1A1 in colorectal cancer (CRC) metastasis. The data obtained from GSE41657 dataset and 24 surgical resected CRC samples was analyzed to explore the expression of ALDH1A1 in CRC and its clinical importance. ALDH1A1 expression was increased in CRC tissues and correlated to poor prognosis. ALDH1A1 was highly expressed in CRC cells and ALDH1A1 knocking down led to reduced proliferation, migration, and invasion of CRC cells. In terms of the mechanisms, ALDH1A1 knockdown or inhibitor caused the significantly reduced gene expression of Notch1, JAG1, and HES1. ALDH1A1 activates Notch signaling pathway to promote CRC growth and development. Our study demonstrated that ALDH1A1 could promote CRC cell proliferation, migration, and invasion via activating the Notch signaling pathway. Targeting ALDH1A1 might be promising for inhibition of CRC metastasis.



**25COASOCT10**

**Title: Antineoplastic potential of *Kushneria avicenniae* pigments via modulation of the BAX/BCL-2 axis and CASP-9 pathway in inducing G2/M arrest and apoptosis in liver and breast cancer.**

Almetwaly, H., Elmetwalli, A., El-Amier, Y.A. *et al.*

*Med Oncol* 42, 400 (2025).

<https://doi.org/10.1007/s12032-025-02949-1>

**Abstract:** Since cancer continues to be a chief cause of disease and mortality worldwide, new and efficient treatment approaches are desperately needed. Natural substances have become a foremost source of bioactive molecules with intriguing cytotoxic effects, particularly those originating from microbes. The cytotoxic potential of pigments derived from the halophilic bacteria *Kushneria avicenniae* HA346018, which was isolated from mangrove environments, is investigated in this work. These pigments' cytotoxic, apoptotic, and cell cycle-modulating properties were assessed in human HepG2 and MCF-7 cell lines. Both cancer cell lines revealed a dose-dependent decrease in cell viability, indicating the pigment extract's potent cytotoxic effects in vitro. HepG2 and MCF-7 cells have computed IC50 values of  $52.7 \pm 3.8$   $\mu\text{g/mL}$  and  $48.3 \pm 4.1$   $\mu\text{g/mL}$ , respectively. Its notable selective cytotoxicity highlighted the pigment's potential as a targeted therapy, which revealed much less toxicity against normal WI-38 cells. A notable concentration of cells in the G2/M phase and a considerable change in cell cycle progression were seen by flow cytometric analysis, indicating the extract's potential to cause cell cycle arrest. The regulation of cyclin-dependent kinases (CDKs) and DNA damage response pathways was associated with this inhibition at the G2/M checkpoint. Moreover, Annexin V-FITC/PI labeling and subsequent flow cytometric analysis verified that the pigment caused both early and late apoptotic events. The mitochondrial mechanisms that mediated the apoptosis were the elevation of pro-apoptotic proteins like Bax and the downregulation of anti-apoptotic proteins like Bcl-2, which eventually led to caspase activation. These results establish *Kushneria avicenniae* pigments as a viable source of bioactive chemicals with therapeutic potential for breast and liver malignancies by offering new mechanistic insights into their apoptosis-inducing effect in cancer cell lines. This study encourages more investigation into natural compounds obtained from microorganisms as potential substitutes for traditional cancer therapies.

**25COASOCT11**

**Title: Hesperetin increases membrane progesterone receptor expression in human myeloid leukemia cells and reduces ROS.**

Hosseini, S.S., Esmailzadeh, E., Zangooei, M. *et al.*

*Med Oncol* 42, 398 (2025).

<https://doi.org/10.1007/s12032-025-02975-z>

**Abstract:** Chronic myeloid leukemia (CML) is characterized by high levels of reactive oxygen species (ROS), which contribute to disease progression and drug resistance. In addition, membrane progesterone receptors (mPRs) may play roles in the proliferation and differentiation of leukemia cells, although their significance in CML remains underexplored. Hesperetin (Hst), a citrus flavonoid, has shown anticancer and antioxidant properties. This study aimed to investigate whether Hst affects mPR expression and ROS levels in K562 cells, to provide initial insights into its potential as a complementary approach for CML treatment.

Cell viability was evaluated using an MTT test following treatment with different concentrations of Hst (60–300  $\mu$ M) for 24, 48, and 72 h. Based on these results, 120  $\mu$ M was selected as a moderate sub-cytotoxic concentration for evaluating mPR $\alpha$  and mPR $\beta$  expression and ROS levels using flow cytometry and DCFDA fluorescence. Hst reduced K562 cell viability in a time- and dose-dependent manner, with IC<sub>50</sub> values of approximately 327  $\mu$ M (24 h), 247  $\mu$ M (48 h), and 213  $\mu$ M (72 h). Based on these results, 120  $\mu$ M Hst was used as a moderate sub-cytotoxic dose to evaluate its effects on both mPR $\alpha$  and mPR $\beta$  expression and ROS levels, which were significantly altered compared to untreated cells ( $P < 0.05$ ). According to our results, Hst shows promising in vitro effects on K562 cells and may be considered for further preclinical research as a potential complementary agent for CML treatment.

## 25COASOCT12

**Title: Natural Nrf2 activators modulate antioxidant gene expression and apoptosis in leukemic K-562 cells.**

Patergiannakis, IS., Georgiou-Siafis, S.K., Papadopoulou, L.C. *et al.*  
*Med Oncol* 42, 396 (2025).

<https://doi.org/10.1007/s12032-025-02946-4>

**Abstract:** Natural products (NPs) have long been used in traditional medicine and continue to be explored for their chemopreventive and therapeutic properties. Many of their biological effects are mediated through redox-sensitive pathways, such as the nuclear factor erythroid 2-related factor 2 (Nrf2), a key regulator of antioxidant responses and cellular defense mechanisms. This study aimed to evaluate the antioxidant capacity, cytotoxicity, pro-apoptotic activity, and Nrf2-modulating effects of 22 natural product extracts traditionally used in ethnomedicine in a human leukemic K-562 cell model. The extracts were assessed for total phenolic content (TPC), radical scavenging activity (DDPH and ABTS assays), cytotoxic effects (AlamarBlue assay), apoptosis induction (caspase-3 activity), and regulation of Nrf2 target genes (*HO-1*, *NQO1* and *GCLC*) via RT-qPCR. The extracts exhibited a wide range of antioxidant and cytotoxic activities. *Punica granatum*, *Rhodiola rosea*, and *Thymus vulgaris* showed high phenolic content and antioxidant potential. *R. rosea* displayed the most potent cytotoxic effect, whereas *Hypericum perforatum* induced the highest caspase-3 activity. Gene expression revealed that *T.vulgaris*, *R.rosea*, *Moringa oleifera*, *Withania somnifera*, *Salvia officinalis* and *Euphrasia officinalis* upregulated all three Nrf2 target genes, with *T.vulgaris* showing the greatest induction. These findings highlight the pharmacological potential of traditionally used natural products as modulators of redox signaling and apoptosis inducers in leukemia cells. The activation of the Nrf2 pathway by the selected extracts supports further investigation of their potential.

## 25COASOCT13

**Title: Bioengineered and biodegradable 3D scaffold for controlled drug delivery of 5-fluorouracil-loaded nanoparticle for bone tumor treatment.**

Ma, H., Shi, J. & Zhang, W.  
*Med Oncol* 42, 395 (2025).

<https://doi.org/10.1007/s12032-025-02891-2>

**Abstract:** The main goal of the present was to develop an anticancer scaffold based on chitosan nanoparticles (CsNPs) loaded with 5-FU against bone tumor. The synthesized Cs/5-FU NPs were incorporated into an alginate hydrogel to obtain a functional scaffold. The results showed that the Cs/5-FU NPs have spherical morphology with a  $112.3 \pm 34.1$  nm diameter and have a hydrodynamic size of around  $321.0 \pm 11.2$  nm and the zeta potential of NPs was  $31.4 \pm 8.1$  mV. SEM imaging showed that both hydrogels have a porous micro structure and the pores are interconnected and were biodegradable (lost around 70–85% of their initial weight during 28 days). The MTT assay showed that the Nanocomposite suppressed the cells growth and significantly induced anticancer cells effects, and significantly suppressed the migration/invasion potential of the cells. The intracellular Reactive Oxygen Species (ROS) measurement and mitochondrial membrane potential ( $\Delta\Psi_m$ ) measurement assay showed that the Nanocomposite elevated the intracellular ROS and disrupted the  $\Delta\Psi_m$ , and subsequently induced apoptosis. The results indicate that the fabricated anticancer scaffold can be applied as an implantable scaffold for controlled and localized drug delivery of chemotherapeutic agents to bone tumor cells.

## 25COASOCT14

**Title:** Antiproliferative and apoptotic effects of Pervari honey on SH-SY5Y neuroblastoma cells.

Altin-Celik, P., Derya-Andeden, M., Eciroglu-Sarban, H. *et al.*  
*Med Oncol* 42, 394 (2025).

<https://doi.org/10.1007/s12032-025-02963-3>

**Abstract:** Neuroblastoma is a complex and heterogeneous pediatric malignancy. Treatment options for neuroblastoma include surgery, chemotherapy, radiotherapy, autologous stem cell transplantation, and emerging immunotherapies. However, these approaches often coincide with oxidative stress, highlighting the potential role of natural antioxidants in chemoprevention and chemotherapy. Honey has long been recognized for its medicinal properties, including antimicrobial, anti-inflammatory, and antioxidant effects. Pervari honey (PH), produced by bees that forage on a diverse array of native flora, is a distinctive honey originating from southeastern Türkiye. This study evaluated the antiproliferative, anti-tumor, apoptotic, and inflammatory effects of PH on SH-SY5Y human neuroblastoma cells. Cell viability was measured using an MTT assay, while apoptosis was evaluated using an Annexin V-FITC/7-AAD staining test. The RT-qPCR method was used to quantify the expression of *IL-1 $\beta$* , *IL-6*, *TNF- $\alpha$* , *NF- $\kappa$ B*, *Caspase-3*, *MMP-2*, *MMP-9*, *BAX*, and *BCL-2* genes. PH significantly reduced SH-SY5Y cell viability in a dose- and time-dependent manner ( $p < 0.05$ – $p < 0.01$ ). It induced apoptosis by upregulating *BAX* and *Caspase-3* while downregulating *BCL-2* ( $p < 0.05$ – $p < 0.001$ ). Additionally, it increased *NF- $\kappa$ B* expression ( $p < 0.05$ – $p < 0.001$ ) and modulated inflammatory (*IL-1 $\beta$* , *IL-6*, and *TNF- $\alpha$* ) cytokines ( $p < 0.05$ – $p < 0.01$ ). *MMP-2* and *MMP-9* levels were significantly elevated ( $p < 0.05$ – $p < 0.001$ ), suggesting enhanced extracellular matrix remodeling. These in vitro findings indicate that PH may exert anti-tumor potential and possess immunomodulatory properties. Furthermore, in vitro and in vivo studies are needed to explore its therapeutic applicability.

**25COASOCT15**

**Title: Protective effects of valencene, a natural sesquiterpene, against benzo(a)pyrene-induced lung cancer in Swiss albino mice.**

Pant, J., Marwah, H., Mittal, P. *et al.*

*Med Oncol* 42, 393 (2025).

<https://doi.org/10.1007/s12032-025-02962-4>

**Abstract:** Lung cancer remains a leading cause of cancer-related mortality worldwide, necessitating the development of novel chemopreventive and therapeutic agents. Valencene, a natural sesquiterpene, has shown potential bioactive properties, but its efficacy against benzo(a)pyrene (B(a)P)-induced lung carcinogenesis remains underexplored. This study investigated the protective and therapeutic effects of Valencene on B(a)P-induced lung cancer in mice, focusing on its impact on body weight, lung weight, oxidative stress biomarkers, serum marker enzymes, and histopathological alterations. Mice were divided into four groups: normal control, B(a)P-induced disease control, Valencene pre-treatment (B(a)P + Valencene), and Valencene post-treatment [B(a)P followed by Valencene]. Body and lung weights were recorded, while oxidative stress markers [superoxide dismutase (SOD), catalase (CAT), glutathione peroxidase (GPx)] and serum enzymes (adenosine deaminase (ADA), aryl hydrocarbon hydroxylase (AHH)) were analyzed. Histopathological examination assessed lung tissue integrity. B(a)P induction caused significant body weight loss ( $15.7 \pm 0.25$  g vs. control  $33.61 \pm 0.03$  g,  $p < 0.01$ ) and increased lung weight ( $360 \pm 1.39$  mg vs. control  $286.33 \pm 1.93$  mg,  $p < 0.01$ ), indicating cancer-associated metabolic and pathological changes. Valencene pre-treatment significantly attenuated these effects (body weight:  $26.33 \pm 0.05$  g; lung weight:  $303.16 \pm 5.05$  mg,  $p < 0.01$ ), whereas post-treatment showed moderate recovery. Oxidative stress biomarkers (SOD, CAT, GPx) were significantly restored by Valencene ( $p < 0.001$ ), with pre-treatment exhibiting superior efficacy. Additionally, Valencene normalized serum ADA and AHH levels, suggesting anti-carcinogenic activity. Histopathological analysis confirmed that pre-treatment preserved lung architecture, while post-treatment partially reversed carcinogenic damage. Valencene demonstrates potent chemopreventive and therapeutic effects against B(a)P-induced lung cancer, primarily by mitigating oxidative stress, reducing tumor burden, and preserving tissue integrity. Pre-treatment was more effective than post-treatment, highlighting its potential as a prophylactic agent. These findings support further exploration of Valencene as a complementary strategy in lung cancer management.

**25COASOCT16**

**Title: Carvedilol sensitizes paclitaxel-resistant gastric cancer AGS cells to paclitaxel: influences on apoptotic regulators, Notch, PI3K/AKT, ERK1/2 signaling pathways, and miR-34a expression.**

Niapour, A., Hosseinzadeh, S., Mohebi, Y. *et al.*

*Med Oncol* 42, 392 (2025).

<https://doi.org/10.1007/s12032-025-02966-0>

**Abstract:** The occurrence of drug resistance is a leading cause of successful therapy failure in gastric cancer patients. This study aimed to investigate the potential resensitizing effect of carvedilol (CVL) in paclitaxel (PTX) resistant gastric cancer (AGS-Rpac) cells. AGS-Rpac cells were co-treated with various concentrations of PTX and CVL. Cellular viability was

measured, and the combination index was calculated. The formation of reactive oxygen species (ROS) and the induction of apoptosis were measured. The expressions of key apoptotic genes, the Notch signaling pathway, and miR-34a were investigated. Protein levels of essential ABC transporters, apoptotic regulators, Notch, PI3K/AKT, and ERK1/2 signaling pathways were also assessed. CVL displayed a distinguished synergistic effect. Co-treatment with CVL and PTX significantly reduced the viability of AGS-Rpac cells and increased intracellular ROS levels. A significant increase in early and late apoptotic cells was observed in the combination-treated group. Modulations in the expression profiles of the BCL-2 and CASP-3 genes favored apoptosis. The expression levels of *Notch1*, *HES1*, and *HEY1* genes and proteins were reduced following treatment with CVL alone and in combination. The diminished levels of miR-34a were upregulated following treatment with CVL alone, and more significantly in combination-treated groups. The levels of P-gp, MRP-1, cleaved-CASP3, P53, HIF-1 $\alpha$ , PI3K, p-AKT, and p-ERK1/2 decreased while the pro-CASP3 level was diminished in CVL + PTX-treated cells. Our findings suggest that CVL could be repurposed as a co-treatment candidate, capable of overcoming PTX resistance, inducing apoptosis, enhancing miR-34a expression, reducing the expression of efflux transporters, and inhibiting essential survival signaling pathways.

## 25COASOCT17

**Title: NFATC3 enhances osteosarcoma progression by increasing PD-L1 and CXCL2 levels.**

Liang, F., Tang, B., Chen, C. *et al.*

*Med Oncol* 42, 388 (2025).

<https://doi.org/10.1007/s12032-025-02850-x>

**Abstract:** Osteosarcoma (OS), in which immune cells play an important role in the development and progression of OS, is the most common malignant bone tumor in the adolescent population. In this study, we performed bioconfidence analysis and experimental confirmation of the expression of the immune gene NFATC3 in OS and its function. qRT-PCR revealed high expression of NFATC3 in several OS cell lines, including 143B, SJSA, HOS, MG63, and MNNG, which was validated by multiple osteosarcoma sequencing datasets. MNNG overexpression of NFATC3 increased the proliferation and migration of MNNG cells. Single-cell sequencing analysis of the OS microenvironment revealed increased expression of NFATC3 in T cells and macrophages. Next, we further analyzed the expression of NFATC3 in the OS microenvironment using single cells. Finally, we explored the mechanism by which NFATC3 affects OS progression. Our results revealed that the overexpression of NFATC3 promoted the expression of PD-L1 ligands and the upregulation of inflammatory factors (IL-1 $\beta$  and TNF- $\alpha$ ). The results from the construction of a tumor cell and macrophage coculture system revealed that the overexpression of NFATC3 promoted the expression of CXCL2 in M0 macrophages. In conclusion, our study suggests that NFATC3 drives the development of OS by promoting tumor cell proliferation and remodeling the immune microenvironment.

## 25COASOCT18

**Title: Annexin A2: regulating glioma's fate and a potential therapeutic target.**

Liu, W., Zhao, X., Regmi, M. *et al*



*Med Oncol* 42, 386 (2025).

<https://doi.org/10.1007/s12032-025-02799-x>

**Abstract:** High recurrence and mortality in glioma are linked to aggressive proliferation. Recent strategies focus on genetic interventions, with Annexin A2 (ANXA2) emerging as a promising target. We wanted to evaluate ANXA2's prognostic value and its role in tumor progression, aiming to establish it as a viable therapeutic target. Bioinformatics analysis of public databases (The Cancer Genome Atlas, Chinese Glioma Genome Atlas, Rembrandt) was performed to validate ANXA2's prognostic significance. Functional assays (on cell lines U87 and U251) and in vivo studies were conducted to examine the impact of ANXA2 on cell proliferation, invasion, apoptosis, cell cycle progression, and tumor volume. Additionally, the relationship between ANXA2 and the Mitogen-Activated Protein Kinase (MAPK) signaling pathway was explored by analyzing key proteins' expression levels and phosphorylation states. Elevated ANXA2 expression correlated with poorer survival rates in glioma, showing variable expression across different grades and subtypes. Silencing ANXA2 impaired glioma cell motility and proliferation, induced apoptosis, altered cell cycle distribution, and reduced tumor volumes in vivo, at least partially through the MAPK pathway. This way, our study validates ANXA2 as a significant prognostic marker for glioma, contributing to tumor progression through the MAPK pathway, underscoring its potential as a therapeutic target.

## 25COASOCT19

**Title: Differences in the expression of *CMTM3* and *SSTR2* genes in right and left colon tumors: A molecular insight into colorectal cancer.**

Binen, T., Akbaş, E., Çolak, T. *et al.*

*Med Oncol* 42, 382 (2025).

<https://doi.org/10.1007/s12032-025-02961-5>

**Abstract:** Colorectal cancer (CRC) is a prevalent and lethal malignancy influenced by genetic, epigenetic, and environmental factors, with diverse molecular subtypes and varying incidence rates across different populations. The anatomical, histological, morphological, and genetic differences between the right and left colons contribute to disparities in tumor incidence, clinical presentation, prognosis, and therapeutic responses, depending on the tumor's localization. We aimed to investigate the expression patterns of the *CMTM3* and *SSTR2* genes both of which are hypermethylated and potentially involved in the development and progression of colorectal tumors in tumors originating from the right and left colon. The study consisted of 89 histopathologically diagnosed tumour tissue samples, 42 from the right colon and 47 from the left colon, and 89 healthy tissue samples from the same individuals adjacent to the tumour tissue. The expression of the *CMTM3* and *SSTR2* genes was analysed using the comparative CT ( $\Delta\Delta CT$ ) method in real-time PCR. Our findings demonstrated a significant upregulation of *CMTM3* and *SSTR2* expression in tumor tissues compared to adjacent normal tissues ( $p < 0.05$ ). Notably, *CMTM3* expression was significantly higher in left-sided colon tumors ( $2^{-\Delta\Delta CT} = 20.95$ ) compared to those originating from the right colon ( $2^{-\Delta\Delta CT} = 14.13$ ) ( $p = 0.027$ ). This study is the first to suggest that elevated *CMTM3* expression may be associated with the increased incidence and distinct molecular behavior of left-sided colorectal tumors. Results provide novel insights into the molecular heterogeneity of

colorectal cancer, emphasizing the importance of tumor localization in understanding disease mechanisms and informing targeted therapeutic strategies.

## 25COASOCT20

**Title: The effect of dendrosomal nanocurcumin on Wnt/ $\beta$ -catenin signaling pathway via PIWIL2 in MCF-7 breast cancer cells.**

Ghasri, A., Bahri Hampa, S., Mirzaee Godarzee, M. *et al.*

*Med Oncol* 42, 381 (2025).

<https://doi.org/10.1007/s12032-025-02960-6>

**Abstract:** Breast cancer ranks as one of the most prevalent cancers impacting women worldwide, posing significant treatment challenges due to chemotherapy resistance and high recurrence rates. This study investigates the therapeutic potential of Dendrosomal Nanocurcumin (DNC), a novel formulation aimed at enhancing curcumin's bioavailability. The focus is on its impact on the Wnt/ $\beta$ -catenin signaling pathway via the modulation of the PIWIL2 protein in MCF-7 breast cancer cells. The Wnt/ $\beta$ -catenin signaling pathway is crucial for controlling cell proliferation, differentiation, and apoptosis. Its dysregulation is strongly linked to breast cancer progression. PIWIL2, a member of the PIWI subfamily of Argonaute proteins, plays a role in RNA silencing, DNA methylation, histone modification, gene transcription regulation, and interactions with oncogenic pathways. These functions highlight its importance in gene regulation, stem cell maintenance, and cancer progression. In this study, MCF-7 cells were treated with Dendrosomal Nanocurcumin at a dose of 20 $\mu$ M for 48 h, based on the IC<sub>50</sub> determined from the MTT assay. Real-time PCR analysis revealed that DNC treatment significantly reduced the expression levels of  $\beta$ -catenin ( $p < 0.0001$ ), Cyclin D1 ( $p < 0.0001$ ), and PIWIL2 ( $p < 0.00001$ ), while significantly increasing the expression of GSK3 $\beta$  ( $p < 0.0001$ ). These findings were supported by Western blot analysis, which showed a significant decline in both phosphorylated and non-phosphorylated forms of  $\beta$ -catenin and PIWIL2 proteins. This suggests that DNC disrupts the Wnt/ $\beta$ -catenin signaling pathway by reducing the stability and cytoplasmic accumulation of  $\beta$ -catenin. The reduction in  $\beta$ -catenin likely prevents its nuclear translocation and the subsequent activation of target genes like Cyclin D1, thus inhibiting cell proliferation and promoting apoptosis. Furthermore, a significant decrease in PIWIL2 protein levels in DNC-treated cells indicates that DNC targets PIWIL2, further inhibiting the Wnt/ $\beta$ -catenin signaling pathway and reducing the oncogenic potential of MCF-7 breast cancer cells. These findings highlight the potential of DNC as an effective treatment option for breast cancer, particularly in overcoming resistance to conventional therapies. Further research is necessary to gain a comprehensive understanding the mechanisms of DNC and its clinical efficacy, offering hope for enhanced breast cancer treatment strategies.

## 25COASOCT21

**Title: Effects of PELP1 on proliferation, metastasis and angiogenesis of epithelial ovarian cancer.**

Xie, L., Sun, C., Mao, Y. *et al.*

*Med Oncol* 42, 379 (2025).

<https://doi.org/10.1007/s12032-025-02908-w>

**Abstract:** To investigate the effects of Proline-, Glutamic acid- and Leucine-rich protein 1(PELP1) on the biological behaviors of epithelial ovarian cancer (EOC) cells and its role in promoting angiogenesis through the regulation of VEGFA expression and secretion. Bioinformatics analysis was performed to evaluate the correlation between PELP1 and VEGFA. The expression levels and subcellular localization of PELP1 and VEGFA in EOC cell lines were assessed using Western blot (WB), quantitative real-time PCR (qRT-PCR) and immunofluorescence. Functional assays, including EdU proliferation assays, wound healing assays, Transwell invasion assays and WB were conducted to examine the effects of PELP1 overexpression. Conditioned medium (CM) from PELP1-overexpression cells was used to culture human umbilical vein endothelial cells (HUVECs) and angiogenesis was evaluated using Transwell migration, wound healing, and tube formation assays. VEGFA expression and secretion were analyzed by immunofluorescence, qRT-PCR, and enzyme-linked immunosorbent assays (ELISA). WB and ELISA were performed to validate the effects of the VEGFA inhibitor (HY-117661) on both the expression and secretion of VEGFA. Functional rescue experiments, including migration and tube formation assays, were conducted to verify whether PELP1 regulated angiogenesis through VEGFA. Bioinformatics analysis revealed a positive correlation between PELP1 and VEGFA. Both proteins were significantly upregulated in EOC cells compared to normal ovarian epithelial cells. Overexpression of PELP1 enhanced proliferation, migration, invasion and the expression of metastasis-associated proteins, including N-cadherin and Vimentin. Additionally, PELP1 upregulated VEGFA expression and secretion, which subsequently promoted HUVEC migration and angiogenesis. PELP1 promotes EOC progression by enhancing cellular proliferation, metastasis and angiogenesis through the regulation of VEGFA. These findings suggest that PELP1 could serve as a potential therapeutic target for EOC.

## 25COASOCT22

**Title: Targeting miR-32-5p suppresses c-MYC-driven proliferation and induces apoptosis in MCF-7 breast cancer cells.**

Khoder, A.I., El-Sayed, I.H. & Ali, Y.B.M.

*Med Oncol* 42, 377 (2025).

<https://doi.org/10.1007/s12032-025-02935-7>

**Abstract:** Progress in molecular medicine has resulted in novel cancer therapies, with microRNAs (miRNAs) recognized as promising instruments for cancer detection and treatment. MicroRNAs are tiny non-coding RNA sequences that manipulate gene expression at the post-transcriptional stage and are involved in cellular differentiation and death. miR-32-5p demonstrates oncogenic activity in several cancers, while c-MYC oncogene is a well-known driver of cancer, promoting tumor growth by stimulating cell proliferation, blocking apoptosis, and suppressing immune responses. This study aimed to examine how inhibiting miR-32-5p affected the behavior of breast tumor cells (MCF-7), particularly focusing on changes in cellular apoptosis and proliferation, and to investigate its relationship with c-MYC expression. A locked nucleic acid (LNA)-based inhibitor was used to knock down miR-32-5p in MCF-7 breast cancer cells. Cell viability was assessed using MTT assays at 24, 48, and 72 h post-transfection. Apoptotic and necrotic cell populations were differentiated using Annexin-V labeling with Propidium iodide. Expression levels of miR-32-5p and c-MYC were evaluated using quantitative Real-Time PCR before and after transfection with the miR-

32-5p inhibitor. Inhibition of miR-32-5p significantly reduced MCF-7 cell viability at 48 h post-transfection ( $P < 0.002$ ) and increased apoptotic cells to approximately 17% (vs. 0.3% in controls,  $P < 0.05$ ), concomitant with significant downregulation of c-MYC mRNA ( $P < 0.006$ ). The lowest level of miR-32-5p expression was observed at 48 h following transfection, with levels gradually increasing by 72 h. This study is the first to demonstrate a plausible regulatory relationship between miR-32-5p and c-MYC in breast tumor cells. The significant reduction in cell viability and increase in apoptosis following miR-32-5p inhibition, likely mediated through c-MYC downregulation, suggests a plausible pathway that may be targeted for therapeutic intervention in breast cancer.

## 25COASOCT23

**Title: Expression and clinical significance of CD155, FGL1, Galectin-9, and PD-L1 in breast cancer with neoadjuvant chemotherapy.**

Zeng, Y., Zhao, B., Yan, M. *et al.*

*Med Oncol* 42, 375 (2025).

<https://doi.org/10.1007/s12032-025-02914-y>

**Abstract:** Neoadjuvant chemotherapy (NACT) plays a pivotal role in modulating the immune microenvironment. However, its impact on immune checkpoint expression and the prognostic significance of immune checkpoints in breast cancer (BC) remain unclear. In this retrospective study, we used immunohistochemistry assays to evaluate PD-L1, CD155, FGL1, and Galectin-9 expression in pre- and post-NACT BC samples. CD155 expression before NACT was significantly elevated in triple-negative breast cancer (TNBC) and showed a tendency to be associated with pathological complete and partial responses. FGL1 was highly expressed in HER2-positive BC and TNBC before NACT. After treatment, higher CD155 expression was more frequently observed in patients with advanced pathological lymph node stages (pN2–N3) than in those with lower stages (pN0–N1). Comparison of paired pre-treatment and residual cancer tissues revealed a significant decrease in PD-L1, CD155, and Galectin-9 expression following NACT. Notably, decreased CD155 expression significantly correlated with improved therapeutic response, particularly in patients with high Ki-67 expression. Patients with reduced CD155 expression after NACT had more favourable disease-specific survival than those with unchanged and increased expression. Moreover, decreased CD155 expression in residual BC showed a trend toward improved overall survival. Changes in PD-L1 and Galectin-9 expression after therapy were not associated with patient survival or pathological response. We conducted further analysis using the METABRIC database and found high CD155 expression after chemotherapy was related to decreased CD8<sup>+</sup> T cell infiltration and poor outcome in TNBC. Our findings indicated that NACT induced significant changes in immune checkpoint expression in BC. PD-L1, CD155, and Galectin-9 expression were reduced in post-treatment samples compared to pre-treatment samples. Specifically, unchanged or elevated CD155 expression after NACT was associated with poor disease-specific survival. Further more, high CD155 expression after chemotherapy was related to decreased CD8<sup>+</sup> T cell infiltration and poor outcome in TNBC.

## 25COASOCT24

**Title: Ephrin B3 drives tumorigenesis and inflammation in cutaneous squamous cell carcinoma.**

Kang, N., Wang, Z., Feng, Y. *et al.*

*Med Oncol* 42, 374 (2025).

<https://doi.org/10.1007/s12032-025-02922-y>

**Abstract:** Dysregulation of Eph receptor-ephrin signaling contributes to tumorigenesis, yet the specific role of Ephrin B3 in cutaneous squamous cell carcinoma (cSCC) remains poorly understood. This study identifies Ephrin B3 as a critical oncogenic driver in cSCC, demonstrating its significant overexpression in cSCC tissues and association with poor prognosis. To elucidate its tumor-promoting mechanisms, we generated Ephrin B3 knockout (*Efnb3*<sup>-/-</sup>) and wild-type (*Efnb3*<sup>WT</sup>) mouse models of DMBA/TPA-induced skin carcinogenesis. Strikingly, Ephrin B3 deletion significantly inhibited cSCC carcinogenesis, while its knockdown in A431 human cSCC cells inhibited proliferation, migration, and invasion, underscoring its pivotal role in tumor aggressiveness. Integrative label-free proteomic analysis revealed cytokeratin 19 (CK19) as the most differentially expressed protein in *Efnb3*<sup>WT</sup> versus *Efnb3*<sup>-/-</sup> mice, establishing a novel molecular connection between Ephrin B3 and CK19. Further mechanistic studies demonstrated that Ephrin B3 positively regulated the NOTCH1 signaling pathway through CK19. Additionally, Reactome pathway analysis implicated Ephrin B3 in inflammation-mediated carcinogenesis through the MAPKs pathway. Consistent with this, *Efnb3* deficiency mitigated inflammatory responses in an acute skin inflammation model, suggesting its role in shaping a pro-tumorigenic microenvironment. Collectively, these findings not only establish Ephrin B3 as a potential prognostic biomarker for cSCC but also reveal its dual mechanistic role in fostering tumorigenesis via the CK19-NOTCH1 axis and amplifying inflammation through MAPKs signaling. This study provides groundbreaking insights into multifaceted contributions of Ephrin B3 in cSCC pathogenesis and opens new avenues for targeted therapeutic intervention.

## 25COASOCT25

**Title: ROCK inhibition suppresses glioblastoma via a PTEN-associated reduction in PI3K/AKT signaling.**

Uzunhisarcıklı, E., Bozkurt, N.M. & Sağlam, A.

*Med Oncol* 42, 372 (2025).

<https://doi.org/10.1007/s12032-025-02952-6>

**Abstract:** Glioblastoma is the most common primary malignant brain tumor. It is aimed to elucidate the role of ROCK in the regulation of PI3K signaling inhibited by PTEN and to evaluate the effects of ROCK inhibitors Thiazovivin and GSK 429286 on glioblastoma as a new therapeutic strategy. U87 MG and L929 cell lines were used to research the cytotoxic effect of ROCK inhibitors Thiazovivin and GSK 429286. 3-(4,5-dimethylthiazol-2-yl)-2,5-diphenyltetrazolium bromide (MTT) method and xCELLigence real-time cell analyzer were used to determine its effect on cell viability. To assess the impact of ROCK inhibitors on PTEN protein levels, PTEN expression in cell lysates was quantitatively determined in vitro using the PTEN ELISA Kit. Total protein concentration was measured using the BCA protein assay kit, p-Akt and PTEN protein level was determined by the western blot method. Showed that GSK 429286 and Thiazovivin significantly reduced U87 MG cell viability even at low concentrations. When IC<sub>50</sub> values were examined, it was understood that THV (IC<sub>50</sub>: 11.02 μM) showed a more potent cytotoxic effect at lower concentrations compared to GSK 429286 (IC<sub>50</sub>: 89.58 μM). At 50 μM, Thiazovivin and GSK 429286 concentration caused a



significant increase in PTEN activity compared to the control and Temozolomide groups, even at low concentrations. THV 50  $\mu$ M significantly increased PTEN expression compared to control ( $p < 0.05$ ). GSK 50  $\mu$ M, THV 1  $\mu$ M, and THV 10  $\mu$ M groups showed significantly reduced p-Akt expression ( $p < 0.05$ ). Considering the effects on healthy cells, Thiazovivin being more effective at low doses suggests it may be a more selective agent. Our findings indicate that ROCK inhibitors may have cytotoxic effects on glioblastoma cells by affecting cell death mechanisms via a PTEN-associated reduction in PI3K/AKT signaling.

## 25COASOCT26

### **Title: Epigenetic reprogramming of mast and cancer cells modifies tumor-promoting cytokine networks.**

Scholnik-Cabrera, A., Ramírez-Yautentzi, M., Soria-Castro, R. *et al.*

*Med Oncol* 42, 371 (2025).

<https://doi.org/10.1007/s12032-025-02941-9>

**Abstract:** Mast cells (MC) play a crucial role in the tumor microenvironment (TME) by promoting tumor progression and immune evasion through the secretion of inflammatory mediators. Here, we investigate the impact of epigenetic reprogramming using a drug repurposing combination—hydralazine, a DNA methylation inhibitor, and valproate, a histone deacetylase inhibitor (HDACi)—on MC–cancer cell interactions. Human cancer cell lines (Ca Ski, MDA-MB-468, and A549) that secrete stem cell factor (SCF) were selected from a panel of tumor lines. The HMC-I MC line and the selected cancer cell lines were treated with hydralazine + valproate (HV) for 72 h, and viability assessed via trypan blue exclusion assay revealed consistent reduction across all lines. Conditioned medium (CM) from HV-treated MCs was applied to cancer cells, with MDA-MB-468 displaying resistance. CM from HV-treated cancer cells was then used to evaluate MC migration and chemotaxis, showing reduced mobility in MCs exposed to supernatants from Ca Ski and MDA-MB-468, but not A549. Flow cytometry analysis revealed that HV epigenetically suppressed the expression of pro-tumoral cytokines and MC chemoattractants, with ITAC being the only consistently upregulated cytokine. These findings demonstrate that pharmacological epigenetic reprogramming via HV modulates MC-driven tumor progression and reshapes the cytokine network, highlighting its potential as a novel immunoepigenetic therapeutic strategy in cancer.

## 25COASOCT27

### **Title: Finerenone with Empagliflozin in Chronic Kidney Disease and Type 2 Diabetes**

Rajiv Agarwal, M.D. , Jennifer B. Green, M.D

*N Engl J Med* 2025;393:533-543, [VOL. 393 NO. 6](#)

<https://doi.org/10.1056/NEJMoa2410659>

**Abstract:** Limited evidence exists to support the simultaneous initiation of sodium–glucose cotransporter-2 inhibitors and finerenone, a nonsteroidal mineralocorticoid receptor antagonist, in persons with chronic kidney disease and type 2 diabetes. We randomly assigned participants with chronic kidney disease (estimated glomerular filtration rate [eGFR], 30 to 90 ml per minute per 1.73 m<sup>2</sup> of body-surface area), albuminuria (a urinary albumin-to-creatinine ratio of 100 to  $\leq 5000$  [with albumin measured in milligrams and creatinine measured in grams]), and type 2 diabetes, who were already taking a renin–

angiotensin system inhibitor, in a 1:1:1 ratio to receive finerenone (with empagliflozin-matching placebo) at a dose of 10 or 20 mg per day, empagliflozin at a dose of 10 mg per day (with finerenone-matching placebo), or a combination of finerenone and empagliflozin. The primary outcome was the relative change in the log-transformed mean urinary albumin-to-creatinine ratio from baseline to 180 days. Safety was assessed. At baseline, the urinary albumin-to-creatinine ratio was similar among the participants in the three groups; the median value was 579 (interquartile range, 292 to 1092) among those with available data (265 in the combination-therapy group, 258 in the finerenone group, and 261 participants in the empagliflozin group). At day 180, the reduction in the urinary albumin-to-creatinine ratio with combination therapy was 29% greater than that with finerenone alone (least-squares mean ratio of the difference in the change from baseline, 0.71; 95% confidence interval [CI], 0.61 to 0.82;  $P < 0.001$ ) and 32% greater than that with empagliflozin alone (least-squares mean ratio of the difference in the change from baseline, 0.68; 95% CI, 0.59 to 0.79;  $P < 0.001$ ). Neither agent, alone or in combination, led to unexpected adverse events. Symptomatic hypotension, acute kidney injury, and hyperkalemia leading to drug discontinuation were uncommon. Among persons with both chronic kidney disease and type 2 diabetes, initial therapy with finerenone plus empagliflozin led to a greater reduction in the urinary albumin-to-creatinine ratio than either treatment alone.

## 25COASOCT28

### **Title: Ciprofloxacin versus Aminoglycoside–Ciprofloxacin for Bubonic Plague**

Rindra Vatosoa Randremanana, Ph.D. et.al

N Engl J Med 2025;393:544-555, VOL. 393 NO. 6

<https://doi.org/10.1056/NEJMoa2413772>

**Abstract:** Plague is a high-consequence infectious disease with epidemic potential. Current treatment guidelines are based on weak evidence. We enrolled persons (excluding pregnant persons) in Madagascar who had clinically suspected bubonic plague during 2020–2024. Using an open-label noninferiority design, we compared two treatments included in the national plague guidelines: oral ciprofloxacin for 10 days (ciprofloxacin monotherapy) or injectable aminoglycoside for 3 days followed by oral ciprofloxacin for 7 days (aminoglycoside–ciprofloxacin). The primary end point was treatment failure on day 11, with treatment failure defined as death, fever, secondary pneumonic plague, or alternative or prolonged plague treatment. To show noninferiority of ciprofloxacin monotherapy among patients with laboratory-confirmed or probable infections, the upper boundary of the 95% confidence interval around the risk difference had to be less than 15 percentage points. A total of 933 patients underwent screening; 450 patients with suspected bubonic plague were enrolled and underwent randomization. A total of 220 patients (110 per group) had confirmed infection, and 2 (1 per group) had probable infection. Of the patients who underwent randomization, 53.2% were male, and the median age was 14 years (range, 2 to 72). Ciprofloxacin monotherapy was noninferior to aminoglycoside–ciprofloxacin therapy: among the patients with confirmed or probable infection, treatment failure occurred in 9.0% (10 of 111 patients) in the ciprofloxacin monotherapy group and 8.1% (9 of 111 patients) in the aminoglycoside–ciprofloxacin group (difference, 0.9 percentage points; 95% confidence interval, –6.0 to 7.8). Noninferiority was consistent in other prespecified analysis populations. A total of 5 patients in the ciprofloxacin monotherapy group and 4 patients in the

aminoglycoside–ciprofloxacin group died, and secondary pneumonic plague developed in 3 patients in each group. The incidence of adverse events among patients with confirmed or probable infections was similar in the two groups — 18.0% in the ciprofloxacin monotherapy group and 18.9% in the aminoglycoside–ciprofloxacin group had adverse events, and 7.2% and 5.4%, respectively, had serious adverse events. Oral ciprofloxacin monotherapy for 10 days was noninferior to an aminoglycoside–ciprofloxacin sequential combination for the treatment of patients with bubonic plague.

## 25COASOCT29

### **Title: Ciprofloxacin versus Aminoglycoside–Ciprofloxacin for Bubonic Plague**

Rindra Vatosoa Randremanana, Ph.D.

N Engl J Med 2025;393:544-555, VOL. 393 NO. 6

<https://doi.org/10.1056/NEJMoa2413772>

**Abstract:** Plague is a high-consequence infectious disease with epidemic potential. Current treatment guidelines are based on weak evidence. **Methods** We enrolled persons (excluding pregnant persons) in Madagascar who had clinically suspected bubonic plague during 2020–2024. Using an open-label noninferiority design, we compared two treatments included in the national plague guidelines: oral ciprofloxacin for 10 days (ciprofloxacin monotherapy) or injectable aminoglycoside for 3 days followed by oral ciprofloxacin for 7 days (aminoglycoside–ciprofloxacin). The primary end point was treatment failure on day 11, with treatment failure defined as death, fever, secondary pneumonic plague, or alternative or prolonged plague treatment. To show noninferiority of ciprofloxacin monotherapy among patients with laboratory-confirmed or probable infections, the upper boundary of the 95% confidence interval around the risk difference had to be less than 15 percentage points. **Results**—A total of 933 patients underwent screening; 450 patients with suspected bubonic plague were enrolled and underwent randomization. A total of 220 patients (110 per group) had confirmed infection, and 2 (1 per group) had probable infection. Of the patients who underwent randomization, 53.2% were male, and the median age was 14 years (range, 2 to 72). Ciprofloxacin monotherapy was noninferior to aminoglycoside–ciprofloxacin therapy: among the patients with confirmed or probable infection, treatment failure occurred in 9.0% (10 of 111 patients) in the ciprofloxacin monotherapy group and 8.1% (9 of 111 patients) in the aminoglycoside–ciprofloxacin group (difference, 0.9 percentage points; 95% confidence interval, –6.0 to 7.8). Noninferiority was consistent in other prespecified analysis populations. A total of 5 patients in the ciprofloxacin monotherapy group and 4 patients in the aminoglycoside–ciprofloxacin group died, and secondary pneumonic plague developed in 3 patients in each group. The incidence of adverse events among patients with confirmed or probable infections was similar in the two groups — 18.0% in the ciprofloxacin monotherapy group and 18.9% in the aminoglycoside–ciprofloxacin group had adverse events, and 7.2% and 5.4%, respectively, had serious adverse events. **Conclusions**—Oral ciprofloxacin monotherapy for 10 days was noninferior to an aminoglycoside–ciprofloxacin sequential combination for the treatment of patients with bubonic plague.

## 25COASOCT30

### **Title: Vepdegestrant, a PROTAC Estrogen Receptor Degradar, in Advanced Breast Cancer**

Mario Campone, M.D., Ph.D.

N Engl J Med 2025;393:556-568, VOL. 393 NO. 6

<https://doi.org/10.1056/NEJMoa2505725>

**Abstract:** Vepdegestrant is an oral proteolysis-targeting chimera (PROTAC) estrogen receptor (ER) degrader that directly harnesses the ubiquitin–proteasome system. **Methods**–In this phase 3, open-label, randomized trial, we enrolled patients with ER-positive, human epidermal growth factor receptor 2 (HER2)–negative advanced breast cancer who had received one previous line of cyclin-dependent kinase 4 and 6 inhibitor therapy plus one line of endocrine therapy (and up to one additional line of endocrine therapy). Patients were randomly assigned in a 1:1 ratio to receive vepdegestrant at a dose of 200 mg orally once every day of each 28-day cycle or fulvestrant at a dose of 500 mg, administered intramuscularly, on day 1 and day 15 of cycle 1 and on day 1 of subsequent cycles, with randomization stratified according to *ESR1*-mutation status and presence or absence of visceral disease. The primary end point was progression-free survival as assessed by blinded independent central review among the patients with *ESR1* mutations and among all the patients who underwent randomization. Progression-free survival was estimated with Kaplan–Meier methods and hazard ratios with a stratified Cox proportional-hazards model. **Results**–A total of 624 patients underwent randomization; 313 were assigned to receive vepdegestrant, and 311 to receive fulvestrant. Among the 270 patients with *ESR1* mutations, the median progression-free survival was 5.0 months (95% confidence interval [CI], 3.7 to 7.4) with vepdegestrant and 2.1 months (95% CI, 1.9 to 3.5) with fulvestrant (hazard ratio, 0.58 [95% CI, 0.43 to 0.78];  $P<0.001$ ). Among all the patients, the median progression-free survival was 3.8 months (95% CI, 3.7 to 5.3) with vepdegestrant and 3.6 months (95% CI, 2.6 to 4.0) with fulvestrant (hazard ratio, 0.83 [95% CI, 0.69 to 1.01];  $P=0.07$ ). Adverse events of grade 3 or higher occurred in 23.4% of the patients in the vepdegestrant group and in 17.6% of the patients in the fulvestrant group. Adverse events led to treatment discontinuation in 2.9% and 0.7% of the patients, respectively. **Conclusions**–Among patients with ER-positive, HER2-negative advanced breast cancer, vepdegestrant was associated with significantly longer progression-free survival than fulvestrant in the subgroup with *ESR1* mutations but not in the full patient population.

## 25COASOCT31

### **Title: First-Line Camizestrant for Emerging *ESR1*-Mutated Advanced Breast Cancer**

François-Clément Bidard, M.D., Ph.D

N Engl J Med 2025;393:569-580, VOL. 393 NO. 6

<https://doi.org/10.1056/NEJMoa2502929>

**Abstract:** Mutations in *ESR1* are the most common mechanism of acquired resistance to treatment with an aromatase inhibitor plus a cyclin-dependent kinase 4 and 6 (CDK4/6) inhibitor for advanced breast cancer. Camizestrant, a next-generation selective estrogen-receptor (ER) degrader and complete ER antagonist, has shown antitumor activity in ER-positive advanced breast cancer. **Methods**–We tested patients with advanced breast cancer with ER-positive, human epidermal growth factor receptor 2 (HER2)–negative tumors for *ESR1* mutations in circulating tumor DNA (ctDNA) once every 2 to 3 months. All the patients had received at least 6 months of first-line therapy with an aromatase inhibitor plus a CDK4/6 inhibitor (palbociclib, ribociclib, or abemaciclib). Patients who were found to have

an *ESR1* mutation and did not have radiologic progression were assigned in a 1:1 ratio to switch to camizestrant (75 mg once daily) with a continued CDK4/6 inhibitor plus placebo in place of an aromatase inhibitor or to continue to receive an aromatase inhibitor plus a CDK4/6 inhibitor plus placebo in place of camizestrant. The primary outcome was investigator-assessed progression-free survival. A total of 3256 patients were tested for an *ESR1* mutation. The 315 eligible patients were assigned to switch to camizestrant (157 patients) or to continue to receive an aromatase inhibitor (158 patients). At an interim analysis at a median follow-up of 12.6 months, the median progression-free survival was 16.0 months (95% confidence interval [CI], 12.7 to 18.2) in the camizestrant group and 9.2 months (95% CI, 7.2 to 9.5) in the aromatase-inhibitor group (hazard ratio for progression or death, 0.44; 95% CI, 0.31 to 0.60;  $P < 0.0001$ ). The median time until a deterioration in the patient-reported global health status and quality of life occurred was 21.0 months with camizestrant and 6.4 months with an aromatase inhibitor (hazard ratio, 0.54; 95% CI, 0.34 to 0.84). The frequency of discontinuation because of adverse events was 1.3% with camizestrant and 1.9% with an aromatase inhibitor. In patients with ER-positive, HER2-negative advanced breast cancer with an *ESR1* mutation that emerged during treatment, those who were switched to camizestrant with continuation of a CDK4/6 inhibitor during first-line therapy had significantly longer progression-free survival than those who maintained the aromatase-inhibitor combination.

## 25COASOCT32

### **Title: Overall Survival with Neoadjuvant Nivolumab plus Chemotherapy in Lung Cancer**

Patrick M. Forde, M.B., B.Ch., Ph.D.

N Engl J Med 2025;393:741-752, [VOL. 393 NO. 8](#)

<https://doi.org/10.1056/NEJMoa2502931>

**Abstract:** Neoadjuvant nivolumab plus chemotherapy significantly improved pathological complete response and event-free survival in patients with resectable non–small-cell lung cancer (NSCLC) in a phase 3 trial. Data are needed on overall survival. In this open-label, phase 3 trial, patients with stage IB to IIIA resectable NSCLC were randomly assigned to receive nivolumab plus chemotherapy or chemotherapy alone for three cycles, followed by surgery. The primary end points were event-free survival and pathological complete response. Here, we report the results of the planned analysis of overall survival. A total of 358 patients were concurrently assigned to receive nivolumab plus chemotherapy (179 patients) or chemotherapy alone (179 patients). The final analysis of overall survival significantly favored neoadjuvant nivolumab plus chemotherapy over chemotherapy (hazard ratio for death, 0.72; 95% confidence interval [CI], 0.523 to 0.998;  $P = 0.048$ ). At a median follow-up of 68.4 months, the 5-year overall survival was 65.4% with nivolumab plus chemotherapy and 55.0% with chemotherapy alone, with consistency across most subgroups. In exploratory analyses, the 5-year overall survival in the nivolumab-plus-chemotherapy group was 95.3% (95% CI, 82.7 to 98.8) among the patients with a pathological complete response and 55.7% (95% CI, 46.9 to 63.7) among those without such a response; survival was 75.0% among the patients with presurgery clearance of circulating tumor DNA (ctDNA) and 52.6% among those without such clearance. No new safety signals were observed. Three



cycles of neoadjuvant nivolumab plus chemotherapy significantly improved overall survival among patients with resectable NSCLC as compared with chemotherapy alone.

### 25COASOCT33

#### **Title: Elinzanetant for Vasomotor Symptoms from Endocrine Therapy for Breast Cancer**

Fatima Cardoso, M.D., Susanne Parke, M.D. et.al.

N Engl J Med 2025;393:753-763, VOL. 393 NO. 8

<https://doi.org/10.1056/NEJMoa2415566>

**Abstract:** Women receiving endocrine therapy for hormone receptor (HR)–positive breast cancer or its prevention among those at high risk for breast cancer commonly have vasomotor symptoms. Data are lacking on the effects of elinzanetant, a neurokinin-targeted therapy shown to be effective in treating vasomotor symptoms, in this population. We performed a phase 3 trial involving women 18 to 70 years of age with moderate-to-severe vasomotor symptoms associated with endocrine therapy for HR-positive breast cancer or its prevention. Women were randomly assigned in a 2:1 ratio to receive once-daily elinzanetant at a dose of 120 mg for 52 weeks or once-daily placebo for 12 weeks followed by once-daily elinzanetant at a dose of 120 mg for 40 weeks. The primary end points were the change in the mean daily frequency of moderate-to-severe vasomotor symptoms from baseline to week 4 and to week 12. A total of 316 participants were assigned to the elinzanetant group and 158 to the placebo–elinzanetant group. At baseline, the mean daily frequency of moderate-to-severe vasomotor symptoms was 11.4 episodes (95% confidence interval [CI], 10.7 to 12.2) in the elinzanetant group and 11.5 episodes (95% CI, 10.5 to 12.5) in the placebo–elinzanetant group. At week 4, the mean change from baseline in the mean daily frequency of moderate-to-severe vasomotor symptoms was –6.5 episodes (95% CI, –7.2 to –5.8) among those who were receiving elinzanetant and –3.0 episodes (95% CI, –3.9 to –2.2) among those who were receiving placebo (least-squares mean difference, –3.5 episodes; 95% CI, –4.4 to –2.6;  $P < 0.001$ ). At week 12, the mean change was –7.8 episodes (95% CI, –8.5 to –7.1) among those receiving elinzanetant and –4.2 episodes (95% CI, –5.2 to –3.2) among those receiving placebo (least-squares mean difference, –3.4 episodes; 95% CI, –4.2 to –2.5;  $P < 0.001$ ). During weeks 1 through 12, a total of 220 participants (69.8%) receiving elinzanetant and 98 (62.0%) receiving placebo reported at least one adverse event that occurred while receiving elinzanetant or placebo, with the most common being headache, fatigue, and somnolence. Serious adverse events occurred during weeks 1 through 12 in 8 participants (2.5%) receiving elinzanetant and 1 participant (0.6%) receiving placebo. Elinzanetant led to a significantly lower frequency of vasomotor symptoms associated with endocrine therapy than placebo.

### 25COASOCT34

#### **Title: Phase 3 Trial of Inhaled Molgramostim in Autoimmune Pulmonary Alveolar Proteinosis**

Bruce C. Trapnell, M.D., Yoshikazu Inoue, M.D., Ph.D

N Engl J Med 2025;393:764-773, VOL. 393 NO. 8

<https://doi.org/10.1056/NEJMoa2410542>

**Abstract:** Autoimmune pulmonary alveolar proteinosis (aPAP) is a rare disease characterized by progressive surfactant accumulation and hypoxemia caused by autoantibodies against

granulocyte–macrophage colony-stimulating factor (GM-CSF), which alveolar macrophages require to clear surfactant. Molgramostim is a formulation of inhaled recombinant human GM-CSF, but its efficacy and safety in patients with aPAP have not been studied sufficiently. **Methods**—In this phase 3, double-blind, placebo-controlled trial, we randomly assigned patients with aPAP to receive molgramostim at a dose of 300 µg or placebo once daily for 48 weeks. The primary end point was the change from baseline to week 24 in the diffusing capacity of the lungs for carbon monoxide (DLCO), which was adjusted for hemoglobin concentration and expressed as a percentage of the predicted value. Secondary end points adjusted for multiplicity were the change from baseline in DLCO at 48 weeks and the change from baseline in the St. George’s Respiratory Questionnaire total (SGRQ-T) and activity (SGRQ-A) scores (scores range from 0 to 100, with lower scores indicating better quality of life) and in exercise capacity at 24 and 48 weeks. A total of 164 patients underwent randomization: 81 were assigned to receive molgramostim and 83 to receive placebo. The least-squares mean change in DLCO from baseline to week 24 was 9.8 percentage points (95% confidence interval [CI], 7.3 to 12.3) with molgramostim and 3.8 percentage points (95% CI, 1.4 to 6.3) with placebo (estimated treatment difference, 6.0 percentage points; 95% CI, 2.5 to 9.4;  $P<0.001$ ). The least-squares mean change in DLCO from baseline to week 48 was 11.6 percentage points (95% CI, 8.7 to 14.5) with molgramostim and 4.7 percentage points (95% CI, 1.8 to 7.6) with placebo ( $P<0.001$ ), and the least-squares mean change in the SGRQ-T score at week 24 was −11.5 points (95% CI, −15.0 to −8.0) and −4.9 points (95% CI, −8.3 to −1.5), respectively ( $P=0.007$ ). No significant between-group difference in the change in SGRQ-A score was observed at 24 weeks, so no statistical inference was drawn with respect to subsequent secondary end points. The percentage of patients with at least one adverse event and the percentage with at least one serious adverse event were similar in the two groups. Once-daily inhaled molgramostim led to a greater increase in pulmonary gas transfer than placebo in patients with aPAP.

## 25COASOCT35

### **Title: Adjuvant Cemiplimab or Placebo in High-Risk Cutaneous Squamous-Cell Carcinoma**

Danny Rischin, M.D., Sandro Porceddu, M.D.

N Engl J Med 2025;393:774-785, [VOL. 393 NO. 8](#)

<https://doi.org/10.1056/NEJMoa2502449>

**Abstract:** Patients who have cutaneous squamous-cell carcinoma with high-risk features are at risk for recurrence after definitive local therapy. The benefit of systemic adjuvant therapy options has not been well established in clinical trials. **Methods**—In a phase 3, randomized trial, we enrolled patients with local or regional cutaneous squamous-cell carcinoma, after surgical resection and postoperative radiotherapy, at high risk for recurrence owing to nodal features (extracapsular extension with largest node  $\geq 20$  mm in diameter or at least three involved nodes) or nonnodal features (in-transit metastases, T4 lesion [with bone invasion], perineural invasion, or locally recurrent tumor with  $\geq 1$  additional risk feature). Patients were assigned in a 1:1 ratio to receive adjuvant cemiplimab (350 mg) or placebo, administered intravenously every 3 weeks for 12 weeks, followed by a dose increase to 700 mg administered every 6 weeks for up to 36 weeks ( $\leq 48$  weeks total). The primary end point was disease-free survival. Secondary end points included freedom from locoregional recurrence,

freedom from distant recurrence, and safety. Results-A total of 415 patients were assigned to cemiplimab (209) or placebo (206). The median follow-up was 24 months. Cemiplimab was superior to placebo with respect to disease-free survival (24 vs. 65 events; hazard ratio for disease recurrence or death, 0.32; 95% confidence interval [CI], 0.20 to 0.51;  $P < 0.001$ ). The estimated 24-month disease-free survival was 87.1% (95% CI, 80.3 to 91.6) with cemiplimab and 64.1% (95% CI, 55.9 to 71.1) with placebo. Cemiplimab led to lower risks of locoregional recurrence (9 events, vs. 40 with placebo; hazard ratio, 0.20; 95% CI, 0.09 to 0.40) and distant recurrence (10 vs. 26 events; hazard ratio, 0.35; 95% CI, 0.17 to 0.72). Adverse events of grade 3 or higher occurred in 23.9% of the patients who received cemiplimab and in 14.2% of those who received placebo; discontinuation due to adverse events occurred in 9.8% and 1.5%, respectively. Conclusions-Adjuvant cemiplimab therapy led to longer disease-free survival than placebo among patients at high risk for recurrence of cutaneous squamous-cell carcinoma.

### 25COASOCT36

#### **Title: Aficamten or Metoprolol Monotherapy for Obstructive Hypertrophic Cardiomyopathy**

Pablo Garcia-Pavia, M.D., Ph.D.

N Engl J Med 2025;393:949-960, VOL. 393 NO. 10

<https://doi.org/10.1056/NEJMoa2504654>

**Abstract:** Beta-blockers have been the initial treatment for symptomatic obstructive hypertrophic cardiomyopathy (HCM) despite limited evidence of their efficacy. Aficamten is a cardiac myosin inhibitor that reduces left ventricular outflow tract gradients, improves exercise capacity, and decreases HCM symptoms when added to standard medications. Whether aficamten as monotherapy provides greater clinical benefit than beta-blockers as monotherapy remains unknown. Methods-We conducted an international, double-blind, double-dummy trial in which adults with symptomatic obstructive HCM were randomly assigned in a 1:1 ratio to receive aficamten (at a daily dose of 5 mg to 20 mg) plus placebo or metoprolol (at a daily dose of 50 mg to 200 mg) plus placebo. The primary end point was the change in peak oxygen uptake at week 24; secondary end points were improvement at week 24 in New York Heart Association (NYHA) functional class and changes at week 24 in Kansas City Cardiomyopathy Questionnaire clinical summary score (KCCQ-CSS), left ventricular outflow tract gradient after the Valsalva maneuver, N-terminal pro-B-type natriuretic peptide (NT-proBNP) level, left atrial volume index, and left ventricular mass index. Results-A total of 88 patients were assigned to the aficamten group and 87 to the metoprolol group. The mean age of the patients was 58 years, 58.3% were men, and the mean left ventricular outflow tract gradient was 47 mm Hg at rest and 74 mm Hg after the Valsalva maneuver. At 24 weeks, the change in the peak oxygen uptake was 1.1 ml per kilogram of body weight per minute (95% confidence interval [CI], 0.5 to 1.7) in the aficamten group and -1.2 ml per kilogram per minute (95% CI, -1.7 to -0.8) in the metoprolol group (least-squares mean between-group difference, 2.3 ml per kilogram per minute; 95% CI, 1.5 to 3.1;  $P < 0.001$ ). Patients who received aficamten had significantly greater improvements in NYHA class, KCCQ-CSS, left ventricular outflow tract gradient, NT-proBNP level, and left atrial volume index than patients who received metoprolol. No significant difference in left ventricular mass index was observed. Adverse events appeared to be similar in the two

treatment groups. Conclusions-Among patients with symptomatic obstructive HCM, aficamten monotherapy was superior to metoprolol monotherapy in improving peak oxygen uptake and hemodynamics and decreasing symptoms.

### 25COASOCT37

#### **Title: Mavacamten in Symptomatic Nonobstructive Hypertrophic Cardiomyopathy**

Milind Y. Desai, M.D, Anjali T. Owens, M.D.

N Engl J Med 2025;393:961-972, VOL. 393 NO. 10

<https://doi.org/10.1056/NEJMoa2505927>

**Abstract:** Mavacamten is approved to treat adults with symptomatic obstructive hypertrophic cardiomyopathy (HCM). However, its effects in nonobstructive HCM remain uncertain. **Methods-**We conducted a phase 3, international, double-blind, placebo-controlled, clinical trial to determine whether mavacamten improves functional capacity and patient-reported health status among adults with symptomatic nonobstructive HCM. Patients were randomly assigned in a 1:1 ratio to receive mavacamten (starting at 5 mg per day and adjusted up to a maximum of 15 mg per day on the basis of left ventricular ejection fraction) or placebo (with sham dose adjustment) for 48 weeks. The two primary end points were the change from baseline to week 48 in peak oxygen uptake and in the 23-item Kansas City Cardiomyopathy Questionnaire clinical summary score. **Results-**We randomly assigned 289 patients to receive mavacamten and 291 to receive placebo. The mean ( $\pm$ SD) age of the patients was 56 $\pm$ 15 years, and 46% were women. From baseline to week 48, the least-squares mean change in peak oxygen uptake was 0.52 ml per kilogram of body weight per minute (95% confidence interval [CI], 0.09 to 0.95) in the mavacamten group and 0.05 ml per kilogram per minute (95% CI, -0.38 to 0.47) in the placebo group (between-group difference, 0.47 ml per kilogram per minute; 95% CI, -0.03 to 0.98;  $P=0.07$ ). The least-squares mean change in the KCCQ-CSS was 13.1 points (95% CI, 10.7 to 15.5) in the mavacamten group and 10.4 points (95% CI, 8.0 to 12.8) in the placebo group (between-group difference, 2.7 points; 95% CI, -0.1 to 5.6;  $P=0.06$ ). Reductions in ejection fraction and interruptions in the trial regimen were more common with mavacamten than with placebo. **Conclusions-**Among patients with nonobstructive HCM, mavacamten did not result in a significantly greater improvement in peak oxygen uptake or decrease in symptoms than placebo.

### 25COASOCT38

#### **Title: Multidomain Rehabilitation for Older Patients with Myocardial Infarction**

Elisabetta Tonet, M.D. et.al.

N Engl J Med 2025;393:973-982, VOL. 393 NO. 10

<https://doi.org/10.1056/NEJMoa2502799>

**Abstract:** The benefit of rehabilitation interventions in patients who are 65 years of age or older with myocardial infarction and impaired physical performance remains unclear. **Methods-**In this multicenter, randomized trial conducted in Italy, we assigned older patients with impaired physical performance 1 month after myocardial infarction in a 2:1 ratio to receive either an intervention consisting of control of cardiovascular risk factors, dietary counseling, and exercise training (intervention group) or usual care (control group). The primary outcome was a composite of cardiovascular death or unplanned hospitalization for cardiovascular causes within 1 year. **Results-**A total of 512 patients underwent randomization

(342 to the intervention group and 170 to the control group). The median age of the patients was 80 years, and 36% were women. A primary-outcome event occurred in 43 patients (12.6%) in the intervention group and in 35 patients (20.6%) in the control group (hazard ratio, 0.57; 95% confidence interval [CI], 0.36 to 0.89;  $P=0.01$ ). Cardiovascular death occurred in 14 patients (4.1%) in the intervention group and in 10 patients (5.9%) in the control group (hazard ratio, 0.69; 95% CI, 0.31 to 1.55). Unplanned hospitalization for cardiovascular causes occurred in 31 patients (9.1%) in the intervention group and in 30 patients (17.6%) in the control group (hazard ratio, 0.48; 95% CI, 0.29 to 0.79). There were no serious adverse events associated with the intervention. Conclusions—Among older patients with impaired physical performance 1 month after myocardial infarction, a multidomain rehabilitation intervention resulted in a lower incidence of cardiovascular death or unplanned cardiovascular hospitalization within 1 year than usual care.

## 25COASOCT39

### **Title: Marburg Virus Disease in Rwanda, 2024 — Public Health and Clinical Responses**

Sabin Nsanzimana, M.D., Ph.D.

N Engl J Med 2025;393:983-993, [VOL. 393 NO. 10](#)

<https://doi.org/10.1056/NEJMoa2415816>

**Abstract:** On September 27, 2024, Rwanda reported an outbreak of Marburg virus disease (MVD), after a cluster of cases of viral hemorrhagic fever was detected at two urban hospitals. **Methods**—We report key aspects of the epidemiology, clinical manifestations, and treatment of MVD during this outbreak, as well as the overall response to the outbreak. We performed a retrospective epidemiologic and clinical analysis of data compiled across all pillars of the outbreak response and a case-series analysis to characterize clinical features, disease progression, and outcomes among patients who received supportive care and investigational therapeutic agents. **Results**—Among the 6340 patients with suspected MVD who underwent testing, 66 had laboratory-confirmed MVD, 51 (77%) of whom were health care workers. The median estimated incubation period was 10 days (interquartile range, 8 to 13), and symptom onset occurred a median of 2 days (interquartile range, 1 to 3) before hospital admission. The results of epidemiologic investigations were highly suggestive of a zoonotic origin of the outbreak: an index patient was identified who had been exposed to Egyptian fruit bats at a mining site. The case fatality rate in the outbreak was 23% (15 deaths among 66 patients). Remdesivir and the monoclonal antibody MBP091 were used under expanded access and clinical trial protocols. In addition, 1710 frontline workers and high-risk contacts received the chimpanzee adenovirus 3–vectored vaccine ChAd3-MARV under emergency use authorization in a phase 2 clinical trial. **Conclusions**—Implementation of containment measures, advanced supportive care, and access to investigational countermeasures may have contributed to reduced mortality from MVD in this outbreak. Enhancing surveillance, improving infection prevention and control in health care settings, and ensuring timely deployment of medical countermeasures will be critical for mitigating the effects of future filovirus disease outbreaks.

## 25COASOCT40

### **Title: Dexmedetomidine- or Clonidine-Based Sedation Compared With Propofol in Critically Ill Patients: The A2B Randomized Clinical Trial.**



Walsh TS, Parker RA, Aitken LM, et al.

*JAMA*. 2025;334(1):32–45.

<https://doi.org/10.1001/jama.2025.7200>

**Abstract:** Importance Whether  $\alpha_2$ -adrenergic receptor agonist–based sedation, compared with propofol-based sedation, reduces time to extubation in patients receiving mechanical ventilation in the intensive care unit (ICU) is uncertain. Objective To evaluate whether dexmedetomidine- or clonidine-based sedation reduces duration of mechanical ventilation compared with propofol-based sedation (usual care). Design, Setting, and Participants Pragmatic, open-label randomized clinical trial conducted at 41 ICUs in the UK including adults who were within 48 hours of starting mechanical ventilation, were receiving propofol plus an opioid for sedation and analgesia, and were expected to require mechanical ventilation for 48 hours or longer. The median time from intubation to randomization was 21.0 (IQR, 13.2–31.3) hours. Recruitment occurred from December 2018 to October 2023; the last follow-up occurred on December 10, 2023. Interventions The bedside algorithms used targeted a Richmond Agitation-Sedation Scale score of –2 to 1 (unless clinicians requested deeper sedation). The algorithms supported uptitration in the dexmedetomidine- and clonidine-based sedation intervention groups and supported downtitration for propofol-based sedation followed by sedation primarily with the allocated sedation (dexmedetomidine or clonidine). If required, supplemental use of propofol was permitted. Main Outcomes and Measures The primary outcome was time from randomization to successful extubation. The secondary outcomes included mortality, sedation quality, rates of delirium, and cardiovascular adverse events. Results Among the 1404 patients in the analysis population (mean age, 59.2 [SD, 14.9] years; 901 [64%] were male; and the mean APACHE II score was 20.3 [SD, 8.2]), the subdistribution hazard ratio (HR) for time to successful extubation was 1.09 (95% CI, 0.96–1.25;  $P = .20$ ) for dexmedetomidine ( $n = 457$ ) vs propofol ( $n = 471$ ) and was 1.05 (95% CI, 0.95–1.17;  $P = .34$ ) for clonidine ( $n = 476$ ) vs propofol ( $n = 471$ ). The median time from randomization to successful extubation was 136 (95% CI, 117–150) hours for dexmedetomidine, 146 (95% CI, 124–168) hours for clonidine, and 162 (95% CI, 136–170) hours for propofol. In the predefined subgroup analyses, there were no interactions with age, sepsis status, median Sequential Organ Failure Assessment score, or median delirium risk score. Among the secondary outcomes, agitation occurred at a higher rate with dexmedetomidine vs propofol (risk ratio [RR], 1.54 [95% CI, 1.21–1.97]) and with clonidine vs propofol (RR, 1.55 [95% CI, 1.22–1.97]). Compared with propofol, the rates of severe bradycardia (heart rate  $<50$ /min) were higher with dexmedetomidine (RR, 1.62 [95% CI, 1.36–1.93]) and clonidine (RR, 1.58 [95% CI, 1.33–1.88]). Compared with propofol, mortality was similar over 180 days for dexmedetomidine (HR, 0.98 [95% CI, 0.77–1.24]) and clonidine (HR, 1.04 [95% CI, 0.82–1.31]). Conclusions and Relevance In critically ill patients, neither dexmedetomidine nor clonidine was superior to propofol in reducing time to successful extubation.

## 25COASOCT41

**Title: Clinical Validation of a Circulating Tumor DNA–Based Blood Test to Screen for Colorectal Cancer.**

Shaukat A, Burke CA, Chan AT, et al.

*JAMA*. 2025;334(1):56–63.

<https://doi.org/10.1001/jama.2025.7515>

**Abstract:** Importance Colorectal cancer screening is widely recommended but underused. Blood-based screening offers the potential for higher adherence compared with endoscopy or stool-based testing but must first be clinically validated in a screening population. Objective To evaluate the clinical performance of an investigational blood-based circulating tumor DNA test for colorectal cancer detection in an average-risk population using colonoscopy with histopathology as the reference method. Design, Setting, and Participants Prospective, multicenter, cross-sectional observational study enrolling participants between May 2020 and April 2022 who were asymptomatic adults aged 45 to 85 years, at average risk of colorectal cancer, and willing to undergo a standard-of-care screening colonoscopy. Participants, staff, and pathologists were blinded to blood test results, and laboratory testing was performed blinded to colonoscopy findings. The study was conducted at 201 centers across 49 US states and the United Arab Emirates. Site-based and mobile phlebotomy were used for blood collection. Exposures Participants were required to complete a screening colonoscopy after blood collection. Main Outcomes and Measures The primary end points were sensitivity for colorectal cancer, specificity for advanced colorectal neoplasia (colorectal cancer or advanced precancerous lesions), negative predictive value for advanced colorectal neoplasia, and positive predictive value for advanced colorectal neoplasia. The secondary end point was sensitivity for advanced precancerous lesions. Results The median age of participants in the evaluable cohort (n = 27 010) was 57.0 years, and 55.8% were women. Sensitivity for colorectal cancer was 79.2% (57/72; 95% CI, 68.4%-86.9%) and specificity for advanced colorectal neoplasia was 91.5% (22 306/24 371; 95% CI, 91.2%-91.9%). The negative predictive value for advanced colorectal neoplasia was 90.8% (22 306/24 567; 95% CI, 90.7%-90.9%) and the positive predictive value for advanced colorectal neoplasia was 15.5% (378/2443; 95% CI, 14.2%-16.8%). All primary end points met prespecified acceptance criteria. The sensitivity for advanced precancerous lesions was 12.5% (321/2567; 95% CI, 11.3%-13.8%), which did not meet the prespecified acceptance criterion. Conclusions and Relevance In an average-risk colorectal cancer screening population, a blood-based test demonstrated acceptable accuracy for colorectal cancer detection, but detection of advanced precancerous lesions remains a challenge, and ongoing efforts are needed to improve test sensitivity.

## 25COASOCT42

### Title: Robotic vs Laparoscopic Surgery for Middle and Low Rectal Cancer: The REAL Randomized Clinical Trial.

Feng Q, Yuan W, Li T, et al.

*JAMA*. 2025;334(2):136–148.

<https://doi.org/10.1001/jama.2025.8123>

**Abstract:** Importance Robotic surgery for rectal cancer is widely used, but data on long-term oncological outcomes are still lacking. Objective To compare the 3-year locoregional recurrence rates of middle and low rectal cancer in patients who underwent robotic surgery vs conventional laparoscopic surgery. Design, Setting, and Participants In this multicenter, superiority, randomized clinical trial, patients with middle or low rectal adenocarcinoma (cT1-T3, N0-N1, or ycT1-T3 Nx) and no distant metastasis were enrolled at 11 centers across 8 provinces in China from July 2016 to December 2020. Among the 1742 consecutive

patients assessed for eligibility, 1240 were eligible and randomized. Follow-up continued until December 31, 2023. **Interventions** Patients were randomized 1:1 to undergo robotic or conventional laparoscopic rectal cancer resection. **Main Outcomes and Measures** The primary outcome was the 3-year locoregional recurrence rate. The primary analysis was performed as randomized, but excluded patients deemed ineligible after randomization. The secondary outcomes included disease-free survival; overall survival; and urinary, sexual, and defecation function. **Results** Of the 1240 patients enrolled, 1171 were included in the primary analysis (586 in the robotic surgery group; mean age, 59.1 [SD, 11.0] years; and 356 were men [60.8%] vs 585 in the laparoscopic surgery group; mean age, 60.7 [SD, 9.8] years; and 354 were men [60.5%]). The median follow-up time was 43.0 months (IQR, 36.7-60.0 months). The 3-year locoregional recurrence rate was 1.6% (95% CI, 0.6%-2.6%) in the robotic group vs 4.0% (95% CI, 2.4%-5.6%) in the laparoscopic group (hazard ratio [HR], 0.45 [95% CI, 0.22-0.92], log-rank  $P = .03$ ; adjusted HR, 0.39 [95% CI, 0.19-0.80]). The 3-year disease-free survival rate was higher in the robotic group (87.2%) vs the laparoscopic group (83.4%) (HR, 0.74 [95% CI, 0.56-0.98], log-rank  $P = .04$ ; adjusted HR, 0.67 [95% CI, 0.50-0.89]). No significant between-group difference was observed in 3-year overall survival (94.7% in the robotic group vs 93.0% in the laparoscopic group). Patients in the robotic group also had better urinary function, male and female sexual function, and defecation function at 3 and 6 months after surgery and better urinary function and male sexual function at 12 months after surgery. **Conclusions and Relevance** Compared with conventional laparoscopic surgery, robotic surgery significantly improved long-term oncological outcomes in patients with middle or low rectal cancer. With additional real-world clinical data and modern, improved training programs for surgeons, robotic surgery could be the preferred choice for patients with middle or low rectal cancer.

## 25COASOCT43

### **Title: Screening Colonoscopy Yields Among Adults Aged 45 to 49 Years After Lowering the Colon Cancer Screening Age.**

Lee JK, Jensen CD, Hendel J, Udaltsova N, Corley DA, Levin TR.

*JAMA*. 2025;334(5):449–452.

<https://doi.org/10.1001/jama.2025.7494>

**Abstract:** In response to rising colorectal cancer incidence rates among adults younger than 50 years, in 2021, the US Preventive Services Task Force (USPSTF) updated its guidelines to recommend that average-risk adults begin colorectal cancer screening at age 45 years.<sup>1</sup> Other groups have made similar recommendations.<sup>2-4</sup> However, there are few reports on screening colonoscopy neoplasia yields among younger adults following the USPSTF guideline change. We investigated colorectal neoplasia yields at screening colonoscopy among adults aged 45 to 49 years vs 50 to 54 years who were members of Kaiser Permanente Northern California (KPNC), a large integrated health system that provides comprehensive inpatient and outpatient services to more than 4.5 million Northern California members. **Methods**—This study was approved by the KPNC Institutional Review Board, with informed consent waived. Individuals were eligible if they were aged 45 to 54 years, underwent their first screening colonoscopy in 2021-2024, and had 12 months or longer of membership prior to colonoscopy. Exclusion criteria included history of inflammatory bowel disease, family history of colorectal cancer, personal history of colorectal cancer or adenoma, incomplete

screening colonoscopy (ie, inadequate bowel preparation and/or did not reach the cecum), or diagnostic indication for the colonoscopy. The study outcomes were colorectal cancer (adenocarcinoma of the colon or rectum); advanced serrated lesion (sessile serrated adenoma  $\geq 10$  mm or traditional serrated adenoma); advanced adenoma (ie, any adenoma with villous or tubulovillous histology or high-grade dysplasia or any adenoma  $\geq 10$  mm); any sessile serrated lesion; or any adenoma. Robust Poisson regression was used to estimate the adjusted risk ratios (aRRs) for outcomes between age groups, with 50- to 54-year-olds serving as the reference group. Regression models were adjusted for sex, race and ethnicity, Charlson comorbidity score, body mass index, and tobacco smoking history. Results A total of 12 031 eligible patients underwent a screening colonoscopy in 2021-2024, including 4380 aged 45 to 49 years and 7651 aged 50 to 54 years (Table 1). Females comprised 47.3% of the overall cohort, 42.8% were White, 78.7% had a Charlson comorbidity score of zero, median body mass index was 26.5 (IQR, 23.6-30.4) (calculated as weight in kilograms divided by height in meters squared), and 24.0% had a history of tobacco smoking.

## 25COASOCT44

**Title: Survival outcomes in small intestine tumors: The role of duodenum, jejunum, and ileum**

Hongwei Wu, Xiaobao Yang, Wei Guo

International Journal of Cancer, Volume157, Issue3

<https://doi.org/10.1002/ijc.35379>

**Abstract:** Small intestine tumors are rare, with variable prognostic factors. The impact of tumor location on survival outcomes remains controversial. This study explores the influence of tumor location (duodenum, jejunum, ileum) on survival. We analyzed data from the SEER database for small intestine cancer patients diagnosed between 2010 and 2017. Survival outcomes by tumor location were assessed using the Kaplan–Meier method and competing risk models, stratified by adenocarcinoma (ADC), neuroendocrine tumor (NET), and gastrointestinal stromal tumor (GIST). Propensity score matching (PSM) was employed to adjust for confounders. The cohort included 6047 patients: 2611 with duodenum, 2584 with ileum, and 852 with jejunum tumors. ADC was predominant in the duodenum (51.4%), while NET was most common in the ileum (84.21%). Overall, the ileum tumors had the best prognosis, and duodenum tumors had the worst ( $p < .001$ ). In ADC, duodenum tumors had the poorest overall (OS) and disease-specific survival (DSS) ( $p < .001$ ) with no significant impact of location in GIST ( $p > .05$ ). The competing risk model indicated better prognosis for jejunum versus duodenum in ADC (HR = 0.80,  $p = .048$ ) and similar risks between ileum and duodenum tumors (HR = 0.99,  $p = .94$ ), while location did not affect prognosis in GIST and NET ( $p > .05$ ). Post-PSM, survival curves reconfirmed no significant difference between duodenum and ileum ADC ( $p > .05$ ). Tumor location significantly influences prognosis in small intestine ADC, with duodenum tumors showing the worst outcomes. Location was not a significant prognostic factor in GIST and NET.

## 25COASOCT45

**Title: Pregnancy and pregnancy outcomes after adolescent and young adult cancer in the AYA horizon study**

Hazel B. Nichols

International Journal of Cancer, Volume157, Issue3

<https://doi.org/10.1002/ijc.35383>

**Abstract:** Lower birth rates and higher pregnancy loss are observed after childhood cancer. Studies specific to adolescent and young adult (AYA) cancer rarely have information on pregnancies that do not end in live birth, fertility preservation strategies, or detailed cancer treatment information to assess these risks. To address this gap, we examined pregnancy outcomes after cancer in a cohort of 30,020 AYAs with detailed clinical records. We identified 6021 survivors of AYA cancer matched to 23,999 AYAs without cancer enrolled in the Kaiser Permanente California health systems during 2004–2016. Of these, 950 survivors had  $\geq 1$  pregnancy during follow-up through 2018. Hazard ratios (HR) and 95% confidence intervals (CI) for pregnancy were estimated using multivariable subdistribution hazard models accounting for competing risks. Relative risks (RR) and 95% CIs for pregnancy loss were calculated with multivariable Poisson regression with generalized estimating equations. Pregnancy was less common after AYA breast (HR = 0.57; 95% CI: 0.50, 0.66) or gynecologic cancer (HR = 0.55; 95% CI: 0.42, 0.73) compared to AYAs without cancer. Among AYAs with cancer, some alkylating and platinum chemotherapy agents, but not gonadotoxic radiation, were associated with a lower likelihood of pregnancy. Use of assisted reproductive technologies was not common, and 69% of pregnancies after AYA cancer resulted in live birth. Pregnancy loss was not statistically significantly elevated for any cancer type. Among survivors, pregnancy loss was more common at older ages, with smoking during pregnancy, and among those who received cyclophosphamide. Our findings inform reproductive counseling and prenatal care for reproductive age cancer survivors.

## 25COASOCT46

**Title: Low type-2 immune effectors modulate atopic diseases' protective role in pancreatic cancer risk**

Jiangchuan He, Bilal Alashkar Alhamwe et.al.

International Journal of Cancer, Volume157, Issue3

<https://doi.org/10.1002/ijc.35397>

**Abstract:** Studies reported that atopic individuals exhibit a 36% reduced risk of developing pancreatic ductal adenocarcinoma (PDAC); however, the underlying molecular mechanisms remain unclear. This study examines the specific role of type-2 immune response in the atopy–PDAC inverse association. To endotype atopic conditions using type-2 immune effectors (i.e., eosinophils and immunoglobulin-E[IgE]) and investigate their protective effect against PDAC risk, IgE levels were measured in 688 PDAC cases and 558 controls from the PanGenEU case–control study. ‘IgE-sensitization’ was defined as having  $>100$  kU/L total IgE with lab-tested sensitization to  $\geq 1$  food- or aeroallergens. Atopic conditions were determined using the European Community Respiratory Health Survey questionnaire. The UK Biobank cohort's 544 PDAC cases and 92,038 nested controls were categorized based on a threshold of  $0.15 \times 10^9$  eosinophil cells/L plus self-reported atopy. Odds ratios (ORs) with 95% confidence intervals (CIs) were estimated using multivariable logistic regression. Restricted cubic splines were applied to examine the nonlinear relationship between type-2 immune effectors and PDAC risk. PDAC risk was not linearly associated with type-2 immune effectors levels. Compared to low IgE-sensitized non-atopic individuals, the low IgE-sensitized atopic population had significantly reduced PDAC risk (OR = 0.56, 95% CI:



0.35–0.84). Similar trends were observed among atopic individuals with low eosinophil counts (OR = 0.67, 95% CI: 0.47–0.95). Atopic conditions were inversely associated with PDAC risk, particularly among those with low levels of type-2 immune effectors. This indicates the protective effect of atopy against PDAC risk is modulated by low type-2 immune response.

## 25COASOCT47

**Title: Prospective evaluation of 92 protein biomarkers for early detection of endometrial cancer**

Victoria Cooley, Renée Turzanski Fortner et.al.

International Journal of Cancer, Volume157, Issue3

<https://doi.org/10.1002/ijc.35428>

**Abstract:** The human epididymis protein 4 (HE4) remains the best available endometrial cancer (EC) biomarker; however, its discrimination between cases and cancer-free individuals is limited and might be improved when combined with other protein markers. We evaluated the discrimination capacity of 92 proteins as potential early detection biomarkers for EC in nested case–control studies in the European Prospective Investigation into Cancer and Nutrition (EPIC) (63 cases, 123 controls) and Janus (75 cases, 146 controls) cohorts, evaluating blood samples taken  $\leq 2$  years prior to diagnosis. Proteins were measured with the Olink Target 96 Oncology II panel assays. Areas under the receiver operating characteristic curves (AUCs) were calculated using logistic regression. The discrimination between cases and controls of top-performing proteins was modest (EPIC: HE4, CA125, CAIX, and S100A4; Janus: HE4, CA125, FURIN, CXCL13, and IL6; AUC range: 0.65 [S100A4], 0.76 [HE4, EPIC] within 0 to <12 months of blood collection) and decreased as the time between blood draw and cancer diagnosis increased (12–24 months AUC range: 0.49 [S100A4], 0.69 [CA125, Janus]). The combination of these other markers with HE4 did not improve discrimination. HE4 and other candidate proteins had limited discrimination between EC cases and controls and hence do not appear to be useful for early detection of this disease in women at average population risk.

## 25COASOCT48

**Title: Impact of exercise on sexual health, body image, and therapy-related symptoms in women with metastatic breast cancer: The randomized controlled PREFERABLE-EFFECT trial**

Martina E. Schmidt, Anouk E. et.al.

International Journal of Cancer, Volume157, Issue3

<https://doi.org/10.1002/ijc.35429>

**Abstract:** The understanding and treatment of sexual health problems, impaired body image, and other non-life threatening but burdensome symptoms of women with metastatic breast cancer (mBC) is still insufficient. We studied the factors associated with such symptoms and investigated whether these problems could be alleviated by a structured exercise intervention. In the multinational PREFERABLE-EFFECT study, 355 women with mBC were randomly assigned to usual care ( $n = 178$ ) or a 9-month supervised exercise program ( $n = 177$ ). Breast cancer-specific functions and symptoms (EORTC QLQ-BR42) were assessed at baseline, 3, 6 (primary timepoint), and 9 months. Linear regression models and linear mixed models for

repeated measures were calculated. At baseline, participants were  $55.4 \pm 11.2$  years old, 52.4% were undergoing endocrine therapy, and 25.4% chemotherapy. Baseline sexual functioning was low, with 94.3% reporting no or little sexual activity. Age and depressive symptoms were negatively associated with sexual functioning. Among sexually active women, 46.2% felt no or little sexual enjoyment and 37.3% suffered from vaginal dryness. Body image was reported as low by 23.7%. Exercise significantly improved sexual functioning (6-months between-group difference (BGD) = 5.6, 95% CI [1.9, 9.4], effect size (ES) = 0.28) and vaginal symptoms (BGD = -7.1 [-11.7, -2.5], ES = 0.25), compared to usual care. Effects on body image were marginal (BGD = 4.0 [-0.2, 8.3], ES = 0.14). Among participants undergoing chemotherapy ( $n = 90$ ), exercise reduced chemotherapy side-effects (BGD = -8.2 [-15.4, -1.0], ES = 0.48). In conclusion, women with mBC often experience sexual and vaginal problems and other treatment-related side-effects. A 9-month supervised exercise program vs. control was effective in improving sexual functioning and vaginal symptoms among women with mBC.

## 25COASOCT49

**Title: Real-world treatment patterns and outcomes based on *RAS/BRAF* status in metastatic colorectal cancer—Analysis of the Prospective Dutch Colorectal Cancer cohort**

Sietske C. M. W. van Nassau et al.

International Journal of Cancer, Volume 157, Issue 3

<https://doi.org/10.1002/ijc.35410>

**Abstract:** The treatment landscape for metastatic colorectal cancer (mCRC) has evolved into a continuum of care with an essential role for biomarkers and molecular subgroups. Treatment guidelines are primarily based on trial results; however, populations and outcomes differ from clinical practice. To support the interpretation of trial results and to assist in tailored patient counseling, we evaluated real-world treatment patterns and outcomes according to *RAS/BRAF* status. We included all patients diagnosed with *BRAF*<sup>V600E</sup>-mutated mCRC in 2015–2020, participating in the Prospective Dutch Colorectal Cancer cohort study, plus a 1:2 random selection of patients with *RAS*-mutated and double wild-type mCRC. We evaluated differences in administered lines of treatment (LOTs), local treatment, attrition rates, treatment duration, progression-free survival (PFS) and overall survival (OS). 178 *BRAF*<sup>V600E</sup>-mutated, 221 *RAS*-mutated, and 174 double wild-type patients were included. Of *BRAF*<sup>V600E</sup>-mutated patients, 26% received  $\geq 3$  LOTs, compared to 42% and 47% of the *RAS*-mutated and double wild-type patients, respectively ( $p = .002$ ). Local treatment was performed in 25% of *BRAF*<sup>V600E</sup>-mutated, 43% of *RAS*-mutated, and 49% of double wild-type patients ( $p < .001$ ). Median OS from diagnosis was 15.4, 24.1, and 32.6 months, respectively ( $p < .001$ ) and loss of prognostic value of *RAS/BRAF* was observed from the 3rd LOT onwards ( $p = .17$  and  $p = .54$ ). This paper provides a comprehensive overview of the treatment landscape of mCRC per *RAS/BRAF* status in daily clinical practice. The observed substantial treatment heterogeneity within and between molecular subgroups underlines the importance of collecting real-world data to address post-trial knowledge gaps and to optimize individualized counseling for all mCRC patients.

**25COASOCT50****Title: TNF signature in advanced melanoma patients treated with immune checkpoint inhibitors: Results from the MELANFα clinical study**

Mathieu Virazels, Amélie Lusque

International Journal of Cancer, Volume157, Issue3

<https://doi.org/10.1002/ijc.35416>

**Abstract:** Resistance to immune checkpoint inhibitors (ICI) in cancer patients is not fully understood, and predictive biomarkers are lacking. MELANFα (NCT03348891) is an open-label, prospective, multicenter cohort of 60 patients with advanced melanoma receiving ICI (bithera: ipilimumab + nivolumab; monotherapy: pembrolizumab or nivolumab). The primary objective was to evaluate whether changes in plasma TNF between baseline (W0) and week 12 (W12) identified patients with non-progressive disease at W12. Secondary and exploratory objectives were to assess the association between plasma TNF, tumor response, and changes in circulating T cells. Plasma TNF increased along therapy, but its W12/W0 fold change was not associated with non-progressive disease at W12. However, plasma TNF levels at W12 were significantly higher in non-responders than in responders across therapies ( $p = .0129$ ). The remodeling of circulating T cell subpopulations was mostly triggered by bithera. Increased proportions of circulating central memory and effector memory CD8 T cells after bithera were positively and negatively associated with response to treatment, respectively. In this cohort, circulating T cells from responders and non-responders also displayed distinct molecular characteristics. Indeed, responders showed an increased proportion of CD8 T cells with low enrichment of TNF-related pathways and high cytotoxic potential, while non-responders displayed increased proportions of circulating CD8 EM T cells enriched for TNF-related pathways and directed toward cytokine expression. In conclusion, our study shows that elevated plasma TNF and enriched TNF pathways in T cells are associated with poorer clinical outcomes, reinforcing the notion that TNF may dampen ICI efficacy.

**25COASOCT51****Title: Efficacy and safety of autologous CIK cell therapy plus Toripalimab with or without chemotherapy in advanced NSCLC: A phase II study**

Runbo Zhong, Tianqing Chu, Liwen Xiong et.al.

International Journal of Cancer, Volume157, Issue3

<https://doi.org/10.1002/ijc.35422>

**Abstract:** Advanced non-small cell lung cancer (NSCLC) with positive PD-L1 expression requires more effective therapeutic options. This study aims to evaluate the efficacy and safety of autologous cytokine-induced killer (CIK) cell therapy combined with the anti-PD-1 antibody toripalimab, with or without chemotherapy, as a first-line treatment for advanced NSCLC. This phase II trial enrolled 40 patients with PD-L1-positive, driver mutation-negative advanced NSCLC between July 2020 and December 2022. Patients were randomly assigned to Arm A (toripalimab + CIK cells + chemotherapy) or Arm B (toripalimab + CIK cells). Progression-free survival (PFS), overall survival (OS), overall response rate (ORR), and safety profiles were evaluated. Subgroup analyses were conducted based on the number of CIK cell cycles received. Arm A showed a significantly longer median PFS compared to Arm B (20.0 vs. 6.0 months,  $p = 0.0038$ ), while median OS was not reached in Arm A versus

17.0 months in Arm B ( $p = 0.0479$ ). ORR was 47.4% in Arm A and 60.0% in Arm B. Patients receiving four or more cycles of CIK cells had significantly improved PFS and OS. No new safety concerns were identified. The combination of CIK cells and toripalimab, with or without chemotherapy, demonstrates promising efficacy and safety in patients with advanced PD-L1-positive NSCLC. The addition of chemotherapy may further enhance therapeutic outcomes, making it a potentially superior strategy compared to CIK cells combined with the anti-PD-1 antibody alone.

## 25COASOCT52

**Title: GREM1 deficiency induced bone marrow adipose niche promotes B-cell acute lymphoblastic leukemia disease progression**

Lili Song, Rui Zhang, Liya Pan

International Journal of Cancer, Volume157, Issue3

<https://doi.org/10.1002/ijc.35418>

**Abstract:** Relapse and disease progression are the primary causes of treatment failure and subsequent mortality in children with B-cell acute lymphocytic leukemia (B-ALL). At diagnosis and during treatment, dyslipidemia and the bone marrow adipose microenvironment are commonly observed in pediatric leukemia. However, the intricate connection between these factors and disease progression remains largely unexplored. We found that abnormal triglyceride accumulation increased the risk of death. Further investigation into the adipogenic potential of BM-MSCs revealed a correlation between higher adipogenicity and elevated serum TG levels, which subsequently led to the rapid proliferation of leukemia cells and heightened the risk of post-relapse mortality. Through RNA sequencing, Gremlin1 (GREM1) was identified as an important factor affecting adipogenicity. Silencing of *GREM1* in BM-MSCs induced adipogenic differentiation, partly through the BMP/SMAD signaling pathway. In an in vitro co-culture model, shGREM1-MSCs promoted B-ALL cell proliferation and induced drug resistance to dexamethasone, while increasing sensitivity to L-asparaginase. Furthermore, GREM1-deficient BM-MSCs promoted B-ALL disease progression in xenograft models. This study provides new insights into overcoming drug resistance, relapse, and death by elucidating the novel mechanism by which GREM1 deficiency induces adipogenic differentiation of BM-MSCs and promotes B-ALL disease progression.

## 25COASOCT53

**Title: A strategy for multimodal integration of transcriptomics, proteomics, and radiomics data for the prediction of recurrence in patients with IDH-mutant gliomas**

Tiffanie Chouleur, Christèle Etchegaray et.al.

International Journal of Cancer, Volume157, Issue3

<https://doi.org/10.1002/ijc.35441>

**Abstract:** Isocitrate dehydrogenase-mutant gliomas are lethal brain cancers that impair quality of life in young adults. Although less aggressive than glioblastomas, IDH-mutant gliomas invariably progress to incurable disease with unpredictable recurrence. A better classification of patient risk of recurrence is needed. Here, we describe a multimodal analytical pipeline integrating imaging, transcriptomic, and proteomic profiles using machine learning to improve patient stratification with novel signatures of patient risk of recurrence

based on gene expression, protein level, and imaging. Additionally, we describe the biological characteristics of IDH-mutant glioma subtypes categorized by positron emission tomography (PET) and histology, and we reinforce the integration of positron emission tomography (PET) metrics in the classification of IDH-mutant gliomas. We identify a gene signature (KRT19, RUNX3, and SCRT2) and a protein signature (ATXN10, EIF4H, ITGAV, and NCAM1) associated with an increased risk of early recurrence. Furthermore, we integrated these markers with imaging-derived features, obtaining a better stratification of IDH-mutant glioma patients in comparison to histomolecular classification alone.

## 25COASOCT54

### **Title: Selpercatinib in *RET* Fusion–Positive Non–Small Cell Lung Cancer: Final Safety and Efficacy, Including Overall Survival, From the LIBRETTO-001 Phase I/II Trial**

[Oliver Gautschi, MD](#) et.al.

Journal of Clinical Oncology, [Volume 43, Number 15](#)

<https://doi.org/10.1200/JCO-24-02076>

**Abstract:** LIBRETTO-001 (ClinicalTrials.gov identifier: [NCT03157128](#)) is a registrational phase I/II, single-arm, open-label trial of selpercatinib in RET-dependent cancers. With 19 months of additional follow-up, we report the final efficacy and safety results of selpercatinib in patients with *RET* fusion–positive non–small cell lung cancer (NSCLC) who had previously received platinum-based chemotherapy (N = 247) or were treatment-naïve (N = 69). The objective response rate (ORR) was 62% for pretreated patients and 83% for treatment-naïve patients. Duration of response (DoR) was 31.6 months for pretreated and 20.3 months for treatment-naïve patients (median follow-up approximately 38 months). Median progression-free survival (PFS) was 26.2 months for pretreated and 22.0 months for treatment-naïve patients (median follow-up approximately 40 months). Median overall survival was 47.6 months in pretreated patients and was not reached in the treatment-naïve group (median follow-up approximately 43 months). At the 3-year landmark estimate, 57% of pretreated and 66% of treatment-naïve patients were alive. Among 26 patients with measurable CNS metastases at baseline, the CNS-ORR was 85% with a CNS-DoR of 9.4 months and CNS-PFS of 11.0 months. The safety profile of selpercatinib was consistent with previous reports. With substantial additional follow-up, selpercatinib continued to show durable responses and intracranial activity, with a manageable safety profile in patients with *RET* fusion–positive NSCLC.

## 25COASOCT55

### **Title: Prognostic Models From Transcriptomic Signatures of the Tumor Microenvironment and Cell Cycle in Stage III Colon Cancer From PETACC-8 and IDEA-France Trials**

[Claire Gallois, MD, PhD](#) et.al.

Journal of Clinical Oncology, [Volume 43, Number 15](#)

<https://doi.org/10.1200/JCO.23.02262>

**Abstract:** Purpose-The objective of this work was to establish prognostic models in stage III colon cancer (CC) on the basis of transcriptomic signatures of the tumor microenvironment (TME) and cell cycle from the PETACC-8 (training set) and IDEA-France (validation set) trials. Patients and Methods- 3'RNA sequencing was performed in 1,733 patients from the



PETACC-8 trial and 1,248 patients from the IDEA-France trial. Four transcriptomic signatures were analyzed: T-cell and macrophage M2 signatures, the expression of CXCL13, and a score on the basis of the Oncotype DX CC Recurrence Score using the same formula from the stromal score and the cell cycle score. The Immune Proliferative Stromal (IPS) score was defined as the number of dichotomized signatures that fall under the category of a dismal prognosis (from 0 to 4). Time to recurrence (TTR) was defined as the time from the date of random assignment to local and/or metastatic relapse and/or death because of CC, whichever occurs first. Results-High Oncotype-like and M2 scores and low CXCL13 expression and T-cell score were associated with a shorter TTR. A multivariable model including these signatures and all known prognostic factors applied to the IDEA-France cohort by obtaining a value of this model for each patient showed TTR significantly different depending on the quartile of this value and a 3-year rate of patients without recurrence ranging from 56% for the lowest quartile to 89% for the highest quartile ( $P < .0001$ ). The IPS score was significantly associated with TTR in multivariable analysis. Conclusion-Using transcriptomic data of patients with stage III CC from two large-scale adjuvant trials, a prognostic model on the basis of signatures of the TME and the cell cycle provides important information in addition to known prognostic factors for patient stratification on risk of recurrence.

## 25COASOCT56

### **Title: Letetresgene Autoleucel in Advanced/Metastatic Myxoid/Round Cell Liposarcoma**

Sandra P. D'Angelo, MD et.al.

Journal of Clinical Oncology, Volume 43, Number 15

<https://doi.org/10.1200/JCO-24-01466>

**Abstract:** Purpose-The cancer/testis antigen New York esophageal squamous cell carcinoma 1 (NY-ESO-1) is a promising target in myxoid/round cell liposarcoma (MRCLS). Methods-In this pilot study, we assessed the adoptive T-cell therapy NY-ESO-1c<sup>259</sup>T letetresgene autoleucel (lete-cel) in patients with human leukocyte antigen (HLA)-A\*02:01-, HLA-A\*02:05-, and/or HLA-A\*02:06-positive advanced/metastatic NY-ESO-1-expressing MRCLS. Patients underwent a reduced-dose (cohort 1) or standard-dose (cohort 2) lymphodepletion regimen (LDR). The primary end point was investigator-assessed overall response rate (ORR). Safety was assessed through adverse event (AE) reports. Correlative biomarker analyses were performed post hoc. The trial is registered at ClinicalTrials.gov (identifier: [NCT02992743](https://clinicaltrials.gov/ct2/show/study/NCT02992743)). Results-Of 23 enrolled patients, 10 in cohort 1 and 10 in cohort 2 received lete-cel. Investigator-assessed ORR was 20% (95% CI, 2.5 to 55.6) and 40% (95% CI, 12.2 to 73.8), median duration of response was 5.3 months (95% CI, 1.9 to 8.7) and 7.5 months (95% CI, 6.0 to not estimable [NE]), and median progression-free survival was 5.4 months (95% CI, 2.0 to 11.5) and 8.7 months (95% CI, 0.9 to NE) in cohorts 1 and 2, respectively. AEs included cytokine release syndrome and cytopenias, consistent with T-cell therapy/LDR. Post hoc correlative biomarkers showed T-cell expansion and persistence in both cohorts. Conclusion- To our knowledge, this study is the first demonstrating the clinical promise of lete-cel in HLA-/NY-ESO-1-positive patients with advanced MRCLS.

**25COASOCT57**

**Title: Trend and Provider- and Organizational-Level Factors Associated With Early Palliative Care Billing Among Patients Diagnosed With Distant-Stage Cancers in 2010-2019 in the United States**

Xin Hu, PhD

Journal of Clinical Oncology, Volume 43, Number 15

<https://doi.org/10.1200/JCO-24-01935>

**Abstract:** Purpose-Early integration of specialized palliative care (PC) is recommended by clinical guidelines for advanced-stage cancers, but real-world evidence of its use is limited. We examined the recent trend of early PC billing among Medicare beneficiaries with distant-stage cancers and associated provider- and organization-level factors. Methods-Using SEER-Medicare data, we identified Medicare Fee-For-Service beneficiaries 65.5 years and older diagnosed with distant-stage female breast, colorectal, non-small cell lung, small cell lung, pancreatic, or prostate cancers in 2010-2019 with a survival of  $\geq 6$  months. Early PC billing was identified by diagnosis codes or hospice and palliative medicine (HPM) specialty codes on outpatient claims within first 3 months of cancer diagnosis or up to hospice admission date, whichever came first. Annual percentages of patients receiving early PC were assessed. We attributed treating physicians and organizations to patients and identified provider- and organization-level factors associated with early PC billing and the between-provider and between-organization variation in early PC billing using multivariable regressions. Results-Among 102,032 patients treated by 18,908 unique physicians, the percentage with early PC billing increased from 1.44% to 10.36% in 2010-2019 ( $P < .001$ ). Treating physician's early PC referrals in the previous year and organizations' employment of any HPM specialist were associated with 3.01 percentage points (ppts, 95% CI, 2.50 to 3.52) and 4.54 ppts (95% CI, 3.65 to 5.42) higher likelihood of early PC billing. Between-provider variation in early PC was considerable but declined from 51.0% in 2010-2013 to 45.3% in 2017-2019. Similar patterns were found for between-organization variation. Conclusion- Despite growth in early PC billing among patients with distant-stage cancers in 2010-2019, its level remained low. Provider and organizational characteristics such as referral patterns and availability of HPM specialists within the organization may be important drivers for early PC utilization.

**25COASOCT58**

**Title: Randomized, Open-Label, Phase III Study of Tilsotolimod in Combination With Ipilimumab Versus Ipilimumab Alone in Patients With Advanced Refractory Melanoma (ILLUMINATE-301)**

Adi Diab, MD et.al.

Journal of Clinical Oncology, Volume 43, Number 15

<https://doi.org/10.1200/JCO.24.00727>

**Abstract:** Purpose-There are limited treatment options for advanced melanoma that have progressed during or after immune checkpoint inhibitor therapy. Intratumoral (IT) immunotherapy may improve tumor-specific immune activation by promoting local tumor antigen presentation while avoiding systemic toxicities. The phase 3 ILLUMINATE-301 study (ClinicalTrials.gov identifier: [NCT03445533](https://clinicaltrials.gov/ct2/show/study/NCT03445533)) evaluated tilsotolimod, a Toll-like receptor-9 agonist, with or without ipilimumab in patients with anti-PD-1 advanced refractory melanoma. Methods-Patients with unresectable stage III-IV melanoma that

progressed during or after anti-PD-1 therapy were randomly assigned 1:1 to receive 24 weeks of tilosotolimod plus ipilimumab or 10 weeks of ipilimumab alone. Nine IT injections of tilosotolimod were administered to a single designated lesion over 24 weeks. Intravenous ipilimumab 3 mg/kg was administered once every 3 weeks from week 2 in the tilosotolimod arm and week 1 in the ipilimumab arm. The primary end point was efficacy measured using objective response rate (ORR; independent review) and overall survival (OS). Results-A total of 481 patients received tilosotolimod plus ipilimumab (n = 238) or ipilimumab alone (n = 243). ORRs were 8.8% in the tilosotolimod arm and 8.6% in the ipilimumab arm, with disease control rates of 34.5% and 27.2%, respectively. Median OS was 11.6 months in the tilosotolimod arm and 10 months in the ipilimumab arm (hazard ratio, 0.96 [95% CI, 0.77 to 1.19];  $P = .7$ ). Grade  $\geq 3$  treatment-emergent adverse events occurred in 61.1% and 55.5% of patients in the tilosotolimod and ipilimumab arms, respectively. Conclusion- Combining IT tilosotolimod with ipilimumab did not significantly improve the ORR or OS compared with ipilimumab alone in patients with anti-PD-1 advanced refractory melanoma.

## 25COASOCT59

### **Title: High-Dose Methotrexate in Children and Young Adults With ALL and Lymphoblastic Lymphoma: Results of the Randomized Phase III Study UKALL 2011**

Amy A. Kirkwood, MSc et.al.

Journal of Clinical Oncology, Volume 43, Number 15

<https://doi.org/10.1200/JCO-24-01851>

**Abstract:** Purpose-UKALL 2011 randomly assigned children and young adults (younger than 25 years) with ALL or lymphoblastic lymphoma. The aims were to reduce induction toxicity (randomization 1 [R1]), CNS relapse risk (randomization 2 [R2]–interim maintenance [R2IM]), and maintenance morbidity (R2pulses). Methods-R1 compared induction dexamethasone (dex) for 28 days (6 mg/m<sup>2</sup>; standard) with 14 days (10 mg/m<sup>2</sup>; short). R2 was a factorial randomization resulting in four arms: high-dose methotrexate (HDM) with pulses, HDM without pulses, standard interim maintenance (SIM) with pulses (standard of care), and SIM without pulses. The primary end points were reduction in steroid-related toxicity (R1), CNS relapse rate (CNSR, R2IM), and bone marrow relapse rate (BMR, R2pulses; ALL only, noninferiority margin 5%). Event-free survival (EFS) was an additional primary end point for both randomizations. Results-Of 2,750 eligible patients registered between April 2012 and December 2018, 1,902 were randomly assigned to R1 and 1,570 to R2. Median follow-up is 99 (R1) and 87 months (R2). There were no differences in steroid-related toxicity between short and standard dex (23.8% v 25.5%;  $P = .41$ ) and CNSR between SIM and HDM (0.98 [95% CI, 0.65 to 1.49];  $P = .94$ ; 5-year rates: SIM 5.3% and HDM 5.5%). EFS was no different between R1 and R2IM arms. BMR in the no pulses arm was noninferior (+1.7% increase at 5 years [95% CI, -1.5 to 4.1]; hazard ratio [HR], 1.19 [95% CI, 0.87 to 1.62];  $P = .27$ ). Although the EFS in the no pulses arm was inferior (1.34 [95% CI, 1.05 to 1.73];  $P = .021$ ), this was not significant for relapse (HR, 1.24 [95% CI, 0.96 to 1.62];  $P = .10$ ). Conclusion-Shorter duration of induction dex does not reduce steroid-related toxicity and HDM does not improve CNSR within a UKALL treatment backbone. Omission of pulses is noninferior for BMR.

**25COASOCT60****Title: Phase I, First-in-Human Study of FOR46 (FG-3246), an Immune-Modulating Antibody-Drug Conjugate Targeting CD46, in Patients With Metastatic Castration-Resistant Prostate Cancer**

Rahul R. Aggarwal, MD et.al.

Journal of Clinical Oncology, Volume 43, Number 15

<https://doi.org/10.1200/JCO-24-01989>

**Abstract:** Purpose-FOR46, a fully human antibody conjugated to monomethyl auristatin E, targets a tumor-selective epitope of CD46, which is overexpressed in metastatic castration-resistant prostate cancer (mCRPC). FOR46 demonstrates potent nonclinical activity in enzalutamide-resistant CRPC models. Patients and Methods-This was a phase I, first-in-human, dose escalation/expansion study in patients with progressive mCRPC after treatment with  $\geq$ one androgen signaling inhibitors (ClinicalTrials.gov identifier: [NCT03575819](https://clinicaltrials.gov/ct2/show/study/NCT03575819)). The starting dose of FOR46 was 0.1 mg/kg given intravenously every 3 weeks. The primary objective was to determine the maximally tolerated dose (MTD). Whole-blood mass cytometry (cytometry by time of flight) was used to characterize peripheral immune response and CD46 expression in CRPC tissue that underwent central pathology review. Results-Fifty-six patients were enrolled. Dose-limiting toxicities included neutropenia (n = 4), febrile neutropenia (n = 1), and fatigue (n = 1). The MTD was 2.7 mg/kg using adjusted body weight. The most common grade  $\geq$ 3 adverse events across all dose levels were neutropenia (59%), leukopenia (27%), lymphopenia (7%), anemia (7%), and fatigue (5%). One grade 3 febrile neutropenia event was observed. There were no treatment-related deaths. In the efficacy evaluable subset (patients with adenocarcinoma treated with a starting dose  $\geq$ 1.2 mg/kg, n = 40), the median radiographic progression-free survival was 8.7 months (range, 0.1-33.9). Fourteen of 39 evaluable patients (36%) achieved a PSA50 response. The confirmed objective response rate was 20% (5 of 25 RECIST-evaluable patients). The median duration of response was 7.5 months. Responders had a significantly higher on-treatment frequency of circulating effector CD8<sup>+</sup> T cells. Conclusion- FOR46 demonstrated encouraging preliminary clinical activity with a manageable safety profile. Targeting CD46 elicited an immune priming effect that was associated with clinical outcomes.

**25COASOCT61****Title: Explaining the Relationships Between Age, Endocrine Therapy Persistence, and Risk of Recurrence in Hormone Receptor–Positive Early Breast Cancer: A Nationwide Cohort Study**

Elise Dumas, PhD et.al.

Journal of Clinical Oncology, Volume 43, Number 16

<https://doi.org/10.1200/JCO.24.01131>

**Abstract:** Purpose: Young age is associated with increased risk of recurrence in hormone receptor (HR)–positive early-stage breast cancer (eBC). Lack of adherence to endocrine therapy (ET) is a potential reason for the lower survival proportions observed in younger patients, but the survival benefits of improving adherence to ET in young patients remain unknown. Materials and Methods: Using data from the French National Health Data System and target trial emulation methods, we considered three sustained ET persistence strategies (allowing treatment gaps of no more than 30, 90, or 180 continuous days) and estimated the

5-year disease-free survival (DFS) benefit of sustained ET persistence compared with observed ET persistence. Results: A total of 121,601 patients with HR-positive eBC were included in the analyses, of whom 29.8% was younger than 50 years at diagnosis. Younger patients had lower DFS and were more likely to discontinue ET than older patients. In patients 34 years and younger, strict ET persistence ( $\leq 30$ -day gaps) improved 5-year DFS proportions from 74.5% to 78.8% (4.3 percentage points [95% CI, 2.6 to 7.2]) compared with observed persistence. ET persistence strategies allowing for  $\leq 90$ -day and  $\leq 180$ -day gaps reduced the 5-year DFS benefit in patients 34 years and younger to 1.3 (95% CI, 0.2 to 3.7) and 1.0 (95% CI, -0.2 to 3.4) percentage points, respectively. By contrast, DFS benefits of improved ET persistence in patients after 50 years old did not exceed 1.9 percentage points, compared with observed persistence, regardless of the persistence definition. Conclusion: The survival benefit that could be achieved with strict ET persistence in women 34 years and younger with HR-positive eBC highlights the need for tailored strategies to improve ET persistence in this population.

## 25COASOCT62

### **Title: Endocrine Therapy Omission in Estrogen Receptor–Low (1%-10%) Early-Stage Breast Cancer**

Grace M. Choong et.al.

Journal of Clinical Oncology, Volume 43, Number 16

<https://doi.org/10.1200/JCO-24-02263>

**Abstract:** Purpose: Adjuvant endocrine therapy (ET) improves overall survival (OS) in estrogen receptor (ER)–positive early-stage breast cancer (BC). However, the benefit of ET for those with ER-low BC (ER 1%-10%) is unclear. Methods: Using the National Cancer Database, we studied patients with high-risk stage I to III, ER-low BC (defined as immunohistochemistry 1%-10%) who received (neo)adjuvant chemotherapy and did or did not initiate ET. OS was analyzed with ET initiation as a time-dependent covariate using Cox proportional hazards regression. Results: Of 10,362 patients with stage I to III ER-low BC, 7,018 received chemotherapy and met inclusion criteria. ET omission was 42% at 12 months and more common in patients with tumors that were progesterone receptor–negative, human epidermal growth factor receptor 2–negative, higher-grade (grade 2/3) and higher Ki-67 ( $\geq 20\%$ ; all  $P < .001$ ) and those who received neoadjuvant chemotherapy (NAC;  $P < .001$ ). With a median follow-up of 3 years, 586 deaths were observed. In a multivariable analysis, ET omission was associated with a higher risk of death (hazard ratio [HR], 1.23 [95% CI, 1.04 to 1.46];  $P = .02$ ), with a greater impact in those with higher ER levels: ER 1%-5% (HR, 1.15 [95% CI, 0.91 to 1.45];  $P = .24$ ) versus ER 6%-10% (HR, 1.42 [95% CI, 1.00 to 2.02];  $P = .048$ ). Among patients treated with NAC ( $n = 4,377$ , 62%), ET omission was associated with worse OS in those with residual disease (RD; HR, 1.26 [95% CI, 1.00 to 1.57];  $P = .046$ ) but not in those who achieved a pathologic complete response (HR, 1.06 [95% CI, 0.62 to 1.80];  $P = .84$ ). Conclusion: In ER-low, early-stage BC, ET omission is associated with significantly worse OS, especially in patients with RD after NAC and those with higher (6%-10%) ER levels. Until prospective data are available, patients with ER-low BC should be counseled regarding the potential benefit of ET.



**25COASOCT63****Title: Methotrexate, Doxorubicin, and Cisplatin Versus Methotrexate, Doxorubicin, and Cisplatin + Ifosfamide in Poor Responders to Preoperative Chemotherapy for Newly Diagnosed High-Grade Osteosarcoma (JCOG0905): A Multicenter, Open-Label, Randomized Trial**

Hiroaki Hiraga, PhD et.al.

Journal of Clinical Oncology, Volume 43, Number 16

<https://doi.org/10.1200/JCO-24-01281>

**Abstract:** Purpose: Our previous NEOCO phase II studies on high-grade osteosarcoma suggested that administering ifosfamide (IF; 16 g/m<sup>2</sup> [4g/m<sup>2</sup> once on day 1, then 2g/m<sup>2</sup> once on days 2-7] × six) to patients showing a poor response (PrRsp) to preoperative chemotherapy with methotrexate, doxorubicin, and cisplatin (MAP) improves their prognoses. In this Japan Clinical Oncology Group (JCOG) study, JCOG0905, we aimed to investigate the efficacy and safety of IF in patients with PrRsp. Methods: JCOG0905 is a multicenter, open-label, multi-institutional, randomized trial. Eligible patients (50 years and younger) had resectable, high-grade osteosarcoma (stage II or III, Union for International Cancer Control TNM) of the extremities, limb girdles, and thoracic wall. After two MAP cycles and tumor resection, patients with PrRsp were randomly assigned to either the MAP or MAP plus 15 g/m<sup>2</sup> (3g/m<sup>2</sup> once daily on days 1-5) × six IF (MAP + IF [MAPIF]) group. The primary end point was disease-free survival (DFS); secondary end points were overall survival (OS) and safety. The planned sample size was 100 patients with a one-sided  $\alpha$  of .1 and a power of 0.7, assuming a 3-year DFS of 50% and 65% for MAP and MAPIF, respectively. This trial is registered with the Japan Registry of Clinical Trials (jRCT; jRCTs031180126). Results: Of the 287 patients registered between February 2010 and August 2020, 51 and 52 patients with PrRsp were assigned to the MAP and MAPIF groups, respectively. As of March 2022, DFS did not differ between groups (hazard ratio [HR], 1.05 [95% CI, 0.55 to 1.98]) and OS was numerically inferior in the MAPIF group (HR, 1.48 [95% CI, 0.68 to 3.22]). Nine and zero patients in the MAPIF and MAP groups discontinued treatment because of adverse events, respectively. Conclusion: Evidence from JCOG0905 does not support the addition of IF for patients with PrRsp.

**25COASOCT64****Title: NOTCH1 Mutation and Survival Analysis of Tislelizumab in Advanced or Metastatic Esophageal Squamous Cell Carcinoma: A Biomarker Analysis From the Randomized, Phase III, RATIONALE-302 Trial**

Zhihao Lu, MD et.al.

Journal of Clinical Oncology, Volume 43, Number 16

<https://doi.org/10.1200/JCO-24-01818>

**Abstract:** Purpose: Although multiple agents targeting PD-1 have been approved as second-line treatment for esophageal squamous cell carcinoma (ESCC), only a fraction of patients derive long-term survival. Hence, reliable predictive biomarkers are urgently needed. Methods: Comprehensive tumor genomic profiling and transcriptome sequencing were performed on samples from the RATIONALE-302 study. We also conducted single-cell RNA sequencing analysis on Notch1 knockdown ESCC murine models to further explore the potential molecular mechanisms underlying anti-PD-1 benefit. Results: We identified

NOTCH1 mutation as a potential predictive biomarker for longer overall survival (OS) with tislelizumab versus chemotherapy (18.4 months v 5.3 months; hazard ratio, 0.35 [95% CI, 0.17 to 0.71]). At the transcriptional level, type I IFN (IFN-I)/toll-like receptor expression signatures were positively associated with OS benefit of tislelizumab, whereas B-cell and neutrophil signatures predicted unfavorable OS. Exploratory analyses showed that the presence of NOTCH1 mutation correlated with enrichment of IFN-I signatures and reduced infiltration of B cells and neutrophils. In murine models, comparative single-cell transcriptome analyses further revealed that Notch1 deficiency facilitated a more immunologically activated tumor microenvironment which potentiated anti-PD-1 treatment. Conclusion: Our data provide novel insights for anti-PD-1 treatment selection using NOTCH1 mutations and may provide a rationale for combination therapy in ESCC.

## 25COASOCT65

### **Title: Improved Survival and Prognostication in Melanoma Patients With Brain Metastases: An Update of the Melanoma Graded Prognostic Assessment**

Paul W. Sperduto, MD, et.al.

Journal of Clinical Oncology, Volume 43, Number 16,

<https://doi.org/10.1200/JCO-24-01351>

**Abstract:** Purpose: Survival for patients with melanoma has recently improved. The propensity of melanoma to metastasize to the brain remains a common and serious feature of this disease. The purposes of this study were to evaluate prognostic factors for patients with newly diagnosed melanoma brain metastases (MBMs) in a large cohort treated with modern multimodal therapies, compare those results with those in prior eras, and update the Melanoma Graded Prognostic Assessment (GPA). Methods: Univariable and multivariable (MVA) analyses of prognostic factors and treatments associated with survival were performed on 1,796 patients with newly diagnosed MBM treated between January 01, 2015, and December 31, 2021, using a multi-institutional retrospective database. Multiple imputation was used to address missingness of potential predictors. Significant variables in combined MVA were used to update the Melanoma GPA. Comparisons were made with legacy cohorts. Results: Median survivals for cohorts A (1985-2007, n = 481), B (2006-2015, n = 823), and C (2015-2021, n = 1,796) were 6.7, 9.8, and 16.6 months and median follow-up times were 40.1, 43.6, and 48.8 months, respectively. In combined MVA, significant prognostic factors for survival were higher Karnofsky Performance Status, fewer MBMs, absence of extracranial metastases, lower serum lactate dehydrogenase, and no immunotherapy before MBM. These factors were incorporated into the updated Melanoma GPA. The combined median and 3-year survivals for patients with GPA 0-1, 1.5-2, and 2.5-4.0 were 5.4, 13.2, and 43.2 months and 12.4%, 28.8%, and 51.6%, respectively. Conclusion: Prognostic factors have changed and survival has improved for patients with MBM but varies widely by GPA. The updated Melanoma GPA calculator (BrainMetGPA), available free online, can be used to estimate survival, individualize treatment, stratify clinical trials, guide surveillance, and augment clinical trial eligibility. Multidisciplinary treatment is essential. Trials are needed to elucidate the optimal sequencing of various therapeutic modalities.

**25COASOCT66****Title: Maintenance Chemotherapy in Patients With High-Risk Rhabdomyosarcoma: Long-Term Survival Analysis of the European *Paediatric Soft Tissue Sarcoma Study Group RMS 2005* Trial**Authors: [Gianni Bisogno, MD, PhD](#)Journal of Clinical Oncology, [Volume 43, Number 16](#)<https://doi.org/10.1200/JCO-24-02850>

**Abstract:** The European Paediatric Soft Tissue Sarcoma Study Group (EpSSG) RMS 2005 trial evaluated maintenance chemotherapy in high-risk rhabdomyosarcoma (RMS). Patients were randomly assigned to either discontinue treatment (standard arm) or receive six 28-day cycles of vinorelbine (25 mg/m<sup>2</sup>) once per day on days 1, 8, and 15, plus once daily low-dose cyclophosphamide (25 mg/m<sup>2</sup>; experimental arm). Initial results showed improved overall survival (OS), but disease-free survival (DFS) improvement was not statistically significant. This report presents mature survival outcomes after extended follow-up. Between April 2006 and December 2016, 186 patients were enrolled in the standard arm and 185 in the experimental arm. After a median follow-up of 122.1 months from diagnosis and 114 months from random assignment, recurrence, progression, or death occurred in 103 patients (61 standard arm, 42 experimental arm). The 10-year DFS was 66.5% (95% CI, 59 to 74) in the standard arm versus 77.1% (95% CI, 70.3 to 82.5) in the experimental arm ( $P = .025$ ). Corresponding 10-year OS rates were 70.8% (95% CI, 63.3 to 77.0) and 82.9% (95% CI, 76.6 to 87.7;  $P = .0099$ ). Long-term results of the RMS2005 trial confirm the survival benefit of maintenance chemotherapy with vinorelbine and low-dose cyclophosphamide for patients with high-risk RMS.

**25COASOCT67****Title: Taltrectinib in *ROS1*+ Non-Small Cell Lung Cancer: TRUST**

Maurice Pérol, MD

Journal of Clinical Oncology, [Volume 43, Number 16](#)<https://doi.org/10.1200/JCO-25-00275>

**Abstract:** Purpose-Taltrectinib is an oral, potent, CNS-active, selective, next-generation *ROS1* tyrosine kinase inhibitor (TKI). We report integrated efficacy and safety from registrational taltrectinib studies in *ROS1*+ non-small cell lung cancer. Methods- TRUST-I and TRUST-II were phase II, single-arm, open-label, nonrandomized, multicenter trials. Efficacy outcomes were pooled from TRUST-I and TRUST-II pivotal cohorts. The safety population comprised all patients treated with once-daily oral taltrectinib 600 mg pooled across the taltrectinib clinical program. The primary end point was independent review committee-assessed confirmed objective response rate (cORR). Secondary outcomes included intracranial (IC)-ORR, progression-free survival (PFS), duration of response (DOR), and safety. Results-As of June 7, 2024, the efficacy-evaluable population included 273 patients in TRUST-I and TRUST-II. Among TKI-naïve patients ( $n = 160$ ), the cORR was 88.8% and the IC-cORR was 76.5%; in TKI-pretreated patients ( $n = 113$ ), the cORR was 55.8% and the IC-cORR was 65.6%. In TKI-naïve patients, the median DOR and median PFS were 44.2 and 45.6 months, respectively. In TKI-pretreated patients, the median DOR and median PFS were 16.6 and 9.7 months. The cORR in patients with G2032R mutation was 61.5% (8 of 13). Among 352 patients treated with taltrectinib 600 mg once daily, the most

frequent treatment-emergent adverse events (TEAEs) were GI events (88%) and elevated AST (72%) and ALT (68%); most were grade 1. Neurologic TEAEs were infrequent (dizziness, 21%; dysgeusia, 15%) and mostly grade 1. TEAEs leading to discontinuations (6.5%) were low. Conclusion-Taletrectinib showed a high response rate with durable responses, robust IC activity, prolonged PFS, favorable safety, and low rates of neurologic adverse events in TKI-naïve and pretreated patients.

## 25COASOCT68

### **Title: Novel Postneoadjuvant Prognostic Breast Cancer Staging System**

David J. Winchester, MD

Journal of Clinical Oncology, Volume 43, Number 17

<https://doi.org/10.1200/JCO-24-01739>

**Abstract:** Purpose-Prognostic staging after neoadjuvant chemotherapy (NACT) is not included in American Joint Commission on Cancer (AJCC) staging. This study addressed this deficiency by including responses to therapy with standardized staging variables in a validated prognostic staging system for patients treated with NACT. Methods-The National Cancer Database was queried to identify 140,605 patients treated with NACT between 2010 and 2018. Three response categories (no response, partial response, and complete response [pCR]) were created on the basis of comparison of clinical and post-NACT pathologic staging. Univariate and multivariate analyses of clinical stage, estrogen receptor, progesterone receptor, human epidermal growth factor receptor 2 (HER2), and grade were analyzed for each category. Predictive models for each response category were validated using the bootstrap technique. Calibration plots compared predicted and observed 3-year survival probabilities in the training and validation data sets. Results-Each validated model demonstrated statistically significant survival differences in the postneoadjuvant prognostic stage assignment. Of all patients with a pCR, 94.2% were assigned to postneoadjuvant ypStage I compared with 35.5% of patients with no response. Advancing clinical stage had a progressive but small impact on overall survival (OS) with pCR (high-grade, triple-negative breast cancer [TNBC]: cStage I, 97% v cStage IIIB/IIIC, 91%; grade 2 luminal A: 97% v 91%) but was associated with a profound decrease in OS with no response for TNBC or HER2+ disease (high-grade TNBC 89% v 50%) and less profound for grade 2 luminal A disease with no response (97% v 81%). Conclusion-We present a novel, validated prognostic staging system that predicts OS according to the response to NACT. These data will provide AJCC stage assignments for a growing proportion of patients treated with NACT.

## 25COASOCT69

### **Title: Hematopoietic Stem Cell Transplantation Outcomes for High-Risk AML: A Report From the Children's Oncology Group**

Benjamin J. Huang, MD

Journal of Clinical Oncology, Volume 43, Number 17

<https://doi.org/10.1200/JCO-24-01841>

**Abstract:** Purpose-Hematopoietic stem cell transplantation (HSCT) is used as consolidation for pediatric patients with high-risk AML in first complete remission (CR1). The definition of high-risk AML has evolved considerably over the past two decades with the successive identification of new unfavorable risk factors. We conducted a cross-study analysis to

determine whether HSCT improves the outcomes of patients with contemporarily defined high-risk AML. **Methods-** We combined data from AAML0531 and AAML1031, the last two phase III clinical trials completed by the Children's Oncology Group (COG). These two trials established the prognostic importance of measurable residual disease (MRD) and several high-risk cryptic cytogenetic/molecular (CM) alterations, which were applied to reclassify patients in the current COG phase III clinical trial, AAML1831. We compared the outcomes after HSCT in CR1 with those after chemotherapy alone in CR1 in the redefined high-risk group. **Results-** Our study cohort comprised 463 patients with high-risk CM alterations and 72 patients with standard-risk (SR) CM results with positive MRD at end of induction I. In all, 33.9% and 45.8% of these groups underwent HSCT in CR1, respectively. HSCT was associated with decreased relapse and improved disease-free survival (DFS) in both groups. In the high-risk CM group, 5-year DFS was 26.0% (95% CI, 20.6 to 31.6) and 49.8% (95% CI, 41.7 to 57.4;  $P < .001$ ) in patients receiving chemotherapy alone and HSCT, respectively. In the SR CM and MRD+ groups, DFS was 16.9% (95% CI, 4.3 to 36.7) compared with 50.9% (95% CI, 32.7 to 66.5;  $P = .032$ ). HSCT was also associated with improvement in outcomes based on multivariable analysis and across subgroups defined by clinical trial and by high-risk CM subtype, with the exception of chromosome 7 or 5 loss. **Conclusion-** HSCT was associated with improved outcomes in pediatric patients with contemporarily defined high-risk AML.

## 25COASOCT70

### **Title: Toxicity Within 6 Months of Heterogeneous Fluorodeoxyglucose-Guided Radiotherapy Dose Escalation for Locally Advanced Non–Small Cell Lung Cancer in the Scandinavian Randomized Phase III NARLAL2 Trial**

Tine Schytte, PhD et.al.

Journal of Clinical Oncology, Volume 43, Number 17

<https://doi.org/10.1200/JCO-24-01386>

**Abstract:** Purpose-Radiation dose escalation for locally advanced non–small cell lung cancer (LA-NSCLC) has been challenged by toxicity concerns. The Scandinavian phase III multicenter dose-escalation trial NARLAL2 (ClinicalTrials.gov identifier: [NCT02354274](https://clinicaltrials.gov/ct2/show/study/NCT02354274)) used a novel approach to dose escalation: heterogeneous escalation driven by the fluorodeoxyglucose positron emission tomography–avid region, with strict normal tissue dose constraints. We report early toxicity within 6 months of random assignment. **Materials and Methods-** Patients were recruited from seven institutions in Scandinavia. Eligibility criteria included performance status 0-1, NSCLC stage IIB-IIIB, and feasibility of delivering 66 Gy/33 fraction treatment plan. Patients were randomly assigned between standard (66 Gy) and heterogeneously dose-escalated radiotherapy. Two treatment plans were made for each patient before random assignment with matched mean lung dose and  $V_{20Gy}$ , and strict dose constraints for all normal tissues. Toxicity was evaluated weekly during radiotherapy, and every 3 months after random assignment. Concurrent chemotherapy was cisplatin/carboplatin and vinorelbine. **Results-** Between January 2015 and March 2023, 350 patients were randomly assigned. The as-treated analysis included 178 patients in the standard and 172 in dose-escalated (mean tumor dose 88 Gy) arms. Median gross tumor and planning target volumes were, respectively, 54 cm<sup>3</sup> and 321 cm<sup>3</sup> (standard arm) and 61 cm<sup>3</sup> and 339 cm<sup>3</sup> (escalated arm). No difference in early toxicity between the two arms was observed. Grade 2 esophagitis



during radiotherapy was 28.1% and 25.6%, grade 3 esophagitis 7.3% and 4.1%, grade 2 pneumonitis 15.7% and 20.3%, and grade 3 pneumonitis 3.9% and 5.8% in standard and escalated arms, respectively. For both arms, the maximum grade of early toxicity aggregated over all toxicities was 35% and 1% for grades  $\geq 3$  and 5, respectively. Four patients died from potential treatment-related toxicity. Conclusion-Heterogeneous dose escalation did not increase early toxicity despite delivery of 88 Gy mean dose to the primary tumor, demonstrating this as an attractive strategy for LA-NSCLC radiotherapy dose escalation.

## 25COASOCT71

**Title: Neoadjuvant FOLF(IRIN)OX Chemotherapy for Resectable Pancreatic Adenocarcinoma: A Multicenter Randomized Noncomparative Phase II Trial (PANACHE01 FRENCH08 PRODIGE48 study)**

Lilian Schwarz, PhD et.al.

Journal of Clinical Oncology, Volume 43, Number 17

<https://doi.org/10.1200/JCO-24-01378>

**Abstract:** Purpose-Despite limited RCTs, neoadjuvant chemotherapy (NAC) shows promise for resectable pancreatic adenocarcinoma (rPAC). Few prospective results are available on completing the full therapeutic sequence and oncologic outcomes with NAC. Methods-The PANACHE01-PRODIGE48 phase II trial randomly assigned 153 patients with rPAC (2:2:1) to four cycles of NAC (modified leucovorin, fluorouracil, irinotecan, and oxaliplatin [mFOLFIRINOX], arm 1; leucovorin, fluorouracil, and oxaliplatin [FOLFOX], arm 2) or up-front surgery (control) across 28 French centers (February 2017-July 2020). The primary objective was to evaluate the feasibility and efficacy of these NAC regimens. Two binary primary end points included 1-year overall survival (OS) postrandomization and the rate of patients completing the full therapeutic sequence. Event-free survival (EFS) assessed time to failure, defined as progression before surgery, unresectable/metastatic disease at surgery, recurrence, or death. Results- The primary objective was achieved for arm 1. In the intention-to-treat population, 70.8% (90% CI, 60.8 to 79.6) and 68% (90% CI, 55.5 to 78.8) completed the therapeutic sequence in arm 1 and arm 2, respectively. Within 12 months postrandomization, 84.3% (90% CI, 75.3 to 90.9) and 71.4% (90% CI, 59.0 to 81.8) of the patients were alive in arm 1 and arm 2, respectively. Treatment was safe and well-tolerated in both NAC arms. Arm 2 was stopped after interim analysis for lack of efficacy ( $H_0$  rejection for 1-year OS). One-year EFS rates were 51.4% (95% CI, 41.0 to 64.3), 43.1% (95% CI, 31.3 to 59.5), and 38.7% (95% CI, 24.1 to 62.0) in arm 1, arm 2, and control arm, respectively. Conclusion- The feasibility and efficacy of mFOLFIRINOX in the perioperative setting are confirmed concerning therapeutic sequence completion and oncologic outcomes, supporting ongoing trials (PREOPANC3, Alliance AO21806). Further research is needed to identify patients who benefit from NAC (ClinicalTrials.gov identifier: [NCT02959879](https://clinicaltrials.gov/ct2/show/study/NCT02959879); EudraCT: 2015-001851-65).

## 25COASOCT72

**Title: Sequential Infusion of Mesenchymal Stem Cell for Graft-Versus-Host Disease Prevention in Haploidentical Hematopoietic Stem Cell Transplantation: An Open-Label, Multicenter, Randomized Controlled Clinical Trial**

Han Yao, MD, PhD

Journal of Clinical Oncology, Volume 43, Number 17

<https://doi.org/10.1200/JCO-24-02119>

**Abstract:** Purpose-The aim of this open-label, multicenter, randomized controlled trial was to determine the efficacy and safety of sequential umbilical cord-derived mesenchymal stem cell (UC-MSC) infusion for graft-versus-host disease (GVHD) prevention within 3 months of haploidentical hematopoietic stem cell transplantation (haplo-HSCT). Methods-This open-label study evaluated UC-MSC infusion (administer  $1 \times 10^6/\text{kg}$  4 hours before the commencement of day 0, once weekly for the first month after transplantation, once every 2 weeks for the second month, and once during the third month, totaling eight doses). The primary end point was the 2-year cumulative incidence of severe chronic GVHD (cGVHD). Results- In the primary analysis, 192 qualified participants between age 18 and 60 years with haplo-HSCT in three transplant centers in China were enrolled and randomly assigned to the MSC and control groups. In the primary analysis, the estimated 2-year cumulative incidence of severe cGVHD and all grades of cGVHD was lower in the MSC group than in the control group ( $P = .033$  and  $P = .022$ ). The cumulative incidence of grade 1 to 4, 2 to 4, and 3 to 4 acute GVHD (aGVHD) in patients in the MSC group significantly decreased (all  $P < .001$ ). The 3-year GVHD-free and relapse-free survival (GRFS) rate in the MSC group was 62.4%, which was significantly higher than that in the control group (32.0%, hazard ratio [HR], 0.34,  $P < .001$ ). MSC infusion did not influence the cumulative incidence of relapse ( $P = .34$ ) and nonrelapse mortality ( $P = .45$ ). Conclusion-Our findings suggest that sequential infusion of MSCs within 3 months after haplo-HSCT significantly reduced both the incidence and severity of cGVHD and aGVHD, manifesting as a better GRFS rate for patients.

## 25COASOCT73

**Title: Efficacy and Safety of Anti-B-Cell Maturation Antigen Chimeric Antigen Receptor T-Cell for the Treatment of Relapsed and Refractory AL Amyloidosis**

Eyal Lebel, MD

Journal of Clinical Oncology, Volume 43, Number 17

<https://doi.org/10.1200/JCO-24-02252>

**Abstract:** Purpose-The use of anti-B-cell maturation antigen (BCMA) chimeric antigen receptor T-cell (CART) therapy for AL amyloidosis (AL) is limited owing to patient frailty. HBI0101 anti-BCMA CART was the first proof of concept for its applicability to AL. This report addresses the AL patient cohort treated to date within the phase Ia/Ib clinical trial. Methods-After lymphodepletion, most AL patients were infused with  $800 \times 10^6$  CARTs. Results- Sixteen patients were treated, with a median of four previous lines of therapy (range, 3-10), 14/16 were triple class refractory, and 6/16 were refractory to belantamab. Most patients (13/16) had cardiac involvement, including five with MAYO stage IIIa/IIIb at study entry. Cytokine release syndrome was frequent (14/16) but mostly low grade (grade 3: 3/16, no grade 4/5). No neurologic toxicity or treatment-related deaths were observed. There were five grade 3 AL-related organ deteriorations resolved quickly with supportive care. The overall hematologic response rate was 15/16 (94%) and complete response (CR) was 12/16 (75%). Minimal residual disease negativity was achieved in 9/14 evaluable patients. Most patients (8/13 evaluable) achieved an objective organ response. Seven patients died during long-term follow-up, three while in CR/very good partial response, and the median overall survival was 10.1 months (95% CI, 5.8 to not reached). Conclusion-This largest clinical trial

of AL patients treated with anti-BCMA CART demonstrates acceptable and manageable toxicity in a highly frail and resistant population with remarkable efficacy, leading to fast organ responses. Among patients with baseline advanced cardiac disease, deaths in the first year were frequent, suggesting that this effective therapy should be considered earlier in the course of therapy. Anti-BCMA CART may become a powerful tool for improving organ function and survival in patients with AL.

## 25COASOCT74

**Title:** IFN- $\gamma$  promotes the progression of iMCD by activating inflammatory monocytes

Xuejiao Yin et.al.

*Blood* (2025) 146 (1): 76–88.

<https://doi.org/10.1182/blood.2024027689>

**Abstract:** A deeper understanding of the immune landscape in patients with idiopathic multicentric Castleman disease (iMCD) is essential to establish early prognostic stratification and uncover novel therapeutic targets. We used single-cell RNA sequencing of peripheral blood mononuclear cells (PBMCs) from a cohort of 15 patients with iMCD and 4 healthy controls. To explore the sources of interleukin-6 (IL-6), we included lymph node and bone marrow samples for comparison with PBMCs. Our results indicate that IL-6 primarily originates from the lymph nodes, particularly from activated B cells. Similarly, in peripheral blood, activated B cells are also the main source of IL-6. IL-6 receptor is primarily expressed in monocytes in PBMCs, with CCL monocytes showing the strongest activation of the IL-6 signaling pathway. This suggests that CCL monocytes in iMCD may play an important role in driving peripheral inflammatory storms. CellChat analysis reveals that during disease flares, CCL monocytes interact with specific natural killer (NK)/NKT cells through enhanced type II interferon (IFN-II) signaling, whereas this interaction significantly diminishes during remission, indicating a significant role for IFN-II in the pathogenesis of iMCD. Notably, serum IFN- $\gamma$  levels positively correlate with both disease severity and treatment resistance, a finding validated by a large independent iMCD cohort. Our findings confirm that the IL-6 pathway remains central to iMCD pathogenesis and highlight a significant role for IFN-II pathway activation in amplifying inflammatory storms. Our findings provide valuable biomarkers for assessing disease severity and identify new therapeutic targets for iMCD.

## 25COASOCT75

**Title:** Large-scale dependency and drug screens to characterize the therapeutic vulnerabilities of multiple myeloma with 1q+

Romanos Sklavenitis-Pistofidis et.al.

*Blood* (2025) 146 (1): 89–103.

<https://doi.org/10.1182/blood.2024025102>

**Abstract:** The development of targeted therapy for patients with multiple myeloma (MM) is hampered by the low frequency of actionable genetic abnormalities. Gain or amplification of chromosome 1q (1q+) is the most frequent arm-level copy number gain in patients with MM and is associated with higher risk of progression and death despite recent therapeutic advances. Thus, developing targeted therapy for patients with MM with 1q+ stands to benefit a large portion of patients in need of more effective management. Here, we used large-scale dependency screens and drug screens to systematically characterize the therapeutic

vulnerabilities of MM with 1q+ and displayed increased sensitivity to myeloid cell leukemia-1 (MCL1) and phosphatidyl inositol 3-kinase (PI3K) inhibitors. Using single-cell RNA sequencing, we compared subclones with and without 1q+ within the same patient tumors and demonstrated that 1q+ is associated with higher levels of *MCL1* and the PI3K pathway. Furthermore, by isolating isogenic clones with different copy number profiles for part of the chromosome 1q arm, we observed increased sensitivity to MCL1 and PI3K inhibitors with arm-level gain. Lastly, we demonstrated synergy between MCL1 and PI3K inhibitors and dissected their mechanism of action in MM with 1q+, uncovering a cytostatic effect. In conclusion, this study highlights that MM with 1q+ may present enhanced sensitivity to MCL1 and PI3K inhibitors, enabling their use at lower doses without sacrificing efficacy, and may thus accelerate the development of targeted therapy for patients with MM and 1q+.

## 25COASOCT76

**Title: Cell-autonomous dysregulation of interferon signaling drives clonal expansion of *SRSF2*-mutant MDS stem/progenitor cells**

Kouhei Takashima

*Blood* (2025) 146 (1): 115–122.

<https://doi.org/10.1182/blood.2024025670>

**Abstract:** Myelodysplastic syndromes (MDSs) are myeloid malignancies often driven by mutations in genes encoding splicing factors (SFs). How these mutations drive the clonal expansion of MDS stem/progenitor cells to outcompete normal hematopoietic stem/progenitor cells (HSPCs) remains unexplained. Although a role for inflammatory processes in promoting clonal expansion of mutant HSPCs and MDS pathogenesis has been proposed, the specific mechanisms implicated remain incompletely understood. In this study, using human isogenic induced pluripotent stem cell–based models of *SRSF2*-mutant MDS and primary cells from patients with MDS, we show that the *SRSF2* P95L mutation downregulates basal STAT1 expression. STAT1 downregulation dampens interferon (IFN) signaling in MDS stem/progenitor cells, which, unlike normal HSPCs, show resistance to the suppression of clonogenic ability by IFNs. Treatment with the proteasome inhibitor bortezomib increased STAT1 protein levels and restored the sensitivity of *SRSF2*-mutant cells to inflammatory stimuli. These results indicate that rewiring of STAT1 signaling by *SRSF2* mutations blunts responsiveness to IFNs, conferring clonal fitness to *SRSF2*-mutant HSPCs against normal HSPCs in the presence of inflammatory stimuli. Our study provides a novel mechanistic link between SF mutations and inflammatory dysregulation and suggests proteasome inhibition as a potential strategy to treat MDS with *SRSF2* mutations.

## 25COASOCT77

**Title: Outcomes in patients with *ETV6::RUNX1* or high-hyperdiploid B-ALL treated in the St. Jude Total Therapy XV/XVI studies**

Katelyn Purvis et.al.

*Blood* (2025) 145 (2): 190–201.

<https://doi.org/10.1182/blood.2024024936>

**Abstract:** Children with *ETV6::RUNX1* or high-hyperdiploid B-cell acute lymphoblastic leukemia (B-ALL) have favorable outcomes. The St. Jude (SJ) classification considers these patients low risk, regardless of their National Cancer Institute (NCI) risk classification,

except when there is slow minimal residual disease (MRD) response or central nervous system/testicular involvement. We analyzed outcomes in children (aged 1-18.99 years) with these genotypes in the SJ Total XV/XVI studies (2000-2017). Patients with *ETV6::RUNX1* (n = 222) or high-hyperdiploid (n = 296) B-ALL had 5-year event-free survival (EFS) of  $97.7\% \pm 1.1\%$  and  $94.7\% \pm 1.4\%$ , respectively. For *ETV6::RUNX1*, EFS was comparable between NCI standard-risk and high-risk patients and between SJ low-risk and standard-risk patients. Of the 40 NCI high-risk patients, 37 who received SJ low-risk therapy had excellent EFS ( $97.3\% \pm 2.8\%$ ). For high-hyperdiploid B-ALL, NCI high-risk patients had worse EFS than standard-risk patients ( $87.6\% \pm 4.5\%$  vs  $96.4\% \pm 1.3\%$ ;  $P = .016$ ). EFS was similar for NCI standard-risk and high-risk patients classified as SJ low risk ( $96.0\% \pm 1.5\%$  and  $96.9\% \pm 3.2\%$ ;  $P = .719$ ). However, EFS was worse for NCI high-risk patients than for NCI standard-risk patients receiving SJ standard/high-risk therapy ( $77.4\% \pm 8.2\%$  vs  $98.0\% \pm 2.2\%$ ;  $P = .004$ ). NCI high-risk patients with *ETV6::RUNX1* or high-hyperdiploid B-ALL who received SJ low-risk therapy had lower incidences of thrombosis ( $P = .013$ ) and pancreatitis ( $P = .011$ ) than those who received SJ standard/high-risk therapy. MRD-directed therapy yielded excellent outcomes, except for NCI high-risk high-hyperdiploid B-ALL patients with slow MRD response, who require new treatment approaches. Among NCI high-risk patients, 93% with *ETV6::RUNX1* and 54% with high-hyperdiploid B-ALL experienced excellent outcomes with a low-intensity regimen.

## 25COASOCT78

**Title:** Single-cell analysis of the multiple myeloma microenvironment after  $\gamma$ -secretase inhibition and CAR T-cell therapy

David G. Coffey

*Blood* (2025) 145 (2): 220–233.

<https://doi.org/10.1182/blood.2024025231>

**Abstract:** Chimeric antigen receptor (CAR) T cells and bispecific antibodies targeting B-cell maturation antigen (BCMA) have significantly advanced the treatment of relapsed and refractory multiple myeloma. Resistance to BCMA-targeting therapies, nonetheless, remains a significant challenge. BCMA shedding by  $\gamma$ -secretase is a known resistance mechanism, and preclinical studies suggest that inhibition may improve anti-BCMA therapy. Leveraging a phase 1 clinical trial of the  $\gamma$ -secretase inhibitor (GSI), crenigacestat, with anti-BCMA CAR T cells (FCARH143), we used single-nuclei RNA sequencing and assay for transposase-accessible chromatin sequencing to characterize the effects of GSI on the tumor microenvironment. The most significant impacts of GSI involved effects on monocytes, which are known to promote tumor growth. In addition to observing a reduction in the frequency of nonclassical monocytes, we also detected significant changes in gene expression, chromatin accessibility, and inferred cell-cell interactions after exposure to GSI. Although many genes with altered expression are associated with  $\gamma$ -secretase-dependent signaling, such as Notch, other pathways were affected, indicating GSI has far-reaching effects. Finally, we detected monoallelic deletion of the BCMA locus in some patients with prior exposure to anti-BCMA therapy, which significantly correlated with reduced progression-free survival (PFS; median PFS, 57 vs 861 days). GSIs are being explored in combination with the full spectrum of BCMA-targeting agents, and our results reveal



widespread effects of GSI on both tumor and immune cell populations, providing insight into mechanisms for enhancing BCMA-directed therapies.

## 25COASOCT79

**Title:** Acute promyelocytic leukemia: long-term outcomes from the HARMONY project  
Maria Teresa Voso et.al.

*Blood* (2025) 145 (2): 234–243.

<https://doi.org/10.1182/blood.2024026186>

**Abstract:** Treatment outcomes for acute promyelocytic leukemia (APL) have improved with the widespread use of targeted therapy with all-*trans* retinoic acid (ATRA) and arsenic trioxide (ATO). Our study aimed to validate these data in a large patient cohort, and to redefine prognostic factors. Leveraging the HARMONY Platform, we analyzed 1438 newly diagnosed patients with APL, diagnosed between 1999 and 2022. Patient data derived from the 2 international multicenter Gruppo Italiano Malattie EMatologiche dell'Adulto (GIMEMA)-APL0406 and National Cancer Research Institute (NCRI)-AML17 trials and 4 European registries: the Haemato Oncology Foundation for Adults in the Netherlands, Belgium and Luxembourg (HOVON), AML Study Group (AMLSG), Swedish AML Registry, and Study Alliance Leukemia (SAL). The study cohort included 721 males and 717 females, with a median age of 50.5 years (range, 16-94 years). Of 1309 patients starting therapy, 562 received ATRA-ATO, and 747 idarubicin-based chemotherapy (AIDA-like CHT). Early death (ED) occurred in 85 of 1438 patients (5.9%) at a median of 9 days after APL diagnosis and was independently associated with increasing age and high Sanz risk score (odds ratio [OR], 1.06; 95% confidence interval [CI], 1.04-1.08; and OR, 4.65; 95% CI, 2.55-8.51, respectively). The median follow-up was 5.5 years (interquartile range, 3.2-7.5 years). ATRA-ATO regimen was associated with the best outcome, reaching 91% 7-year overall survival (vs 81% for AIDA-like CHT; hazard ratio [HR], 2.14; 95% CI, 1.51-3.05), 89% event-free survival (vs 71% for AIDA-like CHT; HR, 2.72; 95% CI, 2.01–3.69), and 3% relapse (vs 13% for AIDA-like CHT; HR, 4.19; 95% CI, 2.38-7.39;  $P < .001$  for all outcomes). The survival advantage of ATRA/ATO was independent of patients' age, Sanz risk score, and treatment scenario. Our study confirms the superiority of ATRA-ATO over ATRA-chemotherapy in patients with APL. Reducing the risk of ED still represents an unmet medical need, in particular in older patients and in high-risk APL.

## 25COASOCT80

**Title:** Ruxolitinib combined with dexamethasone for adult patients with newly diagnosed hemophagocytic lymphohistiocytosis in China

De Zhou et.al.

*Blood* (2025) 146 (3): 318–327.

<https://doi.org/10.1182/blood.2024026139>

**Abstract:** Hemophagocytic lymphohistiocytosis (HLH) is a severe hyperinflammatory syndrome, and the overall survival (OS) of adult patients is poor. Ruxolitinib, a Janus kinase 1/2 (JAK1/2) inhibitor, has shown promise in treating HLH and exerts synergistic effects when combined with dexamethasone. Our pilot study preliminarily demonstrated that the combination of ruxolitinib and dexamethasone (Ru-D regimen) had a high response rate and led to favorable short-term survival outcomes in adult patients with HLH. In this prospective

phase 2 clinical trial, we propose the Ru-D regimen as a first-line treatment for adults newly diagnosed as having HLH with unknown triggers. A total of 28 Chinese patients were enrolled, and the median follow-up time was 25.1 months (range, 0.87-34.0). The 2-month OS rate (the primary end point) was 85.7%, which exceeded our expected 2-month OS rate of 75%. The 6-month and 2-year OS rates were 67.9% (19/28) and 53.6% (15/28), respectively. The median OS of patients with lymphoma-associated HLH (LAHS) was 5.8 months, and most of these patients had natural killer/T-cell lymphoma. In contrast, the 2-year OS rate of patients without LAHS was 75%. The overall response rate was 85.7% (24/28); of 28 patients, 5 (17.9%) achieved a complete response during the Ru-D regimen. Overall, the Ru-D regimen was well tolerated in patients with HLH. This study demonstrates the efficacy and safety of the Ru-D regimen in adults newly diagnosed as having HLH with unknown triggers and warrants a phase 3 randomized controlled study.

### 25COASOCT81

**Title: An unbiased genomewide screen uncovers 7 genes that drive hematopoietic stem cell fate from mouse embryonic stem cells**

Luis G. Palma

*Blood* (2025) 146 (3): 328–340.

<https://doi.org/10.1182/blood.2024027742>

**Abstract:** Hematopoietic stem cells (HSCs) possess the ability to long term reconstitute all the blood lineages and generate all blood cell types. As such, the in vitro generation of HSCs remains a central goal in regenerative medicine. Despite many efforts and recent advancements in the field, there is still no robust, reproducible, and efficient protocol for generating bona fide HSCs in vitro. This suggests that certain regulatory elements have yet to be uncovered. Here, we present a novel and unbiased approach to identifying endogenous components to specify HSCs from pluripotent stem cells. We performed a genomewide CRISPR activator screening during mesodermal differentiation from mouse embryonic stem cells. After in vitro differentiation, mesodermal KDR<sup>+</sup> precursors were transplanted into primary and secondary immunodeficient NSG mice. This approach led to the identification of 7 genes (*Spata2*, *Aass*, *Dctd*, *Eif4enifl*, *Gucal1a*, *Eya2*, and *Net1*) that, when activated during mesoderm specification, induce the generation of hematopoietic stem and progenitor cells. These cells are capable of serial engraftment and multilineage output (erythroid, myeloid, and T and B lymphoid) in vivo. Single-cell RNA sequencing further revealed that activating these 7 genes biases the embryoid bodies toward intraembryonic development, instead of extraembryonic, increasing the number of mesodermal progenitors that can generate HSCs. Our findings underscore the importance of differentiation during the first germ layer specification to generate definitive blood stem cells.

### 25COASOCT82

**Title: Ruxolitinib combined with dexamethasone for adult patients with newly diagnosed hemophagocytic lymphohistiocytosis in China**

De Zhou et.al.

*Blood* (2025) 146 (3): 318–327.

<https://doi.org/10.1182/blood.2024026139>

**Abstract:** Hemophagocytic lymphohistiocytosis (HLH) is a severe hyperinflammatory syndrome, and the overall survival (OS) of adult patients is poor. Ruxolitinib, a Janus kinase 1/2 (JAK1/2) inhibitor, has shown promise in treating HLH and exerts synergistic effects when combined with dexamethasone. Our pilot study preliminarily demonstrated that the combination of ruxolitinib and dexamethasone (Ru-D regimen) had a high response rate and led to favorable short-term survival outcomes in adult patients with HLH. In this prospective phase 2 clinical trial, we propose the Ru-D regimen as a first-line treatment for adults newly diagnosed as having HLH with unknown triggers. A total of 28 Chinese patients were enrolled, and the median follow-up time was 25.1 months (range, 0.87-34.0). The 2-month OS rate (the primary end point) was 85.7%, which exceeded our expected 2-month OS rate of 75%. The 6-month and 2-year OS rates were 67.9% (19/28) and 53.6% (15/28), respectively. The median OS of patients with lymphoma-associated HLH (LAHS) was 5.8 months, and most of these patients had natural killer/T-cell lymphoma. In contrast, the 2-year OS rate of patients without LAHS was 75%. The overall response rate was 85.7% (24/28); of 28 patients, 5 (17.9%) achieved a complete response during the Ru-D regimen. Overall, the Ru-D regimen was well tolerated in patients with HLH. This study demonstrates the efficacy and safety of the Ru-D regimen in adults newly diagnosed as having HLH with unknown triggers and warrants a phase 3 randomized controlled study.

## 25COASOCT83

**Title:** An unbiased genomewide screen uncovers 7 genes that drive hematopoietic stem cell fate from mouse embryonic stem cells

Luis G. Palma

*Blood* (2025) 146 (3): 328–340.

<https://doi.org/10.1182/blood.2024027742>

**Abstract:** Hematopoietic stem cells (HSCs) possess the ability to long term reconstitute all the blood lineages and generate all blood cell types. As such, the in vitro generation of HSCs remains a central goal in regenerative medicine. Despite many efforts and recent advancements in the field, there is still no robust, reproducible, and efficient protocol for generating bona fide HSCs in vitro. This suggests that certain regulatory elements have yet to be uncovered. Here, we present a novel and unbiased approach to identifying endogenous components to specify HSCs from pluripotent stem cells. We performed a genomewide CRISPR activator screening during mesodermal differentiation from mouse embryonic stem cells. After in vitro differentiation, mesodermal KDR<sup>+</sup> precursors were transplanted into primary and secondary immunodeficient NSG mice. This approach led to the identification of 7 genes (*Spata2*, *Aass*, *Dctd*, *Eif4enifl*, *Gucal1a*, *Eya2*, and *Net1*) that, when activated during mesoderm specification, induce the generation of hematopoietic stem and progenitor cells. These cells are capable of serial engraftment and multilineage output (erythroid, myeloid, and T and B lymphoid) in vivo. Single-cell RNA sequencing further revealed that activating these 7 genes biases the embryoid bodies toward intraembryonic development, instead of extraembryonic, increasing the number of mesodermal progenitors that can generate HSCs. Our findings underscore the importance of differentiation during the first germ layer specification to generate definitive blood stem cells.

**25COASOCT84**

**Title: Clinical phenotype and pathophysiological mechanisms underlying qualitative low VWF**

Ferdows Atiq et.al.

*Blood* (2025) 146 (3): 369–381.

<https://doi.org/10.1182/blood.2024028035>

**Abstract:** Previous reports have highlighted that some patients with low von Willebrand factor (VWF) with significant bleeding were diagnosed based on an isolated but persistent reduction in plasma VWF activity levels in the 30 to 50 IU/dL range. These patients had plasma VWF antigen (VWF:Ag) levels >50 IU/dL and thus had qualitative low VWF (low VWF–QL) rather than quantitative low VWF. Although the clinical importance of functional VWF defects in type 2 von Willebrand disease (VWD) is well recognized, the translational implications of mild functional defects in patients with low VWF–QL have not been defined. To address this clinically important question, we combined low VWF data sets from the low VWF in Ireland cohort and the low VWF in Erasmus MC studies. Overall, we observed that low VWF–QL was common and accounted for ~50% of our combined low VWF cohort. Importantly, our findings demonstrated that many of these patients with mild isolated functional VWF defects in the 30 to 50 IU/dL range had significant bleeding phenotypes, although their plasma VWF:Ag levels were within the normal range. In addition, we further showed that low VWF–QL is a distinct clinicopathological entity compared to type 2 VWD. Finally, our studies highlighted that low VWF–QL is predominantly caused by abnormalities in VWF biosynthesis within endothelial cells that are occurring largely independent of identifiable pathological *VWF* sequence variants. Cumulatively, these novel observations have important clinical implications for the diagnosis and management of patients with mild functional VWF defects.

**25COASOCT85**

**Title: Platelet NLRP6 protects against microvascular thrombosis in sepsis**

Huimin Jiang et.al.

*Blood* (2025) 146 (3): 382–395.

<https://doi.org/10.1182/blood.2025028739>

**Abstract:** Sepsis is characterized by a systemic inflammation and microvascular thrombosis induced by infection. The nucleotide-oligomerization domain–like receptor family pyrin domain containing 6 protein (NLRP6) possesses both proinflammatory and anti-inflammatory abilities with cell type–specific or tissue-specific functions. However, the role of cell type–specific NLRP6 in sepsis remains poorly understood. In this study, we detected NLRP6 expression in platelets. By using platelet-specific NLRP6 knockout mice and the cecal ligation and puncture model of sepsis, we demonstrated that deletion of platelet NLRP6 increased the mortality; enhanced microvascular thrombosis in the lung and liver; and promoted platelet activation, platelet-neutrophil interactions, as well as the neutrophil extracellular trap (NET) formation after sepsis. Platelet function analysis in vitro showed that deletion of NLRP6 enhanced platelet aggregation, activation, and granules release. In addition, NLRP6 deletion promoted platelet NF-κB signaling via sustaining transforming growth factor-β activated kinase 1–binding protein 1 (TAB1) expression independent of the inflammasome. Moreover, inhibition of NF-κB signaling abolished the aggravated effects of

the absence of platelet NLRP6 on the intravascular microthrombosis and NET formation in sepsis and increased the overall survival. Mechanistically, NLRP6 facilitated the interaction between tripartite motif-containing protein 21 (TRIM21) and TAB1 in activated platelets, resulting in K48-linked polyubiquitination of TAB1 and subsequent degradation. Finally, sepsis plasma triggered TAB1 degradation mediated by NLRP6/TRIM21 in normal healthy platelets through toll-like receptor 4/myeloid differentiation primary response 88. Our study identifies a novel protective role of platelet NLRP6 in microvascular thrombosis during sepsis, implying it as a novel target for the treatment of sepsis.

## 25COASOCT86

**Title: Itacitinib for the prevention of IEC therapy-associated CRS: results from the 2-part phase 2 INCB 39110-211 study**

Matthew J. Frigault et.al.

*Blood* (2025) 146 (4): 422–436.

<https://doi.org/10.1182/blood.2024026586>

**Abstract:** Cytokine release syndrome (CRS) and immune effector cell (IEC)-associated neurotoxicity syndrome (ICANS) are common complications after IEC therapy for hematologic malignancies. This 2-part phase 2 study (INCB 39110-211) investigated the safety and efficacy of itacitinib, a potent, highly selective Janus kinase 1 inhibitor with broad anti-inflammatory activity, for the prevention of CRS and ICANS in patients who received commercial CD19-directed IEC therapy. Patients in part 1 received 200 mg itacitinib once daily 3 days before IEC therapy (axicabtagene ciloleucel [axi-cel], brexucabtagene autoleucel, or tisagenlecleucel) through day 26 with guidelines for use of other CRS/ICANS interventions. In part 2 (double-blind), patients were randomized to receive 200 mg itacitinib twice daily or placebo 3 days before IEC therapy with axi-cel. The primary end point was the proportion of patients with CRS grade  $\geq 2$  by day 14 using the American Society for Transplantation and Cellular Therapy consensus grading system. Overall, 111 patients were enrolled (63 in part 1; 48 in part 2); 109 patients were analyzed for efficacy and 110 for safety. By day 14, grade  $\geq 2$  CRS occurred in fewer patients on 200 mg twice daily itacitinib (17.4%) than on placebo (56.5%;  $P = .003$ ). The proportion of patients with grade  $\geq 2$  ICANS by day 28 was lower than with placebo (8.7% vs 21.7%). Itacitinib was well tolerated, with pyrexia being the most common treatment-emergent adverse event (200 mg itacitinib twice daily, 43.5%; placebo, 50.0%), and itacitinib-related cytopenias were manageable. Itacitinib did not affect IEC therapy efficacy (objective response rate at 6 months, 39.1% [200 mg itacitinib twice daily] vs 26.1% [placebo]).

## 25COASOCT87

**Title: Project EVOLVE: an international analysis of postimmunotherapy lineage switch, an emergent form of relapse in leukemia**

Sara K. Silbert et.al.

*Blood* (2025) 146 (4): 437–455.

<https://doi.org/10.1182/blood.2024026655>

**Abstract:** Lineage switch (LS), defined as the immunophenotypic transformation of acute leukemia, has emerged as a mechanism of relapse after antigen-targeted immunotherapy, which is associated with dismal outcomes. Through an international collaborative effort, we



identified cases of LS after a host of antigen-targeted therapies (eg, CD19, CD22, CD38, and CD7), described how LS was diagnosed, reviewed treatment approaches, and analyzed overall outcomes for this form of postimmunotherapy relapse. Collectively, 75 cases of LS were evaluated, including 53 (70.7%) cases of B-cell acute lymphoblastic leukemia (B-ALL) transforming to acute myeloid leukemia (AML), 17 (22.7%) cases of B-ALL transforming to mixed phenotypic acute leukemia (MPAL)/acute leukemias of ambiguous lineage (ALAL), and 5 (6.7%) cases of rare LS presentation (ie, T-cell ALL to AML). An additional 10 cases with incomplete changes in immunophenotype, referred to as “lineage drift” were also described. With a primary focus on the 70 cases of LS from B-ALL to AML or MPAL/ALAL, LS emerged at a median of 1.5 months (range, 0-36.5) after immunotherapy, with 81.4% presenting with LS within the first 6 months from the most proximal immunotherapy. Although most involved *KMT2A* rearrangements ( $n = 45$ , 64.3%), other rare cytogenetic and/or molecular alterations were uniquely observed. Treatment outcomes were generally poor, with remission rates of <40%. The median overall survival after LS diagnosis was 4.8 months. Outcomes were similarly poor for those with rare immunophenotypes of LS or lineage drift. This global initiative robustly categorizes lineage changes after immunotherapy and, through enhanced understanding, establishes a foundation for improving outcomes of LS.

## 25COASOCT88

**Title:** Lymphoid Neoplasia| July 24, 2025

**NKG2D-mediated cytotoxicity of CD4 cytotoxic T cells in multiple myeloma**

Sojeong Kim et.al.

*Blood* (2025) 146 (4): 456–470.

<https://doi.org/10.1182/blood.2024025875>

**Abstract:** Emerging evidence indicates that CD4<sup>+</sup> T cells contribute to antitumor immunity beyond their traditional roles as helpers or regulators. However, the specific subset of CD4<sup>+</sup> T cells mediating beneficial outcomes in patients with multiple myeloma remains unclear. Here, we performed single-cell RNA sequencing and T-cell receptor sequencing on CD4<sup>+</sup> T cells sorted from the bone marrow of patients across the stages of myeloma progression. We identified several distinct states of CD4<sup>+</sup> cytotoxic T lymphocytes (CTLs) that were significantly increased and clonally expanded in patients with myeloma. CD4<sup>+</sup> CTLs displayed transcriptional and phenotypic characteristics indicative of cytotoxicity, demonstrating their ability to directly kill myeloma cells. This cytotoxicity, however, was abrogated by NKG2D blockade. Notably, the abundance of NKG2D<sup>+</sup>CD4<sup>+</sup> CTLs correlated with improved survival in patients with myeloma. Our findings suggest that harnessing CD4<sup>+</sup> CTLs could lead to novel strategies for enhancing immunotherapy outcomes in multiple myeloma.

## 25COASOCT89

**Title:** Delineating *Mpl*-dependent and -independent phenotypes of *Jak2* V617F–positive MPNs in vivo

Nicolas Papadopoulos

*Blood* (2025) 146 (4): 482–495.

<https://doi.org/10.1182/blood.2024026711>

**Abstract:** The *Jak2* V617F mutation stands as the main driver of myeloproliferative neoplasms (MPNs) by constitutively activating signaling through several type I cytokine receptors, namely the erythropoietin receptor, the thrombopoietin receptor (TpoR)/myeloproliferative leukemia (Mpl) protein, and the granulocyte colony-stimulating factor receptor. Among these, TpoR assumes a pivotal role in hematopoietic stem cell renewal and differentiation, being positioned as a key driver of MPNs alongside mutated *Jak2*. However, the impact of TpoR/Mpl absence in the context of *Jak2* V617F in vivo has been explored only through a transgenic *Jak2* V617F mouse model, in which regulation of *Jak2* expression does not depend on its natural promoter. In this study, we use a novel mouse model expressing *Jak2* V617F under its endogenous promoter at the heterozygous state within a *Mpl* knockout background. Our findings indicate that erythrocytosis, leukocytosis, and moderate splenomegaly with mild perivascular fibrosis of the spleen persist even in the absence of Mpl expression. Notably, the inherent growth-stimulating effect induced by *Jak2* V617F remains consistent across diverse early hematopoietic progenitor populations in the absence of Mpl but is reduced at the stem cell level and does not allow clonal expansion in competitive transplantation. Our results delineate *Mpl*-dependent and -independent phenotypes induced by *Jak2* V617F and confirm that inhibiting Mpl expression at the stem cell level negates the long-term advantage of the mutant clone. Consequently, although Mpl emerges as a major player in *Jak2* V617F-positive MPNs, our study underscores that it is not the exclusive contributor, broadening the spectrum for therapeutic intervention.

## 25COASOCT90

**Title:** Shear-dependent platelet aggregation by ChAdOx1 nCoV-19 vaccine: a novel biophysical mechanism for arterial thrombosis

Yiyao Catherine Chen et.al.

*Blood* (2025) 146 (4): 496–503.

<https://doi.org/10.1182/blood.2024027675>

**Abstract:** Rare thrombotic events associated with ChAdOx1 nCoV-19 (ChAdOx1) vaccination have raised concerns; however, the underlying mechanisms remain elusive. Here, we report a novel biophysical mechanism by which ChAdOx1 directly interacts with platelets under arterial shear conditions, potentially contributing to postvaccination arterial thrombosis. Using microfluidic post assays, we demonstrate that ChAdOx1 induces shear-dependent platelet aggregation, distinct from conventional von Willebrand factor-mediated adhesion. This interaction is mediated by platelet integrin  $\alpha_{IIb}\beta_3$  and requires biomechanical activation, explaining the absence of significant binding under static conditions. Molecular dynamics simulations and docking studies reveal preferential binding of ChAdOx1's penton arginine-glycine-aspartic acid (RGD) motif to the activated conformation of  $\alpha_{IIb}\beta_3$ . Inhibiting integrin  $\alpha_{IIb}\beta_3$  completely abolishes ChAdOx1-induced platelet aggregation, whereas blocking glycoprotein (GP) Ib has minimal effect, confirming a mechanism that bypasses the conventional GPIb-dependent platelet adhesion pathway. Mutagenesis of the RGD motif to AAA eliminates platelet binding, verifying the specificity of this interaction. These findings provide a potential explanation for the association between ChAdOx1 vaccination and arterial thrombotic events, distinct from vaccine-induced immune thrombotic thrombocytopenia. Our results highlight the importance of considering biomechanical factors in vaccine-related

thrombotic complications and suggest that shear-dependent integrin activation may be another determinant in the pathogenesis of these rare adverse events.

**Surgical Oncology****25COASOCT01:****Title: Pelvic lymph-node dissections in bladder and prostate cancer surgery and the risk of postoperative venous thromboembolism,**

Juhana Rautiola, Johan Björklund, Renata Zelic, Francesco Pellegrino, Per Henrik Vincent, Peter Wiklund, Markus Aly, Henrik Falconer, Olof Akre,

European Journal of Surgical Oncology, Volume 51, Issue 10, 2025, 110326,

<https://doi.org/10.1016/j.ejso.2025.110326>.

**Abstract:** To evaluate the risk of venous thromboembolic events in patients operated with radical cystectomy or radical prostatectomy and pelvic lymph-node dissection. Patients operated with radical cystectomy for bladder cancer or with radical prostatectomy for prostate cancer from 1997 through 2016 were identified from Swedish nationwide registers. We estimated odds ratios of association between lymph-node dissection and pulmonary embolism and deep venous thrombosis (DVT) using logistic regression adjusted for the probability of having lymph-node dissection. In total, 6069 patients operated with radical cystectomy and 36 911 patients with radical prostatectomy were included. The risk of pulmonary embolism and DVT after radical cystectomy with lymph-node dissection was 1,89 % and 2,29 %, and without lymph-node dissection 1,99 % and 2,35 %, respectively. After radical prostatectomy and lymph-node dissection the risk for pulmonary embolism and DVT were 0,97 % and 1,36 %, and without lymph-node dissection 0,42 % and 0,49 %, respectively. Pelvic lymph-node dissection during a radical cystectomy was not associated with pulmonary embolism (OR 0,99; 95 % CI 0,65–1,51) or DVT (OR 0,99; 95 % CI 0,68–1,48), whereas lymph-node dissection during radical prostatectomy was associated with higher odds of both pulmonary embolism (OR 2,29; 95 % CI 1,67–3,09) and DVT (OR 2,95; 95 % CI 2,27–3,85). Pelvic lymph-node dissection did not increase the risk of venous thromboembolism after a cystectomy, whereas we found an increased relative risk of venous thromboembolic events associated with radical prostatectomy with lymph-node dissection.

**Keywords:** Lymph-node dissection; Venous thromboembolism; Prostate cancer; Bladder cancer; Survival

**25COASOCT02:****Title: Survival outcomes and prognostic factors in surgically resected lung carcinoids: A 25-year retrospective analysis,**

Luca Bertolaccini, Giovanni Caffarena, Francesca Spada, Lavinia Benini, Eleonora Pisa, Renato Lobrano,

European Journal of Surgical Oncology, Volume 51, Issue 10, 2025, 110366,

<https://doi.org/10.1016/j.ejso.2025.110366>.

**Abstract:** Carcinoids are rare neuroendocrine lung cancers with a prognosis related to stage and grade. Radical and complete surgical resection is the only curative treatment. However, some prognostic factors influencing survival outcomes must be fully understood. This study aims to evaluate the clinical and pathological characteristics of lung carcinoids and identify key predictors of recurrence-free survival and overall survival. A retrospective analysis was conducted on patients with histologically confirmed lung carcinoids (typical and atypical) who underwent surgical resection between January 1998 and December 2023. Clinical data,

including age, gender, smoking status, tumor laterality, TNM stage, and pathological features, were collected. Survival outcomes were analyzed using Kaplan-Meier curves, log-rank tests, and Cox proportional hazards regression models. The cohort of 524 patients had a median age of 62 years, with 65.6 % females. Most carcinoids were typical (73.7 %) and located on the right side (59.4 %). Advanced tumor stage and higher mitotic counts were significantly associated with poorer survival. No significant impact on survival was observed for surgical techniques or factors such as age, sex, or histology. In particular, laterality shows no statistically significant difference in OS between the two groups ( $p = 0.35$ ). In our extensive series of patients with resected lung carcinoids, tumor stage and mitotic count were critical predictors of survival. While surgical resection is essential, these findings underscore the importance of precise staging and pathological evaluation to inform treatment decisions and enhance patient outcomes.

**Keywords:** Lung neuroendocrine tumors; Lung cancer; Tumour location; Ki-67 index; Mitotic count; Necrosis

### 25COASOCT03:

**Title:** Micro-lymphatic invasion impact prognosis of intrahepatic cholangiocarcinoma independent of lymph node metastasis and micro-vascular invasion,

Chaoqun Wang, Ying Zhu, Haoting Sun, Xiaojia Liu, Bolun Zhu, Jintong Luo, Lu Lu, Baobing Yin,

European Journal of Surgical Oncology, Volume 51, Issue 10, 2025, 110387,

<https://doi.org/10.1016/j.ejso.2025.110387>.

**Abstract:** To evaluate the prognostic significance of micro-lymphatic invasion (MLI), independent of lymph node metastasis (LNM) and micro-vascular invasion (MVI) in patients with intrahepatic cholangiocarcinoma (ICC). We conducted a retrospective cohort study of 137 ICC patients who underwent curative resections between January 2017 and December 2022 in Huashan Hospital. Patients were categorized based on MLI and MVI status, determined by D2-40,  $\alpha$ -SMA, CD34, CK19 immunostaining in multi-sites of tumor and para-tumor. Recurrence-free survival (RFS) and overall survival (OS) were compared between groups. The median OS was 34 months, with 1-year, 2-year, and 3-year OS rates of 90.7 %, 69.4 %, and 39.5 %, respectively. Patients with LNM exhibited significantly poorer OS (median 18 months) and RFS (median 7 months) compared to those without LNM (38 vs. 18 months). Furthermore, MLI was associated with reduced OS (24 months for MLI (+) vs. >60 months for MLI (-)) and RFS (12 vs. >60 months). Among patients without LNM, those with MLI(+) exhibited significantly poorer OS and RFS compared to those without MLI, mirroring the poor prognosis of patients with potential LNM. MVI (+) showed a trend towards reduced OS (24 vs. 36 months), and significantly impacted RFS (12 vs. 18 months). Additionally, multivariate analysis identified carcinoembryonic antigen, carbohydrate antigen 19-9, perineural invasion and MLI as independent prognostic factors for OS. For RFS, carbohydrate antigen 19-9, tumor size, perineural invasion and MLI were found to be independent prognostic factors. The results of the study highlight the critical importance of incorporating MLI into prognostic evaluations.

**Keywords:** Micro-lymphatic invasion; Prognosis; Intrahepatic cholangiocarcinoma



**25COASOCT04:****Title: Impact of diaphragmatic intervention in cytoreductive surgery with heated intraperitoneal chemotherapy for colorectal carcinoma,**

Tiffany Williams, Raymond Hayler, Celine Garrett, Shoma Barat, Ruwanthi Wijayawardana, European Journal of Surgical Oncology, Volume 51, Issue 10, 2025, 110306,

<https://doi.org/10.1016/j.ejso.2025.110306>.

**Abstract:** To evaluate the impact of diaphragmatic intervention for patients with colorectal carcinoma undergoing cytoreductive surgery (CRS) and heated intraperitoneal chemotherapy (HIPEC) on overall survival and morbidity. Peritoneal Carcinomatosis Index (PCI) was used to stratify patients by low and high-volume. Analysis was performed on a prospectively maintained database, from September 1996 to November 2021. Patient demographics, operative information such as PCI, as per the Jacquet and Sugarbaker description, CC score and HIPEC agent was recorded. Postoperative complications were recorded. Patients were assessed by histological subtype, colorectal carcinoma, and then separated into low and high-volume PCI (PCI < 15). Patient cohort was divided into CRS with diaphragm intervention (DI) and CRS with no diaphragm intervention (NDI). Four-hundred and thirty-five patients over this time course were diagnosed with colorectal carcinoma, and 140 (29.9 %) patients had diaphragm involvement at time of surgery. Overall survival for patients with diaphragm involvement was a median of 26.1 months, compared to NDI at 42.4 months ( $p < 0.001$ ). Post-operative complications were greater in the patients with diaphragmatic intervention, particularly intra-abdominal collections (DI 30.0 % (n = 42) vs NDI 22.0 % (n = 65);  $p < 0.001$ ), and pleural effusions (DI 16.4 % (n = 23) vs NDI 13.2 % (n = 39);  $p < 0.001$ ). When considering PCI, for low volume cohort, DI patients' median overall survival was 32.7 months compared to NDI patients with a median overall survival of 45.7 months ( $p = 0.015$ ). For the high-volume cohort, PCI > 15, DI involvement median overall survival was 18.5 months, compared to NDI patients median overall survival of 20.7 months ( $p = 0.282$ ). CRS/HIPEC should be utilised in patients who have colorectal carcinoma and diaphragmatic disease, as overall survival is improved for patients. Greater rates of post operative complications are noted in this cohort and thus should be considered early in the post-operative period. CA19.9 should be considered an important, however not essential, aspect of pre-operative workup, with further investigation required.

**25COASOCT05:****Title: The association between low muscle mass and sarcopenic obesity, survival, and major complications in patients with advanced ovarian cancer undergoing primary cytoreductive surgery: A retrospective study,**

Niina Norppa, Antti Tolonen, Milja Reijonen, Auni Lindgren, Synnöve Staff, Irina Rinta-Kiikka, Sami Saarelainen, Otso Arponen,

European Journal of Surgical Oncology, Volume 51, Issue 10, 2025, 110286,

<https://doi.org/10.1016/j.ejso.2025.110286>.

**Abstract:** The aim of this study is to determine whether imaging-derived estimates of muscle mass or sarcopenic obesity are associated with survival and surgery-related complications in patients with advanced epithelial ovarian cancer treated with primary cytoreductive surgery (PCS). A skeletal muscle index (SMI) was determined by normalizing the muscle area at the level of third lumbar vertebra with the patient's height. Patients with SMI < 38.5 cm<sup>2</sup>/m<sup>2</sup> were

deemed to have low muscle mass, and those with SMI  $<38.5 \text{ cm}^2/\text{m}^2$  and body mass index  $>25 \text{ kg}/\text{m}^2$  were deemed to be affected by sarcopenic obesity. The relationships between low SMI and sarcopenic obesity, 1-year, 3-year, and overall survival were studied with Cox regression and Kaplan–Meier methods. The effect of SMI and sarcopenic obesity on surgery-related major complications (Clavien–Dindo  $\geq$  IIIB) was studied with logistic regression models. Ninety-two patients were retrospectively included, of whom 35 (38.0 %) and 12 (13.0 %) had low muscle mass or were affected by sarcopenic obesity, respectively. Among 73 (79.3 %) patients with high-grade serous OC, the 1-year survival rates were 66.7 % and 95.3 % (hazard ratio [HR] 9.19 [95 % confidence interval (CI): 1.85–45.75]) and the 3-year survival rates were 58.3 % and 68.8 % (HR 2.95 [95 % CI: 1.10–7.92]) for patients with and without sarcopenic obesity, respectively. Neither low muscle mass nor sarcopenic obesity was associated with major complications. Sarcopenic obesity was a marker of poor 1-year and 3-year survival in patients with high-grade serous OC. Neither low muscle mass nor sarcopenic obesity was associated with major complications in PCS.

**Keywords:** Ovarian cancer; Primary cytoreductive surgery; Computed tomography; Body composition analysis; Sarcopenia; Sarcopenic obesity

## 25COASOCT06:

**Title:** Comparison of subcutaneous tunnel-assisted periareolar incision versus conventional uniportal video-assisted thoracoscopic surgery (VATS) for pulmonary nodules: A prospective, randomized, controlled trial,

Zhenyuan Yang, Maohui Chen, Jianghong Wu, Guanglei Huang, Taidui Zeng, Hongmu Li, Shuliang Zhang, Chun Chen, Chunyu Zhou, Bin Zheng,

European Journal of Surgical Oncology, Volume 51, Issue 10, 2025, 110353,

<https://doi.org/10.1016/j.ejso.2025.110353>.

**Abstract:** Recent investigations into subcutaneous tunneled periareolar incisions for thoracoscopic pulmonary resection have established procedural safety and feasibility. Nevertheless, a critical gap persists in prospective evidence. To address this, we conducted a prospective controlled trial comparing perioperative complications and incisional cosmetic outcomes between single-port pulmonary resection performed via subcutaneous tunneled periareolar approaches versus conventional lateral thoracic approaches. 174 patients were randomized 1:1 to either the subcutaneous tunnel periareolar incision group or the conventional single-port group. All demographic, perioperative and follow-up data were prospectively collected and analyzed according to the standardized protocol. Neither group required intraoperative conversion to multi-port or open chest surgery. Operative duration was significantly longer in the periareolar incision group ( $P < 0.05$ ). No statistically significant difference in postoperative complications was observed between the cohorts ( $P = 0.686$ ). Compared to the conventional single-port approach, the periareolar incision group exhibited significantly reduced rates of clinically significant pain. The results of POSAS scale showed that the scar evaluation results were better in the periareolar incision group. Incisional cosmesis satisfaction was significantly higher in female patients who underwent periareolar incision than in those who underwent conventional single-port approach ( $P < 0.001$ ), while there was no similar finding in male patients ( $P = 0.222$ ). All patients reported minimal or no alterations in nipple sensitivity, with no significant functional impact on daily activities. The subcutaneous tunneled periareolar approach for single-port

thoroscopic resection demonstrates equivalent safety to conventional VATS while conferring superior cosmetic outcomes.

**Keywords:** Subcutaneous tunneled periareolar incision; Single-port thoroscopic surgery; Prospective randomised controlled trial; cosmetic satisfaction; Postoperative pain

#### 25COASOCT07:

**Title: Prognostic role of peritoneal lavage cytology: Proposal for staging laparoscopy criteria in biliary tract cancer,**

Yoshiyuki Shibata, Atsushi Oba, Gaku Shimane, Tatsunori Miyata, Jun Tauchi, Hayato Baba, Aya Maekawa,

European Journal of Surgical Oncology, Volume 51, Issue 10, 2025, 110369,

<https://doi.org/10.1016/j.ejso.2025.110369>.

**Abstract:** The role of radical resection for CY-positive BTC remains controversial and needs reassessment in the era of effective multi-agent chemotherapy. To evaluate the clinical significance of peritoneal lavage cytology (CY) in the perioperative management of biliary tract cancer (BTC) and propose novel staging laparoscopy (SL) criteria. We reviewed the medical records of 782 patients with BTC, excluding those with cancer of the papilla of Vater. Patients were classified based on CY and metastatic (M) status. Among 782 BTC patients, 38 (4.9 %) were CY-positive. Patients were categorized as follows: CY1M0 resected group (n = 10, 1.3 %), CY0M0 resected group (n = 637, 81.5 %), M1 resected group (n = 50, 6.4 %), and M1 unresected group (n = 70, 9.0 %). The postoperative median overall survival was 58.8, 19.5, 19.3, and 13.5 months respectively ( $p < 0.001$ ). Postoperative recurrence occurred in 9 patients (90.0 %), 306 patients (48.0 %), and 43 patients (86.0 %) in the CY1M0, CY0M0, and M1 resected group, respectively. Multivariate analysis of pre- and intra-operative factors revealed that CY positivity was independently associated with postoperative recurrence (odds ratio, 7.18; 95 % confidence interval, 1.28–134.83;  $p = 0.022$ ), along with other significant factors. A combination of cT3/T4 and cN-positive status was the good indicator of staging laparoscopy, achieving a detection rate of 28.8 % and accuracy of 85.2 %. CY positivity is associated with postoperative recurrence and poor prognosis and can be considered equivalent to M1 status. Staging laparoscopy may be indicated for patients with a combination of cT3/T4 and cN positivity.

**Keywords:** Peritoneal lavage cytology; Biliary tract cancer; Prognosis; Surgical resection; Staging laparoscopy

#### 25COASOCT08:

**Title: Pain management after minimally invasive gastrectomy: do we need epidural analgesia?,**

E. Azizi, Y. Okumura, B. Sunde, M. Lindblad, M. Nilsson, I. Rouvelas, J. Grip, F. Klevebro, European Journal of Surgical Oncology, Volume 51, Issue 10, 2025, 110232,

<https://doi.org/10.1016/j.ejso.2025.110232>.

**Abstract:** Epidural analgesia (EDA) has been the gold standard postoperative pain management in gastric cancer surgery for many years. As minimally invasive techniques have reduced surgical trauma, the necessity of EDA is being questioned. This study aimed to evaluate if minimally invasive gastrectomy without EDA was associated with shorter hospital stay and fewer complications compared to operations with EDA. All patients undergoing

minimally invasive gastrectomy for cancer at Karolinska University Hospital (Jan 2015–Aug 2023) were included and divided into groups operated with and without EDA. Data were collected prospectively in an institutional database and retrospectively from medical records. The primary outcome was the length of hospital stay. Among 211 patients, 43 (20.4 %) had EDA, and 168 (79.6 %) did not, with 12 (7 %) of the latter requiring EDA postoperatively. The median hospital stay was one day longer in group with EDA (median days 7 vs 6  $p < 0.001$ ), supported by multivariable adjusted analysis with a coefficient of  $-1.76$  days (95 % CI:  $-9.01, -2.26$   $p = 0.003$ ). Patients with EDA had lower pain scores (NRS 0–24h, 0 vs 2  $p < 0.001$ ) but required longer postoperative norepinephrine infusion (11.5h vs 0h  $p < 0.001$ ) and one day longer stay in the high-dependency care unit ( $p < 0.001$ ). Overall (55.8 % vs 39.9 %,  $p = 0.060$ ) and severe surgical complications (20.9 % vs 9.5 %,  $p = 0.039$ ) were more common in the EDA group. Minimally invasive gastrectomy without EDA can be associated with improved outcomes including shorter hospital stays, fewer postoperative complications, reduced postoperative norepinephrine use, and decreased high-dependency care duration.

**Keywords:** Minimally invasive surgery; Gastric cancer; Epidural analgesia; Enhanced recovery; Postoperative complications; Pain management

## 25COASOCT09:

**Title: Robot-assisted vs. open radical cystectomy: octogenarians vs. non octogenarians,** Michele Nicolazzini, Mattia Longoni, Fabian Falkenbach, Andrea Marmioli, Quynh Chi Le, Calogero Catanzaro,

European Journal of Surgical Oncology, Volume 51, Issue 10, 2025, 110345,

<https://doi.org/10.1016/j.ejso.2025.110345>.

**Abstract:** We quantified the effect of robot-assisted radical cystectomy (RARC) vs. open radical cystectomy (ORC) on adverse in-hospital outcomes in octogenarians ( $\geq 80$  years) relative to non-octogenarians. Propensity score matching (PSM), multivariable logistic and Poisson regression models focused on adverse in-hospital outcomes in octogenarian and non-octogenarian patients treated with RARC vs. ORC, identified in National Inpatient Sample (2008–2019). Overall, 13,922 RC patients were included. In 2002 octogenarians, after one-to-two PSM, 430 of 430 (100 %) RARC patients vs. 860 of 1572 (54.7 %) ORC patients were included. Octogenarians treated with RARC exhibited lower rates of adverse in-hospital outcomes than those treated with ORC in two of 12 examined categories: blood transfusions rate (18.6 vs. 28.1 %, OR 0.57) and prolonged length of stay (LOS) (17.7 vs. 25.5 %, OR 0.62), all  $p < 0.01$ . In 11,920 non-octogenarians, after one-to-two PSM, 2639 of 2639 (100 %) RARC patients vs. 5278 of 9281 (56.9 %) ORC patients were included. Non-octogenarians treated with RARC exhibited lower rates of adverse in-hospital outcomes than those treated with ORC in six of 12 examined categories: blood transfusion (12.6 vs. 23.2 %, OR 0.47), prolonged LOS (18.8 vs. 26.1 %, OR 0.66), overall complications (57.8 vs. 62.9 %, OR 0.82), respiratory (9.1 vs. 11.5 %, OR 0.78), wound (2.2 vs. 4.3 %, OR 0.50) and infectious complications (4.2 vs. 5.6 %, OR 0.74), all  $p < 0.05$ . RARC offers more favorable in-hospital outcomes profile relative to ORC in both octogenarians and non-octogenarians. However, the magnitude of RARC benefit over ORC is less pronounced in octogenarians than in non-octogenarians.

**Keywords:** Robotic radical cystectomy; Radical cystectomy; Robotic surgery; Elderly; Octogenarians; Urinary bladder neoplasms; Complications; NIS; Perioperative outcomes

#### 25COASOCT10:

**Title:** Laparoscopic radical gastrectomy is a protective factor for clinical outcomes in gastric cancer patients with sarcopenia,

Dingye Yu, Weizhe Chen, Fengmin Zhang, Hongting Huang, Tianyu Yu, Guowei Huang, Haojie Jiang, Qiantong Dong, Zhen Yu, Jiyu Li,

European Journal of Surgical Oncology, Volume 51, Issue 10, 2025, 110299,

<https://doi.org/10.1016/j.ejso.2025.110299>.

**Abstract:** Sarcopenia is common among individuals afflicted with gastric cancer (GC), and can culminate in unfavorable prognoses. Nevertheless, the efficacy of surgical interventions in GC patients with sarcopenia remains ambiguous. This study compared the prognostic value of laparoscopic and open radical gastrectomy in GC patients with sarcopenia. GC patients with preoperative sarcopenia who underwent radical gastrectomy were enrolled in our study. The patients' outcomes were stratified based on the surgical approach. After correcting for bias in clinical characteristics using propensity score matching, the prognoses of two groups were compared, and independent risk factors for postoperative complications, overall survival (OS) and disease-free survival (DFS) were analyzed. Our study included a total of 136 individuals after propensity score matching, with a postoperative complication rate of 39.0 %. Compared with patients who underwent open gastrectomy, those who opted for laparoscopic gastrectomy exhibited a lower incidence of surgical complications (13.2 % vs 35.3 %,  $P = 0.003$ ) and better prognoses. By conducting a comprehensive analysis of statistical results, it had been determined that laparoscopic surgery was identified as an independent protective factor for surgical complications ( $OR = 0.244(0.098-0.607)$ ;  $P = 0.004$ ), OS ( $HR = 0.522(0.0.297-0.919)$ ;  $P = 0.024$ ), and DFS ( $HR = 0.459(0.234-0.902)$ ;  $P = 0.024$ ). Laparoscopic gastrectomy achieves a better long-term prognosis and significantly reduces the incidence of postoperative surgical complications for GC patients with sarcopenia.

**Keywords:** Sarcopenia; Gastric cancer; Laparoscopic radical gastrectomy; Prognosis

#### 25COASOCT11:

**Title:** Synchronous hepatectomy and splenectomy for patients with BCLC stage 0/A hepatocellular carcinoma and clinically significant portal hypertension: A multicenter retrospective cohort study,

Tianyin Shao, Hongwei Huang, Qi Cheng, Feng Xia, Zhanguo Zhang, Songqing He, Deyu Li, Bangde Xiang,

European Journal of Surgical Oncology, Volume 51, Issue 10, 2025, 110351,

<https://doi.org/10.1016/j.ejso.2025.110351>.

**Abstract:** Liver transplantation is restricted by high costs and donor shortages, necessitating exploration of alternative treatments for hepatocellular carcinoma (HCC) with significant portal hypertension (CSPH). This study examined whether synchronous hepatectomy and splenectomy (HS) improves survival over hepatectomy (H) in patients with BCLC stage 0/A HCC and CSPH. A total of 525 patients with BCLC stage 0/A HCC and CSPH from 12 centers were under review. Among these, 300 patients underwent H (H group) and 225



underwent HS (HS group). Propensity score matching resulted in 157 matched pairs of patients. The study compared both short-term and long-term outcomes between the two groups. The HS group had higher rates of massive intraoperative bleeding (15.3 % vs. 6.4 %), abdominal bleeding (5.1 % vs. 0.6 %), and portal vein thrombosis (14.0 % vs. 3.8 %), but no significant differences in 30-day mortality or overall morbidity. In terms of long-term outcomes, the HS group showed better overall survival (59.0 vs. 48.0 months,  $P = 0.031$ ) and recurrence-free survival (41.0 vs. 28.0 months,  $P = 0.017$ ), with lower incidences of variceal bleeding (1.9 % vs. 7.6 %) and liver failure mortality (3.8 % vs. 13.4 %). Multivariate analysis identified splenectomy as a significant prognostic factor for improved OS and RFS. HS could be a reasonable alternative for patients with BCLC stage 0/A HCC and CSPH. This combined therapeutic strategy enhances long-term survival through various mechanisms while maintaining an acceptable level of perioperative risk.

**Keywords:** Hepatocellular carcinoma; Portal hypertension; Hepatectomy; Splenectomy

## 25COASOCT12:

**Title:** Robotic versus open level III-IV inferior vena cava thrombectomy: A multicenter, retrospective, propensity-matched analysis,

Liangyou Gu, Lin Yao, Qingbo Huang, Yonghui Chen, Peng Wu, Cheng Peng, Huaikang Li, European Journal of Surgical Oncology, Volume 51, Issue 10, 2025, 110327, <https://doi.org/10.1016/j.ejso.2025.110327>.

**Abstract:** The safety and efficacy of robotic inferior vena cava thrombectomy (IVCTE) for level III-IV thrombus with a comparison to open IVCTE is still unclear. This study aimed to compare robotic vs open IVCTE for renal tumors with level III-IV tumor thrombus. We performed a retrospective analysis of patients who underwent R-IVCTE or O-IVCTE in four academic tertiary centers between 2015 and 2023. Propensity score-matching analysis was performed. Perioperative data and prognosis were reviewed. Progression-free survival and overall survival were analyzed by Kaplan-Meier survival curve, and comparison between groups was performed by log-rank test. A total of 34 and 70 patients underwent R-IVCTE and O-IVCTE, respectively. After matching, baseline characteristics were comparable (30 vs 30 patients). Of the matched cohorts, robotic procedures were associated with longer operative time (508 vs 322 min;  $p < 0.001$ ), lower rate of cardiopulmonary bypass (33.3 % vs 66.7 %;  $p = 0.010$ ), longer ICU stay (5 vs 2 days,  $p = 0.001$ ), shorter postoperative hospital stay (10 vs 13 days,  $p = 0.021$ ). Patients undergoing R-IVCTE had a higher level of serum aminotransferase and aspartate aminotransferase than those undergoing O-IVCTE at 1–2 days after surgery, and the difference had disappeared at 1 week after surgery. No difference was observed between the two approaches regarding estimated blood loss, complications, pathological variables and oncological outcomes. R-IVCTE can be feasible and safe in selected cases of renal tumors with level III-IV tumor thrombus, which may achieve similar perioperative and oncological outcomes compared to O-IVCTE.

**Keywords:** Renal cell carcinoma; Inferior vena cava; Tumor thrombus; Nephrectomy; Robotics

## 25COASOCT13:

**Title:** Heterogeneity in prognosis for early-stage hepatocellular carcinoma after hepatectomy: A multicenter analysis of 4,623 patients across five major staging systems,

Lan-Qing Yao, Hui-Xuan Fan, Fu-Jie Chen, Yu-Chen Li, Alfred Wei Chieh Kow, Yi-Fan Li, Ying-Jian Liang,

European Journal of Surgical Oncology, Volume 51, Issue 10, 2025, 110383,

<https://doi.org/10.1016/j.ejso.2025.110383>.

**Abstract:** Multiple staging systems for hepatocellular carcinoma (HCC) have led to heterogeneous definitions of “early-stage” disease, potentially affecting treatment decisions and outcomes. This study aimed to quantify the prognostic variations among patients undergoing curative hepatic resection for “early-stage” HCC, as defined by five major staging systems. In this multicenter study, 4623 patients who underwent curative resection for newly diagnosed HCC (2014–2023) across 11 tertiary hospitals were analyzed. Early-stage disease was defined according to: AJCC-TNM stage I, BCLC stage 0/A, within Milan criteria, HKLC stage I/IIa, and CNLC stage I. Overall survival (OS), time to recurrence (TTR), and prognostic performance (C-index and Akaike information criterion) were compared. The proportion of early-stage classification varied substantially: TNM stage I (49.3 %), BCLC stage 0/A (71.4 %), within Milan criteria (49.3 %), HKLC stage I/IIa (53.1 %), and CNLC stage I (76.3 %). Five-year OS rates ranged from 67.4 % (CNLC stage I) to 74.9 % (within Milan criteria), with cumulative recurrence rates varying from 39.5 % (TNM stage I) to 46.3 % (BCLC stage 0/A). Prognostic performance analysis showed modest differences among staging systems (C-indices: 0.651–0.678 for OS; 0.679–0.715 for TTR), with BCLC demonstrating marginally better discriminatory ability. This large-scale analysis reveals clinically relevant heterogeneity in long-term oncologic prognosis among early-stage HCC patients across different staging systems, with variations in 5-year survival approaching 8 %. These findings highlight the urgent need for a more precise and unified definition of early-stage HCC to standardize prognostic assessment and treatment allocation globally.

**Keywords:** Hepatocellular carcinoma; Early-stage; Resection; Survival; Recurrence

## 25COASOCT14:

**Title:** Association between the type of pre-existing adenoma and response of rectal cancer to neoadjuvant therapy,

Sameh Hany Emile, Nir Horesh, Zoe Garoufalia, Anjelli Wignakumar, Michal Perets, Ebram Salama, Steven D. Wexner,

European Journal of Surgical Oncology, Volume 51, Issue 10, 2025, 110319,

<https://doi.org/10.1016/j.ejso.2025.110319>.

**Abstract:** Several factors influence response to neoadjuvant therapy (NAT) for locally advanced rectal cancer. One potentially relevant factor not previously studied is the type of pre-existing adenoma. We aimed to investigate the association between the type of pre-existing adenoma and response of rectal cancer to NAT and examine the tumor characteristics by adenoma type. This study was a retrospective review of patients with stage II–III rectal adenocarcinomas from the NCDB (2004–2017) who underwent proctectomy after NAT. Rectal cancers were classified and compared by the type of pre-existing adenomas: villous adenoma (VA), tubular adenoma (TA), and tubulovillous adenoma (TVA)-associated carcinomas. Case-control analysis of failure of response to NAT was conducted, including type of pre-existing adenoma as a potential covariate. 2760 patients (69.6 % male; mean age: 59.9 years) with stage II (44.8 %) or stage III (55.2 %) rectal cancers were included. Most adenomas were TVA (78.4 %), followed by VA (21.1 %) and TA (0.5 %). 55.5 % of patients

showed complete response (10 %) and partial (downstaging; 45.5 %) response after NAT. 64.3 % of TA-associated rectal carcinomas failed to respond to NAT compared to 46.4 % and 43.9 % of VA and TVA-associated carcinomas, respectively ( $p = 0.388$ ). Independent predictors of failure of response to NAT were stage II disease (OR: 1.85,  $p < 0.001$ ), high tumor grade (OR: 1.94,  $p = 0.007$ ), LVI (OR: 3.34,  $p < 0.001$ ), PNI (OR: 1.69,  $p = 0.032$ ), and elevated pretreatment CEA (OR: 1.54,  $p = 0.002$ ). TA-associated carcinomas exhibited the lowest response to NAT, although not statistically significant. Predictors for failure of response to NAT were stage II disease, high tumor grade, LVI and PNI, and elevated pretreatment CEA levels.

**Keywords:** Association; Pre-existing adenoma; Response; Rectal cancer; Neoadjuvant therapy; NCDB

### 25COASOCT15:

**Title:** Comparison of short- and mid-term outcomes of robotic versus laparoscopic gastrectomy in high-risk patients with gastric cancer: a nationwide, multicentre cohort study,

Wen-wu Qiu, Ze-Ning Huang, Tai- Yuan Li, Li Zhang, Jun-Jun She, Bao-Qing Jia, Xin-Gan Qin,

European Journal of Surgical Oncology, Volume 51, Issue 10, 2025, 110294,

<https://doi.org/10.1016/j.ejso.2025.110294>.

**Abstract:** To compare short-term and mid-term outcomes of robotic gastrectomy (RG) versus laparoscopic gastrectomy (LG) in high-risk gastric cancer (GC) patients. Patients with  $\geq 1$  of the following criteria were defined as high-risk: age  $\geq 80$  years; BMI  $\geq 30$  kg/m<sup>2</sup>; ASA grade  $\geq$  III; and clinical T stage (cT4). Finally, 2001 patients who underwent radical gastrectomy between August 2016 and June 2019 at eight high-volume hospitals were included and underwent 1:1 propensity score matching (PSM) with 534 patients in each group. After PSM, the RG group experienced less intraoperative blood loss (111.35 vs. 132.46 ml;  $P < 0.001$ ) and a lower incidence of intraoperative massive haemorrhage (2.81 % vs. 5.62 %;  $P = 0.022$ ), postoperative grade I–II complications (9.93 % vs. 13.86 %;  $P = 0.047$ ), medical complications (3.93 % vs. 8.61 %;  $P = 0.002$ ), pneumonia (3.37 % vs. 7.30 %;  $P = 0.004$ ), and pleural effusion (0.00 % vs. 0.75 %;  $P = 0.045$ ) than the LG group. However, RG were associated with longer operative time (225.13 vs 210.51 min,  $P < 0.001$ ) and significantly higher costs (\$11,990 vs \$8,040,  $P < 0.001$ ). The three-year cumulative mortality rate (RG: 18.74 % vs. LG: 21.54 %,  $P = 0.280$ ) and 3-year disease-free survival rate (RG: 78.97 % vs. LG: 75.45 %,  $P = 0.220$ ) exhibited no statistically significant differences between surgical approaches. The 3-year overall recurrence rate was not significantly different between the RG and LG groups (22.47 % vs. 19.66 %;  $P = 0.294$ ). RG yielded better short-term outcomes and comparable mid-term prognoses than LG for patients with high-risk resectable gastric cancer.

**Keywords:** Gastric cancer; High-risk patients; Robotic; Laparoscopic gastrectomy

### 25COASOCT16:

**Title:** Axillary surgery in early breast cancer: real-world analysis of the INSEMA-trial at three certified university breast cancer centers in Germany regarding the omission of sentinel lymph node biopsy,

Nikolas Tauber, Anna-Christina Rambow, Clara Gasthaus, Franziska Fick, Isabell Grande-Nagel,

European Journal of Surgical Oncology, Volume 51, Issue 10, 2025, 110392,

<https://doi.org/10.1016/j.ejso.2025.110392>.

**Abstract:** Recent trials such as INSEMA and SOUND have demonstrated the oncological safety of omitting sentinel lymph node biopsy in selected patients with hormone receptor-positive, HER2-negative early breast cancer. However, the implications for adjuvant treatment decisions in routine clinical practice remain unclear. We conducted a retrospective multicenter cohort study from university breast cancer centers, analyzing 867 patients diagnosed between 2020 and 2024 who met INSEMA criteria: cT1, G1-2, age  $\geq 50$  years, clinically node-negative, undergoing breast-conserving surgery. We evaluated the incidence of pathologically positive lymph nodes, frequency of postoperative upgrades in tumor stage or grading, and potential impact on adjuvant therapy decisions, including indications for CDK4/6 inhibitors, secondary axillary surgery or radiation. Sentinel lymph node biopsy revealed occult lymph node metastases in 14.3 % (n = 124) of patients, with a false-negative rate of 10.5 % when micrometastases and isolated tumor cells were excluded. In 11.6 % of cases, nodal positivity led to relevant therapeutic changes, including chemotherapy, axillary radiation, or potential adjuvant CDK4/6 inhibitor therapy. Moreover, 18.8 % of patients would have required secondary axillary surgery due to postoperative upgrades in tumor characteristics. The number needed to operate to prevent one invasive recurrence with CDK4/6 inhibitors varies significantly based on age and clinical tumor size, ranging from 1:333 (maximum) to 1:111 (minimum). While omission of sentinel lymph node biopsy appears safe in selected patients, our real-world data suggest that axillary staging retains clinical relevance for guiding personalized treatment, unless other prognostic tests like gene expression profiles are used.

**Keywords:** Early breast cancer; Sentinel lymph node biopsy; CDK4/6 inhibitors; Axillary surgery; de-escalation; Real-world data

## 25COASOCT17:

**Title:** Is adjuvant chemotherapy beneficial in NSCLC patients over 75? Insights from a retrospective analysis,

Yohann Vincent, Faustine Enoch, Vanessa Pauly, Anne-Laure Couderc, Pascale Tomasini, Laurent Greillier,

European Journal of Surgical Oncology, Volume 51, Issue 10, 2025, 110307,

<https://doi.org/10.1016/j.ejso.2025.110307>.

**Abstract:** Lung cancer remains the leading cause of cancer-related mortality worldwide. In resected stage II–III Non-Small Cell Lung Cancer (NSCLC), adjuvant chemotherapy (ACT) improves survival, but its benefit in elderly patients remains unclear due to the lack of dedicated studies. We conducted a retrospective study to assess benefit and predictive factors of ACT in NSCLC patients over 75-years-old. We conducted a single-centre retrospective study at Marseille University Hospital using the EPITHOR database. Patients over 75-year-old who underwent anatomical lung resection with a theoretical ACT indication were included between 2013 and 2022. Survival outcomes were compared between ACT and non-ACT groups. The primary endpoint was 5-year mortality without recurrence, with relapse as a competing event. Exploratory outcome were 5-year overall survival and risk factors for

recurrence. Among 129 eligible patients, 36 received ACT and 93 did not. ACT group patients were younger, had a more favourable perioperative course, and were more likely to have lymph node-positive disease (N+) (63.9 % vs. 43.0 %,  $p = 0.031$ ), especially N2 involvement. ACT significantly decreased mortality without recurrence in univariate analysis (HR = 0.257 [95 % CI: 0.080–0.819],  $p = 0.022$ ), but this benefit disappeared in multivariate analysis (HR = 0.461 [95 % CI: 0.144–1.473],  $p = 0.191$ ). Similarly, ACT was associated with lower overall mortality in univariate analysis but lost significance in multivariate analysis. Oncologists preferentially offer ACT to healthier elderly patients with N+ status. While ACT appears feasible, its benefit must be balanced considering competing risks of death in elderly patients. Identifying high-risk subgroups, including those with N2 disease, is crucial to refine treatment strategies in this population.

**Keywords:** Adjuvant chemotherapy; Elderly patients; Non-small cell lung cancer; Postoperative

## 25COASOCT18:

**Title:** Potential for omitting sentinel lymph node biopsy in patients with human epidermal growth factor receptor 2-positive or triple negative breast cancer with non-breast pCR after neoadjuvant chemotherapy,

Dong Seung Shin, Jiwon Park, Hyunwoo Lee, Woong Ki Park, Se Kyung Lee,

European Journal of Surgical Oncology, Volume 51, Issue 10, 2025, 110331,

<https://doi.org/10.1016/j.ejso.2025.110331>.

**Abstract:** Pathologic complete response (pCR) after neoadjuvant chemotherapy (NACT) predicts favorable outcomes in HER2-positive and triple-negative breast cancer (TNBC). While breast and axillary pCR often coexist, some patients with residual breast disease still achieve axillary pCR. This study evaluated axillary pCR rates and factors in this subgroup, and the potential to omit sentinel lymph node biopsy (SLNB) in selected patients. We retrospectively reviewed 1043 patients with HER2-positive or TNBC who did not achieve breast pCR after NACT and underwent surgery between 2008 and 2021 at a single institution. Clinicopathological features were compared between axillary pCR and non-pCR groups. Logistic regression analyses identified predictors of axillary pCR. Axillary pCR was observed in 648 (62.1 %) of 1043 patients who did not achieve breast pCR after NACT. The axillary pCR rate was 91.3 % in clinically node-negative (cN0) patients and 55.4 % in cN-positive patients. Axillary pCR rates decreased as the size of the residual breast tumor increased in both cN0 and cN-positive patients. Axillary pCR rates exceeded 94 % in patients with cN0 and residual tumor size of 1 cm or less. Multivariable analysis identified lower clinical N stage, smaller residual breast tumor size, and absence of lymphovascular invasion as independent predictors of axillary pCR. A substantial proportion of HER2-positive or TNBC patients without breast pCR after NACT achieved axillary pCR, especially those with cN0 status and small residual tumors. These results support the potential omission of SLNB in selected patients and highlight the need for prospective validation and predictive model development.

**Keywords:** Breast neoplasm; Neoadjuvant chemotherapy; Pathologic complete response; Sentinel lymph node biopsy



**25COASOCT19:**

**Title: Quantitative radiomic analysis of computed tomography scans using machine and deep learning techniques accurately predicts histological subtypes of non-small cell lung cancer: A retrospective analysis,**

Suhrud Panchawagh, Arita Halder, Saloni Haldule, Vivek Sanker, Devansh Lalwani, Rachel Sequeria, Harshika Naik, Atman Desai,

European Journal of Surgical Oncology, Volume 51, Issue 10, 2025, 110376,

<https://doi.org/10.1016/j.ejso.2025.110376>.

**Abstract:** Non-small cell lung cancer (NSCLC) histological subtypes impact treatment decisions. While pre-surgical histopathological examination is ideal, it's not always possible. CT radiomic analysis shows promise in predicting NSCLC histological subtypes. To predict NSCLC histological subtypes using machine learning and deep learning models using Radiomic features. 422 lung CT scans from The Cancer Imaging Archive (TCIA) were analyzed. Primary neoplasms were segmented by expert radiologists. Using PyRadiomics, 2446 radiomic features were extracted; post-selection, 179 features remained. Machine learning models like logistic regression (LR), Support vector machine (SVM), Random Forest (RF), XGBoost, LightGBM, and CatBoost were employed, alongside a deep neural network (DNN) model. RF demonstrated the highest accuracy at 78 % (95 % CI: 70 %–84 %) and AUC-ROC at 94 % (95 % CI: 90 %–96 %). LightGBM, XGBoost, and CatBoost had AUC-ROC values of 95 %, 93 %, and 93 % respectively. The DNN's AUC was 94.4 % (95 % CI: 94.1 %–94.6 %). Logistic regression had the least efficacy. For histological subtype prediction, random forest, boosting models, and DNN were superior. Quantitative radiomic analysis with machine learning can accurately determine NSCLC histological subtypes. Random forest, ensemble models, and DNNs show significant promise for pre-operative NSCLC classification, which can streamline therapy decisions.

**Keywords:** Lung cancer; Computed tomography; Radiomics; Histopathology; Artificial intelligence; Machine learning; Classification

**25COASOCT20:**

**Title: Real-world quality of life outcomes after prepectoral implant-based breast reconstruction with or without titanium-coated mesh (TiLOOP® Bra Pocket): A prospective cohort study,**

Moritz Hamann, Elena Bensmann, Anne Androlat, Jasmin Festl, Gitti Saadat, Michael Braun, European Journal of Surgical Oncology, Volume 51, Issue 10, 2025, 110311,

<https://doi.org/10.1016/j.ejso.2025.110311>.

**Abstract:** To evaluate quality of life (QoL) one year after immediate prepectoral direct-to-implant breast reconstruction (DTIBR) with and without a titanium-coated mesh (TiLOOP® Bra Pocket). In this prospective study (March 2021–February 2024), 309 DTIBR patients were analyzed. QoL was assessed preoperatively and postoperatively using the Breast-Q questionnaire (psychosocial well-being, sexual well-being, satisfaction with breasts, and physical well-being of the chest). Influencing factors were identified via linear regression. One-year follow-up (FUP) included 235 unilateral (85.8 %) and 31 bilateral (92.2 %, 61 breasts) DTIBR cases. After excluding 14 patients (autologous reconstruction, ADM use, or both prior and additional postoperative RT), 282 remained: 203 (71.7 %) with TiLOOP® Bra Pocket, 61 (21.9 %) without implant coverage, and 18 (6.4 %) using “dual-

plane” techniques. Mean scores showed increased psychosocial well-being (71.2–73.9) but declines in sexual well-being (64.3–60.3), satisfaction with breasts (67.3–65.2), and chest-related physical well-being (83.1–76.4). Higher preoperative scores predicted postoperative declines across all QoL domains. Older age correlated with better psychosocial ( $B = 0.189$ ,  $p = 0.032$ ) and physical well-being ( $B = 0.259$ ,  $p = 0.008$ ). TiLOOP® Bra Pocket improved psychosocial well-being ( $B = 4.971$ ,  $p = 0.038$ ). Satisfaction with breasts was lower with pending symmetrizing procedures ( $B = -13.771$ ,  $p < 0.001$ ) or complications ( $B = -6.543$ ,  $p = 0.049$ ). Postoperative RT reduced physical well-being ( $B = -7.309$ ,  $p = 0.008$ ). DTIBR results in high QoL, influenced by complications, postoperative RT, age, and preoperative satisfaction. Patients should be counseled considering these factors.

**Keywords:** Breast reconstruction; Direct-to-implant; Prepectoral reconstruction; TiLOOP® Bra Pocket; Quality of life (QoL); Breast-Q questionnaire

## 25COASOCT21:

**Title:** Adherence and response to supervised home-based exercise prehabilitation of unfit patients scheduled for pancreatic surgery,

Nicole D. Hildebrand, Allard G. Wijma, Bart C. Bongers, Sander S. Rensen, Marcel den Dulk, Joost M. Klaase, Steven W.M. Olde Damink,

European Journal of Surgical Oncology, Volume 51, Issue 10, 2025, 110302,

<https://doi.org/10.1016/j.ejso.2025.110302>.

**Abstract:** Exercise prehabilitation yields promising results in major surgery, including pancreatic surgery. Whereas most prehabilitation studies focus on effectiveness, objectively assessed adherence data supporting feasibility of preoperative physical exercise programs are scarce. This study aimed to assess participation rate, adherence, and effectiveness of a partly supervised, home-based exercise prehabilitation program in unfit patients scheduled for pancreatic surgery. In this prospective multicentre study, thirty unfit patients (oxygen uptake [VO<sub>2</sub>] at ventilatory anaerobic threshold [VAT]  $\leq 13$  mL/kg/min and/or VO<sub>2</sub> at peak exercise [VO<sub>2peak</sub>]  $\leq 18$  mL/kg/min) participated in a four-week home-based exercise prehabilitation program consisting of three personalized high-intensity interval training sessions per week on a remotely monitored cycle ergometer. The primary outcome was program feasibility, defined as participation rates and adherence to frequency, intensity, and time of each training session. Secondary outcomes were individual responses to the program. Participation rate was 63.8 % (30/47 eligible patients, median age 71 years [IQR 65–76], 16 females, 80 % malignancy). Five patients (16.6 %) dropped out. Overall adherence to the number of training sessions was 91.1 %. Adherence to frequency and intensity diminished during the second half of the program. Nevertheless, aerobic capacity improved (VO<sub>2peak</sub> +12.4 %,  $p < 0.001$ ; VO<sub>2</sub> at the VAT +16.3 %,  $p = 0.002$ ). Ultimately, twenty patients underwent surgery, without mortality but with major complications in 25.0 %. Objective assessment of adherence to a 4-week partly supervised home-based exercise prehabilitation program by unfit patients scheduled for pancreatic surgery was high, suggesting that even suboptimal execution of a training program still improves aerobic capacity, especially in the least fit patients.

**Keywords:** Pancreatic neoplasms; Exercise; Prehabilitation; Adherence; Surgery

**25COASOCT22:****Title: Transcriptomic classifiers do not reliably predict lymph node involvement in breast Cancer: Insights from three large cohorts,**

Leslie Dalton, Emad Rakha,

European Journal of Surgical Oncology, Volume 51, Issue 10, 2025, 110354,

<https://doi.org/10.1016/j.ejso.2025.110354>.

**Abstract:** Lymph node (LN) status remains one of the most critical prognostic indicators in breast cancer. A reliable molecular surrogate for LN involvement could offer substantial clinical benefits, including improved risk stratification and more selective use of surgical staging. This study investigates the potential of mRNA expression profiles to serve as predictors of LN status. mRNA expression data from three large cohorts, TCGA (n = 749), METABRIC (n = 1895), and SCAN (n = 3273), were used to generate six train-test permutations. Two machine learning algorithms, AdaBoost and XGBoost (gradient boosting), were applied to classify LN status and Nottingham histological grade (used as a benchmark). A total of 15,707 genes were assessed as predictors. Model performance was evaluated using the area under the receiver operating characteristic curve (AUC). In a separate analysis, time-to-event data (SurvObj) were modelled using the FastCox library in R to generate 1000 random survival models. The survival probabilities generated were then repurposed to predict LN status and grade. For LN prediction, the highest AUC achieved was 0.613 using XGBoost and 0.604 using AdaBoost. In contrast, histological grade molecular prediction yielded significantly higher accuracy, with maximum AUCs of 0.901 (XGBoost) and 0.880 (AdaBoost). Cramér's V analysis across all genes showed limited concordance with LN status. Additionally, models derived from survival probabilities consistently yielded AUCs below 0.6 when applied to LN prediction, indicating that strong survival predictors did not translate into accurate LN classifiers. Despite utilizing a comprehensive transcriptomic dataset and advanced machine learning algorithms, mRNA expression alone did not reliably predict LN status. Currently, no mRNA-based model serves as a clinically viable alternative to surgical LN assessment. Future efforts should explore integrative approaches that combine molecular, spatial, and clinical data to enhance our understanding and prediction of lymphatic dissemination in breast cancer.

**Keywords:** Transcriptomics; Lymph node status; Prediction; Breast cancer

**25COASOCT23:****Title: Salvage abdominoperineal resection for anal squamous cell carcinoma after radiotherapy or chemoradiotherapy: analysis of the French prospective cohort FFCD-ANABASE,**

Clara Naessens, Cécile Evin, Karine Le-Malicot, Claire Lemanski, Magali Rouffiac, David Tougeron,

European Journal of Surgical Oncology, Volume 51, Issue 10, 2025, 110346,

<https://doi.org/10.1016/j.ejso.2025.110346>.

**Abstract:** Salvage abdominoperineal resection (APR) is indicated for local failure following definitive chemoradiotherapy or radiotherapy for squamous cell carcinoma (SCCA), at the cost of morbidity and reduced quality of life. This study evaluated outcomes after salvage APR. The FFCD-ANABASE cohort is a prospective multicenter cohort including patients treated for non-metastatic SCCA in France between 2015 and 2020. Among the 1015 patients

included in FFCD-ANABASE, 78 underwent salvage APR. After excluding patients with a pathological complete response (pT0N0), the final efficacy analysis cohort comprised 66 patients. We analyzed disease-free survival (DFS), overall survival (OS), locoregional and metastatic relapse rates, post-operative morbidity and prognostic factors in patients who underwent salvage APR for local failure. With a median follow-up of 58.6 months after APR, the locoregional relapse rate was 21.2 % and the metastatic relapse rate was 9.1 %. An R0 resection was achieved in 80.8 % of cases. Five-year DFS and OS rates were 45.8 % [95 %CI: 33.3-57.4], and 50.2 % [95 %CI: 37.1-62.0]. In multivariate analysis, R0 margins (HR: 0.24 [95 %CI: 0.10-0.61]), and tumor size before chemoradiotherapy <4 cm (HR: 0.33 [95 %CI: 0.12-0.91]) were associated with better DFS; whereas no factor was significantly associated with OS. Post-operative morbidity was reported in 65 patients (83.3 %), with 34 of them (52.3 %) experiencing major complications, classified as Clavien-Dindo III-V. Salvage APR results in high post-operative morbidity and poor oncological outcomes. Our study found that complete resection margins was favorable prognostic factor, suggesting the need for additional perioperative treatment.

**Keywords:** Anal cancer; Squamous cell carcinoma; Chemoradiotherapy; Salvage surgery; Abdominoperineal resection

## 25COASOCT24:

**Title: The effect of PuraBond® on postoperative pain following transoral resections of primary oral or oropharyngeal neoplastic mucosal lesions: A blinded randomised controlled study (PuraBond® PROOF),**

Randa Ghazal Asswad, James Constable, Ahmed Abdelrahman, Paul Banks, Zoe Mellor, Terry M. Jones,

European Journal of Surgical Oncology, Volume 51, Issue 10, 2025, 110322,

<https://doi.org/10.1016/j.ejso.2025.110322>.

**Abstract:** RADA16 (PuraBond®) is a novel, synthetic agent that forms a transparent, self-assembling scaffold, mimicking human extracellular-matrix to promote haemostasis. We hypothesise this physical barrier provides effective analgesia for upper aerodigestive tract surgical wounds through nociception blockade during swallowing. This study evaluated PuraBond®'s efficacy on postoperative pain following transoral resection of oral/oropharyngeal mucosal lesions. A prospective, blinded, single-centre, randomised controlled trial was conducted, comparing intraoperative PuraBond® application versus no topical agent. Patients undergoing transoral resection of dysplasia/malignancy of the oral cavity or oropharynx were recruited. Stratification factors included lesion site, electrosurgery versus laser technique, and concurrent neck dissection. The primary outcome measure was pain scores measured using a visual analogue scale over 30-days postoperatively. In total, 68 patients were recruited (70% oropharyngeal, 30% oral; PuraBond® n = 32, control n = 36) and analysed. Mean pain scores over the study period were 2.56 and 3.41 for PuraBond® and control groups respectively. The control arm had higher baseline adjusted pain scores at all timepoints, but none of these were individually statistically significant. Cumulative results however demonstrated a significantly greater increase in pain from preoperative baseline for the control group over the entire 30-day period (0.61, 95% CI 0.12–1.10, p = 0.016), with the most noticeable clinical difference during the initial week (0.77, 95% CI 0.18–1.36, p = 0.011). Although underpowered with regards to haemorrhage events, these were three-

times lower with PuraBond® ( $p = 0.266$ ). PuraBond® use following head and neck mucosal resections is a safe and potentially useful surgical adjunct in reducing postoperative pain. The opportunity exists, via adequately-powered studies, to assess whether the trend towards reduced haemorrhage is significant and reproducible.

**Keywords:** Transoral surgery; Oral cavity; Oropharynx; Neoplasia; Surgical wound; Pain; Hemostasis; RADA16

#### 25COASOCT25:

**Title:** Enhancing prognostic accuracy in gastric cancer: The TNrrM staging system versus the AJCC TNM system,

Hao-Xiang Zhang, Ze-Ning Huang, Xing-Qi Zhang, Yi-Hui Tang, Yu-Qin Sun, Cai-Ming Weng,

European Journal of Surgical Oncology, Volume 51, Issue 10, 2025, 110362,

<https://doi.org/10.1016/j.ejso.2025.110362>.

**Abstract:** An accurate staging system is crucial for the management of gastric cancer (GC) patients. This study aimed to propose a novel staging system (TNrrM) based on the regional lymph node ratio (rLNR), defined as the ratio of the number of metastatic lymph nodes (LNs) to the number of examined LNs within each LN station. The study included 3263 GC patients, with 2143 in the development set and 1120 in the validation set. For each patient, the rLNR for each LN station was calculated, and the total rLNR was obtained by summing the rLNR values of all LN stations. Optimal cut-off values for total rLNR were determined using X-tile to define the Nrr staging system. Based on combinations of T and Nrr staging, 5-year overall survival (OS) curves were generated, and the TNrrM staging system was defined by grouping stages with similar prognosis. The prognostic value of TNrrM was compared with the 8th edition of the AJCC TNM staging system, showing that TNrrM staging had higher AUC values for predicting 12- to 60-month OS, better calibration, and an increased net benefit as revealed by decision curve analysis (DCA). Stratified analysis demonstrated that TNrrM staging could effectively distinguish subgroups within TNM IIB to IIIC stagings. Incorporating the rLNR, the TNrrM staging system significantly enhances prognostic accuracy for GC patients compared with the AJCC TNM system, with similar results found in the validation set.

**Keywords:** Gastric cancer; Regional lymph node ratio; TNM staging system; Novel staging system; Prognosis

#### 25COASOCT26:

**Title:** Long term outcomes of breast primary sarcomas and malignant phyllodes tumors: 20 years observational analysis of the BEAM\* study group. (\*the breast European association for mesenchymal tumors),

Alejandro M. Sanchez, Flavia De Lauretis, Angela Bucaro, Chiara V. Pirrottina, Niccolò Borghesan,

European Journal of Surgical Oncology, Volume 51, Issue 10, 2025, 110265,

<https://doi.org/10.1016/j.ejso.2025.110265>.

**Abstract:** Primary breast sarcomas (PBS) and malignant phyllodes tumors (MPT) represent less than 1 % of breast malignancies. Current evidence relies on heterogeneous retrospective series, resulting in controversial therapeutic approaches. This study aimed to analyze long-



term outcomes in a large multicentric cohort treated with consistent strategies. We conducted a multicentric retrospective study involving 113 patients treated for PBS (n = 42), MPT (n = 47), and mixed cases (MC, n = 24) at 11 European breast units between 2000 and 2020. Primary endpoint was disease-free survival (DFS). Secondary endpoints included overall survival (OS), local recurrence rate (LRR), and positive margin, re-excision, and axillary involvement rates. Survival analyses were performed using the Kaplan-Meier method and log-rank test. With a median follow-up of 95 months, the 10-year OS, DFS, and LRR for the entire cohort were 75.2 %, 61.9 %, and 18.4 %, respectively. Mixed cases exhibited the poorest outcomes (10-year OS: 57.6 %, DFS: 46.1 %), followed by PBS (OS: 67.5 %, DFS: 46.5 %). MPT demonstrated better survival rates (OS: 89.2 %, DFS: 82.9 %). Significant survival factors included histological subtype, surgical margins, and age. Notably, adjuvant chemotherapy was linked to worse outcomes (HR 5.11, 95 % CI 2.16–12.09,  $p < 0.001$  for OS), likely indicating selection bias for high-risk patients. This study represents the largest European series with a homogeneous treatment approach and long-term follow-up. MC emerge as a distinct high-risk entity, with outcomes akin to angiosarcomas. While surgery remains the cornerstone of treatment, our data challenge the current paradigm regarding adjuvant chemotherapy, highlighting the need for new strategies, particularly for high-risk subtypes.

## 25COASOCT27:

### **Title: Analysis of influencing factors for achieving textbook outcome after laparoscopic right posterior sectionectomy of hepatocellular carcinoma,**

Changyan Zhu, Jiali Wu, Xiuyuan Wang, Weixing Zhang, Zhiqiang Fu, Yuqiu Hu,

European Journal of Surgical Oncology, Volume 51, Issue 10, 2025, 110328,

<https://doi.org/10.1016/j.ejso.2025.110328>.

**Abstract:** Textbook outcome (TO) is a comprehensive indicator used to assess postoperative outcomes and quality of care. This study analyzes the incidence and influencing factors of TO after laparoscopic right posterior sectionectomy (LRPS) in hepatocellular carcinoma (HCC) patients. A retrospective cohort study was conducted on HCC patients who underwent LRPS at Sun Yat-sen Memorial Hospital from January 2018 to June 2023. Patients were divided into TO and non-TO groups. Univariable and multivariable logistic regression analyses identified factors influencing TO achievement. A total of 115 HCC patients underwent LRPS, with 70.4 % (82/115) achieving TO. Univariable logistic regression analysis identified smoking history, preoperative alanine transaminase, preoperative R-glutaminase transferase, operative time, intraoperative blood loss, blood transfusion and lymphovascular invasion as risk factors. Multivariable logistic regression analysis revealed smoking history (OR: 9.92, 95 % CI: 2.60–37.82,  $P = 0.001$ ), preoperative alanine transaminase (OR: 3.43, 95 % CI: 1.11–10.57,  $P = 0.032$ ), preoperative R-glutaminase transferase (OR: 3.34, 95 % CI: 1.16–9.65,  $P = 0.026$ ), and intraoperative blood loss (OR: 1.25, 95 % CI: 1.07–1.47,  $P = 0.005$ ) as independent risk factors. The combined index of these factors showed the greatest predictive value for TO (AUC: 0.821, 95 % CI: 0.74–0.90,  $P < 0.001$ ). TO is a reliable measure for LRPS outcomes. Factors such as no smoking history, preoperative alanine transaminase  $\leq 50$  U/L, preoperative R-glutaminase transferase  $\leq 60$  U/L, and intraoperative blood loss  $< 325$  mL are associated with higher TO achievement.

**Keywords:** Laparoscopic right posterior sectionectomy; Textbook outcome; Hepatocellular carcinoma; Influencing factor

## 25COASOCT28:

**Title:** Long-term muscle-sparing benefits of proximal gastrectomy in elderly patients with upper-third early gastric cancer: A propensity score-matched analysis,

Zhen Tian, Youlei Zhang, Yifan Cheng, Daorong Wang,

European Journal of Surgical Oncology, Volume 51, Issue 10, 2025, 110373,

<https://doi.org/10.1016/j.ejso.2025.110373>.

**Abstract:** As the global population ages, surgical strategies must shift from focusing solely on cancer control to prioritizing functional longevity. Laparoscopic proximal gastrectomy (LPG) has emerged as a potential organ-preserving alternative to laparoscopic total gastrectomy (LTG) for early upper-third gastric cancer (GC). However, the comparative efficacy of LPG versus LTG in elderly patients remains uncertain, as this population is more vulnerable to surgical stress due to age-related multimorbidity and frailty. We conducted a retrospective analysis of patients aged  $\geq 65$  years who underwent either LPG with double-tract reconstruction (LPG-DTR) or LTG for upper-third cT1-2N0M0 GC between January 2018 and December 2021. Propensity score matching (PSM) was used to mitigate selection bias, generating comparable cohorts ( $n = 51$  per group). Comparative analyses focused on perioperative outcomes and longitudinal nutritional parameters, quantified by percentage body weight loss (BWL) and skeletal muscle index (SMI) over 3 postoperative years. LPG-DTR and LTG demonstrated similar surgical outcomes, including operative time, blood loss, and hospitalization, with comparable early and late complication rates. Over the 3-year follow-up, LPG-DTR exhibited significantly superior skeletal muscle preservation compared to LTG, as evidenced by smaller declines in the SMI at Year 2 ( $-5.89\%$  vs.  $-9.54\%$ ,  $P = 0.011$ ) and Year 3 ( $-7.23\%$  vs.  $-10.69\%$ ,  $P = 0.039$ ). Additionally, the LPG-DTR group had less pronounced body weight loss at the 2 year ( $-4.71\%$  vs.  $-9.55\%$ ,  $P = 0.031$ ) and 3 year ( $-5.63\%$  vs.  $-10.2\%$ ,  $P = 0.011$ ) postoperatively. The risk of severe skeletal muscle loss increased over time, particularly in patients older than 75 (OR 2.05,  $P = 0.025$ ), those who underwent LTG (OR 1.89,  $P = 0.031$ ), and males (OR 3.73,  $P = 0.006$ ). Both groups had similar 3-year overall survival rates ( $86.3\%$  vs.  $88.2\%$ ,  $P = 0.777$ ), with age  $>75$  (HR 2.946,  $P = 0.012$ ) and preoperative sarcopenia (HR 1.795,  $P = 0.039$ ) being independent predictors of poorer survival. These findings suggest that LPG-DTR is as safe as LTG, offering superior preservation of skeletal muscle mass and nutritional status without compromising oncological outcomes. LPG-DTR may provide a function-preserving alternative for treating elderly patients with upper-third early GC.

**Keywords:** Proximal gastrectomy; Total gastrectomy; Gastric cancer; Elderly

## 25COASOCT29:

**Title:** Perioperative dynamic changes of systemic inflammatory biomarkers predict tumor recurrence following curative-intent resection of hepatocellular carcinoma,

Jingming Lu, Fumin Wang, Yaoxing Ren, Yu An, Francesca Ratti, Hugo P. Marques, Silvia Silva,

European Journal of Surgical Oncology, Volume 51, Issue 10, 2025, 110320,

<https://doi.org/10.1016/j.ejso.2025.110320>.

**Abstract:** Hepatic inflammation during liver resection induces immune dysregulation. We sought to investigate how surgical stress reshapes systemic inflammation and affects tumor recurrence following surgical resection of hepatocellular carcinoma (HCC). Patients who underwent curative resection of HCC between 2000 and 2022 were identified from an international multicenter cohort. We longitudinally quantified perioperative inflammatory dynamics, particularly neutrophil-to-lymphocyte ratio (NLR) and systemic immune-inflammation index (SII). The primary endpoint was recurrence-free survival (RFS). Model performance was validated through bootstrap resampling (1000 iterations) and ROC analysis. A total of 745 patients were included. Among the dynamic changes of inflammation cells count, only changes in NLR at postoperative day 3 versus preoperative value ( $\Delta\text{NLR}_3$ ) was identified as a strong predictor associated with HCC recurrence (HR 1.005, 95 % 1.002–1.009;  $p = 0.002$ ). The optimal cutoff value of  $\Delta\text{NLR}_3$  was defined as 47, and patients with  $\Delta\text{NLR}_3 \geq 47$  had 75 % increased risk of tumor recurrence versus individuals with  $\Delta\text{NLR}_3 < 47$  (HR 1.75, 95 % CI 1.35–2.28,  $p < 0.001$ ). Moreover,  $\Delta\text{NLR}_3$  could be utilized in differentiating high-versus low-recurrence risk patients with early staged HCC. By combining  $\Delta\text{NLR}_3$  with tumor-associated risk factors, we created an InfTumMod model, which demonstrated very good predictive accuracy of 70 % relative to tumor recurrence within the first three years following surgical resection of HCC. The  $\Delta\text{NLR}_3$  index reflected systemic inflammation and risk of tumor recurrence. The InfTumMod model incorporated inflammation index and tumor characteristics, which can help identify patients at higher risk of recurrence and mortality.

**Keywords:** Hepatocellular carcinoma; Neutrophil-to-lymphocyte ratio; Inflammation; Recurrence; Prediction model

## 25COASOCT30:

**Title:** A retrospective analysis of 44 diminutive rectal neuroendocrine neoplasms that were not suitable for local treatment,

Zhijie Wang, Qian Liu,

European Journal of Surgical Oncology, Volume 51, Issue 10, 2025, 110348,

<https://doi.org/10.1016/j.ejso.2025.110348>.

**Abstract:** Diminutive rectal neuroendocrine neoplasms (NENs) are often treated by local excision, but the presence of regional nodes or distant metastasis is reported in an increasing number of reports. We retrospectively recruited 44 patients with rectal NENs below 2 cm. These patients were not suitable for local excision due to invasion of the muscularis propria, involvement of regional lymph nodes or distant metastasis. A multivariate logistic regression model was conducted to identify the risk factors for distant metastasis. Survival analysis was performed to evaluate their prognosis. Among 44 patients, 11 (25 %) had NENs smaller than 1 cm, and 33 (75 %) had NENs 1–2 cm in size. Thirty-seven patients (84.1 %) had regional node metastasis, and 14 (31.8 %) presented distant metastasis. The depth of tumor invasion (odds ratio [OR] = 20.57, 95 % confidence interval [CI]: 2.17–194.95,  $P = 0.008$ ) was identified as the dominant risk factor for distant metastasis. The median overall survival (OS) was 86 months in the whole cohort, and the 1-year, 3-year and 5-year OS rates were 88.5 %, 81.9 % and 73.0 %, respectively. Poor histological differentiation (hazard ratio [HR] = 11.65, 95 % CI: 2.75–49.38,  $P = 0.001$ ) and metastatic disease (HR = 7.45, 95 % CI: 1.73–32.03,  $P = 0.007$ ) were significantly associated with worse OS. Diminutive rectal NENs are still at

risk of regional and even distant metastasis. A prudent attitude should be maintained with respect to choosing local excision as size alone is not a sufficient criterion for treatment decisions.

**Keywords:** Rectum; Neuroendocrine; Neoplasm; Metastasis; Size

### 25COASOCT31:

**Title:** The role of pathological response in predicting the benefit of adjuvant therapy after neoadjuvant chemoimmunotherapy in patients with esophageal cancer,

Maohui Chen, Yizhou Huang, Rujing Zhang, Bingqiang Cai, Yongcong Zhang,

European Journal of Surgical Oncology, Volume 51, Issue 10, 2025, 110360,

<https://doi.org/10.1016/j.ejso.2025.110360>.

**Abstract:** Neoadjuvant chemoimmunotherapy has demonstrated significant survival benefits in esophageal squamous cell carcinoma (ESCC), but the value of postoperative adjuvant therapy remains controversial. Tumor regression grade (TRG) serves as a crucial pathological indicator of response to neoadjuvant treatment, yet its role in guiding adjuvant therapy is unclear. This study aimed to investigate the prognostic significance of TRG in postoperative adjuvant therapy. This multicenter retrospective cohort study included 169 thoracic ESCC patients who underwent R0 resection after neoadjuvant chemoimmunotherapy between January 2019 and December 2022. Patients were stratified into TRG 0–1 (good response) and TRG 2–3 (poor response) groups. Survival outcomes were analyzed using Kaplan-Meier and Cox regression models. With a median follow-up of 34 months, adjuvant immunotherapy significantly improved 3-year overall survival (OS) compared to no adjuvant therapy (82.1 % vs. 66.3 %,  $p = 0.042$ ), though no significant difference in disease-free survival (DFS) was observed. Subgroup analysis revealed that adjuvant therapy notably improved OS in patients with TRG 0–1 (93.2 % vs. 73.3 %,  $p = 0.015$ ), but not in TRG 2–3. Multivariate analysis confirmed adjuvant immunotherapy as an independent protective factor in TRG 0–1 ( $HR = 0.22$ ,  $p = 0.015$ ), while vascular invasion was an adverse factor in TRG 2–3. Additionally, patients with pathological lymph node involvement (yPN+) benefited from adjuvant immunotherapy ( $HR = 0.41$ ,  $p = 0.019$ ). TRG and lymph node status may serve as valuable markers to identify ESCC patients who benefit from adjuvant immunotherapy, facilitating personalized postoperative treatment strategies.

**Keywords:** Esophageal cancer; Neoadjuvant therapy; Adjuvant therapy; Survival; Tumor regression grade; Lymph nodes

### 25COASOCT32:

**Title:** Textbook Outcomes and Minimally Invasive Techniques in Resectable Gallbladder Cancer: A Global Cohort Study,

Simone Cremona, Benedetto Ielpo, Marcello di Martino, Mauro Podda, Gregorio Di Franco, Niccolò Furbetta,

European Journal of Surgical Oncology, Volume 51, Issue 10, 2025, 110284,

<https://doi.org/10.1016/j.ejso.2025.110284>.

**Abstract:** Surgery for resectable gallbladder cancer (GbC) encompasses complex operative management, and evaluating surgical quality through textbook outcome (TO) is crucial. This study aimed to assess TO incidence and impact in a global cohort, identify independent predictors, and evaluate TO rates of minimally invasive (MI) techniques, including robotic

(ROB) and laparoscopic (LPS). This cohort study included patients undergoing curative-intent hepatectomy and lymphadenectomy for GbC (T1b–T3) from 2012 to 2023 in 41 hospitals. TO was defined as the absence of intraoperative transfusion, major complications, readmission, reoperation, or 90-day mortality, alongside negative margins and  $\geq 6$  retrieved lymph nodes. MI-TO additionally required no conversion. A 1:1 propensity score matching compared TO in open (OPEN) and MI approaches. Data were analyzed from July to November 2024. Among 667 patients (MI, 361; OPEN, 306), TO was achieved in 205 (30.7 %), with no difference between OPEN and MI. ROB independently increased TO (odds ratio, 4.297;  $p = 0.002$ ), achieving higher MI-TO (37.8 % vs. 23.2 %;  $p = 0.003$ ), better lymphadenectomy ( $\geq 6$  nodes: 55.3 % vs. 40.6 %;  $p = 0.009$ ), and fewer OPEN conversions (1.2 % vs. 13.7 %;  $p < 0.001$ ) than LPS. TO correlated with lower mortality (HR, 0.506;  $p = 0.001$ ) and recurrence (HR, 0.682;  $p = 0.027$ ). TO in resectable GbC is achieved in one-third of cases, with significant long-term benefits. MI is effective, with ROB outperforming LPS in MI-TO measures. These results establish a benchmark for centers to enhance outcomes.

**Keywords:** Textbook outcomes; Gallbladder cancer; Laparoscopy; Robotic; Open surgery; Radical cholecystectomy; Lymphadenectomy

### 25COASOCT33:

**Title:** Optimizing the pathological diagnosis of diffuse malignant peritoneal mesothelioma,

F.L. Nava, S. Kusamura, M. Shimonovitz-Moore, T. Cavalleri, D. Baratti, M. Guaglio, A.D. Cabras, G. Colletti, M. Deraco, M. Milione,

European Journal of Surgical Oncology, Volume 51, Issue 10, 2025, 110377,

<https://doi.org/10.1016/j.ejso.2025.110377>.

**Abstract:** Diffuse malignant peritoneal mesothelioma (DMPM) is the most common histological type of peritoneal mesothelioma (PM). Accurate histology and Ki67 assessment are crucial for treatment and prognosis, yet intra-tumoral heterogeneity may hinder preoperative diagnostics. A standardized diagnostic pathway is lacking. This study evaluates factors influencing the diagnostic accuracy on Ki67 and sarcomatoid component. This retrospective study analysed 98 patients (2008–2022). Concordance between preoperative and post-CRS-HIPEC histological subtype and Ki67-class ( $\leq 9$  % vs.  $> 9$  %) was estimated using the k-index. Fisher's exact test assessed the impact of biopsy type (core-needle vs. surgical), biopsy number (single vs. multiple), and specimen quantity (slides and blocks) on histotype and Ki67 concordance. Diagnostic performance was evaluated for both core-needle and surgical biopsy. Concordance was moderate for Ki67 (k-index = 0.4) and optimal for histotype (k-index = 0.8). No significant differences were found between biopsy types for histotype ( $p = 0.60$ ) or Ki67 ( $p = 1.00$ ). Diagnostic accuracy was unaffected by biopsy number ( $p = 0.16$  histotype,  $p = 0.50$  Ki67) or volume ( $p = 0.30$  histotype,  $p = 0.60$  Ki67). Surgical biopsy had Sensibility (Se) = 80 %, Specificity (Sp) = 98 %, Positive Predictive Value (PPV) = 80 %, Negative Predictive Value (NPV) = 98 % for sarcomatoid identification, and Se = 86 %, Sp = 82 %, PPV = 79 %, NPV = 88 % for Ki67. Core-needle biopsy showed Se = 60 %, Sp = 100 %, PPV = 100 %, NPV = 50 % for Ki67. Surgical biopsy remains the current gold standard for PM diagnosis, but core-needle biopsy could be considered for lesions accessible via interventional radiology.



**Keywords:** Peritoneal mesothelioma; Diagnostic pathway; Core-needle biopsy; Surgical biopsy; Ki67

**25COASOCT34:**

**Title:** Detection rate of sentinel lymph nodes in early-stage endometrial cancer according to age,

A. Giudici, G. Schivardi, T. Meschini, S. Restaino, A. Mariani, G. Bogani, F. Raspagliesi, D. Fumagalli,

European Journal of Surgical Oncology, Volume 51, Issue 10, 2025, 110380,

<https://doi.org/10.1016/j.ejso.2025.110380>.

**Abstract:** Sentinel lymph node (SNL) mapping plays a crucial role in staging patients with an apparent early-stage endometrial cancer. Older age may be associated with lower detection rates due to factors such as decreased lymphatic flow; but consensus is lacking. This study aims to evaluate the impact of age on the SNL detection rate in patients undergoing minimally invasive surgical staging for endometrial cancer. This multicenter retrospective study included apparent early-stage endometrial cancer patients undergoing minimally invasive surgical staging, including SLN mapping across four ESGO-accredited centers (2020–2023). Patients were categorized into two age groups: <65 years, defined as younger adults and ≥65 years, defined as older adults. Univariate and multivariate logistic regression models were used to identify predictors of bilateral mapping. Overall, 642 patients were identified: 342 (53.3%) patients were classified as younger adults and 300 (46.7%) as older adults. The overall bilateral SLN detection rate was 89.3%, with no or unilateral detection in 10.7% of patients. Older adults had a significantly lower bilateral detection rate than younger adults (85.0% vs. 93.0%,  $p = 0.005$ ). Multivariate analysis identified age ≥65 years as the only independent predictor of failed bilateral mapping (OR 2.2, 95 % CI 1.3–3.8,  $p = 0.003$ ). Other clinical, surgical, and pathological factors were not associated with mapping failure. Age ≥65 is independently associated with decreased bilateral SLN detection in early-stage endometrial cancer. Nevertheless, SLN biopsy remains a feasible and reliable staging method in older adults when performed using standardized techniques by experienced surgeons.

**Keywords:** Endometrial cancer; Sentinel lymph node; Detection rate; Age

**25COASOCT35:**

**Title:** Prognostic significance of molecular classification in high-risk endometrial cancer patients undergoing sentinel lymph node mapping,

Laguna Olmos Mariano, Padilla-Iserte Pablo, Diaz-Feijoo Berta, Arencibia Sánchez Octavio, European Journal of Surgical Oncology, Volume 51, Issue 10, 2025, 110385,

<https://doi.org/10.1016/j.ejso.2025.110385>.

**Abstract:** The adoption of selective sentinel lymph node biopsy (SLNB) as a viable alternative to lymphadenectomy, along with the redefinition of nodal risk groups based on molecular classification, has significantly changed the management of early-stage, high-risk preoperative endometrial cancer. A retrospective, multicenter study was conducted under the auspices of the Spanish Gynecologic Oncology Group to evaluate recurrence rates and oncologic outcomes in patients stratified by molecular risk. Three groups were compared: SLNB alone (G1), SLNB combined with pelvic and/or para-aortic lymphadenectomy (G2),

and pelvic and/or para-aortic lymphadenectomy without SLNB (G3). The primary endpoint was recurrence rate; secondary endpoints included disease-free survival (DFS), overall survival (OS), recurrence patterns. A total of 221 patients from 14 centers were included, with a median follow-up of 24.4 months (IQR 17–42). Forty-four patients (19.9 %) experienced recurrence. Relapse rates were 15.4 % in G1, 15.8 % in G2, and 22.2 % in G3 ( $p = 0.479$ ). DFS rates were 84.6 % in G1, 84.1 % in G2, and 77.8 % in G3 ( $p = 0.56$ ). OS rates were 94.2 %, 90.9 %, and 92.6 %, respectively ( $p = 0.651$ ). Among the 44 patients with documented recurrence, seven had nodal recurrences, with only two occurring in the group managed with SLNB alone. In this study, patients with early-stage, high-risk preoperative endometrial cancer—classified by molecular subgroups—showed no significant differences in relapse rates, disease-free survival, or overall survival across the three management strategies. Further prospective studies with longer follow-up are warranted to validate these preliminary findings.

**Keywords:** Endometrial carcinoma; Molecular classification; Sentinel lymph node biopsy; Recurrence rate; Recurrence-free survival; Overall survival

### 25COASOCT36:

**Title:** Tumor-Boundary Response Index (TBRI)- A promising indicator for predicting outcomes in colorectal liver metastases receiving neoadjuvant therapy: Insights from a single-center retrospective study,

Yin-Chen Gu, Mei Yang, Yan Geng, Bo Zhang, Bao-Rui Tao, Sen-Feng Ying, Rong-Quan Sun,

European Journal of Surgical Oncology, Volume 51, Issue 10, 2025, 110291,

<https://doi.org/10.1016/j.ejso.2025.110291>.

**Abstract:** Tumor regression grade (TRG) and histopathological growth pattern (HGP) reflect the response of colorectal liver metastases (CRLM) to neoadjuvant therapy (NAT) from the perspectives of the tumor and its microenvironment, respectively. Based on these two indicators, this study aimed to develop a prognostic index for CRLM undergoing surgery after NAT. 237 patients who underwent curative-intent resection following NAT from 2012 to 2022 were selected. Correlations between HGP and TRG were assessed. Cox regression analyses were employed to determine the optimal cut-off point for constructing the Tumor-Boundary Response Index (TBRI). Kaplan-Meier analyses of overall survival (OS), disease-free survival (DFS) and hepatic relapse-free survival (hRFS) were used to evaluate the prognostic value. The predictive ability of TBRI, Fong's clinical risk score (CRS) and Genetic And Morphological Evaluation (GAME) score was compared by time-dependent receiver operating characteristic (ROC) analysis. Calibration plot was utilized to assess the goodness of fit. Desmoplastic HGP (dHGP) exhibited an inverse correlation with TRG in lesions. TBRI stratified patients into four tiers based on whether HGP is predominant desmoplastic ( $>50\%$ ) and whether TRG is  $\leq 3$ , showing significant prognostic value in OS, DFS and hRFS (median OS for TBRI 1–4: 78.6, 42.6, 27.8 and 22.5,  $p < 0.001$ ; median DFS for TBRI 1–4: 22.4, 12.4, 10.9 and 6.5 months,  $p < 0.001$ ; median hRFS for TBRI 1–4: 29.2, 12.9, 10.9, 6.8,  $p < 0.001$ ). Additionally, TBRI surpassed CRS and GAME score with superior discriminatory power and displayed exceptional consistency. TBRI demonstrated a promising ability to predict the postoperative survival of CRLM patients receiving NAT.

**Keywords:** Tumor-Boundary response index; Colorectal liver metastases; Neoadjuvant therapy; Histopathological growth pattern; Tumor regression grade

**25COASOCT37:**

**Title:** Video-assisted total transthoracic liver resection for colorectal liver metastasis, safety and feasibility,

P.D. Gobardhan, E.J. Veen, A.M. Rijken, N. Ayez,

European Journal of Surgical Oncology, Volume 51, Issue 10, 2025, 110389,

<https://doi.org/10.1016/j.ejso.2025.110389>.

**Abstract:** Laparoscopic resection of colorectal liver metastasis (CRLM) located in posterosuperior segments of the liver remains challenging. The primary aim of this study was to evaluate the safety and feasibility of video-assisted total thoracoscopic approach. The secondary aim was to assess the short-term outcomes associated with this technique. Patients undergoing a video-assisted total thoracoscopic resection of CRLM between 2016 and 2020 at the Amphia Hospital were included. Retrospective assessment of complication rate, conversion rate, postoperative outcomes (radicality of resection) and short-term oncological outcomes (disease-free survival) was performed. A total of 15 patients were included in the study. In 14 patients a totally transthoracic liver resection was performed. A wedge resection was not feasible in 1 patient due to difficult anatomy, this patient underwent an ablation. Peri-operative and short- and long-term outcomes are comparable to abdominal laparoscopic liver resections. No postoperative deaths were observed within 90 days. The video-assisted total transthoracic approach is a safe and feasible option for posterosuperior liver metastasis surgery and further studies are warranted to assess the long-term outcomes of this approach.

**Keywords:** Total transthoracic laparoscopic liver surgery

**25COASOCT38:**

**Title:** Immunological and prognostic significance of vessels encapsulating tumor clusters (VETC) in hepatocellular carcinoma,

Tomohiko Taniai, Koichiro Haruki, Juha P. Väyrynen, Kazutaka Gomisawa, Shun Sato, Kenei Furukawa,

European Journal of Surgical Oncology, Volume 51, Issue 10, 2025, 110381,

<https://doi.org/10.1016/j.ejso.2025.110381>.

**Abstract:** Vessels encapsulating tumor clusters (VETC) has been identified as a poor prognostic indicator in hepatocellular carcinoma (HCC). However, the detailed tumor microenvironment in VETC-positive HCC remains unclear. We investigated the prognostic significance of VETC and elucidated the immune cell profile of VETC-positive HCC. We enrolled 229 patients who underwent hepatic resection for HCC. We performed immunohistochemistry for CD34, CD8 and CD163, combined with digital image analysis, on resected specimens to evaluate their immune profile in both the tumor center and invasive margin. The relationships between VETC and clinicopathological features, including immune cell densities were investigated. A total of 78 patients (34 %) had VETC-positive HCC. Univariate and multivariate analyses revealed that VETC was significantly associated with poor disease-free ( $p = 0.001$  and  $p = 0.023$ ) and overall survival ( $p = 0.001$  and  $p = 0.032$ ). VETC-positive HCC exhibited higher serum PIVKA-II levels (217 mAU/ml vs. 40 mAU/ml,  $p = 0.001$ ), moderate/poor differentiation (92 % vs. 75 %,  $p = 0.002$ ), larger tumor size

(4.8 cm vs. 3.0 cm,  $p < 0.001$ ), and microvascular invasion (32 % vs. 11 %,  $p < 0.001$ ). The densities of CD8+ cells and CD163+ cells in the tumor center were significantly lower in VETC-positive HCC compared with those in VETC-negative HCC ( $p < 0.001$  and  $p = 0.024$ , respectively). A similar trend was observed in densities of CD8+ cells and CD163+ cells in the invasive margin ( $p = 0.061$  and  $p = 0.064$ , respectively). VETC may regulate immune cell infiltration into tumors, especially in the tumor center, and serves as a poor prognostic indicator in HCC.

**Keywords:** Vessels encapsulating tumor clusters; Tumor microenvironment; Hepatocellular carcinoma

#### 25COASOCT39:

**Title:** Clinical determinants of outcome following pelvic exenteration for locally advanced or locally recurrent rectal cancer,

Laura E. Gould, E Toby Pring, Alison Wallace, Nicola Hodges, Elaine M. Burns, Colin W. Steele, Campbell SD. Roxburgh, John T. Jenkins,

European Journal of Surgical Oncology, Volume 51, Issue 10, 2025, 110347,

<https://doi.org/10.1016/j.ejso.2025.110347>.

**Abstract:** To assess the impact of clinical factors on survival in patients undergoing pelvic exenteration (PE) with curative intent for locally advanced rectal cancer (LARC) or locally recurrent rectal cancer (LRRC). Retrospective analysis of consecutive patients undergoing PE between January 2008 and July 2021 at a tertiary referral centre. Baseline characteristics, comorbidities and neoadjuvant therapy were recorded. Influence of comorbidity was assessed using the validated Charlson comorbidity index and ASA performance status (ASA). Preoperative inflammation was quantified using clinically relevant values derived from haemoglobin concentration, serum albumin, neutrophil to lymphocyte ratio (NLR), platelet to lymphocyte ratio (PLR), and modified Glasgow Prognostic Score (mGPS). Influence of each factor on overall survival (OS), disease free survival (DFS) and local recurrence free survival (LRFS) were assessed using Cox regression analysis. 388 of 506 resections met the inclusion criteria over this period. 256 PE for LARC and 132 PE for LRRC. Only mGPS  $\geq 1$  and ASA III were significant on multivariate analysis as negative prognostic markers for OS, DFS and LRFS in patients with LARC with Hazard ratios ranging from 1.94 to 3.82. For patients with LRRC ASA III was associated with reduced OS ( $p = 0.005$ ) and LRFS ( $p = 0.039$ ). Despite broadly similar baseline clinical characteristics for LARC and LRRC there are significant differences in the effect of these factors upon long term outcomes. Key clinical factors that influence survival are readily identifiable and easy to measure preoperatively. These factors may help stratify and quantify the risk of recurrence in LARC; however, further prognostic clinical markers for LRRC remain to be fully elucidated.

**Keywords:** Pelvic exenteration; Rectal cancer; Locally advanced; Recurrent; Outcome; Survival

#### 25COASOCT40:

**Title:** Impact of frailty on surgical and survival outcomes following cytoreductive surgery with hyperthermic intraperitoneal chemotherapy,

Zirong Bai, Laura Barker, Cherry Koh, Michael Solomon, Rihan Shahab, Kate Alexander,

European Journal of Surgical Oncology, Volume 51, Issue 10, 2025, 110323,

<https://doi.org/10.1016/j.ejso.2025.110323>.

**Abstract:** Frailty is increasingly recognised as a predictor of poor surgical outcomes. However, its impact in determining outcomes following cytoreductive surgery (CRS) with hyperthermic intraperitoneal chemotherapy (HIPEC) remains underreported. Thus, this study aims to determine the association between preoperative frailty and surgical outcomes including survival in patients undergoing CRS + HIPEC. This retrospective cohort study included patients who underwent CRS + HIPEC at the Royal Prince Alfred Hospital between May 2017 and June 2024. Frailty was assessed preoperatively using the Clinical Frailty Scale (CFS), with patients classified as frail (CFS  $\geq 4$ ) or not frail (CFS  $< 4$ ). Other outcomes included surgery duration, intensive care unit (ICU) and hospital stays, postoperative complications, recurrence rates, and survival. Subgroup analyses were performed based on age group ( $< 65$  years versus  $\geq 65$  years). Of the 466 patients included, 60 (12.9 %) were classified as frail. Frailty was associated with longer surgery durations (median: 10.0 vs. 9.8 h;  $p = 0.015$ ), longer ICU stay (median: 5.5 vs. 5.0 days;  $p = 0.037$ ), hospital stay (median: 21.0 vs. 17.0 days;  $p < 0.001$ ), and worst survival outcomes ( $p = 0.002$ ). Age-stratified analysis revealed that frailty was associated with prolonged hospital stay across both subgroups. Among patients aged  $\geq 65$  years, frailty was also significantly associated with longer surgery durations ( $p < 0.001$ ) and length of ICU stay ( $p = 0.013$ ). Preoperative frailty was associated with worse postoperative outcomes in patients undergoing CRS + HIPEC. These findings highlight the importance of routine frailty assessments to guide surgical planning and improve patient care. Future research should explore interventions such as prehabilitation to mitigate the adverse effects of frailty and optimise outcomes in this vulnerable population.

**Keywords:** Frailty; Cytoreductive surgery; Postoperative outcomes; Survival; Cancer

## 25COASOCT41:

**Title: Oncological and functional outcomes of proximal versus total gastrectomy for advanced proximal gastric cancer: A propensity score-matched study,**

Hung-Hsuan Yen, Young-Jen Lin, Chun-Chieh Huang, Chi-Chuan Yeh, Po-Chu Lee, I-Rue Lai,

European Journal of Surgical Oncology, Volume 51, Issue 10, 2025, 110370,

<https://doi.org/10.1016/j.ejso.2025.110370>.

**Abstract:** Proximal gastrectomy (PG) is considered an alternative to total gastrectomy (TG) for proximal gastric cancer (PGC), but its use in advanced stages remains debated. Additionally, data on both oncological and functional outcomes are limited. We conducted a retrospective study on patients with pathological stage II-III PGC undergoing PG with additional distal lymph node sampling or TG with standard D2 lymphadenectomy from 2013 to 2023. Propensity score-matching was applied to adjust for tumor size and stage between these two groups at a 1:1 ratio. We evaluated the procedural safety, oncological, and functional outcomes. After matching, 48 patients in each group were analyzed, with comparable clinicopathological characteristics. A temporal trend toward increased use of laparoscopic PG was noted. PG was associated with significantly more laparoscopic surgeries, shorter hospital stays and less blood loss compared to TG. Postoperative complication rates were similar between the two groups. Five-year overall (59.0 % for PG vs. 44.2 % for TG;  $p = 0.494$ ) and recurrence-free (46.5 % for PG vs. 48.2 % for TG;  $p = 0.981$ )



survival rates were comparable. In multivariate Cox regression analysis, tumor size >7 cm emerged as the only independent risk factor for overall survival, after adjustment for gastrectomy type and other high-risk features, including Borrmann type IV and serosal invasion. Functional outcomes, including weight and hemoglobin changes, showed no significant differences between groups within 24 months postoperatively. PG provides comparable oncological outcomes to TG for advanced PGC in carefully selected patients. However, no significant long-term functional benefits were observed.

**Keywords:** Advanced proximal gastric cancer; Proximal gastrectomy; Total gastrectomy; Oncological outcomes; Functional outcomes

## 25COASOCT42:

**Title:** Implementing robot-assisted minimally invasive gastrectomy (RAMIG) for gastric cancer in a European tertiary referral center,

Lianne Triemstra, Cas de Jongh, Hylke J.F. Brenkman, Bas L.A.M. Weusten, Jan Erik Freund, Richard van Hillegersberg, Jelle P. Ruurda,

European Journal of Surgical Oncology, Volume 51, Issue 10, 2025, 110342,

<https://doi.org/10.1016/j.ejso.2025.110342>.

**Abstract:** Our European tertiary referral center implemented robot-assisted minimally invasive gastrectomy (RAMIG) in September 2020, following experience with robot-assisted esophagectomy and multiquadrant surgery using the DaVinci Xi robot. RAMIG implementation was evaluated. This single-center prospective cohort study compared 111 MIG patients (2014–2023) with the initial 75 RAMIG patients (2020–2023), operated by two experienced robotic upper-GI surgeons. After propensity-score-matching, surgical, oncological, and textbook outcomes for overall/distal/total RAMIG and MIG were compared. Cumulative sum (CUSUM) analysis assessed learning curves for operating time and nodal yield. Additionally, the transition from laparoscopic-circular stapled (MIG/RAMIG) to robot-assisted handsewn anastomosis (RAMIG-only) was evaluated. After propensity-score-matching, 75 RAMIG and 75 MIG patients were analyzed; 68% underwent total gastrectomy, and 78% neoadjuvant therapy. Postoperative complications, blood loss, hospitalization, R0-resections, and textbook outcomes were similar between groups ( $p > 0.05$ ). Distal RAMIG showed longer median operating time (214 versus 191 min;  $p = 0.032$ ), but less severe complications (13 % versus 38 % grade  $\geq 3$ A;  $p = 0.041$ ). Total RAMIG showed higher median nodal yield (35 versus 22 nodes;  $p < 0.001$ ). CUSUM-analysis showed plateaus for distal/total RAMIG at cases 10 and 24 for operating time, and 8 and 17 for nodal yield. Robot-assisted handsewn esophagojejunostomy seemed to show reduced anastomotic leakage (9% versus 28%), postoperative complications (45% versus 59%), and 30-day mortality (0% versus 5%). Implementing RAMIG in our tertiary referral center resulted in similar perioperative outcomes with improved nodal yield, despite longer operating times. The robotic technique facilitated modification to handsewn esophagojejunostomy. Short learning curves (8–24 cases) for experienced robotic surgeons support adaption towards RAMIG.

**Keywords:** Implementation; RAMIG; Gastrectomy; Gastric cancer; Robot-assisted handsewn anastomosis

**25COASOCT43:**

**Title:** Randomized controlled trial comparing single-use negative-pressure wound therapy (sNPWT) with standard dressings during tissue expander-to-implant exchanges. Assessment of risk factors for impaired wound healing and clinical indications for sNPWT,

Maja Molska, Magdalena Wojciech, Karolina Pieszko, Sławomir Cieśla, Dawid Murawa,  
European Journal of Surgical Oncology, Volume 51, Issue 10, 2025, 110355,  
<https://doi.org/10.1016/j.ejso.2025.110355>.

**Abstract:** Breast reconstruction is a key step in the physical and social recovery of breast cancer patients. Optimal wound healing is crucial not only for aesthetic outcomes but also for the uninterrupted continuation of adjuvant oncologic therapy, which can significantly impact overall prognosis. The study compared single-use negative pressure wound therapy (sNPWT) with standard dressings during the second stage of breast reconstruction - tissue expander-to-implant exchanges. Additionally, it aimed to identify factors associated with an increased risk of impaired wound healing and postoperative complications, to determine clinical conditions in which the prophylactic use of sNPWT is most beneficial. The study evaluated 38 women undergoing the second stage of two-stage breast reconstruction after unilateral mastectomy. Each patient received either sNPWT or a standard dressing postoperatively, with allocation randomized and independent of both physician and patient. Scar characteristics, including elasticity, temperature, healing, and appearance, were assessed. A significant difference in skin elasticity in favor of sNPWT was observed after 7 days, while the most pronounced difference was seen after 6 months (mean 0.688 vs. 0.480). No significant differences were found in temperature. Visually, sNPWT-treated scars appeared narrower and less prominent. The mathematical model identified radiotherapy as the only factor significantly associated with poor healing (p-value = 0.025). Compared to standard dressings, sNPWT demonstrates clear advantages in improving scars' elasticity and aesthetic appearance. Its application significantly reduces postoperative complications, including the risk of implant loss, making it a valuable option in breast reconstruction.

**Keywords:** Breast reconstruction; sNPWT; Scar; Wound healing; Mathematical model; Variable selection

**25COASOCT44:**

**Title:** Cosmetic outcome and patient satisfaction following percutaneous thermal ablation of early-stage breast cancer; results of an open label randomized phase 2 trial,

Sophie M. Wooldrik, Elles M.F. van de Voort, Gerson M. Struik, Bart J.M. Schouten,  
European Journal of Surgical Oncology, Volume 51, Issue 10, 2025, 110305,  
<https://doi.org/10.1016/j.ejso.2025.110305>.

**Abstract:** The aim of the present study is to assess patient reported cosmetic outcome and satisfaction following percutaneous thermal ablation and subsequent breast-conserving surgery. Cosmetic outcome and patient satisfaction were assessed in postmenopausal women diagnosed with unilateral invasive cT1N0M0 breast cancer who participated in a randomized phase 2 treat-and-resect trial comparing the efficacy of radiofrequency ablation (RFA), microwave ablation (MWA) and cryoablation (CA). Cosmetic outcome was measured subjectively with the BCTOS-13 and the Beast-Q questionnaires (0–100 score), and objectively with BCCT.core software at baseline, after thermal ablation and after surgery.

Patient satisfaction was defined as satisfaction with the technique (4 point scale), recommendation of the technique to others (yes/no), and the preference for surgery of thermal ablation after completion of both treatments. Forty-one patients were included in the study. The overall median cosmetic outcome was good after thermal ablation, and intermediate after surgery (1.6 vs 1.8;  $P = 0.07$ ). Most domains of the BREAST-Q were scored higher after thermal ablation, 95 % of patients were very satisfied or satisfied with the technique, and 91 % would prefer thermal ablation over surgery. Differences between the different techniques were limited. On the BCCT.core, 94 % of cases were rated as good or excellent after thermal ablation, compared to 80 % after surgery. The present study demonstrates that patient reported and objectivated cosmetic outcomes are good both after thermal ablation and breast-conserving surgery. Patient satisfaction was outstanding following thermal ablation, with a preference for thermal ablation observed in a group of patients who underwent both treatment options.

**Keywords:** Radiofrequency ablation; Cryosurgery; Cryoablation; Microwave ablation; Early-stage breast cancer; Breast Neoplasms; Minimally invasive treatment; Cosmetic outcome; Patient satisfaction

## 25COASOCT45:

**Title:** The Clock and the Scalpel: Does delayed Robot-assisted radical prostatectomy affect pathological progression and upgrading in prostate cancer?,

Shigeki Koterazawa, Takayuki Goto, Masashi Kubota, Kei Mizuno, Takayuki Sumiyoshi, Naoto Takaoka,

European Journal of Surgical Oncology, Volume 51, Issue 10, 2025, 110357,

<https://doi.org/10.1016/j.ejso.2025.110357>.

**Abstract:** We investigated whether surgical delay may be associated with histological progression in patients treated with robotic-assisted radical prostatectomy (RARP) for prostate cancer (PCa). Patients diagnosed with localized (cT1-2cN0cM0) PCa who underwent RARP between 2011 and 2022 were retrospectively reviewed. Surgical delay was categorized into four groups based on the time from biopsy to RARP: 0–3, 4–6, 7–12, and >12 months. The primary outcome was adverse pathological outcomes (pT3–T4 disease, lymph node invasion, or positive surgical margin). The secondary outcome was Gleason grade group (GG) upgrading. A total of 2362 (39.3 %) patients underwent RARP within 0–3 months after biopsy, 3045 (50.6 %) within 4–6 months, 454 (7.5 %) within 7–12 months, and 154 (2.6 %) after more than 12 months. Patients who underwent RARP within 4–6 months (OR = 0.95, 95 % CI 0.85–1.06), 7–12 months (OR = 0.91, 95 % CI 0.76–1.12), and >12 months (OR = 1.04, 95 % CI 0.73–1.47) did not have significantly increased odds of adverse pathological outcomes than those undergoing surgery within 0–3 months. Subgroup analyses for the low-to-intermediate-risk and high-risk groups showed no significant differences in adverse pathology outcomes. However, surgical delays >6 months were significantly associated with increased likelihood of GG upgrading. Although delayed RARP did not compromise adverse pathological outcomes, it was a risk factor for GG upgrading, particularly beyond 6 months. Thus, prolonged delays should be approached with appropriate monitoring.

**Keywords:** Grade group upgrading; Lymph node invasion; Positive surgical margin; pT3–T4 disease; Surgical delay

**25COASOCT46:**

**Title: Prognostic impact of total (Ipsilateral) retroperitoneal lipectomy vs. complete resection in retroperitoneal liposarcoma: A retrospective cohort study with nomogram,** Qisheng Hao, Qingze Li, Hongliang Liu, Kang Fu, Lichao Cha, Ke Yao, Mingkai Gong, Guofei Dong,

European Journal of Surgical Oncology, Volume 51, Issue 10, 2025, 110374,

<https://doi.org/10.1016/j.ejso.2025.110374>.

**Abstract:** Retroperitoneal liposarcoma (RPLS), the most common retroperitoneal sarcoma, poses significant therapeutic challenges due to high recurrence rates. This study evaluates the long-term outcomes of total (Ipsilateral) retroperitoneal lipectomy (TRL) versus complete resection (CR) and develops prognostic nomograms. A retrospective analysis was conducted on 208 RPLS patients who underwent surgical treatment at the Department of Retroperitoneal Tumor Surgery, Affiliated Hospital of Qingdao University, between January 2015 and December 2022. Patients were stratified into the Complete Resection (CR) group (n = 152) and the TRL group (n = 56). Kaplan-Meier analysis and log-rank tests were used to compare overall survival (OS) and recurrence-free survival (RFS). Patients were randomly divided into training (70 %) and validation (30 %) cohorts. Univariate and multivariate Cox regression analyses identified independent prognostic factors, which were incorporated into nomograms. Model performance was assessed using the area under the curve (AUC), concordance index (C-index), calibration curves, and decision curve analysis (DCA). Among 208 included patients, the TRL group demonstrated significantly higher OS and RFS rates compared to the CR group. Surgical approach, subtype, and types of tumor occurrence were independent predictors of OS. Surgical approach, subtype, and duration significantly influenced RFS. TRL may improve long-term survival outcomes in RPLS patients and could serve as a potential independent protective prognostic factor, though this requires validation through multicenter external studies. The developed nomograms for OS and RFS show promising predictive performance and potential clinical application value, but their generalizability needs to be further confirmed by external validation.

**Keywords:** Retroperitoneal tumor; Liposarcoma; Prognostic model; Total (ipsilateral) retroperitoneal lipectomy; Surgical oncology

**25COASOCT47:**

**Title: Hepatic clearance of remnant liver for assessing lobar difference of liver function in patients with perihilar cholangiocarcinoma: single center experience,**

Atsushi Miki, Yasunaru Sakuma, Jun Watanabe, Hideki Sasanuma, Atsushi Shimizu, Takumi Teratani,

European Journal of Surgical Oncology, Volume 51, Issue 10, 2025, 110297,

<https://doi.org/10.1016/j.ejso.2025.110297>.

**Abstract:** Perihilar cholangiocarcinoma with large hepatic resection is associated with high risk for morbidity and mortality. To improve outcomes, assessment of remnant liver function is crucial. A total of 70 patients with perihilar cholangiocarcinoma were examined retrospectively. Liver function was evaluated <1 month preoperatively by hepatic clearance of remnant liver using <sup>99m</sup>Tc-galactosyl serum albumin (GSA) scintigraphy and computed tomography, and clinicopathological data and outcomes were analyzed in comparison GSA scintigraphy with liver function test based on computed tomography volumetry. There was no

postoperative 90-day mortality, with 10 patients of posthepatectomy liver failure (PHLF) Grade A, 10 of Grade B, and 1 of Grade C. Area under the curve of receiver operating curve showed better prediction power for PHLF compared to remnant liver volume/body surface area or future liver remnant/body weight, especially in patients with incomplete change of liver function. In univariable analysis,  $<150$  ml/min cutoff of hepatic clearance of remnant liver and  $>1750$  ml intra-operative blood loss were significant risk factors for PHLF. In multivariable analysis,  $<150$  ml/min cutoff was a significant risk factor for PHLF. The area under the curve of hepatic clearance of remnant liver indicated better predictivity in patients with incomplete change of liver function compared with complete change of liver function. The hepatic clearance of remnant liver may have predictive power in patients with incomplete changes in liver function compared to computed tomography-based methods. Preoperative measurement of hepatic clearance of remnant liver may assist in risk stratification for surgical management.

**Keywords:** Perihilar cholangiocarcinoma; GSA scintigraphy; Liver failure; Outcome; Liver function test; Portal vein embolization

## 25COASOCT48:

**Title:** Preoperative ASAP score predicts recurrence and survival following curative hepatic resection for hepatitis B virus-related hepatocellular carcinoma: A multicenter cohort study,

Dongxu Yin, Zixuan Wang, Chao Li, Huixuan Fan, Zichao Tu, Yongkang Diao, Zijie Tang, European Journal of Surgical Oncology, Volume 51, Issue 10, 2025, 110361,

<https://doi.org/10.1016/j.ejso.2025.110361>.

**Abstract:** The ASAP score, integrating age, sex, alpha-fetoprotein (AFP), and protein induced by vitamin K absence or antagonist-II (PIVKA-II), has demonstrated value for early detection of hepatocellular carcinoma (HCC) in patients with chronic hepatitis B virus (HBV) infection. This study sought to assess whether the ASAP score could also predict recurrence and survival following curative resection of HBV-related HCC. This multicenter study included patients undergoing curative hepatic resection for HBV-related HCC. The ASAP score was calculated preoperatively. The primary endpoints were time-to-recurrence (TTR) and overall survival (OS). The optimal ASAP cutoff was identified using X-tile analysis. Multivariate Cox regression model was used to evaluate the independent prognostic significance of the ASAP score. In total, 752 patients were analyzed. The optimal cutoff value for preoperative ASAP was 4.8. Patients in the high ASAP group ( $\geq 4.8$ ) had significantly higher recurrence rates (5-year: 73.4 % vs. 52.1 %,  $P < 0.001$ ) and poorer survival outcomes (5-year OS: 30.7 % vs. 58.1 %,  $P < 0.001$ ) compared with those in the low ASAP group ( $< 4.8$ ). On multivariate Cox regression analysis, a high ASAP score remained independently predictive of TTR (HR 1.264; 95 % CI 1.010–1.582;  $P = 0.031$ ) and OS (HR 1.266; 95 % CI 1.017–1.608;  $P = 0.033$ ). Moreover, the ASAP score exhibited good predictive performance for both TTR and OS. Preoperative ASAP score independently predicts recurrence and survival outcomes in patients undergoing curative resection for HBV-related HCC. Given its simplicity and accessibility, the ASAP score may facilitate individualized postoperative surveillance and improved risk stratification for these patients.

**Keywords:** Hepatocellular carcinoma; Alpha-fetoprotein; Protein induced by vitamin K absence or antagonist-II; Hepatitis B virus; Survival; Recurrence



**25COASOCT49:**

**Title: Interpretable machine learning model for predicting perioperative Clavien-Dindo III/IV complications of rectal cancer anterior resection after neoadjuvant therapy: a real-world study,**

Boyue Kang, Yihuan Qiao, Jiawei Song, Zecheng Zhang, Qi Wang, Jun Zhu, Jipeng Li,

European Journal of Surgical Oncology, Volume 51, Issue 10, 2025, 110365,

<https://doi.org/10.1016/j.ejso.2025.110365>.

**Abstract:** This study constructed machine learning (ML) models based on 10 different algorithms using the ratio of preoperative and postoperative hematological indicators to predict the risk factors for perioperative Clavien-Dindo grade III/IV complications after anterior resection in rectal cancer patients who underwent neoadjuvant therapy. Rectal cancer patients undergoing anterior resection after neoadjuvant therapy at the Xijing Hospital of Digestive Diseases were retrospectively collected from January 2011 to December 2021. Receiver Operating Characteristic (ROC) curves, calibration curve, Decision Curve Analysis (DCA), accuracy, sensitivity, specificity, positive predictive value (PPV), negative predictive value (NPV) and F1 score were used to evaluate the model performance. The Shapley Additive exPlanation (SHAP) algorithm was used to interpret the feature importance of the best model. The dynamic hematological ratio characteristics before and after surgeries were integrated to construct the predictive models and identify the optimal one. Gradient Boosting Machine (GBM) was considered the best-performing model with the area under the test set curve (AUC: 0.939, 95 %CI: 0.905–0.972), accuracy: 0.903, sensitivity: 0.836, specificity: 0.907. The interpretable SHAP algorithm revealed that hemoglobin, red blood cell ratio and serum calcium ratio were the crucial factors influencing the predictions of the model. GBM was identified as the optimal predictive model. This model, by predicting the occurrence of perioperative Clavien-Dindo III/IV complications in patients who underwent neoadjuvant therapy and anterior resection, has identified the significant role of hemoglobin, red blood cell ratio and serum calcium ratio, providing guidance for clinical practice. The integration of SHAP provides a clear interpretation of the model's predictions.

**Keywords:** Neoadjuvant therapy; Rectal cancer; Machine learning; SHAP; Surgery

**25COASOCT50:**

**Title: Defining replicability and evaluating reliability of intra-operative cytological bone margins assessment. A study to strengthen previous findings in advanced oral cancer,**

Giuditta Mannelli, Chiara Marzi, Lara Comini, Annarita Palomba, Tiziana Tatti,

European Journal of Surgical Oncology, Volume 51, Issue 10, 2025, 110308,

<https://doi.org/10.1016/j.ejso.2025.110308>.

**Abstract:** Curative intent in advanced oral cavity squamous cell cancer (OCSCC) implies clear resection margins (R0). Controlling resection margin is a pivotal point as R status, which is under the direct control of surgeons, continues to be the most important predictor for survival. However, intra-operative bone resection margin analysis still presents technical challenges preventing its routine clinical application. To introduce intra-operative cytological bone margins analysis by overcoming the previously reported technical limitations and confirming its reproducibility and reliability, to support intra-operative microscopically-guided resection. A total amount of 296 cytological samples and 148 cytological controls were obtained intra-operatively from surgical resection bone-margins in 74 patients affected

by OCSCC with pre-operative suspicious bone cancer infiltration. Both techniques ICAB (intra-operative cytological assessment of bone margins) and ICICAB (intra-operative cell isolation cytological assessment of bone margins) were compared with the corresponding histological final report and evaluated as potential diagnostic intra-operative tool. ICICAB demonstrated perfect accuracy, correctly identifying all positive and negative results as confirmed by the histological exam. Accordingly ICICAB could reliably identify cancer cells from the region of interest (ROI) analyzed. The development and assessment of a reproducible and standard intra-operative bone margins analysis, would help in reducing the discrepancy between pre-operative and final cancer-infiltrative bone status, with a following significant difference in both functional and survival outcomes for advanced OCSCC patients, through an additional reduction in costs and time-consuming rates.

**Keywords:** Oral cancer; Bone infiltration; Cytology; Intraoperative surgical margin control; Bone margins

#### 25COASOCT51:

**Title:** The role of hyperthermia on abdominal tissue concentrations of cisplatin during and after intraperitoneal chemotherapy – insights from a porcine model,

Christina Harlev, Mats Bue, Elisabeth Krogsgaard Petersen, Mads Kristian Duborg Mikkelsen,

European Journal of Surgical Oncology, Volume 51, Issue 10, 2025, 110378,

<https://doi.org/10.1016/j.ejso.2025.110378>.

**Abstract:** Epithelial ovarian cancer remains a leading cause of mortality among gynecological malignancies, with a high incidence of peritoneal carcinomatosis at diagnosis. Hyperthermic intraperitoneal chemotherapy (HIPEC) has emerged as a promising treatment for advanced-stage epithelial ovarian cancer, potentially improving recurrence-free and overall survival rates. The study aimed to investigate the impact of hyperthermia on cisplatin concentrations in healthy abdominal tissues by comparing HIPEC with normothermic intraperitoneal chemotherapy (NIPEC) in a novel porcine model. Sixteen cancer-free pigs underwent cytoreductive surgery followed by either HIPEC or NIPEC, with cisplatin administered intraperitoneally. Microdialysis was used to measure local cisplatin concentrations in various abdominal tissues over a 6-h period. The analysis revealed no statistically significant or clinically relevant difference in cisplatin concentrations between the HIPEC and NIPEC groups. In both groups, cisplatin concentrations were consistently higher in the peritoneum than in other tissues, and plasma levels were significantly lower than those in abdominal tissues. Hyperthermia did not enhance cisplatin's tissue penetration, suggesting that NIPEC may be an effective alternative to HIPEC, particularly for fragile and elderly patients. Future studies should investigate whether hyperthermia improves cisplatin delivery and cytotoxicity in tumor-infiltrated peritoneal tissues.

**Keywords:** Cisplatin; Intraperitoneal chemotherapy; HIPEC; NIPEC; Microdialysis; Pharmacokinetics

#### 25COASOCT52:

**Title:** Pretracheal (No.106pre) lymph node metastasis in esophageal carcinoma: A sign of widespread disease progression, but potentially treatable as oligometastatic disease through neoadjuvant chemotherapy followed by surgery - A multicenter cohort study,

Shota Igaue, Takeo Fujita, Junya Oguma, Koshiro Ishiyama, Kazuma Sato, Daisuke Kurita, Yuto Kubo,

European Journal of Surgical Oncology, Volume 51, Issue 10, 2025, 110289,

<https://doi.org/10.1016/j.ejso.2025.110289>.

**Abstract:** Oligometastatic disease in esophageal carcinoma includes metastases to distant organs and extra-regional lymph nodes. Pretracheal lymph node metastasis (No. 106pre in the Japanese classification) is classified as an M1 lymph node metastasis and has a poor prognosis. However, documentation is limited and has often focused on heterogeneous cohorts from earlier times. The present study examines the outcomes of pretracheal lymph node resection in modern neoadjuvant therapy followed by surgery. This multicenter retrospective cohort study, conducted at two cancer centers in Japan, included esophageal carcinoma patients with clinical pretracheal lymph node metastasis who underwent neoadjuvant chemotherapy followed by esophagectomy. Short-term and long-term outcomes were analyzed. In total, 110 patients were included, of whom 94 were negative, and 16 were positive for pathological pretracheal lymph node metastasis (p106pre(-) and p106pre(+)). The 106pre(+) group exhibited more advanced disease and a higher average number of metastatic lymph nodes (10.0). The 3-year overall survival rate was 66.6 % in the p106pre(-) group and 29.9 % in the p106pre(+) group, significantly poorer but not as poor as previously reported. Multivariate analysis identified ypN3 as the most potent independent prognostic factor, while pathological 106pre metastasis was not an independent prognostic factor. In this multicenter study, patients with esophageal carcinoma with clinical pretracheal lymph node metastasis who underwent esophagectomy with lymph node resection after neoadjuvant chemotherapy had better outcomes than those previously reported. Some patients achieved long-term survival, suggesting that pretracheal lymph node metastasis can be considered oligometastatic disease.

**Keywords:** Neoadjuvant chemotherapy; Esophageal carcinoma; Pretracheal lymph node metastasis; 106pre lymph node metastasis

## 25COASOCT53:

**Title:** Exploratory randomized pilot study comparing speech, swallowing, and quality of life outcomes following different types of primary closure after partial glossectomy for early tongue carcinoma,

Vikas Hansraj Maheshwari, Rohit Nayyar, Harit Chaturvedi, Akshat Malik, European Journal of Surgical Oncology,

Volume 51, Issue 10, 2025, 110309,

<https://doi.org/10.1016/j.ejso.2025.110309>.

**Abstract:** Primary closure is a common reconstructive option for smaller defects following partial glossectomy for early-stage tongue carcinoma (T1 and T2). However, the optimal technique of closure in terms of functional outcomes remains unclear. This study aimed to compare speech, swallowing, and quality of life (QOL) outcomes between different methods of primary closure. This exploratory randomized pilot study was conducted between 2022 and 2023. A total of 36 patients undergoing partial glossectomy for early tongue carcinoma were randomized pre-operatively into three groups: horizontal closure, rotational closure, or healing by secondary intention. Functional outcomes, including speech and swallowing, were assessed pre-operatively, at one week, and one month post-operatively using the Speech

Perceptual Index, Speech Intelligibility Score, Functional Oral Intake Scale (FOIS), Speech handicap index(SHI) and MD Anderson Dysphagia Inventory (MDADI).There were no statistically significant differences between the three groups in terms of speech, swallowing, or quality of life outcomes across all time points evaluated.For smaller partial glossectomy defects(<30 %) in early tongue carcinoma, the choice of closure technique — whether horizontal, rotational, or healing by secondary intention — does not significantly affect speech, swallowing, or quality of life outcomes.

**Keywords:** Oral cancer; Tongue cancer; Speech; Swallowing; Quality of life; Reconstruction

#### 25COASOCT54:

**Title: Investigating the relationship between tongue diagnosis features and gastric cancer: A machine learning-based prediction model,**

Pengfei Tian, Zonglin Chen, Biaojie Fang, Xintian Wang, Xin Yu, Mingdian Lu,

European Journal of Surgical Oncology, Volume 51, Issue 10, 2025, 110352,

<https://doi.org/10.1016/j.ejso.2025.110352>.

**Abstract:** Gastric cancer (GC) remains a major cause of cancer-related mortality, particularly in China, where early detection is hindered by reliance on invasive, resource-intensive methods like gastroscopy. This study aimed to develop a non-invasive diagnostic tool integrating tongue features derived from traditional Chinese medicine (TCM) with machine learning (ML) to enhance early GC detection. A prospective, propensity score-matched cohort of 292 participants (146 GC, 146 non-GC) was analyzed. Standardized protocols captured tongue features (color, morphology, coating) alongside gastroscopic findings. Seven ML algorithms, including GBDT, LightGBM, and XGBoost, were trained on multimodal clinical and imaging data. Feature selection was performed using LASSO regression, and model performance was evaluated through stratified 5-fold cross-validation and a 30 % independent test set. Association rule mining (FP-Growth) was employed to explore predictive tongue-gastroscopy patterns. GC patients exhibited more frequent bluish-purple (42 %), cracked (87 %), swollen (86 %), and prickly tongues (67 %), as well as grayish-black coatings (29 %). Non-GC individuals more often showed pale white tongues (40 %) and peeled coatings (71 %). FP-Growth identified combinations such as cracked tongue, grayish-black, and thin coatings as predictors of hemorrhagic GC (confidence = 88.89 %). LASSO highlighted key predictors including prickly tongue and CA19-9. Among the models, GBDT achieved the best performance (test AUC = 0.980, F1 = 0.932). SHAP analysis confirmed the predictive value of both tongue features and tumor markers. TCM-based tongue diagnostics combined with ML provides a promising, non-invasive tool for early GC detection.

**Keywords:** Gastric cancer; Machine learning; Tongue feature; Traditional Chinese medicine (TCM); Non-invasive diagnostics

#### 25COASOCT55:

**Title: Comparison between sub-lobar resection and lobar resection for clinical stage IA (tumor size  $\leq 2$  cm) lung invasive mucinous adenocarcinoma with tumor spread through air spaces: A multi-center real-world study,**

Hanbo Pan, Weicheng Kong, Hui Yin, Yaofeng Shen, Hang Chen, Zhen Ge, Wanyu Li, Jiaqi Zhang,

European Journal of Surgical Oncology, Volume 51, Issue 10, 2025, 110364,  
<https://doi.org/10.1016/j.ejso.2025.110364>.

**Abstract:** Tumor spread through air spaces (STAS) has emerged as a significant prognostic factor in clinical stage IA (cIA) invasive mucinous adenocarcinoma (IMA) of the lung. However, it remains unclear whether sub-lobar resection (SR) offers survival outcomes comparable to those of lobar resection (LR) in this cohort. This study aimed to assess the efficacy of SR in patients with STAS-positive cIA (tumor size  $\leq 2$  cm) IMA using large-scale, multi-center, real-world data. We retrospectively reviewed consecutive patients with peripheral cIA ( $\leq 2$  cm) STAS-positive IMA who underwent SR or LR between 2012 and 2020 at seven high-volume institutions across five Chinese cities. The primary endpoint was overall survival (OS), and the secondary endpoint was recurrence-free survival (RFS). Propensity-score matching (PSM) was employed to mitigate selection bias. Among 567 included patients, PSM yielded 179 patients undergoing SR and 388 patients undergoing LR. Over a median follow-up of 6.2 years, SR demonstrated comparable 5-year OS (78.7 % versus 81.6 %, hazard ratio (HR) = 0.976, 95 % confidence interval (CI) = 0.693–1.375,  $P = 0.890$ ) and RFS (69.0 % versus 71.8 %, HR = 1.017, 95 % CI = 0.752–1.376,  $P = 0.914$ ) to LR. Subgroup analysis revealed that SR improved 5-year OS in patients aged  $\geq 70$  years (73.1 % versus 67.2 %, HR = 0.636, 95 % CI = 0.404–0.969,  $P = 0.040$ ). Additionally, SR yielded similar outcomes in patients with visceral pleural invasion and exhibited a statistically nonsignificant trend toward lower survival in those with pathological N1-2 disease. Furthermore, LR, segmentectomy, and wedge resection yielded comparable 5-year OS and RFS. Among patients with cIA ( $\leq 2$  cm) STAS-positive IMA, SR provides 5-year OS and RFS outcomes comparable to LR and may confer a survival advantage among patients aged  $\geq 70$  years. These findings support the efficacy of SR and suggest that it should not be considered an adverse prognostic factor in this patient cohort.

**Keywords:** Lung invasive mucinous adenocarcinoma; Spread through air spaces; Sub-lobar resection; Lobar resection; Overall survival

## 25COASOCT56:

**Title:** Cytoreduction and hyperthermic intraperitoneal chemotherapy for rare forms of ovarian carcinoma: A single-center retrospective cohort study,

Jovica Vasiljević, Stojan Latinčić, Miljan Čeranić, Ljiljana Marković-Denić, Jovana Todorović,

Asian Journal of Surgery, Volume 48, Issue 10, 2025, Pages 6010-6017,  
<https://doi.org/10.1016/j.asjsur.2025.06.036>.

**Abstract:** Ovarian cancer (OC) is the third most common gynecological cancer with 313,959 newly diagnosed cases in 2020. and followed by 207,252 deaths. The rare epithelial forms of OC include Low-grade serous carcinoma, Endometrioid carcinoma, Mucinous carcinoma, Clear cell carcinoma, Carcinosarcoma, Brenner and Borderline carcinoma. This retrospective single group cohort study included 61 patients with rare form of ovarian epithelial carcinoma who were treated with cytoreductive surgery (CRS) and HIPEC in the period from 2014 to 2021. The mean age of patients was 55.6 years (SD 55.6  $\pm$  12.9), followed by Low-grade serous carcinoma as the most common form with 28 (45.9 %) patients. PCI  $\leq 20$  was presented in 39 of 61 patients. The Peritoneal Cancer Index (PCI) showed a significant difference in survival based on a cutoff of 20, with better outcomes for scores  $\leq 20$  ( $p =$



0.031). Complete cytoreduction (CC 0/1) was achieved in 98.4 % of cases. After three years the majority of patients (67.2 %) were alive, with a 32.8 % mortality rate. Endometrioid Ovarian Cancer (EMOC) and Mucinous Ovarian Cancer (MOC) showed promising outcomes, with survival rate of 3-years (85.7 % and 75.0 %). Multivariate analysis showed the significant impact of Age  $\geq 65$  years (HR = 2.50), PCI >20 (HR = 2.62), and total hospital stay (HR = 1.16) on mortality. Rare epithelial forms of ovarian cancer can be treated with cytoreductive surgery and HIPEC with acceptable mortality and morbidity. Our findings suggest that younger patients (under 65 years) and those with a lower peritoneal cancer index (PCI  $\leq 20$ ) had better survival outcomes following CRS-HIPEC.

**Keywords:** Rare ovarian cancer; Cytoreduction; HIPEC; PCI; PSS (prior surgical score)

#### 25COASOCT57:

**Title:** Ultrasound-guided acupotomy release combined with corticosteroid injection for carpal tunnel syndrome: A multicenter retrospective study,

Guo-Rui Luan, Xiang Shang, De-Hong Meng, Cun-Bin Liu, Shi-Yu Luo, Yong-Hui Yang, Yang-Chun Song, Han-Qing Zhao, Hou-Shan Fang,

Asian Journal of Surgery, Volume 48, Issue 10, 2025, Pages 6054-6061,

<https://doi.org/10.1016/j.asjsur.2025.06.066>.

**Abstract:** The outcomes, both immediate and prolonged, associated with ultrasound-guided acupotomy release in conjunction with corticosteroid injection for patients suffering from carpal tunnel syndrome (CTS) are delineated. A retrospective analysis was undertaken involving patients diagnosed with CTS who underwent treatment comprising acupotomy release alongside corticosteroid injection during the period from January 2021 to April 2024. A total of 138 patients with CTS were incorporated into this investigation (72 in the corticosteroid injection cohort and 66 in the acupotomy with corticosteroid injection cohort). The outcomes of ultrasound-guided corticosteroid injection revealed comparable or even superior enhancements in Visual Analog Scale and Boston Carpal Tunnel Questionnaire scores within the initial two weeks post-treatment when juxtaposed with the combined acupotomy release and corticosteroid injection approach. Conversely, the latter exhibited more pronounced advancements in median nerve neuroelectrophysiological evaluations and imaging assessments after four weeks of intervention. This investigation suggests that ultrasound-guided acupotomy release paired with corticosteroid injection yields more prolonged therapeutic benefits, whereas corticosteroid injection alone demonstrates enhanced short-term efficacy.

**Keywords:** Acupotomy; Carpal tunnel syndrome; Corticosteroid; Median nerve; Transverse carpal ligament; Ultrasound

#### 25COASOCT58:

**Title:** Robotic surgery in newborns and infants under 12-months: Is it feasible?,

Carlos Delgado-Miguel, Juan I. Camps,

Asian Journal of Surgery, Volume 48, Issue 10, 2025, Pages 6032-6036,

<https://doi.org/10.1016/j.asjsur.2025.03.364>.

**Abstract:** Robotic surgery in pediatric patients has some difficulties compared to adults, such as reduced cavities due to children's small size that lead to decreased working space. This limitation has restricted this type of approach in newborn and infant patients. We present a

retrospective review of our first 100 consecutive robotic cases in children under 12-months. A retrospective single-center study was performed among consecutive children under 12-months who underwent robotic surgeries between 2010 and 2020. A three-arm robot (5-mm trocars) with one 12-mm camera arm was used. Demographic data, type of robotic procedure, surgery time and postoperative complications were analyzed. A total of 100 patients were included (51 males; 49 females), with a median age of 5 months at surgery (IQR: 3–8 months) and a mean weight of  $6.2 \pm 1.9$  kg. We performed 147 robotic-assisted procedures: 66 funduplications, 43 gastrostomies, 19 pull-throughs, 8 pyloroplasties, 3 congenital diaphragmatic hernia repairs, 2 nephrectomies, 1 adrenal tumor, 1 liver cyst, 1 mediastinal cyst, 1 common bile duct cyst, 1 intestinal duplication cyst and 1 Ladd's procedure. Median surgery time was 130 min with some differences among different procedures (IQR: 103–202 min). No intraoperative complications or conversion to open or laparoscopic technique were described. Postoperative complications were found in 6 patients (2 required reoperation). During long-term follow-up (median 6.5 years; IQR 3.8–9.4), we reported 4 % of reintervention. Although robotic surgery in newborns and infants are still controversial, it is feasible and safe to perform by well-trained surgeons, with a very low complication rate.

**Keywords:** Robotic surgery; Children; Neonatal surgery; Fundoplication; Pull-through

## 25COASOCT59:

**Title: Comparisons of clinical features between pediatric and adult patients with surgically resected abdominal lymphatic malformations: An observational study of a large cohort,**

Min Yang, Cong-xia Yang, Yu-jia Zhang, Jiang-yuan Zhou, Tong Qiu, Zi-xin Zhang, Yi Ji, Asian Journal of Surgery, Volume 48, Issue 10, 2025, Pages 6047-6053,

<https://doi.org/10.1016/j.asjsur.2025.06.038>.

**Abstract:** Abdominal lymphatic malformations (ALMs) are a rare subgroup of lymphatic anomalies that may manifest differently between paediatric and adult patients. We aimed to systematically compare the clinical features of ALMs in terms of patient sex and clinical presentation, cyst content and location, preoperative complications and surgical treatment regimens between paediatric and adult patients. Data from patients who were surgically treated and pathologically diagnosed as ALMs were retrospectively compared between paediatric ( $\leq 18$  years) and adult ( $> 18$  years) patients. We ultimately enrolled 320 patients with ALMs, including 162 paediatrics and 158 adults. There were significantly more female patients in the adult group ( $P = 0.001$ ). Acute abdominal disease occurred more frequently in paediatric patients ( $P < 0.001$ ), but ALMs were more often detected by incidental health checkups in adults ( $P < 0.001$ ). Furthermore, ALMs were more often detected in the small intestinal mesentery ( $P < 0.001$ ), large intestinal mesentery ( $P = 0.034$ ) and greater omentum ( $P < 0.001$ ) in paediatric patients, while ALMs in adults were more frequently located in the retroperitoneum ( $P < 0.001$ ) and spleen ( $P < 0.001$ ). Simultaneous resection of ALMs and the intestine was performed more frequently in paediatric patients ( $P < 0.001$ ). Acute abdomen ( $P < 0.001$ ) was an independent risk factor for preoperative complications in paediatric patients with ALMs, while incidental detection ( $P = 0.003$ ) and retroperitoneum ( $P = 0.046$ ) were found to be independent protective factors against preoperative complications in adult patients with ALMs. ALMs in children and adults are rare vascular anomalies with different

clinical features and risk factors for preoperative complications. Our study provides a deep understanding of ALMs for clinicians.

**Keywords:** Lymphatic malformations; Abdominal site; Surgical resection; Paediatrics; Adults; Preoperative complications

#### 25COASOCT60:

**Title:** Long-term outcomes and genetic mutation patterns in early-onset colorectal cancer,

Kien Trung Le, Vinh Ngoc Truong Pham, Minh Duc Do, Thinh Huu Nguyen, Trung Thien Tran,

Asian Journal of Surgery, Volume 48, Issue 10, 2025, Pages 6018-6024,

<https://doi.org/10.1016/j.asjsur.2025.06.149>.

**Abstract:** This study aimed to evaluate long-term outcomes and mutation patterns in early-onset colorectal cancer (EOCRC) patients. A retrospective study was conducted on 67 colorectal cancer (CRC) patients under 40 years old. Patients were stratified by tumor location, disease stage, and genetic mutation status. Comparative analysis assessed their characteristics and clinical outcomes. Among EOCRC cases, 94 % were sporadic. The male-to-female distribution was nearly equal, with tumors predominantly localized in the left colon. The mean interval from symptom onset to diagnosis was 2.5 months. A majority (68.7 %) were diagnosed at an advanced stage (III–IV). Notably, left-sided colorectal cancer (LCC) had a significantly higher prevalence of advanced-stage disease than right-sided colorectal cancer (RCC) ( $p = 0.012$ ). However, prognosis did not significantly differ by tumor location. Overall survival (OS) and disease-free survival (DFS) were 49 months (95 % CI, 45–54) and 48 months (95 % CI, 43–53), respectively. Germline mutations were identified in 17.9 % of cases, with over half occurring in Lynch syndrome (LS)-associated genes. Somatic mutations were found in 94 % of cases, with TP53, APC, and KRAS being the most frequently mutated genes (65.7 %, 38.8 %, and 35.8 %, respectively). No significant association was observed between these mutations and OS, and disease stage remained the only independent prognostic factor. The majority of EOCRC cases are sporadic, with prognosis appearing independent of tumor location. The mean OS and DFS were 49 months and 48 months, respectively. No significant prognostic impact was observed for individual somatic mutations in TP53, APC, or KRAS.

**Keywords:** Early-onset colorectal cancer; Long-term outcomes; Gene mutations; Vietnam

#### 25COASOCT61:

**Title:** Antecolic vs retrocolic gastrojejunostomy after laparoscopic gastrectomy for cancer. A multicenter propensity matched analysis,

M. Milone, S. Vertaldi, M. Manigrasso, A. D'Amore, M.S. Alfano, A. Agrusa, G. Anania, G.L. Baiocchi,

Asian Journal of Surgery, Volume 48, Issue 10, 2025, Pages 6025-6031,

<https://doi.org/10.1016/j.asjsur.2025.06.214>.

**Abstract:** Intracorporeal Roux-en-Y reconstruction has been shown to be the most effective reconstruction method after minimally invasive distal gastrectomy. The aim of this study is to compare postoperative complications and early outcomes after antecolic and retrocolic gastro-jejunal anastomoses reconstructions. A multicentric retrospective cohort study was

designed to compare only laparoscopic Roux-en-Y procedures with intracorporeal antecolic and retrocolic reconstruction of gastro-jejunal anastomoses performed on posterior wall of the stomach from January 2009 to December 2019. After performing propensity score matching analysis (PSM), data from 258 patients were analysed. Intraoperative data included fashion of gastro-jejunal anastomosis; length and type of cartridge used; total operative time. To evaluate safety and efficacy of anastomoses, early postoperative complications and recovery outcomes were examined. Operative time was statistically significant lower for the antecolic group ( $192,88 \pm 42,60$  min vs.  $227,09 \pm 81,26$  min;  $p < 0,001$ ). No differences between the two groups were identified in the incidence of postoperative complications neither in recovery outcomes. Both antecolic and retrocolic techniques are reliable and effective to perform, since the route of the alimentary limb does not affect the incidence of postoperative complications and gastric emptying function. Considering its safety and efficacy and the shorter operative time, the antecolic approach with a large stapled anastomosis could be recommended.

**Keywords:** Antecolic; Retrocolic; Gastrojejunostomy; Gastrectomy; Gastric cancer

## 25COASOCT62:

**Title:** Extended arch repair with aortic-femoral/iliac bypass if necessary for treating lower extremity malperfusion secondary to acute type A aortic dissection,

QiYi Chen, YuLin Wang, KeJie Shao, Hao Lai, ChunSheng Wang, Qiang Ji,

Asian Journal of Surgery, Volume 48, Issue 10, 2025, Pages 6037-6046,

<https://doi.org/10.1016/j.asjsur.2025.05.254>.

**Abstract:** In patients with acute type A aortic dissection (ATAAD) complicated by lower extremity (LE) malperfusion (MP), the optimal surgical approach and its outcomes remain a topic of debate. This study aimed to assess both in-hospital and midterm outcomes of our strategy, which involves extended arch repair with additional aortic-femoral or iliac bypass when required, for managing ATAAD with LE-MP. The study included 92 patients with ATAAD and LE-MP and 588 without MP who underwent surgical repair at our center over a 7-year period. From this cohort, 90 matched pairs (1:1) were selected. In-hospital and midterm outcomes were compared between groups in both unmatched and matched cohorts. Additional outcomes, including rates of lower-limb ischemia resolution after central repair alone, limb loss, and bypass patency, were documented. In total, 81 (88.0 %) LE-MP patients achieved resolution of lower-limb ischemia following extended arch repair alone, while 11 required additional aortic-femoral or iliac bypass procedures during the initial repair. Postoperatively, four (4.3 %) LE-MP patients underwent re-intervention due to persistent limb ischemia, with one (1.1 %) eventually requiring a minor amputation. In-hospital mortality for ATAAD patients with LE-MP was 15.2 %, significantly higher than that observed in ATAAD patients without MP ( $p < 0.001$ ). LE-MP was associated with elevated operative mortality and morbidity in both multivariable and propensity score analyses, and a high cumulative mortality in Cox regression (HR 3.6, 95 % CI 2.2–5.7,  $p < 0.001$ ). Patent aortic-femoral or aortic-iliac bypass was observed in six (85.7 %) patients during a median follow-up period of 26.1 months. Preoperative LE-MP in ATAAD patients is linked to poorer outcomes. Extended arch repair with selective aortic-femoral or iliac bypass may represent an effective strategy for treating ATAAD with LE-MP.

**Keywords:** Acute type A aortic dissection; Low extremity malperfusion; Extended aortic arch repair; Extra-anatomic bypass

### 25COASOCT63:

**Title:** Robot-assisted cortical bone trajectory versus traditional pedicle screws in the treatment of lumbar spinal stenosis with osteoporosis: A retrospective cohort study,

Ruizhao Zhao, Yuyu Fan, Junjie Qiao, Lixiang Ding, Wei Qu, Xiutong Fang,

Asian Journal of Surgery, Volume 48, Issue 10, 2025, Pages 6062-6069,

<https://doi.org/10.1016/j.asjsur.2025.06.215>.

**Abstract:** The aging population has led to a rise in the incidence of lumbar degenerative diseases, especially lumbar spinal stenosis (LSS). When conservative treatment fails, surgical intervention has become the preferred approach. The emerging cortical bone trajectory (CBT) screw technique and the traditional pedicle screw technique remain subjects of debate. A retrospective cohort study was conducted to compare the early efficacy of robot-assisted CBT and traditional pedicle screw (TPS) in the treatment of LSS in patients with Osteoporosis. A total of 110 patients underwent robot-assisted posterior lumbar interbody fusion (PLIF) between September 2018 to June 2021. They were divided into two groups, the CBT group (N = 55) and the TPS group (N = 55). The general information, surgical related data, postoperative related indicators and functional scores for the two groups were analyzed to evaluate the differences between the two screw placement methods. The CBT group demonstrated significantly lower the intraoperative blood loss, length of surgical incision and visual analogue scale (VAS) scores at 6 months after operation compared with TPS group ( $P < 0.05$ ). The difference of blood glucose at 1 week after operation was statistically significant ( $P < 0.05$ ). The rate of screw loosening, adjacent facet joint invasion and the degree of paraspinal muscle fat infiltration in the CBT group were significantly lower than those in the TPS group as at the last follow-up ( $P < 0.05$ ). Compared to TPS instrumentation, PLIF with robot-assisted CBT screw provides better short-term symptom relief, a lower rate of screw loosening, and reduced adjacent facet joint invasion and paraspinal muscle fat infiltration.

**Keywords:** TiRobot system; Cortical bone trajectory; Traditional pedicle screws lumbar spinal stenosis; Posterior lumbar interbody fusion; Paraspinal muscle fat infiltration

### 25COASOCT64:

**Title:** Short-term and long-term outcomes of laparoscopic surgery for T4b colon cancer: Comparison with open colectomy,

Yasuhiro Takeda, Hiroshi Sugano, Atsuko Okamoto, Takafumi Nakano, Yuya Shimoyama,

Naoki Takada, Yuta Imaizumi, Masahisa Ohkuma, Makoto Kosuge, Ken Eto,

Asian Journal of Surgery, Volume 48, Issue 10, 2025, Pages 6004-6009,

<https://doi.org/10.1016/j.asjsur.2025.06.001>.

**Abstract:** Recent studies have shown that laparoscopic surgery is widely accepted as the optimal procedure for colon cancer resection. However, the safety and feasibility of laparoscopic surgery for T4b colon cancer remain controversial. This study aimed to compare the outcomes of laparoscopic and open surgery for locally advanced colon cancer requiring multivisceral resection. Patients who underwent planned curative resection of T4b colon cancer between 2008 and 2019 were enrolled. We compared short- and long-term outcomes between the two groups. A total of 49 consecutive patients who underwent multivisceral



resection for T4b colon cancer were included. Of these, 22 (44.9 %) underwent laparoscopy, while 27 (55.1 %) underwent open surgery. Their clinicopathological characteristics were similar. Compared to open surgery, laparoscopic surgery resulted in significantly less blood loss and a shorter postoperative hospital stay, despite a longer operative time. Although all postoperative complications were more common in the open surgery group ( $p = 0.043$ ), there was no significant difference between the two groups for major complications (Clavien–Dindo grade  $\geq 3a$ ). The two groups showed similar pathologic factors, and there were no significant differences in disease-free survival (DFS) or overall survival (OS) between them (5-year DFS: 56.4 % vs. 57.0 %,  $p = 0.907$ ; 5-year OS: 94.4 % vs. 77.5 %,  $p = 0.224$ ). The most commonly resected adjacent structure was the abdominal wall. Laparoscopic surgery for T4b colon cancer requiring combined resection of other organs achieved acceptable outcomes and is a useful treatment option.

**Keywords:** Colon cancer; Laparoscopic colectomy; Multivisceral resection; T4

#### 25COASOCT65:

**Title:** Is pre-operative electromyography a reliable tool in differentiating acute and chronic facial palsy? A preliminary evaluation in patients treated with triple innervation facial reanimation,

Fabiana Allevi, Nicole Abate, Federico Bolognesi, Filippo Tarabbia, Dimitri Rabbiosi, Martina Maddalena Bellasio, Alessandro Lozza, Federico Biglioli,

Journal of Cranio-Maxillofacial Surgery, Volume 53, Issue 10, 2025, Pages 1667-1674,

<https://doi.org/10.1016/j.jcms.2024.04.001>.

**Abstract:** Electromyographic evaluation is a reliable tool for confirming facial palsy and assessing its severity. It allows differentiating facial paresis and paralysis, and further distinguishes acute palsies, still showing muscle fibrillations, from chronic cases. This article aims to show that EMG fibrillations might represent a better criterion to differentiate acute and chronic palsies than the standard 18–24 months' cut-off usually employed for classification and treatment purposes. We performed a cohort study using the eFACE tool for comparing triple innervation facial reanimation results in patients with EMG fibrillation treated <12 months, 12–18 months, and >18 months from paralysis onset. Patients showed a statistically significant post-operative improvement in all eFACE items, both in the whole sample and in the three groups. Only the deviation from the optimal score for the gentle eye closure item in group 2 didn't reach statistical significance ( $p = 0.173$ ). The post-operative results were comparable in the three groups, as the Kruskal-Wallis test showed a difference only for the platysmal synkinesis item scores, which were significantly lower in group 3 ( $p = 0.025$ ). EMG should represent a further tool to wide the group of paralysis patients that could be treated as recent facial palsy patients; Further prospective studies on pre-operative EMG fibrillations might allow for further refinement of the technique selection process.

**Keywords:** Facial palsy; Electromyography; Facial reanimation; Facial paralysis; Recent facial palsy; Acute facial palsy; Muscular fibrillations

#### 25COASOCT66:

**Title:** Comprehensive three-dimensional morphological changes in perioral soft tissue following bimaxillary orthognathic surgery in patients with skeletal Class III malocclusion,

Chi Zhang, Yuan Si, RuoYuan Li, Yule Xu, Yuan Li, Jinwei Qin, Hua Wang, Han Ge, Dongmiao Wang, Jie Cheng,

Journal of Cranio-Maxillofacial Surgery, Volume 53, Issue 10, 2025, Pages 1675-1682,

<https://doi.org/10.1016/j.jcms.2025.07.006>.

**Abstract:** This study aimed to comprehensively evaluate the three-dimensional morphological changes in perioral soft tissue in patients with skeletal Class III malocclusion after combined orthognathic-orthodontic treatment. In total, 68 eligible patients with skeletal Class III malocclusion who underwent bimaxillary surgery and orthodontics between January 2019 and January 2023 were included. Cone-beam computed tomography data were collected for each patient at three stages: pre-treatment (T0), 1 week before surgery (T1), and on completion of treatment (T2). Perioral soft-tissue changes, including upper/lower lip vermilion thickness, alar width, and nasolabial and mentolabial angles, were measured via image reconstruction and 3D measurements using Dolphin Software. Upper/lower lip thickness increased after preoperative orthodontics (T0–T1), while decreased upper lip thickness and increased lower lip thickness were observed after orthognathic surgery (T1–T2) and the whole treatment (T0–T2). Increased alar width and nasolabial angle, along with decreased mentolabial angle, were observed after orthognathic surgery. Lip thickness significantly correlated with incisor inclination in both jaws. Alar width, alar base width, and nasolabial angle positively correlated with maxillary anteroposterior or vertical movement. Collectively, our results comprehensively delineate perioral soft-tissue changes in patients with skeletal Class III malocclusion following combined orthodontic-orthognathic surgery, and underscore the necessity of incorporating perioral soft-tissue changes into treatment planning.

**Keywords:** Orthognathic surgery; Class III malocclusion; Perioral soft tissue; CBCT; 3-Dimensional measurement

## 25COASOCT67:

**Title: Three-dimensional morphometric analysis of alar asymmetry in unilateral secondary cleft nasal deformity: implications for non-cleft alar reduction in surgical planning,**

Qingqing Li, Guang Zhang, Wenjun Di, Mengmeng Zhang, Menghao Deng, Tianyi Gu, Yongqian Wang,

Journal of Cranio-Maxillofacial Surgery, Volume 53, Issue 10, 2025, Pages 1696-1703,

<https://doi.org/10.1016/j.jcms.2025.07.010>.

**Abstract:** Preoperative surgical planning for alar reduction remains challenging due to the lack of objective references in traditional measurements. Therefore, this study aimed to objectively quantify preoperative bilateral alar symmetry using 3D best-fit alignment analysis, and to establish an evidence-based threshold for alar morphological deviation for alar reduction in secondary cleft rhinoplasty. 26 patients with unilateral secondary cleft nasal deformity were retrospectively assessed: 13 underwent secondary cleft rhinoplasty alone and 13 received concurrent alar reduction. Preoperative 3D facial images were processed with best-fit alignment analysis to quantify alar morphological deviation between the cleft and non-cleft alar surfaces. Symmetry scores were also assessed by plastic surgeons using a four-point Likert scale (1 = poor, 2 = fair, 3 = good, 4 = excellent), based on pre- and postoperative standard photographs. In both groups, the cleft-side alar exhibited a distinctly

smaller size compared with the non-cleft side. The combined alar reduction group showed significantly larger preoperative alar morphological deviation ( $2.49 \pm 0.52$  mm versus  $1.19 \pm 0.35$  mm;  $p < 0.05$ ). Morphological deviation analysis revealed a surgical threshold of 1.5–2 mm. Postoperative symmetry scores were significantly improved in both groups. 3D best-fit alignment analysis is a reliable method for objectively quantifying alar asymmetry. Non-cleft alar reduction is recommended during secondary rhinoplasty when preoperative alar morphological deviation reaches 2 mm.

**Keywords:** Alar asymmetry; Secondary cleft nasal deformity; 3D best-fit alignment; Alar reduction

#### 25COASOCT68:

**Title:** The accuracy of dual energy CT on evaluation of bone invasion caused by oral squamous cell carcinoma – a comparison to MRI,

Veronique C.M.L. Timmer, Genevieve A.J.C. Crombag, Sander M.J. van Kuijk, Lauretta A.A. Vaassen, Peter A.W.H. Kessler, Alida A. Postma,

Journal of Cranio-Maxillofacial Surgery, Volume 53, Issue 10, 2025, Pages 1731-1737,

<https://doi.org/10.1016/j.jcms.2025.07.005>.

**Abstract:** Bone marrow edema (BME) is a key sign of bone invasion by malignancies, alongside cortical involvement. Dual-energy CT virtual non-calcium (VNCa) reconstructions can visualize BME in the head and neck, but its role in evaluating bone invasion by oral squamous cell carcinoma (OSCC) remains underexplored. This study aimed to evaluate the accuracy of Dual energy CT (DECT) and additional virtual non-calcium (VNCa) reconstructions in detecting OSCC-related bone invasion in comparison to MRI using histology as reference standard. This retrospective study included 59 consecutive participants (mean age  $68 \text{ years} \pm 12$ , 33 male) with primary OSCC who underwent both contrast-enhanced DECT and MRI. DECT weighted average (DECT WA) and DECT VNCa reconstructions were assessed for bone invasion based on the presence of cortical erosion, cortical disruption and cortical erosion combined with BME. DECT WA(erosion) showed a sensitivity and specificity of 95 % and 86 % comparable to MRI (92 % and 86 % respectively). Addition of VNCa-reconstructions to DECT WA did not improve sensitivity or specificity (84 % and 86 % respectively). Overall, accuracy of DECT is excellent and comparable to MRI for detecting bone invasion caused by OSCC. However, additional diagnostic benefits of VNCa reconstructions could not be shown in this study.

**Keywords:** Oral squamous cell carcinoma; Bone invasion; Dual energy CT; Virtual non calcium reconstruction; MRI; Accuracy

#### 25COASOCT69:

**Title:** A comparison of isolated midface and forehead fractures and pattern of fractures of the midface and forehead in cases with panfacial fractures – A study from 2007 to 2024 on 6588 patients,

Ákos Bicsák, Leonie Koch, Stefan Hassfeld, Lars Bonitz,

Journal of Cranio-Maxillofacial Surgery, Volume 53, Issue 10, 2025, Pages 1704-1710,

<https://doi.org/10.1016/j.jcms.2025.07.012>.

**Abstract:** This study analyses upper and midface fracture patterns and demographics from 2007 to 2024 in a highest-level German interregional trauma centre, comparing isolated and

pan-facial fractures to improve diagnostics and treatment. The data from our Maxillofacial Trauma Registry was analyzed by demographic methods,  $\chi^2$ -test for group comparison, and Wilcoxon ranked test. In this study of 5459 isolated and 1129 panfacial fracture cases, males predominated (ratios: 2.1:1 and 3.4:1, respectively). Male patients peaked at ages 20–30, while females peaked at 80+. Average ages were similar across groups (46.3 vs. 46.2 years). Yearly panfacial cases declined steadily, while isolated cases showed volatility after 2020. Statistical tests revealed significant differences in fracture distributions “far from the cranial base” ( $p = 0.047$ ) but not “near the cranial base” ( $p = 0.807$ ), highlighting biomechanical implications. Young males and older females are the most fracture-prone groups. The fracture distribution highlights the biomechanical significance of the cranial base. While demographic shifts and pandemic-driven case volatility necessitate ongoing monitoring for effective healthcare planning.

**Keywords:** Facial bone fractures; Head and neck injury; Midface; Maxilla; Cranial base

## 25COASOCT70:

### **Title: Three-dimensional cephalometric analysis of morphological characteristics in children with bilateral craniofacial microsomia,**

Chen Li, Zhipu Ge, Xiaojun Tang, Zhiyong Zhang, Xiaolei Jin, Wei Liu,

Journal of Cranio-Maxillofacial Surgery, Volume 53, Issue 10, 2025, Pages 1820-1827,

<https://doi.org/10.1016/j.jcms.2025.07.024>.

**Abstract:** Craniofacial microsomia (CFM), the second most common congenital craniofacial anomaly, is poorly characterized in bilateral cases because conventional cephalometry cannot accurately assess facial asymmetry. This study aims to characterize craniofacial morphology in children with bilateral CFM using three-dimensional (3D) cephalometric analysis. A retrospective 3D cephalometric analysis was conducted on 8 bilateral CFM patients and 10 age-/sex-matched normal patients as controls. A coordinate system was established with three reference planes: the Frankfurt Horizontal Plane (FHP), the Midsagittal Plane (MSP) and the Nasion Perpendicular Plane (CP). Fifteen linear and angular measurements assessed maxillary, mandibular, chin, and occlusal parameters. Subgroups were stratified by bilateral mandibular deficiency severity according to Pruzansky-Kaban classification (Group A: similar; Group B: different). Statistical comparisons utilized independent t-tests (CFM vs. controls) and Mann-Whitney U tests (subgroups), with Pearson's correlation analysis exploring variable relationships. Bilateral CFM patients exhibited significant reductions in ramal height (Co-Go:  $p < 0.001$ ) and mandibular body length (Go-Me:  $p < 0.001$ ), a posteriorly inclined occlusal plane (OP-FHP:  $27.63^\circ \pm 5.50^\circ$  vs.  $8.13^\circ \pm 3.33^\circ$ ,  $p < 0.001$ ), and pronounced chin retrusion (Me-NP:  $46.08 \pm 6.66$  mm vs.  $8.28 \pm 7.71$  mm,  $p < 0.001$ ) and lateral deviation (Me-MSP:  $5.84 \pm 4.64$  mm vs.  $1.73 \pm 0.93$  mm,  $p < 0.05$ ). Me-NP and Me-MSP differed significantly in subgroup analyses. Pearson correlation analysis revealed strong associations between Me-NP and Me-MSP and OP-MSP, posterior maxillary height (U6-FHP) and Co-Go. Bilateral CFM is mainly characterized by posteriorly inclined occlusal plane and pronounced mandibular retrognathia. The occlusal plane and chin will consistently deviate toward the more severely affected side. When bilateral mandibular involvement is similar in extent, chin deviation tends to be mild, resulting in less severe facial asymmetry.

**Keywords:** Bilateral craniofacial microsomia; Facial asymmetry; Three-dimensional cephalometry; Mandibular hypoplasia; Occlusal cant

**25COASOCT71:****Title: AI-driven CBCT segmentation and 3D modeling of the anterior surface of maxilla for computer-assisted surgery: a comparison of multiple algorithms,**

Hei Yuet Lo, Pui Hang Leung, Yu-xiong Su, Yiu Yan Leung, Andy Wai Kan Yeung, Wei-fa Yang,

Journal of Cranio-Maxillofacial Surgery, Volume 53, Issue 10, 2025, Pages 1683-1690,

<https://doi.org/10.1016/j.jcms.2025.07.007>.

**Abstract:** The maxilla is frequently involved in virtual surgical planning (VSP), serving as a base for osteotomies and designing patient-specific devices. However, segmenting thin bone structures like the anterior surface of the maxilla is challenging, often resulting in defects that compromise VSP. Our study aimed to compare various segmentation and 3D modeling algorithms for the anterior surface of the maxilla in CBCT, to serve as a reference for clinical practice. The study included 20 patients preparing for orthognathic joint surgery. Various segmentation and 3D modeling algorithms were compared, including manual segmentation, threshold segmentation, 3D hole repairing, and AI segmentation, using Mimics Viewer and Blue Sky Plan software. The accuracy of each segmentation method was evaluated using the Dice Similarity Coefficient (DSC) and 95 % Hausdorff distance (HD95). Additionally, the clinical applicability of the 3D models was qualitatively evaluated using questionnaires focused on surface consistency, structural completeness, surface smoothness and noise, accuracy of anatomical features, and overall suitability for virtual surgical planning. Statistical analysis was performed using non-parametric tests. For segmentation accuracy, threshold segmentation and 3D hole repairing achieved significantly higher DSC and HD95 compared with other algorithms. AI segmentation in Mimics Viewer achieved a DSC of  $0.90 \pm 0.03$  and an HD95 of  $0.72 \pm 0.50$  mm, less than 1 mm. With regard to the qualitative assessment of clinical applicability, the score for Mimics Viewer was 3 (IQR: 3–4;  $p < 0.001$ ), which outperformed the other algorithms for accuracy of anatomical features. Blue Sky Plan had the lowest median DSC ( $0.78 \pm 0.12$ ) and highest HD95 ( $2.02 \pm 0.80$  mm). 3D hole repairing using 3-matic gave the best performance in terms of both accuracy and quality assessment for the anterior surface of the maxilla. AI-driven segmentation using Mimics Viewer, designed specifically for craniomaxillofacial surgery, provides optimal performance and could be a valuable tool in VSP.

**Keywords:** CBCT segmentation; 3D modeling; Maxilla; Computer-assisted surgery; Artificial intelligence; Virtual surgical planning; Patient-specific surgical plates; Thin bone

**25COASOCT72:****Title: Costal cartilage graft harvesting for auricular reconstruction: donor-site morbidity assessment,**

Journal of Cranio-Maxillofacial Surgery,

Laura Tognin, Jacopo Benerecetti, Michela Bergonzani, Francesca Zito, Giovanni Lilloni, Andrea Varazzani, Marilena Anghinoni, Volume 53, Issue 10, 2025, Pages 1691-1695,

<https://doi.org/10.1016/j.jcms.2025.07.008>.

**Abstract:** Auricular reconstruction is a challenging procedure, and the use of autologous costal cartilage represents the gold standard for the treatment of congenital microtia. Since adolescents are a significant demographic for congenital reconstruction, age-related psychosocial factors must be considered. The aim of this study was to evaluate postoperative



patient perception of donor-site morbidity following costal cartilage graft harvesting and its impact on social and physical activities. We included patients treated at the University Hospital of Parma (Italy) between 2010 and 2020. Data collected included: scar evaluation, asymmetry of the thoracic profile, sport participation before and after surgery, physical limitation, donor-site long-term discomfort, postoperative pain. A total of 100 patients were enrolled in the study (58 males and 42 females; mean age: 13.58 years), reporting good long-term aesthetic results at the thoracic site, with female patients showing slightly better outcomes. The majority (82 %) participated in sports before surgery, and 70 % continued the same activities afterward. Minimal chest deformity or thorax asymmetry was reported by 30 patients (30 %). The study confirms that postoperative donor-site morbidity following costal cartilage graft harvesting is low. Sporting activities do not appear to be significantly affected by ear reconstruction procedures, supporting social and psychological development in growing patients.

**Keywords:** Auricular reconstruction; Congenital microtia; Costal cartilage harvesting; Donor-site morbidity

#### **25COASOCT73:**

**Title: Efficiency and outcomes in microvascular anastomosis: A meta-analysis of mechanical versus manual techniques,**

Chaim Ohayon, Niv Gross, Tal Capucha, Shaged Carasso, Yotam Shkedy, Adi Rachmiel, Omri Emodi,

Journal of Cranio-Maxillofacial Surgery, Volume 53, Issue 10, 2025, Pages 1720-1730,

<https://doi.org/10.1016/j.jcms.2025.07.015>.

**Abstract:** Microvascular anastomosis plays a critical role in free flap transfers, aiming to reduce ischemia time, minimize vessel trauma, and optimize ease of use. This meta-analysis compares coupler devices and hand-sewn techniques for venous anastomosis across all types of free flaps, with a subgroup analysis focused on head and neck reconstruction. A comprehensive literature search following PRISMA guidelines was conducted across multiple databases up to November 6, 2024. Eighteen retrospective comparative studies met the inclusion criteria from an initial pool of 3184 articles. The overall flap loss rate was 1.53 % for coupler devices and 2.32 % for hand-sewn techniques. Thrombosis occurred in 2.91 % of coupler cases versus 3.17 % for hand-sewn. Anastomosis time was notably shorter with coupler devices (7.5 min) compared to hand-sewn methods (32.2 min). In head and neck reconstruction, the coupler group showed even more favorable outcomes: flap loss was 0.66 % versus 3.08 %, thrombosis rates were 1.7 % versus 3.88 %, and anastomosis times were 7.5 versus 17 min. These findings suggest that coupler devices are a safe and time-efficient alternative to traditional hand-sewn techniques in free flap surgery, particularly in head and neck reconstruction.

**Keywords:** Coupler device; Free flap; Reconstruction; Meta-analysis; Microsurgery

#### **25COASOCT74:**

**Title: Evaluation of Uncertain Resection for Localized Non-small Cell Lung Cancer: The Crucial Prognosis of Suboptimal Lymph Node Assessment,**

Romain Vergé, Axel Rouch, Pierre Rabinel, Claire Renaud, Mathilde Cazaux, Laurent Brouchet,

The Annals of Thoracic Surgery, Volume 120, Issue 4, 2025, Pages 637-645,  
<https://doi.org/10.1016/j.athoracsur.2025.02.004>.

**Abstract:** Surgery is the cornerstone of treatment for early-stage non-small cell lung cancer (NSCLC). The concept of “uncertain resection” (R[un]) describes cases where complete tumor excision with clear margins is achieved but without comprehensive lymph node assessment or pleural cytology. This study aimed to establish R(un) as a prognostic factor in localized NSCLC patients and explore its heterogeneity. This single-center retrospective study was conducted at Toulouse University Hospital. Consecutive patients who underwent surgery for localized NSCLC between 2008 and 2018 were included. Resection status, particularly R(un), was reclassified retrospectively. Overall survival and disease-free survival were analyzed, and a Cox proportional hazards regression model was used to assess whether R(un) and its newly proposed subcategories were independent predictors of survival. Among 1108 patients, 732 (66.1%) were classified as R0, 291 (26.2%) as R(un), and 85 (7.7%) as R1. Our study demonstrated that R(un) was an independent prognostic factor, with adjusted hazard ratios of 1.26 (95% CI, 1.03-1.52) for overall survival and 1.23 (95% CI, 1.03-1.46) for disease-free survival. A proposed classification system with 3 R(un) subcategories revealed a continuum between uncertain and incomplete resections ( $P < .001$ ). This study validated the updated resection classification for localized NSCLC and highlighted the significant prognostic impact of suboptimal lymph node assessment. These results underscore the heterogeneity among R(un) patients and the need for precise resection assessment to improve outcomes.

## 25COASOCT75:

### **Title: Extended Sleeve Lobectomy After Neoadjuvant Immunochemotherapy for Centrally Located Non-small Cell Lung Cancer,**

Jiawei Chen, Ze-Rui Zhao, Hongsheng Deng, Chao Yang, Zhongqiao Mo, Lei Fan, Jianxing He, Shuben Li,

The Annals of Thoracic Surgery, Volume 120, Issue 4, 2025, Pages 646-654,  
<https://doi.org/10.1016/j.athoracsur.2025.03.033>.

**Abstract:** Extended sleeve lobectomy (ESL) is proposed as an effective alternative to pneumonectomy for patients who are not amenable to standard sleeve lobectomy (SSL), which is designed to preserve more lung parenchyma and improve postoperative quality of life. However, the safety and feasibility of ESL after neoadjuvant immunochemotherapy remain unclear. Between 2019 and 2023, 94 patients with central non-small cell lung cancer (NSCLC) received neoadjuvant immunochemotherapy, followed by pneumonectomy, ESL, or SSL, in 2 high-volume centers. Perioperative, surgical, pathologic, and survival outcomes were meticulously analyzed to evaluate the impact of neoadjuvant immunochemotherapy. ESL, SSL, and pneumonectomy were performed in 18, 42, and 34 patients, respectively. Patients who underwent ESL had a poorer predicted postoperative forced expiratory volume in 1 second percentage than those who underwent pneumonectomy ( $P < .01$ ), if pneumonectomy was to be conducted. R0 resection was confirmed in 90 patients (95.7%), including 17 (94.4%) in ESL, 41 (97.6%) in SSL, and 32 (94.1%) in pneumonectomy ( $P = .72$ ). Postoperative complications were predominantly observed in patients who underwent pneumonectomy (32.4%). Kaplan-Meier curves showed no difference between ESL and SSL. Compared with pneumonectomy, ESL had a longer event-

free survival ( $P = .04$ ).ESL after neoadjuvant immunochemotherapy is a viable and safe option for selected patients with centrally located NSCLC to avoid pneumonectomy, especially when SSL is insufficient for R0 resection.

**25COASOCT76:****Title: Association Between Participation in a Quality Collaborative and Value in Lung Cancer Surgery,**

Callie K. VanWinkle, Whitney Fu, Kristen P. Hassett, Michael P. Thompson, Rishindra M. Reddy, Kiran Lagisetty, Sidra N. Bonner,

The Annals of Thoracic Surgery, Volume 120, Issue 4, 2025, Pages 656-663,

<https://doi.org/10.1016/j.athoracsur.2025.02.027>.

**Abstract:** In this study, the association between participation in a statewide thoracic surgery collaborative quality initiative (CQI) and value for resection of lung cancer is evaluated. Robust multipayer claims data from the Michigan Value Collaborative, a quality initiative with the goal of improving health care value and quality across Michigan, were leveraged to identify patients undergoing lung cancer resection at Michigan hospitals from 2015 to 2020. We identified patients who did and did not receive their care at a hospital participating in a statewide thoracic surgery CQI. There were 16 CQI hospitals and 38 non-CQI hospitals identified at which patients underwent resection for lung cancer. Multivariable logistic and linear regression analyses were performed to compare surgical outcomes and total surgical episodes for patients receiving care within the CQI compared with those outside of the CQI. A total of 4857 patients undergoing resection for lung cancer were identified, with mean (SD) age of 68.3 (8.6) years; 2599 (53.5%) were women. Patients receiving surgery within CQI hospitals had significantly lower mortality compared with patients at non-CQI hospitals (1.5% vs 2.6%;  $P < .04$ ). A similar pattern was found for all complications (48.4% vs 60.6%;  $P < .001$ ) and for specific complications, including acute respiratory failure (11.1% vs 25.5%;  $P < .001$ ), pneumonia (6.4% vs 10.1%;  $P < .001$ ), pneumothorax (20.3% vs 25.3%;  $P < .001$ ), and renal failure (5.9% vs 9.3%;  $P < .001$ ). Last, CQI hospitals had significantly lower mean 30-day total surgical episode payments (\$26,470.42 vs \$28,561.56;  $P < .001$ ). This study found association between participation in a CQI and improved value in lung cancer surgery.

**25COASOCT77:****Title: Time to definitive treatment in rectal cancer care coordination,**

Alexis L. Woods, Axenya Kachen, Rebeka A. Dejenie, Sean M. Flynn, Robert J. Kucejko, Erik R. Noren, Ankit Sarin, Miquell Miller,

The American Journal of Surgery, Volume 248, 2025, 116333,

<https://doi.org/10.1016/j.amjsurg.2025.116333>.

**Abstract:** Timely initiation of rectal cancer treatment improves outcomes, and standard of care is to receive definitive treatment within 60 days of diagnosis. A retrospective review of rectal cancer patients (2013–2023) at a tertiary cancer center was performed. Statistical analysis was conducted on patients stratified to time-to-treatment within 60 days and patient sociodemographics. 182/342 (53.2 %) rectal cancer patients had time-to-treatment  $\leq 60$  days. Unified care was significantly faster than fragmented care (57.5 vs 77.4 days,  $p = 0.002$ ). Factors associated with time-to-treatment  $> 60$  days: sex ( $p = 0.03$ ), age ( $p = 0.004$ ), insurance

( $p = 0.006$ ), Healthy Places Index quintile ( $p = 0.02$ ), distance from hospital ( $p = 0.01$ ). Multivariable analysis associated delays with females (OR 1.74 [95 % CI 1.05–2.91],  $p = 0.03$ ), and living >60 miles from the hospital (60–100 miles OR 2.49 [95 % CI 1.09–5.85],  $p = 0.03$ ; >100 miles OR 2.87 [95 % CI 1.05–8.25],  $p = 0.04$ ). In this study, 46.8 % of rectal cancer patients initiated definitive treatment >60 days from diagnosis. Unified care improved time-to-treatment. Female sex and living >60 miles from the hospital were associated with delays.

**Keywords:** Rectal cancer; Time-to-treatment; Care coordination; Outcomes; Definitive treatment

## 25COASOCT78:

**Title:** Postoperative survival evaluation of patients with Siewert II adenocarcinoma of esophagogastric junction: a population-based study,

Gangzhi Zhang, Yan Chen, Dan Jin, Ziqi Sui,

The American Journal of Surgery, Volume 248, 2025, 116536,

<https://doi.org/10.1016/j.amjsurg.2025.116536>.

**Abstract:** To explore the influencing factors of postoperative survival in Siewert II adenocarcinoma of esophagogastric junction (AEG). The eligible patients and 28 variables were extracted from the Surveillance, Epidemiology, and End Results database. The association of each variable with overall survival (OS) was explored by univariable COX regression analysis. Multivariable COX analysis was then conducted to determine the independent factors. Kaplan-Meier method was used to compare the OS difference between 2 groups. Totally 3568 patients were enrolled, of whom 2344 patients died. There were 23 variables showing the differences between alive and dead groups (all  $P < 0.05$ ). Univariable COX and LASSO regression analyses identified 7 key features associated with OS, including age, income, M stage, chemotherapy, systemic therapy plus surgical procedures, liver metastasis, and tumor size. The M stage and tumor size were the key factors associated with postoperative survival of patients with Siewert II AEG.

**Keywords:** SEER; Adenocarcinoma of esophagogastric junction; Association; Survival; Risk model

## 25COASOCT79:

**Title:** Optimal port site skin closure method following minimally-invasive surgery: A systematic review and network meta-analysis of randomised clinical trials,

E.P. Kerin, M.G. Davey, L. Bouz Mkabaah, N.E. Donlon,

The American Journal of Surgery, Volume 248, 2025, 116542,

<https://doi.org/10.1016/j.amjsurg.2025.116542>.

**Abstract:** For minimally-invasive surgery (MIS), there are numerous acceptable port-site closure techniques with no consensus on the method used. To identify optimal port site postoperative wound closure method following MIS with respect to complication rates and cosmetic outcome. Network meta-analysis (NMA) was performed in accordance with PRISMA-NMA guidelines for RCTs comparing at least two methods of port-site closure. Nineteen RCTs were identified evaluating eight methods of wound closure in 1,932 patients; across three types of suture, three forms of tissue glue, staples and paper-tape. At NMA, there was no significant difference in wound complication, infection, dehiscence or

pain rate irrespective of closure method, albeit a trend towards higher rate of dehiscence for adhesives. At NMA, wound cosmesis was superior for adhesives at both early and late postoperative follow-up. This study validates the use of tissue adhesives with respect to primary closure of port sites following MIS while highlighting potential associated risks.

## 25COASOCT80:

**Title: Female gender and racial minority status is associated with Poor clinical outcomes and higher healthcare resource utilization in necrotizing fasciitis: Analysis of a Nationwide database in the United States,**

Muhammad Ahmad Nadeem, Mohamed A. Quazi, Samia Aziz Sulaiman, Amir Humza Sohail, Aqsa Munir,

The American Journal of Surgery, Volume 248, 2025, 116303,

<https://doi.org/10.1016/j.amjsurg.2025.116303>.

**Abstract:** Necrotizing fasciitis is a rapidly progressive infection associated with high mortality and complications. It mainly involves subcutaneous tissue and fascia. More quality data on disparities in clinical outcomes of necrotizing fasciitis must be provided. Our study aims to identify gender and racial disparities in necrotizing fasciitis outcomes. We used data from the Nationwide Inpatient Sample database from 2016 to 2020. As appropriate, the Chi-square and t-test were used to test for associations between categorical and continuous variables. Multivariate logistic regression models, adjusted for key confounders, were used to obtain odds ratios for in-hospital mortality and various complications. Similarly, multivariate linear regression models were created for continuous outcome variables. Among 118,775 patients with necrotizing fasciitis, women (adjusted odds ratio [aOR] 1.18, 95 % confidence interval [CI]: 1.07–1.30,  $p = 0.001$ ), Asian (aOR 1.49 (95 % CI: 1.10–2.02,  $p = 0.01$ ), and Hispanic (aOR: 1.16; 95 % CI: 1.0–1.35;  $p = 0.045$ ) patients had significantly higher in-hospital mortality than White patients. In comparison with men, women were more likely to require invasive mechanical ventilation and blood transfusions and develop ARDS. They are less likely to develop AKI, acute myocardial infarction, or venous thromboembolism and require non-invasive mechanical ventilation ( $p < 0.05$  for all comparisons). Similarly, certain racial minority groups were also at a heightened risk for complications, such as AKI requiring hemodialysis, ARDS, venous thromboembolism, sudden cardiac arrest, and need for blood transfusion, among others ( $p < 0.05$  for all comparisons). As compared to white patients, African American (1.7 days longer,  $p < 0.001$ ), Asian (4.3 days longer,  $p < 0.001$ ), and Hispanic (0.6 days longer,  $p = 0.048$ ) patients had a significantly longer length of hospital stay. Asian, African American, and Hispanic patients also had substantially higher hospitalization costs, amounting to an additional \$17,596.07 ( $p < 0.001$ ), \$5899.60 ( $p < 0.001$ ), and \$4356.55 ( $p < 0.01$ ), respectively, versus White patients. Native American patients did not have any significant difference in the cost of hospitalization as compared to White patients. Females and racial minorities are at increased risk of mortality and higher healthcare resource utilization in necrotizing fasciitis. There is a need to develop equitable management strategies and health policy interventions to address these disparities effectively.

**Keywords:** Necrotizing fasciitis; Disparities; Gender; Race



**25COASOCT81:****Title: Higher Distressed Communities Index is associated with more aggressive features in papillary thyroid cancer,**

Joy Zhou Done, Alexandra Helbing, Rachel Stemme, Darci Foote, Jennine Weller, Mingzhao Xing, Lilah F. Morris-Wiseman, Aarti Mathur,

The American Journal of Surgery, Volume 248, 2025, 116520,

<https://doi.org/10.1016/j.amjsurg.2025.116520>.

**Abstract:** We sought to identify associations between living in an economically distressed community and the oncologic features and mutational status of papillary thyroid cancer (PTC). Patients with PTC were identified retrospectively. Community distress was estimated using the Distressed Communities Index (DCI). Logistic regression was used to assess associations between DCI, oncologic features, and tumor mutational status. Among 1062 patients, those from “at risk” (9.6%) or “distressed” (7.1%) communities were more likely to have tumors >4 cm (aOR 2.13, 95% CI 1.15–3.95), experience disease recurrence (aOR 1.84, 95% CI 1.16–2.91), and die due to thyroid cancer (aOR 3.56, 95% CI 1.26–10.05) compared to those in “prosperous” (41.6%) communities. No associations were found between DCI and tumor mutations or multifocality. Patients from “distressed” communities are diagnosed with more advanced thyroid cancer with higher rates of recurrence and death despite no differences in tumor mutational profile.

**Keywords:** Papillary thyroid cancer; Tumor mutations; Distressed communities index; Economic distress; Thyroid cancer outcomes

**25COASOCT82:****Title: The path to liver transplantation for low MELD patients: A comparative analysis of deceased and living donor grafts in the perfusion technology era,**

Lauren E. Matevish, Jason Guo, Yanik J. Bababekov, Andrew D. Shubin, Nicolas Goldaracena, Mark R. Pedersen,

The American Journal of Surgery, Volume 248, 2025, 116512,

<https://doi.org/10.1016/j.amjsurg.2025.116512>.

**Abstract:** Patients with low MELD scores remain at substantial risk for waitlist removal. We investigated modern outcomes and graft utilization for low MELD patients undergoing liver transplant (LT) in the US. Adult LT recipients with low MELD scores (match MELD  $\leq$  20) from 2022 to 2023 were identified from the UNOS database and stratified by receipt of a donation-after-circulatory-death (DCD), donation-after-brain-death (DBD), or living donor (LD) graft. Demographic and outcome data were compared. Of 5946 recipients, 21.7 % underwent DCD transplant and 15.7 % LDLT. Both LD and DCD recipients spent less time on waitlist compared to DBD recipients (LD 4.4, DCD 5.0 months vs. DBD 6.0 months,  $p < 0.001$ ). Only DCD grafts preserved with static-cold-storage (SCS) had lower 1-year graft survival rates. Male sex led to higher odds of DCD-LT, while female sex and diagnosis of malignancy or cholestatic disease increased odds of LDLT. Both LD and DCD LT should be nationally encouraged to increase LT access for low MELD patients.

**25COASOCT83:****Title: A pilot study on the impact of da Vinci 5's force feedback on clinical outcomes: Does it lead to less tissue trauma in colorectal surgery?,**

Grace C. Chang, Upinder Sidhu, Debra Lai, Gabriela Vargas, Sai Shah, Laila Rashidi,  
The American Journal of Surgery, Volume 248, 2025, 116518,  
<https://doi.org/10.1016/j.amjsurg.2025.116518>.

**Abstract:** The Da Vinci 5 (DV5) platform's force feedback (FFB) may enhance tactile cues for surgeons. We compare DV5 FFB levels and surgical outcomes in colorectal surgery, focusing on complex versus non-complex cases. A retrospective analysis of colectomies performed with the DV5 between April and July 2024 was conducted. Primary outcomes included time to bowel function and length of stay (LOS). Secondary outcomes included case complexity, complications, operative time, console time, and readmission rates. Among 68 surgeries, the mean time to bowel function was 0.8 days, with no significant differences by force feedback ( $p = 0.12$ ). LOS averaged 1.4 days across feedback levels ( $p = 0.12$ ). Lower force was applied to tissue as FFB setting was higher. Force on tissue was higher in complex cases (2.40 vs. 1.83 N,  $p = 0.007$ ). A trend toward lower force was observed with high feedback settings (1.54 vs. 1.85 N,  $p = 0.0646$ ). Operative and console times were significantly longer in complex cases ( $p = 0.0002$  and  $p = 0.0003$ , respectively). Complications and readmission rates were similar across complexity levels. Preliminary data suggest that FFB does decrease the total amount of force applied without significantly affecting primary outcomes like bowel function and LOS. As expected, operative and console times increase with case complexity. Enhanced FFB may reduce time in non-complex cases and decrease force applied to tissue but has a more pronounced impact in complex surgeries. Further research is needed to clarify its role in clinical outcomes.

## 25COASOCT84:

**Title:** Postoperative pancreatic fistula after pancreaticoduodenectomy: A contemporary analysis of a large national database,

Felipe B. Maegawa, Francisco Tustumi, Ankit D. Patel, Mihir Shah, David Kooby, Arie Szomstein,

The American Journal of Surgery, Volume 248, 2025, 116535,  
<https://doi.org/10.1016/j.amjsurg.2025.116535>.

**Abstract:** Despite the surgical refinement and the rise of minimally invasive surgery (MIS), postoperative pancreatic fistula (POPF) remains a common complication after pancreaticoduodenectomy. The ACS-NSQIP was queried, identifying patients who underwent pancreaticoduodenectomy from 2018 to 2023. A trend analysis and factors associated with POPF (Grade B/C) were examined. In total, 28100 patients were identified. The rate of POPF (Grade B/C) significantly increased from 2018 to 2023, from 13.3 % to 15.7 % (Cochran-Armitage trend test:  $p = .0007$ ). Race was independently associated with increased POPF: Asians and other races versus whites, OR:1.42, 95 %CI:1.22–1.64 and OR:1.29, 95 %CI:1.11–1.41, respectively. Preoperative chemotherapy exerted a protective effect against POPF, OR:0.60, 95 %CI:0.54–0.67. The surgical approach was not associated with POPF. Race was independently associated with receiving preoperative chemotherapy: Asians and other races versus Whites: OR:0.57, 95 %CI:0.48–0.68 and OR:0.42, 95 %CI:0.38–0.47, respectively. The rate of POPF (Grade B/C) after pancreaticoduodenectomy is still prevalent, and racial disparities is significantly associated with its development.

**25COASOCT85:****Title: Examining disparities in management and outcomes among unhoused patients with traumatic brain injury,**

Sean Kim, Stephen Park, Steven Forman, Shea Gallagher, Chais Ugarte,

The American Journal of Surgery, Volume 248, 2025, 116526,

<https://doi.org/10.1016/j.amjsurg.2025.116526>.

**Abstract:** This study aims to investigate any differences in management and hospital outcomes between unhoused and housed patients with traumatic brain injury (TBI). We conducted a 3-year retrospective study (2019–2021). Patients with a head Abbreviated Injury Scale  $\geq 3$  were included and divided into two cohorts: unhoused (UH) and housed underinsured (HUI). Logistic regression assessed the association between the unhoused status and our study outcomes. A total of 1172 patients were identified. There was no significant difference in the rate of acute interventions for TBI, including intracranial pressure monitoring and neurosurgical procedures. Unhoused status was associated with a lower rate of withdrawal of care (3.7 % vs. 11.1 %,  $p = 0.012$ ). After adjusting for confounding factors, UH patients had increased odds of brain death (adjusted odds ratio [AOR]: 8.54,  $p < 0.001$ ) and prolonged ventilator days (AOR: 3.62,  $p = 0.048$ ). Our results suggest that unhoused status may have an influence on end-of-life medical decisions following TBI.

**Keywords:** Traumatic brain injury; Unhoused; Management; Outcome; Disparity

**25COASOCT86:****Title: High usability, low adoption: The struggle of a perioperative patient decision aid for extended thromboprophylaxis after major abdominal cancer surgery,**

Victoria Ivankovic, Abdelrahman Noureldin, Celine Dainhi, Mary Farnand, Rebecca C. Auer, Sameer Apte,

The American Journal of Surgery, Volume 248, 2025, 116415,

<https://doi.org/10.1016/j.amjsurg.2025.116415>.

**Abstract:** Clinical guidelines recommend 30-day extended venous thromboembolism (VTE) prophylaxis after major abdominal cancer surgery, though equipoise exists among experts. We developed a patient decision aid (PtDA) to support patient decision-making and evaluated its perioperative usability. Patients undergoing major abdominal cancer surgery and discharging healthcare professionals at two academic centers were recruited. Usability was assessed using the Post Study System Usability Questionnaire (PSSUQ) for patients and the Pragmatic Assessment Tool (pCAT) for clinicians. PtDA revisions occurred iteratively every three participants. Of 108 eligible patients, 79 (73%) enrolled, and 20 (25%) completed the PtDA. Among them, 65% used it to decide on extended VTE prophylaxis. The median PSSUQ score was 2 (IQR 2–3.75). Fifteen clinicians completed the pCAT, reporting more facilitators than barriers to its implementation. The PtDA was highly useable, but low completion rates suggest systemic barriers that require further study to improve implementation.

**Keywords:** Venous thromboembolism; Perioperative decision-making; Usability; Shared decision making

**25COASOCT87:**

**Title: Don't blame it on the alcohol! Alcohol and Trauma Outcomes: A 10 year retrospective single-center study,**

Joseph C. Nowacki, Eli Jones, Isabella Armento, Krystal Hunter, Justin Slotman, Anna Goldenberg-Sandau,

The American Journal of Surgery, Volume 248, 2025, 116444,

<https://doi.org/10.1016/j.amjsurg.2025.116444>.

**Abstract:** Alcohol use is associated with injury. Although ACS guidelines require screening injured patients for alcohol misuse, outcome data remains inconclusive. This single-center, 10-year (2013–2023) retrospective study examined patients with ISS >15 at a Level I trauma center. Patients from an institutional registry were grouped by blood alcohol content (BAC): positive (>80 mg/dL, BAC-P) or negative (BAC-N). Of 517 patients, 401 were BAC-N and 116 BAC-P. BAC-P patients were younger, mostly male, with lower GCS, higher ISS, and higher Shock Indexes ( $p < 0.001$ ). They required emergency surgery more often ( $p = 0.023$ ), ICU care ( $p < 0.001$ ), and had longer hospital stays (12.1 vs. 8.9 days,  $p = 0.003$ ). Mortality rates were similar between groups. BAC-P patients received more aggressive interventions, possibly mitigating alcohol-related harm. Though BAC-P trauma patients had more severe injuries and required more aggressive care, the lack of difference in mortality suggests that targeted, evidence-based management strategies may benefit intoxicated trauma patients.

**Keywords:** Surgery; Trauma; Alcohol; Resuscitation; Pre-hospital

**25COASOCT88:**

**Title: Effects of socioeconomic factors on biliary disease in patients with sickle cell,**

Jeduthun Harris, Ahmad Zeineddin, Sandy Li, Juan Carmona, Quyen D. Chu, Terrence M. Fullum, Edward E. Cornwell, Mallory Williams,

The American Journal of Surgery, Volume 248, 2025, 116524,

<https://doi.org/10.1016/j.amjsurg.2025.116524>.

**Abstract:** There are approximately 100,000 patients with sickle cell disease (SCD) in America with 134,000 SCD-related admissions annually costing \$1.1 billion. Cholecystectomy is the most common procedure in those patients. We evaluate the impact of socioeconomic factors on peri-operative outcomes. The Nationwide Inpatient Sample was queried for patients with SCD and gallbladder disease between 2006 and 2015. Patients were stratified by insurance and hospital type. Outcomes included perioperative vaso-occlusive crisis (VOC), post-operative morbidity, and mortality. A total of 1779 patients were included. Most patients had Medicaid (49 %), then Private insurance (29 %). Urban-Teaching hospitals cared for 75 % of patients. Complications were lowest with private insurance. On logistic regression, odds of VOC were 1.57 [1.05–2.33] with Medicare and 1.51 [1.13–2.01] with Medicaid. Majority of patients with SCD undergoing cholecystectomy have Medicaid and receive care in urban teaching hospitals. Perioperative VOC was lowest with private insurance and significantly higher with Medicare and Medicaid.

**25COASOCT89:**

**Title: Original scientific paper in-hospital and post-discharge outcomes with autologous versus prosthetic repair of traumatic abdominal vascular injuries: a 10-year review of the PROOVIT registry,**

Negar Nekooei, Danielle Brabender, Stephen Park, Christine Bent, Anaar Siletz, Kazuhide Matsushima,

The American Journal of Surgery, Volume 248, 2025, 116413,

<https://doi.org/10.1016/j.amjsurg.2025.116413>.

**Abstract:** Abdominal vascular injury (AVI) often coincides with bowel injury and abdominal contamination. Prosthetic materials may be necessary for vascular reconstruction, but outcomes are poorly understood. We examined outcomes in patients undergoing autologous vs. prosthetic open repair of AVI using a national database. This retrospective cohort study (2013–2023) utilized the PROOVIT registry. Patients with abdominal aorta, inferior vena cava, iliac artery/vein, renal vein, or portal vein injuries who underwent open repair and survived  $\geq 72$  h were included. Univariate and multivariate analyses assessed the association between repair type and in-hospital vascular complications, including re-intervention, amputation, and bowel resection, as well as re-intervention outcomes specifically. Post-discharge data was also reviewed. A total of 142 patients met inclusion criteria, with 124 (87.3%) undergoing autologous repair, primarily as primary repairs with only 5 autologous vein grafts, and 18 (12.7%) undergoing prosthetic repair, including synthetic grafts and bovine pericardial patches, predominantly for arterial injuries (iliac artery, abdominal aorta). In univariate analysis, no significant differences were observed in in-hospital vascular complications, re-intervention, and infection. In adjusted analysis, prosthetic repairs showed a higher risk of in-hospital vascular complications (aOR 5.253,  $p = 0.017$ ), but comparable risk of re-interventions (aOR 3.046,  $p = 0.138$ ). Follow-up data ( $N = 36$ ) revealed 2 complications (5.6%): one infection (autologous) and one thrombosis (prosthetic). Notably, no prosthetic repair required revision due to infection, either in-hospital or during extended follow-up. Prosthetic repairs may be associated with higher overall complication rates compared to autologous repairs. However, despite the increased complexity of prosthetic repairs and adjustment for injury severity, the autologous cohort did not demonstrate a clear advantage in terms of re-intervention rates. Future studies with more homogeneous cohorts are needed to further confirm or refute the impact of different graft materials on patient outcomes.

**Keywords:** PROOVIT; Vascular trauma; Synthetic graft; Autologous repair; Prosthetic repair

## 25COASOCT90:

**Title: Ten-year outcomes of sleeve gastrectomy in a single-center series of 156 patients: weight loss and need of revisional surgery,**

Arnaud Liagre, Francesco Martini, Olivier Van Haverbeke, Hubert Boudry, Niccolo Petrucciani,

The American Journal of Surgery, Volume 248, 2025, 116525,

<https://doi.org/10.1016/j.amjsurg.2025.116525>.

**Abstract:** The long-term sustainability of sleeve gastrectomy (SG) has been questioned. The aim of the article is to evaluate the results of SG at 10-year follow-up in a high-volume referral center for bariatric surgery. Data of patients who underwent SG between 2004 and 2010 were analyzed. Revisional surgery was proposed in case of weight recurrence (WR), non-response to primary bariatric metabolic surgery or gastroesophageal reflux (GERD) resistant to medical treatment. SG was performed in 156 patients, with mean BMI of 47.6 kg/m<sup>2</sup>. After 10 years, 117 out of 153 patients were evaluated (32 patients lost to follow-up (20.5 %) and four died due to causes unrelated to SG). Mean follow-up duration was 144  $\pm$



13 months. Forty-six patients (39.4 %) did not receive any further bariatric surgery. In this population, the average BMI was 35.1 kg/m<sup>2</sup>, EWL was 55.2 % and TWL was 25.5 % 10 years after SG. 71 patients underwent a second bariatric procedure (60.6 %). The average time between SG and redo-surgery was 51.9 months. Reasons for conversion were weight regain (WR) (53 %), non-response (38 %), GERD resistant to medical treatment (7 %), and gastric stricture (1.4 %). A high BMI (from 46 to over 50) was most often associated with a second bariatric surgery. The present series reports a high rate of revisional surgery after SG at 10 years, for weight recurrence or GERD. On the other hand, patients who did not need revisional surgery had good outcomes in terms of WL and QoL. Patients with lower BMI (<41) at the time of SG experienced the lower rate of WR, non-response and revisional surgery.

**Keywords:** Sleeve gastrectomy; Ten years; Revisional surgery; Weight recurrence; Non-response; Gastroesophageal reflux disease

### 25COASOCT91:

**Title:** Exploring actionable targets to address disparities in thyroid cancer survival: A study of patients with aggressive variants of papillary thyroid cancer,

Alberto J. Monreal, Anthony N. Eze, Samantha M. Thomas, Kimberly S. Johnson, Randall P. Scheri, Hadiza S. Kazaure,

The American Journal of Surgery, Volume 248, 2025, 116428,

<https://doi.org/10.1016/j.amjsurg.2025.116428>.

**Abstract:** Despite compromised survival, disparities studies on aggressive variants of papillary thyroid cancer (PTC) are sparse. Using the NCDB (2004–20), adult Non-Hispanic Whites (NHW), Non-Hispanic Asians or Pacific Islanders (NHAPI), Hispanics, and Non-Hispanic Blacks (NHB) with aggressive variants were abstracted. Mortality risk was estimated using Hazard Ratios (HR). NHB patients had larger tumors ( $p < 0.001$ ) but lower thyroidectomy rates ( $p = 0.04$ ). For all patients, cancer stage posed the strongest mortality risk (HRs Stage II–IV vs. Stage I: 2.75, 4.18, 8.04,  $p < 0.001$ ), however, this was substantially higher by stage for NHBs (HRs Stage II–IV: 4.78, 7.57, 10.49,  $p < 0.001$ ). Age  $\geq 55$  years was the strongest risk factor for Hispanics ( $p < 0.001$ ); non-private insurance was the strongest risk factor for NHAPI, NHBs, and NHWs. Beyond health insurance, actionable targets to improve PTC survival vary by race/ethnicity. For NHBs, higher clinical stage and worse survival by stage might indicate compromised access to optimal care. For Hispanics, improved follow-up, particularly for patients  $\geq 55$  years, may enhance survival.

**Keywords:** Thyroid cancer; Papillary thyroid cancer; Aggressive variants; Race; Ethnicity; Survival; Endocrine surgery

### 25COASOCT92:

**Title:** ErgoEd: a pre-post trial investigating the effect of ergonomic education on laparoscopic surgeons' ergonomic risk scores,

Frances Dixon, Parveen Vitish-Sharma, Achal Khanna, Barrie D. Keeler,

The American Journal of Surgery, Volume 248, 2025, 116398,

<https://doi.org/10.1016/j.amjsurg.2025.116398>.

**Abstract:** This pre-post trial investigates whether ergonomic education using the STEPS model (Screen, Table, Equipment, Posture, Stance) can improve laparoscopic surgeons'

ergonomic risk. Intraoperative photographs taken at 1-min intervals were used to calculate risk through the objective Rapid Entire Body Assessment (REBA) scale. Surgeons were reobserved immediately after an educational video, then again 4–6 weeks later. Cognitive strain (modified NASA-TLX), subjective outcomes, and knowledge retention were also assessed. Ten surgeons were recruited from colorectal, general, and gynaecology. There was no difference in REBA between baseline (REBA = 5.0) and early reobservation (REBA = 4.5) [ $p = 0.058$ ], but between baseline and late reobservation (REBA = 4.5) there was a significant reduction [ $p = 0.028$ ]. The overall scores for each day remained in the “medium risk” category. Knowledge retention was good (90 % correct answers). All found the education worthwhile and subsequently made changes to their practice. Ergonomic education is desired and deemed very important by surgeons, and reduces both their ergonomic risk and subjective experience of pain, but laparoscopic surgery remains ergonomically “medium risk” overall. Further solutions must be found to reduce risk.

**Keywords:** Ergonomics; Minimally invasive surgery; Education

### 25COASOCT93:

**Title:** Impact of surgeon race, ethnicity, and gender on perceptions of professional behavior in the operating room,

Zamaan Hooda, Justin A. Olivera, Emily Rodriguez, Shanique Ries, Rajika Jindani, Lovette Azap,

The American Journal of Surgery, Volume 248, 2025, 116298,

<https://doi.org/10.1016/j.amjsurg.2025.116298>.

**Abstract:** Surgeons’ behaviors may be perceived differentially by operating room (OR) personnel, and implicit biases may have potential impact on those perceptions. We aimed to characterize OR team responses to surgeon behaviors based on perceived demographic traits of the surgeon. This multi-institutional, randomized study surveyed OR personnel responses to five scenarios of surgeon behaviors. Participants were randomized to six different surgeon descriptors, with gender, race, and ethnicity implied by name. Chi-squared analyses assessed differences in responses. 296 individuals completed the survey, with responses found to be dependent on perceived surgeon demographics. In scenarios describing an impatient surgeon and shouting surgeon, Black woman (BW) and Hispanic woman (HW) surgeons’ behaviors were seen as more inappropriate ( $p \leq 0.01$  for both). Respondents were more likely to report BW surgeons arriving late for surgery ( $p < 0.01$ ), and directly address Black and Hispanic surgeons omitting the time-out ( $p = 0.03$ ). Our findings highlight the demographic associations with perceptions of surgeon behaviors, with gender and race resulting in harsher expectations of Black women. Work is needed to better understand and mitigate such inequities.

**Keywords:** Disruptive behavior; Implicit bias; Surgeon behavior; Work environment

### 25COASOCT94:

**Title:** Timing of excisional debridement and its effects on outcomes in geriatric burn patients: A retrospective analysis,

Riddhi Mehta, Kartik Prabhakaran, Anna Jose, Michelle Bravo, Aryan Rafieezadeh, Rishwanth Vetri,

The American Journal of Surgery, Volume 248, 2025, 116528,

<https://doi.org/10.1016/j.amjsurg.2025.116528>.

**Abstract:** Optimal timing for excisional debridement in geriatric burns remains unclear. We hypothesized that early debridement (ED:  $\leq 72$  h) is associated with improved outcomes. A 6-year (2017–2022) analysis of the TQIP database was done to isolate geriatric ( $\geq 65$  years) burn patients (2nd or 3rd degree with TBSA  $\geq 10$  %) undergoing excisional debridement. Propensity score matching (1:1) adjusted for demographics, injury severity, and frailty. Outcomes were mortality, complications, length of stay (LOS), and discharge disposition. After matching 882 patients, ED ( $n = 294$ ) was associated with lower rates of sepsis (2.4 % vs. 7.1 %) and deep vein thrombosis (2.0 % vs. 6.1 %) ( $p < 0.05$ ). There was no difference in mortality. ED had shorter hospital (12 vs. 23 days,  $p < 0.001$ ) and ICU LOS (9 vs. 16 days,  $p < 0.001$ ). ED had higher routine discharge (25.9 % vs. 16.3 %,  $p = 0.039$ ). Early excisional debridement within 72 h is associated with reduced complications and shorter hospitalization in geriatric burn patients.

**Keywords:** Burns; Geriatric; Excisional debridement; Frailty; Outcomes research

#### 25COASOCT95:

**Title:** Association of traumatic brain injury with management and outcomes of patients with blunt thoracic aortic injury,

Victor Andujo, Benjamin Chou, Eni Nako, Samantha Durbin, Gregory L. Moneta, Cherrie Z. Abraham,

The American Journal of Surgery, Volume 248, 2025, 116404,

<https://doi.org/10.1016/j.amjsurg.2025.116404>.

**Abstract:** 30% of patients with blunt thoracic aortic injury (BTAI) can have concomitant traumatic brain injury (TBI), with mortality nearing 20%. Conflicting blood pressure goals may influence decision and timing of thoracic endovascular aortic repair (TEVAR). This study analyzed management and outcomes in patients with concomitant TBI/BTAI. Patients with concomitant TBI/BTAI and BTAI were identified in our trauma registry. Descriptive statistics and logistic regression compared management and outcomes. Twenty patients had concomitant TBI/BTAI. 46 patients had BTAI alone. 9 (13%) patients with concomitant TBI/BTAI and 30 (45%) patients with BTAI alone underwent TEVAR. There was no difference in overall mortality (OR 0.29, 0.05–1.55 CI,  $p = 0.12$ ), aortic-related mortality ( $x^2$  3.51,  $p = 0.06$ ), incidence of TEVAR ( $x^2$  1.59,  $p = 0.10$ ) or timing to TEVAR ( $t = -1.6056$ ,  $p = 0.06$ ) between patients with concomitant TBI/BTAI and BTAI alone. There was no difference in outcomes or interventions in patients with TBI/BTA vs BTAI alone in this small, hypothesis-generating single institutional trial.

**Keywords:** Traumatic brain injury; Blunt thoracic aortic injury

#### 25COASOCT96:

**Title:** Exploring the role of quality of life in surgical decision making for patients undergoing pancreatectomy,

Naveen Manisundaram, Jorge I. Portuondo, Carolyn Chen, Mark Bloomston, Carl R. Schmidt, Nicholas J. Zyromski,

The American Journal of Surgery, Volume 248, 2025, 116523,

<https://doi.org/10.1016/j.amjsurg.2025.116523>.

**Abstract:** The influence of baseline health-related quality of life (HRQoL) on peri-operative outcomes in pancreatobiliary (PB) patients is not well established. This study investigated the impact of baseline HRQoL on peri-operative outcomes and the effect of surgery on HRQoL. A secondary post-hoc analysis of a multicenter trial (2011–2016) assessed PB patients undergoing pancreatectomy. Pre-operative and 30-day post-operative FACT-G surveys were analyzed. Logistic regressions determined associations between baseline HRQoL scores and 60-day major complications. Subgroup analysis evaluated change in HRQoL (pre-operative to 30-day scores). Among 391 patients, higher baseline HRQoL (FACT-G overall OR 0.54,  $p = 0.04$ ) was associated with decreased likelihood of developing major complications. Surgery resulted in improvement in HRQoL for patients with chronic pancreatitis (10.2 points) compared to other pathologies (−7 to 3.9 points). Baseline HRQoL was associated with post-operative complications and HRQoL significantly improved for patients with chronic pancreatitis, highlighting the importance of HRQoL on patient-centered outcomes.

#### 25COASOCT97:

**Title: Racial/ethnic and socioeconomic disparities in cancer mortality hotspots: A multi-state geospatial analysis,**

Azza Sarfraz, Mujtaba Khalil, Zayed Rashid, Abdullah Altaf, Jun Kawashima, Shahzaib Zindani, Timothy M. Pawlik,

The American Journal of Surgery, Volume 248, 2025, 116492,

<https://doi.org/10.1016/j.amjsurg.2025.116492>.

**Abstract:** We sought to identify county-level cancer mortality hotspots for breast, colorectal, lung, and prostate cancers, as well as evaluate contributions of structural factors underlying racial/ethnic disparities, and social vulnerability index (SVI). This ecological analysis included states selected to represent high (i.e., Massachusetts), medium (i.e., Ohio), and low (i.e., Mississippi) GDP categories. A cancer hotspot was defined as a county with elevated cancer mortality rates. Cancer hotspots in Mississippi consisted of higher SVI (breast: 95.9 vs. 82.8), lower median household income (\$34,808 vs. \$43,766), and predominantly Black populations (63.7 % vs. 35.1 %) (all  $p < 0.05$ ). Ohio hotspots had higher rates of food insecurity (17 % vs. 13 %), smoking (lung: 29 vs. 23 %), and obesity (colorectal: 41 % vs. 38 %) (all  $p < 0.05$ ). In Mississippi, disparities rooted in structural racism were more prominent, whereas socioeconomic disadvantage was more prominent in Ohio. Cancer mortality hotspots are disproportionately concentrated in low-GDP states, driven by social vulnerability and economic disparities.

**Keywords:** Cancer mortality; Hotspots; Socioeconomic disparities; Social vulnerability index (SVI); Racial disparities; Geospatial analysis

#### 25COASOCT98:

**Title: Projected augmented reality and dynamic infrared thermography enhances profunda artery perforator flap perforator mapping,**

E.L. Meier, H.J.P. Tielemans, R.F. Pronk, D.J.O. Ulrich, S. Hummelink,

Surgical Oncology, Volume 62, 2025, 102274,

<https://doi.org/10.1016/j.suronc.2025.102274>.

**Abstract:** Preoperative perforator mapping of the Profunda Artery Perforator (PAP) flap is hindered by challenges in aligning preoperative images with the intraoperative lithotomy position of the leg. Dynamic Infrared Thermography (DIRT) is a real-time, quick, and non-invasive imaging modality that is increasingly explored for preoperative perforator mapping. This feasibility study demonstrates the application of Projected Augmented Reality to project thermal images of DIRT directly on the skin for the identification of perforators before PAP flap breast reconstructions. A portable self-aligning projection device (Anatomy Projector) was integrated with a thermal sensor to obtain thermal information and automatically project thermal images onto the patient's medial thigh before PAP flap dissection. Projected DIRT hotspots were evaluated with hand-held Doppler (HHD) and compared to locations of intraoperative perforators following a Cartesian coordinate system. Preoperative DIRT examination yielded a projection of 127 DIRT hotspots in 20 PAP flaps. All projected hotspots could be verified with Doppler (100 %) and 82.1 % of intraoperative perforators correlated with a projected DIRT hotspot within a 3 cm radius. Notably, 30.4 % of these matches involved the first appearing DIRT hotspot, and 82.6 % of these matches involved a DIRT hotspot within the first 5 appearing hotspots. This feasibility study pioneers the use of Projected Augmented Reality for the display of thermal images of DIRT directly on the skin for the preoperative perforator identification before PAP flap harvest. High resemblance with HHD and intraoperative perforators was found. Future research should examine the further applications in the intraoperative and postoperative setting.

**Keywords:** Dynamic infrared thermography; Augmented reality; Profunda Artery Perforator (PAP) flap; Free flap surgery; Perforator mapping; Autologous breast reconstruction

## 25COASOCT99:

### **Title: Trend shift from autologous to implant-based breast reconstruction,**

Ekaterina Nedeoglo, Philipp Moog, Jun Jiang, Inessa Suhova, Hans-Günther Machens, Kai Megerle, Haydar Kükrek,

Surgical Oncology, Volume 62, 2025, 102256,

<https://doi.org/10.1016/j.suronc.2025.102256>.

**Abstract:** Breast cancer is the most common type of cancer in women and advances in treatment have shifted the focus towards improving quality of life. Breast reconstruction plays a crucial role in preserving body image for patients undergoing mastectomy. However, significant variations exist in breast reconstruction choices across different countries. Understanding national trends can help optimize patient-centered care. Using data from quality reports, we analyzed breast reconstruction trends in Germany from 2012 to 2021. The study examined overall reconstruction rates, the distribution of reconstruction methods (implant-based vs. autologous), and differences between surgical departments. Breast reconstruction rates in Germany have steadily increased, with up to 38 % of mastectomy patients undergoing reconstruction. The number of implant-based reconstructions rose significantly by nearly 70 % during this period. Most reconstructions were performed in gynecology departments, where the highest increase in implant-based procedures was observed. The reasons for the shift towards implant-based reconstruction are speculative. The increase in contralateral prophylactic mastectomies, the lack of collaboration with plastic surgery departments and the complexity of autologous breast reconstruction could all be plausible explanations for this observation. Further analysis and critical evaluation of current



trends are essential to ensure an individualized, patient-centered approach to breast reconstruction surgery.

**Keywords:**Breast reconstruction; Autologous breast reconstruction; Implant-based breast reconstruction; Skin-sparing mastectomy

#### 25COASOCT100:

**Title: The Qaly study: Quality of life and lower extremity lymphedema in 174 patients after inguinal lymphadenectomy,**

Brett A. Hahn, Alieske Kleeven, Milan C. Richir, Arjen J. Witkamp, Anke M.J. Kuijpers, Surgical Oncology, Volume 62,2025,102257,  
<https://doi.org/10.1016/j.suronc.2025.102257>.

**Abstract:** Lower extremity lymphedema (LEL) can develop in patients who undergo inguinal lymph node dissection (ILND) in the treatment of gynecologic, genitourinary, and skin and soft tissue malignancies. While LEL can negatively impact quality of life, the poorly documented prevalence and severity of lymphedema-related symptoms complicates the ability to identify high-risk patients and improve the selection of candidates for emerging microsurgical interventions. This multicenter, cross-sectional study included patients who underwent ILND between 1990 and 2022 across three medical centers in the Netherlands. Retrospective clinical data, including demographic, surgical, and postoperative variables, were abstracted from medical records. Lymphedema prevalence and severity were assessed using the Lymph-ICF-LL questionnaire, while additional patient-reported outcome measures (PROMs) evaluated quality of life and lower extremity function. Statistical analyses included multivariate logistic and linear regression to identify predictors of lymphedema-related symptoms and their impact on PROMs. Among 174 patients who underwent ILND, 77 % reported lymphedema-related symptoms, which were associated with significantly lower quality of life. Multivariable analysis identified that younger age at time of surgery, medical history of cardiovascular disease, and postoperative complications such as surgical site infections (SSI) and prolonged wound healing were significant predictors of developing lymphedema-related symptoms. Additionally, the presence of lymphedema was strongly linked to poorer physical and mental health PROMs, with malignancy type and surgical factors influencing these outcomes. This study emphasizes the significant burden of lymphedema-related symptoms following ILND, while highlighting the potential role of reconstructive microsurgery in reducing morbidity for high-risk patients.

**Keywords:**Lower extremity lymphedema (LEL); Inguinal lymph node dissection (ILND); Inguinal lymphadenectomy; Quality of life; lymphedema; Patient-reported outcome measures (PROMs)

#### 25COASOCT101:

**Title: Does Tilmanocept based lymphoscintigraphy measure up against colloid-based lymphoscintigraphy for sentinel node biopsy in melanoma and early oral squamous cell cancer?,**

Giuleta Jamsari, Eva Wong, Gopi Elango, Michael Veness, Bradley Camden, David Farlow, Muzib Abdul-Razak, Surgical Oncology, Volume 62,2025,102258,  
<https://doi.org/10.1016/j.suronc.2025.102258>.

**Abstract:** Sentinel lymph node biopsy (SLNB) is crucial in cutaneous melanoma and oral cavity squamous cell carcinoma (OCSCC) as it directs the need for systemic therapy. There has been growing interest in Technetium-99m-labeled Tilmanocept (TL) due to its specific binding capability. This study compares the efficacy of TL to 99mTc-antimony sulphide colloid (ASC), in these two biologically distinct cancers. In this prospective cross-sectional study, 40 patients were included in each radiotracer group. The primary outcomes measured SN identification rate on lymphoscintigraphy and surgical node retrieval rate. Secondary outcomes include pathological status of lymph nodes, false negative rates (FNR), and nodal recurrence. TL had comparable outcome to ASC with a 100 % SN detection and retrieval rate. Both radiotracers had 100 % lymph nodal tissue specificity with an FNR rate of 0 % for both radiotracers in CM and 25 % for TL in OCSCC. There were significant differences between the SN detection and retrieval rates in ASC in CM and OCSCC but not TL, reflecting its superior binding capability. Our study is the first to demonstrate the superior molecular binding capability of TL with minimal migration to the second echelon nodes.

**Keywords:** Tilmanocept; Sulphide colloid; Oral squamous cell carcinoma; Melanoma; Sentinel lymph node; Sentinel lymph node biopsy

## 25COASOCT102:

**Title:** Signal heterogeneity in apparent diffusion coefficient map of magnetic resonance imaging in resectable pancreatic cancer: a new prognostic factor for biological borderline resectable pancreatic cancer,

Michinori Matsumoto, Masashi Tsunematsu, Kenei Furukawa, Koichiro Haruki, Yoshihiro Shirai,

Surgical Oncology, Volume 62, 2025, 102270,

<https://doi.org/10.1016/j.suronc.2025.102270>.

**Abstract:** This study aimed to identify recurrence and prognostic factors in patients with resectable pancreatic cancer (RPC) that may define biological borderline resectable pancreatic cancer (BRPC). This retrospective study included 162 patients with R/BRPC who underwent upfront surgery. Univariate and multivariate analyses were performed to assess the relationship between preoperative factors and disease-free survival (DFS) and overall survival (OS) for RPC. The cutoff value for the coefficient of variation of apparent diffusion coefficient (CVADC) on preoperative magnetic resonance imaging was determined using receiver operating characteristic curve analysis. Surgical outcomes of patients with RPC were stratified by a score, with each independent prognostic factor assigned 1 point. The outcomes of R/BRPC patients were compared according to the score. Of the patients, 145 had RPC, and 17 had BRPC. In RPC patients, serum CA19-9 >500 U/mL ( $p = 0.03$ ) and  $CVADC \geq 0.1$  ( $p = 0.003$ ) were independent recurrence factors, while serum CA19-9 >500 U/mL ( $p = 0.03$ ), superior mesenteric vein/portal vein contact  $<180^\circ$  ( $p = 0.03$ ), and  $CVADC \geq 0.1$  ( $p < 0.001$ ) were independent prognostic factors. RPC patients with a score of 0 had significantly better prognoses than those with scores of 1 or 2–3, and BRPC patients (median DFS: 35.0, 9.8, 9.0, and 7.0 months; median OS: 80.7, 26.5, 16.8, and 17.6 months, respectively). No significant difference in prognosis was found between BRPC patients and RPC patients with scores of 1 or 2–3. Preoperative CVADC in RPC may be a new recurrence and prognostic factor defining biological BRPC.

**Keywords:** Apparent diffusion coefficient; Biological borderline resectable pancreatic cancer; Coefficient of variation

### 25COASOCT103:

**Title:** Surgery versus immunotherapy in locally advanced cutaneous carcinoma of the external ear: A multicenter study,

Francesco Mattioli, Matteo Miglio, Margherita Basso, Giacomo Papi,

Surgical Oncology, Volume 62, 2025, 102271,

<https://doi.org/10.1016/j.suronc.2025.102271>.

**Abstract:** Immunotherapy is a promising therapeutic strategy for cutaneous carcinoma in locally advanced and advanced stages. This study aims to compare the survival outcomes between patients treated with surgery and those treated with cemiplimab. Secondly, we evaluated how adjuvant treatment, tumor stage, and margins status may influence the oncological outcomes in the surgical group. The study included 77 patients with locally advanced cutaneous carcinoma of the external ear treated between 2015 and 2023 with surgery, either followed or not by adjuvant therapy, or treated with cemiplimab. Immunotherapy demonstrated a benefit in the disease-specific survival both at 24 months (HR = 0.09,  $p = 0.02$ ) and at 60 months (HR = 0.11,  $p = 0.04$ ) when compared to patients treated by surgery, with an estimated 5-year survival of 80 % and 55.9 %, respectively (log-rank = 0.03). Conversely, surgery showed a more favorable trend for disease-free survival than cemiplimab (HR 0.58,  $p = 0.08$ ), with a median survival of 25.6 and 14.2 months. Stage IV, compared to stage III, tended to have a worse survival rate when stratified by treatment strategy. The addition of adjuvant therapy improved median disease-specific survival from 12 to 40 months for stage IV. On the other hand, adjuvant radiotherapy did not significantly affect outcomes when stratified by margin status, especially when resection margins were clear ( $p = 0.36$ ). Cutaneous carcinoma of the external ear represents a rare entity, affecting elderly patients and still associated with high complication rates. Emerging therapeutic strategies, which may serve as alternatives to surgery, offer a basis for future adjustments of treatment algorithms for these neoplasms.

**Keywords:** Cutaneous carcinoma; External ear carcinoma; Locally advanced tumors; Surgery; Immunotherapy; Survival

### 25COASOCT104:

**Title:** Prevention in non-oncologic intent sarcoma surgery,

Clare E. Wise, Chris Le, Nicole S. Pham, Christin New, Deborah Ellen Kenney, Raffi Avedian, David Mohler, Robert Steffner,

Surgical Oncology, Volume 62, 2025, 102273,

<https://doi.org/10.1016/j.suronc.2025.102273>.

**Abstract:** Non-oncologic resection of soft tissue sarcomas (STS) continue to be a common referral to multidisciplinary sarcoma centers. While previous literature has reported tumor characteristics and outcomes related to non-oncologic resections, little is known regarding the surgical specialties most likely to excise such a mass and the non-oncological manner in which they do so. Such information can facilitate preventative strategies. The goals of this study are: 1) Investigate the surgical specialties that most often perform unplanned excisions and their diagnostic imaging approach, 2) Identify the frequency of non-oncological

techniques utilized in initial unplanned excisions, and 3) Define indications for the use of radiation (XRT) in patients with initial non-oncologic resections of STS. Patient data were collected from a large tertiary referral sarcoma center between 2005 and 2022. Eligible patients had a diagnosis of soft tissue sarcoma that was excised at an outside institution in a non-oncologic manner and subsequently underwent tumor bed re-excision using wide resection. Data regarding the index procedures at outside hospitals were obtained from referral documents and tumor bed re-excisions, along with follow-up care. A total of 124 patients were identified. Forty-three percent of referrals for non-oncologic resection of soft tissue sarcomas (STS) involved tumors located deep to the fascia. The majority of these referrals originated from General Surgery (N = 54, 44 %), Orthopedic Surgery (N = 35, 28 %), and Plastic Surgery (N = 11, 9 %). Preoperative imaging was conducted in 59 % of cases. General surgeons were less likely to obtain preoperative imaging ( $p = 0.009$ ) and perform MRI scans ( $p = 0.013$ ) than orthopaedic surgeons. The proper orientation of the incision based on location was incorrect for general surgeons in 26 % (N = 20) of cases. General surgeons were less likely to make an appropriate incision ( $p = 0.052$ ) and to use a tourniquet during the initial procedure ( $p < 0.001$ ). There were no differences among surgical subspecialties in the use of local anesthetic, drain use, or excision type regarding the initial non-oncologic resection. Residual disease following tumor bed re-excision was linked to masses removed in the clinic ( $p = 0.030$ ) and initial stage IIIB tumors ( $p = 0.019$ ). Our institutional use of radiation therapy (XRT) correlated with large initial size, high-grade histology, location deep to fascia, and tumors that were re-excised with staged coverage by plastic surgery. Most referrals for initial non-oncologic resection of STS come from general surgery followed by orthopaedic surgery. Indications for pre-operative MRI imaging, incision orientation, and tourniquet use are education targets for general surgeons in training. Interpretation of MRI scans is an education target for orthopaedic surgeons in training. Clinic procedures are associated with residual disease on tumor re-excision. Radiation before tumor bed re-excision can be considered for larger, high-grade tumors that are deep to the fascia and when plastics coverage is planned.

## 25COASOCT105:

**Title:** Effect of antiviral treatment for hepatitis C virus on long-term outcomes in patients undergoing resection for hepatocellular carcinoma,

Hiroyuki Hakoda, Yoshikuni Kawaguchi, Yujiro Nishioka, Yuichiro Mihara, Akihiko Ichida, Surgical Oncology, Volume 62, 2025, 102255,

<https://doi.org/10.1016/j.suronc.2025.102255>.

**Abstract:** Hepatitis C virus infection is a risk factor for hepatocellular carcinoma (HCC). The effect of direct-acting antivirals on prognoses remains unclear. We assessed the prognosis of patients receiving direct-acting antiviral and interferon treatment after the initial resection of hepatitis C virus-related HCC. We retrospectively analyzed patients who underwent initial hepatitis C virus-related HCC resection at The University of Tokyo Hospital between June 2009 and December 2022. Recurrence-free survival (RFS) and overall survival (OS) were assessed using the log-rank test. Cox proportional hazards model analysis was performed to identify the risk factors for RFS and OS. Of 756 patients who underwent HCC resection, 142 had hepatitis C virus-related HCC. Among them, the 5-year OS was significantly better in those receiving antiviral treatment than in those without antiviral treatment (72.2 % vs.

48.9 %,  $P < 0.001$ ); however, RFS did not differ between the groups ( $P = 0.35$ ). RFS and OS did not differ significantly between patients who received direct-acting antivirals and those who received interferon ( $P = 0.09$  and  $P = 0.47$ , respectively). RFS and OS did not differ significantly between patients receiving antiviral treatment before surgery and those after surgery ( $P = 0.11$  and  $P = 0.23$ , respectively). Antiviral treatment improved postoperative prognosis; however, the prognosis did not differ between the types of antiviral treatment in patients with hepatitis C virus-related hepatocellular carcinoma.

**Keywords:** Hepatectomy; Prognosis; Direct-acting antiviral

#### 25COASOCT106:

**Title:** Impact of the completeness of cytoreductive surgery on the prognostic role of the KELIM score in patients treated for ovarian peritoneal metastasis,

Charif Khaled, Lise Sogalaw, Laura Polastro, Maxime Fastrez, Michel Moreau, C. Florin Pop, Isabelle Veys, Vincent Donckier, Gabriel Liberale,

Surgical Oncology, Volume 62, 2025, 102272,

<https://doi.org/10.1016/j.suronc.2025.102272>.

**Abstract:** The two major treatment related prognostic factors for peritoneal metastasis of ovarian cancer (PMOC) are chemosensitivity and completeness of cytoreduction (CC). Chemosensitivity can be assessed by the CA-125 elimination rate constant K (KELIM) score, based on CA-125 kinetics. CC is evaluated by residual macroscopic disease. The aim of this study was to evaluate the prognostic impact of KELIM score versus CC, in a population who underwent complete (CC-0) and near-complete (CC-1) debulking. Monocentric retrospective study including patients with primary PMOC treated with curative intent between January 2010 and December 2021. The Biomarker Kinetics website (CA-125 KELIM Calculator) was used to calculate the KELIM score. Univariate and multivariate analysis were performed to assess the impact of CC and KELIM score on PFS and OS. A total of 111 patients were included in the study. Kaplan-Meier analysis showed that PFS and OS were significantly influenced by KELIM, CC, PCI, and BRCA mutation ( $p < 0.05$ ). Multivariate Cox analysis showed that PFS was significantly influenced by CC (HR = 0.481,  $p = 0.0027$ ), while OS was influenced by KELIM (HR 0.561,  $p = 0.0408$ ). These results suggest that PFS is more impacted by the completeness of the surgery than the KELIM score and the KELIM score influences OS more than the completeness of surgery.

**Keywords:** Ovarian cancer; Peritoneal metastasis; KELIM; Cytoreductive surgery; PCI; Complete surgery

#### 25COASOCT107:

**Title:** Shear wave elastography combined with high-frequency ultrasound for predicting the presence of occult carcinoma contralateral to unilateral papillary thyroid cancer,

Shu-ni Jia, Dong Wang, Zhe-xia Zhao, Ting-ting Xue,

Surgical Oncology, Volume 62, 2025, 102267,

<https://doi.org/10.1016/j.suronc.2025.102267>.

**Abstract:** To investigate the correlation between high-frequency ultrasound (US) signs and shear wave elastography (SWE) parameters of papillary thyroid carcinoma (PTC) in a unilateral lobe and the contralateral lobe occult PTC, and to evaluate the value of SWE in



combination with high-frequency US in predicting contralateral occult carcinoma of the thyroid gland preoperatively, to provide clinicians with assistance in the selection of preoperative surgical approaches. We collected a total of 552 preoperatively diagnosed patients with unilateral thyroid carcinoma and postoperatively pathologically confirmed PTC. High-frequency US and SWE were performed before surgery. Based on the pathologic findings, they were divided into the contralateral occult PTC positive group and the negative group. To investigate the association between the ultrasonographic features of unilateral PTC and the presence of contralateral occult carcinoma by univariate and multivariate analyses, and comparing the accuracy of high-frequency US alone, SWE alone, and SWE combined with high-frequency US in predicting contralateral occult PTC. Univariate analysis showed that the differences between the two groups of extrathyroidal extension (ETE), ipsilateral multifocality, the combination of Hashimoto's thyroiditis (HT), the combination of lymph node metastasis, and Emax and Emean values of the primary tumors were statistically significant ( $P < 0.05$ ). The multifactorial binary logistic regression model showed that the differences between the two groups of extrathyroidal extension, ipsilateral multifocality, lymph node metastasis, HT and high Emax value were all independent predictors of contralateral occult PTC. The ROC curve analysis showed no statistically significant difference between high-frequency ultrasound and SWE in predicting the AUC of contralateral occult PTC (0.739 vs 0.699,  $P = 0.185$ ). The AUC for predicting contralateral occult PTC using high-frequency US combined with SWE was significantly higher than the AUC predicted using high-frequency US and SWE alone (0.794 vs 0.739,  $P = 0.005$ ; 0.794 vs 0.699,  $P < 0.001$ ). SWE combined with high-frequency US improves the prediction of contralateral occult PTC, and the presence of contralateral occult PTC is more likely in the presence of extrathyroidal extension of a unilateral lobe lesion of the thyroid gland, ipsilateral multifocality, metastasis to cervical lymph nodes, high Emax, and the combination of HT.

**Keywords:** Papillary thyroid carcinoma; Contralateral occult carcinoma; Shear wave elastography; Ultrasound; Risk factors

## 25COASOCT108:

**Title:** Diagnostic utility of the preoperative cachexia index for malnutrition in colorectal cancer: A prospective cohort study,

Katarzyna Chawrylak, Wojciech Górski, Katarzyna Sędlak, Radosław Mlak, Marta Kaus,

Surgical Oncology, Volume 62, 2025, 102275,

<https://doi.org/10.1016/j.suronc.2025.102275>.

**Abstract:** Cachexia is a multifactorial syndrome characterized by weight and muscle loss, often linked to malnutrition and inflammation. Malnutrition affects almost 40 % of colorectal cancer (CRC) patients, contributing to worse surgical outcomes, higher morbidity, and increased mortality. This study evaluates the Cachexia Index (CXI) for malnutrition detection in CRC patients. Seventy patients (54.3 % men; median age 65) underwent bioelectrical impedance analysis, blood tests, and nutritional assessments before surgery. Patients were recruited between November 1, 2023, and October 30, 2024. CXI, calculated as  $[\text{Skeletal Mass Index} \times \text{Serum Albumin}] / \text{Neutrophil-to-Lymphocyte-Ratio}$ , was compared with the Subjective Global Assessment. The median CXI was 13.7 (range: 1.9–53.8), with malnourished or at-risk patients exhibiting significantly lower median CXI values (9.5 vs. 14.9;  $p = 0.0262$ ) than well-nourished individuals. Tumor location also influenced CXI;

patients with sigmoid colon tumors had the highest median CXI, while those with caecum tumors had the lowest (22.2 vs. 8.2;  $p = 0.0202$ ). CXI demonstrated 100 % sensitivity and 60 % specificity for malnutrition detection, with a cutoff of  $\leq 12.09$  (AUC = 0.80; 95 % CI: 0.69–0.89;  $p < 0.0001$ ). Malnourished patients had a significantly lower median CXI (9.5 vs. 14.9;  $p = 0.0262$ ). These findings support CXI as a reliable, non-invasive biomarker for malnutrition in CRC patients, with potential applications in personalized nutritional and therapeutic care.

**Keywords:** Colorectal cancer; Cachexia index; Cachexia; Sarcopenia; Surgical outcomes; Subjective global assessment

---

**List of Serials**  
**Abstracted in COAS**  
**COAS, Volume- 2 Issue No. 10, 2025**

1. American Journal of Roentgenology, Volume-225, Issue- 3, 2025
2. Annals of Oncology, Volume-36, Issue- 9, 2025
3. Anticancer Research, Volume 45, Issue 10, 2025
4. Apoptosis, Volume 30, Issue 9 & 10, 2025
5. Archives of Pathology and Laboratory Medicine, Volume-149, Issue - 9, 2025
6. Asian Journal of Surgery, Volume 48, Issue 10, 2025
7. Biochimica Et Biophysica Acta (BBA) Review of Cancer, Volume 1880, Issue 5, 2025
8. Blood , Volume-146, Issue- 1,2,3 & 4, 2025
9. British Journal of Anaesthesia, Volume 135, Issue 4, 2025
10. Cancer Cytopathology, Volume-133, Issue - 10, 2025
11. Cancer Gene Therapy, Volume 32, Issue 10, 2025
12. Cancer, Volume 131, Issue 18, 2025
13. Carcinogenesis, Volume 46, Issue 3, 2025
14. European Journal of Surgical Oncology, Volume 51, Issue 10, 2025
15. International Journal of Cancer , Volume-157, Issue- 3, 2025
16. JAMA.; Volume-334, Issue- 1,2,4 & 5, 2025
17. Journal of American Chemical Society, Volume 147, Issue 36,37, 38 & 39, 2025
18. Journal of Cardiothoracic and Vascular Anesthesia, Volume 39, Issue 10, 2025
19. Journal of Clinical Oncology, Volume 43, Issue- 15, 16 & 17, 2025
20. Journal of Clinical Pathology, Volume- 78, Issue- 9 & 10, 2025
21. Journal of Cranio-Maxillofacial Surgery, Volume 53, Issue 10, 2025
22. Journal of Critical Care, Volume 89, 2025
23. Journal of Pain and Symptom Management, Volume 70, Issue 4, 2025
24. Medical Oncology, Volume- 42, Issue- 9, 2025
25. Nature Cell Biology, Volume 27, Issue 9, 2025
26. New England Journal of Medicine, Volume- 393, Issue- 6,7,8,9 & 10, 2025
27. Surgical Oncology, Volume 62, 2025
28. The American Journal of Surgery, Volume 248, 2025
29. The American Journal of Surgical Pathology, Volume- 49, Issue- 10, 2025
30. The Annals of Thoracic Surgery, Volume 120, Issue 4, 2025
31. Toxicology Letter, Volume 412, 2025
32. Trends in Anaesthesia and Critical Care, Volume 64, 2025

# Current Oncological Abstract Service (COAS)



**Chittaranjan National Cancer Institute**

(An Autonomous Body under Govt. of India, Ministry of Health & Family Welfare)

1st Campus, Hazra: 37, S.P. Mukherjee Road, Kolkata-700026

2nd Campus, New Town: Street Number 299, DJ Block, Action Area I, New Town, Kolkata-700160